# Dilution torque control of a gasoline engine

Maugham, Robin

*Award date:*
2002

*Awarding institution:*
University of Bath

# Dilution Torque Control of a Gasoline Engine

Submitted by Robin Maugham
For the degree of PhD of the University of Bath 2002

## COPYRIGHT







ProQuest LLC
789 East Eisenhower Parkway
P.O. Box 1346
Ann Arbor, MI 48106-1346

## Summary

A continuously variable transmission (CVT) allows a powertrain controller the freedom to develop a required output power at a range of engine torque / speed conditions. This flexibility can be used to maximise fuel efficiency. Due to low frictional and pumping losses a gasoline engine's fuel efficiency is maximised at low speed, high torque conditions. However due to the reduced torque margin available, controlling a gasoline engine in this region compromises transient vehicle response.

In this thesis the use of charge diluents, such as exhaust gas recirculation and excess air, to control engine torque is introduced. Dilution torque control has the potential to maintain the economy gains available using a CVT powertrain whilst improving a vehicle's transient response.

A test rig has been developed to assess the potential of dilution torque control. The test rig is based around an engine fitted with variable cam phasing, which has been modified to include a large bore EGR system and electronic throttle. The test rig allows the effect of five control variables, namely: EGR rate, valve overlap, engine fuelling rate, spark timing and throttle position, to be investigated across a range of engine speed conditions.

Steady state and transient test programs have been undertaken. In order to maximise the quality of data derived from the steady state test program a Design of Experiments (DoE) approach has been applied. This DoE approach features an adaptation developed to minimise the effect of response signal oscillation suffered by high order regression models. Transient investigations were undertaken to characterise the engine's torque response to step changes in charge dilution rate.

Using the steady state DoE models and transient response results a multi-objective optimisation process was undertaken. The optimisation procedure developed control variable settings for power conditions which minimised both fuel consumption and engine transient response. The solutions developed were constrained to meet current emissions legislation. The effect of the optimised power conditions was investigated over a legislative drive cycle, this showed the use of dilution torque control could develop a 6% fuel economy improvement in addition to the transient benefits.

## Acknowledgements

The author would like to express many thanks to Torotrak Development Ltd, the Ford Motor Co. and the EPSRC for supporting this research project financially. Thanks go especially Steve Murray, and Prof. Nick Vaughan, for conceiving and developing this project, and to Dr. Chris Brace for supervising the project alongside Prof. Vaughan. I must also thank Prof. Alec Parker for his input to this work, especially for his thoughts during the later stages.

In particular I would like to thank Brian Eves and Trevor Taylor who have acted as liaisons with Ford and similarly Iain James at Torotrak. Additionally I would like to thank the many technical support staff who assisted me throughout this project. Notably, Alan Brewer for building the test rig, Jeff Brewster and Vejay Singh for the test rig instrumentation work. A special thanks should be given Allan Cox for his continual support, guidance and level headed approach. Similarly Eric Brain, Steve Combes and George Bonwick deserve a special mention for entertaining me and always being available to offer help and advice.

Thanks should also go to all the people in my office who have entertained me over the last few years and given invaluable advice and help, Adrian Cooper, Richard Olafsson, Jon Hall, Dr. Roshan Wijetunge, Dr. Volker Wicke, Matthew Ward, Simon Pickering, Damian Higgs, Paul Newton, and Ben Shalders.

Also my numerous unnamed friends who have managed to enforce some sanity in my life over the past 4 years deserve a massive thank you. Thanks should also go to my family for their support over the last 4 years. Finally a special mention should go to Sam and Catherine Akehurst for their outstanding support, guidance, and help during the last 4 years.

## TABLE OF CONTENT

# INDEX OF FIGURES

# INDEX OF TABLES

ABBREVIATIONS

| | | |
|---|---|---|
| TDC | Top dead centre (prefix: B - before; A - after) | |
| BDC | Bottom dead centre (prefix: B - before; A - after) | |
| CO | Carbon monoxide (prefix: BS - Brake specific) | g/kWh |
| $CO_2$ | Carbon dioxide (prefix: BS - Brake specific) | g/kWh |
| $COV_{imep}$ | Coefficient of variation of indicated mean effective pressure | % |
| CVT | Continuously variable transmission | |
| DoE | Design of Experiments | |
| ECE-15 | Urban component of European drive cycle | |
| ECU | Engine controller unit | |
| EGR | Exhaust gas recirculation | |
| e-line | Engine economy control line | |
| EUDC | Extra urban component of European drive cycle | |
| EVO | Exhaust valve opening (prefix: L-late; E-early) | |
| EVC | Exhaust valve closure (prefix: L-late; E-early) | |
| GDI | Gasoline direct injection | |
| HCCI | Homogenous charge compression ignition | |
| HEGO | Heated exhaust gas oxygen sensor | |
| iEGR | Internal Exhaust gas recirculation | |
| ISAD | Integrated starter alternator damper | |
| IVO | Inlet valve opening (prefix: L-late; E-early) | |
| IVC | inlet valve closure (prefix: L-late; E-early) | |
| MAF | Manifold air flow | |
| MPI | Multi point injection | |
| $NO_x$ | Oxides of nitrogen (prefix: BS - Brake specific) | g/kWh |
| $O_2$ | Oxygen (prefix: BS - Brake specific) | g/kWh |
| OBD | On board diagnostics | |
| $R^2$ | Correlation coefficient | |
| RCON | Research console | |
| TWC | Three way catalyst | |
| uHC | Unburnt hydrocarbons (prefix: BS - Brake specific) | g/kWh |
| UoB | University of bath | |
| VCT | Variable cam timing | |
| VVA | Variable valve actuation | |
| WOT | Wide open throttle | |

# 1 Introduction

The pressures of environmental legislation on the automotive industry have been well documented[1,2,3]. Recently there has been legislative impetus to limit the emissions of green house gases, particularly carbon dioxide ($CO_2$)[4] whose production is proportional to fuel consumption for carbon based fuels. Many technologies are being investigated which have the potential to reduce fuel consumption. Gasoline engined vehicles are particularly problematic due to their high fuel consumption characteristics under throttled conditions. The technologies that have been developed that may help to reduce gasoline engine fuel consumption are:-

- Lean burn and gasoline direct injection (GDI) engines[5]
- Variable valve throttling[6]
- Variable compression ratio[7]
- Homogenous charge compression ignition (HCCI)[10,11]

Although these concepts offer much promise, many of them are far from production feasibility. Another approach to reducing vehicle fuel consumption is to improve the utilisation of the gasoline engine. Work by Takiyama & Morita [12], Hendricks[13] and Kriegier et al[14] has shown that the use of advanced transmission concepts has the potential to improve vehicle fuel consumption. The engines and advanced transmissions tested in these studies are currently in production, but the full potential improvement in fuel economy has yet to come to fruition. The predominant reason for this is that the optimisation that yielded the minimum fuel consumption failed to consider the demands of driveability.

The following sections of Chapter 1 will examine the fuel consumption compromises developed for gasoline engines with conventional transmissions, with particular reference to their transient response. This will be followed by an examination of the advanced transmissions used by Takiyama & Morita [12], Hendriks[13] and Kriegier[14], considering the approaches used to minimise fuel consumption, and the causes of poor transient response. The examination then extends to additional hardware that may be introduced to reduce the necessary compromise in fuel consumption needed to secure adequate transient response. Finally this chapter introduces an engine-transmission matching concept which uses systems fitted to production gasoline engines to achieve high fuel economy, combined with a good transient driveability characteristic.

## *1.1 Types of transmissions*

Throughout the 20th century a number of approaches have been used to transfer motive power from the vehicle prime mover to the driving wheels; of these the most popular has been the conventional discrete ratio transmission.

### 1.1.1 CONVENTIONAL DISCRETE RATIO TRANSMISSIONS

The conventional manual fixed ratio transmission features a set of helically cut gears, a synchromesh mechanism to allow smooth engagement of ratios and a frictional clutch to disengage the transmission from the prime mover[15]. Modern discrete ratio gearboxes typically offer five forward ratios, i.e. four transitional ratios with an overdrive gear for high speed cruising, although sport models have started to offer an additional sixth ratio. The popularity of conventional discrete ratio transmissions is primarily due to market demand, since manual transmissions are cheaper and are perceived to provide a 'sportier' drive. Additional benefits are high mechanical efficiency and the ability to handle large torque reductions within a simple scaleable compact unit[16].

Automatic transmissions have proved very popular in the Northern American market. These transmissions replace the friction clutch, synchromesh arrangement of a manual fixed ratio transmission with a torque converter and an epicyclic geartrain[15]. The fluid coupling torque converter that replaces the clutch allows smooth pull away and transition through different ratios by dissipating the power mismatch that exists between the wheels and the engine. Modern torque converter couplings have relatively small ranges of use, but while in these ranges, transmissions are highly inefficient. Ratio selection is achieved by a series of wet clutch band brake mechanisms selected by an hydraulic control system. Automatic transmissions have proved popular due to the low level of driver input required, however for a given number of units the cost is considerably greater than that of a discrete ratio manual transmission, reportedly up to 68% more[17]. Additionally, as a result of, the influence of the torque converter coupling, this type of transmission is considerably less efficient and larger than a conventional manual transmission. Since this transmission features an automated gear selection device, there is potential to force ratio changes to match engine efficiency regions. However in practice ratio changes are typically scheduled for smooth shift quality.

Figure 1-1 is a speed / torque graph for a fictitious gasoline engine showing the wide open throttle (WOT) line, and the engine motoring line. The plot shows typical fixed ratio gear running lines. Superimposed upon this figure are constant power lines (dotted blue) Additionally superimposed are lines of constant brake specific fuel consumption (BSFC) in red. Although conventional gearboxes offer high mechanical efficiency (up to 98%[17]), It can be seen that it does not necessarily follow that the powertrain as a whole has a high efficiency. For a given steady state vehicle speed, a conventional five ratio gearbox can only develop the required power at five engine operating torque points and it is seldom likely that these points will correspond to the minimum fuel consumption. Furthermore, manual transmissions rely upon the driver to select ratio change points, again, these changes are seldom performed to minimise fuel consumption. Consider the 22 kW power line. This line represents a steady state vehicle velocity of 40 mph (64 km/h). The fifth gear ratio crosses the 22 kW power line in an engine region close to the optimal fuel consumption point. However, it is unlikely that many drivers would have chosen fifth gear while travelling at 40 mph. Fourth gear is a more likely selection, the use of which would develop a 3% fuel consumption penalty.

Manual transmissions have become synonymous with good driveability and much of this can be attributed to the driver's perceptions of features of their transient response. Prior to a transient event the driver makes a decision regarding the acceleration required to perform a particular manoeuvre. From experience the driver then decides whether the current operating point offers the potential to provide the required acceleration. The point labelled '1' represents the 22 kW steady state point in Figure 1-2. If it is deemed that the current engine condition will not provide the required acceleration, a ratio change is made. The point labelled '1B' represents the same power condition following a downshift. A downshift has the effect of increasing the engine speed, and developing a greater margin between the steady state torque condition and the wide open throttle (WOT) torque limit. When the accelerator is subsequently depressed initiating the acceleration, the engine is able to generate the torque available at the WOT limit. The difference between the torque required to maintain the instantaneous vehicle velocity and the torque available at the WOT line is termed the torque margin. It is this torque margin that is used to accelerate the combined vehicle / engine inertia toward the new desired power condition (denoted by point '2' on Figure 1-2). In the transient process described here the driver has direct control over the torque margin through ratio selection and has direct control over other vehicle effects such as shift smoothness and vehicle retardation through de-clutching. Consequently the driver's good expectation of the vehicle transient response will have

been formed in light of his or her own actions, and will match closely the response of the vehicle. It is this input and feedback process which has given the manual transmission the reputation for good transient driveability.

A similar transient operation performed in a conventional automatic transmission will require the same downshifting process; however the driver has no input into this process. Instead the transmission controller must make an assessment of the driver's intention from the translation of the throttle pedal and the current engine torque and speed. As a result the ratio change duration now becomes part of the transient response; since the driver has no direct control over the torque margin the change may be less than smooth leading automatic transmissions to be judged more harshly by drivers.

### 1.1.2 CONTINUOUSLY VARIABLE TRANSMISSIONS

- Mechanisms

More recently another type of transmission has begun to gain market acceptance, the continuously variable transmission (CVT). CVTs have no fixed gear ratio between the engine and driven wheels; instead a 'variator' allows, between mechanical limits, an infinite range of ratios to be developed. Introductions to CVT mechanisms are provided by Wicke[18], Happian-Smith[19], and Setright[16]. From these works the number of different variator mechanisms can be categorised into hydraulic, mechanical, electrical and mechanical traction devices. The mechanical traction type has proved the most popular within the passenger vehicle market. The two predominant mechanical approaches within this category are the pushing v-belt type as developed by Van Doorne, and the traction roller type.

Figure 1-3 is a schematic of the Van Doorne transmission; it is constructed of two variable diameter pulleys and a segmented metal pushing belt, consisting of segmented stamped steel blocks held in shape by tensioned steel bands. Akehurst[20] provides a detailed introduction to the mechanical structure of this transmission type. The transmission ratio is changed by varying the diameter of the input and output pulleys via primary and secondary actuators operated by an hydraulic control system. This type of transmission has limited torque scalability, since the maximum torque transfer is limited by the tensile strength of the belt bands, the compressive strength of the segments [21], and in practice it is primarily limited by the belt pulley friction[20]. In practical applications the greatest torque that can be transferred using Van Doorne pushing belts has been limited to less than 200 Nm for example in the MGF sports car. The type of transmission operates a ratio control

system such that for a given vehicle speed and engine condition, a transmission ratio is determined. The pulley radiuses will remain fixed at this ratio unless the controller identifies a change in either road load or driver demand. It is this type of transmission that Takiyama & Morita[12], Hendriks[13] and Kriegier[14] used to produce the fuel efficiency gains demonstrated.

Figure 1-4 illustrates a traction roller type transmission. The mechanism that is demonstrated in this figure is the toroidal variator currently under development by Torotrak Development Ltd. Nissan have a half torodial version in production in Japan. It features a disc transferring power from one toroidal surface to another. The cavity between the toroidal surfaces is filled with a high traction coefficient hydraulic fluid that augments surface traction to maximise power transfer and transmission efficiency. The power transfer disc operates between one radius on the input toroid and another radius on the output toroid. A force on the positioning mechanism of the power transfer disc must be balanced by the net forces at the points where the disc makes contact with the toroids. As a result the torque which can be transferred through the variator is governed by the positioning arm effort. The subsequent ratio will be developed dynamically as a result of the acceleration / deceleration of the inertias attached to each shaft. As a result the transmission ratio is not fixed in the same manner as that of the Van Doorne type device; instead a change in either input or output torques will have an effect. This type of transmission is said to have a torque control system [22], and as a result has a very fast response characteristic.

Another feature of the Torotrak transmission although not exclusively, is that via a planetary gear set, it is possible to have two paths through which power is transferred. Balancing the powers transferred through the variator with those passed through a geared connection it is possible to develop a geared neutral state, and as a result elevate the requirement for a clutch or torque converter. Devices that can develop a geared neural state are termed infinitely variable transmissions (IVT).

In practice both the Van Doorne and the Torotrak CVT mechanisms discussed, feature a higher overdrive ratio than that fitted to conventional discrete ratio transmissions. This feature of CVTs allows the use of a greater range of engine speed / load conditions during steady state driving.

- Steady state operation

In comparison to conventional discrete ratio gearboxes, CVTs are typically more expensive, heavier and larger; however recent technical advances and market sector targeting are making these disparities less significant[23]. CVTs however offer many potential benefits compared with conventional transmissions. The infinite range of gear ratios available affords a stepless transition throughout the operating region; this offers significant improvements in vehicle smoothness and specific emissions previously caused by de-clutching. Additionally CVTs have the potential to offer improved durability, since slipping clutches are no longer required and neither are the complex synchromesh mechanisms of manual transmissions. However, the greatest benefits are to be achieved by operating a CVT as part of an integrated powertrain, incorporating an electronic throttle. With such systems there is the possibility to develop a required wheel power at a range of engine speed / load conditions. This freedom in engine operating condition enables the development of a range of engine control strategies that may be used to optimise the vehicle's performance for a number of criteria. Figure 1-5 shows the torque / speed representation described earlier, and as before it has brake specific fuel consumption lines superimposed upon it. It is apparent from examination of the figure that for a given power condition the minimum fuel consumption will occur at low speeds and high engine loads. This relationship can be explained by considering the engine losses. In conventional throttle regulated gasoline engines pumping losses are a minimum at high load, WOT conditions, and frictional losses are a minimum at low speed conditions. The solid green line plotted in Figure 1-5 represents a steady state control line for a gasoline engine which has been optimised to produce minimum fuel consumption. In many works [12, 14] this is termed an economy line or an e-line. In order to highlight the improvement in fuel consumption it is useful to compare an operating condition achieved using a CVT featuring an e-line engine control strategy with the corresponding power condition achieved using a conventional transmission. Comparison may be made along the steady state 22 kW line described earlier. As discussed this power condition is unlikely to be achieved in the most efficient gear ratio so here it is considered to be developed at 2400 rev/min, with an engine torque of 80 Nm. A similar condition achieved on the CVT e-line would occur at 1600 rev/min and 130 Nm. Torotrak[23] claim that an optimised engine control profile may offer a 17% fuel consumption improvement and this is consistent with the claims of Hendricks[13] and Takiyama & Morita[12]. Kriegler[14] predicts a 10% improvement for a multipoint fuel injected engine (MPI) over the course of a drivecycle. Brace[24, 25] has shown that similar techniques may be applied successfully to reduce

specific emissions, and that it is possible to develop an ideal operating line which minimises the necessary compromise in satisfying a combination of engine performance criteria.

- Transient operation

As has been shown there is great potential to improve the specific fuel consumption of a vehicle by implementing an integrated CVT controller. However in practice few if any of the fuel consumption benefits have been realised. This is because the described operating lines have not been considered in the light of their implications for the transient response of the vehicle. To demonstrate the implications of the e-line on transient engine response, the excursion considered for a conventional fixed ratio transmission is considered again here for a CVT with an integrated controller. The initial 22 kW steady state operating point is denoted on Figure 1-5 by the point marked '1', while the destination 44 kW power condition is denoted by the point marked '2'. Following a transient demand the integrated controller attempts to liberate the torque margin that is available to the transmission. In the example considered here there is a small (10 Nm) torque margin available. If the available torque margin were used solely to accelerate the engine it would develop an estimated 8 rev/s increase in engine speed. Clearly this is far too small for any practical application. As a result, in order to initiate the acceleration of the engine, the powertrain controller reduces the variator ratio. This has the effect of reducing the power supplied by the engine to the driven wheels, and forcing the vehicle to slow down. In effect the wheel power will be accelerating the engine to a condition where there is sufficient torque margin to allow the transmission ratio to increase. Quite clearly this type of engine controller is not acceptable for inclusion into a production vehicle. In order to have acceptable driveability the control line must be run with a significant torque margin. The engine operating line can be optimised for this application, but since this requires operating at higher engine speeds with greater throttling, the fuel consumption is compromised.

It is therefore apparent that there is a trade off between acceptable vehicle driveability and minimum fuel consumption. This is one of the major reasons that the fuel consumption improvements predicted[13,14,15] have yet to be fully realised in a production vehicle. A compromised control line is shown in Figure 1-6. It is worth noting that at 40 kW the engine control line meets the WOT line thus removing any available torque margin. This loss of torque margin is acceptable because powers above 40 kW will not be used for steady state driving; instead these regions will only be visited during high load conditions

(acceleration up a hill with a trailer) where the driver requires maximum available power. Audi have notably developed an engine control line which produces fuel consumption below that of a conventional fixed ratio manual gearbox, whilst providing good driveability[26]. However, further fuel consumption improvements are possible with this configuration if driveability is sacrificed, therefore the full potential for fuel economy improvement has not been realised.

## *1.2 Approaches to overcome the fuel consumption driveability compromise*

A number of external systems offer the potential to develop the torque margin required for improved driveability. Such systems would enable the engine to operate along an economy control line.

### 1.2.1 HYBRID VEHICLES

The combination of two power generators within a vehicle, typically an internal combustion engine and an electric motor, is referred to as a hybrid powertrain. Development of such systems has received much attention for many years [27]. Hybrids offer a huge potential to overcome the difficulties of the CVT fuel consumption / driveability trade off. Internal combustion engine torque boosting using an electric motor is one possibility available; however, so is using the electric motor as the main motive power source and using the IC engine to keep the electric motor within a certain efficiency region. As a solution solely to the problem of improving the driveability / fuel consumption compromise the use of a hybrid powertrain may be considered to be rather excessive, since hybrid systems offer the potential to significantly reduce fuel consumption in their own right. Furthermore, such a solution would also be punitively expensive to implement. However, with the recent interest in 42 volt automotive systems an interesting mild hybrid solution has been developed.

'Mild' hybrid is a term used to describe a drivetrain fitted with an integrated starter alternator damper (ISAD). This is a single unit, mounted in the location of the current flywheel, that is intended to replace the starter motor, the flywheel and the alternator. A description of the hardware is provided by Nickel[28]. Although little work has been published in this area, it is the author's opinion that such devices may allow the engine to operate closer to the minimum fuel consumption ideal. Following a transient demand, the ISAD could act as a small motor developing the torque margin required to initiate the acceleration of the combined engine and vehicle inertia. Mild hybrid systems could

potentially develop the required torque margin quicker than a conventional throttled engine, because the ISAD reaction time will be less than the filling time of the inlet manifold. Additionally, an ISAD can actively reduce the inertia of the engine, since the flywheel effect would be produced by active control, to allow faster engine acceleration.

Although ISAD systems are not subject to the packaging compromises that effect full hybrid solutions, they are still subject to punitive component costs. Currently there is an impetus move from the current 12 Volt engine system to a 42 Volt, this is principally to reduce component weight and size, thus making ISADs smaller, more common place, and therefore cheaper. Another feature of the move to 42 Volts is that belt driven ancillaries can be electrified which through intelligent control, may allow them to present a smaller drain upon the engine, thus further reducing fuel consumption. However, as with full hybrid vehicles, battery charge management processes have the potential to cause an inconsistent transient response, and this is possibly more detrimental to vehicle driveability than a consistent negative transient characteristic.

### 1.2.2 ELECTRIC TURBOCHARGING

The general premise of electric turbocharging is to use an electric motor either to increase the velocity, and therefore charge compression, of a turbocharger or to initiate the motion of a supercharging device. Katrasnik et al[29] and Panting et al[30] provide introductions to the mechanical structure of such systems, applying their use to the improvement of diesel transient response. Again, although there is very little work examining the potential of electric charge boosting with gasoline engines, the author believes that this offers the potential to partially overcome the fuel consumption / driveability compromise suffered by gasoline engines matched with CVT transmissions. Following a transient demand, the electrical systems could accelerate the supercharger or the turbocharger in order to increase the charge density of the engine and therefore the power available at a given engine speed. Although similar in principle to the ISAD concept, this solution would produce similar levels of torque margin from a smaller, and therefore cheaper electric motor. Unlike the ISAD concept, however, the response of the charging device is unlikely to be faster than a standard throttle response since there are manifold filling and component acceleration issues to consider. Unfortunately in gasoline engines the compression ratio which generates peak efficiency is very close to the compression ratio which causes the initiation of spontaneous combustion (knock). Therefore in order to generate a sizeable torque margin the steady state efficiency, would have to be compromised through the use of a reduced compression ratio. Further adaptation could

mate an electrically driven turbocharger to a sophisticated engine featuring variable compression ratio, (e.g. Saab SVC, Lotus AVC engine, Mayflower $e^3$ engine). In doing so the compression ratio can be decreased during transient events to avoid knock. However, the combination of an electrically assisted turbocharger and a variable compression ratio engine are very expensive and far from production. Furthermore with this concept as with hybrid solutions, there is the possibility that electrical charge management strategies will produce inconsistent transient response characteristics.

### 1.2.3 ZERO INERTIA (ZI) ENGINE CONCEPT

Another possible solution to the fuel economy / driveability trade off is the use of energy stored within an additional flywheel to provide the required torque margin. This area of research has been investigated in the Zero Inertia Powertrain project at Eindhoven University[31,32,33]. The system that has been tested combines the engine, CVT and wheels in a conventional manner but includes an additional flywheel mounted, via a planetary gear system, in parallel with the engine and wheels. Using this system the engine can operate along an e-line during steady state cruising. Following a transient demand, the energy stored within the flywheel can be liberated to provide the torque necessary to accelerate the engine to the required power condition. This system is unlikely to suffer from the inconsistent transient response that may affect the electrical storage type approaches described earlier because the flywheel can be accelerated very quickly, simply by running the engine at a higher load condition. Although not alluded to in the work presented to date, such a system could be used to develop regenerative braking, thus actually providing better fuel economy than an optimised engine CVT combination alone. However this is not to say that the additional flywheel approach is without its disadvantages. Since a regenerative braking system is not being applied, the engine must provide the work to accelerate and over come frictional losses of the additional flywheel and this will to some extent compromise the potential fuel economy gains made possible by operating close to the e-line. Furthermore the additional flywheel, planetary gear set and clutches required in the control of such a system will represent an increase in cost, mass and dimensions for the developed powertrain. There is also the issue of a gyroscopic effects which has not been completely explored.

## *1.3 Dilution torque control*

Gases that are introduced into the combustion chamber but are not combusted, can be collectively termed diluents. Both exhaust gas recirculation (EGR) and lean burn

combustion allow gases that do not play a part in the combustion process to be induced and passed through the combustion chamber. EGR introduces previously combusted gases into the induced air, while lean combustion limits fuelling thereby allowing some fresh air to pass through the combustion chamber.

It is well documented [34,35] that the use of diluents in a gasoline engine can have beneficial effects on both fuel consumption and specific emissions. Additionally introducing diluents into a combustion chamber reduces the torque that an engine can produce. This aspect of the use of dilution has however received little detailed attention. It has been proposed by Murray[36] that the reduction of performance offered by charge dilution, specifically EGR, may be used to regulate engine output torque as an alternative to throttling. It is suggested that in a steady state condition an engine could operate at WOT, thus minimising pumping losses, and the output torque could be modulated by the introduction of charge dilution.

Murray presented Figure 1-7, which shows an engine torque / speed map highlighting the low speed region where EGR dilution may be applied. Murray suggested two EGR strategies. Firstly the use of EGR at WOT conditions to reduce engine torque, thus enabling a minimum fuel consumption strategy to be implemented whilst maintaining good driveability. This region is highlighted in green. The second strategy suggested by Murray was that through throttling the EGR rate could be increased. In this operating region throttling would compromise fuel consumption and the transient response, but the high EGR rates would provide a strategy which minimised $NO_x$ emissions. This region is highlighted in light green.

Figure 1-8 illustrates an engine map showing a steady state control line where, in the low speed region, charge dilution has been used to reduce the WOT torque from the limiting engine torque. In the region where dilution torque control is applied, a torque margin is produced. Comparing the steady state operation of the suggested dilution torque control strategy with a standard optimal fuel economy strategy, it is apparent that to achieve a given power an engine will have to operate at a higher speed. It is therefore expected that any potential fuel economy gains achieved through the beneficial effects of dilution may be reduced by the increase in friction at higher engine speeds.

Considering the same transient excursion examined in Section 1.1.1 for a CVT featuring an optimal fuel control strategy, the engine starts from a 22 kW steady state condition

(point '1'), and is required to produce a new 44 kW power condition, (point '2'). Using dilution control there is clearly a torque margin that could be used to accelerate either the engine or the vehicle.

As long as an engine has a sufficient dilution tolerance such that a useful torque margin may be developed, this proposed control strategy can reduce the fuel consumption / driveability compromise at a fraction of the cost of external torque enhancement systems. It would also not be susceptible to the inconsistent transient response characteristics that could effect hybrid and electrical charge boosting approaches.

## *1.4 Objectives of the work described in this thesis*

The object of this work is to identify and quantify the benefits that can be made to both fuel consumption and vehicle driveability through the use of charge dilution. The work will examine the benefits available when using a standard multi point injection engine, coupled to a continuously variable transmission. It is acknowledged that greater benefits might be obtained using gasoline direct injection (GDI) technologies but at greater expense. Here the intention is to identify a solution that may be implemented in a small passenger vehicle where the expense of a CVT and a GDI engine would make the product prohibitively expensive.

The work will identify the diluent or combination of diluents that offers the greatest fuel economy for improved driveability. The studies will consider the implications of dilution on regulated emissions and include these factors in the determination of the optimal combination of diluent control levels.

Work by Dorey & Martin[37] and List & Schoeggl[38] has shown that the factors that determine driveability are complex and multi faceted. Further work by Wicke et al[18,39], has shown that CVTs can afford a control engineer a great deal of freedom to shape a vehicle's response from a constant engine response. It is therefore considered that the total improvement of vehicle driveability is beyond the scope of this work. Instead the work will concentrate upon the contribution of the engine, seeking to minimise the engine transient response duration and hence maximise the potential to which a vehicle response may be tailored for improved driveability.

Determining the fuel consumption impact of operating a dilution torque control strategy over a legislative drive cycle will conclude the work.

### 1.4.1 LAYOUT OF THE THESIS

Following this chapter in which the operation of conventional and continuously variable transmissions has been compared and the dilution torque control concept has been introduced there are eight further chapters. The following summary describe the content of these chapters.

Chapter 2

This chapter examines aspects of the use of charge diluents. This examination includes methods of dilution development, beneficial effects on specific emissions and fuel consumption, and the conventional control of such diluents in combustion management.

Chapter 3

This chapter describes the mechanical installation of a steady state gasoline engine test rig, including details of specific adaptations to enable full assessment of the potential of torque control via charge dilution.

Chapter 4

The chapter begins by discussing the high experimental cost of investigating multi-variable problems, such as the one to be considered here. It proceeds to examine a number of approaches that have been used to reduce testing requirements, selecting the use of a Design of Experiments (DoE) engine testing program for further use within this study. A detailed introduction to the use of DoE is provided along with details of its application for use in the development of engine models. The work is extended to propose an adaptation to classical DoE methodology such that difficulties associated with modelling high order responses are minimised.

Chapter 5

This chapter considers the quality and implications of the steady state models. The steady state section presents a comparison of the accuracy of the models developed using the novel DoE approach proposed in Chapter 4 and a classical approach. The accuracy is assessed using correlation coefficients and comparison with a secondary set of test results. This second approach is novel in this field and highlights the inaccuracies caused by high order regression model oscillations. The chapter proceeds to examine the main effects of individual variables and fuelling / EGR interactions on engine responses.

This section concludes with an examination of the effects of dilution on engine response maps.

Chapter 6

This chapter considers transient aspects of dilution torque control, discussing the reconstruction of signals relating to events during the transient and the determination of suitable measures of transient initiation. The chapter concludes by examining the relative durations of all engine transient events.

Chapter 7

This chapter selects an optimisation approach suitable to identify global optimal control variables, using the engine model developed. It continues to develop an objective function for use with the optimisation approach. The objective function described incorporates the engine models developed in Chapter 5, with metrics to ensure that all solutions meet suitable emissions levels. The objective function also incorporates metrics to standardise the examination of the engine's transient response.

The chapter concludes with an examination of the control variables identified as optimal for each power condition and an assessment of the potential improvements in fuel consumption that are possible using this control strategy over the course of a legislative drive cycle.

Chapters 8 & 9

These chapters review the conclusions of this work and detail scope for further work arising from this study.

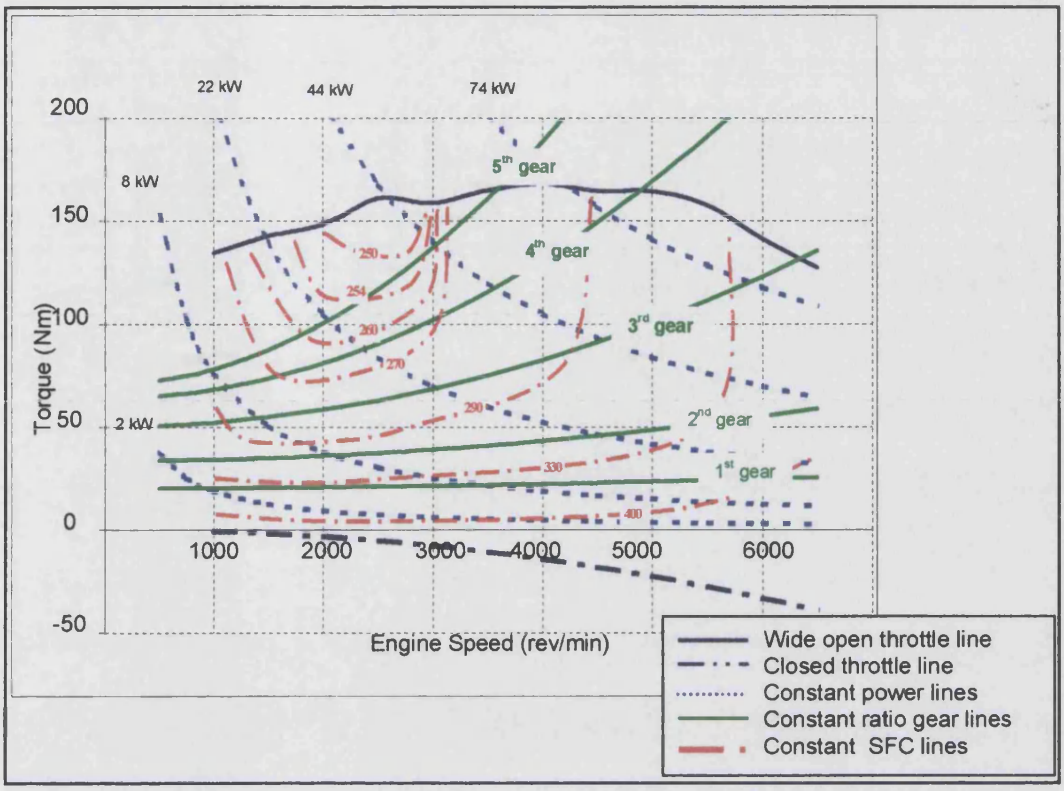


**Figure 1-1 Engine speed torque map showing fixed ratio gear lines**

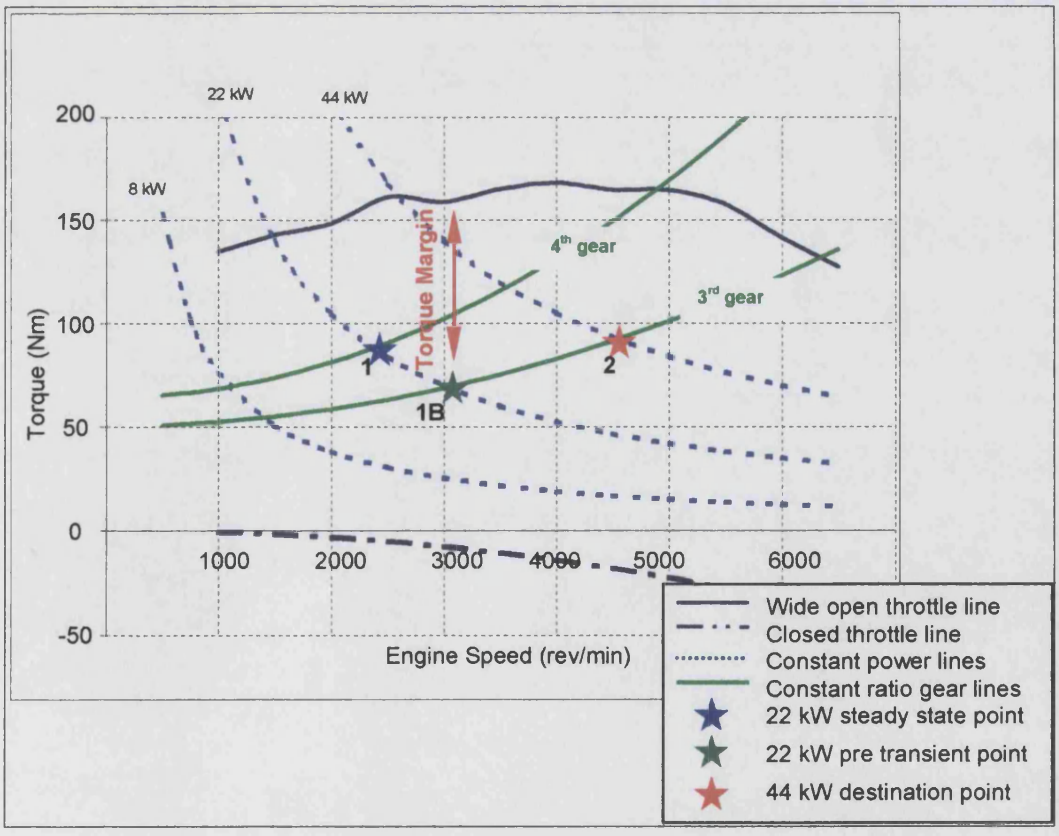


**Figure 1-2 Transient manoeuvre for a conventional transmission**

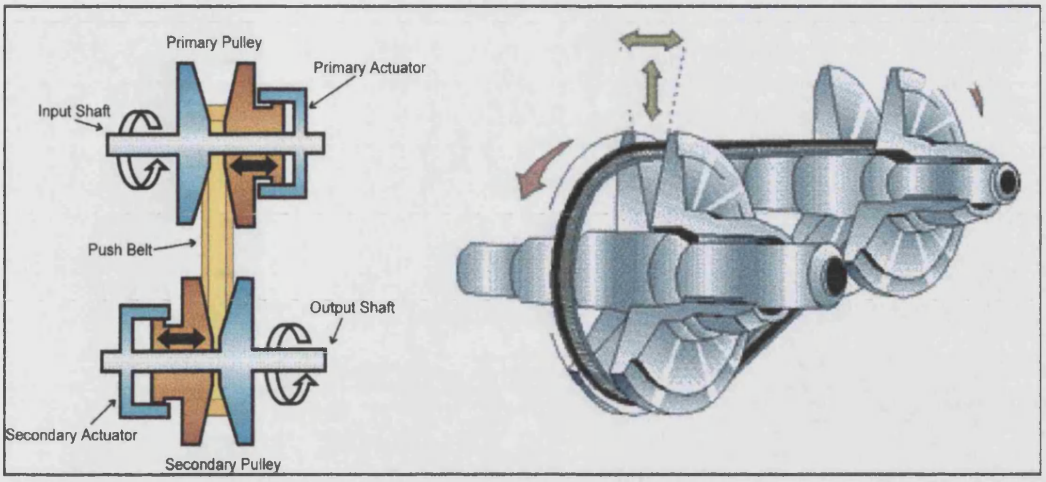


**Figure 1-3 Van Doorne ratio variator**[13]

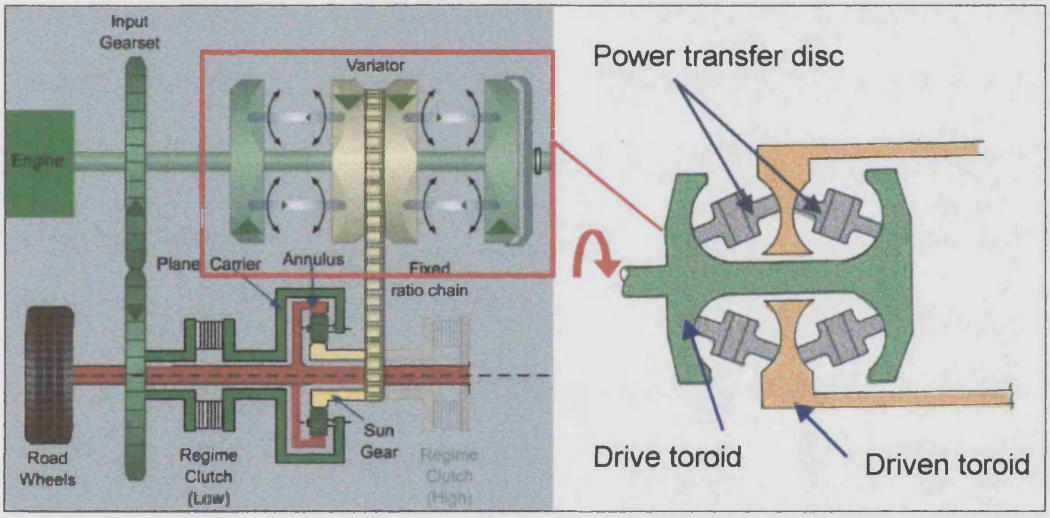


**Figure 1-4 Torotrak ratio variator** [23]

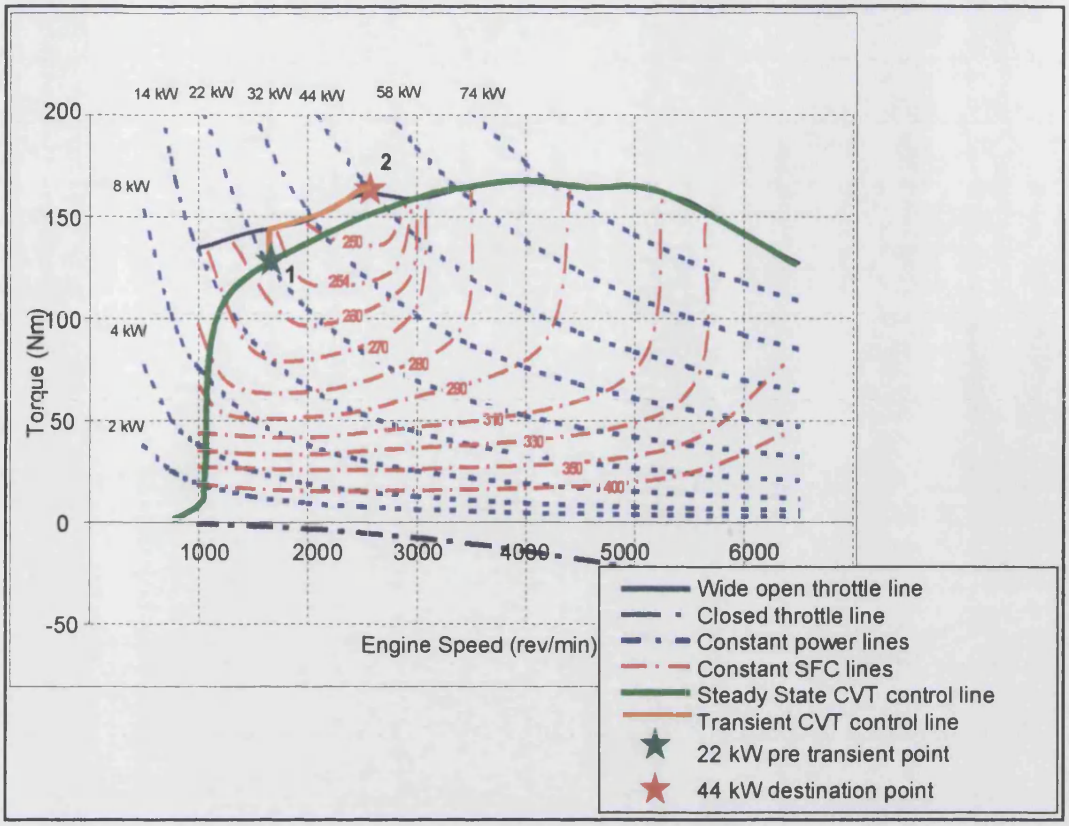


**Figure 1-5 Optimal fuel consumption engine control line**

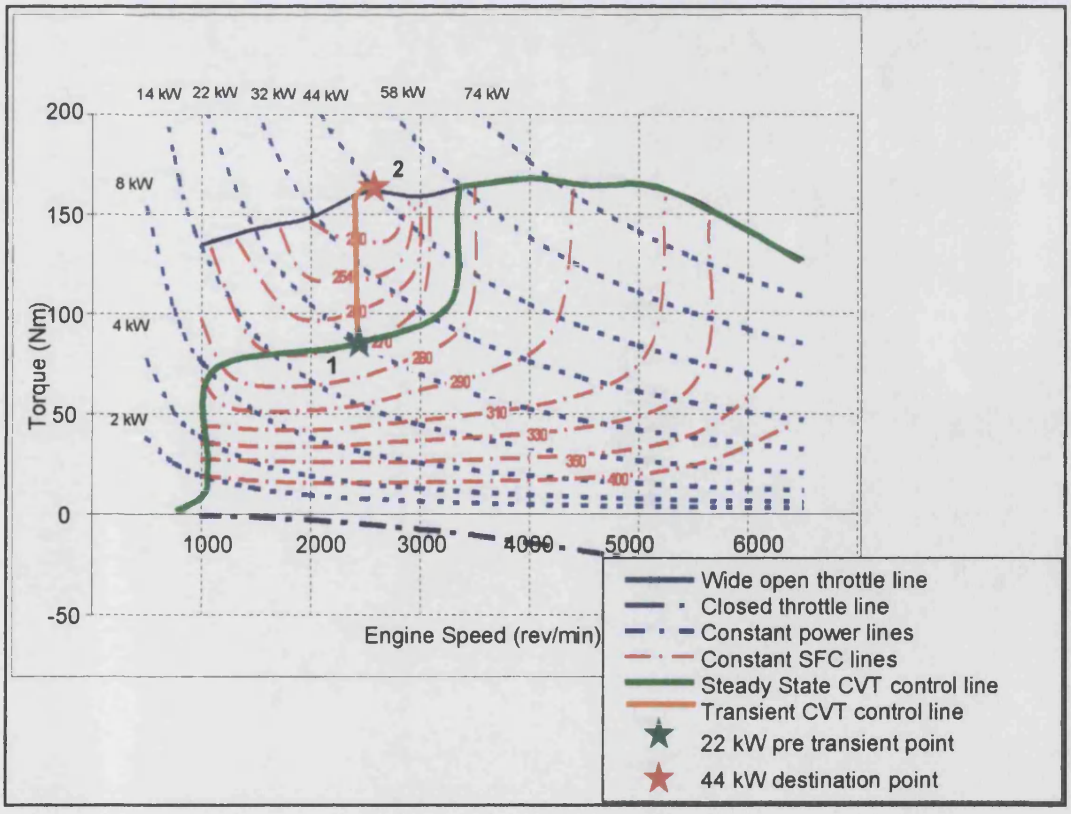


**Figure 1-6 Compromised engine control line**

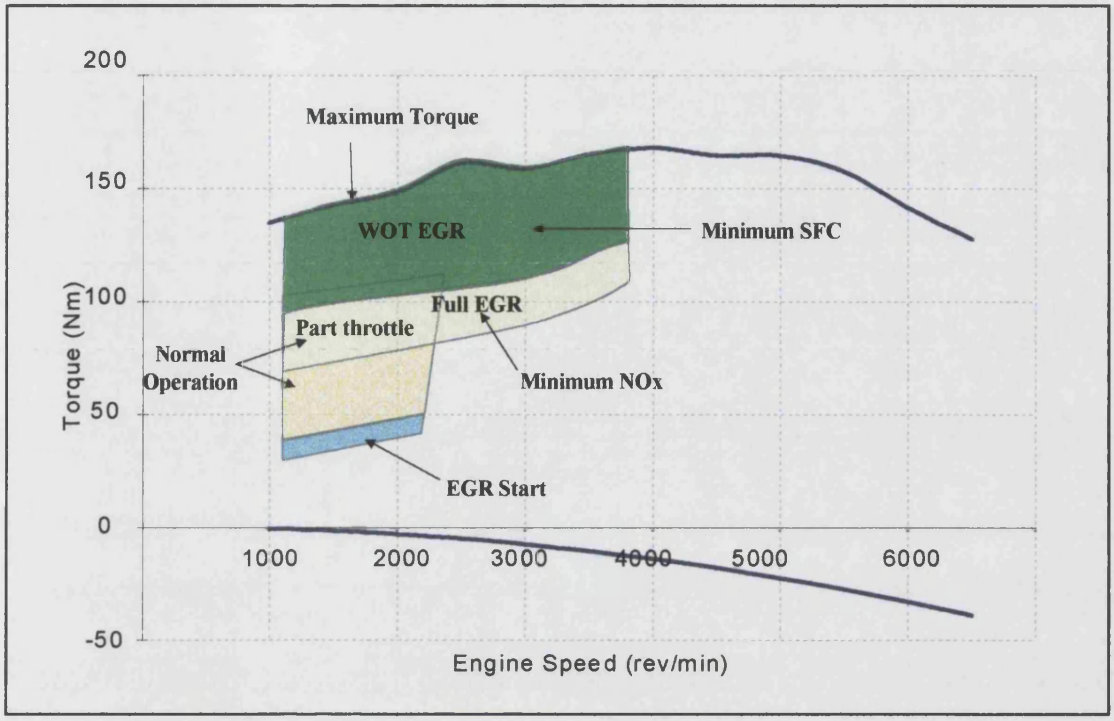


**Figure 1-7 EGR dilution strategy proposed by Murray [36]**

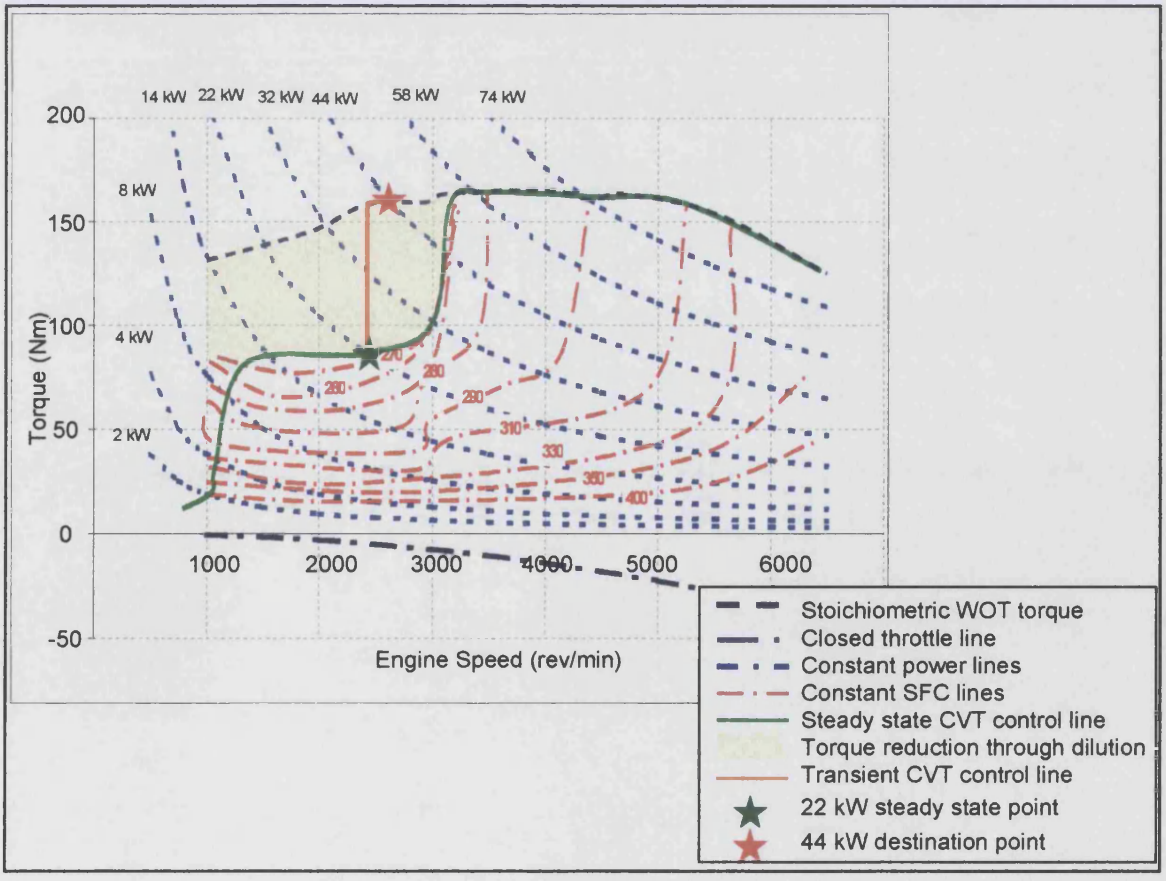


**Figure 1-8 Gasoline engine dilution control strategy**

# 2 Existing work

## *2.1 Scope of Chapter*

This chapter examines the characteristics that have been attributed to the use of charge dilution within the literature. The purpose of this review is to identify whether there is any work that suggests charge dilution has sufficient scope to be used to control engine torque. Additionally this review seeks to develop an understanding of the main approaches used to generate dilution.

The induction of gases additional to those required for a stoichiometric combustion charge is termed charge dilution. Work by Jackson[40] has shown that internal combustion engines can tolerate charge dilution by a wide range of diluents. However, since the reduction of fuelling leading to excess air and the recirculation of exhaust gases are the most readily available forms of diluents, these will represent the majority of the work presented within this chapter. The review will therefore seek to identify the relative benefits of the application of both systems separately and how the combination of both lean and exhaust dilutions may compliment one another.

## *2.2 Use of EGR*

Exhaust gas principally consists of nitrogen, carbon dioxide and in gasoline engines carbon monoxide. Characteristically exhaust gases are hotter than the induced fresh air. The following sections will examine the approaches undertaken to introduce EGR into the induced gases, the effects that have been shown on specific engine performance, additional attributes of the use of EGR and typical EGR control strategies.

### 2.2.1 METHODS OF PRODUCTION

This section will introduce the various approaches that have been used within presented work to introduce EGR into the inlet gas flow. There has been to the author's knowledge no work published which specifically provides a comparison of the different approaches.

Whereas EGR in diesel engines has evolved to a uniform configuration, comprising a large bore external EGR manifold featuring cooling, EGR in gasoline engines has been investigated with a number of configurations. Diana et al[41] investigated the effect of EGR dilution with engines which featured increased compression ratios. This work was undertaken on an engine fitted with a pre-throttle external EGR manifold (termed external

EGR) featuring partial cooling. This is the configuration that has greatest similarity with the systems used on diesel engines. In a pre-throttle external EGR system the EGR flow rate is determined by the EGR valve position, the exhaust manifold pressure and the diameter of the EGR piping. As a result, there is typically a linear EGR response to valve demand leading to simple control of EGR percentage within an inlet gas flow. Furthermore the extra manifold length from the EGR induction point, improves the homogeneity of the induced mixture. However, since the EGR flow joins an induction stream which is at ambient pressure, to achieve large flow rates the EGR manifold must have a large diameter. Diana et al[41] claimed that 25% EGR by volume was possible at full engine load using the system implemented. Many diesel applications use turbochargers to boost specific output; as a result there is a high pressure gradient between the inlet and exhaust manifold, which means that the diameter of the EGR piping can be reduced whilst maintaining large EGR flow rates (in excess of 50%). No work to the author's knowledge has been undertaken to examine the effectiveness of pre-throttle EGR configurations during transient events. However, it is apparent that, due to the extended inlet volume in which the EGR dilution is resident pre-throttle systems will suffer an extreme transient lag while the engine consumes the diluted inlet gases.

Tabata et al[42] performed investigations on an engine featuring a post-throttle external EGR system. This is the system adopted on the majority of production gasoline vehicles featuring EGR. The EGR flow through a post-throttle external system is regulated by similar physical attributes to a pre-throttle external EGR system, with the addition of inlet manifold pressure. As a result, while the engine is operating under throttled conditions the pressure gradient between the inlet and exhaust manifolds is greater. Consequently for part load EGR requirements the diameter of the EGR pipe can be smaller. As a result of the inlet manifold pressure influence upon EGR flow rate within post-throttle EGR configurations, the inlet EGR percentage in these systems is determined by a complex relationship between engine speed, throttle position and EGR valve demand. In consequence the control of such systems is a more challenging problem. Furthermore Yoshizawa et al [43], and Blank et al[44] have recently published work which demonstrates that port induced post-throttle EGR systems suffer from inconsistent EGR / fresh air mixing, Yoshizawa et al[43] has shown that this can result in varying mixture rates being induced into individual cylinders. Yoshizawa et al[43] suggested that typically cylinder four would have a high level of EGR and cylinder one would have a very low level of EGR induced. Since the engine management strategy assumes that the each cylinder induces inlet gases from a homogeneously mixed manifold, this will result in over fuelling cylinder

four and lean fuelling of cylinder one. Similarly the spark timing will be compromised for individual cylinders. Nakajima et al[45] presents a test rig which features a mixing chamber immediately after the throttle and EGR points; such a system would promote improved inlet homogeneity. Yoshizawa et al[43] suggested a more complex multiple inlet port, multiple control valve design in order to develop a homogeneous air EGR mixture. The work of Blank et al[44] goes on to examine the effect of single port post throttle EGR induction during transient events. Blank et al[44] concluded that an engine featuring this configuration would suffer a substantial transient lag due to the volume of EGR resident within the inlet manifold prior to the transient demand. However, Blank et al[44] also concluded that the inlet manifold geometry and the single port design lead to EGR gases becoming trapped within the manifold and consequently reducing the post transient performance of the engine. Blank et al[44] advocated multiple EGR inlet ports distributed throughout the inlet manifold as a means to reduce both of the described aspects of this type of EGR i.e. long transient duration and reduced post transient peak torque. Work by Olbrot et al[46] has characterised the response of a post throttle EGR system. This work showed that the transient duration could vary between 0.17 s and 0.28 s depending upon the initial operating condition.

Osses et al[47] investigated the use of an exhaust throttle to induce an EGR flow. In this configuration the exhaust manifold pressure is increased to such an extent that during the valve overlap period at the beginning of the intake stroke exhaust gases are forced back into the combustion chamber. The work examines the possibility of using this approach to reduce the levels of specific $NO_x$ emissions from a gasoline engine mated to a CVT. This is the only work identified by the author which evaluates an EGR system or concept with specific reference to its use within a CVT powertrain. Exhaust throttling as an approach to develop EGR has no external connection between inlet and exhaust and is thus termed internal EGR (iEGR). Internal EGR developed via exhaust throttling is unique amongst the induction concepts examined here, because of the four EGR approaches described it is the only one which during steady state operation will substantially increase the work required from the engine and therefore its specific fuel consumption. Osses et al[47] failed to demonstrate a practical implementation for such a system, so it is difficult to speculate regarding its transient response. However, if a fast responding exhaust throttle system were possible, this EGR concept may offer the best transient response of any of the EGR induction concepts examined here, since it does not involve large volumes of non-combustible gas in the induction system. Although as presented in the work of Osses et al[47] this system is the least practical of the EGR approaches described, the author of the

current work proposes an approach to its application. Placing the turbine stage of a turbocharger within the exhaust stream and using it to drive an electrical generator would provide a practical means to develop control over exhaust manifold pressure, and could perhaps be used to replace the crank shaft driven alternator. Although this proposed system would compromise steady state fuel consumption, the removal of the alternator may offset this penalty.

A fourth type of EGR system can be developed using specific features available to a variable valve actuation (VVA) system. Since EGR induced through valve timing does not require any external connection between inlet and exhaust manifolds, these systems are also termed iEGR. In contrast to iEGR developed through exhaust throttling, iEGR developed through valve timing offers the greatest potential for dilution engine torque control. To achieve iEGR using valve timing there has to be an overlap period between the inlet valve opening (IVO) and the exhaust valve closing (EVC). If the overlap period occurs during the exhaust stroke, exhaust gas is expelled into the inlet manifold; subsequently during the induction stroke the exhaust gas is drawn back into the combustion chamber. If the overlap period occurs during the induction stroke the fresh charge is drawn from both the inlet and exhaust manifolds. Ahmad and Theobald[48], Stone and Kwan[49] and Gray[50] provide detailed introductions to the various VVA concepts that exist. However these studies do not discuss the potential to achieve iEGR.

Stein et al[51], and Leone et al[52] examined various arrangements of inlet- and exhaust-mounted VVA devices, with the intention of replacing an external EGR system on a gasoline engine. This work was conducted using variable cam phasing devices, the most common VVA devices currently in production. Single cam phasing devices enable control over the overlap period of the inlet and exhaust valves while dual cam phasing devices also enable the point at which the overlap period occurs to be varied. The works of Stein et al[51] and Leone et al[52] present a thorough examination of inlet only, exhaust only, dual equal and dual independent valve timing concepts with a goal of producing similar levels of oxides of Nitrogen ($NO_x$) emissions reduction to that produced by an external EGR system. This work concluded that each of the arrangements could develop enough iEGR to replace an external EGR system; however the greatest potential to develop iEGR was attributed to systems featuring exhaust cam phasing. In practice inlet only phasing devices have proved most popular; this is because these systems have the added benefit of enabling ram charging throughout the engine operating region which has the benefit of increasing output torque. Jankovic et al[53], and Stefanopoulou & Kolmanovsky[54] present

works examining the transient response of such cam phasing technologies. This work suggested that ideally the duration of the transient would simply be limited by the translational characteristics of the cam phasing device. However the research had shown that following a fast transient by the inlet cam phasing device, there is an initial reduction in the engine's output torque. This is caused by an interaction between the cam timing and the slow speed intake manifold filling dynamics[54]. In order to overcome this, Stefanopouiou & Kolmanovsky [54] proposed a controller which uses a first order lag to regulate the translation of the cam phasing device. This work showed that following a transient demand an optimised response can take up to 1.5s. It is noted that this duration seems rather poor compared to the 0.28s transient duration of an EGR system. However neither the works of Stefanopoulou & Kolmanovsky [54] or that of Olbrot et al[46] elaborated sufficiently on the transient investigations to allow this disparity to be explained.

The cam phasing system examined by Stein et al[51] was only capable of manipulating the phasing of conventional cam profiles. Other variable valve actuation concepts have the potential to increase the production of iEGR through the use of more exotic cam profiles. Rao et al[55] presented work investigating the use of an exhaust cam featuring a multiple lobed profile. This work was principally intended to investigate the effect of drawing exhaust gas into the combustion chamber at the end of the intake stroke to assist cold start engine warm up. Rao et al[55] noticed that this system has similar effects on specific emissions and fuel consumption to an external system operating with 20% EGR charge dilution. Edwards et al[56] proposed a similar concept for use with a large diesel engine. This work however showed limited benefits with presently available hardware, primarily because of its application on a large low speed diesel engine. Although the work of Edwards et al [56] has cast a shadow over the potential of this particular implementation of iEGR, it is the author's belief that applied to high speed gasoline engines it could be used to achieve very high rates of iEGR. In practice a vehicle featuring such a double lobe cam profile would suffer reduced peak power. However, the advent of cam switching technologies as implemented in the Honda V-TEC engines[57] means that such a cam profile could be included as an economy profile, within a set of cam profiles. During transients such systems will not be subject to the inlet disturbance discussed for cam phasing concepts, because these systems only effect the timing of an exhaust event consequently there is no interference with the inlet filling dynamics.

In order to develop a VVA system to fully exploit the potential of iEGR the maximum versatility is required. Such a system would offer control over the duration of valve

opening period, the amount of valve lift and valve overlap timing. So far, the majority of mechanisms capable of controlling all these valve characteristics are achieved using electro-hydraulic, electro-pneumatic or solenoid actuation. Schechter & Levin[6] provide a comprehensive introduction to the potential that such valve actuation systems offer. Such fully versatile systems would enable a vast array of actuation options, and subsequently iEGR could be developed for any given operating condition. Such systems are still prohibitively expensive, with limited operating speed range and very complex control requirements. However, during transient events such systems have the potential to rapidly phase between optimal conditions, thus reducing the charge starvation discussed by Stefanopoulou & Kolmanovsky [54].

It is apparent from this discussion that the two EGR concepts that offer the greatest potential for minimum production cost are post throttle external EGR and the use of a large overlap valve phasing device to provide iEGR. These systems are fitted to some currently available engines.

### 2.2.2 BENEFITS AND DISADVANTAGES

- Torque margin available

Although the use of EGR within gasoline engine combustion has received detailed examination within the literature, very little work has discussed the relationship between the induced level of EGR and the reduction in engine torque. This is partially due to the relatively low levels of EGR induced in most experimental studies, but is mainly due to the fact that EGR is typically used at part throttle conditions, where the torque depreciation can be offset by increasing the throttle opening. The reduction in torque expected from the use of EGR charge dilution is principally caused by the reduction of combustible fuel / air mixture drawn into the combustion chamber. Therefore it is reasonable to assume that the reduction in torque associated with the introduction of EGR will be proportional to the reduction in combustible gases. Under extreme conditions poor combustion quality will further reduce the developed engine torque. This hypothesis would appear to be born out by the results presented in the work of Diana et al[41], which investigated the effect that EGR and compression ratio have on fuel consumption. Presented within this work is the effect that different EGR levels have on output engine torque. Detailed examination of these results shows a consistent 0.5 Nm reduction in engine out torque for every 1% increase in EGR. Osses et al[47] presented work with an exhaust throttling system. This work showed that inducing a 30 kPa backpressure (the equivalent of 8% EGR) reduced engine torque by 6%. Osses et al[47] did not establish what proportion of this torque

reduction was associated with the induction increased levels of residual gases. Stefanopoulou & Kolmanovsky [54] has shown that internal EGR developed using a VVA system can develop a 27% torque margin at WOT throttle conditions; as the throttle closes, the torque margin available purely by varying the valve overlap is reduced. The exact specification of the system implemented in this work is not clear however; it is simply described as a cam phasing system, with no details of which set of cams are actuated.

The reductions in engine torque resulting from the induction of EGR discussed above are the only references available. As a result it is apparent that this area of research had to be developed in order to use EGR as a means of torque control.

- Effect of EGR on specific emissions

The use of exhaust gas charge dilution has some benefits in addition to torque reduction Indeed characterising these additional benefits has represented the prime motivation for the investigations discussed so far. Depending upon the approach used to develop it, EGR can have a beneficial effect on both fuel consumption and specific emissions of $NO_x$ and unburnt hydrocarbons (uHC). The following sections will consider work that has examined these benefits.

The mechanism though which oxides of nitrogen are produced within the combustion process is well understood [34],[35]. Much work [34],[35],[42] has demonstrated that EGR can reduce an engine's $NO_x$ emissions. The work of Tabata et al[42] has even suggested that $NO_x$ emissions can be reduced by up to 93% at low speed / low load conditions using an induced charge comprising of 50% EGR. Ladommatos et al[58] proposes that the introduction of EGR reduces the emissions of $NO_x$ via three mechanisms. These are the dilution effects, thermal effects, and chemical effects. In this context the dilution effect is a term used to describe the reduction of available oxygen within combustion gases. The rate of combusted gas cooling has a significant effect upon the rate of $NO_x$ emissions; rapid charge cooling leads to lower $NO_x$ emissions. Exhaust gas is primarily composed of nitrogen and carbon dioxide both of these gases have a relatively high specific heat capacity. As a result combustion charges rich in these gases cool more quickly after a combustion event and have a reduced level of $NO_x$ emissions compared to a non diluted gas mixtures. Dissociation of oxygen from combustion products (e.g. carbon dioxide) allows greater levels of $NO_x$ formation. Dissociation may only occur at very high temperatures; since EGR gases reduce combustion temperature, the dissociation rate

also reduces, thus reducing $NO_x$ emissions. However the work of Tabata et al[42], which examined the effect of EGR strategies on $NO_x$ emissions, failed to discuss these factors or attribute relative importance to them. Work by Ladommatos et al[58] provides a detailed discussion of the relative importance of these effects on $NO_x$ emissions for diesel engines. Ladommatos et al[58] concludes that the dominant factor in the reduction of $NO_x$ emissions for diesel engines is the dilution effect; the reduction in the available oxygen. Since no similar comparison of the importance of $NO_x$ formation criteria has been developed for a gasoline engine, it is believed that the dilution effect is again here the primary cause of $NO_x$ reduction.

Work by Jackson[40] suggests that iEGR is not as effective in reducing $NO_x$ formation as external systems, due to its heating effect on the bulk gas prior to combustion. However this assertion is not born out by the work of Stein et al[51] who suggests that iEGR systems reduce $NO_x$ by a greater margin for a given EGR flow rate. So this issue cannot be resolved from published data.

The negative effect of external EGR on uHC emissions is also well documented [34],[35]; this is due the diluent effect reducing the combustion quality. Work by Tabata et al[42], and Diana et al[41] provide results which concur with this relationship. However iEGR has been shown by Stein et al[51], and Jackson[40] to improve uHC emissions. The later proportion of the exhaust gases contain the majority of the uHC emissions which were stored during combustion in crevice volumes crank case oils[59]. Stein et al[51] explains that iEGR systems predominately recirculate these uHC rich gases thus reducing the uHC emissions.

Carbon monoxide (CO) emissions for both external[42] and internal[51] EGR systems show an interesting relationship with increasing levels of EGR. Diana et al[41] has shown that as external EGR increases CO emissions increase; from 43 g/kWh, to 53 g/kWh at low load conditions. However as the engine load increases the CO penalty reduces until at very high load conditions there is actually a CO benefit with the addition of EGR. While Stein et al[51] have shown that at low loads as the internal EGR increases past 10% the CO emissions levels increase from 20 g/kWh to 30 g/kWh. Here again however as the engine load increases the CO penalty reduces. Neither of these works give sufficient detail to allow this phenomenon to be explained.

The key emissions benefit over lean burn of charge dilution via EGR induction is discussed by Hacohen et al[60] in a paper that compares simulation results. Hacohen et al[60] concluded from this study that regardless of any transient or combustion stability issues, the fact that EGR dilution could be implemented with a stoichiometrically fuelled charge, meant that EGR strategies are superior. This is a key benefit because it means that EGR dilution strategies can use the high conversion efficiency of a three-way catalyst to minimise tailpipe emissions.

- Effect of EGR on fuel consumption

Neame et al[61], Diana et al[41] and Tabata et al[42] report that low to medium (about 10%) EGR strategies may have a beneficial effect on fuel consumption across a large range of throttle positions, while extended EGR strategies (up to 50%) have been shown to have detrimental effects on fuel consumption. Nakajima et al[45] present a detailed investigation of the phenomena which affect fuel consumption of external EGR systems. This work identified the main contributions to the improvement in fuel consumption to be a reduction in pumping losses, reduced heat loss and a reduction in dissociation. Jackson [40] suggests that 40% of the improvement in fuel consumption can be attributed to each of the reduction in pumping losses and the reduction in heat losses, while the 20% remainder is attributed to the reduction in the dissociation level. The increase in fuel consumption observed at higher EGR rates is attributed to the reduction in combustion quality[45] and the reduction in burning rate[42].

Stein et al[51] presented work which showed that valve strategies which increase iEGR have a beneficial effect on fuel consumption. However these tests were undertaken upon an engine fitted with a VVA system; no comparison was made with an engine not featuring a VVA. As such, the fuel consumption implications of the VVA system had not been considered. No work has been presented which examines the direct fuel consumption consequence of the application of a VVA system.

### 2.2.3 APPLICATION AND CONTROL

In vehicle applications EGR has typically been used as a means of controlling part load $NO_x$ emissions. Consequently EGR valve demand is greatest at part throttle conditions at medium to high engine speed conditions. Olbrot et al[46] present the details of a classical EGR controller as fitted to a gasoline engine. This work presents typical values of EGR at given speed / load conditions. The maximum EGR typically tolerated by a gasoline engine at part throttle is shown to be 11%. Olbrot et al[46] suggests that during a transient

operation the engine controller will simply stop the EGR demand and develop the torque margin.

Typically the exhaust flow through external EGR systems is regulated by a pneumatic positional control valve. The vacuum demand to this valve is controlled by an EVR (electronic vacuum regulator) which requires a PWM demand signal. The more advanced control systems, typically fitted to diesel applications, provide a PID control to modulate the demand signal in order to maintain a constant EGR flow. These EGR controllers are developed using either valve position, or pressure difference across an orifice as the feedback signal.

Control of EGR flow rate in diesel applications is a far more complicated problem, since EGR rate has a direct impact on the air fuel ratio and subsequently the levels of smoke produced. Wijetunge et al[62] discuss this problem and in later works[63] develop an integrated EGR, variable geometry turbocharger (VGT) transient positional control system which minimises the impact of the EGR strategy on legislative emissions. However since the EGR rate essentially only affects transient driveability in gasoline vehicles, the complexity of diesel EGR control does not require further attention here.

## *2.3 Use of lean burn*

Lean charge dilution is the reduction of fuelling from a stoichiometric level. This creates a combustion mixture where oxygen is present which will not be used in the combustion process, and this acts as a diluent.

### 2.3.1 RECENT HISTORY

Lean burn engines were seen in the late 70s as a partial solution to improve fuel consumption in response to the energy crisis. However, a period of rapid research and development in this area in the 70s and early 80s was followed by an extended period through the later 80s and early 90s where very little research was focused on the use of lean dilution. This change in fortunes of the lean burn engine was primarily due to exhaust legislation for $NO_x$ emissions. This legislation was finally implemented in Europe in the late 80s and with it research work on high $NO_x$ emitting lean burn engines was moved to research on catalytic converters. It is only recently, with legislative pressure shifting from specific emissions toward a reduction in fuel consumption, that lean combustion concepts

are beginning to resurface. Shillington[2] presents a more detailed examination of the historical influence of legislation on the development of lean burn technologies.

### 2.3.2 METHODS OF PRODUCTION

There are only two main engine configurations that allow the development of lean combustion mixtures: port fuelling and direct injection fuelling.

Port fuelling lean burn engines use a conventional electronic fuel injection system and simply under-fuel a given induced airflow. This type of fuelling control was implemented in studies by Horie et al[57], Stokes et al[64] and Mikulic et al[65]. It is essential in such systems that the airflow into the engine can be measured accurately. Modern fuel injection systems typically feature hot wire anemometers, or manifold pressure sensors, both of which develop accurate airflow measurements. Fuel injection using port mounted injectors produce a homogenous mixture within the port. By simply fuelling only one port in a dual port intake system, a stratified charge can be developed. The CCVS system developed by Honda and described by Horie et al[57] uses the V-TEC cam switching mechanism to selectively switch the flow through a nominally non-fuelled port on and off. During stoichiometric operation both valves are active and the fuelled port is over fuelled to ensure a stoichiometric charge. During homogenous lean conditions only the fuelled inlet valve is open and the induced fresh air is part fuelled. During stratified conditions the non-fuelled port is semi closed, developing a high level of organised charge motion while the fuelled port is under fuelled. A similar system is implemented on the CBR research engine developed by Ricardo and is discussed by Stokes et al[64]. The CBR engine features the additional complication that the non-fuelled port can supply a variable mixture of air and EGR via a complex manifold arrangement.

The major benefits of port fuelled dilution configurations are that the engine components required are very cheap, and control is relatively simple. The inclusion of stratification arrangements require more sophisticated engine control and an increase in product cost.

Gasoline direct injection (GDI) engines are the other main technology used to develop lean burn combustion strategies. These devices use high pressure injectors to deliver fuel directly into the cylinder. Nohira et al[5] describe the development of a direct injection gasoline engine including the complex decisions required during the development of the combustion chamber, the piston bowl profile and the associated control system. As discussed by Nohira et al[5], direct injection still requires the use of air measurement

devices at least as sophisticated as those fitted to port fuelled lean burn engines in order to determine the required fuelling rate. The major benefit of direct injection engine systems is that they allow the development of charge stratification arrangements simply through the timing and shape of the fuelling pulse. If the fuel is injected during the intake stroke it will develop a homogenous charge; if the fuel is injected during the compression stroke it will develop a stratified charge [66].

The injection equipment capable of operating within the high pressures in the combustion chamber is considerably more expensive than port fuel injectors, to the point where direct injection engines have not been offered for sale in small capacity low profit market sectors. Additionally, such systems provide a more complicated control and optimisation problem, including requiring a new variable, injection timing, to be incorporated into the structure of engine controllers. This aspect of GDI engines is touched upon by Sadler et al[67]. However the ability of GDI engines to develop stratified charge mixtures without further engine modifications has led to this becoming the emerging technology in gasoline engine development.

### 2.3.3 BENEFITS AND DISADVANTAGES

-Torque margin development

In a similar manner to the use of EGR to reduce $NO_x$ emissions, lean burn concepts have been seen as an approach to reduce fuel consumption at part load conditions. As a result few papers present details of the reduction in output torque for a specific throttle position and engine speed. Instead the throttle position is modulated to maintain a demanded power condition.

Ma & Finlay[68] presented some results for a lean fuelled engine at WOT over a number of speed conditions. Examination of these data suggests that a maximum torque margin of around 50 Nm would be possible using the system applied by Ma & Finlay[68]. However the work is concerned principally with the development of a predictive emissions measure and does not detail the test engine or dilution level achieved. Sadler et al[67] suggests in a paper that discussed the development of a wide fuelling range tolerant GDI engine that the test engine can operate at air fuel ratios as low as 60:1, and this has the potential to allow throttleless torque control. This suggests a torque margin of at least 90 Nm. However Sadler et al[67] does not present any results which corroborate the throttleless potential of the designed engine.

Even though there is a significant lack of work in this area, it is apparent that the torque margin which is possible will be directly proportional to the reduction in combustible mixture.

- Effect on emissions

The effect of lean burn engines on specific emissions is well documented. Heywood[35] and Stone[34] present classical emissions relationships. Shillington[2] presents possibly the definitive emissions / dilution relationship representation, later used by Stone[34]. It shows that as the lambda value increases, emissions of specific $NO_x$ increase up to lambda 1.1; from this point $NO_x$ emissions reduce. At lambda 1.2, $NO_x$ emissions have returned to the stoichiometric level and by lambda 1.5, $NO_x$ emissions are somewhat lower than 50% of the original value. The initial increase in $NO_x$ emissions can be explained by the increased availability of free oxygen and the increase in flame temperature associated with partially lean mixtures. The subsequent reduction in emissions is due to bulk gas cooling caused by the excess air; this cooling effect reduces flame temperature and hence specific $NO_x$ emissions.

The effect on each of CO and uHC is throughout the majority of the lambda range a reducing one. Greater availability of oxygen leads to greater fuel conversion, so that there are fewer uHC and CO emissions. At extreme lambda dilution conditions these emissions can be seen to increase as a result of reduced combustion stability and the resultant poor fuel combustion.

- Reduction in fuel consumption

The key benefit to a conventional powertrain of lean burn engine strategies is the reduction in specific fuel consumption. Since a lean mixture will develop a reduced amount of work, the engine must consume a greater quantity of fresh air in order to develop an equivalent power. This increase in air consumption is achieved by reducing engine throttling and the reduction in fuel consumption for a given power can almost totally be attributed to the consequent reduction in pumping losses.

Jackson[40] suggests that port fuelled lean gasoline concepts may develop improvements in fuel consumption of up to 10%. This is borne out by the works of Horie et al[57], Shayler et al[69] and Tabata et al[42] who reported fuel economy improvements of 12%, 8.6% and 12% respectively. Jackson[40] continued to suggest that direct injection gasoline concepts allow improvements in fuel consumption of up to 20%. This claim in turn is corroborated

by the results presented by Shiga et al[70] who identified a 14% fuel economy improvement for a lean fuel GDI engine compared with a port injected lean fuelled engine. Shayler et al[69] presents work which suggests a maximum fuel consumption improvement of 20% for a GDI engine compared with a port fuelled engine operating stoichiometrically.

Shiga et al[70] partially attributes the further improvement in fuel consumption of a direct injection engine to additional reductions in pumping losses. However, this work attributes the majority of the improvement to improved cycle efficiency.

- Transient operation

No works to the author's knowledge, have examined the transient response of a gasoline engine under the sole influence of fuelling demand changes. Transient operations have been examined for diesel engines[71] where load is purely controlled by fuelling rate. However, diesel engines have considerably greater inertia than gasoline engines and typically feature high boost turbocharging strategies. As a result little comparison can be drawn between the two types of transient response. It can be predicted however, that fuelling transients will be performed rapidly on either port injected or direct injected gasoline engines as a result of the minimal transportation volumes and rapid injector responses.

### 2.3.4 CONTROL AND APPLICATION

A number of control strategies have been developed for the use of port and direct injection fuelling[5],[66]. Horie et al[57] presents a classical example of lean dilution application to a gasoline engine. In the low to medium load, low to medium speed condition Horie et al[57] proposes the use of a high lean dilution rate (lambda 1.5), but at all other part throttle conditions use a stoichiometric charge. At WOT conditions overfuelling is used to achieve peak power and cooling of the catalyst surface. Nohira et al[5] presented a similar strategy for a direct injection engine: a highly diluted stratified mixture is used within the low speed, low load engine regions and as the engine speed increases, the mixture dilution is reduced and homogenous lean dilution is implemented. For high speed or high engine load conditions a stoichiometric charge is adopted.

Proposals have also been made for more complex uses of lean dilution. Gradin & Angstrom[72] suggested the use of lean charge dilution to replace fuelling enrichment cooling of exhaust gases with turbocharged engines. This application of lean charge dilution would require lean dilution at or near WOT conditions.

The work of Kolmanovsky et al[71] examines the control of a lean burn engine mated to a CVT during the transition from a diluted operating condition to a stoichiometric condition in order to regenerate a lean $NO_x$ trap. This work does not propose a lean burn dilution strategy for a gasoline vehicle; instead it focuses on co-ordination of the control of the engine and CVT to remove torque disturbances during catalyst regeneration cycles.

## *2.4 Combined use of lean burn and EGR*

A number of authors, for example Tabata et al[42] have extended their studies of either lean burn or EGR dilution to examine the effect of a combined dilution strategy. These studies have shown that the combination of these diluents has the potential to reduce engine fuel consumption whilst simultaneously reducing exhaust $NO_x$ emissions. Tabata et al[42] showed that the combination of EGR and lean dilution strategies could further improve fuel consumption (2% better than a purely lean mixture) whilst developing half the $NO_x$ emissions.

Gschweitl et al[73] present work in which the integration of AVL's cameo optimisation programme with a test rig host system is discussed. Within this paper is a dilution application strategy for a direct injection engine. This dilution application adapts the lean burn control strategy proposed by Nohira et al[5] to include a combination of lean burn and EGR dilution in the low speed / low load region.

## *2.5 Engine tolerance of charge dilution*

An engine's dilution tolerance is the maximum level of charge dilution at which it can maintain stable combustion. Combustion stability is typically determined by the coefficient of variation of the indicated mean effective pressure ($COV_{imep}$). Details of the calculation of this measure are presented in Chapter 3. The level of $COV_{imep}$ taken to indicate unacceptable combustion stability varies with research origin. Heywood [35] suggests the use of a limit at 10% $COV_{imep}$, while Fraidi et al[74], Tabata et al[42], Mikulic et al[65], and Shayler et al[69] used 5%; Stokes et al[64], and Jackson [40] use 2%. It is apparent that there is a general trend to develop systems which maintain greater combustion stability.

In a conventionally fuelled spark ignition engine following ignition, a flame kernel is developed. The flame kernel develops into a flame front that propagates throughout the fresh mixture during combustion[35]. Here comparison should be drawn with the

combustion process within a diesel engine, where multiple initiation sites are generated by the high pressure / temperature conditions incident during the compression stroke. From each of these initiation sites a separate flame front is developed.

Very high levels of dilution can inhibit the combustion process described for spark ignition engines in two ways. They can either cause poor mixture quality local to the flame initiation point, or else localised pockets of poor mixture can quench the propagation of the flame front. Again comparison can be drawn with compression ignition engines, which can tolerate much greater levels of charge dilution. This is because in compression ignition combustion multiple flame ignition points develop within regions where the mixture is of a suitable quality. The EGR limit reported for a conventional port fuelled gasoline engine ranges from 28%[42], to 18% [41]. The lean dilution limit for a conventional port fuelled engine ranges from lambda 1.4[42], to lambda 1.6[34].

A number of engine adaptations have been developed to improve the dilution tolerance of a gasoline engine. These operate principally by increasing charge motion, inducing charge stratification and through improved flame ignition devices.

Increasing charge motion improves charge mixing, resulting in better mixture quality throughout a homogeneous charge. Furthermore, increasing charge motion improves the propagation speed of a flame front. Charge motion can be increased via swirl, squish and tumble phenomena. A number of authors[57,64] implemented high swirl concepts on test engines in order to improve dilution tolerance. Swirl induces within the induced charge an axial motion. Using such systems, dilution tolerance was shown to improve from non-swirl conditions by 15% EGR [65] and 0.27 lambda [57]. The disadvantage of high swirl is that the energy used to develop high charge motion is achieved at the cost of volumetric flow rate[34]. In the studies examined swirl is developed by altering the geometry of an inlet port, whilst maintaining an inlet port with non-swirl characteristics; this reduces the compromise in volumetric efficiency. Swirl is controlled by either a valve placed in swirl generating inlet port[64] or through reduced valve opening of swirl port, inlet valve[57].

Other authors preferred the use of tumble charge motion, i.e. the establishment of a radial charge motion, because of its reduced effect on peak engine power (Ando[66]). Arcoumanis et al[75] provide a thorough and detailed explanation of tumble motion. A test rig featuring such charge motion concepts was shown to be capable of dilution limits up to lambda 1.7 [64], but no EGR data were presented. Tumble is achieved either through port

geometry[66] or through piston head profiling[67]. As the quantity of induced charge increases the tumble charge motion breaks down therefore allowing high volumetric efficiency. Consequently there is no need to include a normal flow port or tumble control features.

Squish is generated through incorporating galleries into the piston head profile. During the compression stroke, these galleries cause jets of gas to cross the main bulk of the charge thus inducing charge turbulence. This is an approach more commonly associated with diesel engines; however Evans[76] presented work describing the development of a squish-inducing gasoline piston design. This work did not show any increase in the dilution tolerance of the test engine, but it did demonstrate improved combustion characteristics and fuel consumption.

A final approach to the increase of dilution tolerance with a gasoline engine is the increase of the ignition energy. Nakajima et al[45] presented work showing the dilution improvement possible using two spark plugs per cylinder (10% improvement in tolerable EGR compared with a single spark plug system), while Asik et al[77] and Neame et al[61] demonstrated that a plasma ignition system could be used to allow an engine to tolerate dilution levels as high as 40% EGR. Geiger et al[78] showed that advanced spark plug design could tolerate lean dilutions up to lambda 1.8.

## *2.6 Conclusions*

This research has shown that a number of technologies can be used to develop EGR into the combustion charge. Of these methods external post-throttle EGR and iEGR developed via variable valve actuation strategies offer the greatest potential to develop high EGR dilution rates. Reported transient investigations have shown that an external EGR transient occurs more rapidly than an iEGR transient. This relationship rather contradicts a phenomenological understanding of the system, since due to reduced diluted volumes within the inlet manifold it is to be expected that iEGR systems would offer the quicker transient response.

Research has shown that there are principally two approaches that may be used to develop a lean combustion charge: port injection and GDI. GDI solutions have been shown to have the greater potential to sustain dilution levels; however, it is not apparent that this will directly translate into the development of a torque margin. Additionally this study is intended to identify the potential available for mating conventional, low cost

engines with continuously variable transmissions, and currently GDI engines are high cost items.

As a result of the research a testing program was carried out to investigate the potential to control torque via EGR and lean burn. Both EGR and iEGR via valve phasing have been examined, all lean burn work used port injection.

Work has also been identified which determines a range of methods which may be implemented to increase the dilution tolerance of an engine. These are considered to allow further development should there have been insufficient torque margin available with the engine in its conventional configuration.

# 3 The Structure of the test rig

## *3.1 Scope of test rig*

The majority of testing undertaken on this rig was steady state engine testing used to characterise the engine response over a range of operating conditions. Additionally, a number of transient experiments have been undertaken to characterise the response of the engine following a step change in dilution strategy.

## *3.2 Test engine*

### 3.2.1 ENGINE SPECIFICATIONS

The engine used as the base for this investigation is a 1.7 L Ford Zetec - SE. This is the engine is fitted in versions of Ford's small sports car the Puma. The engine has a peak power of 125 ps (92 kW), achieved at 6300 rev/min and a peak torque of 157 Nm at 4500 rev/min[79]. Figure 3-1 presents a torque speed representation for a standard engine configuration. This engine is based upon the Ford 1.6 L Zetec [79], from which additional displacement is achieved by removing the cylinder liner and coating the surface of the iron engine block with a nickel alloy[79]. A novelty of this engine is that it is the first Ford production engine to feature a variable valve actuation device. The device fitted to this engine varies the overlap duration of the inlet and exhaust valves. Section 3.2.3 describes the device in greater detail. The engine is fitted with an aluminium inlet manifold, rather than the much vaunted[80] plastic manifolds used in the smaller capacity sister variants. The engine also features a close-coupled three-way catalyst (TWC) which is retained on the test rig. The inlet geometry of the 1.7 L Zetec has no specific adaptations to develop swirl charge motion, while Heuser et al[79] described the tumble developed as moderate. Therefore the test engine does not feature any peculiarities that make it particularly tolerant of charge dilution.

The 1.7 L engine has a relatively small displacement for a 'sport' product. However its specific power output at 73 ps/litre is in keeping with market sector trends. Key engine specifications are presented in Table 3-1.

### 3.2.2 ENGINE CONTROL SYSTEM

Engine control is provided by the EEC V engine control unit (ECU). This type of ECU was the first produced by Ford to feature a torque based architecture. In such a controller,

speed and proportion of maximum torque, scale all engine control variable settings e.g. spark timing points are determined from speed and torque via lookup tables. The engine torque is inferred from the airflow into the engine. It was also the first generation of controller fitted to a Ford gasoline engine to feature on board diagnostics (ODB). The EEC V strategy uses engine mounted instrumentation to control the spark timing, the fuel injector pulse width and the variable cam timing (VCT) position. Figure 3-2 provides a schematic of the instrumentation required to develop particular control signals. It can be seen that each system features a multi signal control approach. Here, as an example to illustrate the importance of each signal, the hierarchy of the fuelling control system will be considered. Under normal steady state operation the engine fuel injector pulse width is controlled by the signal from a heated exhaust gas oxygen (HEGO) sensor to the ECU. Whilst in this condition, the fuelling signal is modulated by +/- lambda 0.05. This fluctuation is used to determine that the exhaust sensor is operating accurately. If it is deemed that the sensor has failed, or if the HEGO sensor has not achieved working temperature, the fuelling rate is determined from the signal provided by the hot-wire anemometer, termed the manifold air flow (MAF) sensor, mounted after the air box. If the signal from the MAF sensor does not vary as expected with throttle position, this sensor is also deemed to have failed and the fuelling is scheduled solely from the throttle position and air temperature sensors. This is the multi signal control approach used to ensure that the engine operates under most conditions. As is shown in Figure 3-2 the scheduling of spark timing also features a multi signal controller. However, the scheduling of cam timing does not have this type of robust control mechanism; if any fault conditions are registered by the engine controller this system is returned to a fail safe condition. It is the author's belief that this is a result of the novelty of this feature to the Ford control engineers.

The ECU features a key code recognition engine immobiliser. Originally this system was overridden by fitting the test engine with a production ignition barrel and programming a key into the test ECU's memory. However the key code was erased from the engine memory following a fuse blow. The final solution to this problem was to update the controller with a strategy in which the immobiliser function was removed.

### 3.2.3 VARIABLE CAM TIMING

The engine is fitted with a variable valve actuation system called variable cam timing (VCT). This system varies the relative phase of the inlet valves to the fixed exhaust valves. It should be noted that this is an approach used by manufactures such as BMW, and Toyota[81]; the concept was originally proposed by Alfa Romeo[50]. The mechanism

used to vary angular position is shown in Figure 3-3. The component highlighted is the sliding collar, which transfers rotation from the belt driven cam pulley to the camshaft. The cam pulley has a series of straight cut channels removed from its internal diameter. The camshaft has a series of helically cut channels removed from it outer diameter. The sliding collar features a series of straight cut teeth on both internal and external diameters. The teeth interface with the both sets of channels. The unit is sealed and hydraulic fluid is regulated to either side of the sliding collar. When a cam phasing process is demanded the hydraulic pressure is increased to one side of the sliding collar, forcing the collar to transverse the channel length. Since the collar is constrained by the straight cut channels its motion is purely longitudinal. As the collar moves along the helical spline interface with the camshaft, it causes the camshaft to rotate relative to the driven pulley. Thus the phase of the inlet cam is varied relative to the crank positions and the exhaust valves. The position of the cam is fed back to the ECU via a magnetic pick-up, which monitors the position of a toothed gear. The hydraulic pressure on either side of the sliding collar is regulated by a positional control valve, which is controlled by a PWM signal from the engine ECU.

Figure 3-4 shows the range of valve overlap that this mechanism allows. This system has a maximum overlap duration of 40°. Table 3-2 shows the overlap control as implemented in the engine strategy. Optimal output power is achieved using valve overlaps ranging from 20° to 35° at WOT conditions. Any overlap greater than this will cause an increase in the levels of exhaust gas incident in the combustion charge thus potentially inducing iEGR.

Since the inlet cam profile has been developed to maximise engine power it features a large opening duration (240°). When the valve overlap is at a minimum, the inlet valve opening occurs near to top dead centre. This will force the inlet valve closing to occur after BDC; in effect the inlet valve will remain open during the compression stroke. During the period in the compression stroke when the inlet valve is open, charge will be exhausted from the cylinder. This effect is known as late inlet valve closure (LIVC) throttling, and is particularly prevalent at conditions where there are low levels of manifold charge motion. There is considerable scope on the system fitted, for this characteristic of the VCT system to pay an important role in fuel consumption reduction.

## *3.3 Modifications to engine*

In order to investigate the effect of high dilution rates the engine has been modified to include an external EGR system. Additionally, in order to represent a production integrated powertrain, the standard engine has been modified to incorporate an electronic throttle. The components selected and implementation of these modifications are discussed in the following sections.

### 3.3.1 ELECTRONIC THROTTLE

The inclusion of an electronic throttle allows the test rig to more fully represent the engine as fitted in an integrated powertrain. Furthermore, this adaptation improves testing repeatability and automation of test cell control. The unit supplied by Ford is manufactured by Bosch and features a stepper motor driving a geartrain which controls the position of the butterfly valve. The electronic unit has a slightly reduced internal diameter compared with the cable unit, namely 80 mm rather than 83 mm. This has the effect of reducing the maximum output power by 12 ps (8 kW). The electronic throttle has been fitted as a direct replacement for the standard cable throttle unit. A modification plate had to be manufactured to allow the electronic unit to align with the inlet manifold. The electronic throttle, and the modification plate are shown in Figure 3-5

The electronic unit was designed for a vehicle which does not feature an idle by pass control system; consequently when the throttle is at zero demand position the butterfly plate is $5^{o}$ open. This opening causes very poor idle quality because the idle bypass controller fails to regulate the flow correctly. Communications with Bosch revealed that zero stop opening was set by a hard endstop and reducing the hard stop position improved the quality of idle. However, it was subsequently discovered that the geartrain fitted within the electronic throttle was not designed to absorb the shock loads developed when the butterfly valve performed rapid range swings; the overshooting and impacting upon the throttle body during rapid closure operations was the particular problem. Hence, it was decided to use the original electronic throttle configuration, and disable the idle bypass controller. As a result the idle speed was increased from 800 rev/min to 1400 rev/min.

The stepper motor fitted within the electronic throttle requires a +/- 15 Volt signal. The University of Bath (UoB) have developed a feedback positional controller which interprets a 0-10 Volt demand signal and develops the corresponding stepper motor voltage signal,

The electronic throttle is thus equipped with a positional feedback signal, and this is used within the throttle position demand unit.

The EEC V strategy demands a throttle position signal as a base control input. If this signal is not supplied, the VCT system defaults to a fail safe mode, The feedback position from the electronic throttle unit is scaled to represent the 0-5 Volt signal from the standard cable throttle unit and is presented to the standard ECU throttle position connection.

### 3.3.2 EGR SYSTEM

The second major adaptation to the engine is the inclusion of a large bore external EGR system. This was included to allow high EGR dilution rates even at wide open throttle conditions, The EGR system applied to this test rig was implemented in the year 2000. At that time the works of Yoshizawa et al[43] and Blank et al[44] on EGR configurations to maximise charge homogeneity and to minimise transient implications of EGR configurations had not been published. The EGR arrangement implemented on this rig is similar in design that fitted on Ford 1.8L DI diesel engines. The system consists of a post throttle inlet manifold interface, into which a stainless steel tube is connected. This swings over the engine bell housing and mates with a large bore pneumatically operated EGR valve. This valve is then connected to a tube which runs into the connector in the exhaust manifold. A schematic of the system is provided Figure 3-6. A 30 mm diameter hole bored into the inlet manifold, 50 mm after the throttle mounting, acts as the EGR interface. The EGR tube extends 20 mm into the inlet manifold and the tube end is finished with a 20° chamfer to improve the homogenous mixing of the EGR and fresh charge. A flange is welded 20 mm before the end of the EGR tube; this flange secures the EGR piping to the inlet manifold. The EGR system used 22 mm ID thin walled stainless steel tubing; this was formed using a standard plumber's pipe bender. The pneumatic valve fitted is secured to the first pipe section by a second welded flange. The valve itself is taken from a Ford 1.8 L diesel engine and is pneumatically actuated with a spring return. The valve was selected because it has an appropriate internal diameter and also features a position feedback transducer. The second section of EGR tubing, connecting the valve to the exhaust manifold, is secured using a stainless steel compression fitting. The fitting has been positioned on the top of the exhaust manifold in the location where the HEGO sensor was originally fitted. The HEGO sensor has been relocated to a position above the catalyst mounting flange (Figure 3-7).

As a result of the inclusion of the EGR system it was necessary to move the air temperature sensor of the engine from it original location in the inlet manifold to the airbox. This move was necessitated since the air sensor is used to determine the mass charge of fresh air induced, had it been retained in its original position it would have overread the charge temperature by up to 80 °C.

## *3.4 Mechanical installation*

### 3.4.1 TEST BED DESIGN

The engine is mounted on a test bed frame developed by the University of Bath. This test bed has been designed to mimic many of the features which are used on industrial engine test rigs. It is constructed of two mounting channels each formed from two channel sections, welded a distance apart.

The engine is positioned by its standard mounting points. This necessitates the inclusion of a gearbox bell housing. However, the engine is fitted with a clutch assembly and straight 1:1 drive; as a result the bell housing does not contain a gear set. The drive shaft from the engine is mounted via a universal coupling to a Heenan & Froude MN1 Eddy current dynamometer. The engine dynamometer has been calibrated for work up to 6000 rev/min and is rated up to a maximum power of 110 kW. The load developed by the dynamometer is measured from a torque arm using a strain gauge torque transducer.

### 3.4.2 COOLING

Engine cooling is supplied by a Bowman heat exchanger into which the cooling water flow is regulated by a 24 Volt proportional control flow valve. The engine thermostat has been removed; instead a PID feedback controller that forms part of the test rig host system provides control over engine temperature. The dynamometer also requires a cooling water flow and this is taken from the same supply that provides the Bowman. The cooling water is provided by a blast air cooler supplying a number of cells on a ring main; used water is returned to the cooling system.

The oil system is not fitted with a cooler; instead a centrifugal fan was used to blow test cell air across the oil sump.

### 3.4.3 ENGINE ELECTRICAL SUPPLY

The test engine is fitted with a vehicle electrical loom; this means that there are a large number of superfluous electrical connections, such as those for the headlamps. The loom features a standard fuse box and engine relays and is provided with a 12 Volt supply from a switched channel controlled by the host system. The starter motor and ignition signal are also provided by a switched 12 Volt channel controlled by the host system. The 12 Volt supply is derived from a standard car battery, permanently trickle charged from a standard battery charger.

### 3.4.4 EXHAUST SYSTEM

The engine exhaust down pipe is a standard unit from a vehicle and is connected via a universal coupling to an 80 mm cast pipe which is drawn round into the vacuum exhaust extractor. Fitted within the cast pipe is a regulating valve used to tune the exhaust backpressure to match the 30 kPa (at maximum power) produced by the vehicle's standard exhaust system.

### 3.4.5 FUEL STORAGE AND SUPPLY

The engine is supplied with fuel from a 50 L day tank. Fuel is piped from the day tank through a diesel fuel filter into a Plint fuel measuring system. From the Plint unit the fuel is pressurised using the standard vehicle fuel pump. The fuel then passes through copper tubing to the fuel rail inlet. A fuel return line takes unused fuel back to the reservoir that forms part of the Plint unit. The fuel used in the investigation was standard 95 Ron unleaded gasoline. Fuel was always purchased from the same garage to maintain blend consistency.

## *3.5 Instrumentation*

### 3.5.1 GAS SAMPLING

The inlet and exhaust manifolds are fitted with gas sampling points as illustrated in Figures Figure 3-7 & 3:8. The post catalyst down pipe is also fitted with gas sampling points, to allow the characterisation of the catalyst performance. However, only one emissions tower was available during this study and as a result it was not possible to develop an accurate experimental catalyst model from this rig. The exhaust manifold sampling point was connected to an AVL heated line, while the inlet manifold gases were transported along 6 mm polyethylene tubes. The sample lines were 20 m long and

connected to an AVL CEB X00 emissions tower. The inlet manifold connection allowed determination of the EGR rate via inlet $CO_2$ sampling. The second connection to the inlet manifold was a return line, such that the flow rate measured by the MAF sensor was accurate.

The AVL CEB X00 emissions tower incorporates three non-dispersive infra-red absorption (NDIR) detectors to determine the levels of CO, and exhaust and inlet $CO_2$. It also incorporates a chemiluminescent detector (CLD) which was used to determine the levels of $NO_x$ in the exhaust. A flame ionisation detector (FID) was used to determine the levels of uncombusted fuel in the exhaust gas. A paramagnetic detector (PMD) was used to detect Oxygen.

The analyser was set in the ranges, CO 0 - 6%, exhaust $CO_2$ 0 - 14%, inlet $CO_2$ 0 - 6%, NO 0 - 2000 ppm, uHC 0 - 1000 ppm and $O_2$ 0 - 21%. These ranges were set before every testing session using calibration span gases and where checked after the testing session by resampling the span gases. Variations in analyser accuracy of greater then 1% raised an error flag and required the session to be repeated.

Since the gas paths are very long, the analysers are designed for steady state testing, and the communication update rate between the gas analyser and the host system ran at 1 Hz, this experimental setup is not suitable for transient emissions analysis.

### 3.5.2 PRESSURES

Figures Figure 3-7 & 3:8 show the positioning of pressure sampling points on the engine. It can be seen that there are gas sampling points in both the inlet and exhaust manifolds. The pressure transducers for these tappings are positioned in the transducer box and are connected to the transducers via short lengths of Teflon tubing. Trans-instruments pressure transducers were used to measure the inlet and exhaust pressures. The transducers are rated to 1.6 $bar_{absolute}$ and 2 $bar_{gauge}$ respectively. The oil pressure was measured as part of the host system shut down requirements. An engine instrumentation oil pressure sensor was removed and replaced by a pressure switch and a 1 $bar_{gauge}$ pressure sensor. The pressure in the fuel line was also measured by the host shutdown system. A Murray pressure switch set to 1.5 bar provided a digital shut down signal if the fuel pressure dropped.

### 3.5.3 IN CYLINDER PRESSURE

The spark plug fitted to cylinder number one contained a type 6117b piezoelectric pressure transducer manufactured by Kistler. It features a sensitivity of 16 pC/bar and can measure pressures up to 200 $bar_{gauge}$. The signal from the piezoelectric transducer is passed through an AVL charge amplifier and is subsequently manipulated by an AVL Indiset. The Indiset used, can record up to 1000 pressure signals for data analysis. The data signals were analysed to establish whether the engine was currently in a knocking condition and whether the current engine combustion was sufficiently stable. Combustion stability was assessed by examining the coefficient of variation of indicated mean effective pressure ($COV_{imep}$). $COV_{imep}$ is determined by the following equation:-

$$COV_{imep} = \frac{\sigma_{imep}}{\overline{imep}}$$

Where:- $\sigma_{imep}$ Is the standard deviation of imep

$\overline{imep}$ Is the mean imep

Section 2.5 showed that a range of $COV_{imep}$ measures have been used in other work to determine combustion stability. Here it has been decided to fix the maximum allowable $COV_{imep}$ to 10%. This is because under certain highly throttled conditions the engine as installed on this test rig could develop $COV_{imep}$ variations of up to 10%. It therefore seemed reasonable to set this as the limit for charge dilution strategies on the same test rig. If during a testing procedure the steady state $COV_{imep}$ exceeded 10%, engine variables were adjusted to improve stability and consequent control variable settings were recorded. In order to align the pressure signal with the crank position, an AVL shaft encoder was fitted to the engine crank pulley. This affords the Indiset a 0.1° positional accuracy.

### 3.5.4 TEMPERATURE

In total there are 12 temperature channels. These are:- inlet manifold temperature, four individual exhaust port temperatures, exhaust manifold temperature, exhaust temperature post catalyst, coolant temperatures pre and post Bowman, oil temperature and cell ambient temperature. All temperatures were measured using K-type thermocouples.

### 3.5.5 FUEL MEASUREMENT

Measurement of the fuel flow into this test rig was originally achieved using a Plint fuel flow measurement device. However this apparatus was not designed for high speed, large capacity engine applications and the return flow from the injectors was sufficient to cause large amounts of turbulence in the fuel reservoir and thus false completion signals, leading to very poor testing repeatability and accuracy. Instead the engine ECU's measure of fuel flow was used. The EEC V engine strategy calculates fuel flow based upon an assumption of fuel rail pressure and a calculated relationship between the block temperature and the fuel temperature. Knowledge of the duration of the injector pulse width can yield a measure of the fuelling rate. The use of this fuelling signal can be justified because it was considerably more repeatable than the Plint signal. Its use is considered to be consistent with an ultimate engine application of the technologies under consideration in this study.

An independent measure of fuel consumption was derived from the Spindt air fuel ratio determined from the exhaust gas constituents. Evaluating this ratio with an airflow measurement yields a fuel consumption rate. Comparison of the Spindt derived fuel consumption and the engine control system fuel consumption measure showed a good correlation; therefore confidence was established in both measures. In the experimental study the fuel consumption was determined from the ECU measure alone

### 3.5.6 AIRFLOW MEASUREMENT

The air charge consumed by the engine was measured by two systems. The engine management system uses a hot wire anemometer mounted after the airbox to determine the airflow (MAF) into the engine. Testing demonstrated that this approach to air charge measurement was accurate under most conditions however under WOT, high EGR rate conditions, the signal over read the amount of air induced. The EEC V strategy does not use the MAF signal to schedule fuelling at WOT condition. This is due to a phenomenon referred to in the ECU strategy[82] as blowback, where standing pressure waves in the inlet manifold cause the hotwire anemometer sensor to over read. Thus at WOT the EEC V strategy schedules fuelling solely from a lookup table of speed and throttle position.

An alternative measure of air charge flow was determined from the fitting of a Yokogawa vortex shedding flow meter, The Yokogawa flow meter is connected to the inlet of the airbox via a 160 L plenum. The plenum acts to remove the effects of blowback on the flow

meter. All of the experimental airflow results presented in this thesis are based upon the Yokogawa readings.

## *3.6 Control and data acquisition*

### 3.6.1 CP ENGINEERING HOST SYSTEM

A CP Engineering test rig data acquisition and control host system is fitted to this test rig. This system can read up to 256 input channels, and can provide 20 PID control signals, 20 digital outputs and 20 analogue outputs. The host systems consist of a main control tower, housing signal conditioning cards, the transducer box into which transducer signals are routed, a dynamometer control box and an engine electrical distribution box. The transducer box acts as a collating point for transducer signals. It also contains cold junction compensation for the thermocouple readings. The dynamometer control box encloses a voltage transformer to provide the 24 Volt signal required by the dynamometer and also acts as a collection point for the dynamometer speed and load signals. The engine electrical distribution box houses a number of 12 Volt switching relays. Figure 3-9 presents a schematic of the configuration of the host system.

The CP engineering host system is also capable of interfacing with any electrical equipment fitted with an RS232 connector. Using this interface the host system records measurements by the AVL gas analyser. These signals are updated at a 1 Hz refresh rate.

The host system as supplied to the university has an open architecture allowing the inclusion of specific signal manipulation functions. Here this capacity has been used to display and record corrected engine signals. The host system uses an engine operation package called CADET V12. CADET V12 can display a number of different user sheets, allowing the engineer access to a great deal of information in a range of display formats. Figure 3-10 demonstrates the display set as used on this application.

The host system has a safety shutdown facility; signals from the oil pressure switch, the oil temperature switch, the coolant temperature switch and a number of emergency stop buttons can provide hard engine shut down conditions. The CADET software also allows a user to implement soft shutdown signals. On this engine set-up, these were used to limit the maximum engine speed and switch the engine off should the pressure drop in the fuel line.

As applied to this test cell the host system operates at an 80 Hz base frequency. Base control channels operate at this frequency; these channels are engine speed and engine load for dynamometer control. For transient measurements, the signals can be grouped into either high speed signals or low speed signals. High speed signals are recorded at half base operating frequency - 40 Hz, while low speed signals are recorded at a 1 Hz operating frequency. High and low speed signals are identified on the Table 3-3 and Table 3-4.

The host system has been used to provide closed loop control of a number of items of test rig equipment. This control is established by connecting the demand and feedback signals to a PID control loop. Components controlled in this way are the coolant valve position and the dynamometer demand voltage. The host system is also used to provide a signal to the EGR position controller. However, the host system cannot develop PWM signals, instead a UoB PWM signal generator was manufactured. This signal generator scales a 0 - 10 Volt demand to a PWM signal, such that the CP host system simply supplies the PWM box with a scaled demand signal. A similar approach was used in the control of the throttle position. This is shown in Figure 3-11. Each control loop required PID tuning, which was achieved at representative operating conditions using a regimented strategy. Investigations were made to assess the improvements that might be achieved from retuning the dynamometer PID loop to provide better control during transient operations. However, it was found that this retuning process was unable to provide an operating condition which had sufficient stability to warrant a change in PID values.

The CADET V12 software allows control variable scheduling such that throttle, EGR and speed transient operations can be instigated by the host system. Fuelling rate, spark timing and cam phasing transients cannot be controlled by the host system because they are engine strategy transients and the host system is unable to interface with this engine ECU because the EEC V strategy does not support the ASAP 3 interface.

### 3.6.2 ENGINE STRATEGY CALIBRATION TOOL

Ford had supplied the project with an ECU research interface and control device known as an RCON. The RCON allows engine signals to be manipulated, and recorded at rates of up to 100 Hz. It communicated to a laptop computer, used in this study, via a PC-Anywhere program. Under steady state testing conditions a 60 second RCON data file was recorded for each operating point.

- Fuelling

Manipulating the EEC V strategy using the RCON it was possible to override the fuelling strategy. In the override condition, engine fuelling is scheduled based upon the MAF sensor signal. Lambda ratios may be demanded; the ECU examines the airflow rate and determines a suitable fuelling pulse width. The controller allows lambda fuelling requests in the range 0 - 2 lambda.

- Spark timing

The engine strategy does not allow complete overriding of the spark timing control. Instead a determined spark angle can be incremented or reduced via a user-specified calibration variable. The ECU retains control over the maximum extents of the spark timing range; which were set as -60° to +60° degrees before top dead centre.

- Cam timing

Unlike spark timing and fuelling, the EEC V strategy does not provide an in built calibration tool to control the cam timing. Instead engine look-up tables must be amended in order to vary the valve overlap for a given condition. The limits of operation are in the range 0° - 40° overlap and, any cam position between these limits may be used throughout the operating speed range.

## *3.7 Transient testing*

A number of transient investigations were required to assess the relative response rate of the engine to step changes in charge dilution. This requirement introduced a number of complications to the test rig control and measurement.

### 3.7.1 TRANSIENT DATA ACQUISITION RATE

As discussed the maximum data acquisition rate of the CP host system is 40 Hz, during transient testing every channel was recorded at its maximum frequency. These are shown in Table 3-4. The host system was set to record the data at 100 Hz. The RCON was set to acquire data at 100 Hz sampling frequency; however the maximum channel update frequency was also 40 Hz.

### 3.7.2 TRANSIENT SIGNAL MATCHING

Since there are two systems being used to measure and control one test rig during transient operations, there may be a discrepancy in signal alignment. To overcome this both systems record engine speed and, by comparing these speed trace signals, the two sets of data can be aligned.

Another more complex problem was encountered whilst performing transients involving step changes in EGR rate. An EGR transient requires synchronisation of the EGR and spark timing demand signals. However, the EGR demand signal is controlled by the CP system while the spark signal is controlled by the RCON system. Co-ordination of these demand signals is essential. If the spark timing swing happened too early, there would be a reduction in torque immediately prior to the main transient event. If the spark swing occurred late the spark timing would be significantly advanced for a stoichiometric condition, leading to engine knocking. This problem was partially solved by reducing the number of signals recorded by the RCON to a minimum, thus minimising the lag from a user demand to a transient variable change, and from experience developing an accurate 'feel' for the timing of the two signals. It is acknowledged that this is a less than ideal approach to engine control during transient events. However, no other approach was possible and poor transient results were identified and repeated. In a vehicle operating a dilution control strategy, the timing of these control signals would be scheduled by a single controller and thus this problem would be avoided.

## *3.8 Data handling techniques*

Because each test point produced two data files, and a number of test points were required to provide a partial investigation, data handling techniques were developed. These techniques consisted of data structuring and data processing.

### 3.8.1 DATA STRUCTURING

The host system provides information for each measured point by averaging a series of test points over a minute. The RCON does not provide a similar averaging ability, so instead 60 sample points are saved in a file. The host system was set up such that for each test point an RCON file name identifier could be recorded. Additionally the testing engineer made a paper record of each the conditions for a test point and the appropriate RCON File name. An Excel macro was developed to average the RCON data for each operating condition and record the results with the appropriate CP test data.

### 3.8.2 CORRECTION CALCULATIONS

The Excel macro was adapted to perform correction calculations on all the data including atmospheric corrections, in order to develop standardised performance and emissions results. These calculations were developed in accordance with BS:2534[83] and BS:8178[84] The calculation macro also included the Spindt[85] calculations which, by developing an oxygen, carbon and hydrogen balance between inlet and exhaust charges, can determine the air fuel ratio of the charge. This has been shown to be typically accurate to less than 2% [85].

## *3.9 Calibration procedures*

In order to achieve a consistent quality of test results, a test rig maintenance and calibration procedure was implemented. On a daily level the test rig was inspected for leaks and a conditioning test sequence was run to achieve warm steady state conditions. The conditioning cycle was always completed by examination of 2000 rev/min WOT to make sure that within the bounds defined by the atmospheric conditions the engine had consistent performance characteristics. It was found that the host system had very low drift on the cards and transducers; as a result the calibrations of the dynamometer load cell, the pressure transducer channels and the thermocouple channels were only tested on a monthly basis. Again on a monthly basis the spark plugs were checked for deposits. They were subsequently cleaned and if there were any signs of wear they were replaced. After every 80 hours of engine running the oil and oil filter were replaced.

**Table 3-1 Engine specifications. From Heuser et al[79]**

| Parameter Value | Value |
|---|---|
| Configuration | In-line 4 cylinder 16v |
| Capacity | 1.679 L |
| Bore | 80 mm |
| Stroke | 83.5 mm |
| Overall length | 860 mm |
| Overall height | 620 mm |
| Overall width | 580 mm |
| Inlet valve duration | 240° |
| Range of inlet valve opening | 6° ATDC - 34° BTDC |
| Range of Inlet valve closing | 66° ABDC - 26° ABDC |
| Exhaust valve duration | 216° |
| Exhaust valve opening | 30° BBDC |
| Exhaust valve closing | 6° ATDC |
| Inlet valve lift | 7.81 mm |
| Exhaust valve lift | 6.22 mm |
| Valve overlap range | 0 – 40° |
| Peak power (@ 6300 rev/min) | 92 kW |
| Peak torque (@ 4500 rev/min) | 157 Nm |
| Maximum speed | 6875 rev/min |

**Table 3-2 Standard VCT control position lookup table[86]**

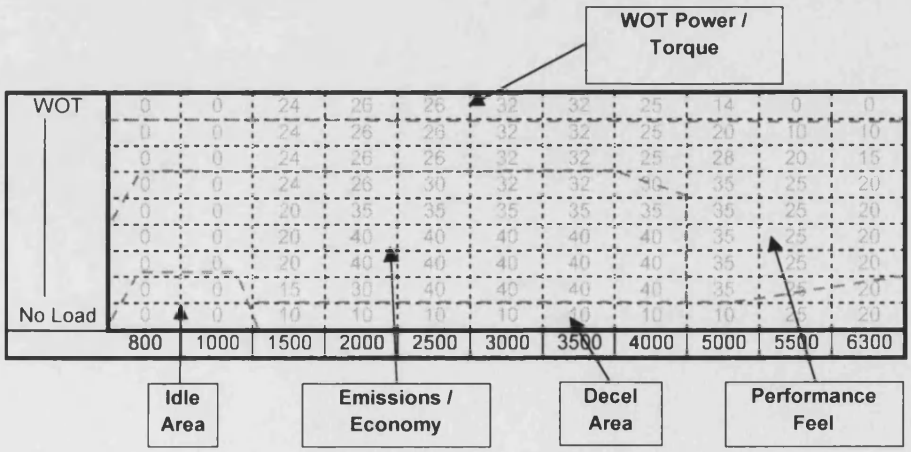

**Table 3-3 Summary of test rig control variables**

| Variable | Controlled by | Range | Frequenc |
|---|---|---|---|
| Throttle position | Electronic throttle unit - host system via UoB +/- 15V box | 0 - 100% | 80 Hz |
| EGR position | Host system PID control loop, providing signal to UOB PWM box | 0- 100% | 40 Hz |
| Engine speed | Heenan & Froode Eddy current dyno host system via PID loop | 0- 7000 rev/min | 80 Hz |
| Engine torque | Heenan & Froode Eddy current dyno host system via PID loop | 0 - 250 Nm | 80 Hz |
| Coolant temperature | Heat exchanger & flow control valve via host system PID loop | 0 - 105 °C | 40 Hz |
| Fuelling rate | RCON engine controller | 0- 2 lambda | 40 Hz |
| Cam overlap | RCON engine controller | 0° - 40° crank | 40 Hz |
| Spark timing | RCON engine controller | + 60° : -60° | 40 Hz |

**Table 3-4 Summary of Response transducers**

| Responses | Measured by |
|---|---|
| Inlet $CO_2$ | AVL CEB gas analyser NDIR |
| Exhaust $CO_2$ | AVL CEB gas analyser NDIR |
| Exhaust CO | AVL CEB gas analyser NDIR |
| Exhaust $NO_x$ | AVL CEB gas analyser PMD |
| Exhaust $O_2$ | AVL CEB gas analyser CLD |
| Exhaust uHC | AVL CEB gas analyser FID |
| Inlet manifold pressure | Trans-Instruments pressure transducer |
| Exhaust manifold pressure | Trans-Instruments pressure transducer |
| Incylinder pressure | Kistler 6117B, AVL charge amplifier, AVL indiskop |
| Inlet manifold temperature post throttle | K-type thermocouple |
| Inlet temperature pre throttle | ECU temperature sensor |
| Exhaust manifold temperature | K-type thermocouple |
| Exhaust port temperature 1-4 | K-type thermocouple |
| Exhaust temperature post catalyst | K-type thermocouple |
| Oil sump temperature | K-type thermocouple |
| Coolant inlet temperature | K-type thermocouple |
| Coolant outlet temperature | K-type thermocouple |
| Fuel Flow | ECU pulse width |
| Airflow 1 | Yokogawa vortex shedding |
| Airflow 2 | Hot wire anemometer |
| Speed 1 | Hall effect sensor 60 tooth wheel dynamometer |
| Speed 2 | Hall effect sensor 38 tooth wheel flywheel |
| Torque | Strain gauge |

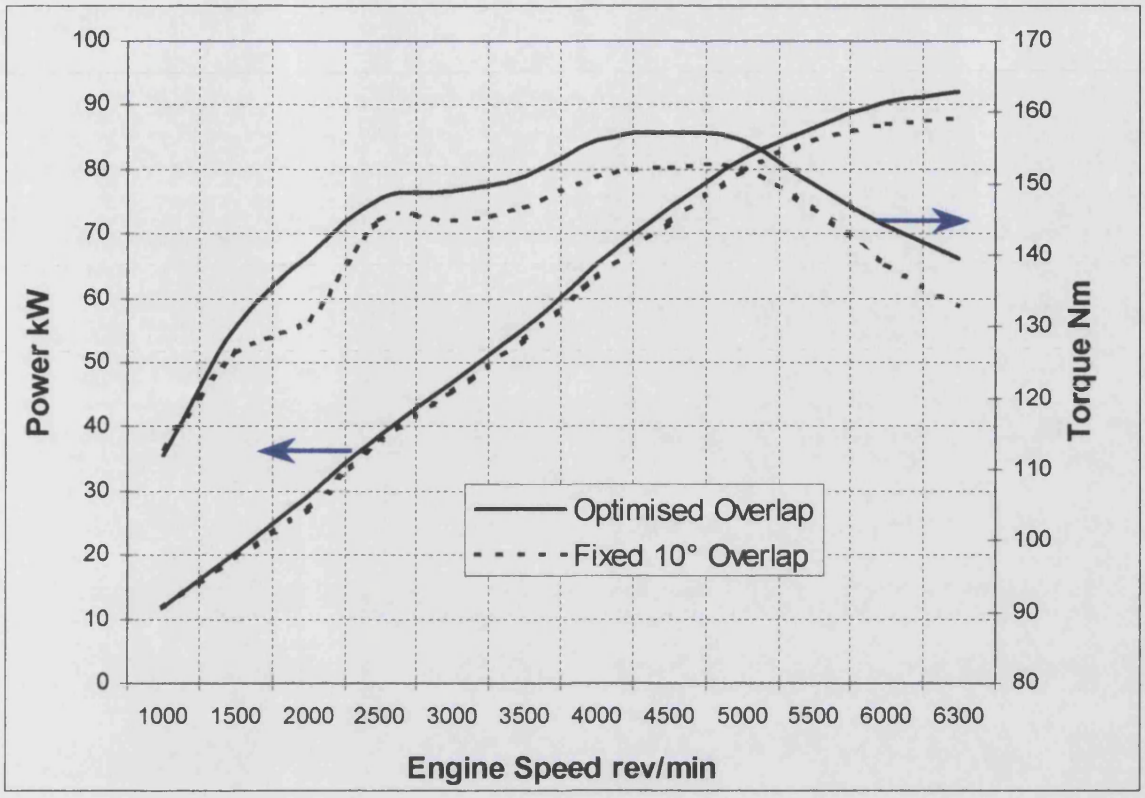


**Figure 3-1 Standard engine torque speed map as supplied Ford[86] Showing the effect of valve timing**

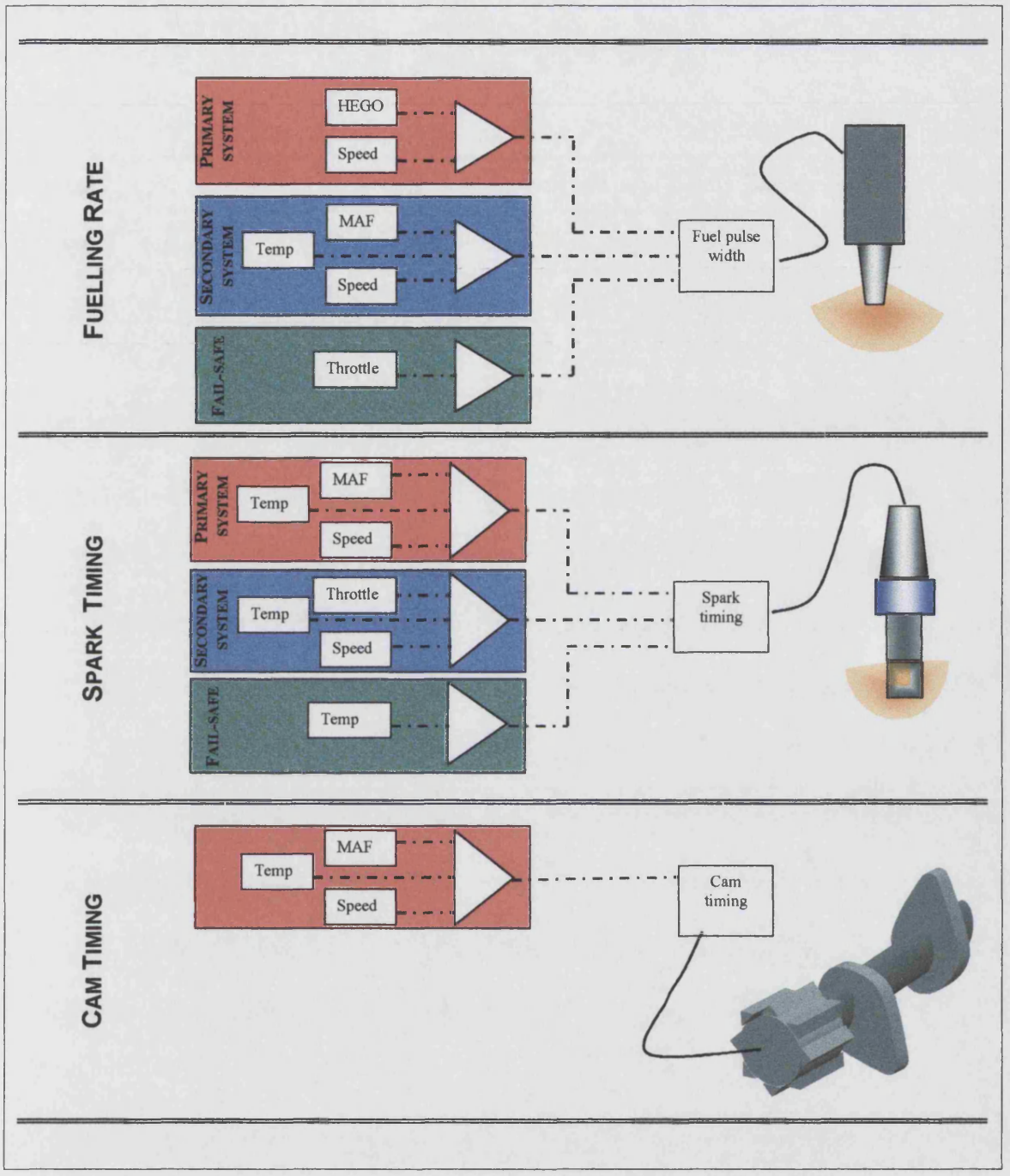


**Figure 3-2 ECU control instrumentation hierarchy for fuelling, spark timing, and cam positioning**

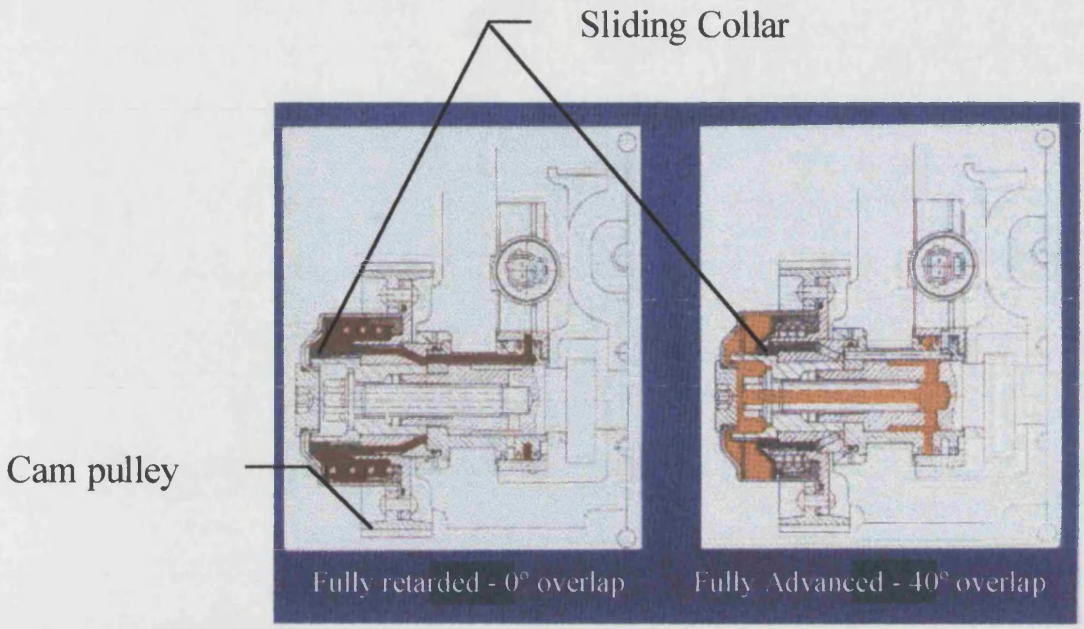


**Figure 3-3 Variable cam timing VCT mechanism[79]**

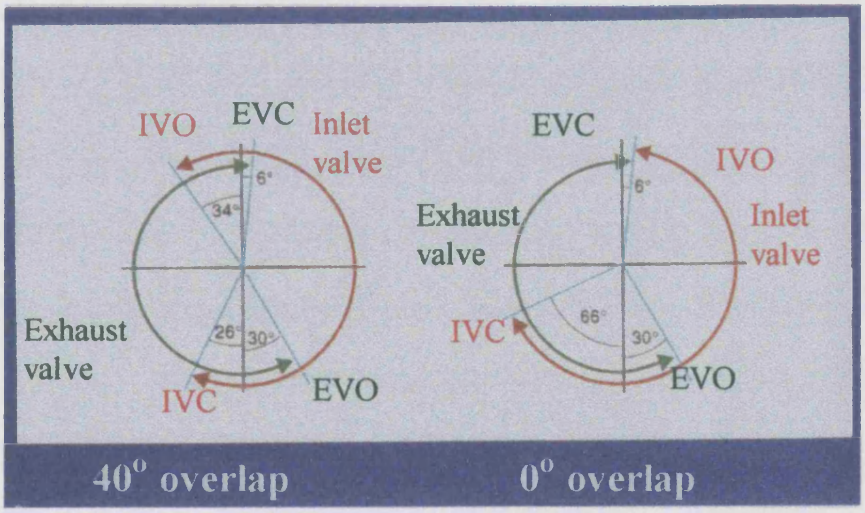


**Figure 3-4 VCT overlap range[79]**

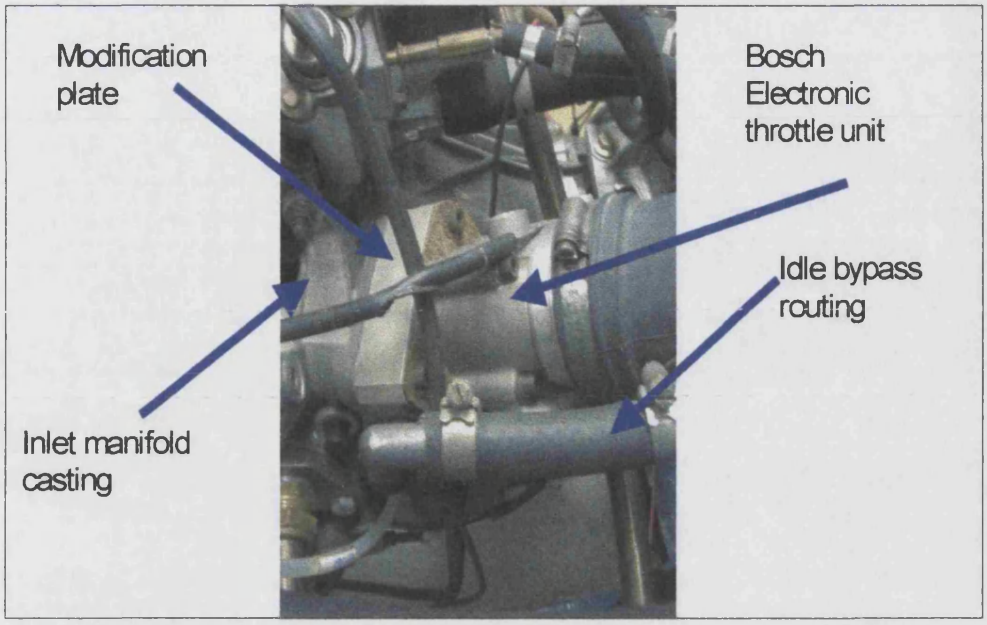


**Figure 3-5 Electronic throttle modification**

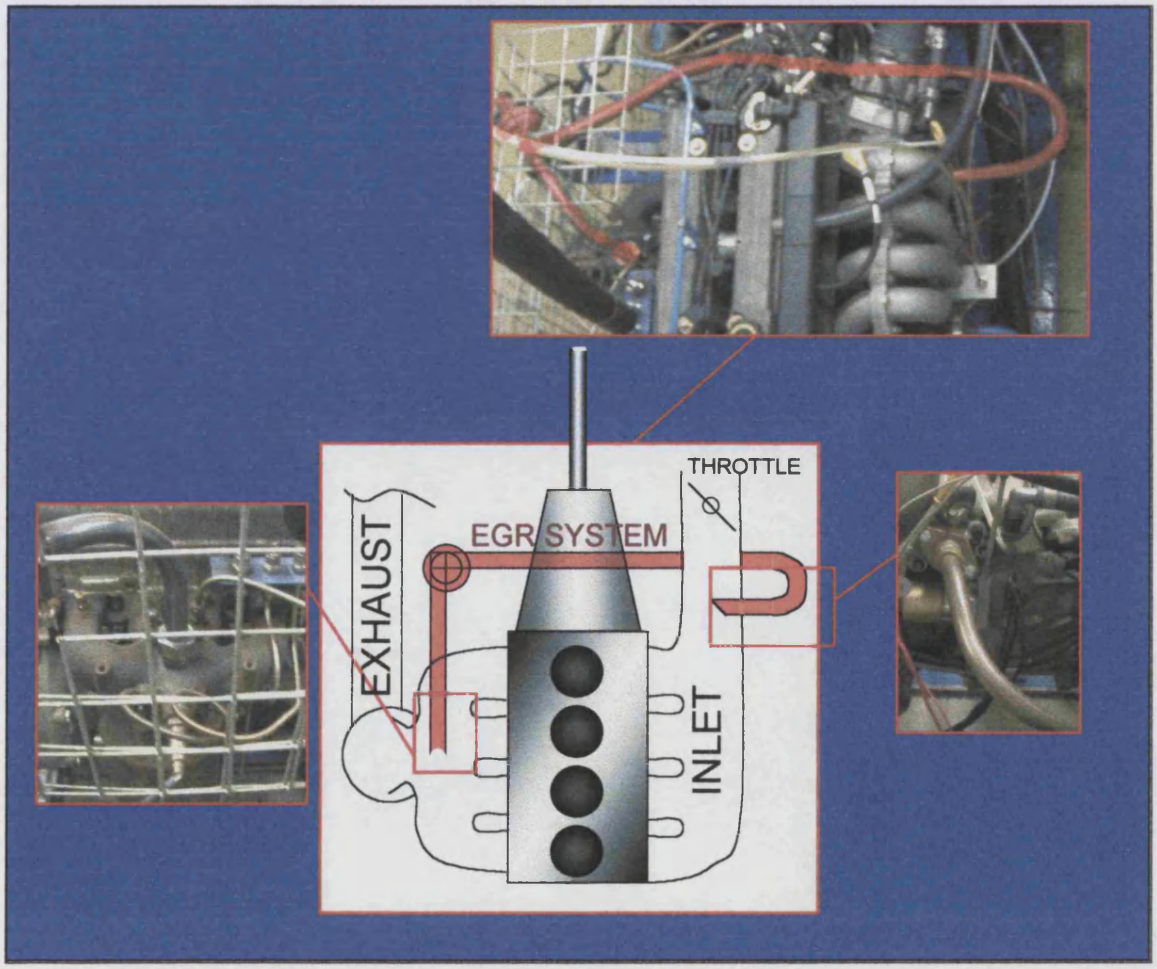


**Figure 3-6 EGR system – showing inlet and exhaust mountings**

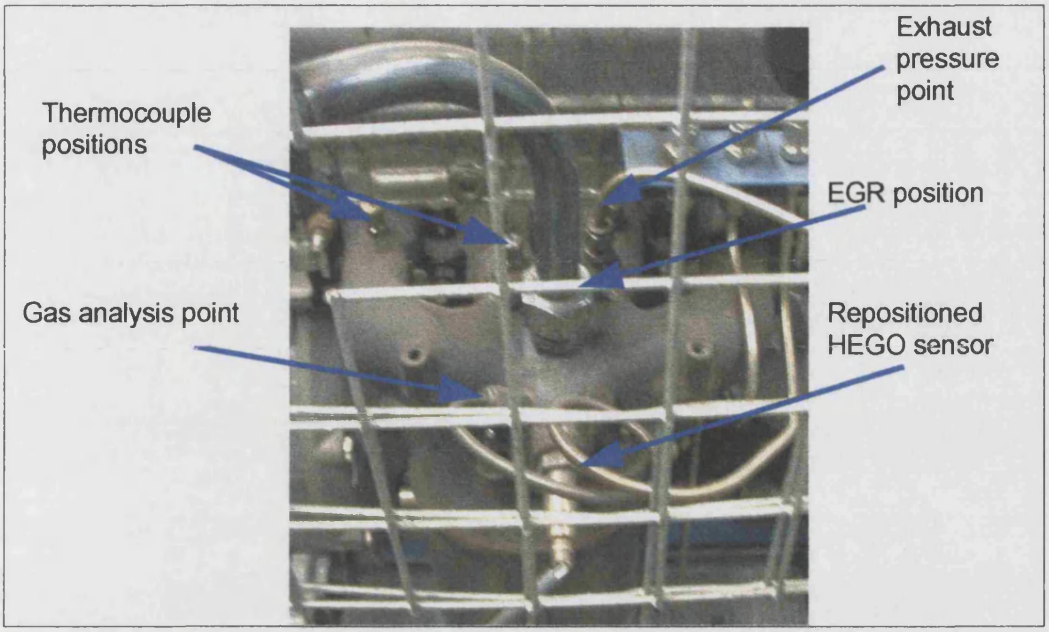


**Figure 3-7 Exhaust manifold - identifying transducer position, details of EGR system and the reposition of the HEGO sensor**

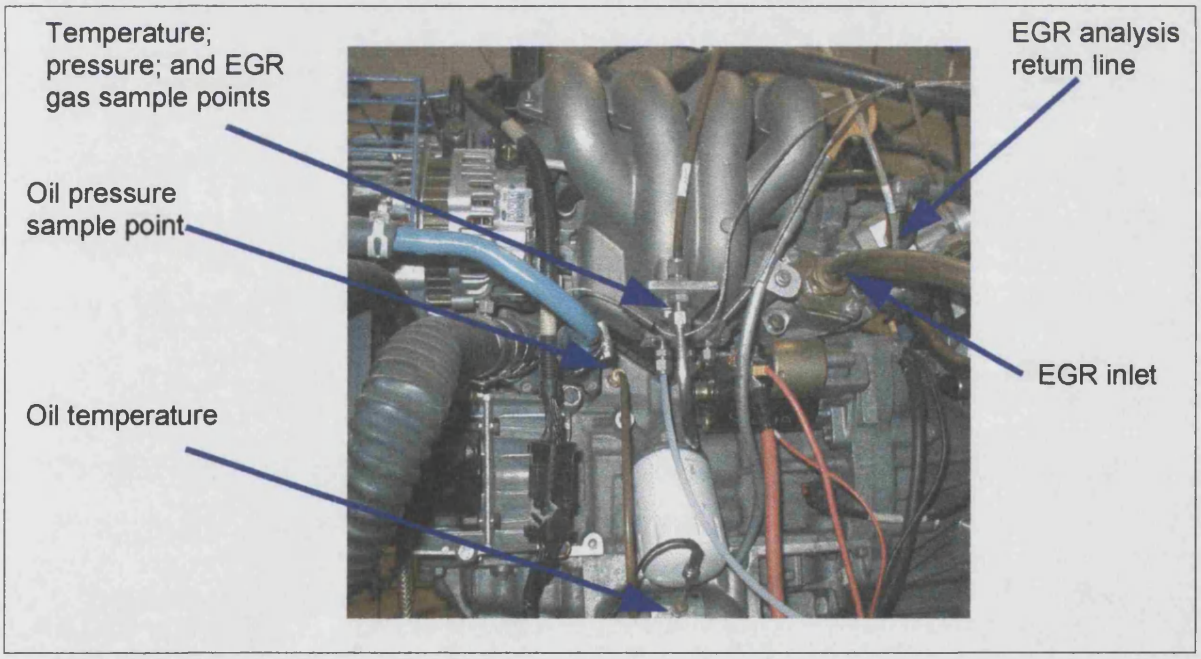


**Figure 3-8 Inlet manifold pressure, temperature and gas sampling points**

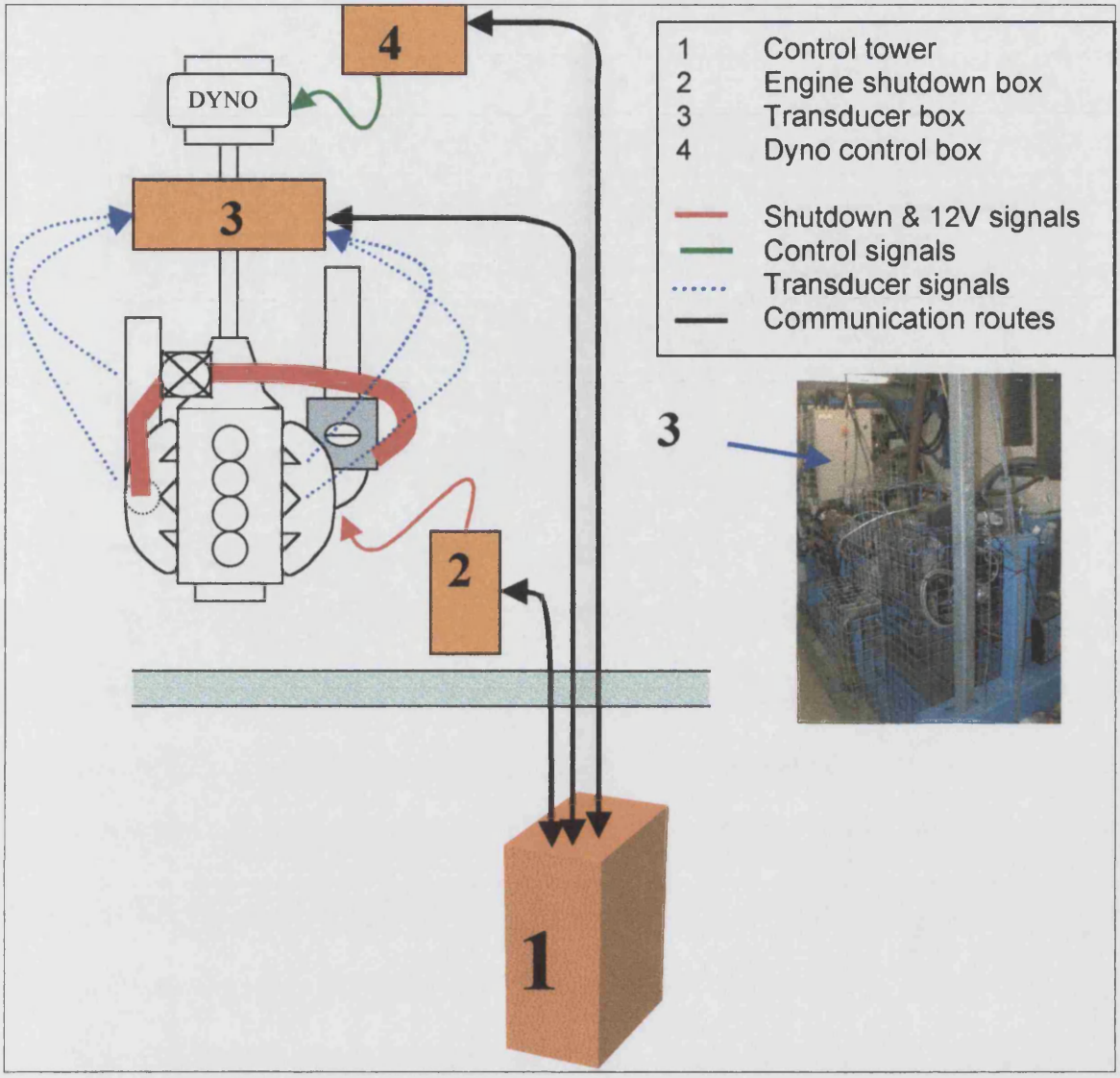


**Figure 3-9 CP host system - physical arrangement**

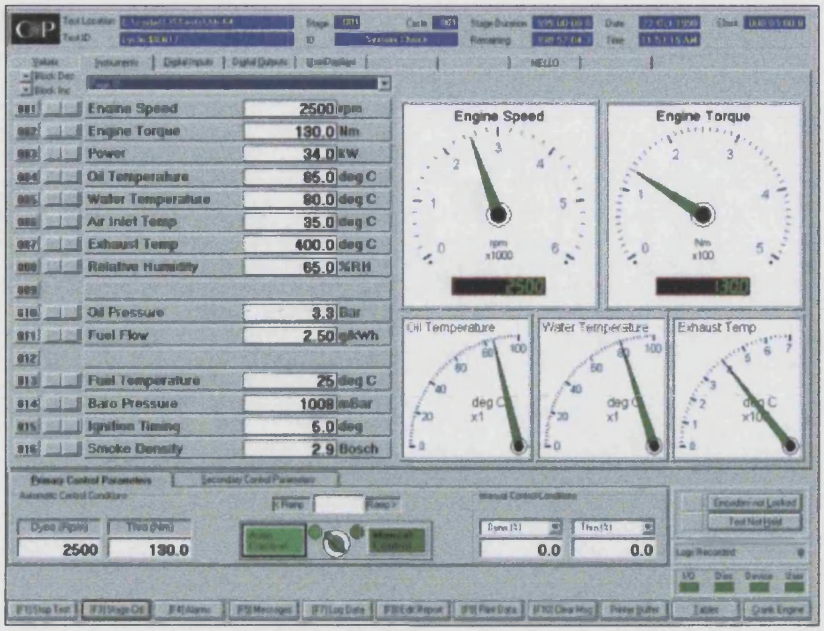


**Figure 3-10 User interface of CP host system**

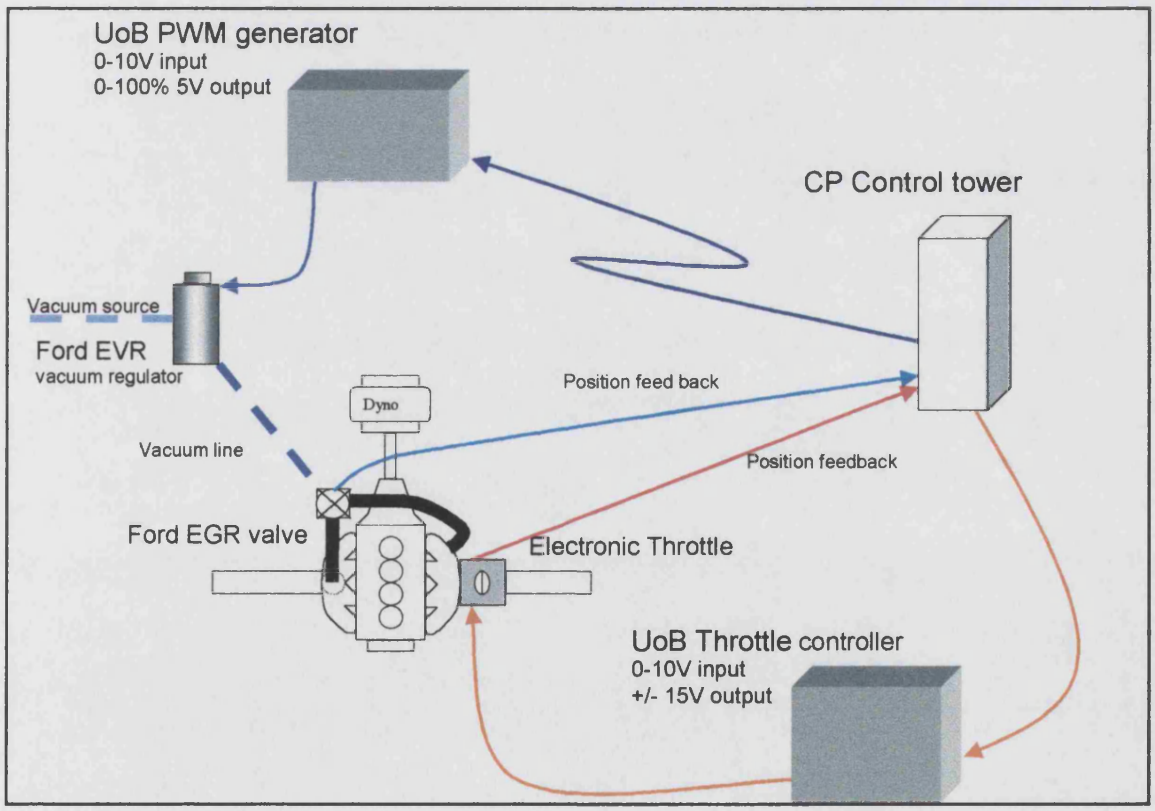


**Figure 3-11 Adaptations to allow host system control of EGR, throttle, position**

# 4 Experimental methodology

In order to establish the viability of dilution torque control it was decided to implement an experimental study. This investigation was designed to establish the effects of charge dilution in steady state operation. The following sections will discuss the testing methodology, which has been selected in order to complete these investigations in a rigorous and efficient manner.

## *4.1 Steady state testing*

During a steady state experiment an operating condition is held for a number of minutes, until the responses of the engine become stable, at which time a test point is recorded. Recently there has been a move toward transient engine testing[87], and inference of steady state conditions from speed ramped investigations[88]. However conventional engine controllers are based upon steady state lookup tables. Therefore using transient engine testing it is difficult to adjust control variables in order to optimise engine responses. Therefore it was decided to conduct the investigation using a conventional steady state procedure.

### 4.1.1 EXPERIMENTAL PROCEDURES

The detail required from an investigation varies depending on the response under investigation and the intended use of the resultant data. In an automotive testing context, investigations are expected to yield large quantities of detailed information. However, the time and testing resource required to generate such levels of information represent an additional delay and cost to the final product. The problem that faces a test engineer is that maximising the quality of information produced by an investigative study mitigates against the requirement to minimise testing effort on the final product.

The engineer has a number of systematic experimental procedures available. Four main approaches are considered here; one variable at a time, approaches based on statistical methods, neural networks and neuro-fuzzy based methods.

### 4.1.2 ONE STEP AT A TIME METHODS

'One step at a time' is a name given to a set of tests where all but one of the variables are kept constant, the remaining variable is systematically varied and the response (the value of the result being examined e.g. BSFC) is recorded. In an industrial situation two

separate methods are used. The perceived importance of the response dictates which method is implemented. If a response is considered important then each variable which directly effects it, will be incremented across its full range, as shown in Figure 4-1. If a response is considered to be of lower importance a less refined testing approach is implemented, this is shown in Figure 4-2. Here the engineer, from experience, proposes a setting for the first variable. The effect of a second variable is investigated until minimum / maximum is found. Freezing the second variable at this condition the first variable is investigated to determine the position of an apparent global optimum condition.

In both cases the selected step increment size is based on the engineer's understanding of the expected response or testing convention. In Figures Figure 4-1 and 4:2 the optimum region is shown in yellow. It is apparent that if the step size is too great the optimum can be missed. Therefore there is pressure to use a small step size, which is in conflict with the desire to minimise testing time and expense.

Thus 'one step at a time' approaches use a relatively large number of experiments to identify a potential optimum and the identified optimum is not necessarily the true global optimum. This, however, is not to suggest that such approaches have no benefits. On the contrary, until recently 'one step at a time' methods were the only approaches that were available to automotive test engineers. As a result there is a reluctance to move to more abstract experimental approaches. The main advantages of one-step at a time approaches are:

- Constant feedback to the test engineer.
  The engineer can identify general trends before all of the testing is complete. In some situations this allows the test engineer to focus the investigation more rapidly. Additionally, due to the discretised nature of the investigation, information becomes available progressively. This is often used to measure the progress of the project.
- Sensitivity to outliers.
  Due to the relatively small significance of individual test points outlying responses (points with error in their measured position) have a limited effect on the quality of the information. It is also easy for a test engineer to identify an outlying response whilst testing; thus the process of re-testing a point is speeded up.
- Tolerance of unsteady operation near to an optimum.
  If an optimum exists close to a region where a response becomes unsteady, then one-step at a time methods are capable of accurately identifying the optimum. This

is not necessarily the case with statistical methods where the accuracy of the model is dependant upon the test points being taken at stable operating conditions.

It is important to note that since each variable is examined separately either of the above approaches can only provide information about single variable effects. It would require a properly structured experimental sequence and statistical analysis to yield information about the effect of changes in multiple variables on a response.

### 4.1.3 STATISTICAL METHODS

These are methods that use statistical approaches to minimise the number of test points required to investigate a problem. The Design of Experiments (DoE) approach, described by Pilley et al[89] is based on the premise that an empirical model of a response may be developed using a curve fit. Test points are selected which enable the coefficients of the response model to be identified. In practice this means that the value of more than one control variable will be changed between experiments. Using the developed model a response surface can be produced which is able to identify optima without the necessity to test at the location of the optimum.

This approach appears to have the characteristics that the test engineer is looking for, namely a minimum number of tests, chosen so that they provide accurate information about the true positions of the global optima. However, there are a number of problems of which the test engineer should be aware:

- Variations of multiple variables
  For test engineers the main problem with statistical methods is that varying more than one variable at a time is intuitively incorrect. Furthermore, using this approach the results are not available until all of the experimentation has been completed. This has effects on the management and managerial perceptions of the project.
- Sensitivity to unsteady operation
  Due to the relatively small number of test points investigated, if a response is measured at a point of unstable operation (e.g. around the knock limit of the engine) or the response is an outlier, it can have a significant effect on the quality of the model produced.
- Reliance on the accuracy of the model assumed.
  The quality of the response model is dependent upon the accuracy of the initial assumption of the form of the system's response. If the model assumed is of too low

an order, important variations can be missed, or if the assumed model is of too high an order, the model may become oscillatory and thus unrepresentative.

Some of the drawbacks of using DoE can be overcome using Bayesian methods [90],[91],[92]. These are methods that refine the application of DoE and require the test engineer to detail his beliefs (based on prior knowledge) and confidence in these beliefs regarding a number of interactions between variables before starting the experiment. Using a DoE approach, an experimental design is systematically developed to test the points that define these relationships. The number of tests and the size of the investigated area are varied depending upon the confidence that the test engineer has in the proposed relationships. Throughout the testing procedure, information derived from the proposed relationship model is replaced by actual test results. Hence the test engineer can monitor the development of the experimental results, which can aid the project management. Additionally since this method requires proposed model relationships, and confidence in these relationships to be stated, an area where results are expected to fall can be defined. Thus any results which fall outside this area can be identified as possible outliers while the experiment is being undertaken.

The author notes that applications of the Bayesian technique to date [91],[92] are still reliant upon the test engineer's perceived order of the response. Although it has not been suggested in the examined literature, the author believes that when fully developed Bayesian methods will have the potential to allow a test sequence to update the order of the assumed model during a testing procedure. An approach based on the examination of systematic variance from the predicted model would identify model order inconsistency. Thus during an experiment the number of tests could be updated to produce a model that better represents the measured response. However, developing Bayesian techniques in this manner is beyond the scope of this work.

### 4.1.4 NEURAL NETWORKS

A third and popular approach [25, 93] for data reduction is the use of neural networks. Neural networks use a series of layers of nodes and connections to develop models of a system. Layers are called typically input, hidden and output, Each node on the first layer is connected to every node on the following layer and so on. The connections from each node apply a weighting function to the influence of that node on the value of each destination node. Using this system, engine control variables (speed, fuelling rate, etc) are

presented to the input nodes and the output nodes are used to represent the engine responses. Test engine data are used to train the neural network such that the weighting for each connection develops the required value for the response. Prediction of a second independent set of data is used to determine the accuracy of the network. These systems have proved very popular because of relative size and prediction speed. Work has been undertaken to integrate the use of neural networks into engine control systems[94]. However large numbers of test points are still required in order to develop the neural network, and the accuracy of a response may vary depending upon the level of engine training undertaken in a particular region. Consequently neural networks are not a very efficient method to reduce engine testing requirements.

### 4.1.5 NEURO-FUZZY METHODS

An approach proposed by Mhller et al[95],[96] allows rapid development of neural network engine representations. It is based on the premise that a complex response (e.g. $BSNO_x$) can be modelled by a number of linear approximations. The number of linear approximations required increases with increasing response complexity and desired information resolution. Mhller et al[96] describe a fuzzy logic process which identifies the number of test points required in separate regions of engine operation in order to develop a characteristic neural network model. The work describes the DoE testing of a small capacity engine. Response complexity was determined from the responses of this engine and used to develop test system with a reduced number of test points for subsequent use as a neural network response map for a larger capacity test engine.

There are a number of drawbacks in the use neuro-fuzzy methods to characterise a test engine; principally that it is not suitable for a one off test program, since this approach requires a detailed test sequence to be conducted before the reduction in test point number can be realised. Additionally, since many responses have very different characteristics, it is necessary to develop a set of test points for each model. If a large number of responses are to be investigated at a reasonable level of detail, then it is possible that this approach may require more experimental points than a DoE approach. This approach has a similar sensitivity to outliers and unsteady operation to that of a DoE approach. However, outliers can be identified more accurately by comparison of test data with the results of the original mapping process.

### 4.1.6 SELECTED EXPERIMENTAL METHODOLOGY

Since the aim of this project is a one-off investigation over the full working range of the test engine, the ideal solution will provide the greatest detail of information with the minimum number of experiments. A statistical method is best suited to this problem. It is noted that this is not the case for all testing situations. For a situation where a rapid optimum is required and there is a significant amount of engineering experience, or where it may be difficult to get steady operation from the test apparatus, one variable at a time methods are the most suitable. Alternatively for situations where a database of information is to be developed, and similar investigations are to be carried out periodically, neuro-fuzzy methods would be particularly suitable.

For this investigation a conventional DoE approach has been selected in preference to the adapted Bayesian technique. This is because there is very little information available on which to base the prediction of the proposed response relationships. As a result it is possible that a Bayesian solution may miss important trends because it is tailored to an inappropriate model.

## *4.2 Previous applications of DoE*

This section will introduce the use of Design of Experiments, including the historical background to the use of DoE and the benefits and difficulties that have been experienced.

### 4.2.1 HISTORY OF DESIGN OF EXPERIMENTS

Design of Experiments was first used and developed for yield optimisation by the agricultural industry in the 1930s. It is particularly suitable to this application because of the long test duration and the constant experimental area, albeit within which there are many variables e.g. soil composition.

The approach was developed in the chemical industry, and was then adopted by manufacturing industry as an aid to quality control. Taguchi provided work that combines some of the greatest developments in this area. The use of the approach proposed by Taguchi is has been a major factor in the improvement in quality of the automotive product. It should be noted that the predominant use of Bayesian techniques (Section 4.1.3) thus far has also been in the field of improving product quality[97].

More recently DoE has been used to develop reduced test point sequences to allow rapid identification of optimal component designs[106].

### 4.2.2 APPLICATIONS IN AUTOMOTIVE TESTING

Pilley et al[89], provide good introductions to the application and use of DoE in the automotive area, while Stevens et al[98] provides a comparative study of the use of neural networks and a DoE approach. This latter work also presents a detailed introduction to DoE, correctly stating that DoE is only effective when examining the influence of independent variables. However, there is a flaw in the case study of DoE presented in this work[98]; the study considers the effects of engine speed, manifold pressure, air fuel ratio, and spark timing on combustion stability ($COV_{imep}$). Clearly manifold pressure is not an independent variable in this test sequence, though it is unlikely that this oversight will effect the test results significantly. However, as an application example it is misleading.

Surprisingly there are very few references that give details regarding one of the key benefits of DoE, the reduction in testing requirements Edwards et al[99], details the use of DoE to develop an MBT spark timing map. Using traditional methods this would require the measurement of 180 test points. A sophisticated DoE experimental sequence was developed which resulted in 56 points being tested to perform the same examination. It can be seen that this represents a significant reduction in the number of tests. However, it is not clear that this example was fully successful, since at some points the timing in the modelled response were over advanced; also the process had a general smoothing effect on the test data, which resulted in optimum conditions being missed.

Stevens et al[98] presented work which used 27 test points to investigate the effects of a 4 control variable problem. Each variable was considered to have a second order response. This is compared to 100 test points used to characterise a similar problem using neural networks. Yan et al[100] discuss the use of statistical experimental methods to identify the engine component configuration required to achieve minimum specific emissions. The experiment examined the effect of six variables on specific emissions over a legislative test cycle. The authors considered that only individual effects were of interest and reduced the test sequence to 18 test points.

Ahlinder et al[101] discuss the use of DoE to investigate rapidly the main variables of a new direct injection gasoline engine. However, this report does not give details of the experimental efficiency improvements and the information regarding the experimental

procedure and the results obtained is limited. Thus it is prudent only to consider this reference as an example of the industrial acceptance of these procedures.

A second key benefit of DoE is the ability to identify optima that were previously not investigated. Edwards et al[102] provides an example of such an investigation. The objective of the work was to optimise the performance of a single cylinder, common rail diesel engine. Six responses were investigated over a range of eight control variables. Subsequent optimisation was achieved through the use of genetic algorithms. Extrapolation of the results for comparison with multi-cylinder engines suggests that, applying the parameter and hardware settings as optimised, this engine would have 'best in class' emissions performance. Ahlinder et al[101], and Lee et al[103] also present work which identifies the position of optimal control variables within a response model developed through a DoE approach. However these studies do not provide an indication of the optimal solution determined before the DoE and subsequent optimisation process.

The third key benefit of the use of DoE is the improvement in the quality of information produced by the experiments, principally that about multi-variable interactions. However, again there are few papers that identify this as a benefit of DoE. Seabrooke[104] produces a large number of plots demonstrating the interactions between many of the variables under investigation, but fails to illustrate that this improvement in information has any perceivable gain. The improvement of information on variable interactions is generally demonstrated by a response surface plot. It is proposed that this benefit, although providing information regarding the intricacies of a problem, is implemented so subtly that the engineer is not aware of the specific cause of the improvement, and this accounts for the lack of references available to define this benefit.

A number of problems have been identified with the use of Design of Experiments. The first is most ably demonstrated by the spark timing example described by Edwards et al[99]. The DoE solution, although producing the correct general form of the solution, failed to identify that the spark timing is retarded at high speeds. Edwards et al[99] implemented stochastic methods, i.e. localised fitting of data through the use of flexible surfaces, to improve the accuracy of the model. However these processes require significantly more experimental points and the characterising equations are more complex than Taylor's series approximations (see 4.3.2). This greater complexity will affect optimisation of these models. Additionally, although the results fit more accurately, the model is still unable to predict the exact position of some of the optima. The inability to predict accurately the

position of optima is due to the natural smoothing effect produced when a reduced number of experiments are used to develop a model for an entire response characteristic.

The inability to predict accurately the position of an optimum using DoE presents a significant limitation to its application. It suggests that it is not suitable to be used as a development tool for final vehicle calibrations. It should be noted, however, that spark timing is the most difficult variable to accurately model, and that this process applied to other variables (e.g. fuelling rate, EGR rate) would produce a model that is very much closer to the ideal settings.

Another difficulty in the use of DoE is the quality of the derived models. Pilley et al[89] experienced a problem with the model derived for BSHC emissions. It was difficult to produce a good data fit due to the low sample levels and small variations relative to the sample 'noise'. The paper gives no details of the apparatus used to measure the value of BSHC. Similar difficulties were reported by Houghton[105] using a DoE approach, and Brace[25] using neural network models.

Edwards et al[99] established that poor communication between experimental engineers and statisticians affected the initial implementation of the use of DoE. He also points out that the nature of DoE provides a poor basis for project management, since the quality of a test sequence cannot be established until all of the testing has been completed.

A further problem associated with the use of DoE is the representation of the quantity of information derived from the study. Since a problem can have more than 3 variables, the design space can have more than 3 dimensions, so it is not possible to graphically represent all of the information in one plot. The work of Seabrooke[104] demonstrates this point; although he considers the experimentation in detail, the presentation of the results is unclear. Pilley et al[89] overcomes this problem by only demonstrating a small fraction of the results achieved. In later work Seabrooke[106] demonstrates the graphical approach of a software package which has been developed at Cosworth. This produces a response surface based on the values of the input variables. The value of these variables can be varied and the response surface is re-plotted as a result. This represents a considerable improvement, however this does not translate very readily to paper.

Recently there has been little work which develops the use of DoE methods. Instead work has tended to concentrate on the integration of DoE within an automated experimental

facility [107],[108]. DoE has started to become the major experimental practice. This surprises the author since a number of implementation issues remain unclear.

## *4.3 Theory of Design of Experiments*

This section will introduce some of the more detailed aspects of Design of Experiments. The sources for this section are Bartee[109], Umetri[110] and Atkinson & Donev[111]. Umetri[110] has been written to complement a software package that Umetrics has developed; as a result this reference only examines problems with relatively simple response characteristics. However, the examples provided give a good introduction to practical application of the theory. Atkinson & Donev[111] provides a deeper statistical description of the area; this can prove abstract in places.

### 4.3.1 DESIGN SPACE

The design space is one of the fundamental concepts in Design of Experiments. This is the area over which control variables are to range during an investigation. The boundaries for this space can be physical (e.g. limiting torque curve) or they may be limited by the interest of the study (e.g. only EGR levels above 20% and below 40%).

For a two variable problem, where the boundary of both variables is valid throughout the investigation, the design space is termed regular and has a rectangular form (Figure 4-3). If the boundaries are not valid throughout the investigation (e.g. the maximum EGR tolerance of an engine reduces as engine speed increases) the design space is termed irregular and has a form that is defined by the physical limits (Figure 4-4). For a 3 variable problem the design space forms a cube, referred in much of the literature as a Latin hyper-cube. Figure 4-5 demonstrates this for the control variables EGR, valve overlap and spark timing.

Each variable in a problem is an axis of the design space. Therefore, in an investigation involving 5 variables there are five dimensions to the design space. Hence, with greater numbers of investigated variables, visualisation of the design space becomes increasingly difficult.

As described by Stevens et al[98], and Pilley et al[89] it is critical that the control variables are independent throughout the design space. For example in a study of the effect of EGR percentage on $BSNO_x$ emissions across an entire throttle range, the EGR percentage in

the inlet is a not an independent variable, since it is a function of throttle position and EGR valve demand. The use of non-independent variables will result in poor and misleading response models

### 4.3.2 REGRESSION MODELLING

The other fundamental concept in Design of Experiments is the regression fitting of data to a mathematical model. Generally a Taylor's series approximation is used as the basis of the mathematical model. The data are fitted to the model using a least squares regression approach. Equation 4.1 is a representation of Taylor's series.

$$f(x) = f(x_o) + f'(x_o)(x - x_o) + \frac{f''(x_o)}{2!}(x - x_o)^2 + \ldots + \frac{f^n(n)(x_o)}{n!}(x - x_o)^n + \ldots \quad (4.1)$$

Where:

| | |
|---|---|
| $f(x_o)$ | is the constant coefficient - zero order term |
| $f'(x_o)(x - x_o)$ | is the 1st order term |
| $\frac{f''(x_o)}{2!}(x - x_o)^2$ | is the 2nd order term |
| $\frac{f^n(n)(x_o)}{n!}(x - x_o)^n$ | is the nth order term |

### 4.3.3 IDEAL FULL FACTORIAL APPROACH

To fully characterise the responses in a design space, investigations would be carried out at every available test point. Therefore the number of tests would be set by the resolution of the instruments. Using the information acquired, a regression fit will determine the coefficients of a mathematical representation.

Should this approach be applied it would yield information that would allow all of the factors in the Taylor's series approximation to be determined. The level of information that could potentially be developed is limited only by the resolution of the test apparatus. However it is apparent that to achieve this level of detail it is necessary to perform a large number of experiments. Since many of the responses that are modelled in this way have relatively simple (low order) forms, this approach provides more information than is appropriate for their subsequent investigation. In addition to increasing testing time and cost, the use of models that are unnecessarily complex will slow down any optimisation regimes applied to the problem.

### 4.3.4 FRACTIONAL FACTORIAL EXPERIMENTAL DESIGN

It is apparent that the full factorial method described is not a practically applicable experimental method. A fractional factorial experimental design represents a more appropriate experimental design model. It uses fewer experimental points to produce a reduced form of the Taylor's series expansion.

The number of tests that are required may be reduced by considering only the factors that are believed to have a significant effect on the response. To achieve this, it is necessary to make a prediction regarding the shape of the perceived response.

Typically responses are considered to be adequetly modelled by second order polynomial models. As an example Equation 4.2 represents a second order Taylor series model. Here using the example of the effect that EGR and valve overlap have upon $BSNO_x$.

$$BSNOx = \beta_o + \beta_1 EGR + \beta_2 CAM + \beta_3 EGR^2 + \beta_4 CAM^2 + \beta_5 (EGR \times CAM) + \xi \quad (4.2)$$

Where

| | |
|---|---|
| EGR | is the instantaneous value of EGR rate |
| CAM | is the instantaneous valve overlap position |
| $\beta_{0\text{-}5}$ | is are the model coefficients as derived from regression fitting |
| $\xi$ | an error term, which includes the accuracy of experimental apparatus |

The minimum number of experimental points required to fully characterise a single variable effect in a second order model is three. Thus to fully characterise a two variable design space nine test points are required, as shown in Figure 4-3.

It should be noted that the test points are positioned at the extreme limits of the design space. On the Figure 4-5 the points which are termed axial and factorial are labelled. The axial test points represent the effect of varying one factor only (i.e. βEGR and βCAM). The combination of the centre and axial points allow the quadratic function to be assessed ($\beta EGR^2$ and $\beta CAM^2$), the corner or factorial points allow the interaction term to be estimated (βEGRCAM).

### 4.3.5 TYPES OF FRACTIONAL FACTORIAL DESIGNS

In a two variable problem the increase in testing efficiency achieved by applying a DoE approach may be relatively small. However as the number of control variables increases, so does the testing efficiency.

Examining three variables to a second order form in a fractional factorial manner, would require 27 test points (Figure 4-6a). As the numbers of variables increase the number of tests points increases by a factor of 3 per additional variable. Thus even a full second order fractional factorial design can require a significant number of test points. By reducing the number of axial points it is possible to reduce the number of test points required to investigate a design space. A reduction in the number of axial test points can be performed without significant effect to the accuracy of the investigation since these points can be inferred by the response from the factorial points. A central composite face centred (CCF) cube is the term used to describe a reduced fractional factorial design of this type. Using a CCF design a similar three control variable, second order problem can be fully characterised using just 15 tests (Figure 4-6b).

If a design space is physically limited at its corner points, although it is possible to remove one or two test points from a CCF design and still develop a response model, it can have significant effect on the accuracy of the model. One solution to the problem of a non-rectangular search space is to use a (CCC) central composite circumscribed design. This design uses star points to extend the area covered by a fractional factorial design (Figure 4-6c). However due to the use of star points, model accuracy at the extremes of the design space can be limited.

Generally the test points are positioned at the corners of the design space as shown in Figure 4-6b. However, if a test engineer believes that the most significant test points occur at the midpoint of a variable's range, then a Box Brehmen design can be applied to the problem (Figure 4-6d).

From the studies described in the literature, which have discussed the use of DoE, a range of designs have been selected and promoted as the optimum for engine applications. Yan et al[100] used a full fractional factorial solution, Pilley et al[89] proposed the use of a centred central composite design matching the test sequence to minimise testing around engine limitations. Stevens et al[98] promoted the use of a Box Brehmen approach, suggesting that this was the optimal arrangement for automotive applications

because of the reduced number of test points where all control variables are at extreme positions. Although this approach minimises the risk of an operating point producing unsteady results, it also seriously degrades the quality of the response model since no combined extreme conditions are tested. Seabrooke[104] investigated a test engine across a range of operating speeds, throttle conditions, EGR rates, fuelling conditions, with inlet and exhaust valve timing to achieve this the study used numerous CCC designs throughout the engine operating range. The justification given for this selection was that the CCC designs offer the potential to characterise third order models from a minimal number of test points. However, it is felt that the use of many discrete DoE designs across a range of speed and throttle conditions represents a compromised application of DoE to engine testing.

The reduced fractional factorial designs described represent a significant reduction to the number of test points required to investigate a problem. This improvement is increased as the number of variables approaches six. However for problems with greater than six variables, engineers can require a testing approach that use fewer tests still. Additionally, the use of fractional factorial designs is fairly limited when presented with an irregular design space.

### 4.3.6 D-OPTIMAL DESIGNS

In an attempt to reduce the number of necessary tests whilst still maintaining high design resolutions (defined in Section 4.4) D-optimal designs have been developed.

D-optimal designs are generated by considering Taylor's series in matrix form, Equation 4.3.

$$y = \beta X + \xi \qquad (4.3)$$

Where y is the response

$\beta$ is the vector of the of coefficients $\beta_0$ - $\beta_n$

X is the matrix of the variables (e.g. EGR, CAM, EGRCAM)

X' is the transpose of the X matrix

$\xi$ is the system error

When considered in terms of β

$$\beta = (X'X)^{-1}X'y \qquad (4.4)$$

Therefore with a limited amount of test resource (as defined by the test engineer), the set of data points that minimises the value of the determinant of $(X'X)^{-1}$ will provide the best representation of the model. An alternative definition is that a D-optimal experimental design will produce the greatest span of a design space for a given number of test points.

The variable matrix 'X' can be defined to represent an irregular design space. Therefore a major benefit to this investigation is the ability to examine irregular design spaces. Figure 4-4 demonstrates the approach that a D-optimal design takes to tackle the problem of an irregular design space.

Pilley et al[89] and Edwards et al[99] used D-optimal experimental design solutions to great effect, reducing a 180 test point design to a 52 test point sequence. Pilley et al[89] and Edwards et al[99] also used D-optimal experimental design in the optimisation of a common rail fuel system. The automated application of DoE by Stuhler et al[107] have also implemented a D-optimal approach to selection of the most suitable experimental design.

## *4.4 Statistical tests for DoE*

Since the use of DoE reduces the number of test points undertaken, establishing confidence in these points is important. Several tests can be applied which examine the validity of the recorded data and the developed model. Residual and correlation tests examine both data accuracy and the suitability of the model. Additionally, replicate checks are made which identify the significance of systematic errors.

### 4.4.1 DESIGN RESOLUTION AND COMPOUNDING

If a problem is investigated using fewer tests than the minimum required for a full fractional factorial design, the validity of the model is reduced. The effects of multiple variable interactions are combined with the effects of single variables during the data regression process. This combination of effects is called compounding. The level of compounding experienced by a particular experimental design may be expressed in terms of the 'design resolution'.

### 4.4.2 RESIDUAL TESTS

It has been noted in Section 4.1.3 that outliers can have a significant influence on the model that is produced by DoE. Figure 4-7 demonstrates the effects that outlying test points can have on a model. The residual is the difference between the modelled and measured position of a test point, and can be used to identify whether a test point requires further investigation.

Along with the model design resolution, examination of residuals can provide a second test of model suitability. Residual plots can be used to identify if the chosen model order is suitable to describe the investigated response. If the test points have an even, but random variation around the predicted values the model is of an appropriate order and represents a good fit (Figure 4-8). However if the test points can be seen to form a curve relative to the modelled response then the order of the model is not appropriate (Figure 4-9).

### 4.4.3 CORRELATION TESTS

Once an experimental design has been run and a response model has been generated it is necessary to examine the quality of the model. The correlation ($R^2$) test examines the amount a point varies from the model. This test investigates the total variance of the residual between predicted and the measured. Equation 4.6 shows the form of the equation used to assess this factor.

$$R^2 = 1 - \frac{\sum_{i=1}^{n}(y_i - \hat{y}_i)^2}{\sum_{i=1}^{n}(y_i - \bar{y}_i)^2} \qquad (4.6)$$

Where :

$R^2$ is the correlation coefficient (1 is a perfect fit, and 0 no fit)

$y_i$ is the measured value at $x_i$.

$\hat{y}_i$ is the estimated response at $x_i$.

$\bar{y}_i$ is the mean response value of $y$

I is the test point under investigation

The range of the $R^2$ can vary between 0 (no fit) and 1 (perfect fit). If the $R^2$ value is low this can indicate that an individual point has a highly weighted effect on the model and should be checked, or that the selected model is not correct.

The $R^2$ test is performed for each response being investigated. Umetri[110] suggests that a model which has an $R^2$ value of greater than 0.7 is an indication of a good model.

### 4.4.4 REPLICATE POINTS & RANDOMNESS

An assessment of the systematic variations within the test apparatus is established by performing replicate point investigations. These are test points where multiple readings are taken progressively throughout the investigation. Replicate points are used to assess the error term in the Taylor's series approximation.

In an attempt to reduce the effects of systematic test rig variations (e.g. component wear) on the results generated, randomness is incorporated into the run order. For example, a high speed run may be followed by a low speed investigation. This can have important repercussions on the overall experimental duration if engine components have to be changed.

## *4.5 Application of DoE to gasoline engine modelling*

As discussed in Section 4.2, the majority of reported applications of DoE have focused on small test regions where second order models can represent the system response accurately. However very few studies have used DoE over large design spaces incorporating wide ranges of engine operation. This section investigates the form of the engine responses of interest over the full operating region. It concludes by establishing what order models are required to develop an accurate representation of the response.

### 4.5.1 INDEPENDENT CONTROL VARIABLES

As discussed earlier (Section 4.3), critical to the effective use of DoE is the examination of independent variables. In this investigation the selection of certain independent variables is clear i.e. speed, lambda ratio and valve overlap, but other independent variables are less apparent. Ideally the remaining control variables would be engine torque load, percentage EGR and total spark timing. This is the approach selected by Seabrooke[104]. However engine load and percentage EGR are dependent variables. Since Seabrooke[104] performed investigations over relatively small test regions it was possible to use the throttle position to regulate engine load. However this approach is not acceptable for the development of a larger engine model. As discussed, Stevens et al[98] used inlet manifold pressure as a control variable. This avoided the difficulty of considering engine torque as a dependent variable over the range of operation investigated. However, with the use of

an external EGR system, manifold pressure becomes a dependent variable. It was chosen here to use throttle position and EGR valve demand as the independent variables.

The selection of the independent variable for spark timing is also dependent upon the application. A total spark timing measure could be used since this is an independent variable. Stevens et al[98] developed a secondary measure of spark timing which was factored by manifold depression and engine speed. This new spark measure was developed to avoid the difficulties faced with finding MBT spark timing. In the current work regression models developed using total spark timing and MBT spark timing were compared. It was found that total spark timing provided marginally better representations. However the application of the resultant engine model must be considered. It is very unlikely that an end user will know the total spark timing required to provide MBT for a specific diluted mixture. Additionally the use of total spark timing would require a very complex design space to ensure that detonation is avoided. Therefore a spark timing measure relative to MBT was selected as the appropriate independent variable.

### 4.5.2 MATHEMATICAL FORMS WHICH REPRESENT THE KEY ENGINE RESPONSES

The engine responses which are of principal importance to this investigation are fuel consumption, output torque, specific emissions ($NO_x$, uHC, $CO_2$, CO, $O_2$), exhaust temperature and induced EGR flow. The majority of previous work suggest that second order models are suitable to represent all engine responses. However these studies have centred upon the application of DoE to small design spaces. Edwards et al[102] presented a case study where a ninth order polynomial was required to model a spark timing map across a range of torque and speed conditions. Hence it is clear that over large design spaces engine responses do not necessarily have a second order form.

In order to identify the general form of the responses, a baseline testing program was undertaken. This program consisted of a series of classical 'one variable at a time' designed experiments used to determine the general form of the engine's responses.

A demonstrates the engine's torque response to perturbations in throttle position. As the throttle opens the principal responses react rapidly until roughly 30% throttle is achieved. The responses to subsequent throttle opening are small. These response characteristics can be justified by considering the induction area developed as a result of each degree of opening by the throttle, and the mass airflow required at the examined engine speed. Also shown in this figure are second, fourth and fifth order models fitted to the torque response.

These models have been included to demonstrate that over the throttle response region a second order model would be far from accurate. Furthermore, to fully represent the torque response the minimum of a fifth order model is required.

Similar procedures have been used to characterise the form of the other responses. The order of the model required to accurately represent the responses are presented in Table 4-1. A more detailed examination of the principal responses to perturbations in the major control variables can be found in Section 5.3.

From Table 4-1 it can be seen that the majority of responses can be modelled accurately by second order Taylor's series models. However, representations of responses to throttle and speed variation require models of fifth and ninth orders respectively.

Due to the complexity of the problem little can be done to reduce the effect of oscillations on a ninth order model. Instead it has been decided to develop individual models for a number of discrete operating speeds.

### 4.5.3 A NOVEL METHOD TO IMPROVE THE ACCURACY OF HIGH ORDER REGRESSION MODELS

As discussed in Section 4.5.2 the difficulty in using high orders in data fitting is that the subsequent model has a tendency to introduce oscillations which were not evident within the original signal. These oscillations can be caused by insufficient quantities of fitting data and minor errors in the recorded signal. Figure 4-11 demonstrates the effect that reducing the number of test points and introducing a minor error into the experimental readings has upon the fifth order model. The data points in blue circles have been used to fit the response model, and the point marked with a blue asterisk has been subjected to a 5% reading error. It can be seen, that the fifth order model produced as a result of the fitting process passes through all of the reduced data test points. However, in the range 40 - 100% throttle, the model is subject to an oscillation that is not evident within the measured data. Using all of the available data to fit the model would remove this oscillation (solid blue line). However increasing the number of test points required tends to compromise the gains in testing efficiency of a DoE experimental solution.

The oscillatory nature of fifth order models fitted from reduced data sets can be very detrimental in the accuracy of subsequent applications of the model. If the model is used, to identify global ideal solutions, such oscillations will mislead the optimisation algorithms.

Algorithms will identify the local maxima and minima as real characteristics and converge to these solutions.

This thesis will propose another approach to developing sophisticated models using reduced data sets that will not be subject to modelling oscillation. The proposed experimental procedure is based on the premise that, over small operating regions, second order models provide accurate representations of test results. Figure 4-12 shows the data used to demonstrate the oscillatory nature of the fifth order curve. Here two-second order curves have been used to represent the data. The choice regarding the regions to be covered by each of the models was determined primarily by the shape of the data. It is obvious that the high rate of change in response characteristic of the low throttle angle region is quite separate from the small rate of change response evident in the high throttle angle region. It is quite apparent that within the regions for which each model is valid there is a very good model fit; furthermore because these models are low order there is no tendency to develop unrepresentative oscillations.

Since the two models do not have a common start / end point it is necessary to extrapolate the models in order to generate a complete response model. Here the high region model was extrapolated over the lower experimental region. The point where the high model intersected the lower model was thus determined to be the cross over point. It is this region, in which the low model switches to the high region model that its accuracy is compromised. This area of poor accuracy is highlighted by a red dashed line in Figure 4-12.

It is apparent from Figure 4-12 that prior to the join point the lower region model provides a good representation of both the test data points and the general form of the response, e.g. variations in local gradient. The same is true of the high region model following the cross over point. It is from this confidence in the model form that an improvement to the model structure was developed. This improvement develops a bridging curve to run between the high and low region models, thereby providing a smooth transition. The process of developing the bridging curve is shown in Figure 4-13. To characterise this bridging model it is necessary to determine the cross over point between the high and low models. At a predetermined distance prior to the cross over point the local value and gradient of the low region response is evaluated. This will be the start of the bridging curve. The same information is determined for the high region model, at a similar predetermined distance. This will be the end of the bridging curve. Using a spline tool, a

bridging curve can be created which has the start / end points developed from the low and high models. The bridging model produced by this tool will have an initial and final gradient that matches the gradients just prior and following its application.

The required bridging model can be developed using a spline. Splines consist of a series of polynomials each valid over a very small range. Subsequently for a known start gradient and position, and known end gradient and position a spline can be produced which will develop a number of polynomials to complete the curve between these points. A function within the spline development tool determines that the progression from one polynomial to the next is smooth. The mathematics involved in the development of splines is very complex, and Mathworks[112] provides an introduction to the complex field of spline development. Fortunately a number of spline fitting tools are available within the Matlab modelling environment, so that it was not necessary to develop a complete understanding of their operation.

Figure 4-14 compares a fifth order modelling solution with a two stage gradient matched solution. Both solutions require the same number of test points, and both solutions have similar correlation coefficients for the generating data set. However as previously discussed, the fifth order solution is subject to oscillations in between the fitting test points which are not evident in the full test data set. The two stage gradient matching solution is not subject to these oscillations; this becomes more apparent when the correlation coefficient is examined for an extended data set including data which was excluded from the generating data. Here the correlation for the fifth order solution drops to 0.9872 whereas the correlation for two stage gradient matched solution remains at 0.9964.

### 4.5.4 Advantages / disadvantages of the two stage gradient matching solution

As may be expected, in comparison to a fifth order Taylor's series regression solution the two stage gradient matching approach requires more computational time to evaluate. However, this computational demand can be justified by the increase in model accuracy produced by the more complex modelling solution. Furthermore, the two stage gradient matching DoE approach offers solutions to some of the problems identified (Edwards et al[99]). Poor feedback during the testing procedure can be overcome, since the quality of high and low region models can be determined independently of one another. Increased testing duration due to the randomness required to negate the effect of systematic errors can be overcome by applying a randomised test sequence within a high / low set of

experiments (e.g. running a high throttle region / high speed test immediately followed by a low region / low speed test).

This section has established which independent variables are to be used in the design space. The work has also determined typical response forms and the development of a method to reduce the influence of high order model oscillations. The following sections will determine the exact form of the design space and the approach to be used to implement this within a DoE test procedure.

## *4.6 Application of DoE to the investigation to be examined in this study*

This section will explore the limits of the design space and use these to develop a test procedure. Certain aspects of the design space have already been identified. The speed range has been selected to cover the low engine speed operation range; up to 3000 rev/min. The cam overlap will be examined over its full working range. However, factors such as charge dilution and spark timing ranges have yet to be identified.

### 4.6.1 DILUTION LIMITS

As discussed in Section 4.5.1 the dilution factors used, as control variables are the demand values. However, a unified dilution measure has been developed which allows the effect of either charge dilution method to be assessed upon a consistent basis.

The unified dilution measure has been developed by balancing the constituents of the inlet and exhaust gases, and through consideration of the thermal effects of charge heating. Appendix A describes in greater detail the development of the unified dilution measure. The dilution measure may be evaluated using the following equation:-

$$\lambda = 1 + (\lambda_{afr} - 1) + (\frac{1}{(1 - EGR_{per})} - 1) + (\frac{T_{inlet}}{T_{ambient}} - 1)$$

Where: $\lambda_{afr}$ Is the classical lean dilution value calculated by:

$$\lambda_{lean} = \frac{AFR_{lean}}{AFR_{stoich}}$$

$EGR_{per}$ Is the classical EGR percentage, calculated by:

$$EGR_{\%} = \frac{EGR_{inlet} - EGR_{ambient}}{EGR_{exhaust} - EGR_{ambient}}$$

$T_{inlet}$ Is the inlet temperature - K

$T_{ambient}$ Is the ambient temperature - 298 K

This unified dilution measure is used in Section 5.3 to assess the effect of dilution levels upon engine response. However when this preliminary work was conducted the unified dilution measure had not been developed as such lean and EGR dilutions are treated separately using the classical measures.

Key to the effectiveness of a DoE test program is that the design space should span the maximum variable range over which the measured responses are stable. Consequently in order to implement a thorough and accurate test program, a preliminary series of 'one variable at a time' tests was undertaken to identify the maximum dilution tolerance of the engine. The lean charge dilution, was increased until the combustion instability, as measured by the $COV_{imep}$, exceeded 10%; this was then determined to be the dilution limit. This procedure was repeated for EGR charge dilution. The whole process was then repeated over a number of engine speed and throttle conditions.

The results of this preliminary engine mapping are presented in Figure 4-15. Since the EGR system implemented upon the test engine cannot develop sufficient EGR flow during WOT operation to achieve unstable combustion. It is apparent that over the engine speed region to be investigated, the variation in WOT maximum dilution tolerance is not substantial, varying from lambda 1.6 at 1200 rev/min to lambda 1.5 at 3000 rev/min. The most apparent variation in dilution limit occurs at part throttle condition, operating with EGR dilution. Here the minimum throttle condition that can tolerate maximum EGR demand varies from 26% throttle and 1200 rev/min to 40% throttle at 3000 rev/min. This variation can be attributed solely to the variation of inlet manifold pressure at these conditions leading to a greater pressure gradient driving the EGR; additionally there is a lower peak combustion pressure, and subsequent flame speed. A similar examination of the minimum throttle position at which the engine can tolerate maximum lean dilution showed that this occurs at a reduced throttle condition compared with the EGR dilution limit. This can be attributed to the fact that, unlike EGR dilution, lean dilution as implemented upon this test engine is homogeneous and consistent for every cylinder. Investigations at low throttle conditions identified that the engine was unable to operate in a stable manner with any dilution present at throttle positions lower than 10%.

Figure 4-16 shows a simplified relationship for fuelling and EGR dilution and throttle position. These are the relationships used to determine the geometrical shape of the design space.

In order to determine the maximum levels of a combination of dilution measures that the engine could tolerate a further series of tests were undertaken. From a fixed EGR demand condition the fuelling was systematically reduced until combustion stability was compromised this identified the maximum total levels of dilution that could be used in combination. Figure 4-17 demonstrates the relationship that was used to incorporate this in to the definition of the design space. It can be seen that at 100% EGR demand a fuelling dilution of 10% was allowed; however, at the maximum fuelling dilution no EGR dilution could be tolerated.

At each of the identified operating limits the valve overlap was tested across its full range to ensure that stable operation was possible. Stone[34] and Heywood[35] suggest spark timing can be varied by as much as 10° retarded from MBT in production engines. The stability of combustion at maximum dilution levels was tested at the extreme spark retardation, but it was found that the engine could only tolerate a range of spark timings up to 6° at these highly dilute mixtures. Rather than make the design space any more complex, it was decided to fix the spark timing range from MBT to 6° retarded from MBT.

### 4.6.2 Final testing schedule

As discussed earlier, engine responses to continuous variations in speed are of a very high order, such that it is very difficult to ascertain if a modelled response is representative of the true engine response. Instead a less efficient, discrete speed solution has been selected, as this offers the flexibility to increase testing density within regions of particular interest without compromising the final model solution. The speed range to be investigated will range from the lowest engine speed at which there is a useful range of power available (1200 rev/min) to a maximum speed where the diluted power equates to a high vehicle cruising velocity (3000 rev/min). Within this speed range samples are taken at discrete engine speed intervals of 200 rev/min. If a discontinuity was observed between discrete models, additional tests could be introduced at 100 rev/min steps. In practice this has not been necessary. However, the operation of the engine at 1600 rev/min proved unstable at all operating conditions. The cause of this instability was difficult to pin point, but it was concluded that it must be as a result of an unfortunate harmonic between the capacity of the test cell and the engine induction system at this speed. Hence it was decided to take test results at speeds 1500 rev/min and 1700 rev/min to avoid this difficult operating point.

At the time when the test schedule was finalised, it was not clear whether the increase in computational demand required to implement a two stage gradient matched solution would allow its implementation within an optimisation routine. As a result, it was deemed necessary to develop a testing solution that had sufficient test points to allow a fifth order regression model to be developed. A fifth order response model requires a minimum of six discrete throttle positions to be examined. A two stage gradient matched solution could be achieved using five discrete throttle positions; this would develop greater continuity between the two models since one throttle response point would be repeated. However, in order to maintain the flexibility to implement either solution, the greater number of test points were selected. As such two second order test sequences were undertaken for each engine speed to be investigated. As discussed in Section 4.5.3, the low test region modelled the response to the rapid change characteristics in the low throttle range (nominally 10 - 30%). The high test region examined the effects from the low region to WOT (nominally 40 - 100%). There was a discontinuity of 10 degrees throttle between the two model regions; this was determined to be a gap size which would be least likely to induce oscillations in a fifth order model.

To implement a full fractional factorial test at each individual speed, testing the effect of five independent variables would require 250 test points. This would mean that to characterise the performance of the engine over the entire operating region of interest would require 2500 test points. It is apparent that even this reduced number of test points would not be a viable proposal and instead a reduced fractional factorial solution would be required. The number of test points required by a CCC design to characterise a 5 variable response problem, each to second order, is $32^{[110]}$. However since the engine's operational limits are bounded by its dilution tolerance, the operational region is not regular, (e.g. at low throttle openings the engine cannot tolerate as much EGR) a D-optimal experimental design must be implemented. The number of test points selected for a given speed was determined through a compromise to maximise the determinant of a given test sequence while maintaining a number of tests that could practically be undertaken in one sitting. Typically experimental sequences consisted of 37 test points. D-optimal experimental solutions were generated by a Umetrics DoE package. All of the experimental designs developed have a design resolution of 'V'. This means that individual variable effects are compounded with three variable interaction effects. In total 628 test points were conducted to develop the steady state engine model. The copies of the test sequences and key responses are included in Appendix B.

The accuracy of the developed response models is to be tested by examining the form of the residuals and calculation of the $R^2$ coefficient. Additionally comparison of modelled responses with that of the second set of test results shall be used to determine which regression modelling solution is most suitable to be developed into an engine model. This model analysis is presented in Chapter 5.

During the testing program the uHC gas analyser was only available intermittently Therefore testing program was scheduled such that uHC data is available at 400 rev/min intervals. It is acknowledged that this is a limitation of the resultant model.

Section 5 presents the results to the testing procedure discussed here.

**Table 4-1 Regression model order required to represent response**

| Response | Speed | Throttle | EGR | Fuel | Cam | Spark timing |
|---|---|---|---|---|---|---|
| Torque | 9 | 5 | 2 | 2 | 2 | 1 |
| BSFC | 8 | 4 | 1 | 2 | 2 | 2 |
| $BSNO_x$ | 8 | 4 | 2 | 2 | 2 | 2 |
| BSuHC | 8 | 3 | 2 | 2 | 2 | 2 |
| $BSCO_2$ | 8 | 5 | 2 | 2 | 2 | 2 |
| BSCO | 8 | 4 | 2 | 2 | 2 | 2 |
| $BSO_2$ | 8 | 3 | 1 | 1 | 2 | 2 |
| EGR per | 5 | 3 | 2 | 1 | 1 | 1 |

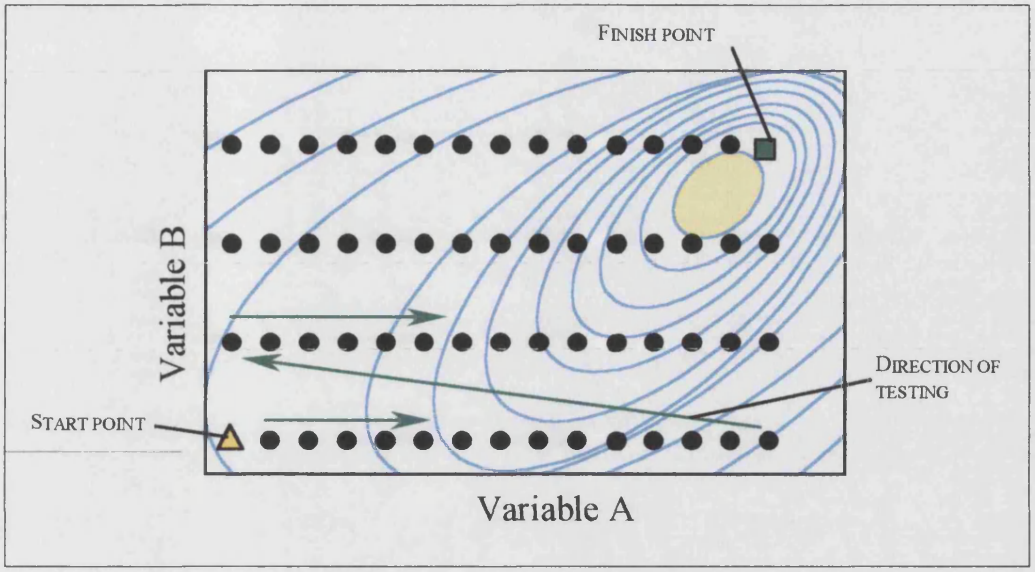


**Figure 4-1 Example of the optimisation approach taken for critical variables**

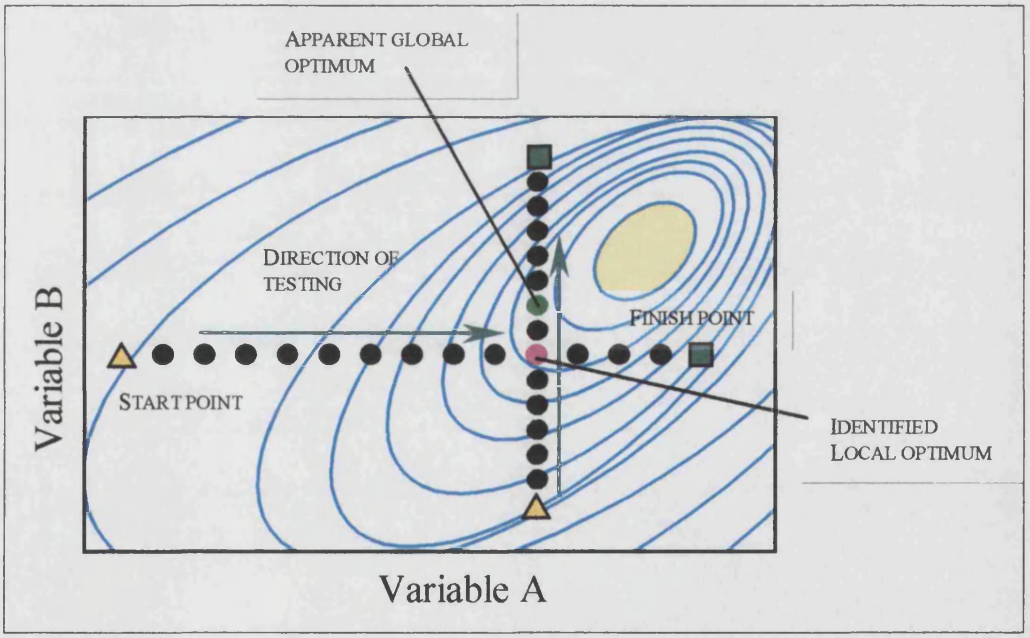


**Figure 4-2 Example of approach for secondary variables**

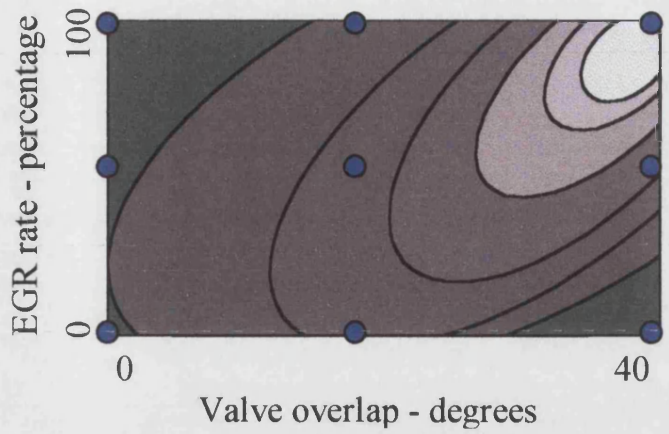


**Figure 4-3 DoE: Design space for a 2 variable problem, showing test points for a fractional factorial investigation**

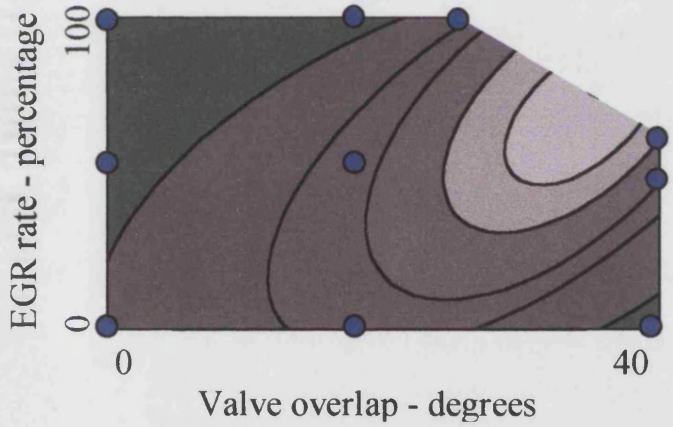


**Figure 4-4 DoE: Irregular 2 variable design space, showing test points for a D-optimal investigation**

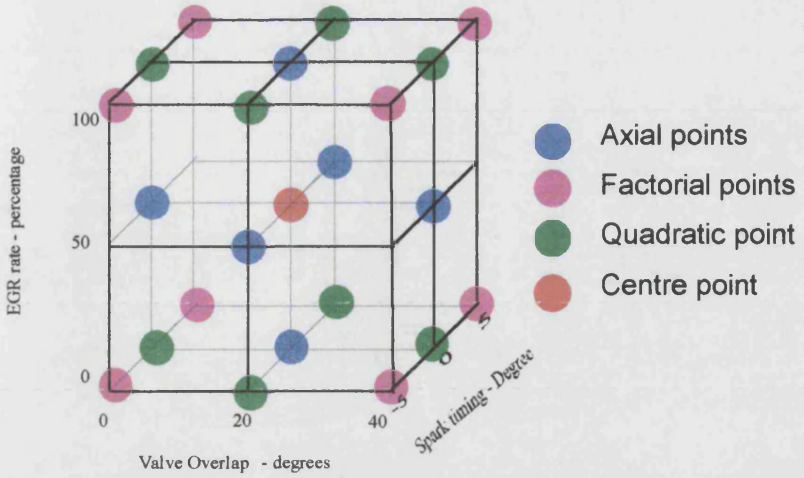


**Figure 4-5 DoE: 3 variable design space**

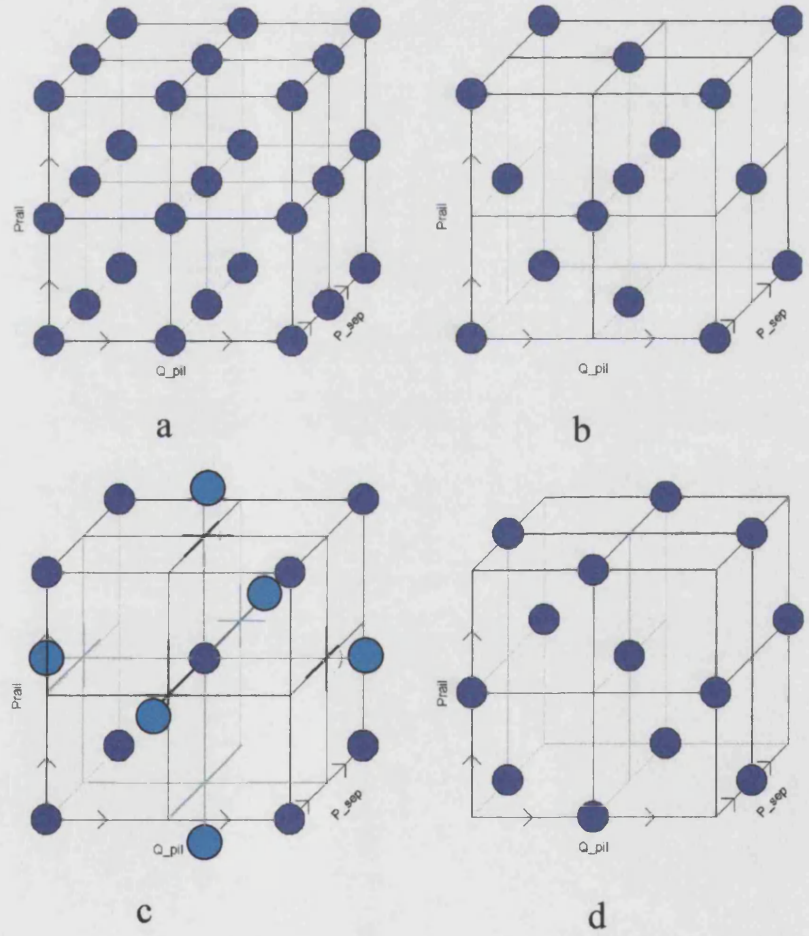


**Figure 4-6 Fractional factorial DOE designs**

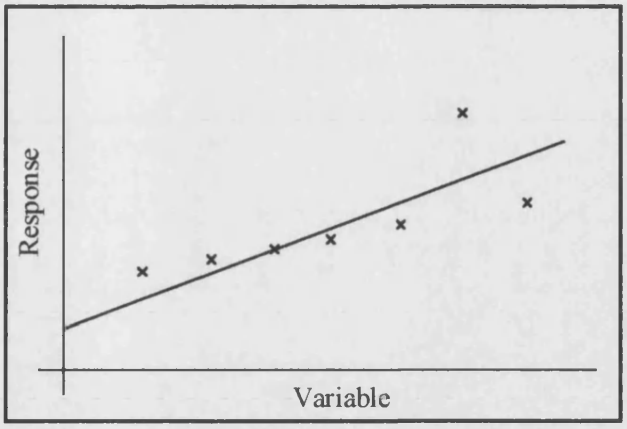


**Figure 4-7 The effect of outliers on regression models**

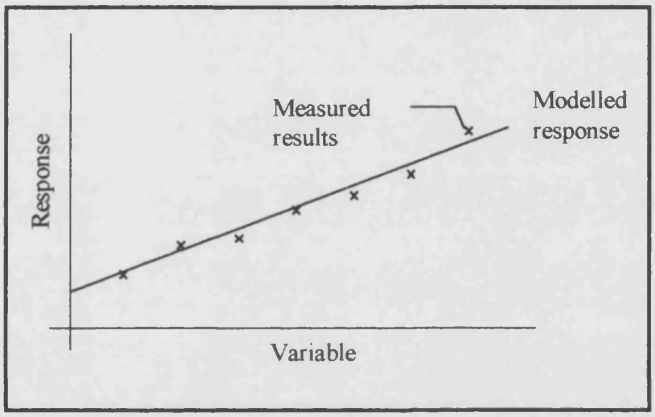


**Figure 4-8 Example of normal relationship between model and experimental data**

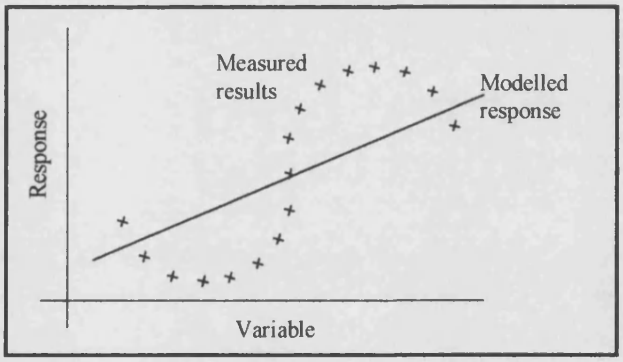


**Figure 4-9 Effect of inaccurate model order on the relationship between predicted and measured data**

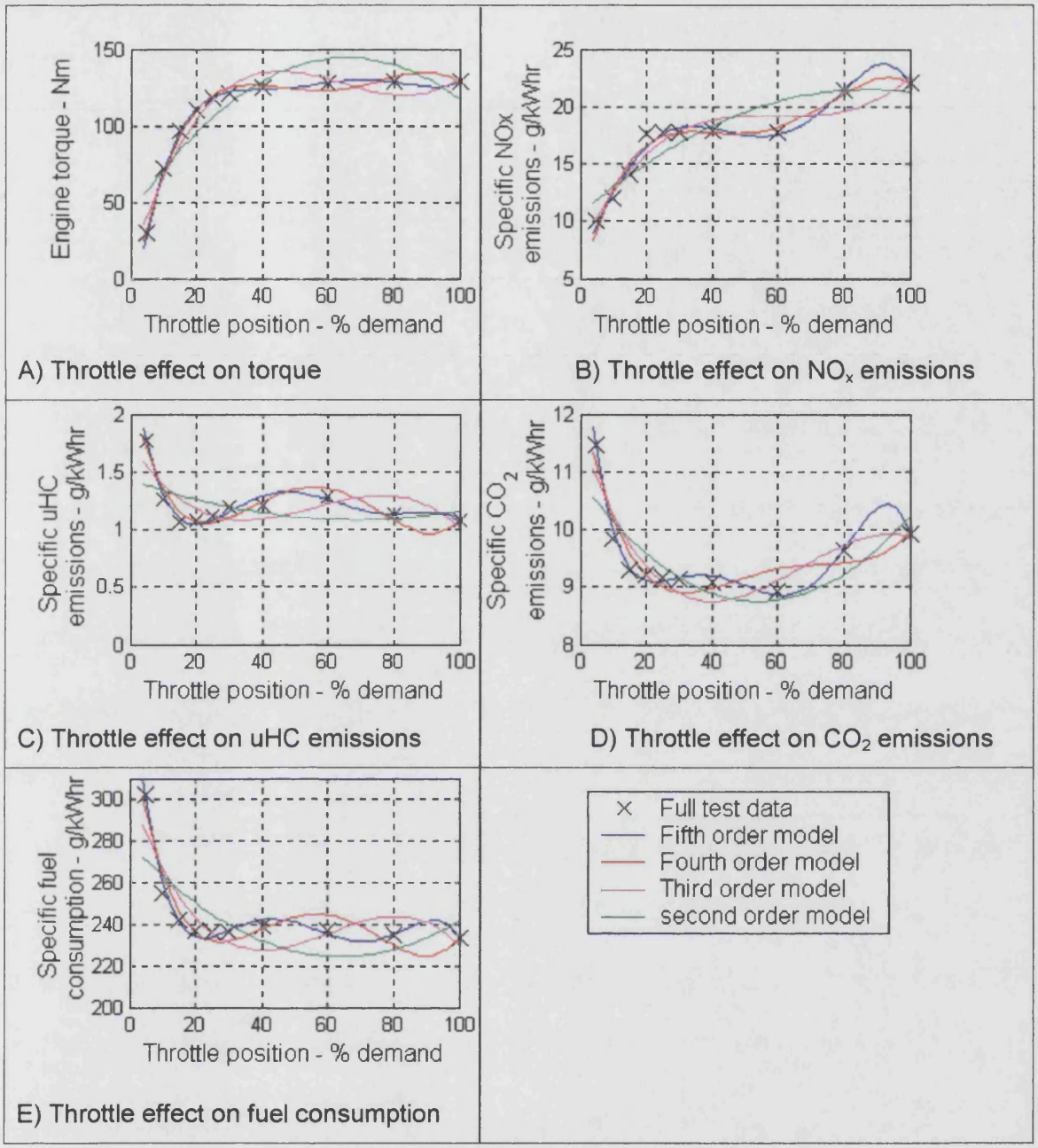


**Figure 4-10 Comparison of the accuracy of different order models to represent the torque response to throttle position**

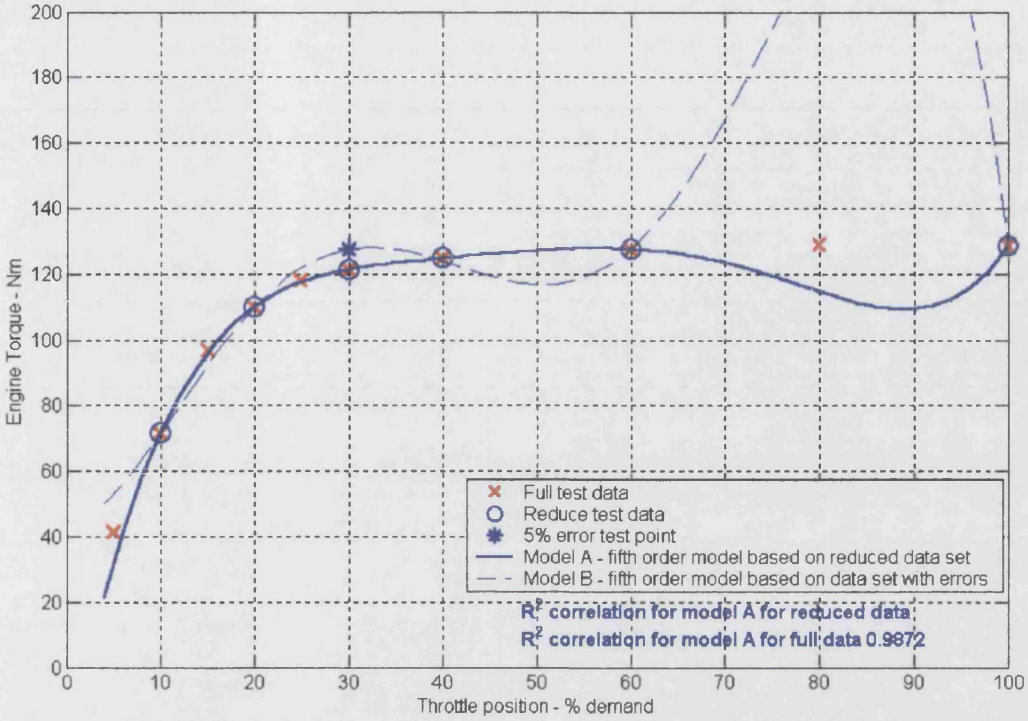


**Figure 4-11 Examination of the effect of small errors on the accuracy of 5th order regression models**

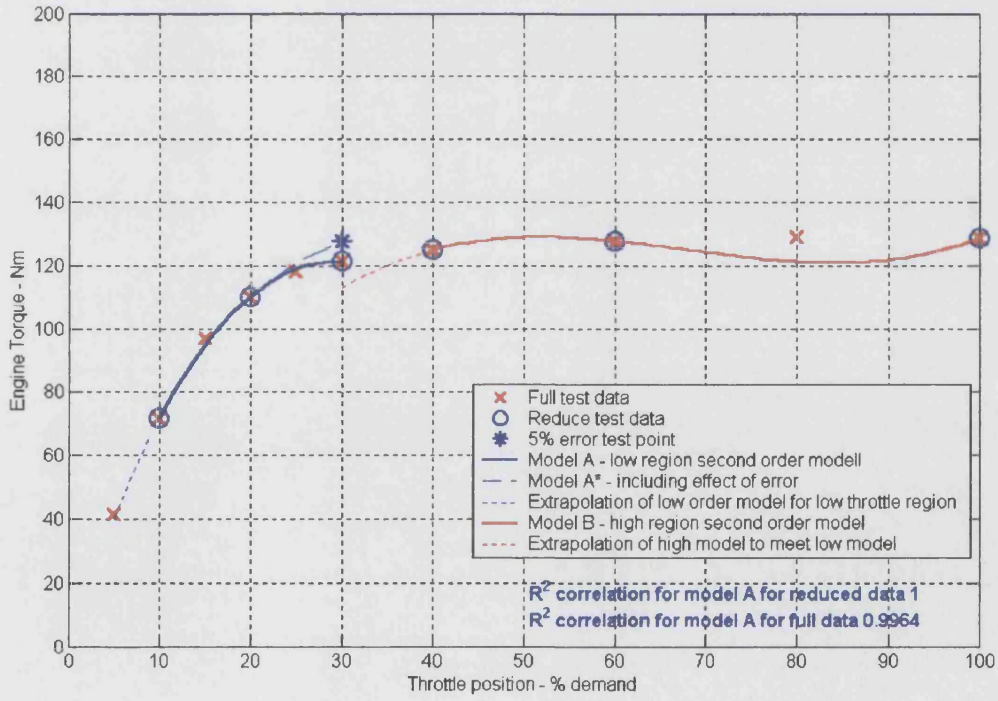


**Figure 4-12 Examination of the use of two second order models to represent engine data**

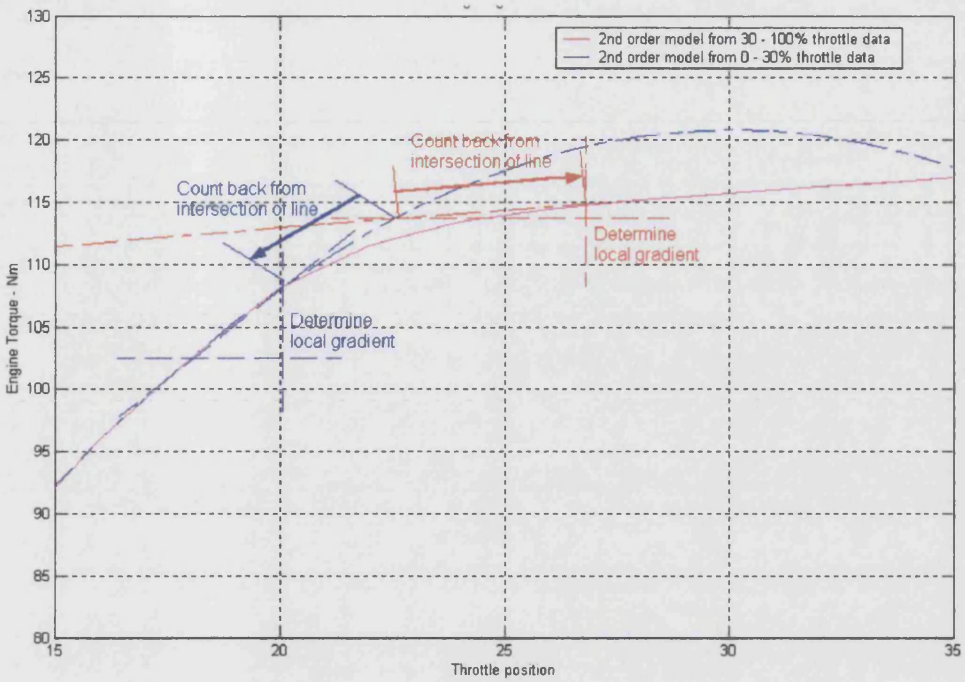


**Figure 4-13 Development of spline curve**

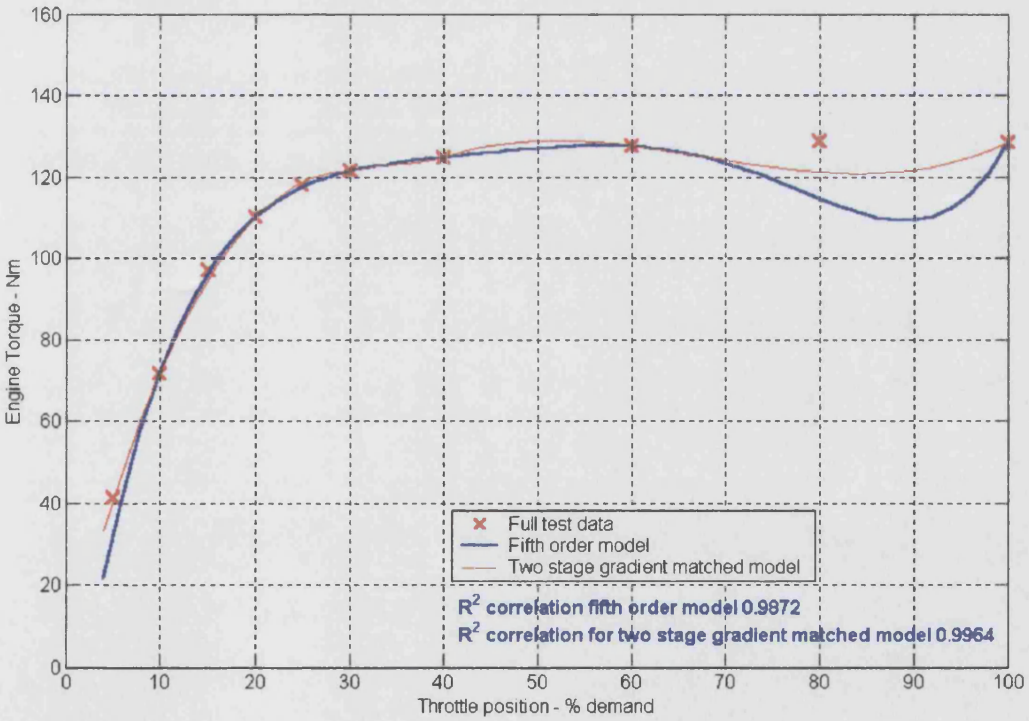


**Figure 4-14 Comparison of a fifth order model with a two gradient matched second order solutions**

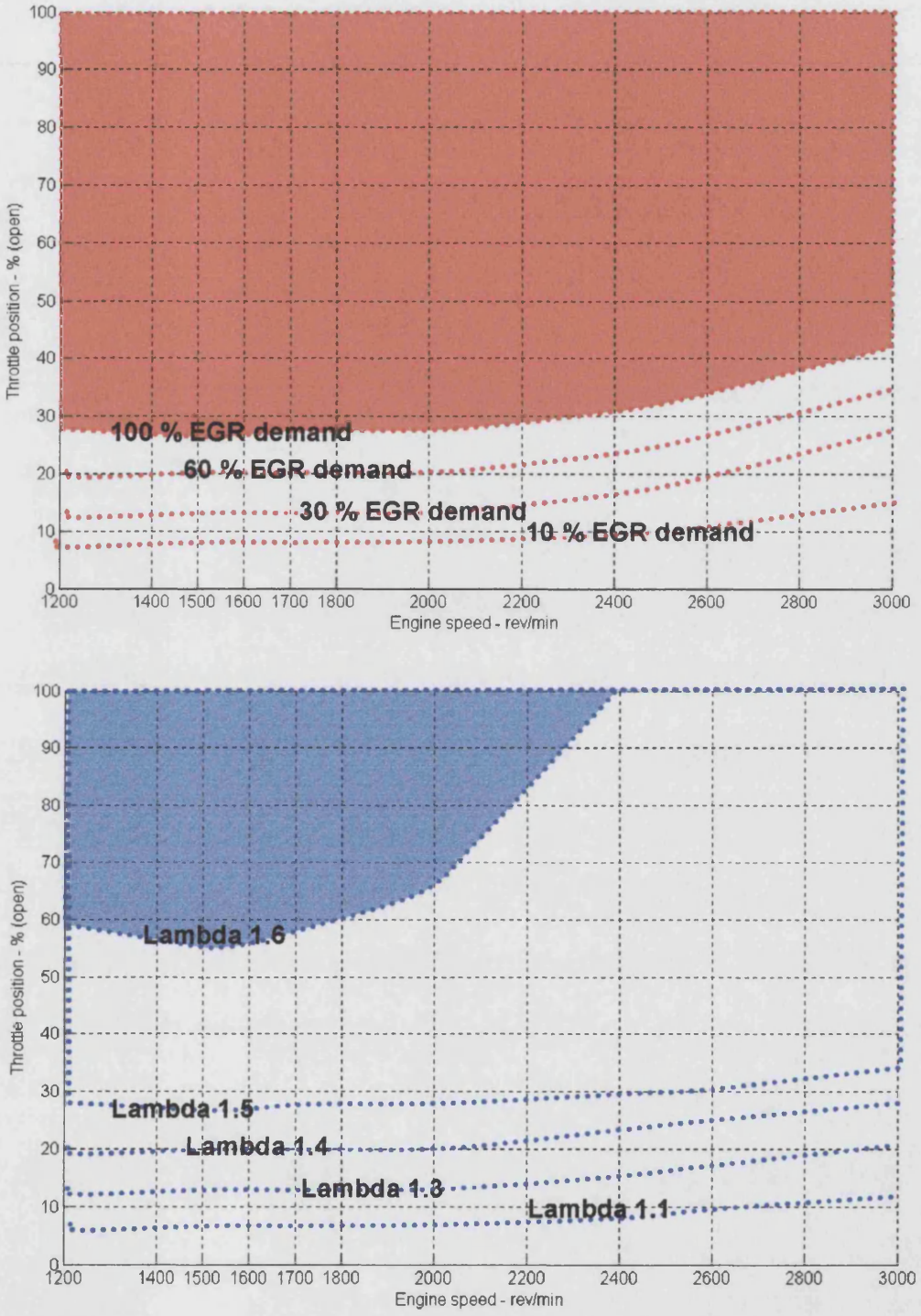


**Figure 4-15 Engine throttle speed map showing dilution limits**

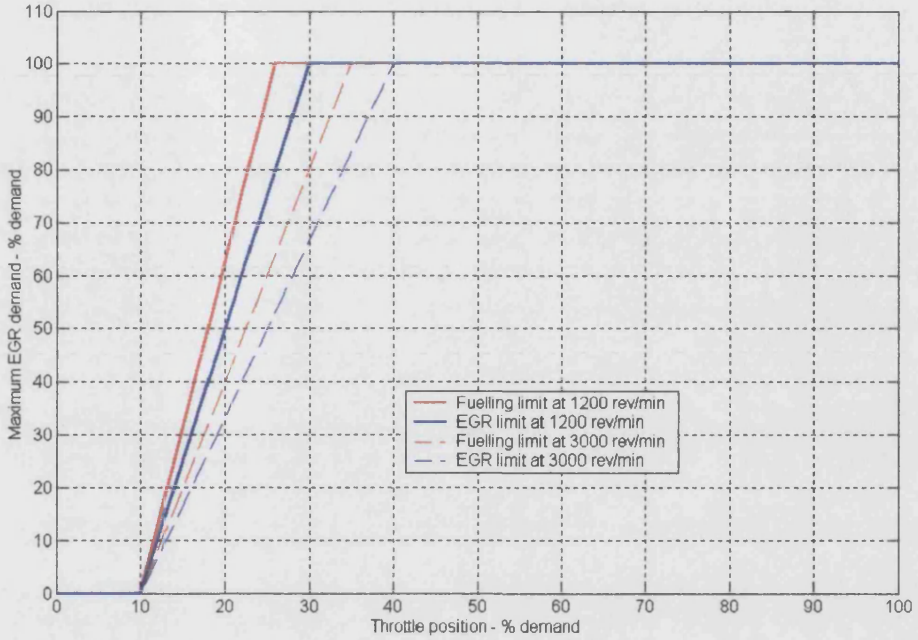


**Figure 4-16 Definition of design space simplified EGR and fuelling limits applied**

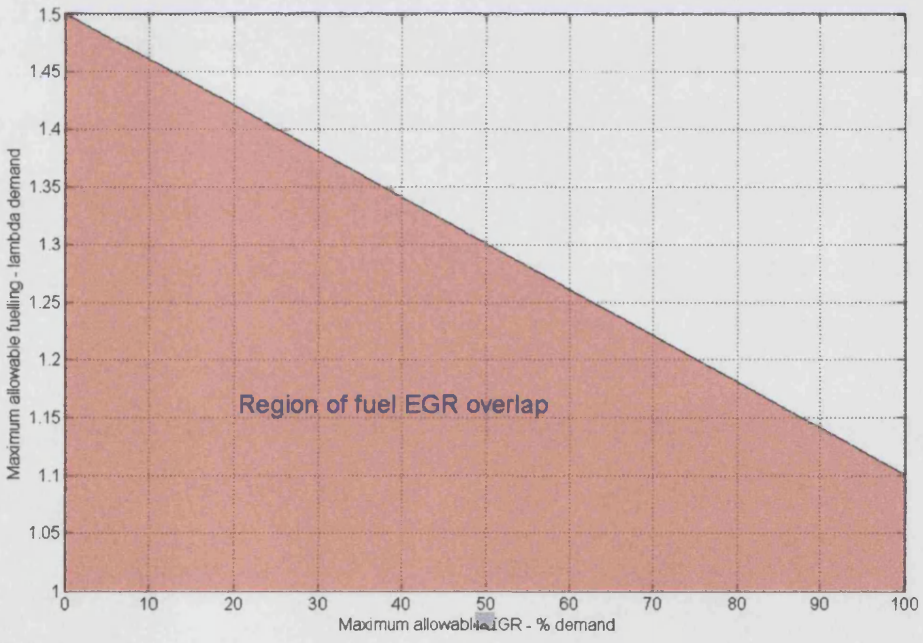


**Figure 4-17 Definition of design space - simplified region of permissible dilution overlap**

# 5 Steady state results

## *5.1 Scope*

This chapter consists of three sections; an examination and selection of a suitable engine model, a main effect examination and a steady state response surface examination. The examination and selection of a suitable engine model section examines the validity of the two engine model approaches described in Section 4.5 and establishes which of the modelling solutions to select for further use. In the steady state analysis section the selected model is used to examine the main effects of each control variable. The section concludes with an examination of the response surface models.

## *5.2 Examination and selection of engine models*

The steady state response regression models are examined in this section. Initially the accuracy of the regression models are examined, and via the examination of measured versus predicated plots of the suitability of the regression model order to represent the measured data is considered. Once confidence is established in the regression models the most suitable model type is selected for the examination of dilution torque control. Appendix C contains tables of the regression coefficients for each of the model types.

### 5.2.1 MODEL ACCURACY

Figure 5-1 shows observed versus predicted torque at ten different speed conditions. For each of these figures the x-axis is the measured torque while the y-axis is the torque predicted the response models. The solid blue line, which runs diagonally through this figure, represents the values where the measured and modelled data are equal. If all of the plotted points lay upon this line, then the model would be a perfect representation of the measured data, and it would have a correlation coefficient of 1. Plotted on the figures are red asterisks and blue crosses. The red asterisks represent the points predicted by the fifth order model; while the crosses represent the data predicted by the two stage gradient matched model. These graphs are presented with outlying points removed. Figures 5:2 to 5:8 have a similar style and show other models. Figure 5.7 has a similar style, but only presents plots for 5 speeds, this is due to the reduced test data density.

Examination of model trends reveals that the observed versus predicted data fall roughly upon the diagonal representing a perfect fit. Response models for torque (Figure 5-1), fuel consumption (Figure 5-2), $NO_x$ (Figure 5-3) and $CO_2$ (Figure 5-4) are particularly

consistent with a good correlation. There is no apparent systematic curvature of the data around this diagonal; as a result it, can be concluded that a suitable regression model order was selected for each response. The second key observation is that at specific speeds the scatter of the observed versus predicted data increases. These variations can be attributed to the effect of engine speed on instrumentation sensitivity. Examination of the 1400 rev/min and 2600 rev/min plots show that these are the speeds particularly affected by large variations. Additionally models for exhaust CO (Figure 5-5), $O_2$ (Figure 5-6) and EGR percentage flow (Figure 5-8) are subject to poor accuracy at zero or minimum readings. This zero error is due to the regression process reducing data, which features a range where results are constant with varying control variable, to a second order model, whose principle gradient is defined by the whole data set.

The correlation coefficient ($R^2$) for both sets of models are presented in Table 5-1 and Table 5-2. This shows that all models have an $R^2$ value of greater than 0.8, typically in the range 0.95 - 0.99. The exception is uHC, where due to the limited model density caused by emissions analyser failure the model accuracy can only be assured for a limited range of test speeds. Umetri[110], suggests that models featuring correlation coefficients greater than 0.8 are good representations . Models with a correlation coefficient greater than 0.9 are considered to be a very good fit. As a result, it was decided that both models represent the test data accurately.

### 5.2.2 Selection of engine Model

This section determines which modelling approach will be used in the remainder of this work. Three measures are used within this selection process. The comparison of $R^2$ values for the modelling test data, however, as shown above both modelling approaches provide good correlations. Therefore, an additional correlation coefficient is presented for the models ability to predict an independent data set, which includes test points not present in the modelling data. Additionally the general form of key regression response models are examined in order to determine whether either of the modelling techniques are subject to response oscillations.

Examination of the $R^2$ coefficient for the modelling data set presented in Table 5-1 and Table 5-2 show that generally the fifth order regression model represents the data with greater accuracy than the two stage gradient based approach. However, typically the error between the models is small (<0.05), and, as has been discussed, these values show that both models are suitable to represent engine responses.

Figure 5-9 presents the torque response surface for the fifth order model. Figure 5-10 presents a similar plot for the two stage gradient matched modelling solution. Figure 5-11 & Figure 5-12 represent similar plots for fuel consumption. These sets of torque and fuel consumption response surface plots represent the engine response at a stoichiometric fuelling condition across a range of speed and throttle conditions. Examination of the response model surface in the throttle region above 40% shows that the fifth order torque and fuel consumption models are subject to signal oscillations. Responses from the two stage gradient matched solution do demonstrate any oscillations in the same regions. The response surface oscillation are highlighted in the figures. It is considered that these oscillatory characteristics are demonstrated sufficiently by these responses that examination of other engine response models is not required.

The response models were used to predict a second data set. The correlation coefficients for this exercise are presented in Table 5-3. It can be seen that for both model types the $R^2$ values are reduced from those of the fitting data. This can partially be attributed to systematic test variations caused by extended test cell running, since these test points were taken after the transient response testing sequence. However, it can be seen that the reduction in the $R^2$ coefficient for the fifth order model is greater than that for the two stage gradient matched solution. Which can be attributed to the error in prediction caused by signal oscillation.

It is apparent from Table 5-1 and Table 5-2 that there is very little difference between the accuracy of the response models when predicting the measured data points. However, it is clear from a visual examination of the response surfaces and the correlation coefficient for an independent data set that the fifth order solution introduces oscillations into the model. These measures have shown that the two stage gradient matched solution does not have such a tendency and therefore is used as the engine model for the remainder of this study.

## *5.3 Steady state engine result investigation*

The response model selected above is used here in the examination of the main effects of each control variable on specific engine performance characteristics. A part of this examination is the determination of the ability of the considered dilution methods to develop a controllable torque margin.

Main effect plots are presented which show the effect of varying just one variable at a time; the equivalent of a one step at a time investigation. The main effect plots are developed by examining the response of the engine model to discrete step changes control variables. During this operation all other control variables were maintained at nominal values.

### 5.3.1 EXAMINATION OF MAIN EFFECTS OF CONTROL VARIABLES

Main effect graphs represent the information that would have been produced if the engine were mapped using a one variable at a time approach. Main effect figures allows the engineer to gain a practical understanding of the importance of individual variables. It is intended that this will be used to clarify some of the unresolved issues identified in the literature review section. Additionally examination of main effect trends for conventional engine control approaches (e.g. throttling, spark timing), allow further credence to be given to the developed response model.

Figure 5-13 shows the main effects of control variables on engine output torque. The figure consists of 6 subplots marked A to F. These are the main effects of:

- A) Throttle position
- B) EGR demand
- C) Fuelling rate
- D) Valve overlap
- E) Spark timing
- F) An interaction between EGR and fuelling dilution.

The nominal control variable settings for each plot are 100% throttle; 0% EGR demand; lambda 1; 20° valve overlap; and MBT spark timing. All main effect plots are varied across the full range of the control variable. Where possible the same Y-axis scale has been used to aid comparison. The effect of the control variables is demonstrated for three speed conditions. These are 1200 rev/min (red line), 2000 rev/min (blue line) and 3000 rev/min (green line). The EGR effect is presented upon a universal lambda scale, the details of which are presented in Appendix A Figure 5-15 through to Figure 5-17 and Figure 5-19 through to Figure 5-22 have a similar style and show the main effect of variations in control variable on other examined responses. The figures include the effects of lean, cam overlap and EGR dilution on engine torque at the nominal WOT conditions, a more complete examination is provided in Section 5.4.

### 5.3.2 MAIN EFFECTS ON ENGINE TORQUE

Considering first the main effect of throttle position on engine torque (Figure 5-13A). The responses are presented from 10% open; this is because, as discussed in Section 4.6.1, 10% open was the minimum throttle position at which charge dilution could be tolerated. It was decided that studies in regions below this throttle opening would be detrimental to the accuracy of the developed engine model. From the relationship presented for 1200 rev/min, it can be seen that, as the throttle position is increased, the engine torque increases rapidly to 115 Nm, which occurs at 20% throttle opening. This rapid increase in torque is followed by a throttle range where the engine torque builds gradually to a maximum value. As the engine speed increases, so the throttle point at which engine torque levels off also increases; not occurring until 40% throttle at 3000 rev/min. This is a classical throttle / torque relationship as discussed by Stone[34].

Figure 5-13B shows that increasing EGR dilution reduces the engine output torque. The torque reduction caused by EGR is greater at high speeds; 20 Nm at 1200 rev/min and 30 Nm at 3000 rev/min. It can be seen that the torque reduction, and dilution level that can be developed varies considerably with speed. This is due to the phenomena which are responsible for the charge dilution. Figure 5-14 shows the effect of EGR valve demand upon the combined dilution lambda, the EGR rate, and the inlet manifold temperature. It is the effects of inlet temperature and EGR rate which combine to develop the lambda value. From this figure it can be seen that the high dilution rates at mid speed conditions are caused by high EGR flow rates and high charge heating effects. At low speed conditions the exhaust gases are relatively cool, therefore although there is a high EGR rate, there is low amounts of thermal dilution. Equally at high engine speed conditions although the exhaust gases are relatively hot, and thus cause high levels of thermal dilution, due to the high mass flow rate through the engine and the geometry of the EGR system there is a reduced EGR dilution rate.

The effect of increasing the air fuel ratio, shown in Figure 5-13C, has a similar effect on engine torque. Lean charge dilution, up to lambda 1.5, offers the potential to develop torque margins of 25 Nm at 1200 rev/min and 45 Nm at 3000 rev/min. Comparison of Figure 5-13B and Figure 5-13C show that EGR and lean dilution levels have a similar effect upon engine torque. It can be seen that for both dilution methods the torque reduction is proportional to the lambda value; approximately 50 Nm/lambda for 1200 & 2000 rev/min and 80 Nm/lambda at 3000 rev/min. This is expected, since the torque reduction is caused by the reduction in combustible charge.

It was hoped that at high cam overlap conditions, those above 30°, internal EGR would act to reduce engine torque. Figure 5-13D shows that, at WOT, the torque margin available via internal EGR is small. However, at very low valve overlaps there is a practicable torque margin; the greatest at 10 Nm (3000 rev/min). This torque margin is developed due to compromised volumetric efficiency. Late inlet valve opening effectively reduces the duration of the induction stroke during which fresh charge can be induced. It is also believed that the torque reduction can be partially attributed to late inlet valve closing; causing an additional throttling effect.

It is apparent from Figure 5-13E that varying spark timing has a limited effect on the engine output torque. Additional studies[115] have shown that sizeable torque margins are possible by controlling spark timing alone, however, such strategies punitively compromise both fuel consumption and uHC emissions.

Figure 5-13F presents the main effect of moving from a purely EGR condition to a pure lean condition. The X-axis of this Figure is presented in terms of percentage lambda for a mixture where the charge dilution is maintained at a constant level. Since the dilution level is constrained, there is minimal effect on engine output torque. This figure is presented here such that in later emissions and fuel consumption sections the effect of combined dilution strategies can be explored.

Figure 5-15 presents BSFC relationships for variations in main control variables. The well known relationship between throttle position and fuel consumption is presented in Figure 5-15A. Specific fuel consumption is high at low throttle opening conditions, due to the affects of pumping losses. As the throttle is opened, the specific fuel consumption decreases. Although the figure gives the impression that specific fuel consumption decreases as engine speed increases, this is not the case. A specific power condition occurs under greater throttling as engine speed increases, thus the power condition achieved at WOT at 1200 rev/min, occurs at 10% throttle opening at 3000 rev/min. As a result, the higher speed condition will have greater fuel consumption for a specific power point.

Figure 5-15B shows the relationship between EGR dilution and fuel consumption. It can be seen that there is a small drop in BSFC as EGR rate increases for low and medium speed conditions. This is due to the reduction in pumping losses. At high speed conditions

EGR causes a small increase in fuel consumption. This is caused by the reduction in combustion stability. Using figure X.xx and figure X.xx it is possible to determine the potential benefit of running a dilution control strategy. Considering a medium speed as an example, a fully diluted EGR condition (to lambda 1.5) develops 100Nm, with a fuel consumption of 235 g/kWh. A similar condition developed purely by charge throttling develops a fuel consumption of 245 g/kWh. Therefore the EGR torque control at this condition offers a 4% fuel consumption improvement.

It can be seen in Figure 5-15C that as the air fuel ratio is increased the fuel consumption is reduced. At low engine speeds a minimum fuel consumption occurs at 1.35 lambda, after this the fuel consumption increases. As the engine speed increases the minimum fuel consumption occurs at lower dilution levels. This is caused by the reduction in combustion stability (Figure 5-22C) and the subsequent reduction in fuel conversion efficiency. At low speeds a greater period is available for flame development; as a result there is greater conversion efficiency and better fuel economy. A comparison of operating condition and fuel consumption reveals that the reduction in fuel consumption caused by operating a lean torque control strategy 14% at 2000 rev/min. The fuel consumption improvement associated with lean charge induction is primarily due to a reduction in pumping losses.

Examination of Figure 5-15D shows that fuel consumption is a minimum at low valve overlap conditions. As discussed in Section 3.2.3 small valve overlap periods lead to greater valve opening during the compression stroke and valve throttling. Therefore, the low fuel consumption at low valve overlap conditions is consistent with the engine experiencing LIVC throttling. A similar trend is not evident at higher speeds; due to greater charge motion reducing the amount of charge exhausted during the compression stroke. A reduction in fuel consumption at cam positions where there is a large degree of valve overlap would suggest that there is a reduction in pumping losses caused by exhaust gas being recirculated internally. Figure 5-15D however shows that this is not observed, instead there is an increase fuel consumption at this valve condition.

Reducing spark timing away from MBT, causes a reduction in the peak combustion pressure Figure 5-16E and thus, a reduction in the specific power from a given quantity of combustible charge. As a result, the specific fuel consumption increases. This relationship is shown in Figure 5-15E. At low engine speeds, this effect increases fuel consumption by

12%. As discussed in Section 4.6.1, it is partially for this reason, that the spark timing range was limited to 6°.

It can be seen from Figure 5-15F, that as a combined lean / EGR dilution strategy changes from a predominately EGR condition, toward a lean fuelling condition the fuel consumption decreases. However this is contrary to the study by Tabata et al[42], who suggested that combining EGR and lean dilution methods could develop lower fuel consumption than either EGR or lean burn used individually. It is possible that this disparity between results, is due to the fact that the Tabata et al[42] study was conducted on an engine featuring a high dilution tolerance stratified charge system. Such that, while the test engine in the current work is operating at its combustion stability limit, the engine examined by Tabata et al[42] was capable of operating under greater levels of dilutions.

### 5.3.3 Main effects on specific $NO_x$ emissions

The correlation of $NO_x$ emissions and throttle position is shown in Figure 5-17A. As the throttle position is increased the specific $NO_x$ emissions increase. Figure 5-16A demonstrates the peak combustion pressure relationship with variations in the control variables. It can be seen that as the throttle position increases the combustion pressure and consequently the combustion temperature also increase. As the cylinder pressure increases so the peak flame temperature increases and greater $NO_x$ emissions are produced as a result.

As discussed in many texts, Figure 5-17B shows, that increasing EGR reduces the production of $NO_x$ emissions. These results show that at high and low engine speed conditions the induction of EGR can result in a 50% reduction in engine $NO_x$. However for medium speed conditions the reduction is less pronounced resulting in 20% reduction in engine out $NO_x$. This discrepancy could be explained by considering the work of Yoshizawa et al[43], which showed that for a single EGR port system the distribution of EGR within the inlet gases was non-homogeneous. As a result, the levels of dilution vary between individual cylinders. At high dilution rates, a large spark advance is required in order to achieve MBT spark timing. However in a cylinder with a low level of charge dilution this high spark advance will take the engine into a region where it has passed MBT and will thus produce very high levels of $NO_x$ emissions.

The $NO_x$ response to variations in fuelling rate are presented in Figure 5-17C. This follows the trend discussed in many texts [34],[35],[2]. As the lambda ratio increases so does the rate

of production of $NO_x$ emissions, this is due to the greater availability of oxygen. This trend continues up to lambda 1.15. After this point dilution charge cooling reduces the emissions of $NO_x$ until, at lambda 1.5 the $NO_x$ levels are approximately 50% of the throttled stoichiometric level.

Work by Leone et al[52] discusses that part of the motivation for fitting a VCT system to the engine was to alleviate the requirement for an external EGR system. As a result, it is expected that at high valve overlap conditions there should be a sizeable reduction in $NO_x$ emissions. Figure 5-17D shows that although there is a reduction, it is not large. The VCT system was intended to replace the external EGR system at part load, since the nominal engine condition presented here are for 100% throttle this is not a representative comparison. Figure 5-18 shows the $NO_x$ reduction effect of cam overlap positions at 30% throttle. It can be seen that a $NO_x$ reduction of 25% is possible. This is the equivalent to the $NO_x$ reduction developed by a conventional external EGR system at this engine condition.

The effect of spark timing on engine $NO_x$ emissions are shown in Figure 5-17E. It can be seen that advancing the spark to the maximum 6° away from MBT reduces $NO_x$ emissions by 20%. This reduction is consistent across the speed range, and is caused by the reduction in peak combustion pressure shown in Figure 5-16E.

Examination of the combined EGR / lean dilution strategy, (Figure 5-17F) shows as the lean percentage of the diluted charge increases the $NO_x$ emissions increase until lean dilution represents 75% of the mixture. From this point onward the charge cooling effects of high rate lean dilution becomes predominant, causing a reduction of $NO_x$ emissions.

### 5.3.4 Examination of the main effects on CO, uHC and $CO_2$ emissions

Figure 5-19A demonstrates the effect of throttle position upon CO emissions. Generally the CO emissions decrease as the throttle opens. This is due to the improvement of combustion stability (Figure 5-22A) that occurs as the throttle is opened. Figure 5-19B demonstrates the effect of EGR dilution upon CO emissions. It can be seen that as suggested in many works e.g. Stone[34] that CO emissions increase with EGR dilution. This increase in emissions is due to the reduction in the quality of charge mixing, leading to a lower fuel conversion efficiency. However, this increase is limited because tight control was maintained over the fuelling of the charge mixture. At low speeds the effect of

EGR upon CO emissions is limited this is due to the greater combustion duration, which leads to improved fuel conversion.

The relationship between CO emissions and lean combustion is shown in Figure 5-19C. Initially as the charge fuelling is reduced the CO emissions drop. This is caused by an improvement in fuel conversion efficiency. However as the fuel dilution increases past 1.3 lambda the rate of CO emissions production increases this is caused by a reduction in combustion stability (Figure 5-22C).

Figure 5-19D and Figure 5-19E show that the effect of valve overlap and spark timing on CO emissions is small. Figure 5-19F shows that as the combined dilution strategy mixture becomes increasingly lean the CO emission reduce significantly until the lean component represents 70% of the induced charge. This is due to the increase in available oxygen, leading to an increase in fuel conversion rate. As the mixture becomes increasingly lean 70 - 100%, the CO emissions begin to increase. This is due to a reduction in combustion stability (Figure 5-22F).

Figure 5-20A shows the effect of throttling upon uHC emissions. It can be seen that as the throttle opens the uHC emissions reduce. This is due to the increase in peak combustion pressure (Figure 5-16A) and combustion stability (Figure 5-22A), leading to improved fuel conversion. Figure 5-20B shows that as the EGR dilution increases, so the mixture quality is compromised and the uHC emissions increase. It can be seen that contrarily to CO emissions, the increase in uHC is greater at low engine speeds. The geometry of the inlet manifold is tailored to charge motion at high engine speeds, therefore at low speed conditions the low charge motion is low leading to a greater propensity for unburned mixture to become resident in cylinder crevices.

Figure 5-20C shows that, due to improved fuel conversion efficiency, as the fuelling rate is reduced the uHC emissions also reduce until lambda 1.2. From this point onward uHC emissions rise rapidly, due to reduced combustion stability (Figure 5-22C). A global feature of Figure 5-20C is that for any fuelling condition the uHC emissions levels are relatively high. This is caused by the relatively high peak combustion pressures which are associated with lean combustion (Figure 5-16C), these lead to greater amounts of gases trapped in crevice volumes, and absorption into engine fluids.

Figure 5-20D shows that for low and medium speed conditions as the valve overlap increases the levels of uHC emissions decrease, until 25°, after this point the uHC levels increase once again. This is due to the high combustion pressure (Figure 5-16D) which occurs at low overlap conditions, and the greater levels of gases passing straight through the combustion chamber, without being combusted, which occurs at large valve overlaps. The characteristic is significantly different at high speed conditions, where increasing valve overlap leads to increased emissions of uHC. This is due to the due to the different charge motion characteristics which are present at high speeds. Here high, inlet port induced, charge motion leads to reduced levels of uHC emissions from crevice volumes. However due to increased charge inertia, as the valve overlap increases the quantity of gases that pass directly through the combustion chamber also increase. It should be noted that the reduction in uHC at large valve overlaps discussed by Leone et al[52] is not evident in Figure 5-20D. This is also believed to be an effect of the nominal WOT conditions used in this example.

Figure 5-20E shows that spark timing has limited effect upon uHC emissions. While Figure 5-20F shows that at any power developed using a combined dilution approach will feature high uHC emissions. This is due to the poor mixture quality and high peak combustion pressures.

Comparison of Figure 5-21 and Figure 5-15 reveals that, as expected, the main effects relationships discussed for fuel consumption also hold for $CO_2$ emissions.

### 5.3.5 THE MAIN EFFECTS ON COMBUSTION STABILITY

Figure 5-22A shows the main effect of control variables upon engine combustion stability. At highly throttled conditions the combustion stability is reduced, while throughout the remainder of the throttle travel the combustion stability is consistently less than 5%.

Figure 5-22B shows the effect of the EGR rate upon combustion stability. It can be seen that for all dilution levels examined the combustion stability is less than 5%. Furthermore it can be seen that as the dilution level increases the combustion stability reduces, this is to be expected since the induction of exhaust gases, reduces the mixture quality and cools the combustion charge. Low speed conditions are subject to the greatest reduction in combustion stability, due to the low levels of in-cylinder charge motion. At high engine speeds the reduced combustion duration also effects combustion stability.

Examination of the combustion quality with varying fuelling dilutions (Figure 5-22C) reveals that for low speed conditions there is high engine stability for all fuel dilutions. Examination of higher speed conditions show that above 1.2 lambda the combustion stability reduces due to reduced combustion duration.

The effect of different valve overlap strategies upon engine combustion stability is presented in Figure 5-22D. It can be seen that at low valve overlap conditions the engine stability is high, as the valve overlap becomes greater the stability reduces. This can be attributed to the levels of residual gases, and the peak combustion pressure (Figure 5-16D) at low overlap conditions. It is expected that combustion stability would be reduced at highly throttled / low valve overlap conditions. This is due to LIVC, leading to a reduction in compression ratio.

Figure 5-22E shows that there is a limited effect of spark timing upon engine combustion stability. For a combined dilution strategy, Figure 5-22F, the engine stability increases until the mixture comprises 50% lean dilution after this point the stability increases once again. It is not apparent why this should be.

## *5.4 Examination of the ability of diluents to enable torque control*

### 5.4.1 EGR TORQUE CONTROL

It has been shown in Figure 5-13B that when presented on the unified dilution measure there is a linear relationship between torque reduction and EGR charge dilution.. The torque reduction is between 50 Nm/lambda at 1200 rpm and 80 Nm/lambda at 3000 rev/min. It can be seen that greater dilution levels and thus torque reductions are available at mid speed conditions.

Figure 5-23 presents the dilution rate which is achieve across the throttle range with the EGR valve wide open. Similarly Figure 5-25 presents the torque margin that can be developed across the throttle range. It can be seen from these figures that for throttle conditions below 10% no torque margin maybe developed through the induction of EGR. This is because, due to combustion stability limitations charge dilution is not utilised at low throttle conditions. For throttle conditions greater than 10% the available torque margin increases to a maximum at 30% demand. It can be seen from Figure 5-23 that at 30% throttle the EGR flow induced is a maximum this is due to the large pressure difference between the inlet and exhaust manifolds. As the throttle opens further the inlet manifold

pressure approaches atmospheric reducing the pressure difference and consequently the EGR flow and torque margin are reduced.

### 5.4.2 Scope of iEGR torque control

It was hoped that by increasing the valve overlap past that required for maximum power internal EGR could be developed and this could be used to produce a sizeable torque margin. It is apparent from the examination of Figure 5-13 that at WOT conditions this has not been the case. It was believed, that the high inlet manifold pressure may have been restricting the internal flow of exhaust gases into the combustion chamber, therefore Figure 5-25 demonstrates the effect of full cam overlap across a throttle demand range. It can be seen that, although the developed torque margin does increase with a reduction in throttle position, the torque margin available via iEGR is never greater than 4 Nm. It is apparent that this is insufficient to act as a practicable torque control mechanism. Interestingly this is contrary to torque margin reported by Stefanopolou[54]. This suggests that the variable valve actuation device implemented in Stefanopolou's[54] study, was capable of phasing inlet and exhaust cam profiles.

A benefit of the use of the DoE test system is that the developed response models can be extrapolated to determine the potential benefits available through modification to a system. Toyota[81] have developed a production engine featuring a cam phasing system capable of developing 60° of valve overlap. If the VCT system, and engine clearances were modified to allow 60° valve overlap there is potential to increase the available torque margin, as shown in Figure 5-26. It can be seen that, at 60° overlap a torque margin of 10 Nm is achievable. Although this represents an increase in torque margin, it is not sufficient to allow practical torque control. Additionally the Toyota system has the greatest overlap presented in the literature for an inlet cam phasing system, it is speculated that increasing the overlap potential further, will be detrimental to the engine efficiency due to reduced compression ratio. Therefore it would appear that torque control via internal EGR developed through inlet cam phasing is not practical with a naturally aspirated engine.

### 5.4.3 Scope of lean fuelling to control engine torque

As shown in Figure 5-13C the torque margin available via lean burn dilution at WOT ranges from 37 Nm at 3000 rev/min to 25 Nm at 1200 rev/min. Figure 5-27 shows the size of the torque margin developed through lean dilution across a throttle range. It can be seen that in the range 0-10% throttle opening no torque margin via lean dilution is available, this is the range where the engine cannot tolerate charge dilution. Then in

throttle range from 10- 30% open the lean torque margin builds rapidly. In the range 30 - 100% the torque margin stabilises, varying by typically less than 5 Nm from the 30% throttle torque margin. Comparing this torque margin to that developed by an EGR strategy across the throttle range (Figure 5-24) it can be seen that the major difference is the profile of the torque margin in the 30 - 100% throttle range. While there is typically only a small variation in torque margin for a lean dilution condition, for an EGR condition there is a minimum of an 8 Nm variation in torque margin. As a result of this throttle torque margin characteristic, it is believed a lean dilution torque margins would be easier to controlled.

## *5.5 Examination of response surfaces for a range of torque control strategies*

Response surface maps are representations of the response models that cover a complete range of engine speeds, over the examined throttle range. The response maps are displayed here in a classical speed / torque manner; since this is the basis for the development of powertrain control lines. These figures are demonstrated in order to identify the potential afforded through the use of dilution charge control. Furthermore, this examination will detail the possibility to optimise an individual power condition through the use of lean, EGR and combined dilution strategies. As an example this examination will consider the effect of optimal fuel consumption strategies upon a specific emission response.

Figure 5-29 is a BSFC response map for a stoichiometrically fuelled, throttle only torque control approach. This plot was developed by imposing dilution limits upon the engine models, then incrementally recording torque and BSFC responses at increasing throttle positions. This was repeated for all speed conditions. The BSFC data was aligned against the torque response in order to develop a torque speed plot. Plotted upon this figure are contour lines (black solid), these highlight speed torque conditions with the same specific fuel consumption condition. Also superimposed upon this figure are lines of constant power, these range from 6 kW through to 38 kW in 4 kW steps. It can be seen that there are no fuel consumption contour lines below 10 kW resulting from the minimum throttle position imposed by the DoE test schedule. Similar characteristics are present upon the BSFC plots for other dilution strategies (FiguresFigure 5-30 to Figure 5-32) and on FiguresFigure 5-33 to Figure 5-36 where contour lines identify points of constant specific $NO_x$ emissions.

Through examination of the fuel consumption, for a classical torque control approach, presented in Figure 5-29, it is a apparent that the lower fuel consumption regions as identified by the darker blue regions, occur as the engine condition approaches WOT operation. It can also be seen, the fuel consumption along a specific power condition is a minimum at low speed / high load conditions, as discussed in Section 1.1.

Examining the fuel consumption plots (Figures Figure 5-29 to Figure 5-32) it is possible to draw some conclusions regarding the characteristics of an optimal control solution. If a 14 kW power condition is considered, for a stoichiometric, throttle only, torque control approach (Figure 5-29) it is apparent that the minimum fuel consumption occurs at the minimum engine speed (1200 rev/min) at 110 Nm. The fuel consumption at this point is 240 g/kWh. Examination of an EGR diluted stoichiometric operating strategy (Figure 5-31) shows that the WOT torque has been reduced, compared to a stoichiometric throttle only condition, by a minimum of 20 Nm at all speed conditions. Additionally, the fuel consumption contours have been compressed. Although this strategy has no significant effect upon the absolute minimum fuel consumption of the engine, in the region where dilution can be tolerated the fuel consumption for a specific speed / load condition has been reduced. If the 14 kW operating point achieved through throttling only control is compared with an EGR dilution control strategy, it can be seen that the minimum fuel consumption occurs at a higher speed of 1500 rev/min. Operating at the optimal EGR dilution condition provides the engine with a 30 Nm torque margin and a 300 rev/min engine speed advantage over a throttle only condition. Whilst still developing a fuel consumption of 240 g/kWh. During a transient operation from the EGR dilution operating condition the torque margin could be liberated quickly, and the engine has a smaller speed range over which to be accelerated. Therefore this condition offers the potential of improved transient response.

Examination of the lean dilution strategy (Figure 5-31) shows a similar trait to EGR dilution in so much as a reduced WOT torque and an increase in fuel consumption contour density. However unlike the EGR strategy, the colours of the constant fuel consumption regions become darker, thus signifying a reduction in both absolute and specific fuel consumption. Optimal fuel consumption, for the same 14 kW operating condition is achieved at 1400 rev/min and 100 Nm using lean dilution. At this operating point there is a torque margin of 25 Nm. Drawing comparison with a throttle only torque control strategy, a lean dilution strategy offers a 25 Nm torque margin and a 200 rev/min transient speed advantage. At this condition the fuel consumption is 220 g/kWh representing a reduction

of 8% percent in fuel consumption compared to both stoichiometric throttled and EGR dilution conditions.

Examination of Figure 5-32 shows that a combined EGR / lean dilution strategy offers similar reductions in WOT torque to EGR dilution strategy. Additionally this torque control approach offers a similar fuel consumption characteristic to that of an EGR strategy. A 14 kW power condition achieved through combined lean and EGR charge dilution has an optimal operating point at 1500 rev/min, 90 Nm. However, at this condition the fuel consumption is 235 g/kWh; a potential fuel saving of 2% compared to the stoichiometric strategy. Additionally the same transient response arguments hold for the EGR strategy at this condition.

This examination is extended to consider the effects of operating condition upon $NO_x$ emissions, to demonstrate to procedure that would need to be followed in order to establish the effects of control strategies upon emissions. Examination of Figure 5-33 shows the specific $NO_x$ emissions for the stoichiometric control strategy. The lighter green areas represent greater specific $NO_x$ emissions. It can be seen that the greatest $NO_x$ emissions occur at high speed / low torque conditions. Since this area is little effected by dilution control strategies this is the case for all considered figures. The $NO_x$ emissions relationship for an EGR dilution strategy is presented in Figure 5-34. It can be seen by the darker green shading that there is a general $NO_x$ reducing characteristic. Figure 5-35 presents the $NO_x$ emissions response map for a lean dilution strategy. It can be seen that over the majority of the engine speed / load conditions where dilution maybe tolerated the $NO_x$ emissions are close to stoichiometric levels. The $NO_x$ emissions for an equal lean / EGR combined dilution strategy are presented in Figure 5-36. this demonstrates a reducing trend compared to both lean and classical throttle torque control approaches.

Continuing the investigation of the 14 kW power condition to examine the exhaust emissions implications of running at the optimal fuel consumption conditions. Considering Figure 5-33, for the stoichiometric operating strategy, it can be seen that at the operating condition which develops minimum fuel consumption (1200 rev/min and 110 Nm) the specific $NO_x$ emissions are 16 g/kWh. Comparatively the emissions for the optimal fuel consumption condition using and EGR only strategy are reduced to 8 g/kWh. The lean condition develops $NO_x$ emissions of 12 g/kWh and the combined condition develops emissions of 6 g/kWh.

However, this is not the complete picture since the tailpipe emissions are effected by the influence of catalytic converters. Three way catalysts (TWC) when at operating temperature in the influence of a steady gas stream have been developed to achieve conversion efficiencies of up to 98%[34]. The $NO_x$ reduction effects of a three way catalyst may only be achieved in a low oxygen exhaust stream, hence they can only be effectively used with the stoichiometric and EGR dilution strategies. Recently a large amount of research has been undertaken to improve the performance of catalysts that reduce $NO_x$ in a oxygen rich exhaust stream. As a result the peak efficiency of $NO_x$ storage catalysts is now very close to that of TWC. However $NO_x$ storage catalysts become saturated and as a result their conversion efficiency falls. Regeneration cycles are required to return the catalyst to peak operating performance. A more detailed examination of the factors that influence catalyst conversion efficiency is presented in Chapter 7.

Similar examinations to the one conducted for NOx emissions could be performed for $CO_2$, CO and uHC. However it is felt that the examination provided for $NO_x$ emissions is sufficient to demonstrate that the identification of optimal fuelling operating conditions has complex affects upon exhaust emissions.

Lee & Reitz[103] developed an optimal engine control strategy by investigating responses surfaces in a similar manner to the comparative discussion presented here. For two or possibly three variables problems this approach may produce a global optimal solution, however for complex response surfaces, or problems of greater than three variables, a computational optimisation approach must be implemented. Since the optimisation to be attempted within this work is of a 6 variable problem, a computational approach is required. The optimisation is presented in Chapter 7.

## *5.6 Conclusions*

It has been shown that both the fifth order and the gradient matched second order regressions models have a high fitting accuracy. Examination of response surface topography and the models' accuracy when predicting a secondary experimental data set identified that the gradient matched modelling approach was most suitable for further investigation.

Section 5.3.2 demonstrated that torque margins greater than 30 Nm can be developed across the operating speed range by application of lean and EGR charge dilution at WOT condition. This margin is sufficient to offer a 3 kW step at 1200 rev/min and a 9 kW step at

3000 rev/min. This is enough torque margin to suggest that there is potential to reduce the throttle requirement in engine torque control. Reduced valve overlap conditions can develop torque margins of up to 10 Nm. Internal exhaust recirculation through large valve overlaps has proved to be disappointing, the maximum torque margin available was 5 Nm at 20% throttle (1200 rev/min). It is apparent that this is not sufficient to provide a practical torque control strategy.

Examination of the response surfaces revealed that for an engine featuring throttle only torque control minimal fuel consumption is achieved at low speed / high torque conditions. A direct comparison of throttle only torque control with dilution control strategies reveal that a given power condition is achieved at higher engine speeds for dilution conditions. This is a result of the reduction in WOT torque. Detailed examination revealed that, for the given power condition, lean dilution has the potential to reduce the specific fuel consumption by 8% compared to a stoichiometric throttle torque control approach. It was concluded that since the engine power is determined by the interaction of six independent variables, and that each of these variables has complex effect upon legislative emissions, a computational method is required in order to establish optimal control variable positions.

**Table 5-1 $R^2$ values for two stage gradient match modelling method**

| | Engine Speed | | | | | | | | | |
|---|---|---|---|---|---|---|---|---|---|---|
| | 1200 | 1400 | 1500 | 1700 | 1800 | 2000 | 2200 | 2400 | 2600 | 3000 |
| Torque | 0.9909 | 0.8739 | 0.9789 | 0.9903 | 0.9895 | 0.9889 | 0.9924 | 0.9834 | 0.6735 | 0.9919 |
| BSFC | 0.9520 | 0.7880 | 0.8918 | 0.8976 | 0.8922 | 0.9379 | 0.9690 | 0.9714 | 0.9147 | 0.9652 |
| BSNOx | 0.9297 | 0.9562 | 0.9185 | 0.9106 | 0.9636 | 0.8588 | 0.9118 | 0.9136 | 0.7211 | 0.9342 |
| BSCO2 | 0.9517 | 0.8432 | 0.8839 | 0.8393 | 0.9831 | 0.9717 | 0.9206 | 0.9327 | 0.7485 | 0.9693 |
| BSCO | 0.9322 | 0.8544 | 0.6568 | 0.8448 | 0.8817 | 0.4249 | 0.6970 | 0.8844 | 0.9409 | 0.9506 |
| BSO2 | 0.9991 | 0.9936 | 0.9951 | 0.9990 | 0.9961 | 0.9885 | 0.9729 | 0.9372 | 0.9914 | 0.9998 |
| BSuHC | 0.7702 | N/A | 0.8154 | 0.6573 | N/A | 0.6307 | N/A | 0.8372 | N/A | 0.6755 |
| EGR % | 0.9879 | 0.9585 | 0.9899 | 0.9844 | 0.9839 | 0.9916 | 0.9932 | 0.9980 | 0.7215 | 0.9958 |

**Table 5-2 $R^2$ values for fifth order regression modelling method**

| | Engine Speed | | | | | | | | | |
|---|---|---|---|---|---|---|---|---|---|---|
| | 1200 | 1400 | 1500 | 1700 | 1800 | 2000 | 2200 | 2400 | 2600 | 3000 |
| Torque | 0.9747 | 0.9594 | 0.9744 | 0.7303 | 0.9868 | 0.9861 | 0.9926 | 0.9867 | 0.8875 | 0.9894 |
| BSFC | 0.9492 | 0.8906 | 0.9392 | 0.8813 | 0.9295 | 0.8993 | 0.9523 | 0.9569 | 0.9152 | 0.9655 |
| BSNOx | 0.9490 | 0.9480 | 0.9466 | 0.5645 | 0.9566 | 0.9439 | 0.9347 | 0.9462 | 0.7891 | 0.9463 |
| BSCO2 | 0.9589 | 0.9493 | 0.9522 | 0.9297 | 0.9847 | 0.9676 | 0.9489 | 0.9392 | 0.9061 | 0.9737 |
| BSCO | 0.9316 | 0.8481 | 0.8215 | 0.8394 | 0.8847 | 0.8439 | 0.8272 | 0.9290 | 0.8050 | 0.9532 |
| BSO2 | 0.9994 | 0.9843 | 0.9973 | 0.9986 | 0.9974 | 0.9930 | 0.9915 | 0.9745 | 0.9878 | 0.9982 |
| BSuHC | 0.4732 | N/A | 0.2293 | 0.5868 | N/A | 0.2127 | N/A | -0.0187 | N/A | 0.1839 |
| EGR % | 0.9802 | 0.9838 | 0.9828 | 0.7252 | 0.9839 | 0.9832 | 0.9864 | 0.9939 | 0.8434 | 0.9960 |

**Table 5-3 $R^2$ for second data set**

2-stage gradient matched solution

| | EGR | Lean | Stoich |
|---|---|---|---|
| Torque | 0.963 | 0.935 | 0.814 |
| BSFC | 0.784 | 0.820 | 0.655 |
| BSNOx | 0.853 | 0.716 | 0.741 |
| BSCO2 | 0.739 | 0.784 | 0.946 |
| BSCO | 0.227 | 0.221 | 0.341 |
| BSuHC | 0.750 | 0.946 | 0.750 |
| BSO2 | 0.319 | 0.920 | 0.450 |
| EGR % | 0.540 | 0.630 | 0.950 |

5th order regression model

| | EGR | Lean | Stoich |
|---|---|---|---|
| Torque | 0.958 | 0.941 | 0.860 |
| BSFC | 0.739 | 0.851 | 0.618 |
| BSNOx | 0.723 | 0.539 | 0.852 |
| BSCO2 | 0.808 | 0.765 | 0.961 |
| BSCO | 0.183 | 0.238 | 0.211 |
| BSuHC | 0.730 | 0.936 | 0.640 |
| BSO2 | 0.450 | 0.890 | 0.450 |
| EGR % | 0.560 | 0.564 | 0.941 |

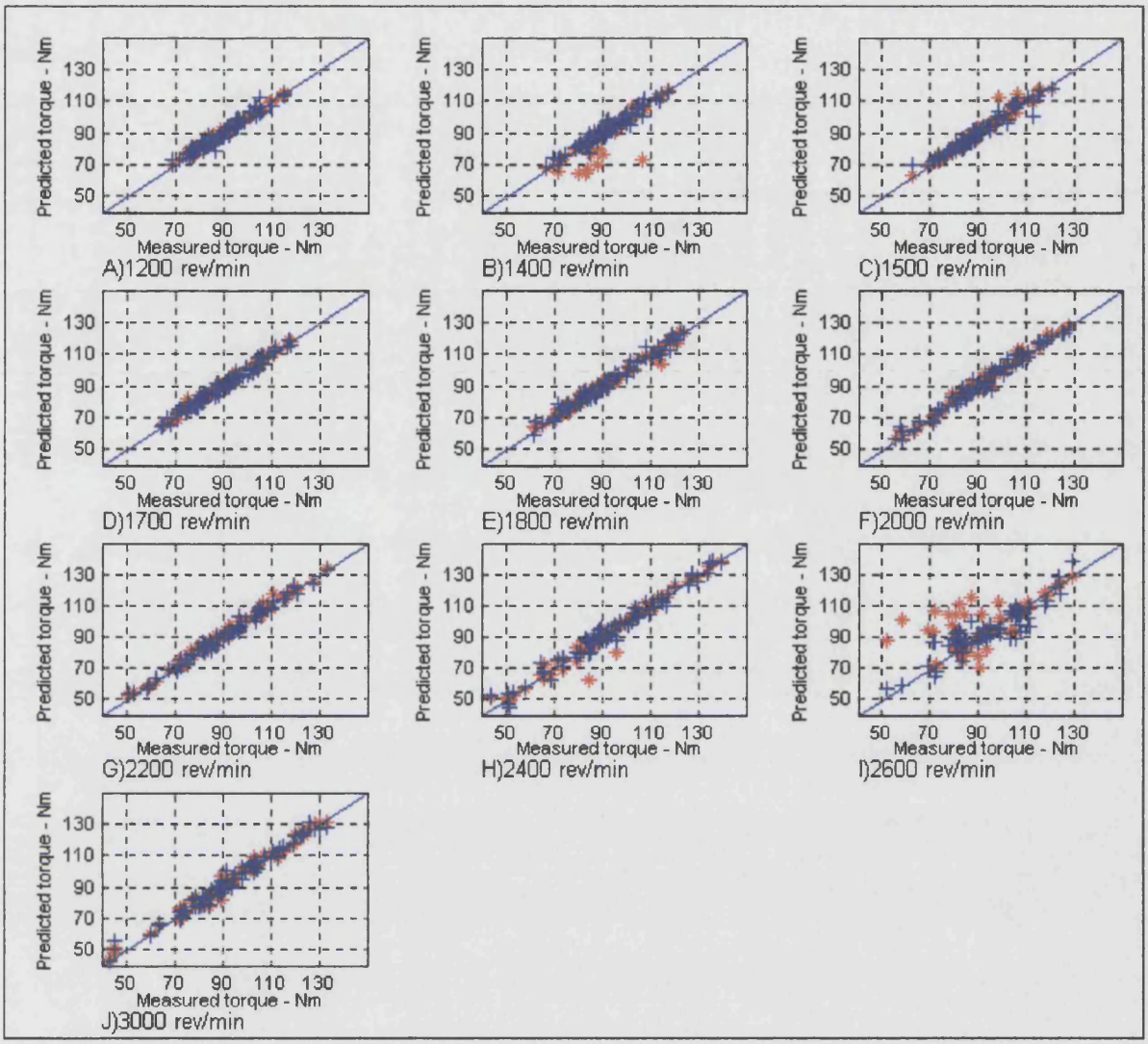


Figure 5-1 Observed versus predicted plot for engine torque response

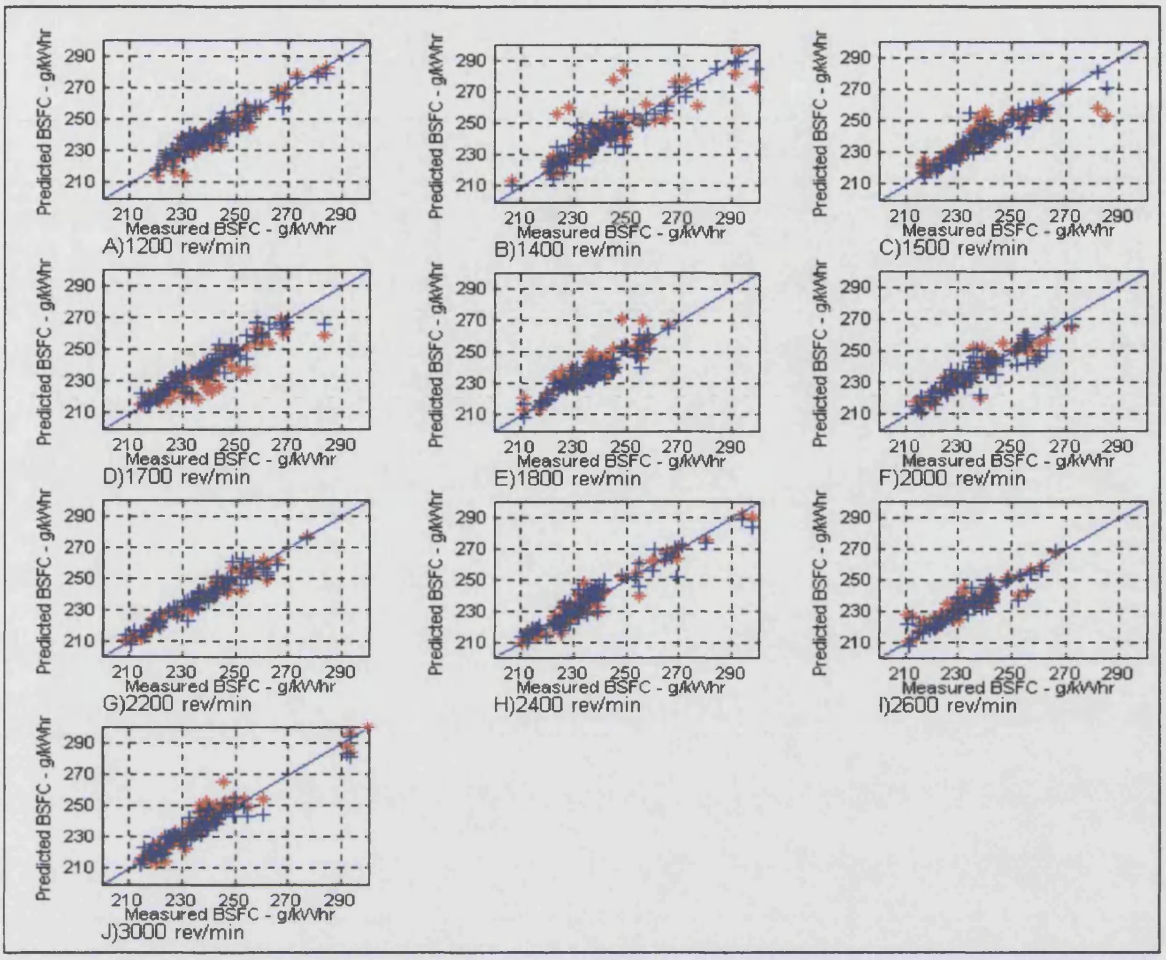


**Figure 5-2 Observed versus predicted plot for specific fuel consumption**

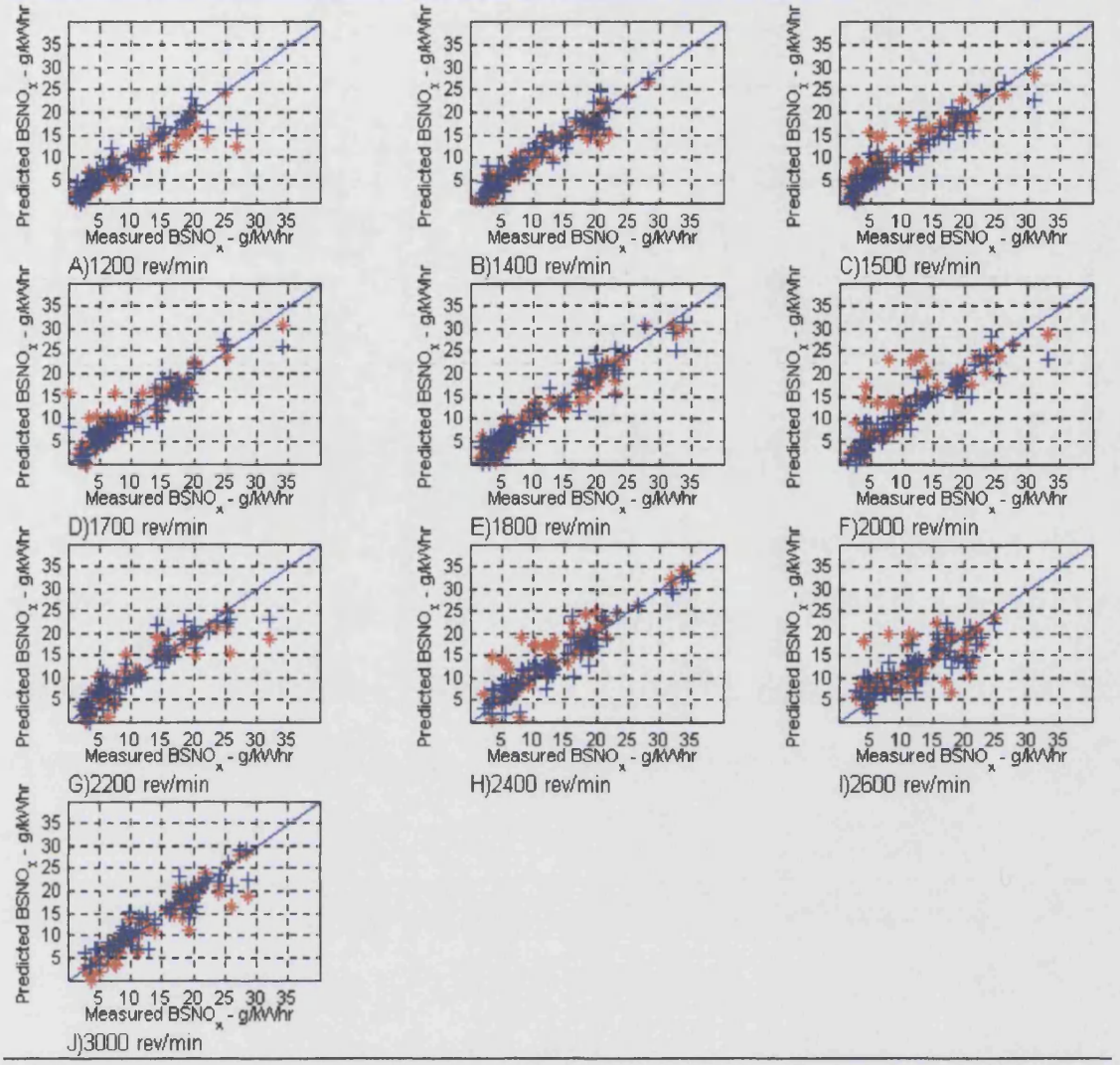


**Figure 5-3 Observed verses predicted plot for specific $NO_x$ emissions**

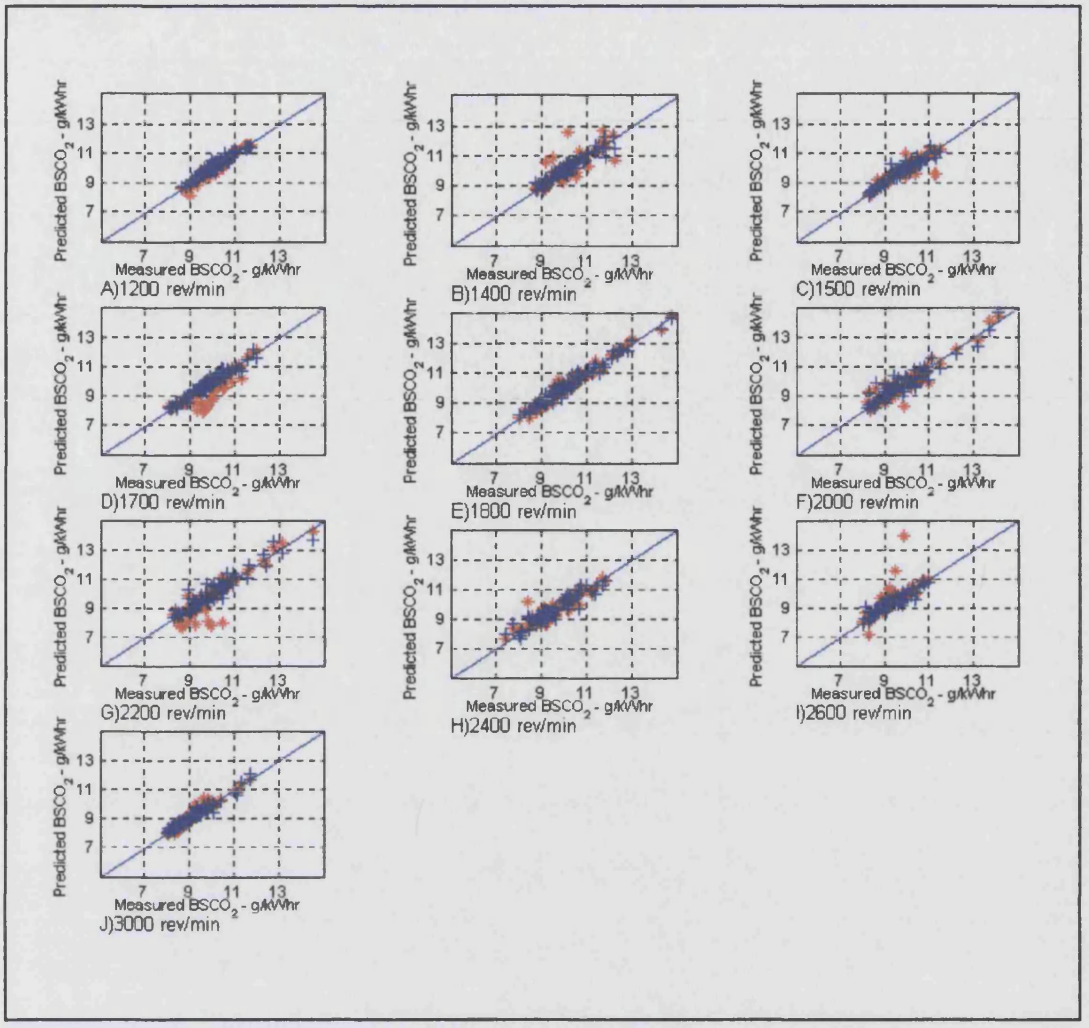


**Figure 5-4 Observed verses predicted plot for specific $CO_2$ emissions**

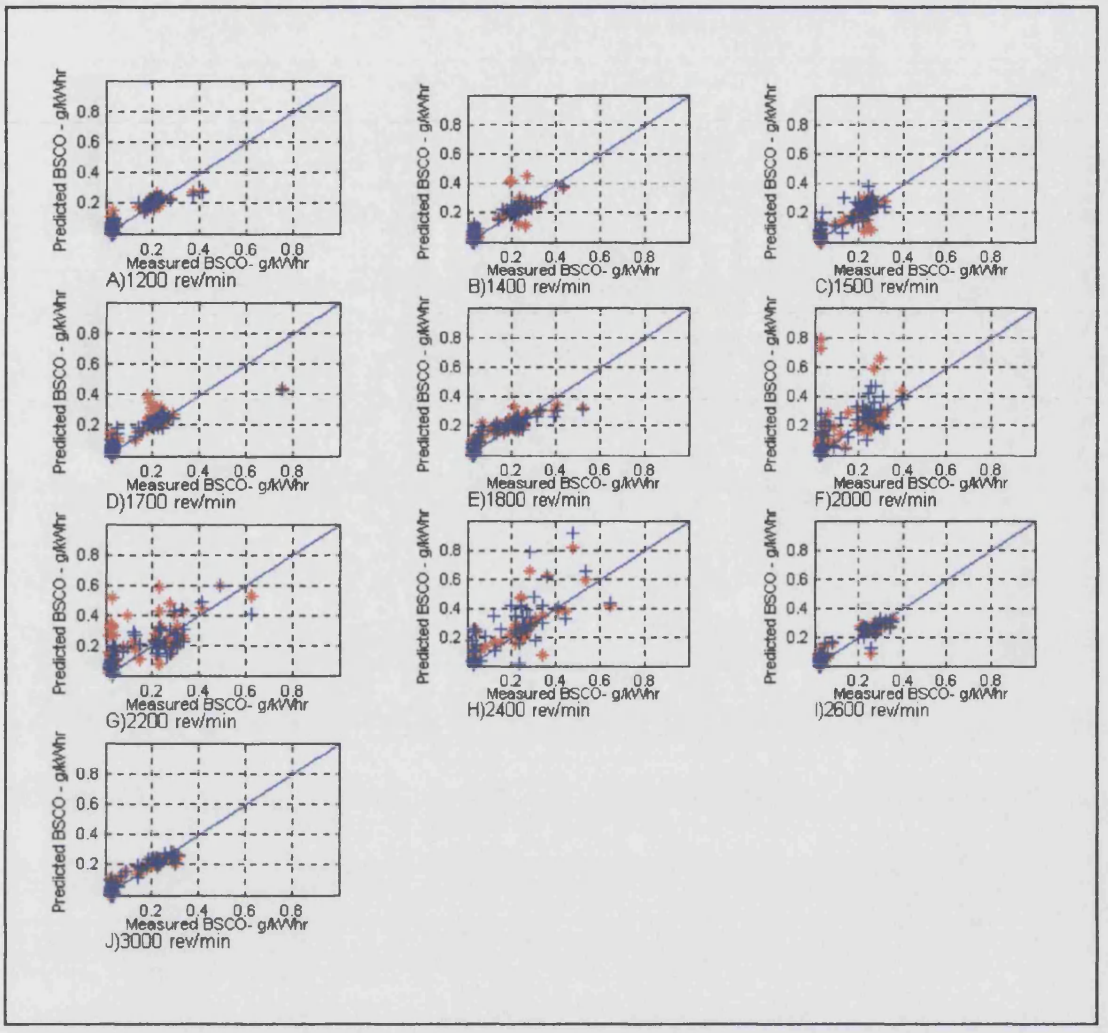


**Figure 5-5 Observed versus predicted plot for specific CO emissions**

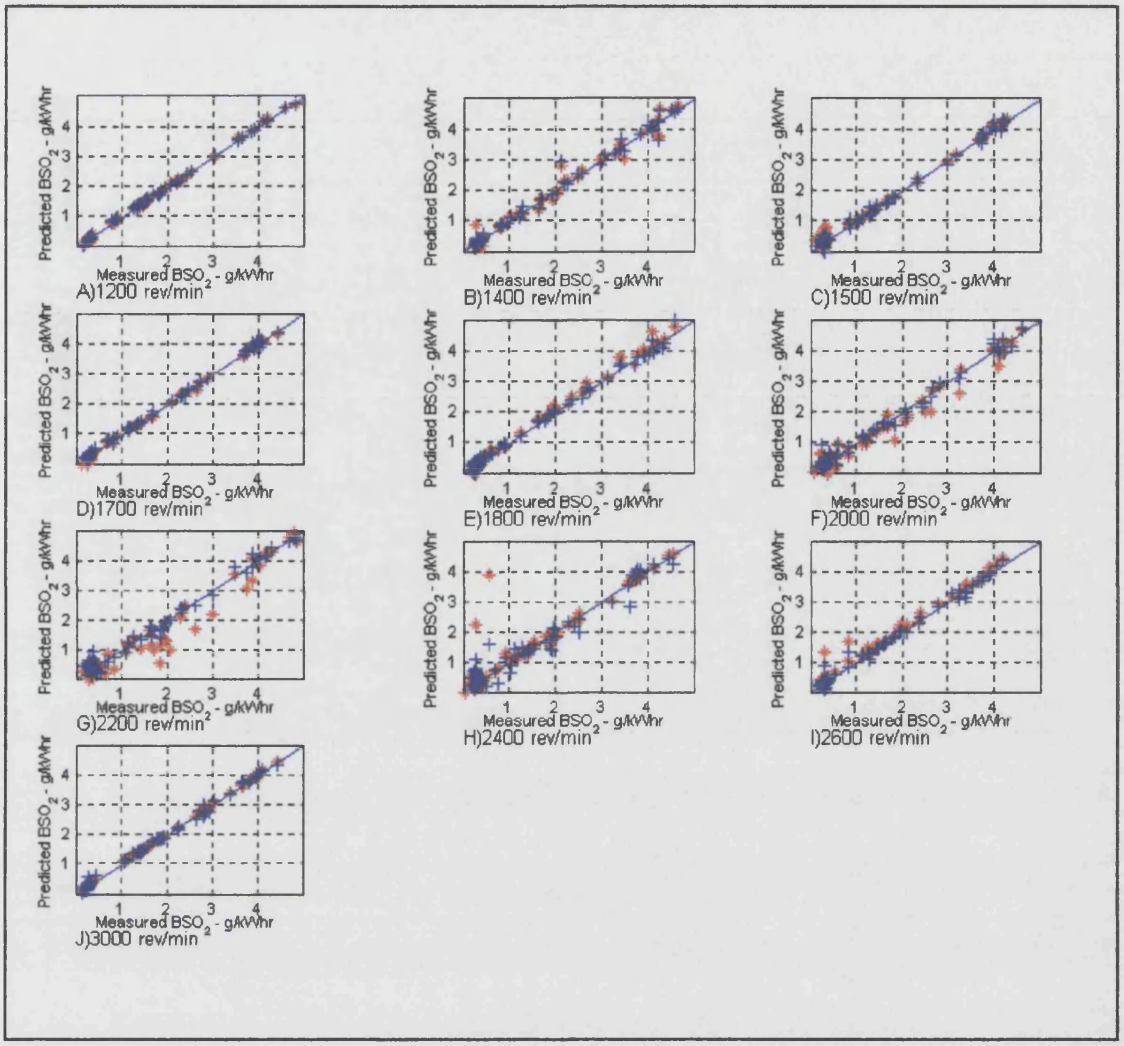


**Figure 5-6 Observed versus predicted plot for specific $O_2$ emissions**

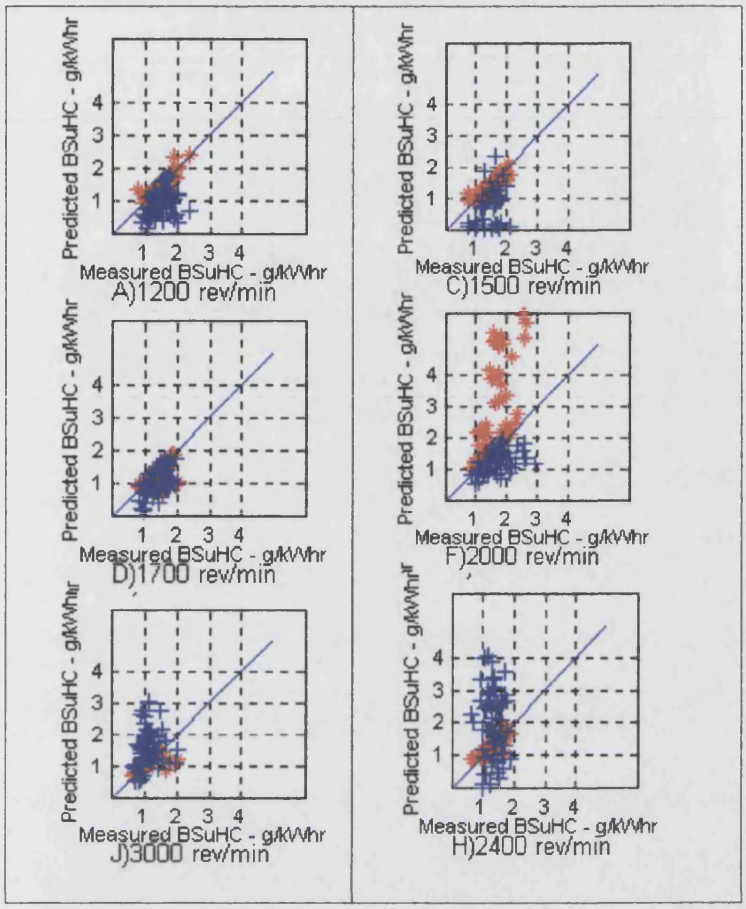


**Figure 5-7 Observed versus predicted plot for specific uHC emissions**

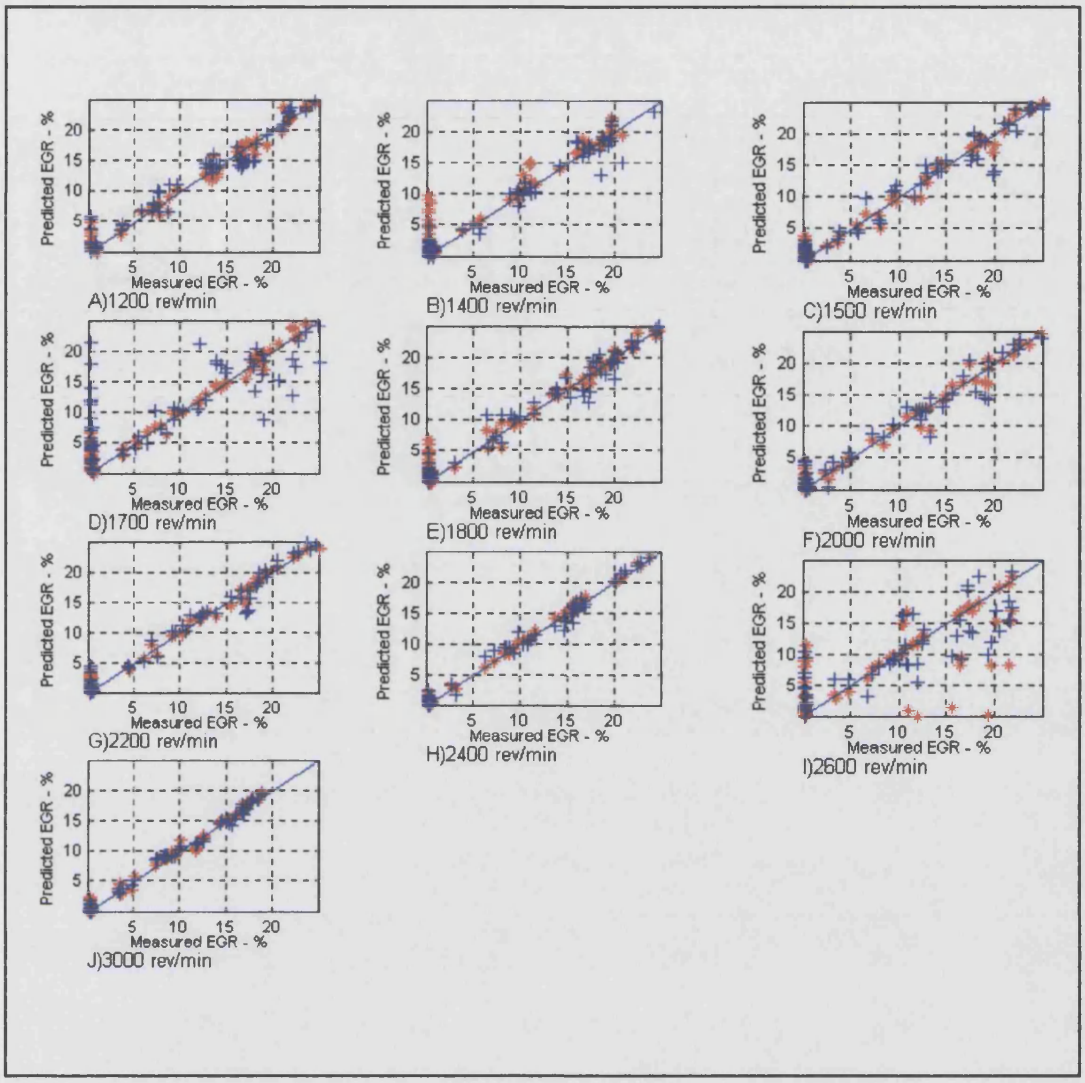


**Figure 5-8 Observed versus predicted plot for percentage EGR response**

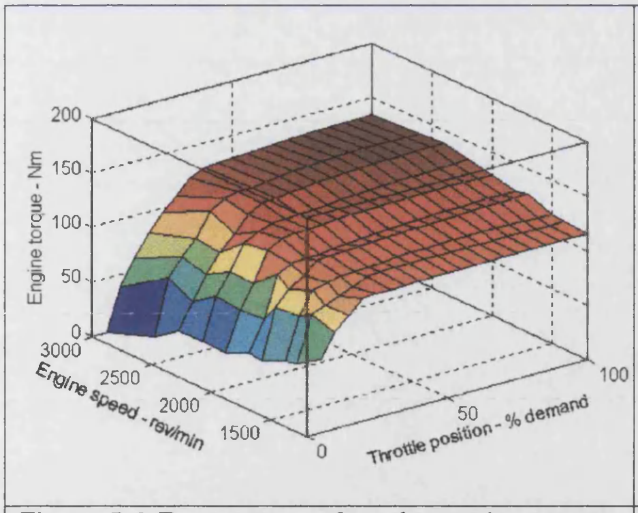


Figure 5-9 Response surface for engine torque - developed via gradient matched solution

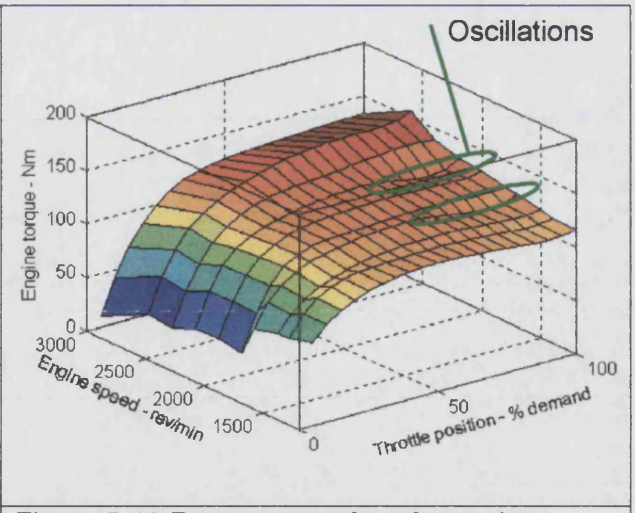


Figure 5-10 Response surface for engine torque - developed via Fifth order regression model

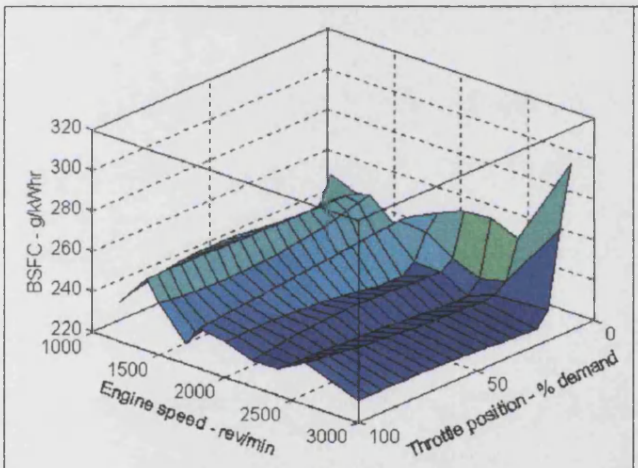


Figure 5-11 BSFC response surface developed using two stage gradient method

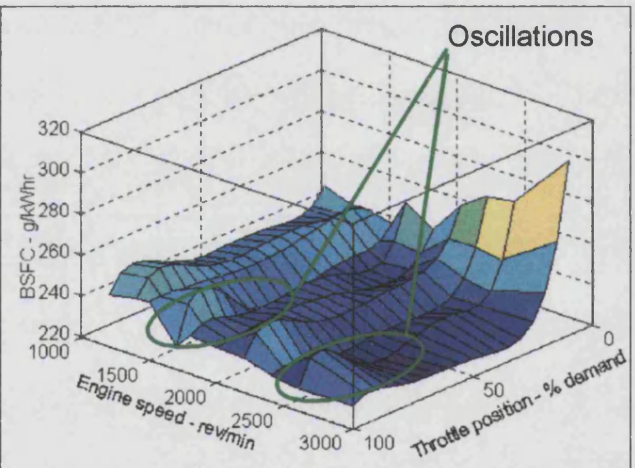


Figure 5-12 BSFC response surface developed using fifth order method

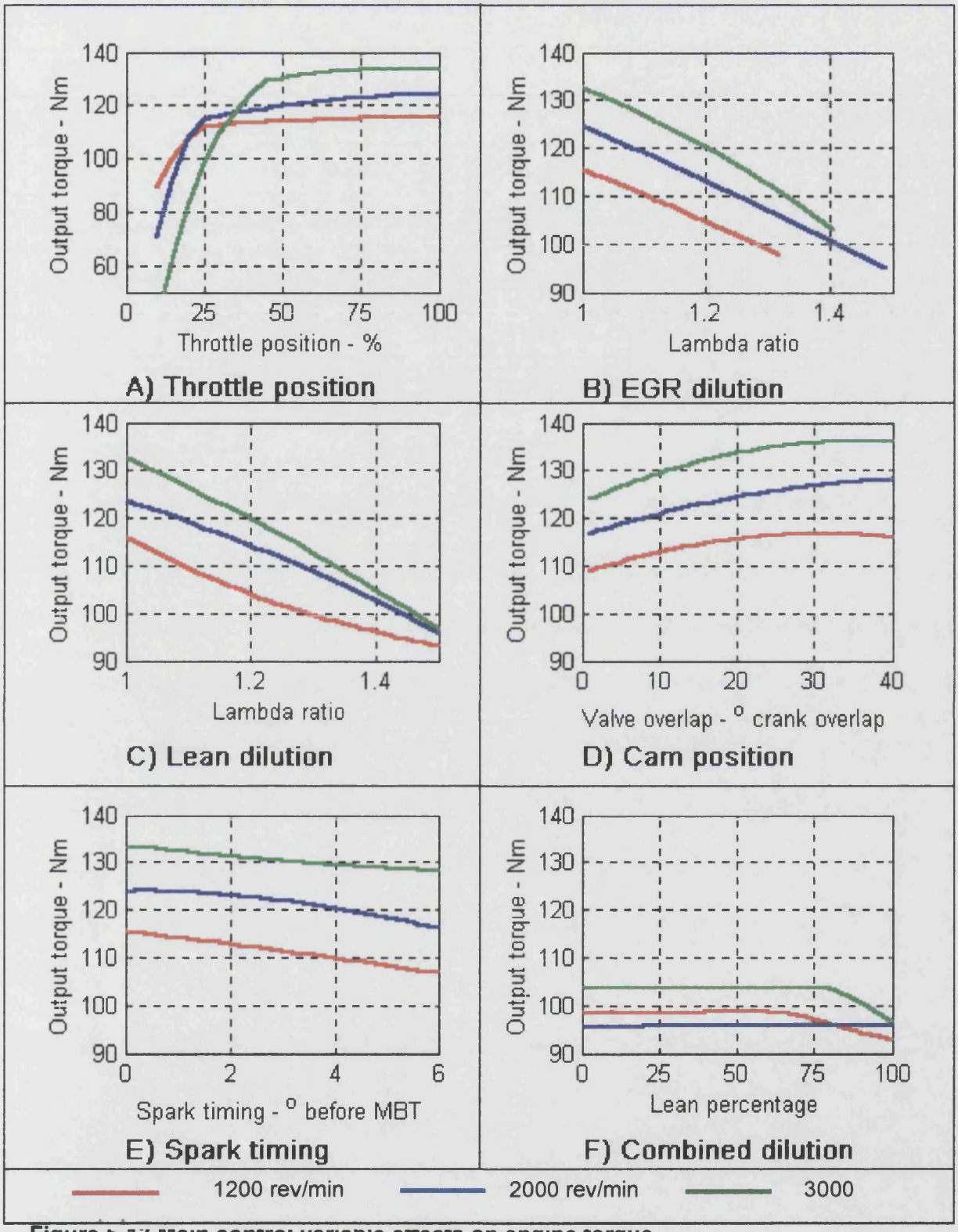


**Figure 5-13 Main control variable effects on engine torque**

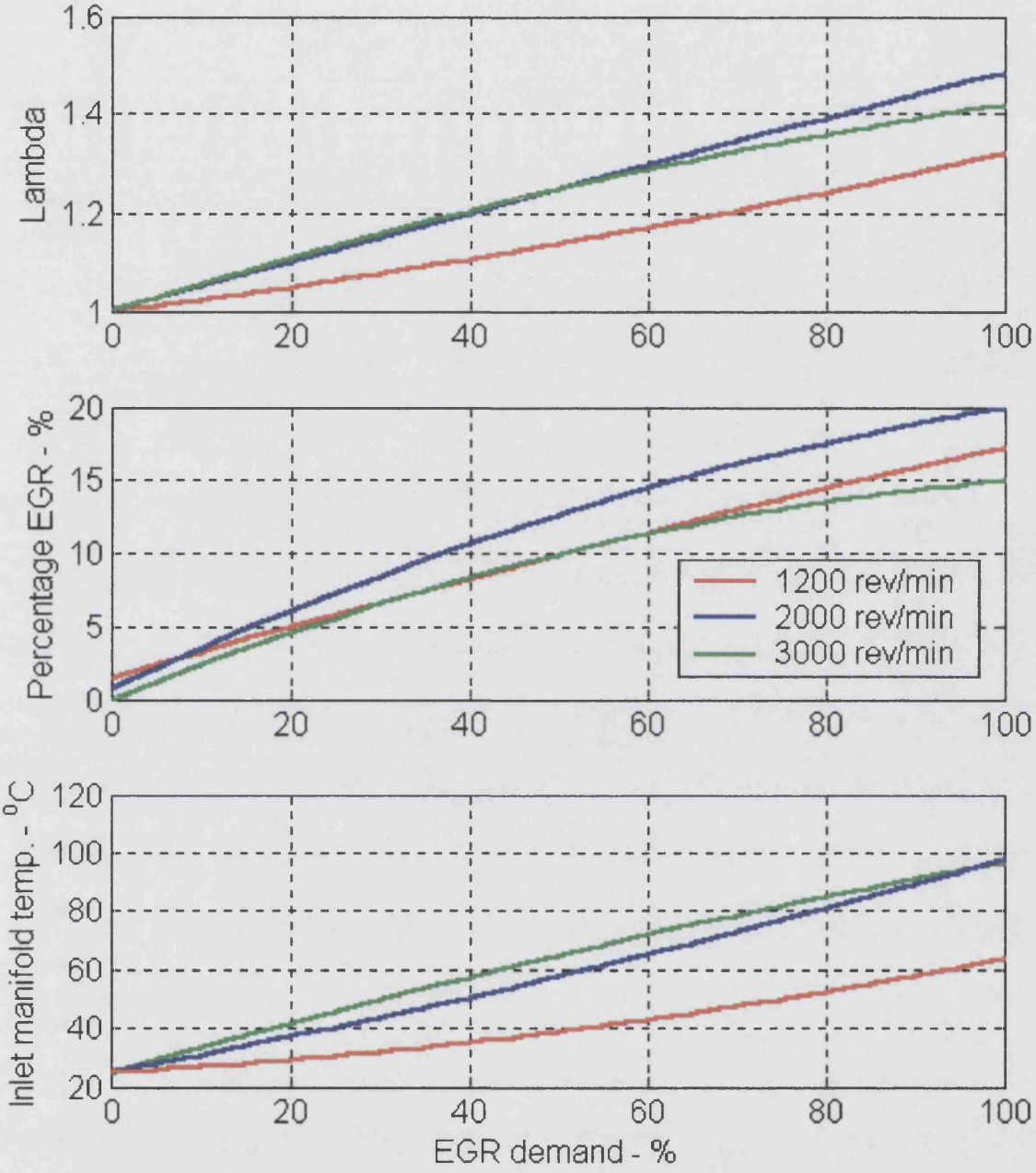


**Figure 5-14 Effect of EGR valve demand upon lambda ratio, EGR percentage and inlet temperature**

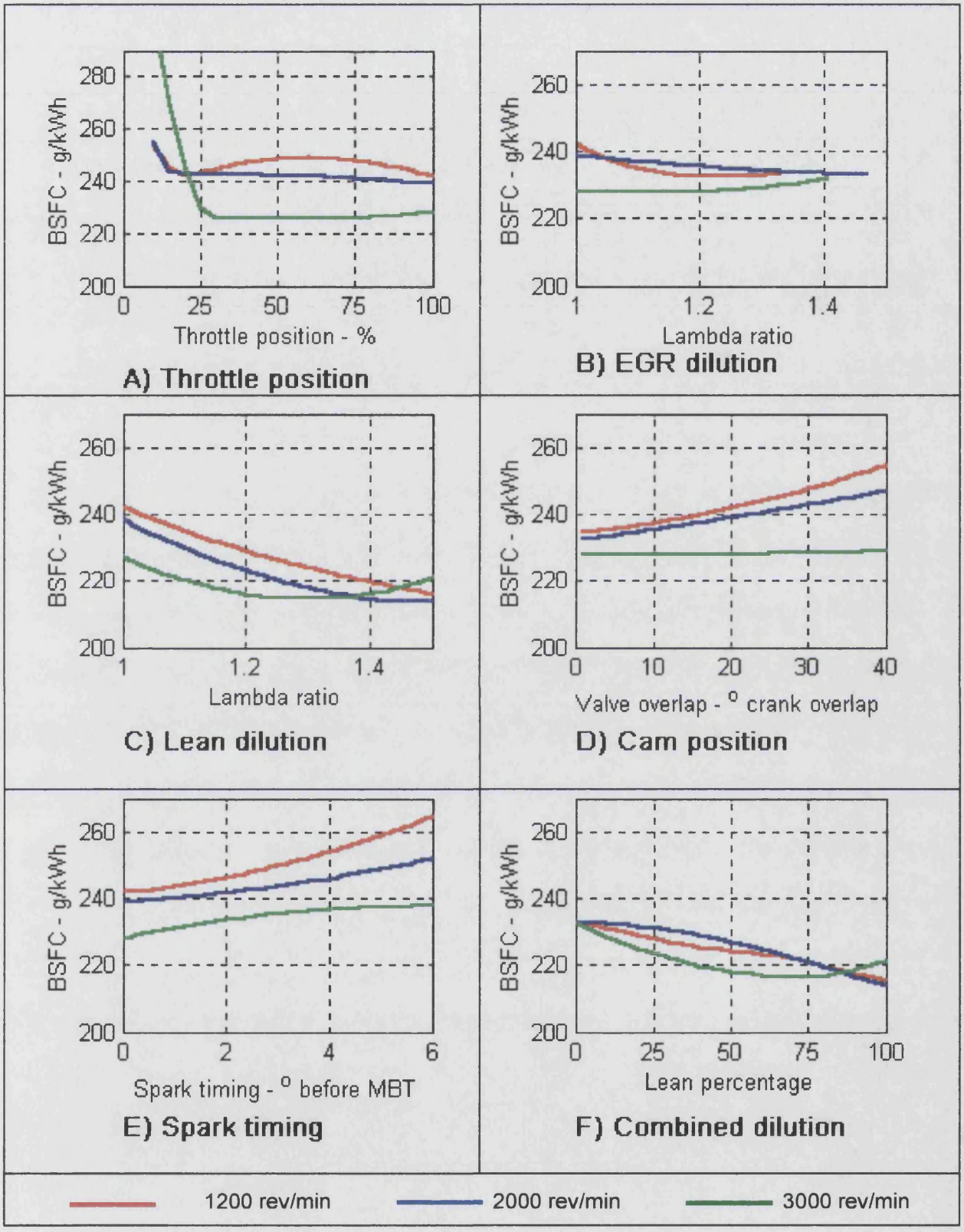


**Figure 5-15 Main control variable effects on specific fuel consumption**

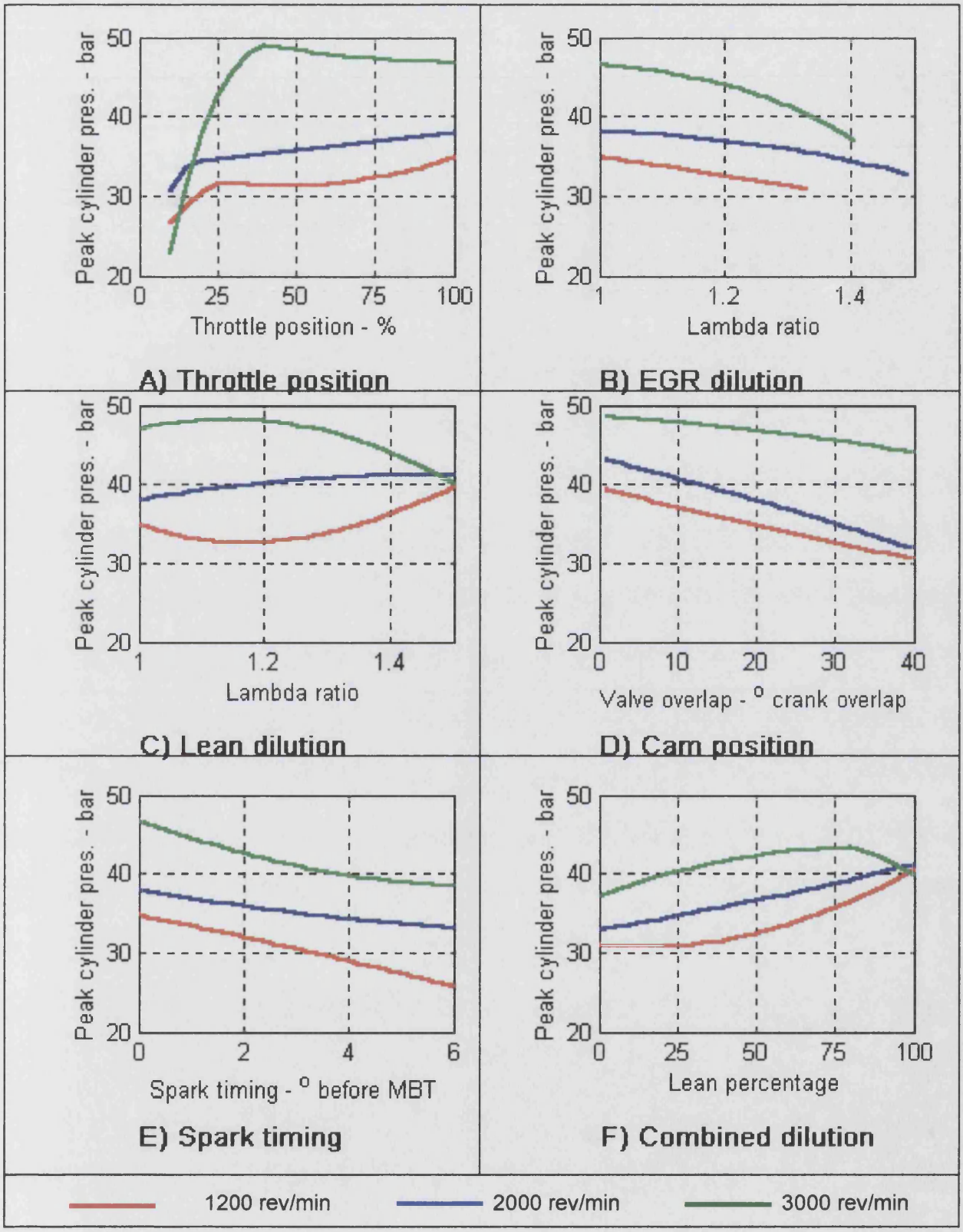


**Figure 5-16 Main effect of control variables on peak combustion pressure**

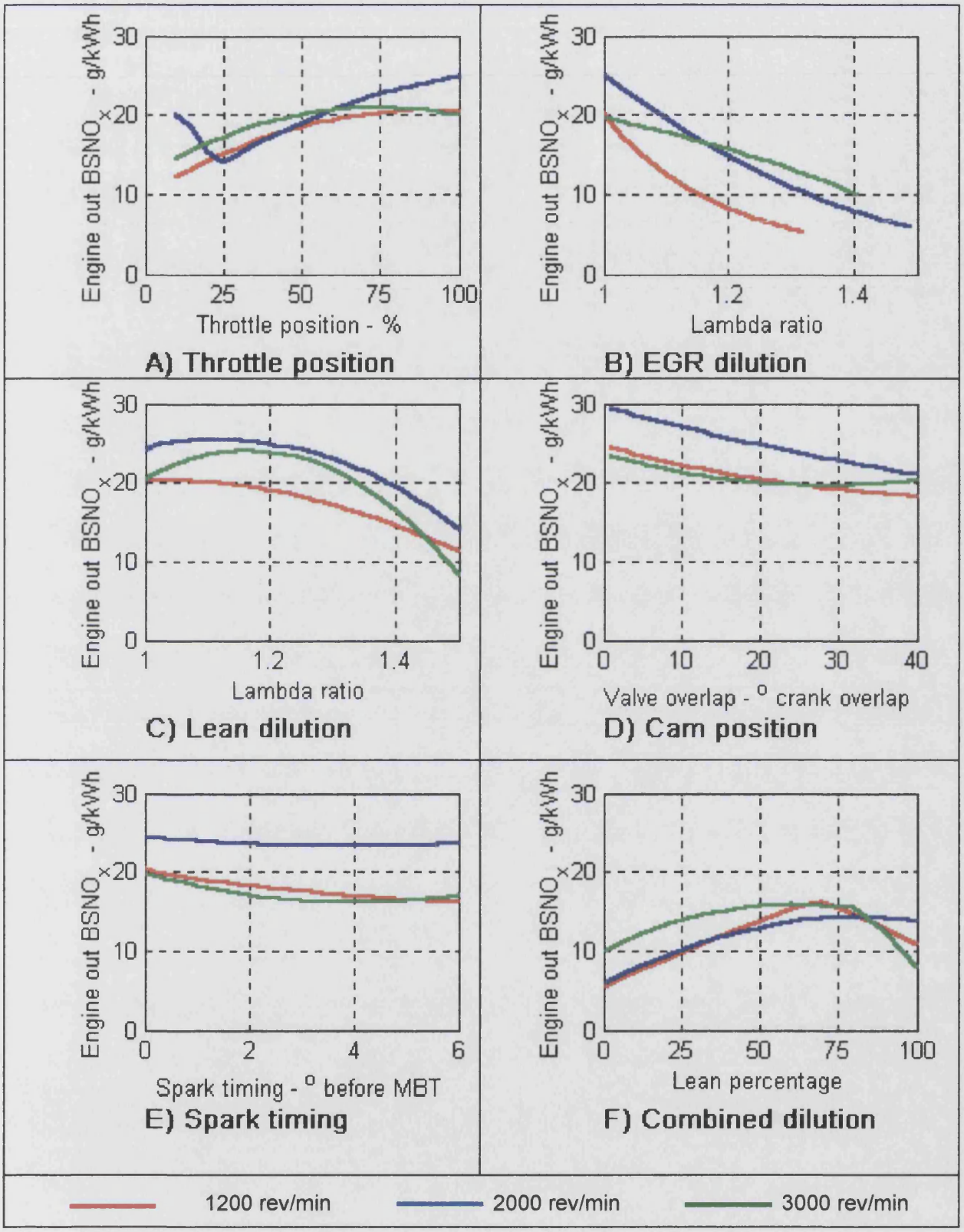


**Figure 5-17 Main control variable effects on specific $NO_x$ emissions**

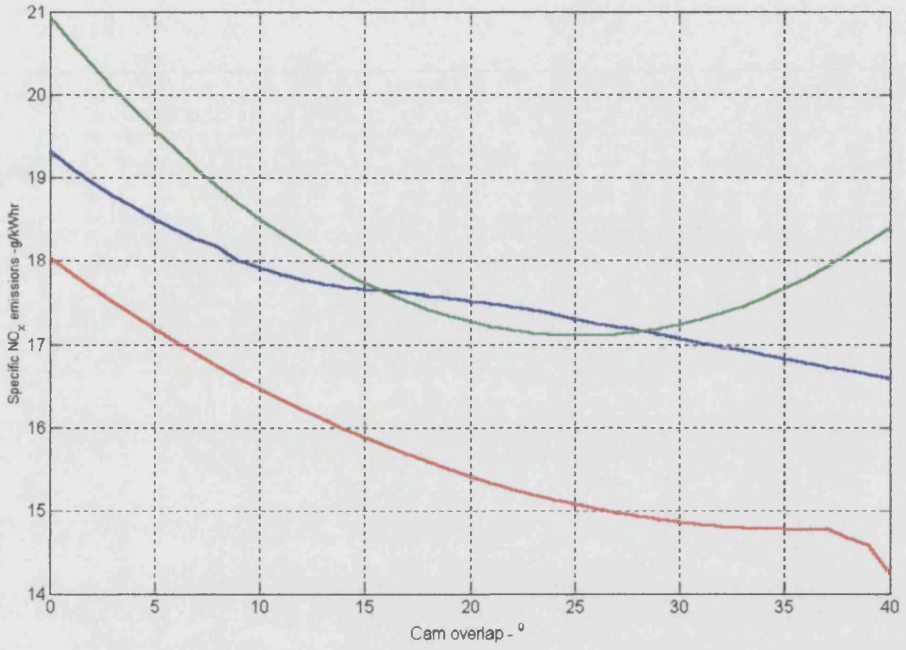


**Figure 5-18 Specific $NO_x$ emissions over cam overlap swings at part throttle conditions**

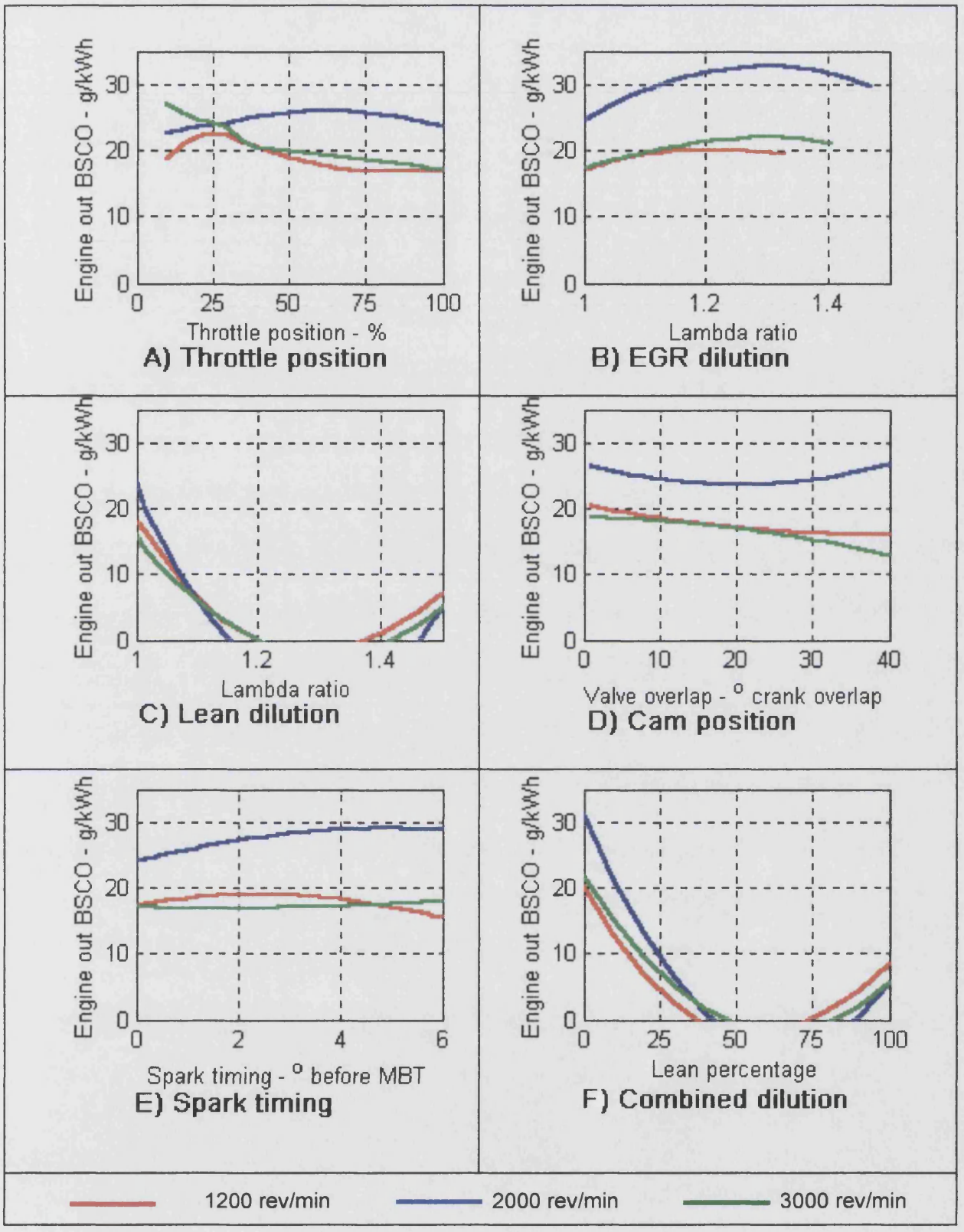


**Figure 5-19 Main control variable effects on specific CO emissions**

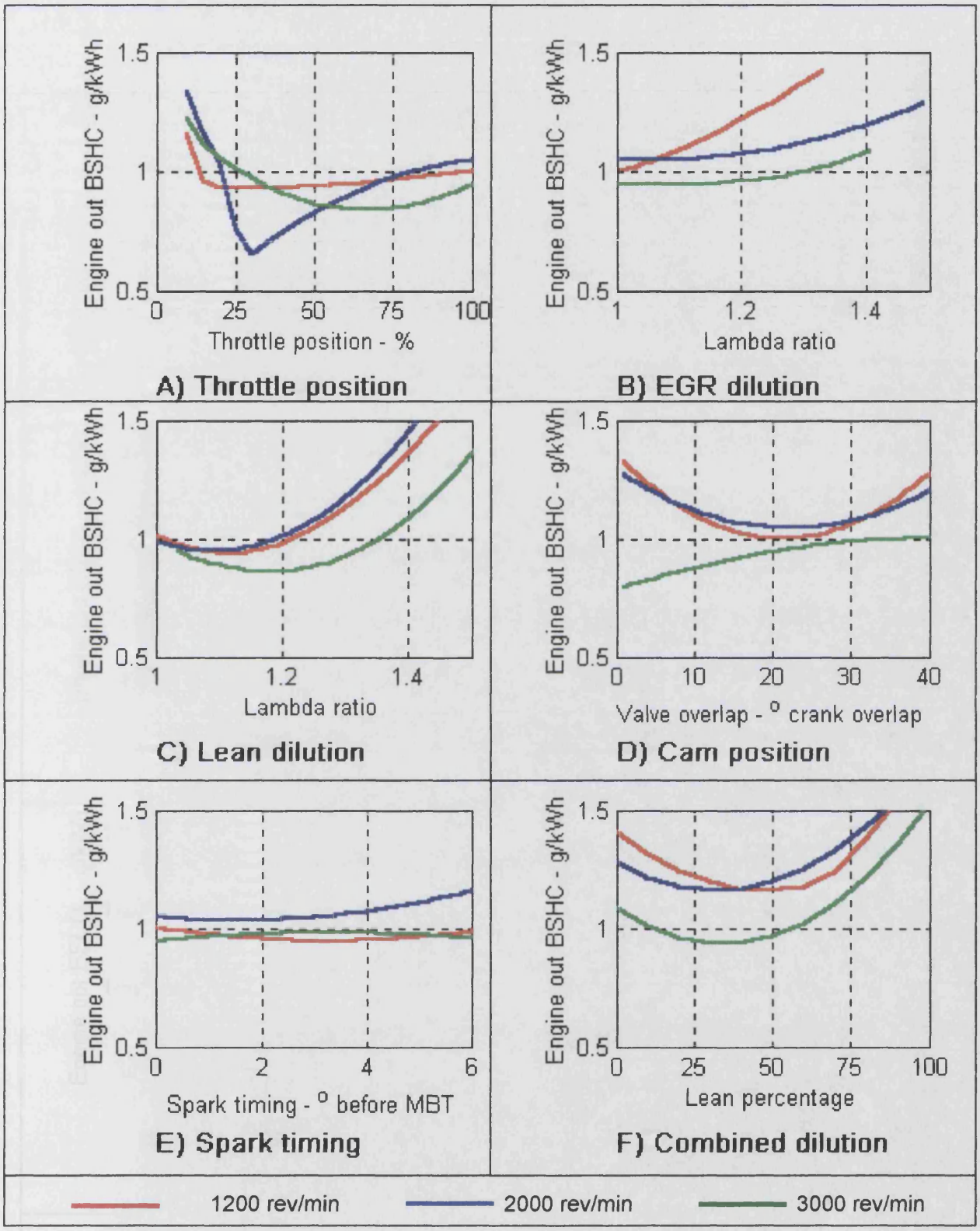


**Figure 5-20 Main control variable effects on specific uHC emissions**

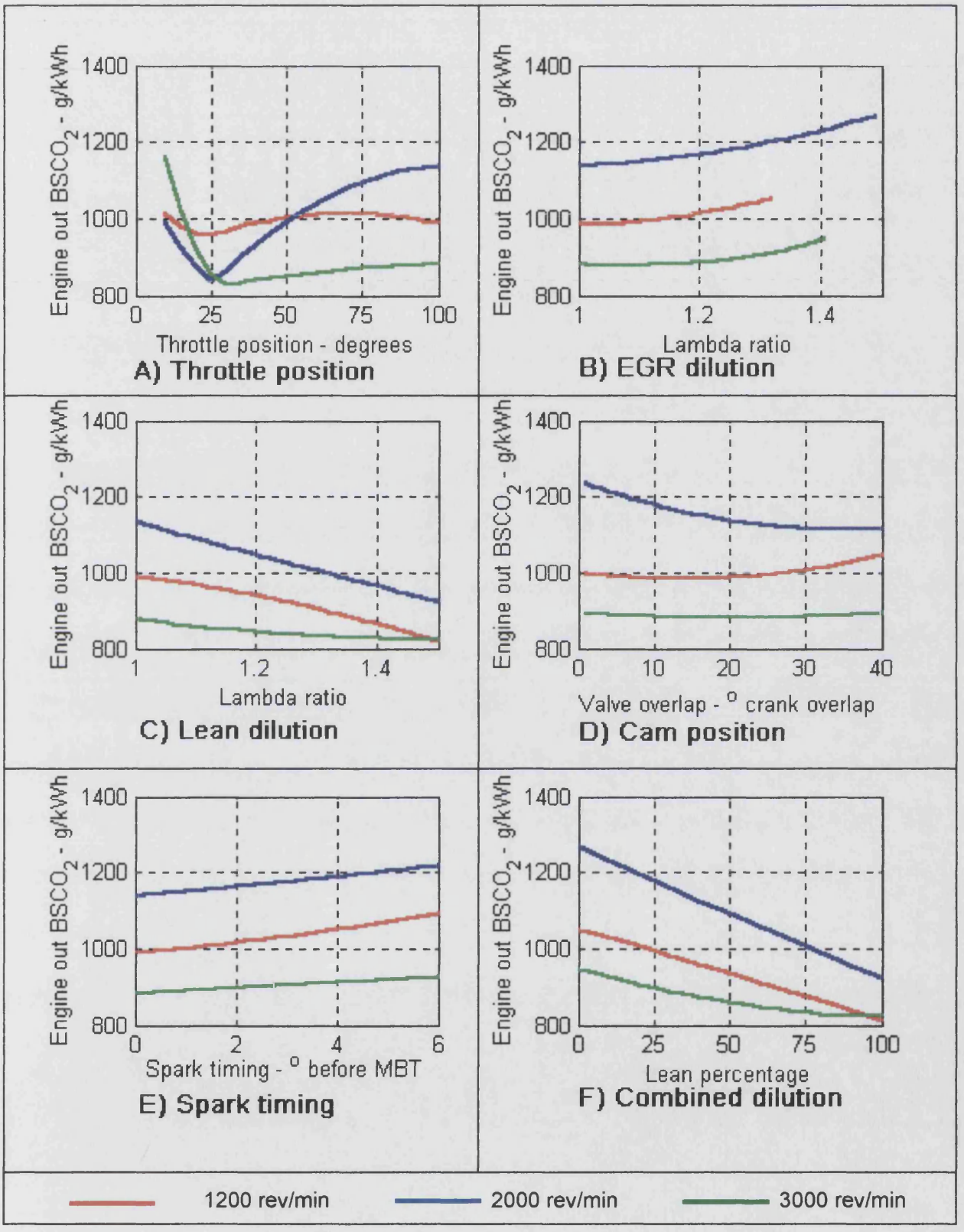


**Figure 5-21 Main effect of control variables on specific $CO_2$ emissions**

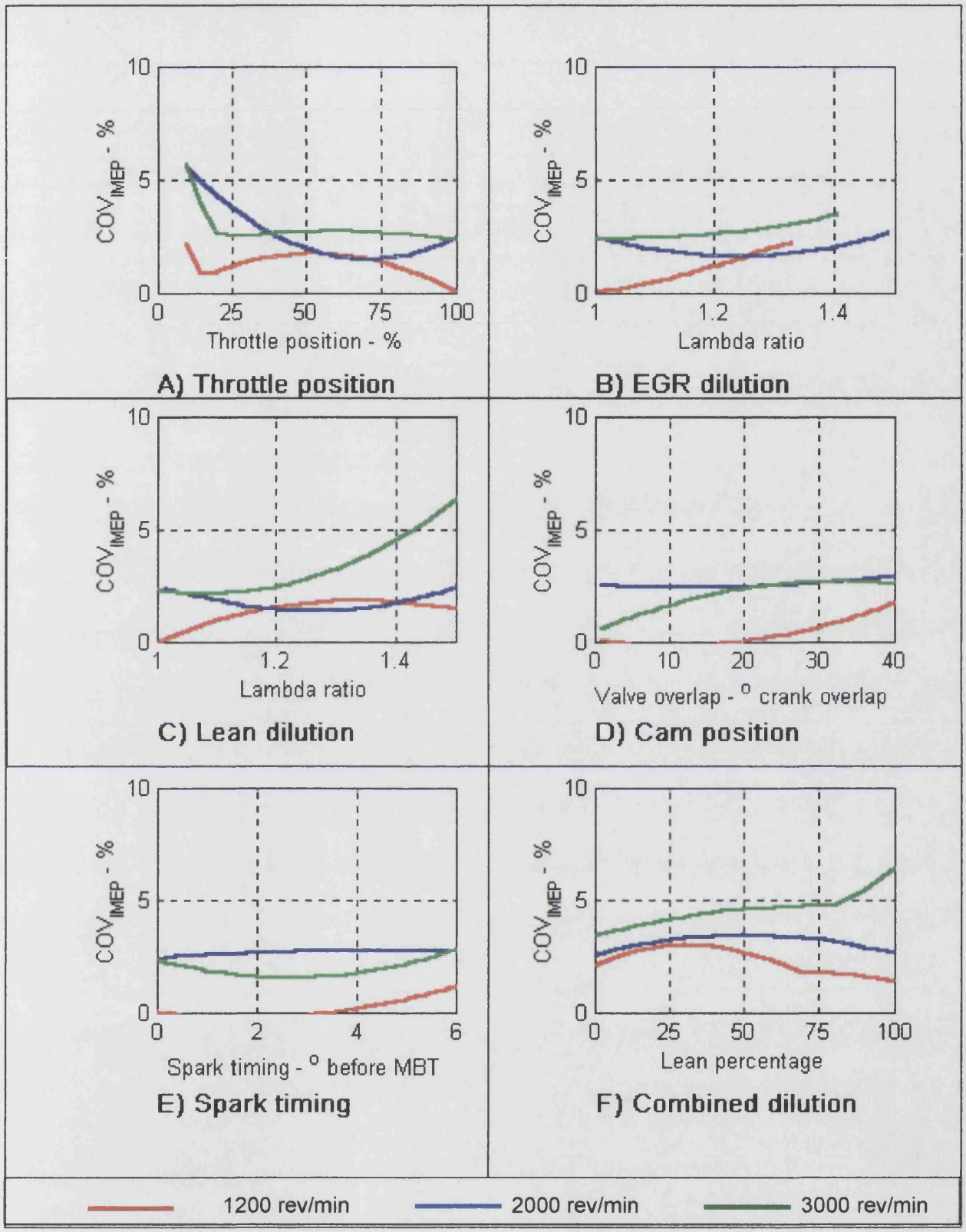


**Figure 5-22 Main affect of control variables on combustion stability**

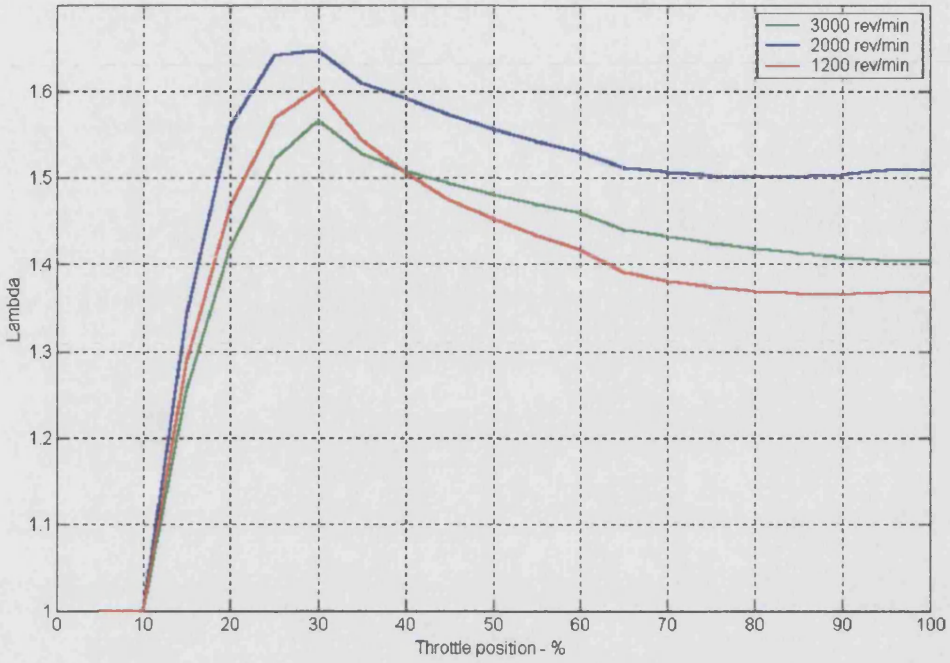


**Figure 5-23 EGR dilution across the throttle range**

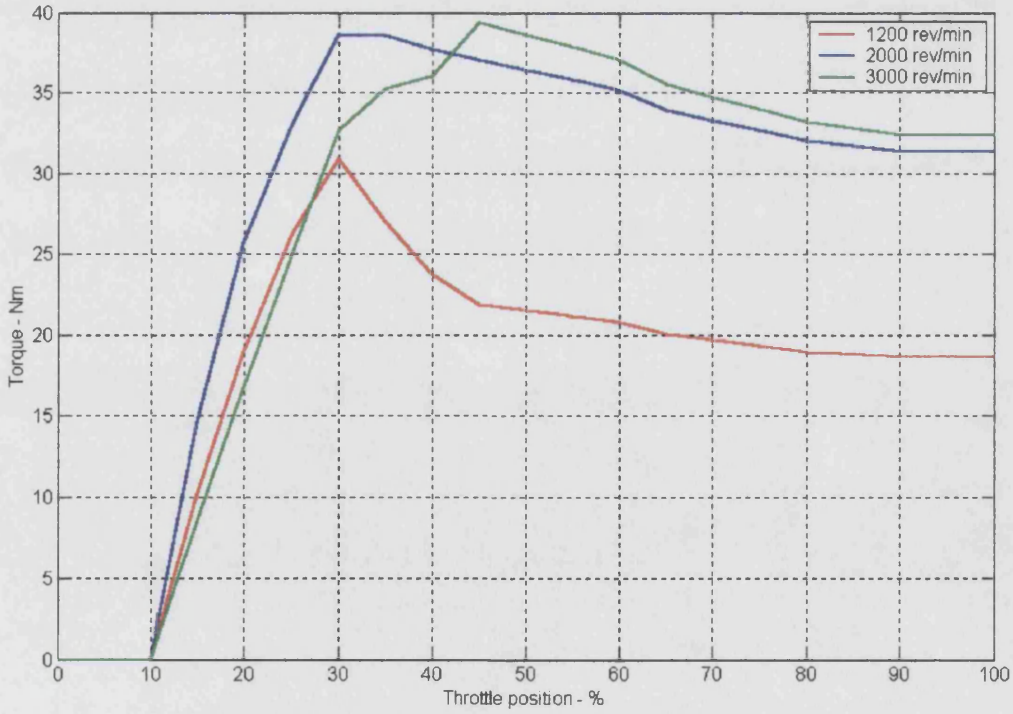


**Figure 5-24 Torque margin developed via EGR dilution across engine throttle range**

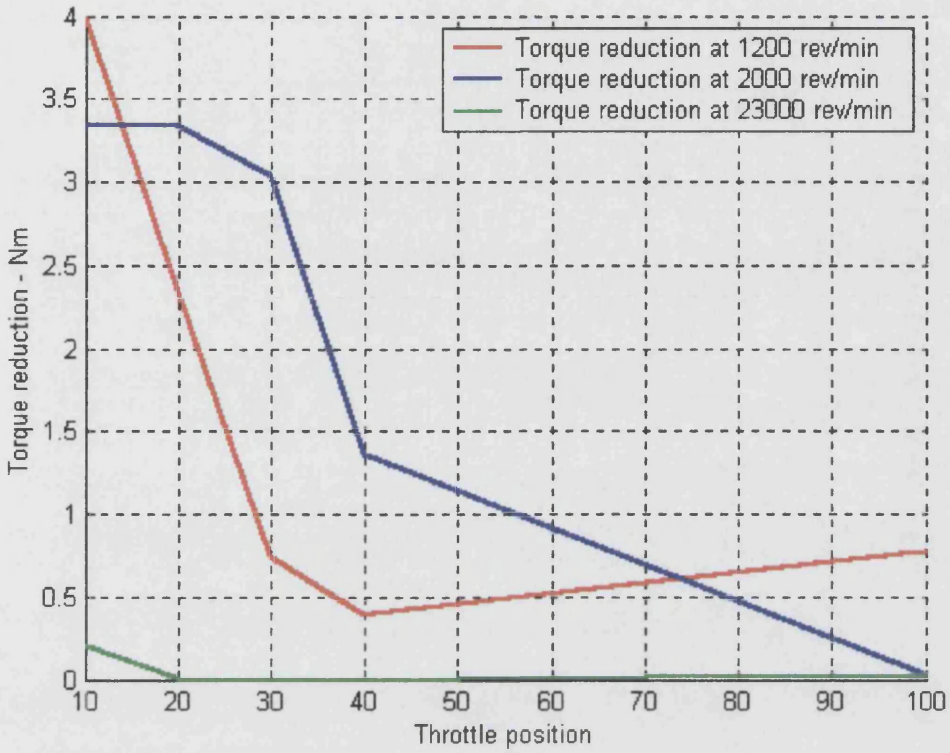


**Figure 5-25 Reduction in engine torque by iEGR charge dilution over full throttle range**

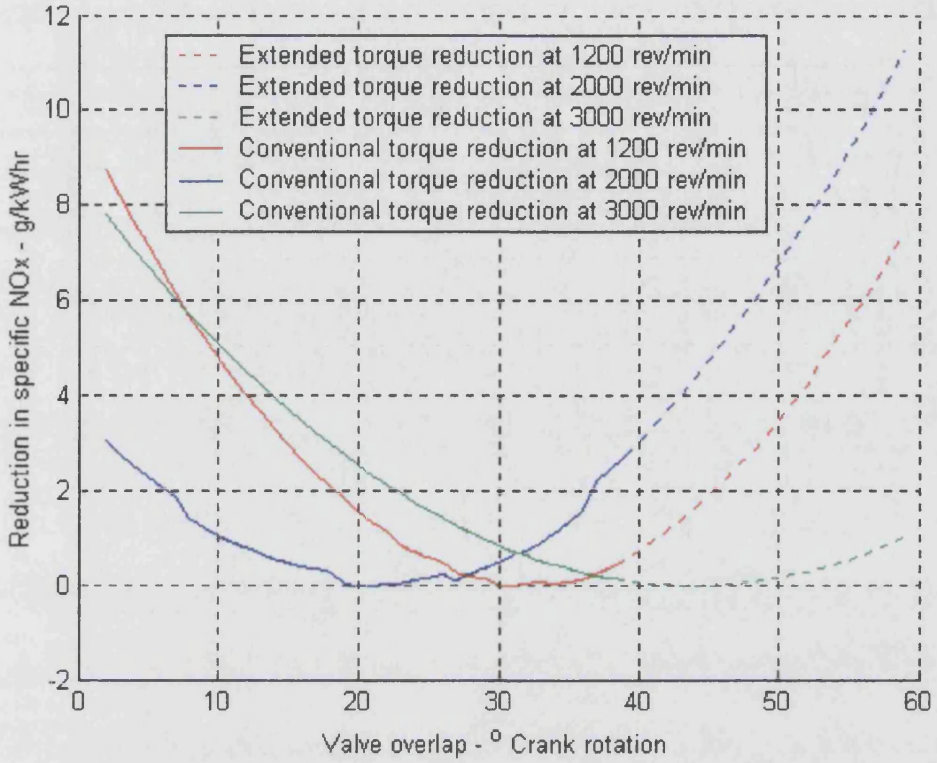


**Figure 5-26 Reduction in engine torque achieved by extending the valve overlap range**

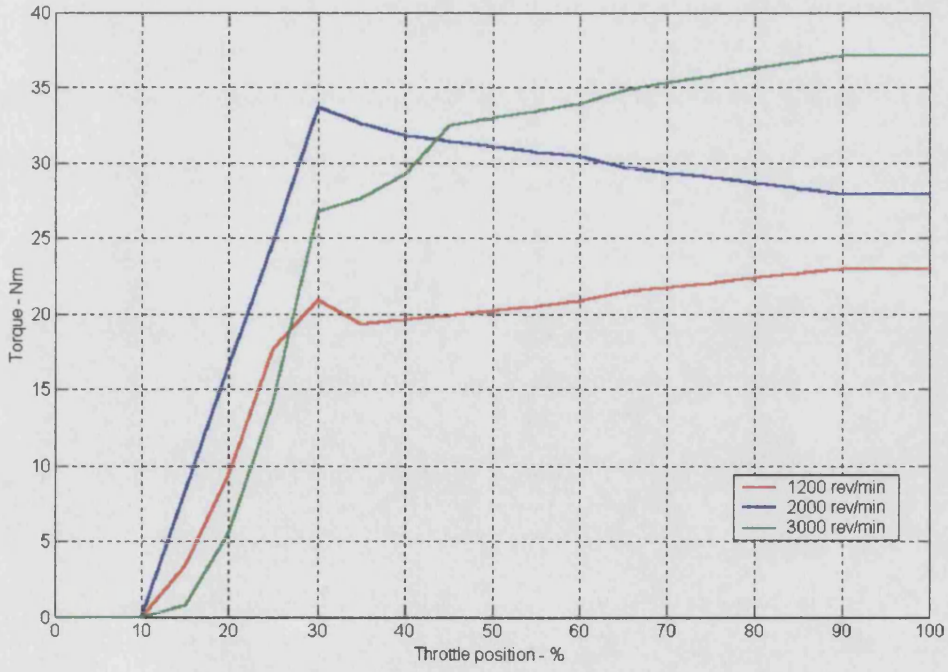


**Figure 5-27 Torque margin available over throttle range for lean charge dilution**

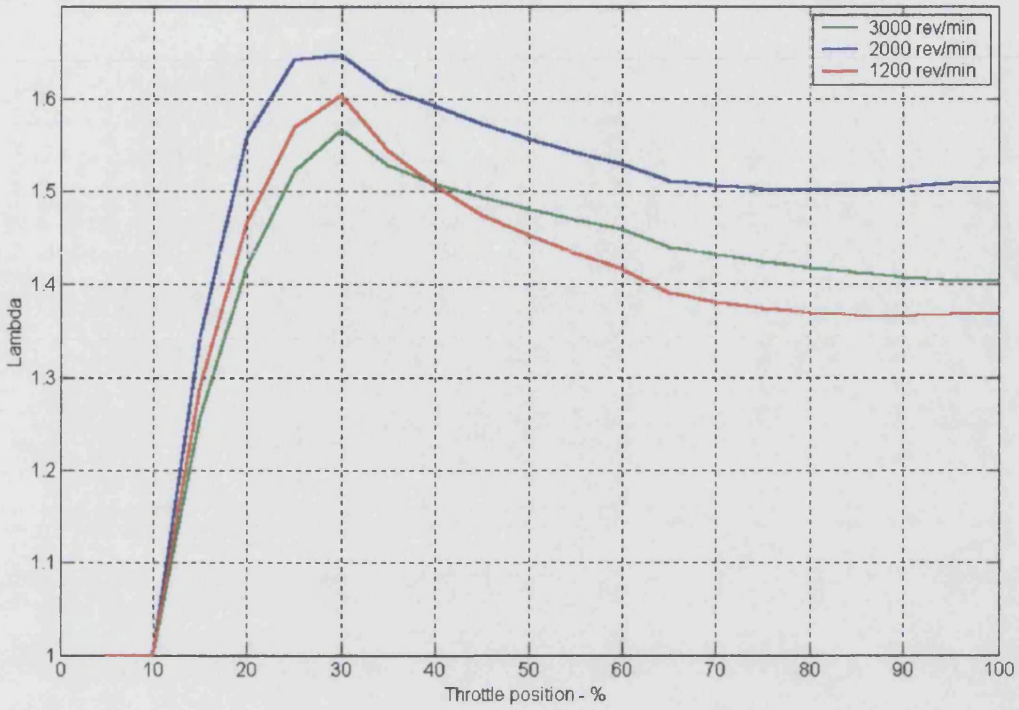


**Figure 5-28 EGR flow rate for 100% EGR demand across a throttle range**

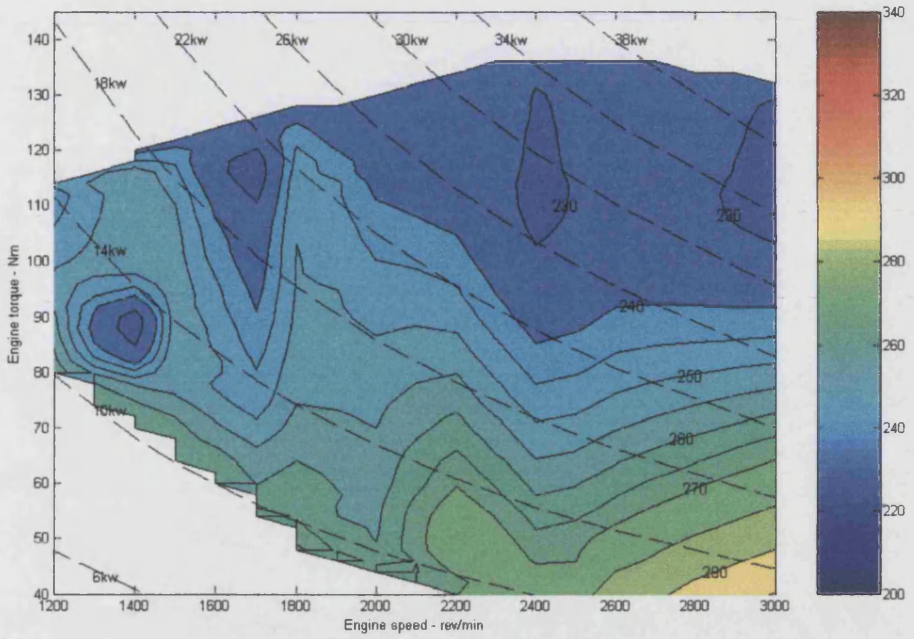


**Figure 5-29 Fuel consumption map for engine - Stoichiometrically fuelled**

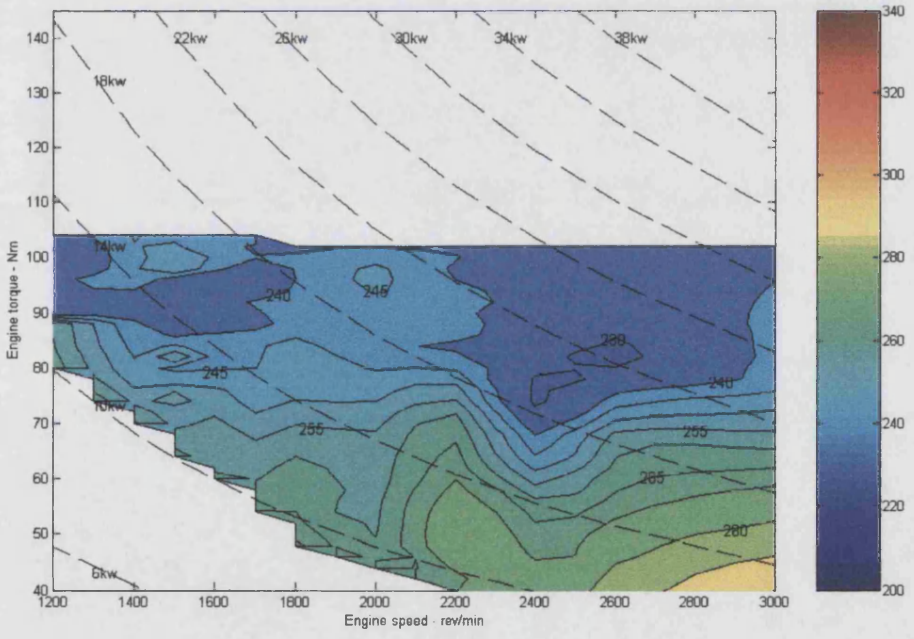


**Figure 5-30 Fuel consumption map for engine - Stoichiometrically fuelled EGR 100% demand**

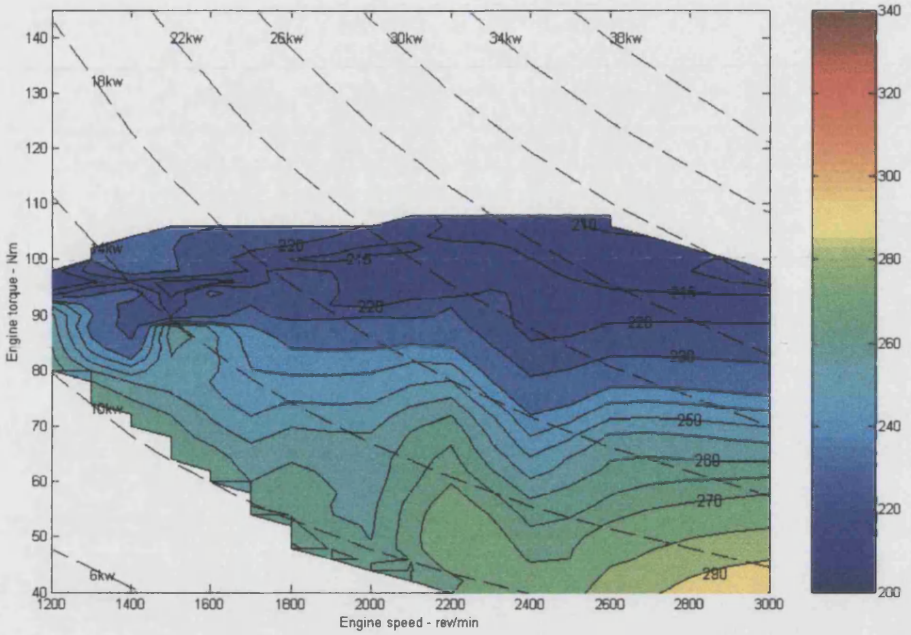


**Figure 5-31 Fuel consumption map for engine - 100% lean demand fuelling**

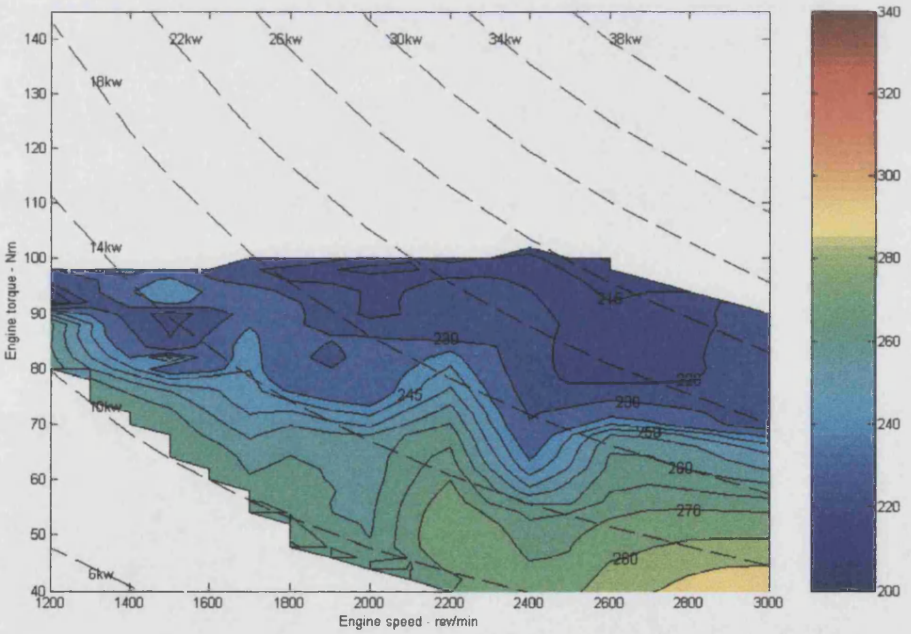


**Figure 5-32 Fuel consumption map for engine - 100% lean demand 100% EGR demand**

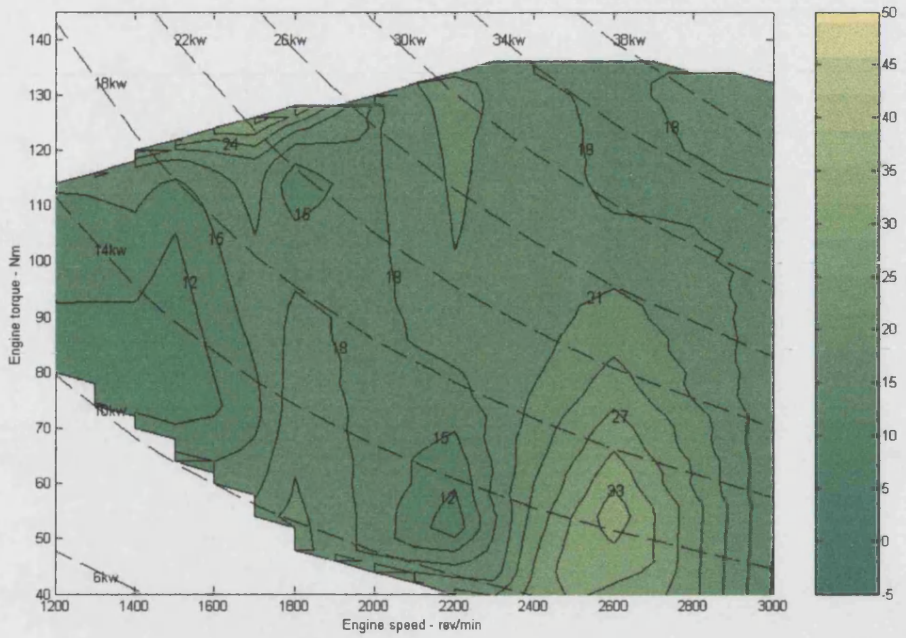


**Figure 5-33 $NO_x$ emissions map of engine torque speed region - stoichiometrically fuelled**

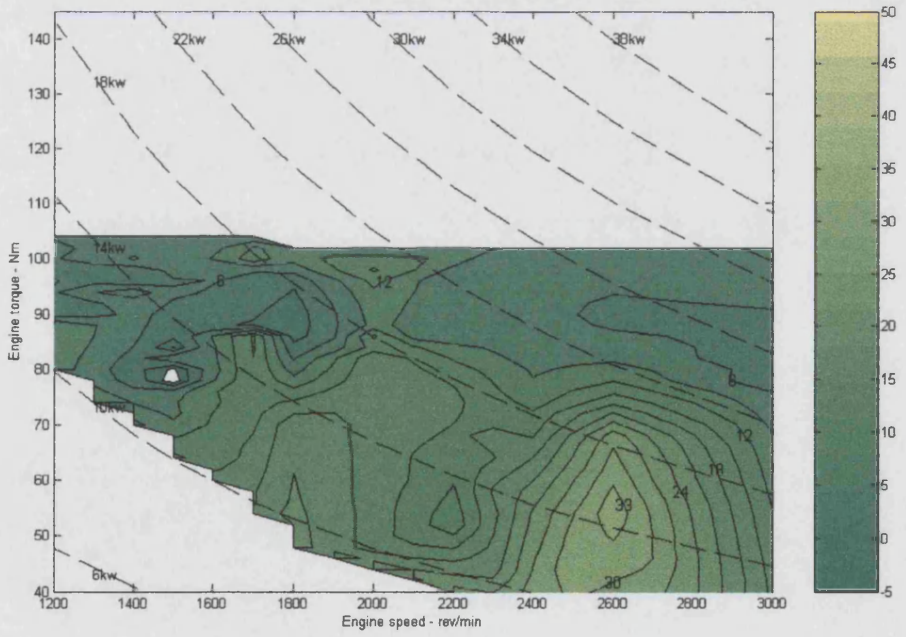


**Figure 5-34 $NO_x$ emissions map of engine torque speed region - stoichiometrically fuelled 100% EGR demand**

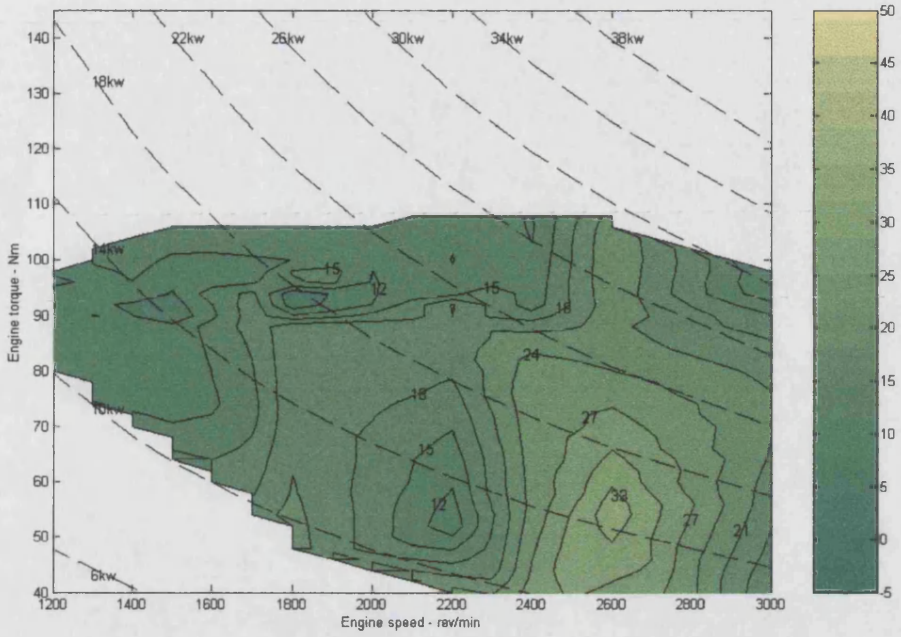


**Figure 5-35 $NO_x$ emissions map of engine torque speed region - 100% lean demand**

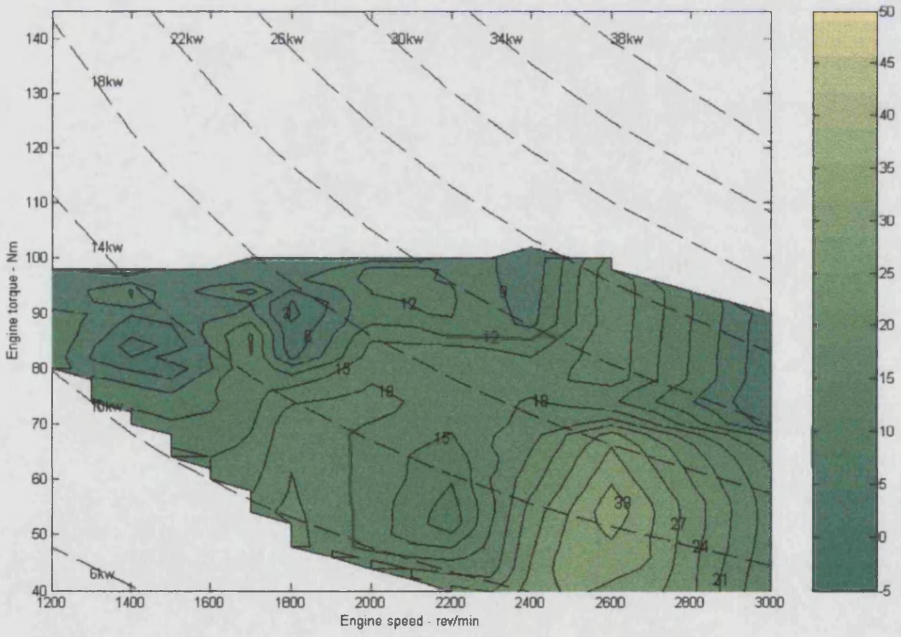


**Figure 5-36 $NO_x$ emissions map of engine torque speed region - 100% lean demand , 100% EGR demand**

# 6 Transient engine response

## *6.1 Scope*

This chapter examines the transient response characteristics associated with step changes to engine control variables. This chapter consists of two main sections, these are transient testing methodology, including signal reconstruction and examination of transient results.

## *6.2 Methodology*

### 6.2.1 TRANSIENT TEST PROCEDURE

The objective of the transient investigations was to develop an understanding of the relative transient performance of different torque control approaches. This meant that it was difficult to apply any formal experimental procedure other than a 'one variable at a time' type approach. Relationships developed as a result of this test program are used to characterise the engine's transient response within the optimisation work.

### 6.2.2 BASELINE TRANSIENT RESPONSE

A baseline characteristic was established as the transient response of the engine to step changes in throttle position. For use within the optimisation work presented in Chapter 7, any developed model was required to be valid over the full range of initial engine speed / throttle position conditions.

The developed test program was structured such that, at each of two separate speed conditions (1500 rev/min and 2600 rev/min) six transients were performed from increasingly open initial throttle conditions. These would allow the development of a model that could predict the engine response to any step change in engine throttling. Transient steps undertaken at the remaining eight speed conditions allow the development of an understanding of the general trend of transient response with engine speed. The initial condition for these transient steps was the throttle position that developed a 100 Nm torque.

### 6.2.3 DILUTION TRANSIENT RESPONSE INVESTIGATIONS

The effect of step changes on transient duration has been investigated at engine speeds of 1500 rev/min and 2600 rev/min. The dilution steps were at 100, 80, 60, 40% EGR, and 1.6, 1.5, 1.4, 1.3 lambda dilution. At all other speed conditions the transient response was investigated from a 100 Nm initial condition, in a consistent manner to the baseline test sequence.

Additionally at 2600 rev/min dilution, transients were examined for a range of combined EGR and lean dilutions. For these tests the fuelling rate was varied systematically from 1.5 to 1.1 and EGR was introduced until the engine output torque was a consistent 100 Nm. These tests were intended to determine if the transient response to a combined dilution strategy is independent of diluent, or if there is some interaction effect between the diluents.

## *6.3 Signal reconstruction: torque signal development*

Figure 6-1 is an example of the raw signals collected for an engine transient. The red and blue curves are engine speed traces. The CP data acquisition equipment records the red curve, while the blue curve is recorded by the RCON ECU interface equipment. These two traces are used to align the data from the independent sets of data acquisition equipment. The yellow trace is the torque response of the engine recorded by a strain gauge load cell mounted to the dynamometer. The green trace is the transient demand signal, in this case a fuelling signal.

The variation in engine speed shown in Figure 6-1 indicates that during a transient manoeuvre there is an engine speed oscillation; therefore the dynamometer controller is not sufficiently quick to develop torque only transients. As a result, the initial torque developed by the engine is used to increase the dynamometer and engine speed. Once the controller has identified that a transient operation is occurring the load increases and as a result the torque signal begins to increase. This slow response of the dynamometer is to be expected since it is controlled via a heavily damped feedback signal.

Since improvements in the dynamometer controller were not practical (Section 3.7), it was decided to reconstruct the torque signal using the engine speed transient information. Examination of the torque signal path from the torque transducer to the data acquisition equipment identified a filter developing a 0.3 s lag. Figure 6-2 presents the characteristic

form of the filter response. Using fast Fourier transforms the effect of the filter was removed from the torque signal. The cyan line on Figure 6-3 demonstrates the change in torque response that occurs as a result of the removal of the effect filter. The torque which causes the engine acceleration can be deduced through knowledge of the second moment of inertia for the rotating masses of the test rig. The test rig was found to have a second moment of inertia of 0.317 $kg/m^3$. This allowed the torque signal to be fully reconstructed, represented by the purple line on Figure 6-3.

## *6.4 Signal reconstruction: identification of transient initiation / completion*

### 6.4.1 IDENTIFICATION OF INITIATION OF TRANSIENT

Important in the determination of the duration of a transient event are the initiation and completion points. Transient demand and establishing the steady state maximum torque are the obvious trigger and completion points. However, examination of engine transients has shown that these are not necessarily ideal indicating points. Figure 6-4 shows similar fuelling, EGR and throttle transient operations. Presented on this figure are the transient demand signals, and normalised feedback signals; throttle position, fuelling rate, and EGR valve position. It can be seen that there is little discrepancy between the demand and feedback signals of the throttle and fuelling transients. However, the same comparison for the EGR transient reveals that there is a discrepancy between demand and feedback positions. Furthermore, there is a sizeable lag between EGR transient demand and the initiation of the transient response. There is an argument to suggest that the 'fairest' way to compare the transient response is via the duration from the demand signal to attainment of steady state torque. However, this becomes a measure of the control actuation systems as well as the engine's ability to react. For throttling and fuelling transients the delay between transient demand and the initial change in feedback signal is small (less than 0.05 s). It is unclear what the reaction time for the EGR system is, however. Since the control system comprises a PID controller, effecting the demand to a PWM vacuum controller, it is unlikely to be as fast as a throttling or fuelling transient. Furthermore, the EGR system is far from an optimal system. As work by Blank et al[44] suggests, in a modern practical application, pneumatic EGR valves would be replaced by electronic units, and these would be mounted flush with the face of the inlet manifold. It can be seen from the red inlet manifold pressure trace in Figure 6-4 that the inlet manifold pressure drops immediately before the EGR transient begins. This is concurrent with the end of the EGR flow through the external EGR system. Consequently it is proposed that using the step change of inlet manifold pressure as the transient initiation point represents

the minimum system and transportation delay that any EGR system could achieve. As such the transient duration presented will represent only the engine's response and not the effects of the EGR controller. As a result, from this point forward the initiation of EGR transients is taken to be the point where there is a marked reduction in inlet manifold pressure.

Figure 6-5 shows two repeated throttling transients from 15% throttle opening at a nominal 1500 rev/min, it can be seen that there is a large fluctuation in the point where the torque margin reaches a steady state condition. This variation in transient response can be attributed to variations in the development of tuning resonances and the fuelling strategy during transient events. On Figure 6-5 the area highlighted in yellow represents the difference in duration for the two transient events to achieve 100% of the torque transient. The area highlighted in purple, identifies the difference in duration between the two transients to achieve 90% of the torque margin. The area highlighted in green covers the range of durations between the two transients to achieve 62% of the torque margin. It is apparent that the development time of the 62% torque margin presented the most consistent measure of the transient duration. As shown in Figure 6-5, the 62% torque occurs during the rapid initial torque development phase. As such this measure will be representative of the initial response characteristic. In the remainder of this work the duration measure used is the time taken from the demand signal until 62% of the total torque margin is achieved.

## *6.5 Transient step results*

A factor which is included within the optimisation work presented in Chapter 7 is a transient response factor. This factor examines the rate at which the engine can move from one operating point to another. In order to develop this transient response measure it is important to have a detailed understanding of the relative duration of the torque margin development. In order to develop this understanding the following section will examine the trends developed from the series of torque transients.

## *6.6 Throttle transients*

Figure 6-6 demonstrates the form of a typical transient response to a step change in throttle position. Identified on this graph is the point of transient demand, the point where peak torque is reached and the throttle position. It can be seen that following a transient demand there is an initial delay period before the throttle starts to move. The delay

represents the period required to operate the stepper motor. Figure 6-6 also shows the inlet manifold pressure response during a transient event, it can be seen that once the throttle translation is initiated there is a delay prior to the manifold pressure increase, this is due to manifold filling effects. As is expected, for this low speed example, the manifold pressure response and consequent engine torque response stabilise at 30% throttle. After this increasing point changes in throttle position have only a limited effect on the torque response. Peak torque is reached 0.6 s after the transient demand signal.

As discussed in Section 6.4 it was difficult to determine a consistent measure of transient duration from the time to peak torque. Instead the duration to 62% was selected as a more consistent measure. It is using this measure that the following relationships have been developed.

### 6.6.1 THROTTLING TRANSIENTS: TRENDS WITH THROTTLE POSITION

Figure 6-7 shows the relative durations for transient initiated from different throttle conditions. It can be seen that the transient duration from heavily throttled conditions (5% open) is considerably larger than from less throttled initial states. This is to be expected, since the torque margin to be developed from a starting position of 10% throttle is 60 Nm at 1500 rev/min, while the torque margin at 40% throttle is 10 Nm. The period required to perform inlet manifold filling is responsible for this greater delay. It can be seen from this series of throttle transient steps that the responses duration with different initial throttle conditions tends toward an asymptotic relationship. Furthermore, the response tends toward a minimum delay that required to energise the throttle stepper motor.

### 6.6.2 THROTTLING TRANSIENTS: TRENDS AT DIFFERENT INITIAL SPEED CONDITIONS

Figure 6-8 demonstrates the transient durations associated with a step from a 100 Nm throttled initial condition to WOT torque across the operating speed range. It can be seen that there is a complex form to this relationship. Initially as the engine speed increases the transient duration decreases however after 2200 rev/min the duration of the transient increases. Finally after 2600 rev/min the transient duration decreases again. This complex relationship can be explained by considering optimality of the cam timing for each of the operating conditions. The manifold is tuned to develop a charge resonance point at 2600 rev/min. At this speed tuned manifold lengths are used to develop a ram charging effect increasing the maximum torque above the level which it would normally develop. This effect only occurs as the throttle approaches WOT, since the throttle obstructs the development of charge resonances below these settings. Therefore a greater throttle

movement is required to reach peak torque, and as previously discussed the electronic throttle has relatively slow translation rate.

## *6.7 EGR transients*

Figure 6-9 shows an EGR torque transient from WOT, 100% EGR demand at 1500 rev/min. As discussed in Section 6.4.1, the transient demand signal is difficult to determine categorically, instead a more consistent measure of transient initiation is the manifold depression caused by the reduction in EGR flow. It can be seen, that following the transient demand there is a small delay, caused by the engine consuming the remaining diluted charge. As the dilution of the bulk gases within the manifold reduce the engine torque increases. Following the initial rise, the rate of increase of engine torque levels. This is caused as the fresh non-diluted charge cool the gases within the inlet manifold. The subsequent final torque development stage until the peak torque occurs with a low rate of torque increase. This is attributed by Blank et al[44] to trapped pockets of EGR which reduce the rate of ingestion of cool fresh charge.

### 6.7.1 EGR TRANSIENTS: TRENDS WITH DIFFERENT EGR LEVELS

Figure 6-10 shows the relationship between transient duration and initial EGR level. This relationship has been presented for WOT at 1500 rev/min. It can be seen that there is an apparent deadband of torque transient response within the region from 0-10% EGR demand. There would appear to be a similar response deadband between 90 – 100% EGR demand. It can also be seen that between these dead band regions there is a roughly linear trend of transient duration with EGR demand.

### 6.7.2 EGR TRANSIENTS: TRENDS WITH DIFFERENT THROTTLE POSITIONS

Figure 6-11 shows the relationship between throttle position and transient duration. It is apparent that the transient duration increases with reduction in throttle position. This is to be expected since as shown in Figure 5-28 as the throttle is closed the EGR level resident in the inlet manifold increases. These transients consist of a combination of effects of the step change in EGR valve position and throttling opening effects.

### 6.7.3 EGR TRANSIENTS: TRENDS WITH DIFFERENT SPEEDS

Figure 6-12 demonstrates the relationship between engine speed and torque margin development duration. Data are provided for transients from steady state points at 100 Nm achieved using EGR dilution at WOT. It can be seen that as engine speed increases

the transient duration decreases. This is to be expected since at higher speeds the engine will consume the diluted charge more rapidly, thus reducing the period until fresh charge can be induced. Furthermore, the greater mass flow rates of fresh charge at higher speeds mean that there is a smaller charge warming effect and a more rapid disposal of stored EGR.

## *6.8 Lean transients*

Figure 6-13 presents a typical transient response from a lean steady state point. The transient demand point, the peak torque and the fuelling response signals are highlighted. It can be seen that there is a demand lag between the transient demand and the change in fuel pulse width. This delay is caused by communication time, and ECU interpretation of the fuelling demand. However this delay is significantly shorter than that for throttling or EGR transients. Following this delay there is a sustained period of rapid torque development until maximum torque is achieved. This differs from throttled and EGR transients because there is no secondary torque development period dependant upon actuator or gas dynamics.

### 6.8.1 LEAN TRANSIENTS: TRENDS WITH DIFFERENT LEAN DILUTIONS

Figure 6-14 demonstrates the effect of increasing lean dilution on transient duration. It can be seen that there is a consistent very small variation in duration for any fuelling step size. This consistency of transient duration is caused by the constant duration of fuelling pulse width transient. In comparison a throttle transient requires throttle translation and manifold filling, while EGR requires pneumatic valve demand alterations, manifold filling and consumption of diluted charge. The transient delay duration for throttle and EGR transients both increase with the size of the developed torque margin. However, for torque margins developed through lean charge fuelling, the transient duration is the rate of change of pulse width, it can be seen that this is sufficiently fast to appear to be constant for any observed change in fuelling.

### 6.8.2 LEAN TRANSIENT: TRENDS WITH DIFFERENT ENGINE SPEEDS

Figure 6-15 demonstrates the effect of engine speed on lean fuelled transient duration. It can be seen that there is a reducing trend on transient duration as engine speed increases. The change in transient duration between high and low speeds is small, 0.2 s. It can be seen by correlating these transient durations with the number of firing strokes that there is a consistent number of firing events between transient demand and initiation

of torque transient. This goes to show that the reduction of transient duration with increasing speed is caused by the increase in firing event frequency.

## *6.9 Spark timing effects on transient durations*

As discussed in Section 5.3.2 torque management using spark timing develops very small torque margins. It is very difficult to accurately assess the endpoint of such transients. As a result it is felt that spark timing transients have similar characteristics to lean transients because of the shared controller and the independence of manifold filling characteristics.

## *6.10 Cam overlap effects on transients durations*

Although iEGR through cam phasing only develops small torque margins (Section 5.4.2), conventional use of cam phasing can develop torque margins of up to 15 Nm. As such it is appropriate to consider the duration of transients of this type.

The profile of a transient performed following the step change in cam demand is presented in Figure 6-16. It can be seen that here again the system has a delay. This delay can be attributed to the ECU interpretation of the transient demand and the activation and translation of the proportional control valve responsible for the state of the cam phasing. Following this delay there are two periods of rapid torque development, separated by a dwell period. The initial torque development can be attributed to the improvement in volumetric efficiency which occurs as the valve overlap increases. The secondary torque development period can be attributed to the development of resonances in the induced charge, leading to ram charging. It can be seen that there is a lag between the degree of valve overlap and the development of the torque margin.

### 6.10.1 CAM OVERLAP: TRENDS WITH DIFFERENT INITIAL CAM POSITIONS

Figure 6-17 presents the relationship regarding the variation of transient duration with variations in initial steady state cam position. It can be seen that there is a proportional relationship between steady state cam overlap and the transient duration. This is because the translation period of the proportional valve and the filling time of the actuation galleries is significant, thus for greater cam phasing translations the delay before torque development initiation is also greater. This relationship is similar to that seen for throttle position. However the translational period of the cam phasing mechanism is considerably greater than that for the throttle mechanism, thus the relationship is exaggerated.

### 6.10.2 CAM TRANSIENTS: TRENDS FROM VARIOUS INITIAL SPEED CONDITIONS

As the engine speed varies, the hydraulic system pressure and magnitude of ram charge effect vary. As a result the transient duration will also vary. This is shown in Figure 6-17. As the engine speed increases the hydraulic system pressure increases since the pump is driven from the crank, consequently the VCT gallery filling time reduces. Contradictorily the valve overlap condition where maximum torque is developed increase with engine speed, as a result the transient duration will also increase.

## *6.11 Combined transients*

Studies have been undertaken to identify whether there is any pattern to the transient duration from mixed torque management control strategies. Figure 6-18 shows the representation of a number of transient operations each from a 100 Nm steady state condition. The initial conditions for the red trace were lean dilution to lambda 1.4 and EGR dilution of 10% (demand). For the green trace the steady state conditions were lambda 1.25 EGR 50% (demand). The initial conditions for the purple trace were lambda 1.1 and EGR 80% (demand). It was hoped that control over combined EGR / lean ratios would allow the shaping of a transient response thus allowing the control engineer another variable to enable the tuning of the transient performance. However, due to the difficulty in accurately co-ordinating the two separate control systems, required to perform these combined transients, it can be seen that no definitive trends are apparent.

## *6.12 Conclusions transient response investigations*

Section 6.5 examines the duration of the torque margin development following a step change in the control variable demand signal. Examination of Figure 6-8, Figure 6-12 and Figure 6-16 shows that for any given torque margin a fuelling control strategy will develop the available torque quickest.

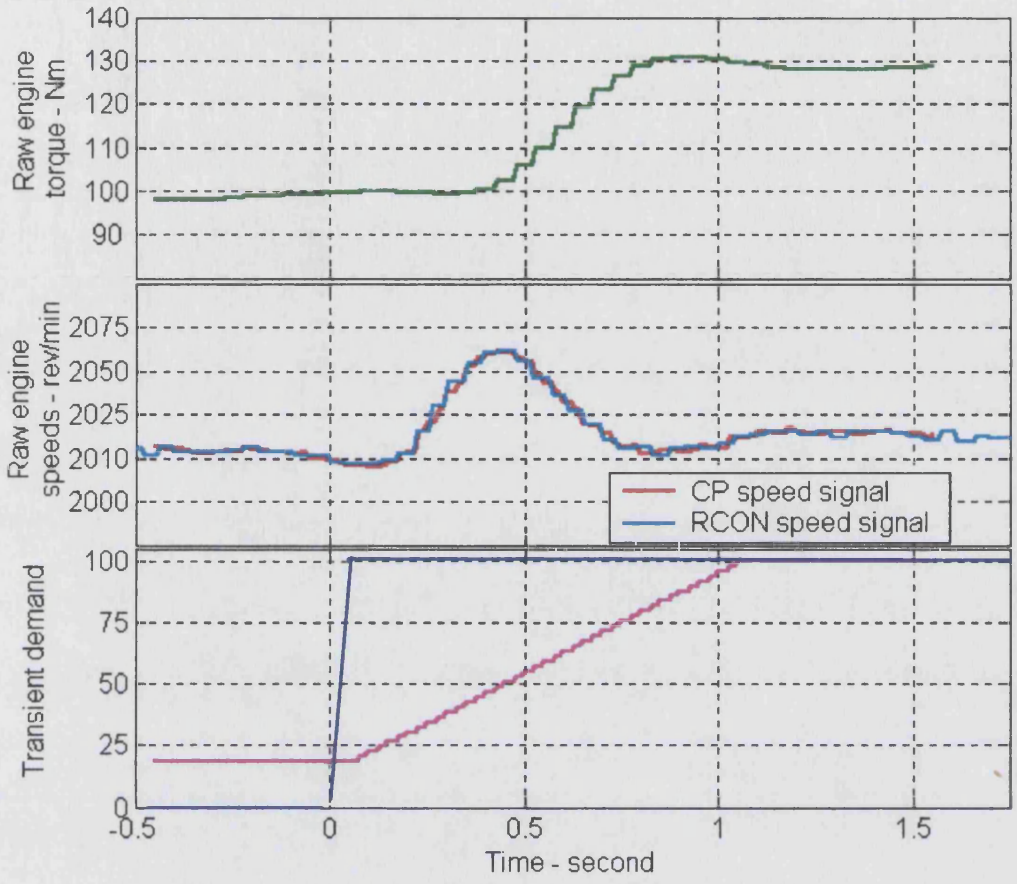


**Figure 6-1 Examination of raw transient signals**

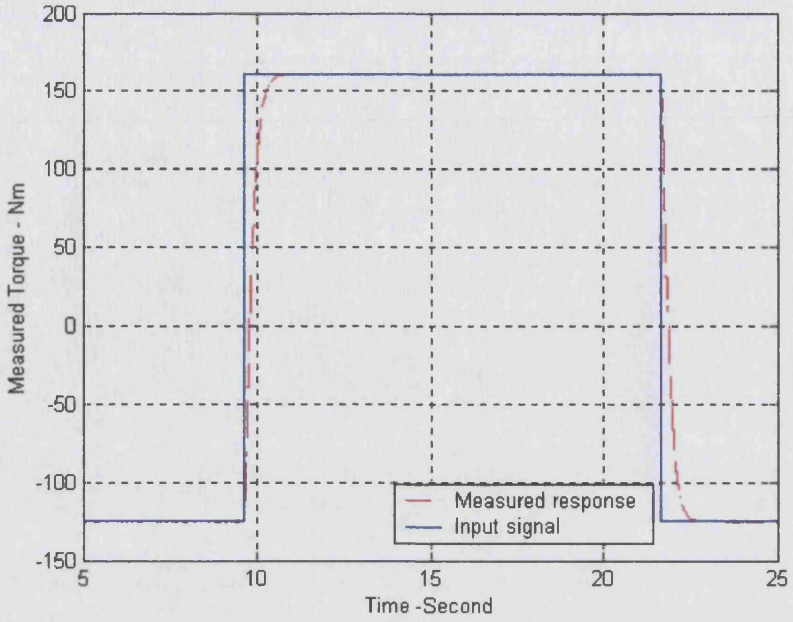


**Figure 6-2 Filter response characterisitic**

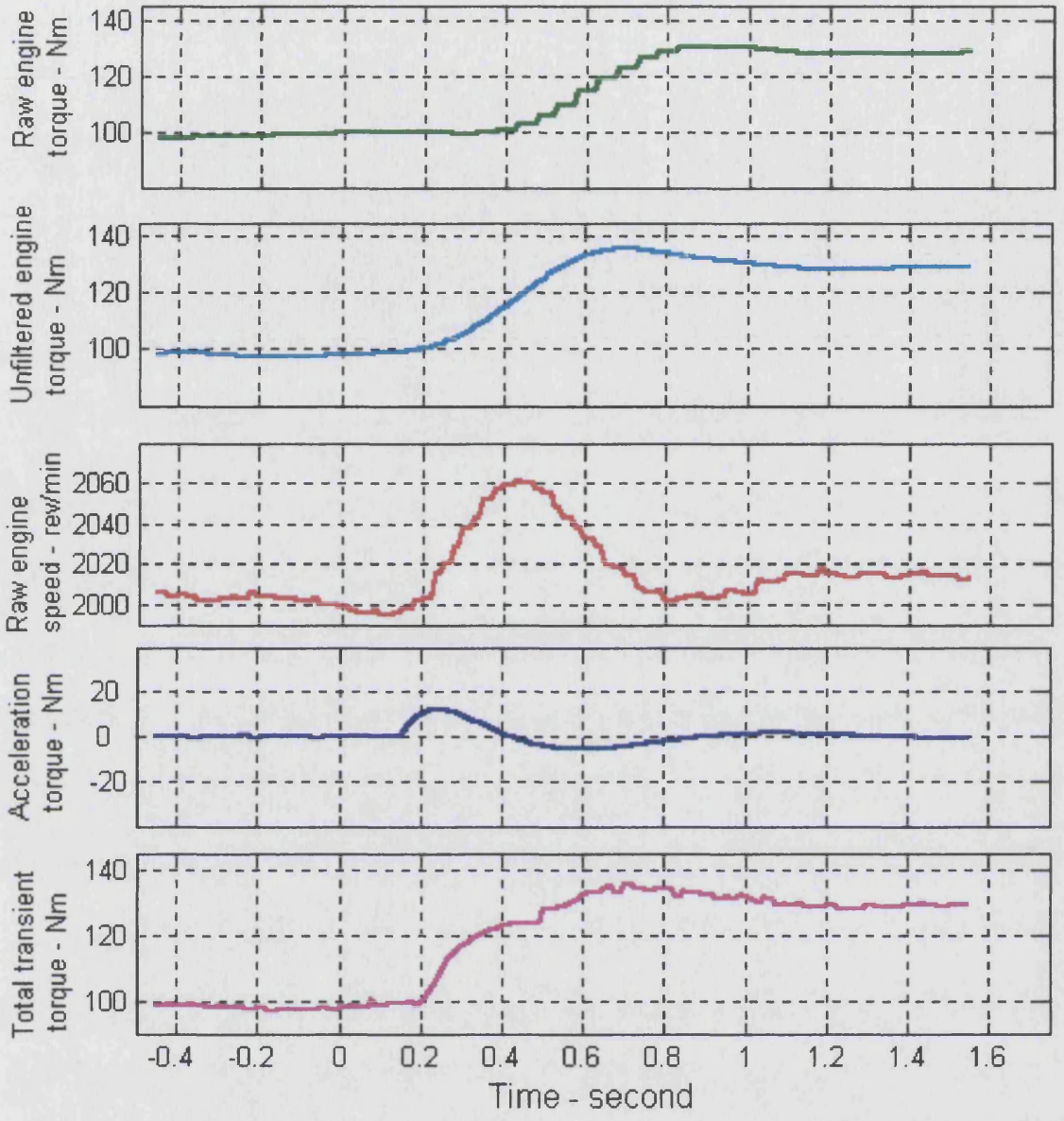


**Figure 6-3 Torque reconstruction**

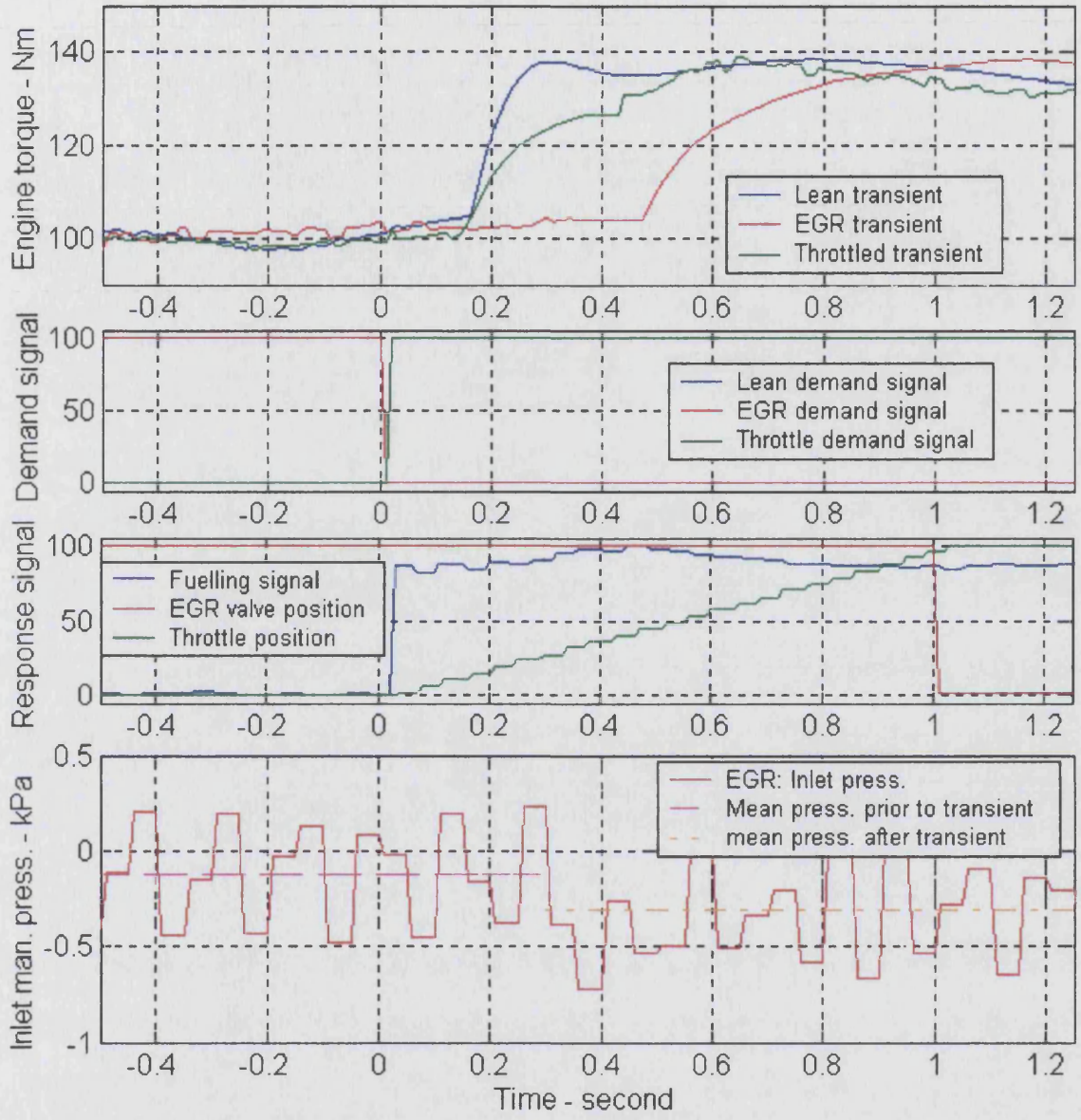


**Figure 6-4 Examination of the transient demand and feedback response characteristics**

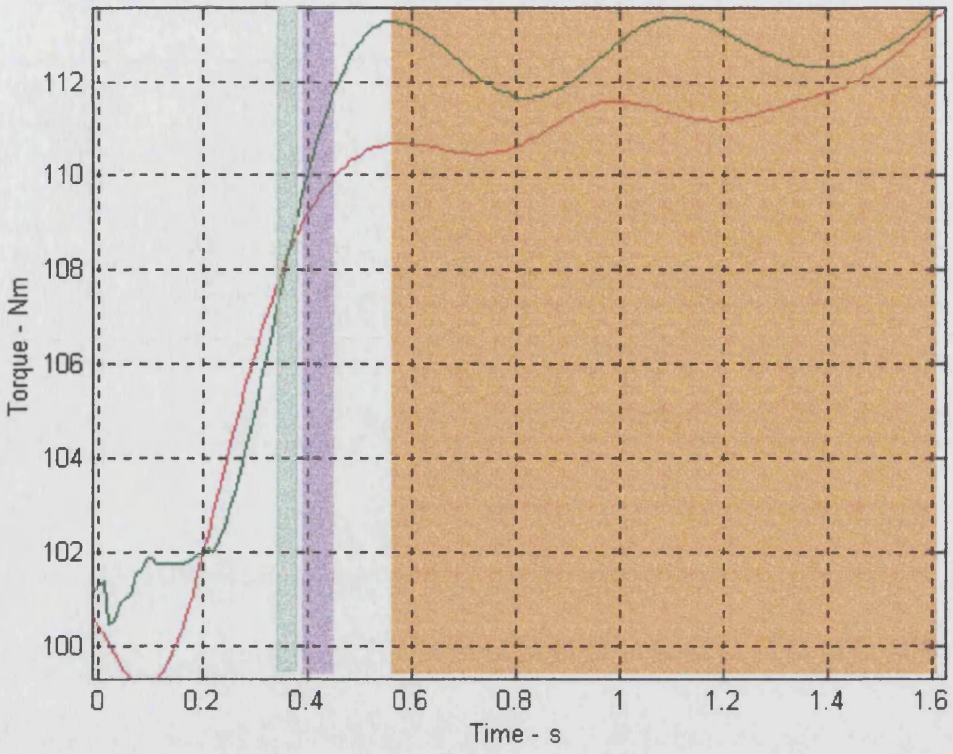


**Figure 6-5 Identification of 62%, 90%, and 100% torque margin transient points**

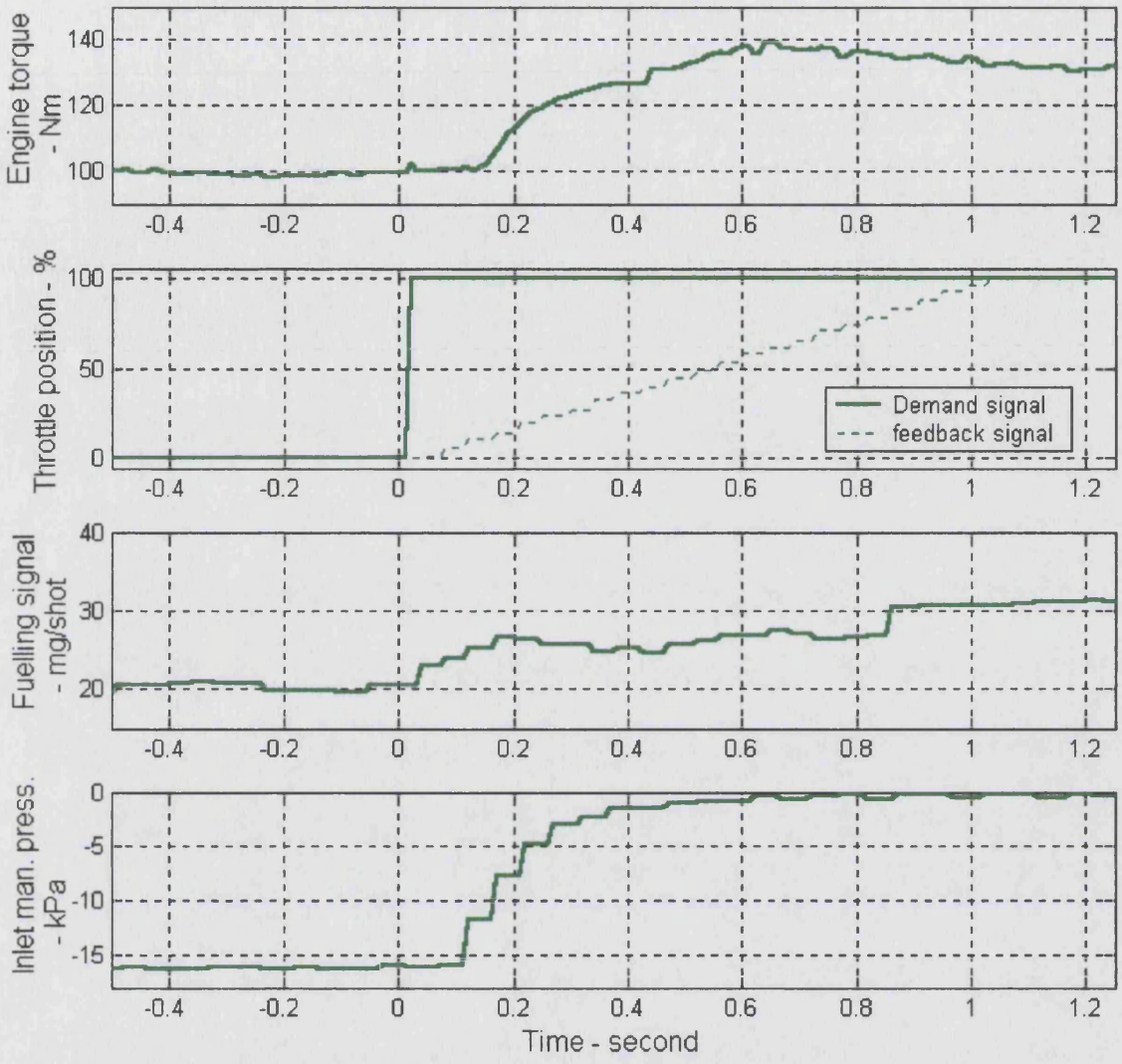


**Figure 6-6 Typical throttle transient - from 10% throttle demand at 1500 rev/min**

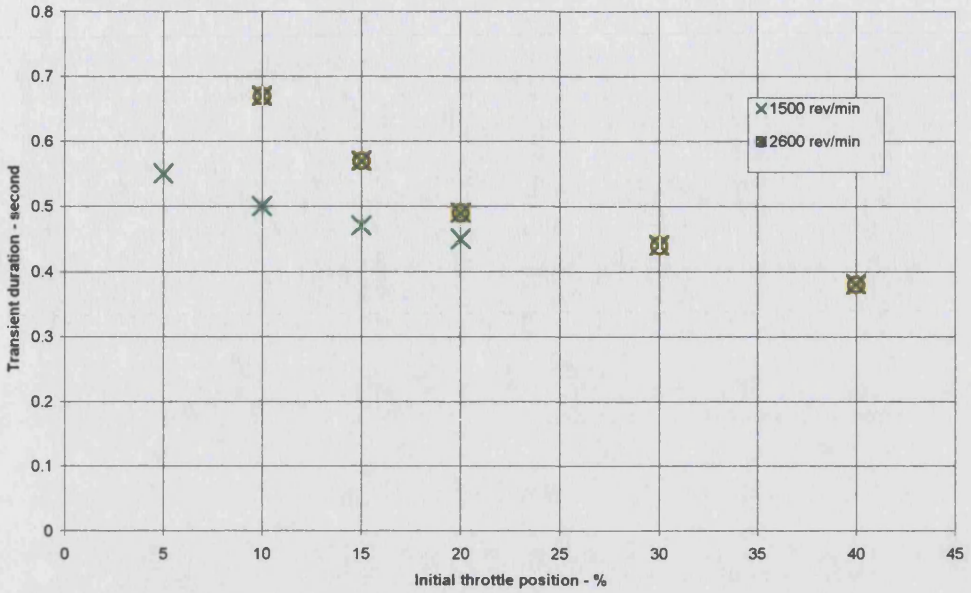


**Figure 6-7 Effect of initial throttle position on duration of transient excursion**

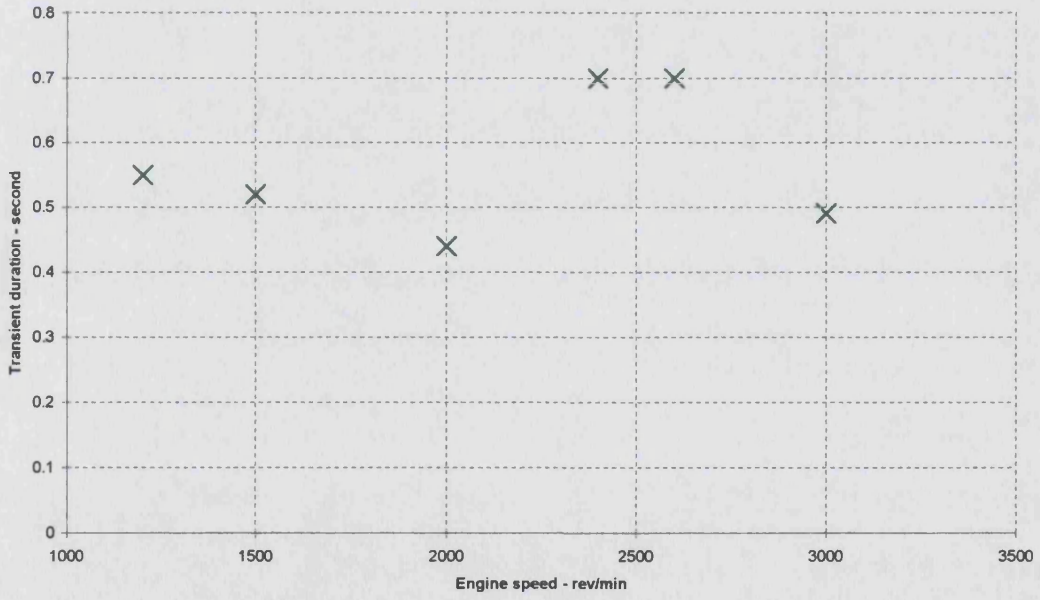


**Figure 6-8 Effect of engine speed on throttle transient duration**

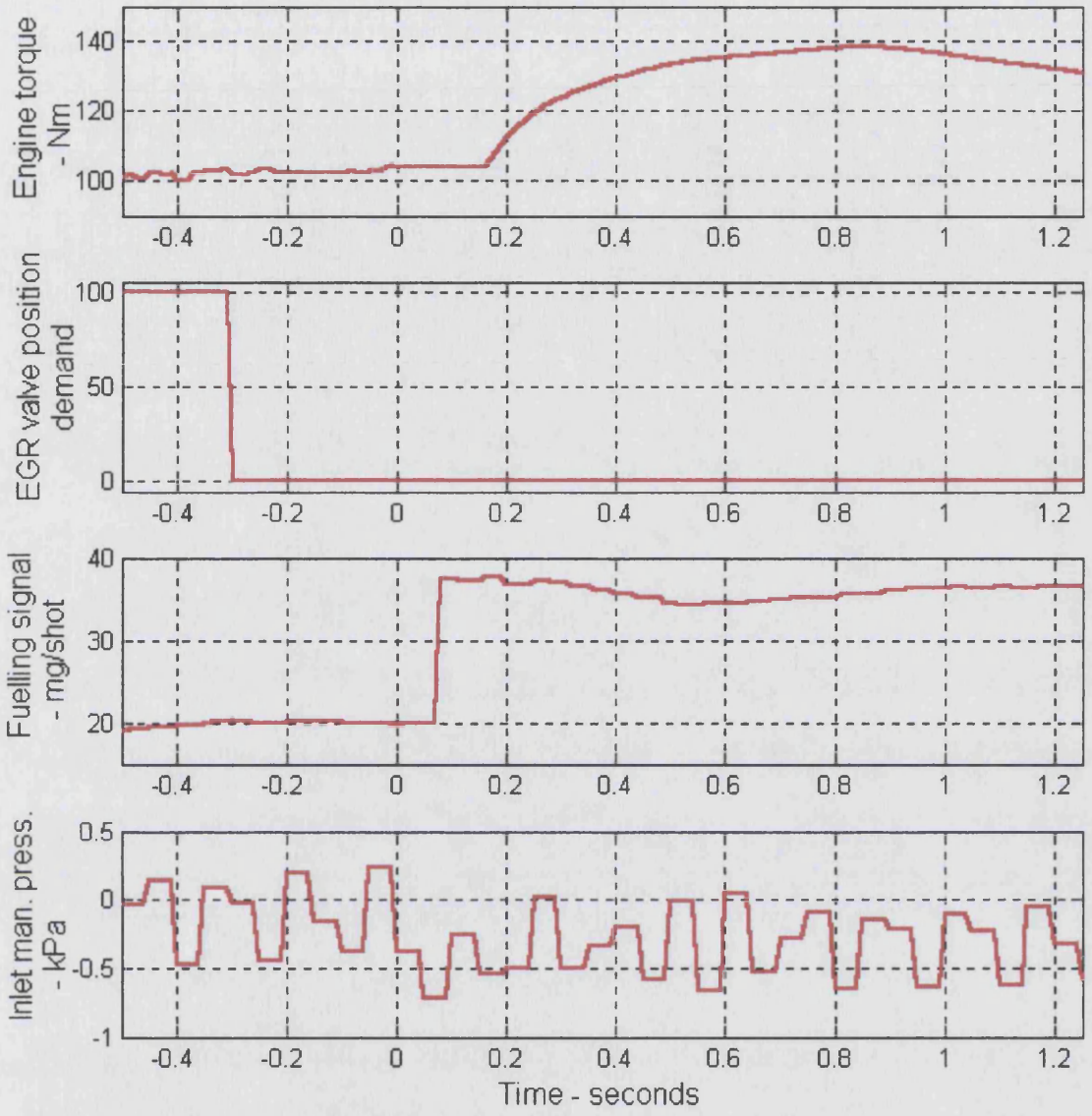


**Figure 6-9 Typical EGR torque transient - from 100% EGR demand at WOT 1500 rev/min**

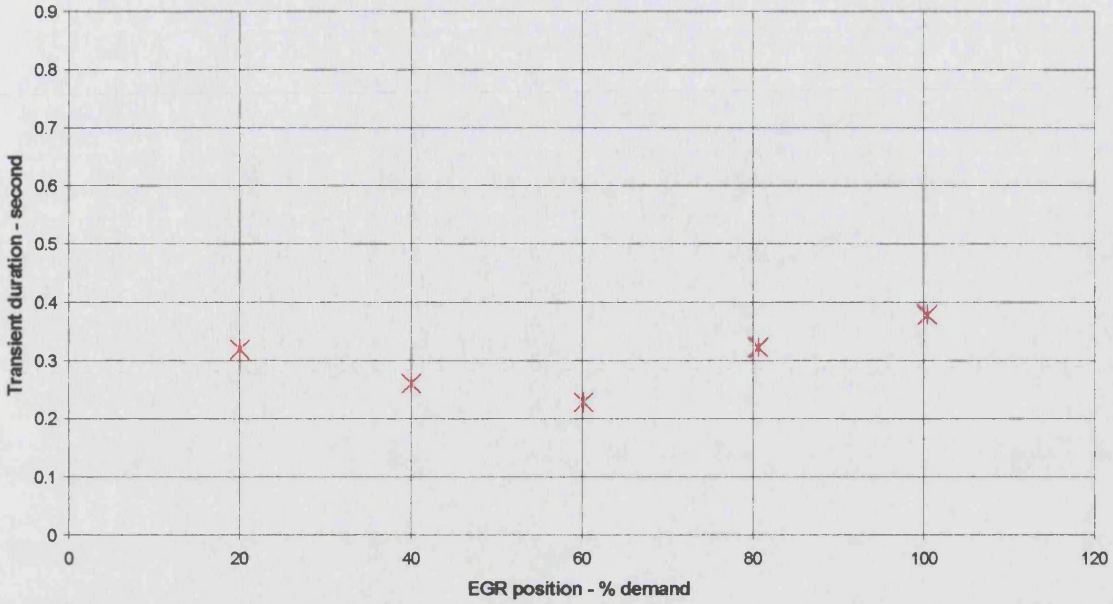


**Figure 6-10 Effect of varying EGR demand positions on transient duration**

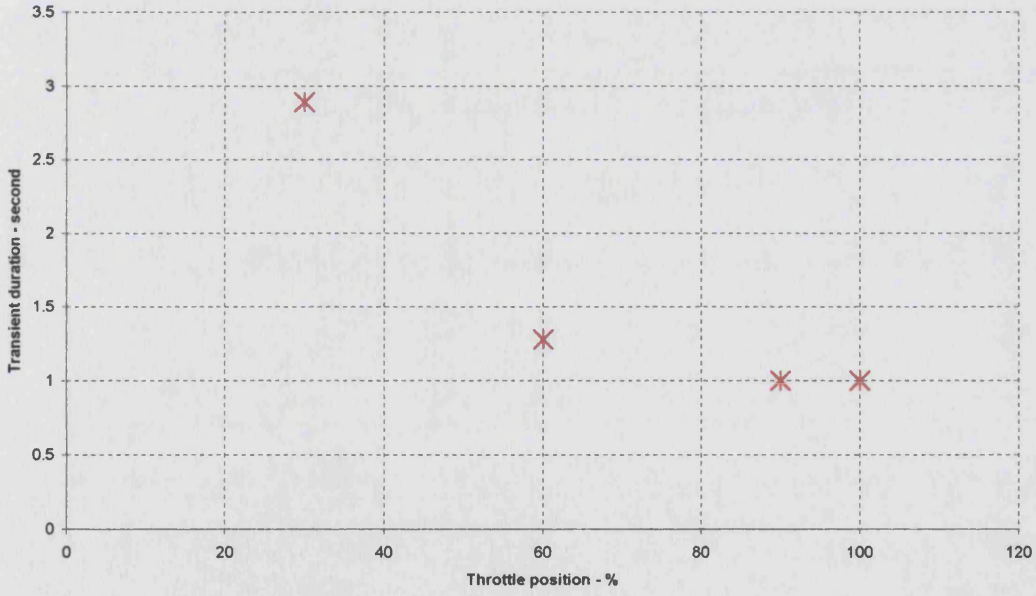


**Figure 6-11 Effects of varying initial throttle condition in transient duration**

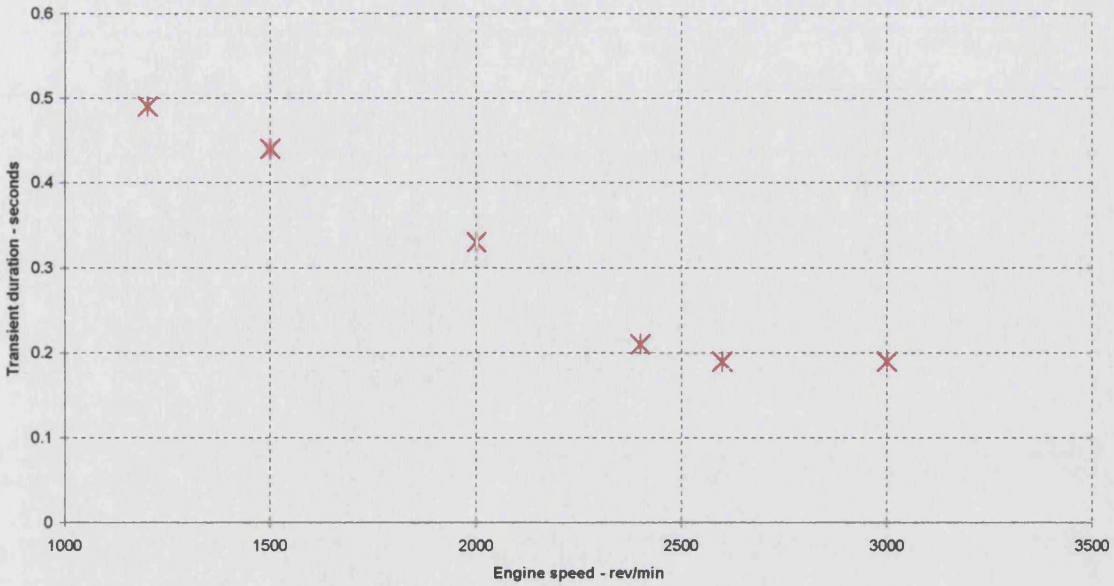


**Figure 6-12 Effect of varying engine speed on transient duration - from 100% EGR demand at WOT**

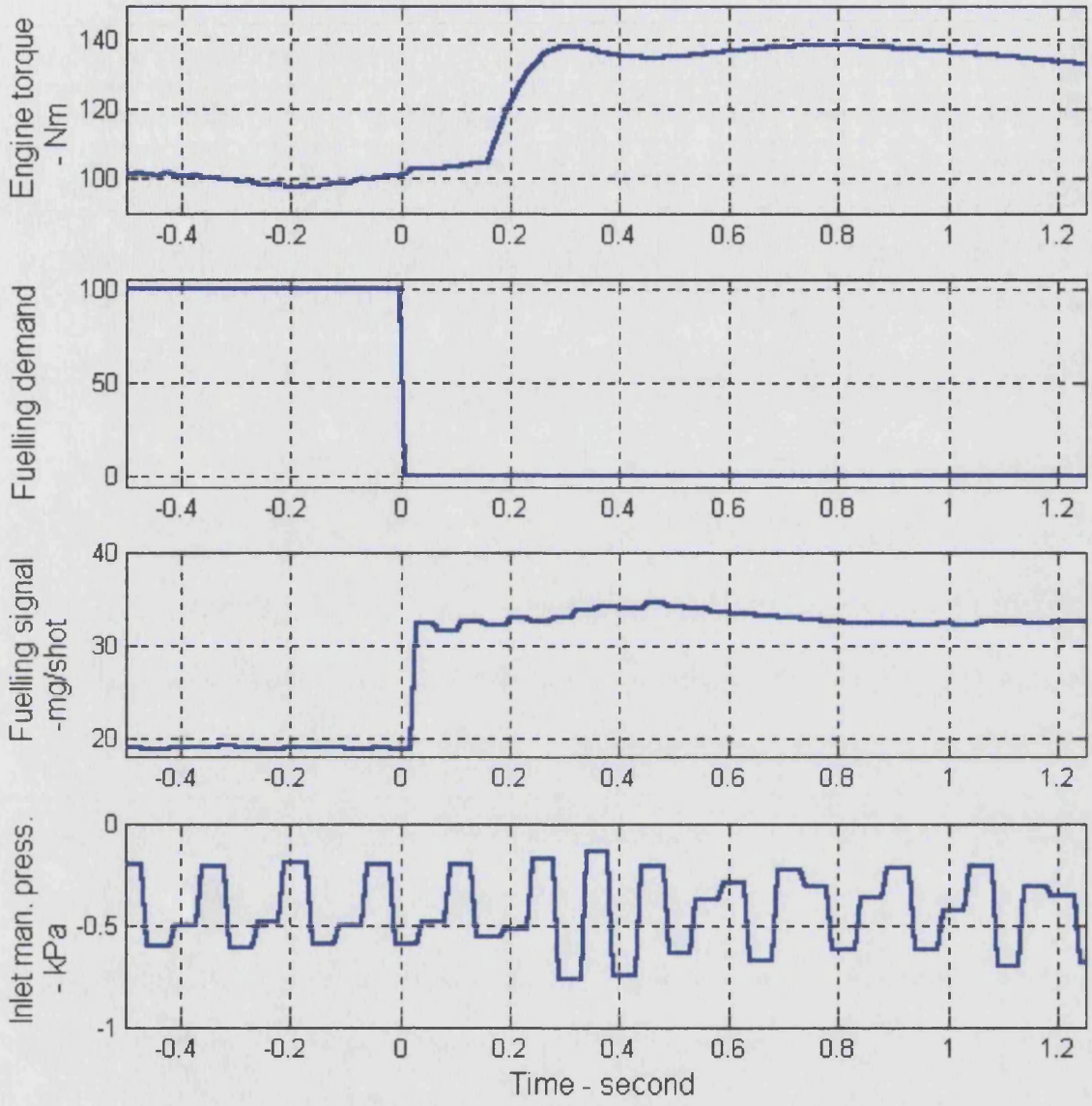


**Figure 6-13 Typical lean transient - from 1.5 lambda; WOT; 1500 rev/min**

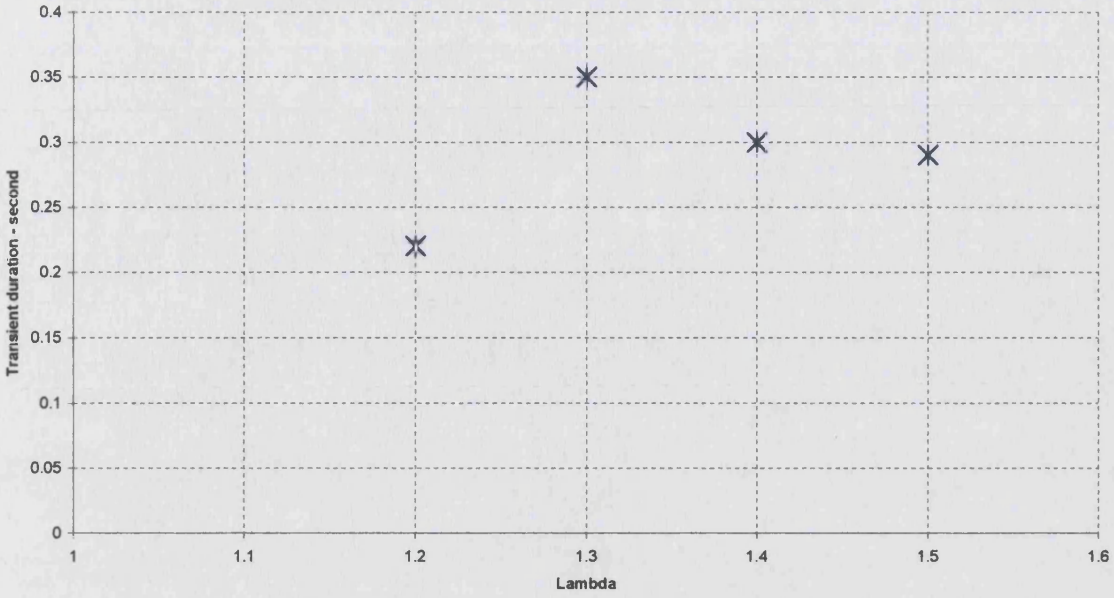


**Figure 6-14 Effect of varying lean dilution level on transient duration**

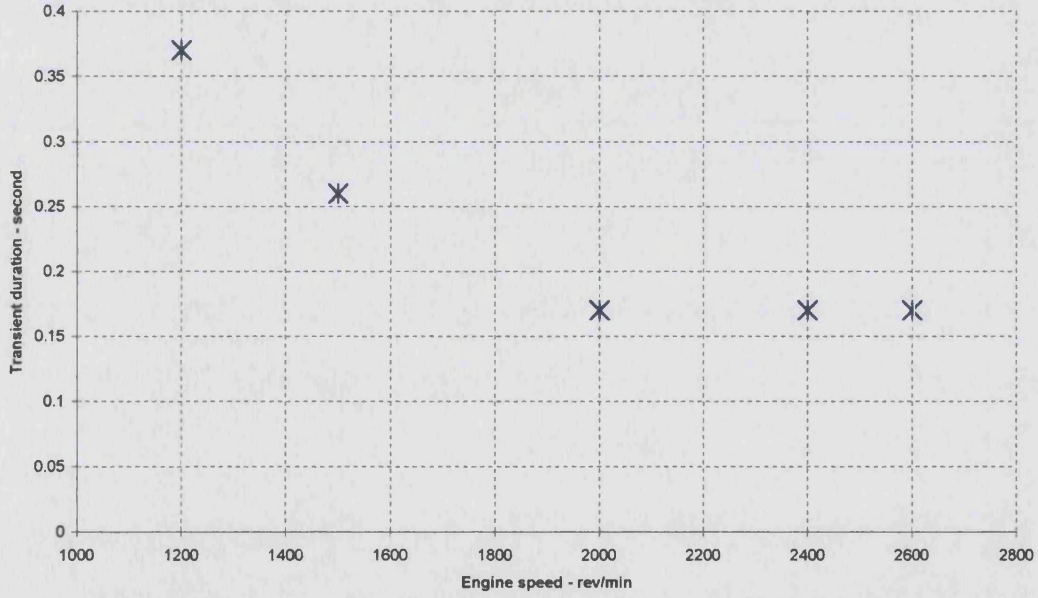


**Figure 6-15 Effect of engine speed on transient duration - from lambda 1.5 WOT**

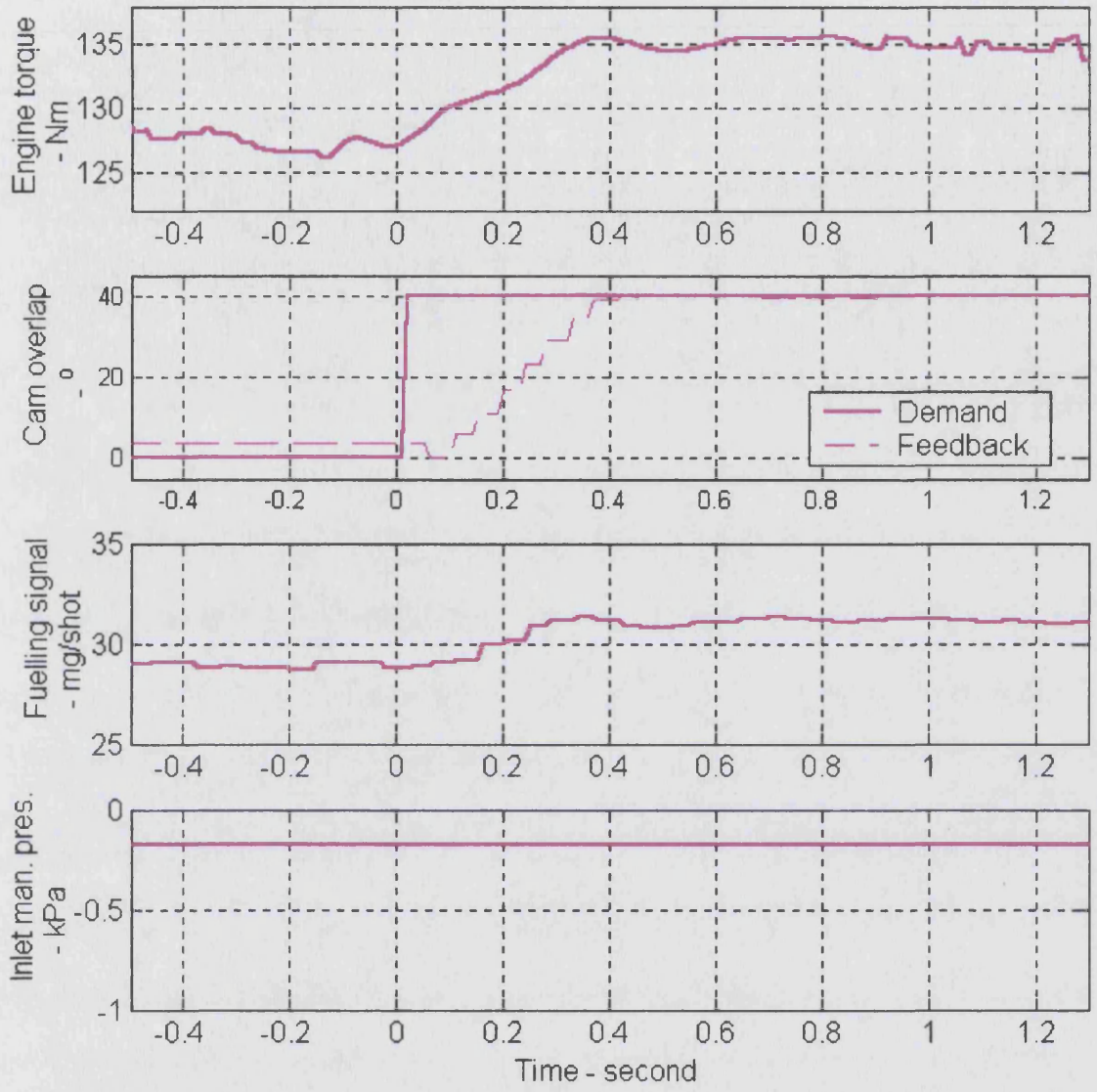


**Figure 6-16 Cam transient from 1500 rev/min WOT**

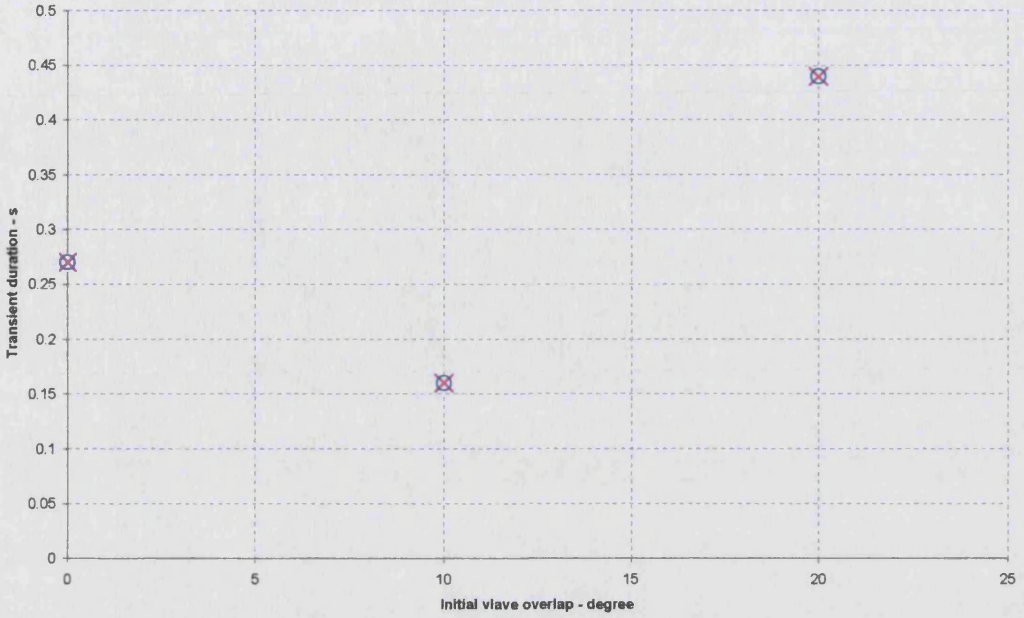


**Figure 6-17 Effect of varying valve overlap on 62% transient duration**

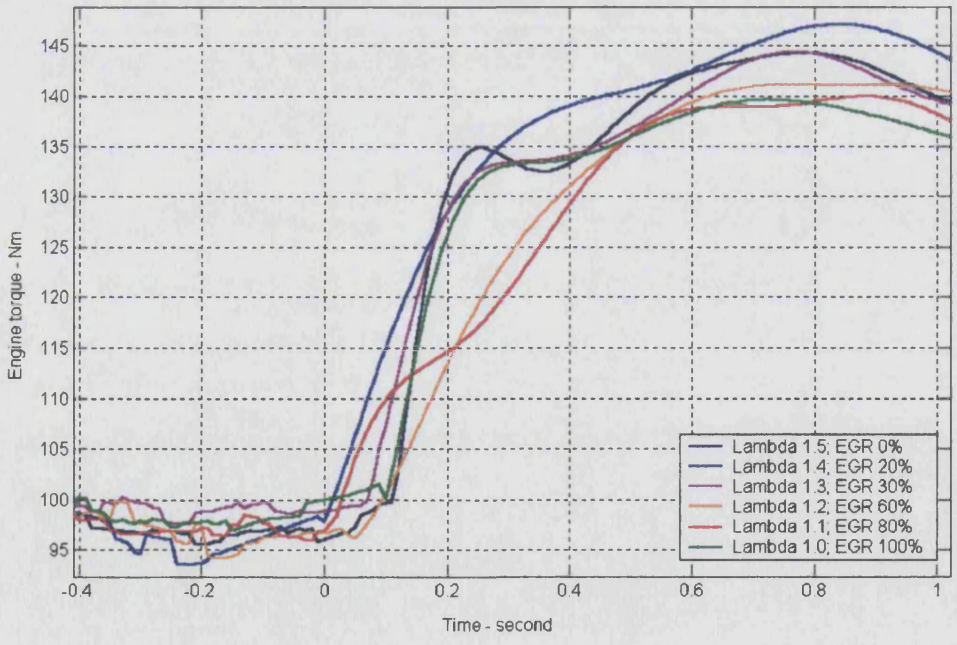


**Figure 6-18 Transient response of combined dilution strategies**

# 7 Development of optimal control lines

## *7.1 Introduction*

The objective of this chapter is to identify optimal engine control variable settings for a range of power conditions to minimise fuel consumption and transient response duration. Initially this work examines the general requirements of optimisation procedures, this is followed by the identification of the optimisation approach to be applied in order to identify the optimal control settings. The work then examines the development of a multi variable objective function, which is used to minimise fuel consumption and transient response duration, whilst restricting viable solutions to ones that have emissions limits within legislative limits. In order to demonstrate the improvement that dilution torque control offers, the fuel consumption performance is considered over the course of an European drive cycle.

The work presented here proposes an optimisation methodology for multiple response objectives. The developed methodology is applied to the reduction of fuel consumption whilst identifying the minimum transient response duration within emissions limits. These optimisation goals were selected since minimising fuel consumption and transient response duration will develop a transmission controller which is not as affected by the trade off which has limited the solutions demonstrated to date. However the methodology could equally be applied to the reduction of specific emissions, whilst maximising fuel consumption.

## *7.2 Introduction to optimisation techniques*

A massive number of optimisation procedures have been developed and it is neither practical or necessary to examine all of the available possibilities here. Instead this work will briefly examine the general structure of optimisation procedures followed by more specific characteristics of gradient and genetic based methods.

### 7.2.1 General characteristics of optimisation procedures

Optimisation procedures regardless of approach have a generally standard structure. This structure consists of 4 stages. These are:

- Stage 1. Initial variable generation
- Stage 2. Assessment of the effects of variable settings (objective function)
- Stage 3. Assessment of relative fitness of variables

- Stage 4. Generation of new solutions function.

The initial variable generation is either produced by random selection or by an engineers assessment of likely optimal settings. The effect of these settings upon a response model is assessed within the objective function. The value of the objective functions response is examined by the fitness assessment code, which influences the proceeding generation of new possible solutions. The effect of this generation upon the objective function is assessed and the stages 2 to 4 are repeated until convergence criteria are met.

### 7.2.2 GRADIENT BASED METHODS

Garbett[116] provides an introduction to gradient based optimisation methods. Gradient based methods examine the response to a number of sets of control variables. Using the resultant information the local gradient of the response surface is determined. Using a process known as steepest decent, the fitness criteria influence the generation code, to produce a new set of control variables along the route of steepest decent. The step size between sets of control variables is varied with gradient such that a route with a large gradient will be interrogated less thoroughly than one with a low gradient. Such gradient based methods converge to a point where all the local gradients are positive.

An advantage of such systems is that by varying evaluation resolution with local gradient they can very quickly converge to an optimal solution.

Gradient based methods are subject to certain disadvantages in there application. Primary among these is the tendency to converge to a local minimum. This is a particular problem when optimising surfaces whose form is more complex than second order. A secondary consideration is that when optimising multiple engine responses, it is frequently the case that individual responses have contradictory optimal control settings (e.g. fuel consumption and transient response). As well as being complex to implement, such multi-response optimisation systems are particularly prone to identification of local minima. Such optimisation approaches also fail to handle none continuous response surfaces, such as surfaces comprising discretised speed responses.

A number of adaptations have been developed to reduce the difficulties discussed above. Multiple starting points has been suggested[116] as a means to minimise the likelihood of the identification of a local minimum. However, to the authors knowledge, no adaptations have been developed to allow gradient methods to be effectively implemented on

discretised models. This limitation has significant implications for the implementation of such an optimisation approach.

Gradient based optimisation procedures have been applied by Brace[25] to produce single variable optimisations of an integrated CVT powertrain. This work used a routine that implemented multiple starting points in order to minimise the probability of identification of a local minimum. This work interrogated a diesel engine model based upon a Neural network. Brace[25] applied the technique to develop optimised engine control lines of single responses. Garbett[116] used regression models to represent a diesel engine, and optimised fuelling and the ratio of an integrated transmission to develop an e-line. This study required the optimisation of a 3 variable problem.

### 7.2.3 EVOLUTIONARY METHODS

Fonseca[117] provides a detailed introduction to evolutionary methods implemented by genetic algorithms (GA). In evolutionary methods a set of control variables is considered to be a chromosome. Each chromosome is comprised of genes that represent individual control variables. Evolutionary methods can be considered to use a shot gun approach to identification of optimal solutions, since initially they generate a large number of random chromosomes, this is the first generation. The response of the objective function is determined for each individual within the first generation and then ranked for fitness. Individuals that produced poor solutions are discarded, while the individuals producing good solutions are maintained to develop the next generation. The next generation is developed by a number of techniques, these include, asexual reproduction, sexual recombination, and mutation.

Genetic algorithms use many approaches to maintain the diversity of the gene pool, therefore they are particularly robust to the identification of local minima. Furthermore the shot gun approach of these techniques means that they can be used to determine the position of an optimum across a discontinuous response surface. This feature of genetic algorithm optimisation means that they can be easily adapted for use in multi-response optimisation applications. Cello[118] provides a discussion regarding the strengths of different multi-response optimisation adaptations to GA's. This work suggests that there are four principal methods used to adapt GA's for use with multi-response problems, these are aggregate functions, Schaffers VEGA, Fonseca and Fleming's MOGA, Srinivas and Deb's NSGA, target vector approaches. Aggregate functions simply combine the effects of two response characteristics in the objective function. The structure of the GA remains the

same but the combined response surface becomes more complex. The weighting of the combination of the two effects within the objective function is an area open to interpretation, and it is for this reason that more complicated adaptations to the GA structure have been developed. VEGA, MOGA and NSGA solutions use adaptations to the assignment of fitness to determine a surface of optimal solutions known as the parento set. Using target vector approaches a response goal is assigned and other responses are optimised within the regions where this goal is met.

The major weakness of genetic algorithm optimisation methods is that a large number of generations are required in order to be certain that a solution is optimal, and that, since an objective function must be evaluated for every individual with a generation they are very computationally expensive. Additionally, GA's are by their very nature dumb optimisation procedures, whereas a correctly developed gradient based method could speculate what benefits would be available if variable ranges could be extended.

#### 7.2.4 SELECTION OF OPTIMISATION APPROACH

The optimisation that is to be undertaken here has three goals; to minimise fuel consumption; to maximise transient response and to meet emissions limits. Simple code for basic gradient based and genetic algorithm optimisation procedures exists, within the Matlab environment. Although it is possible to use a gradient based optimisation approach to achieve the required goals it will necessitate adapting the standard gradient based code. Additionally the use of a gradient based solution will require careful construction of the objective function in order to produce a continuous response surface. However, it is not within the scope of this work to develop sophisticated optimisation techniques, and as a result, it has been decided to use the slower, more robust genetic algorithm solution throughout the rest of this work.

The genetic algorithm code, which forms the basis of the optimisation procedure used within this chapter, has been developed by Sheffield University for the Matlab programming environment.

### *7.3 Development of objective function*

#### 7.3.1 INTRODUCTION TO STRUCTURE OF OBJECTIVE FUNCTION

The objective function is based around the steady state response models developed from the DoE test program. The principal response from the engine model is that of fuel

consumption. This response is scaled by the results from two sub-objective models. These sub-objective models consider the effect of control variable settings upon specific emissions and transient response duration. The combination of the results from the fuel consumption and transient response objective functions is achieved via a simple summing process. The effects of the specific emissions objective function is considered using a target vector approach, such that if the tail pipe emissions are greater than legislative limits, then the control variable settings are rejected. Section 7.4 considers the development of the basic engine model from the regression models developed in Chapter 5. Section 7.5 considers the development of the emissions sub-objective function; examining the development of catalyst models. Section 7.6 considers the development of a sub-objective function for transient response, Section 7.7 examines the combination of the outputs of these objective functions to develop a single objective response value.

## *7.4 Development of steady state engine response model*

Prior to developing the steady state engine model it necessary to determine the methodology within which it will be used, i.e. how the engine model will interact with the optimisation algorithm. It is also important to determine the operating condition to be optimised. It was decided to develop an engine control line throughout the low speed operating region examined in the test program (<3000 rev/min). Subsequently, the control variable settings for operating powers from 2 to 40 kW could be optimised. The optimisation algorithm could be arranged such that all engine variables (i.e. throttle position; EGR rate; fuelling rate; spark timing; cam timing; and engine speed) may be varied continuously across their full range. This approach would require massive numbers of individuals within each generation; because very few individuals would develop control conditions which produced the desired operating power. It was considered that this approach would be too computationally expensive to be implemented with a GA optimisation approach. It was decided that the steady state engine model should contain some intelligence, such that it can determine the required throttle position necessary to achieve a given power while operating using the dilution conditions determined within the chromosome.

Within this model structure evaluating the required throttle condition and valid model ranges require the greatest computational time. It is believed that the extra time that this process requires is significantly shorter than the time which would be required to achieve the same solution using a genetic algorithm that manipulated the 7 available engine variables without any intelligence.

The engine model is also adapted to include the dilution limits of the engine, therefore the lean burn and EGR genes, represent the percentage dilution demanded, and not the actual engine settings.

The response model used for the engine is based upon the two stage gradient matched regression approach described in Section 4.5.3. In this modelling approach the responses to variations in throttle positions are represented by two second order models; high throttle range and low throttle range models. These models are joined by the use of a geometric spline. Since the range of validity for the high and low region models vary with charge dilution, it is necessary to implement a flexible model joining code. This code must identify the region over which the high and low models are valid and then determine the characteristics of the gradient matching spline that links them. The structure of this piece of code is detailed in Figure 7-1.

The regression coefficients for each response are loaded from a substantial 4-dimensional matrix. Each set of response coefficients are loaded in turn, in order to determine all engine responses.

The code as used, optimises each power condition for every available test speed condition. The condition which develops the minimum response value is taken to be the optimal solution.

## *7.5 Catalyst model*

The regression models developed in Chapter 4 and 5, examined engine out rather than tailpipe emissions. As a result, it is necessary to develop a model of catalyst efficiency in order to establish a meaningful evaluation of engine performance.

This section comprises a discussion regarding conventional modelling approaches applied to the three way catalyst (TWC) and high oxygen exhaust stream $NO_x$ reducing catalysts. Simplified models suitable for inclusion within the optimisation routine are then developed. The section concludes by examining the sub-objective function used to assess whether a specific condition meets legislative emissions limits.

### 7.5.1 THREE-WAY-CATALYST MODELLING

The oxidation type catalyst commonly referred to as a three way catalyst is currently fitted to all gasoline powered vehicles within Europe and the United states. This type of catalyst reduces $NO_x$ emissions via a process of oxygen reduction; while it completes the combustion of uHC and CO, resulting in increased emissions of carbon dioxide, water.

Many studies have modelled three way catalysts [119,120]. These models examine the conversion efficiency of catalysts with respect to feed gas rates, wash coat properties, exhaust constituents, catalyst geometry and catalyst light off duration. These studies and the developed models are very complex and not suitable for use within an optimisation routine of the nature of the one implemented here.

### 7.5.2 SIMPLIFED MODELS OF TWC

Two simple models of TWC efficiency have been developed for use within the optimisation procedure. The first simplified catalyst model is based upon pre and post catalyst emissions measurements taken from a 1.6 L Ford Focus. These measurements were taken over the course of a European drivecycle. The subsequent cumulative emissions responses are demonstrated in Figure 7-3. Using the pre and post catalyst emissions data it is possible to develop measures of catalyst efficiency, presented in Figure 7-4. Knowledge of vehicle road load characteristics as defined by the following equations allow the EUDC to considered as a series of power conditions.

$$Power = \frac{c_d \rho v^3}{2} + R.mg.v + mg \sin\theta.v$$

Where:

| | | |
|---|---|---|
| | V | Vehicle speed |
| | $c_d$ | Vehicle drag coefficient |
| | $\rho$ | Density of air |
| | R | Rolling resistance |
| | Mg | Weight of vehicle |
| | $\theta$ | Inclination of road |

Correlating the catalyst performance with the power condition provides a rudimentary model of real world catalyst efficiency. The relationship is useful because the optimisation routine focuses on individual power conditions and because it allows the warm up performance of the catalyst to be to be modelled in a simplified manner.

Due to the HEGO fuelling control employed in the test vehicle, this model is only valid for a tightly controlled range of fuelling conditions, lambda 0.95 - 1.05. However the working envelope of the reduction mechanisms within a TWC is considerably broader than the +/- 0.05 lambda control developed by HEGO fuelling control. Therefore, there was a need for a second model, which could describe the performance of the catalyst under a wider range of engine operating conditions. The second model is intended for use during non-stoichiometric engine operation. It is based upon simple lambda verses catalyst efficiency relationship presented in many texts [121,34]. Figure 7-5 demonstrates the characteristic form of the catalyst efficiencies with a range of lambda values. The second TWC model consists of regression polynomials that represent the classical catalyst lambda / efficiency relationships. The following are the regression polynomials.

$$\xi = \beta_1 + \beta_2.\lambda + \beta_3.\lambda^2 + \beta_3.\lambda^3 + \beta_4.\lambda^4 + \beta_5.\lambda^5$$

Where: $\xi$ Specific catalyst efficiency

$\lambda$ Air fuel ratio

$\beta$ Regression coefficients

During non-stoichiometric operation these models are evaluated within the objective function. Figure 7-2 presents an overview of the catalyst model code identifying the selection of different catalyst models.

### 7.5.3 $NO_X$ REDUCING CATALYSTS

The optimisation examines the operation of the engine into very lean regions. In these regions, because of the oxygen rich exhaust characteristics, $NO_x$ conversion efficiency of a standard TWC is minimal. As a result, any production vehicle operating such a lean charge dilution strategy would use additional approaches to reduce exhaust $NO_x$; typically de-$NO_x$ catalysts, and lean $NO_x$ traps. $NO_x$ traps work by storing $NO_x$ gases in location sites in a catalytic substrate. As the substrate approaches saturation, a period of rich engine running is required to enable the conversion of the stored $NO_x$ into nitrogen and $CO_2$. De-$NO_x$ catalysts operate by continuously converting $NO_x$ back to nitrogen and oxygen. For an aged $NO_x$ storage catalyst the peak of conversion efficiency can be as high as 80% [123]. This compares favourably with de-$NO_x$ catalysts, where conversion efficiency peaks around 30%[122]. Although $NO_x$ storage catalysts require greater controller complexity, their higher conversion efficiency has lead to them becoming the

solution which has predominately been adopted for use with lean running GDI engined vehicles. As a result of their popularity and high conversion efficiency it has been decided to incorporate a simplified model of a $NO_x$ storage catalyst in this work.

### 7.5.4 DEVELOPED $NO_X$ TRAP MODEL

As with traditional TWC, modelling $NO_x$ reducing and particularly $NO_x$ storage catalysts have received considerable attention. There have been a large number of studies which experimentally assess the implications of specific catalyst chemical compositions over the course of a drive cycle, for example[124]. While Ketfi-cherif et al[130] have developed a reduced complexity model which just considers simple chemical processes and gas flow rates.

However detailed modelling of storage catalysts is not within the scope of this work; a $NO_x$ trap model has been included within the optimisation procedure simply to provide an assessment of the scope of possible $NO_x$ emissions reduction.

Hepburn et al[123] have shown that the major factor when determining the conversion efficiency of a storage type catalyst is the temperature of the exhaust feed gas. Hartick et al[127] have gone so far as to propose variable exhaust ducting system, in order to optimise the temperature of the feed gases. Figure 7-6 shows the temperature dependency of an aged storage catalyst, which represents the basis of the model. Hepburn et al[123] also reports that levels of exhaust gas oxygen affect the conversion efficiency, and that feed gas flow rate also affects conversion efficiency. However both of these effects are small compared to the exhaust temperature dependency and have not been considered in this simplified model.

In order to achieve maximum cooling of exhaust gases, and thus maximum conversion efficiency, storage catalysts are usually positioned at the end of the exhaust system, close to the silencer. A comparison of different exhaust geometry configurations has been undertaken by Marshall et al[128], and it is from this work that data has been taken to characterise the cooling effect on the exhaust gases. Marshall et al[128] states that exhaust gas with a temperature of 700 °C will have cooled to 300 °C by the inlet to the storage catalyst. Since the test vehicle in Marshall's[128] study is of a similar class to a vehicle which may host the test engine, it is plausible to consider that the exhaust system will be of similar design. Therefore using standard theory it is possible to determine a heat

transfer coefficient which can be used to characterise the exhaust gas temperature at the inlet to the storage catalyst from any given exhaust temperature / flow rate condition.

$$Q = \dot{m}.C_p.(T_{DENOX\_INLET} - T_{TWC})$$
$$Q = h_c.A.(T_{TWC} - T_{AMBIENT})$$
$$T_{DENOX\_INLET} = \frac{h_c.A}{\dot{m}.C_p}.(T_{TWC} - T_{AMBIENT}) + T_{TWC}$$

Where:

| | | |
|---|---|---|
| | Q | Heat transfer rate |
| | $C_p$ | Specific heat capacity |
| | A | Area of heat transfer surface |
| | T | Temperatures |
| | $\dot{m}$ | Mass flow rate |
| | $h_c$ | Heat transfer coefficient |

This allows the determination of the maximum catalyst efficiency during any regeneration cycle. However, as Hepburn et al[123] explained, once a regeneration cycle has been completed the catalyst efficiency drops as a function of catalyst geometry, exhaust gas constituents, and exhaust mass flow rate, all symptoms of location site filling. As a result, conversion efficiency will reduce from the peak conversion value in an exponential manner toward zero efficiency. It is not possible with the information available to determine the exact decay characteristics of the conversion efficiency. Instead some assumptions were made regarding the engine controller, which may be used to schedule the regeneration cycles. Marshall et al[128] implied that a controller used in a production application, would be sufficiently developed such that it would be capable of predicting the rate of catalyst saturation. The ECU would therefore schedule regeneration cycles to maintain a certain catalyst efficiency. In the model developed here, it is assumed that the regeneration cycles will be scheduled such that the conversion efficiency of the catalyst will not drop below 50% of the peak value. As a result, the objective function uses a mean value model for catalyst efficiency; assuming that the catalyst has a mean efficiency of 75% of the peak value.

Regeneration cycles will have obvious implications toward the fuel consumption of the engine. However applying the model as discussed, it is difficult to characterise the full extent of the fuel consumption penalty. Hepburn et al[123] suggests that a fully saturated catalyst will take 30 seconds to regenerate. The rate at which regeneration cycles occur

will constitute a major factor in the specification of design of the storage catalyst. Although sizing the catalyst could be included in this optimisation process, it has been considered that this would detract from the main focus of the work. Therefore due to lack of information about the specifications of a suitable catalyst it has been decided not to incorporate a regeneration fuelling penalty into the BSFC model. It is acknowledged that this constitutes a compromise in the validity of incorporating a $NO_x$ storage catalyst model within the optimisation procedure.

### 7.5.5 EMISSIONS OBJECTIVE FUNCTION

In order to determine if the exhaust emissions are within legislative limits a sub-objective function has been developed. This sub-objective function examines the predicted tailpipe emissions, if the tailpipe emissions are lower than the limits prescribed by legislative standards then that particular set of control variables is considered to have produced a condition which has 'passed'. If the tail pipe emissions are in excess of the legislative limits then a punitive scaling factor is applied within the main objective function, such that the particular set of control variables is seen to have poor fitness. Figure 7-4 provides a schematic of the structure of the emissions sub-objective model.

Since the optimisation process is to be applied to individual power conditions, the first step in the development of the sub-objective function is to establish allowable emissions limits at each discrete power condition. Little work has been published which details a scheme through which emissions limits can be established for specific discrete drivecycle conditions. As a result, a novel approach to the characterisation of discrete emissions limits as been developed for use within this work. The developed approach is based upon the examination and scaling of measured tailpipe emissions during a legislative cycle. Figure 7-3 shows an European drive cycle and demonstrates the cumulative emissions from a 1.6 L Ford Focus. The large dash lines on the cumulative emissions figures represents the cumulative maximum mass of emissions as prescribed by the EURO IV legislative limits. The short dashed line represents the EURO V limits. It can be seen that the representative vehicle fails to meet the EURO V limits for $NO_x$ emissions. The EURO V limits will not come into force until 2005, as a result it is quite probable that improvements in catalyst warm up, and combustion characteristic will enable the 1.6 L engine to pass the emissions standard. Due to the representative vehicle requiring technological development in order to meet the EURO V standards, it has been decided to use the current EURO IV standard to define the limits for this objective function. It can also be seen that the majority of the emissions produced are developed within the warm-

up period of the catalyst. As discussed earlier owing to combustion stability considerations, dilution charge control can only be applied over higher power ranges, i.e. those of the EUDC drive cycle region. Therefore, outside of these regions it is sensible to consider that the generation of emissions will not vary from that of the test vehicle. As a result, the allowable emissions limits for the ECE-15 region can be considered to be the measured value. Following the ECE-15 region there is a difference between the accumulated emissions and the maximum allowable emissions as defined by the legislative limits. This difference represents the emissions potential that maybe used during the EUDC before the engine operation breaches legislative limits. Apportioning this emissions potential for discrete operating conditions over the course of the EUDC is not a straight forward task. Although the production of $NO_x$ emissions maybe considered to be proportional to engine power, the production of uHC and CO are more prevalent during deceleration and motoring operations. It was decided to apportion the emissions potential according to instantaneous power, i.e. the power determined by the instantaneous speed condition alone excluding acceleration powers. This approach provides reduced peak $NO_x$ allowances but positive declarative allowances for uHC and CO.

Table 7-1 presents the tolerable emissions limits for the discrete power conditions over the EUDC.

## *7.6 Assessment of transient response duration to a step change in demand*

This section examines the difficulty in developing a 'driveability' assessment, justifying the use of transient engine response as a means to maximise vehicle driveability performance. This section then examines the use transient response curves to model the engines transient response. This section of the thesis concludes by determining a sub-objective function which determines a measure of relative transient response.

### 7.6.1 EXAMINATION OF WORK ON VEHICLE DRIVEABILITY

As much recent work [37,38,39] has discussed the development of a measure for drivers' appreciation of a vehicles response to a demand is a very complex problem. Wicke[39] , Dorey & Martin [37], and List & Schoeggl[38] have produced detailed studies investigating the driveability of vehicles performing straight line accelerations. These works have shown that factors such as initial jerk, engine delay time, and the overall profile of the acceleration response, have important parts to play in a drivers assessment of a manoeuvre. Given these complex interactions, it is clearly beyond the scope of this work

to attempt to fully predict driveability. Garbett[116] discusses driveability and examines each of the optimised transmission solutions to determine whether it would be drive-able. Dorey & Martin[37] and List & Schoeggl[38] have attempted to determine the dynamic criteria which can be used to objectively characterise driveability. Wicke[18,39] has gone a step further, correlating the objective driveability assessments with multiple drivers subjective assessments. This work lead to the development of a CVT transient controller which affected CVT response during transient events in order to develop ideal levels of initial engine jerk, vehicle acceleration delay and rate of vehicle acceleration. More recently Dorey & Schoeggl[37] optimised a discrete ratio transmission for driveability. In this work Dorey & Schoeggl[37] used initial jerk as the prime measure of driveability.

As shown by Wicke[18] for vehicles fitted with CVTs, characteristics such as initial jerk can be affected by the CVT controller implementation during transient operations. As a result, using characteristics such as jerk and vehicle acceleration delay in order to characterise a vehicle's driveability is fraught with difficulty. As a result, it has been decided that the driveability assessment to be optimised in this work, will ignore CVT control implications, and dynamics. Instead this assessment of driveability will consider the contribution of the engine, seeking to identify the relative rate of transient response when moving from an initial operating condition to a new desired power condition. This approach can be considered to be more of an assessment of a vehicle's potential under transient situations, than an assessment of actual driveability. It is clear that ignoring CVT dynamics represents a significant compromise, however Wicke[18] has shown that the Torotrak CVT can change ratio significantly quicker than engine speed can rise. Subsequently, the faster a power condition can be met by the engine the greater the potential afforded to the CVT controller to tailor the response of the vehicle to suit drivers tastes.

The duration of an engine transient from an initial power condition to a required power condition can be considered to consist of three factors. The first is purely a delay factor, and represents the controller lag, dead bands of operation, and manifold filling dynamics. The second transient duration factor is the time required to develop the torque margin available at the initial steady state condition. From examination of transient responses, presented in Chapter 6 these factors typically have a value of:

- Throttling: 0.15s delay and 0.28s transient development
- Fuelling: 0.15s delay and 0.1s transient development
- EGR: 0.18s delay and 0.2 - 06s transient development
- Cam: 0.2s delay and 0.4s transient development

The third transient duration factor is the time required to accelerate the engine to the new power condition. This factor is dependent upon difference between the initial speed and the speed where the required power condition is achieved and torque margin available to accelerate the engine over this speed range. To a certain degree there will be an overlap between the second and third transient factors, since as the torque margin is developed it is used to increase the engine speed.

Conventionally modelling these transient factors is achieved using delays, manifold filling models and system inertias. However conventional manifold filling models typically only consider the implications of throttled transients. Applying this approach to modelling lean and cam transients would not produce representative relationships, while adaptation would be required to include external EGR to a filling model. However, in this study there are a wealth of experimental transient results available to allow a more empirical approach to transient response modelling. The adopted modelling strategy, discussed in the following sections uses relationships developed from measured transient results (Section 6.5), to scale 'unit' torque responses, which are used to determine the engine acceleration.

### 7.6.2 TRANSIENT RESPONSE CALCULATION

The transient response of the engine is assessed by considering the time taken to move from the initial power condition to a desired power. To achieve this the engine has to liberate the torque margin available at the initial steady state condition and use this to accelerate the engine. The engine acceleration is governed by the magnitude of the torque margin and the inertia of the rotating masses. This work considers the transient response in an iterative manner; examining the effect that the torque developed during a small time interval has on the engine speed. The response delay and torque development duration for a given type of engine event are characterised by a specific 'unit' response curve. These unit response curves are developed for each type of transient operation (i.e. throttled, fuelling, EGR, and cam phasing transients) from normalised typical response data. When the normalised unit responses are to be evaluated the amplitude of the response is scaled to match the torque margin available at the steady state condition. The duration of the unit torque response is scaled to coincide with mathematical relationships based upon the work presented in Chapter 6; which predicts the time taken to liberate 62% of an available torque margin.

Figure 7-7 presents a global overview of the transient response evaluation code structure.

### 7.6.3 EXAMINATION OF UNIT TORQUE RESPONSE CHARACTERISTICS

This section seeks to confirm that this approximation of engine torque development is valid for a range of initial steady state conditions. Figure 7-8 presents a number of normalised torque responses, for initial throttle conditions from 5% open to 30% open at 1500 rev/min. It can be seen that the response to a 5% throttle step has a rapid profile, while the response to a throttle step from 30% open has a different gradually accelerating profile. Also shown is the selected unit throttle response curve, which is based upon a transient event from 5% throttle performed at 2000 rev/min. The 5% throttle response has been selected, as the basis for the unit torque response, because at other throttle conditions the torque margin is smaller and the effect of signal error on transient duration will be also be smaller. It can be seen that although the unit torque response provides a poor model for the torque step from 30% throttle it provides good representation of the response for steps from 10% and 15% throttle. It is therefore concluded that the unit curves can be used as a basis to characterise the response of the engine.

Figure 7-9 presents a comparison of the unit throttle response with normalised measured data taken for transients from 5% throttle at 1500 rev/min and 2600 rev/min. This plot shows that there is a very good correlation between the unit model and the two transient responses examined. As a result it is concluded that the unit torque approximation is valid across a range of speed conditions.

### 7.6.4 UNIT TORQUE RESPONSE SCALING FACTOR

Figure 6-7 shows the measured 62% duration for transients from a range of initial throttled conditions. It can be seen that these results have an organised form, asymptotically decaying toward a minimum transient duration. The form of these results may be modelled using an exponential curve fit. Figure 6-8 shows the relationship between throttle transient duration and speed condition. It is proposed that at each speed condition there is a similarly profiled asymptotic relationship between transient response and initial throttle position. Therefore the exponential used to model the transient response with throttle condition may be scaled to represent the response from any initial speed / throttle condition. The constant is not scaled since it represents the system minimum response duration.

$$t_{THROT62\%} = \left( c_1 e^{\frac{-THROT}{t1}} + c_2 e^{\frac{-THROT}{t2}} \right).sf + c_3$$

Where:

| | | |
|---|---|---|
| | C | Regression fitted scaling factors |
| | THROT | Initial throttle position |
| | T | Exponential time constant |
| | Sf | Scaling factor for different initial speed conditions |
| | $C_3$ | Non- scaled regression component |

Table 7-2 presents the exponential constants and scaling factors for different speed conditions.

Examination of Figure 6-14 reveals that to characterise the 62% response time of any fuelling transient, is a constant delay for a given speed. Which is a result of the fact that there are no filling dynamics to consider, simply a step change in fuelling rate. As the engine speed increases the number of fuel injection pulses per second increases and as a result the delay before a step change in fuelling is reduced. This is modelled via an additional delay determined by examining Figure 6-15.

$t_{62\%\_LEAN} = f_{LEAN}$

Where: $f_{lean}$ Scaling factor of different speed conditions

This relationship will hold for spark timing transients as well. However since it has been shown that fuelling / spark timing transients are the quickest and that it is unlikely that a spark timing transient will occur independently of either a fuelling transient or an EGR transient it is not necessary to consider them independently.

EGR transients are significantly more complex to model. As shown in Section 5.4.1, due to the pressure difference between the inlet and exhaust manifolds, levels of EGR increase with throttling; peaking at 30% throttle. As the engine speed increases the diluted charge in the inlet manifold is consumed at a faster rate and as a result, EGR transients occur faster. Since EGR transient duration is taken to be initiated when the inlet manifold pressure drops there is no need to consider the valve dynamics.

Due to the limited data available it was not possible to fully characterise the EGR response duration across a continuous range of initial EGR valve conditions. As a result, it

was assumed that there was a linear relationship between EGR valve position and duration of transient response for a given initial speed / throttle position. A scaling factor was applied in order to match the predicted transient response time with measured results. In order to examine the effect of the increased EGR rates for throttle conditions, a throttling factor was developed. This throttling factor was based upon a polynomial regression of measured data. A further scaling factor was applied in order to adjust the transient response for different initial speed conditions.

$$t_{62\%\_EGR} = 0.9.(EGR - 10).f_{THROT}.f_{SPEED} + lag$$

$$f_{THROT} = c_0 + c_1.THROT + c_2.THROT^2 + c_3.THROT^3$$

| | | |
|---|---|---|
| Where: | EGR | Initial EGR demand |
| | $f_{throt}$ | Scaling factor for initial throttle position |
| | $f_{speed}$ | Scaling factor for initial speed position |
| | Lag | Constant lag |
| | THROT | Initial throttle condition |
| | C | Regression coefficients |

As discussed in Section 5.5 for a given engine speed there is an optimal cam timing position for maximum torque; determined by the point where charge resonances cause improved volumetric efficiency. The developed model is based upon the belief that the transient duration will be directly proportional to the gap between the initial cam position and the optimal cam position. Included within this model is a delay to represent the control system and the valve dynamics. A scaling factor is used to modify the response for an initial speed condition. It is believed that this model is suitable since there is insufficient data available to accurately characterise a more detailed model.

$$t_{62\%\_CAM} = (CAM_{OPT} - CAM_{INITIAL}).f_{SPEED}.SPEED + lag$$

| | | |
|---|---|---|
| Where: | $CAM_{opt}$ | Optimal cam overlap for max power |
| | $CAM_{INITIAL}$ | Initial cam overlap |
| | $f_{SPEED}$ | Speed scaling factor |
| | SPEED | Initial speed |
| | Lag | Constant system delay |

When a step change in a number of control variables causes a combined transient operation the algorithm selects the greatest individual transient duration to be

representative of the system response. As shown in Section 6.11, work has been undertaken to verify that it is valid to assume that the transient response duration is not subject to dilution interaction effects; however the results were not conclusive. Despite this, since all of the control variables are independently actuated and, with the exception of EGR, diluent levels are independent of control variable interaction effects, it seems unlikely that a combination of transient response durations would be representative.

### 7.6.5 TRANSIENT DURATION SUB OBJECTIVE FUNCTION

In order to assess the relative transient response a sub-objective function has been developed. The sub-objective function seeks to develop a unit-less measure of transient response, which may be used to scale the fuel consumption metric developed in the engine model section of the objective function.

It was decided to compare the predicted transient duration for a dilution condition with one predicted form a base, stoichiometric only condition. As a result, it has been necessary to develop an engine control line for the examined power conditions limited to develop minimum fuel consumption using only throttle variations. Also included in the requirements for this base engine control line was a minimum torque margin of 10 Nm at any given speed condition. This ensured that the control line at least represented a real world application of a minimum BSFC line. This base engine control line is considered in greater detail in Section 7.8.2.

The transient sub-objective function evaluates the duration of the transient performed from the current steady state condition to a 42 kW power condition. This duration is compared with the equivalent duration for a transient operation instigated from the baseline control variable conditions. The output of the sub-objective function is a ratio of the appropriate transient durations, such that a transient response of less than 1 means that the dilution control variables produces a transient response which is quicker than the base control throttle only condition.

## *7.7 Global objective function*

The global objective function evaluates the specific fuel consumption for a particular operating condition using the engine model. The result of this is subsequently scaled by the result of an emissions sub-objective function. If the control variable conditions produce specific emissions which meet legislative limits then the fuel consumption is scaled by a

factor of 1. If the control variable conditions produce emissions levels which exceed legislative limits then the fuel consumption is scaled punitively. Following this the scaled fuel consumption result is combined with the relative transient duration sub-objective function response. The transient factor response is weighted to give an equal importance to fuel consumption and transient response. A summation of the fuel consumption and weighted driveability performance is used as the final objective response. This response is assessed for its relative fitness, before effecting the next generation; either by being included directly or by becoming a 'parent' for a new individual.

## *7.8 Application of objective function to develop steady state control lines*

This section examines the engine control lines developed using the optimisation process described above and assesses the effect of these control lines on the performance of a vehicle over the EUDC legislative cycle.

### 7.8.1 SOLUTIONS DEVELOPED

Three sets of engine control lines have been developed, these are the 'baseline' best fuel optimised using only the throttle position. The best fuel consumption optimised using all the available variables, and best combined fuel consumption and driveability using all the engine control variables.

### 7.8.2 BASE ENGINE CONTROL LINE - NON DILUTION SOLUTION

Figure 7-10 shows the throttle only base engine control line plotted upon speed / torque axes. It can be seen that the BSFC contours provide greater coverage of the speed/ torque regions this is because the model has been adapted to include further 5% throttle information. The minimum BSFC control line achieved only varying the position of the throttle is shown as a bright green line. It can be seen the control line has a discontinuous profile. This is due to the discrete speed engine model used to develop it. In practice the control line would have a continuos profile and would track with a 10 Nm offset the WOT maximum torque line. However since all control lines will be subject to the same discontinuous profile it considered that this is not a significant limitation of the derived control lines. This base BSFC control line represents a classical e-line as developed in other works.

### 7.8.3 MINIMUM FUEL SOLUTION

Figure 7-11 presents a control line for an engine with the freedom to manipulate all control variables available in order to achieve minimum fuel consumption at a required power. Figure 7-12 gives a break down of the control variable position at each power condition. Figure 7-13 & Figure 7-14 demonstrates the fuel consumption and relative driveability score for each of the power conditions.

Generally it can be seen that this control line develops powers at higher speed / lower torque condition that the throttle only BSFC line. This is due the torque reduction dilution effects. It can seen that this strategy relies predominately upon lean charge dilution, with minimised valve overlap to develop minimum BSFC. EGR dilution is minimised since dilution through this approach does not have such a significant reducing effect upon fuel consumption. It would appear that the spark timing is modulated to control the specific emissions.

Examination of Figure 7-13 demonstrates that fuel consumption is typically 10% reduced for the dilution torque engine control line.

An additional benefit even of this purely fuel consumption optimised condition is that at every power condition the transient engine response is considerably improved. Typically a transient operation requires only 75% of the time required for a condition on the baseline configuration.

### 7.8.4 COMBINED SOLUTION

Figure 7-11 demonstrates the form of the best combined driveability and fuel consumption optimised control line. Figure 7-15 demonstrated the control variable settings for each power condition. Figure 7-13 & Figure 7-14 demonstrates the fuel consumption and relative driveability scores for each of the power conditions.

It can be seen from Figure 7-15 that typically the best combined operating condition occurs at a higher speed, with reduced reliance on lean dilution and increased use of EGR. Examination of Figure 7-13 demonstrates that this combined solution offers an average fuel consumption improvement over the throttle only optimised solution of 5%, although at 10 kW, 18 kW and 30 kW there is a small increase in fuel consumption. Whilst producing transient driveability durations of less than half of the throttle only optimised solutions.

### 7.8.5 Comparison of constant speed conditions

Table 7-3 presents the steady state speeds which each power condition represents. It presents the minimum fuel consumption for a vehicle operating at these power conditions for each of the three optimised control lines. An additional set of results is presented and these are for a stoichiometric throttle condition which has a similar steady state condition to that of the improved driveability control line. Thus it represents a classical driveability controller.

It can be seen that for motorway cruising speeds the minimum BSFC control line provides a 11% improved fuel consumption. While at 50 mph there is a 15% improvement between an optimal combined condition and an equivalent stoichiometric condition.

### 7.8.6 Application of dilution control to EUDC drive cycle.

In order to assess the potential improvement to fuel consumption the optimised engine control lines will be examined over the course of a standard European drive cycle.

The European drive cycle consists of a series of acceleration low speed cruise deceleration processes used to represent city driving (ECE-15) followed by a higher power manoeuvred which consists of an extended acceleration and high speed cruising periods (EUDC). The power conditions for these manoeuvres are also shown in Figure 7-16. It can be seen that only the power conditions achieved during the EUDC exceed the minimum where dilution torque control has any effect. As a result, the investigation of the effect of the dilution control approach will focus specifically upon the EUDC The acceleration periods during the course of the EUDC occur at a low rate; a maximum of 0.1 kW per second. These rates of power variation are sufficiently small that the powertrain controller will not have to implement a rapid transient event. The engine test bed had no means to allow the engine to be motored, consequently there is no experimental deceleration information for this engine. It is felt that dilution torque control will not be used during deceleration processes due to the heavily throttled nature of deceleration phases. Information for the deceleration periods will be taken from test data taken on a 1.6 L Ford Focus used to develop in the development of the catalyst model (Section 7.5).

During the drivecycle simulation the vehicle speed points are considered to be power conditions examined at discrete time intervals. Consequently since the time intervals are

small and there is slow progression through the power range the transition from one power condition to the next is considered to be instantaneous.

Figure 7-16 presents the fuel consumption for an engine operating both an optimised throttle only control strategy and a dilution control strategy. For both cases the engine responses for very low torque settings were determined by extrapolation of the engine regression models.

It can be seen that using the combined optimal fuel and transient response engine control line there is potential for a 3% fuel consumption improvement over the course of the EUDC, whilst meeting specific emissions requirements. This fuel improvement is over a throttle only optimised control strategy, the type of which have been shown to offer a minimum of a 8% improvement over a conventional automatic transmission.

**Table 7-1 Emissions limits for specific power conditions**

| Power cond. | $NO_x$ - g/sec | uHC - g/sec | CO - g/sec |
|---|---|---|---|
| 4 kW | 0.0012 | 0.0027 | 0.03 |
| 6 kW | 0.0014 | 0.0031 | 0.045 |
| 8 kW | 0.0017 | 0.0036 | 0.06 |
| 10 kW | 0.0021 | 0.0042 | 0.064 |
| 12 kW | 0.0022 | 0.0047 | 0.072 |
| 14 kW | 0.0028 | 0.0049 | 0.074 |
| 16 kW | 0.0031 | 0.0051 | 0.079 |
| 18 kW | 0.0034 | 0.0053 | 0.084 |

**Table 7-2 Coefficients for transient reponse models**

| Throttle transients coefficients | | |
|---|---|---|
| | y0 | 0.08943 |
| | a1 | 0.75324 |
| | t1 | 5.88706 |
| | a2 | 0.50985 |
| | t2 | 72.37884 |
| EGR transients coefficients | | |
| | c3 | -7.28E-06 |
| | c2 | 2.05E-03 |
| | c1 | -1.92E-01 |
| | c0 | 7.01E+00 |

**Table 7-3 Specific fuel consumption for steady vehicle speed conditions**

| | | | | | | | | | | | | |
|---|---|---|---|---|---|---|---|---|---|---|---|---|
| | Vehicle speed | mile/h | 30.00 | 35.00 | 40.00 | 45.00 | 50.00 | 55.00 | 60.00 | 65.00 | 70.00 | 75.00 |
| | Vehicle speed | km/h | 48.38 | 56.45 | 64.51 | 72.58 | 80.64 | 88.70 | 96.77 | 104.83 | 112.90 | 120.96 |
| | Vehicle power | kW | 6.95 | 8.77 | 10.90 | 13.38 | 16.25 | 19.56 | 23.34 | 27.66 | 32.54 | 38.03 |
| Minimum fuel consumption | Throttle only | g/kWh | 322.83 | 296.98 | 247.72 | 241.48 | 239.93 | 227.92 | 241.19 | 229.47 | 232.39 | 229.53 |
| | Dilution strategy | g/kWh | 322.83 | 296.98 | 246.07 | 221.96 | 216.34 | 216.23 | 207.23 | 203.60 | 206.73 | 214.49 |
| | Percentage improvement | | 0.00 | 0.00 | 0.67 | 8.08 | 9.83 | 5.13 | 14.08 | 11.28 | 11.04 | 6.55 |
| Optimised driveability and fuel consumption | Throttle only | g/kWh | 323.06 | 299.69 | 265.49 | 253.80 | 255.25 | 244.17 | 228.98 | 230.14 | 228.00 | 228.03 |
| | Dilution driveability | g/kWh | 323.06 | 298.72 | 250.94 | 237.36 | 247.87 | 230.19 | 223.60 | 210.01 | 224.08 | 228.20 |
| | Percentage improvement | | 0.00 | 0.32 | 5.48 | 6.48 | 2.89 | 5.72 | 2.35 | 8.75 | 1.72 | -0.08 |

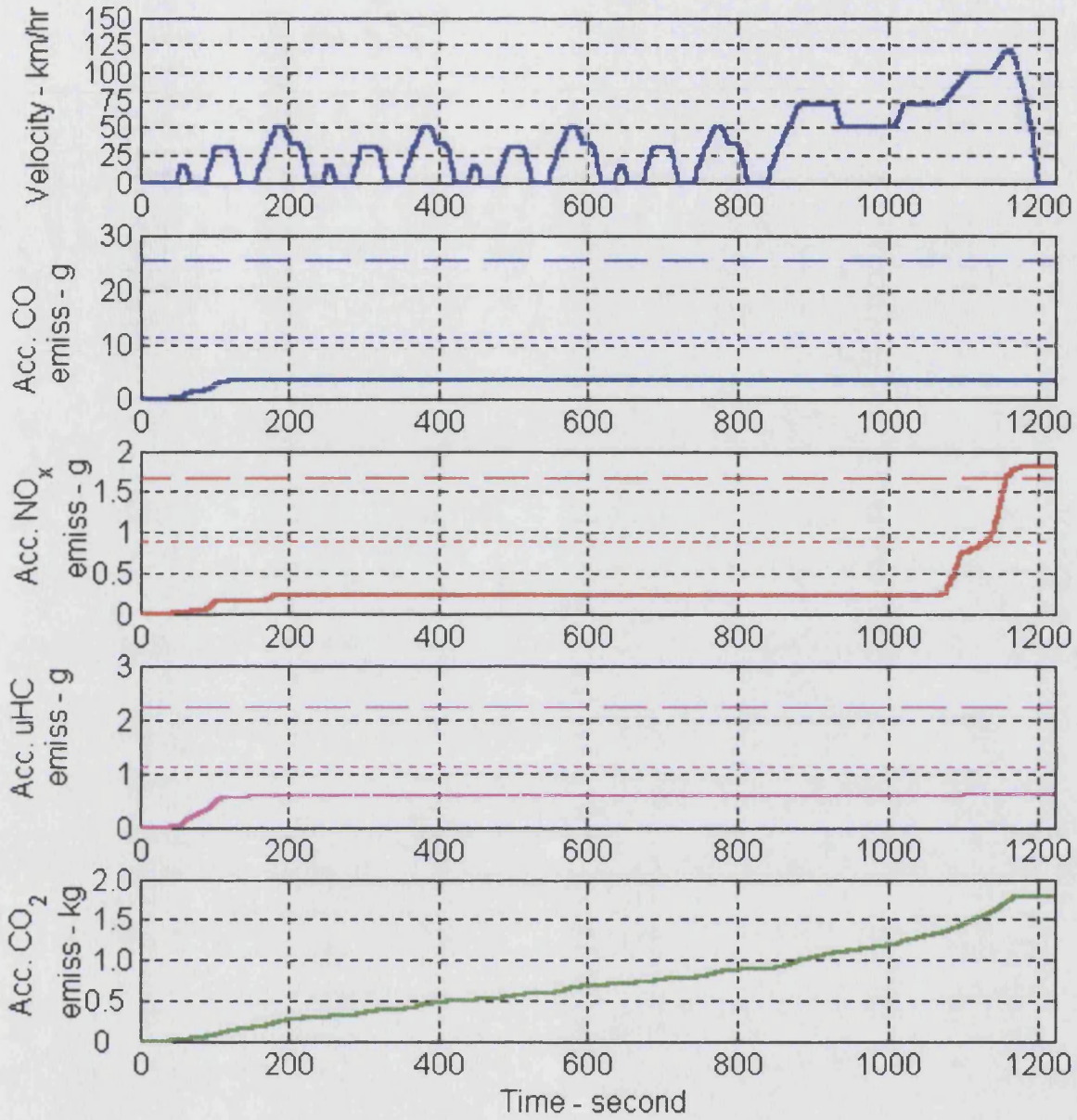


**Figure 7-3 Cumulative emissions for 1.6 L Focus over drive cycle**

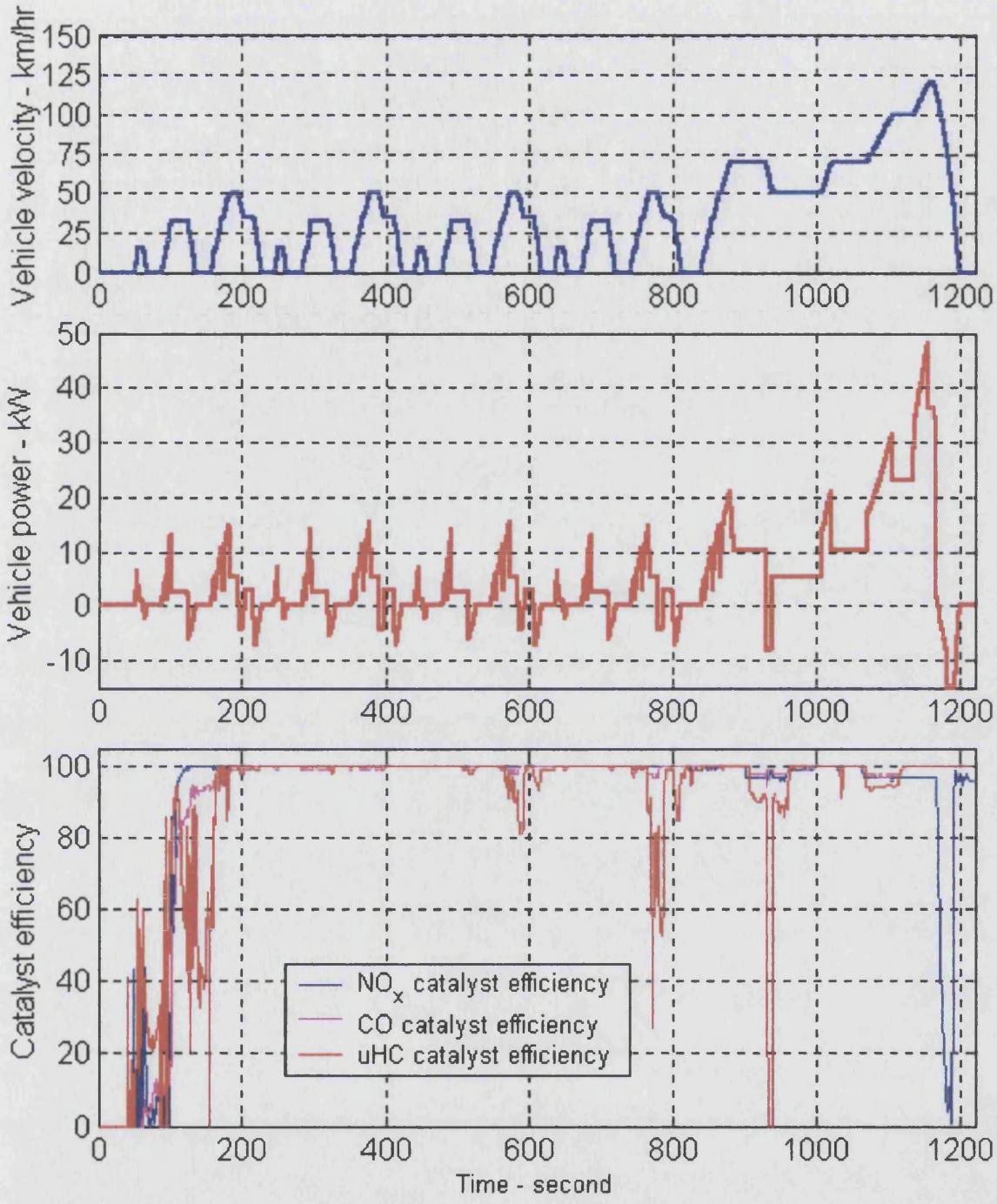


**Figure 7-4 Conversion efficiency of close coupled three way catalyst in 1.6 L Ford Focus**

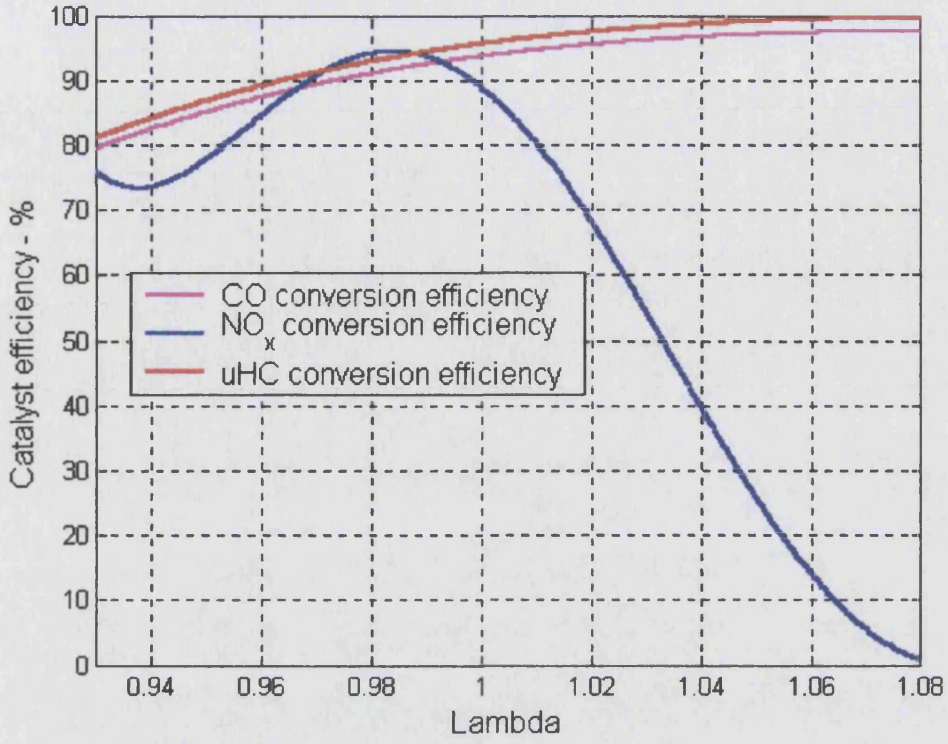


**Figure 7-5 Models used predict the efficiency of three way catalyst for lambda ranges greater than those achieved using HEGO control.**

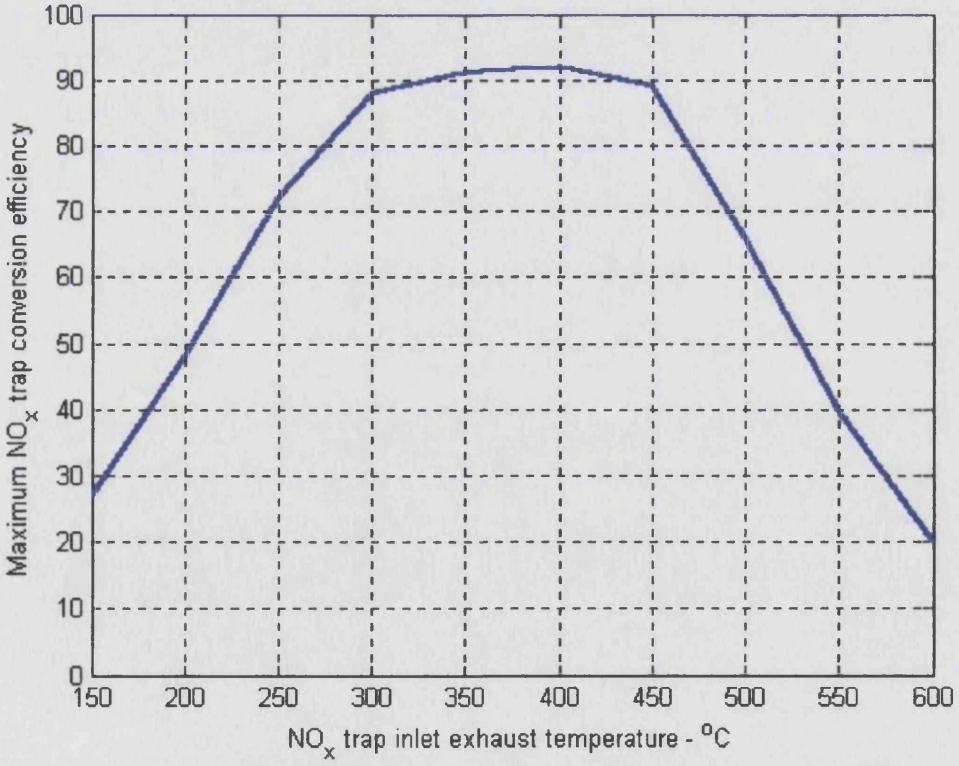


**Figure 7-6 $NO_x$ trap catalyst efficiency with inlet charge temperature**

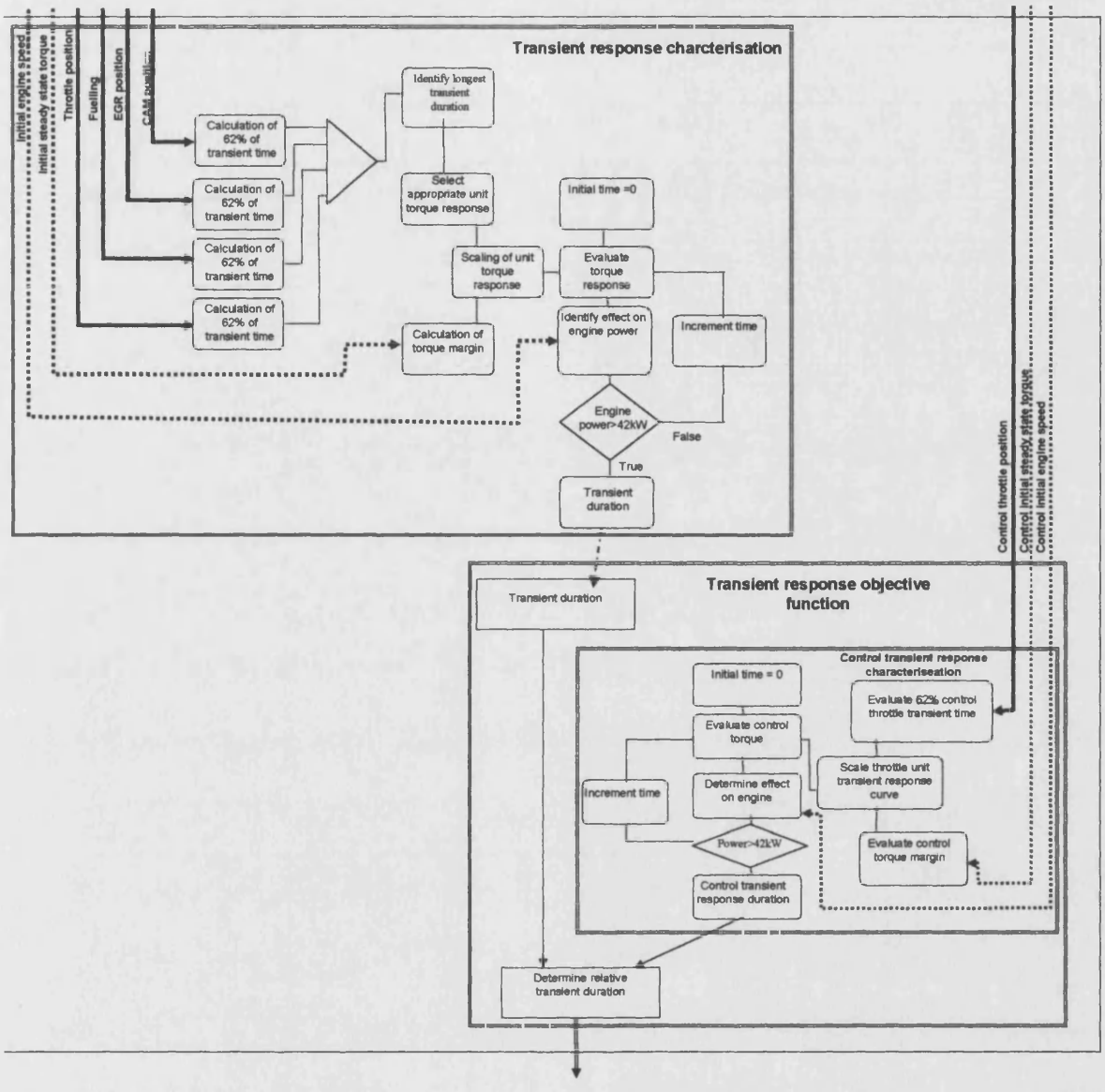


**Figure 7-7 Driveability assessment and sub objective function**

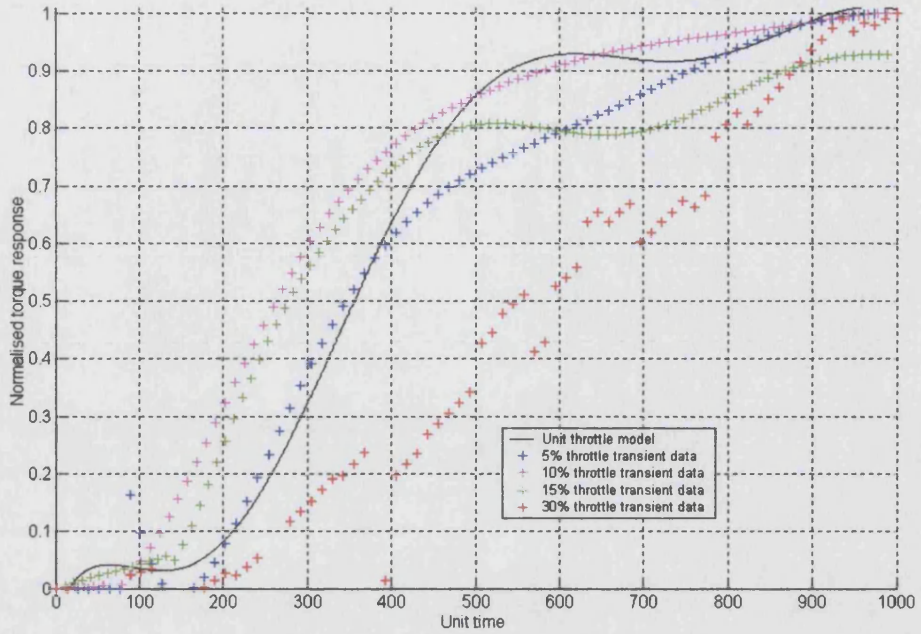


**Figure 7-8 Unit torque response - validity for different initial throttle conditions**

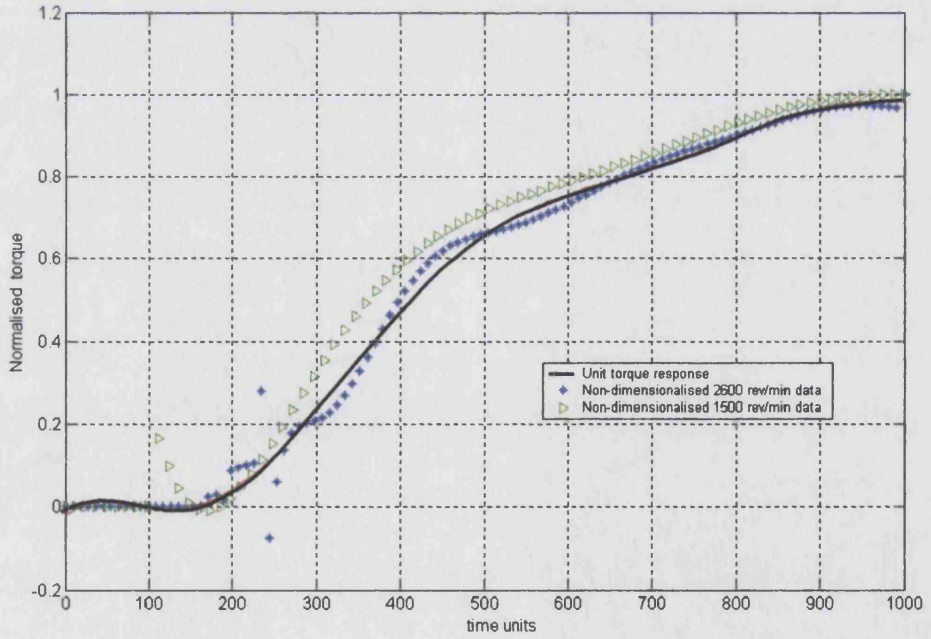


**Figure 7-9 Unit torque development validity for different initial speed conditions**

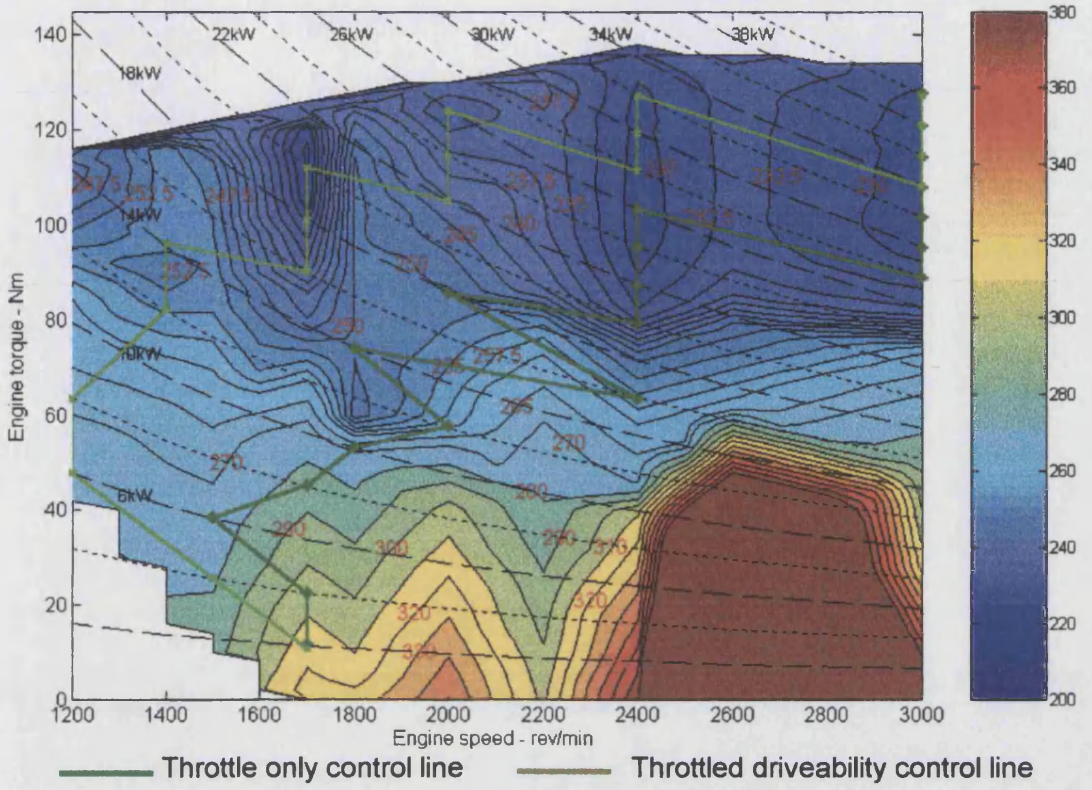


**Figure 7-10 'Control engine control line' throttle only fuel consumption optimisation of engine performance**

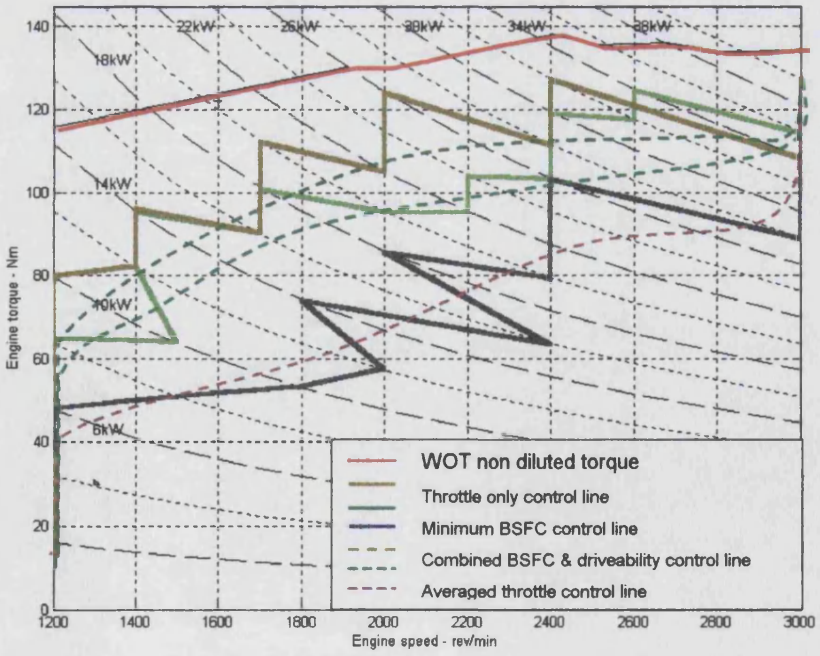


**Figure 7-11 Optimised fuel consumption and transient response engine control line**

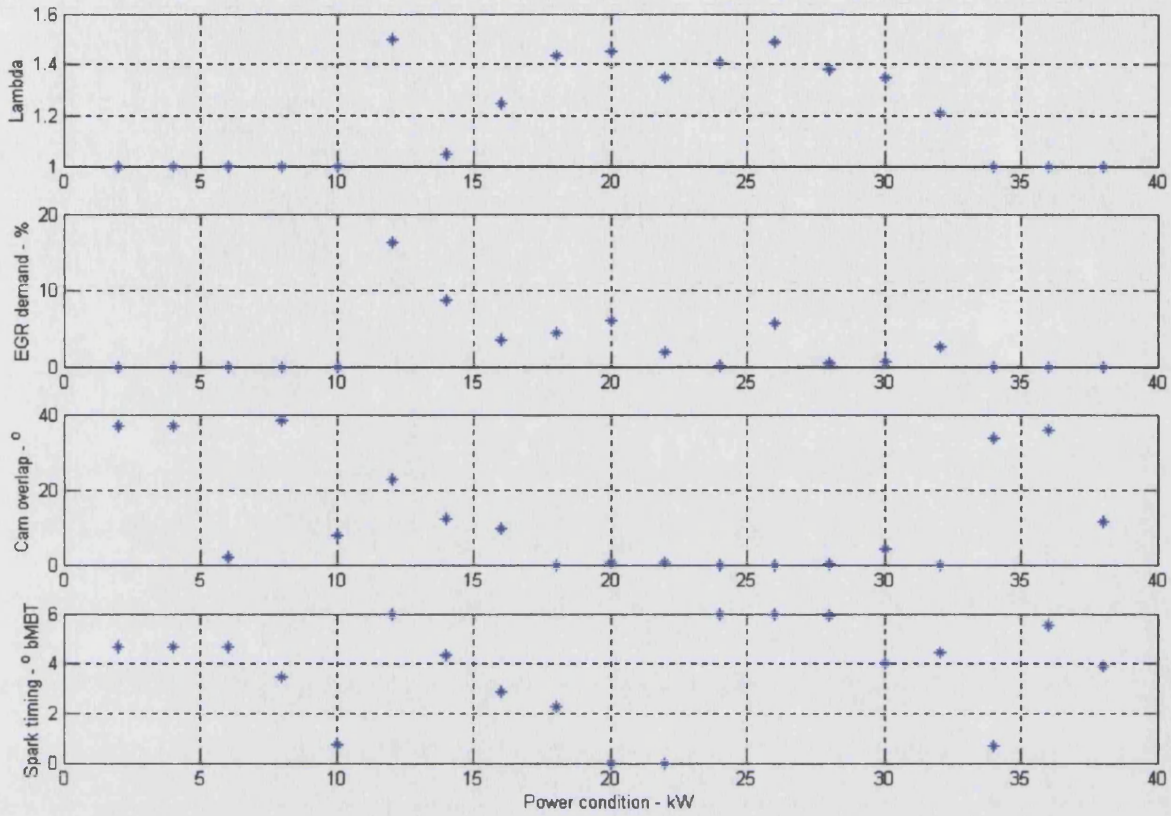


**Figure 7-12 Dilution conditions for minimum BSFC engine controller**

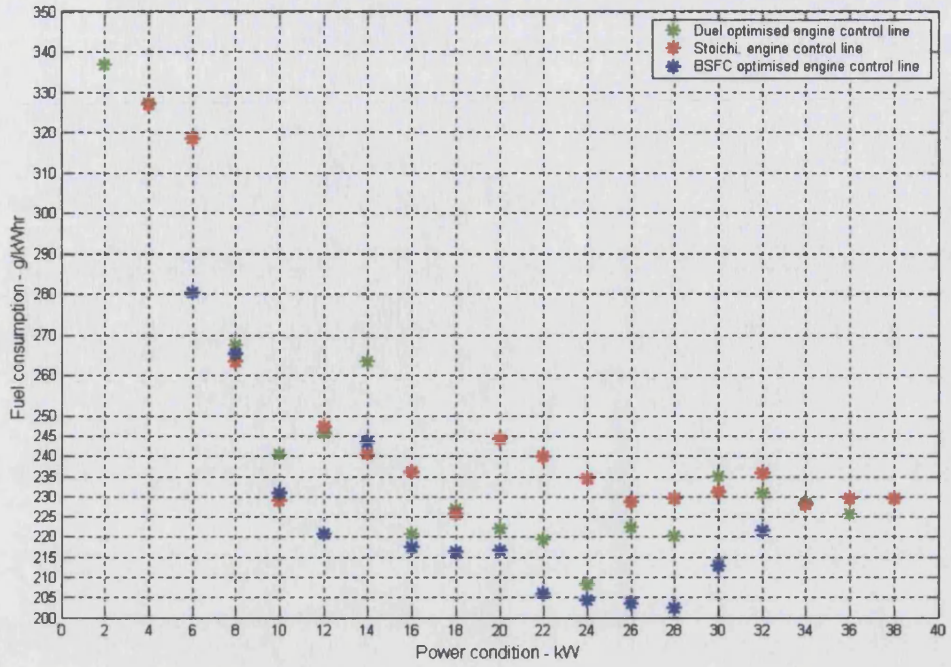


**Figure 7-13 Comparison of fuel consumption characteristics for engine control strategies**

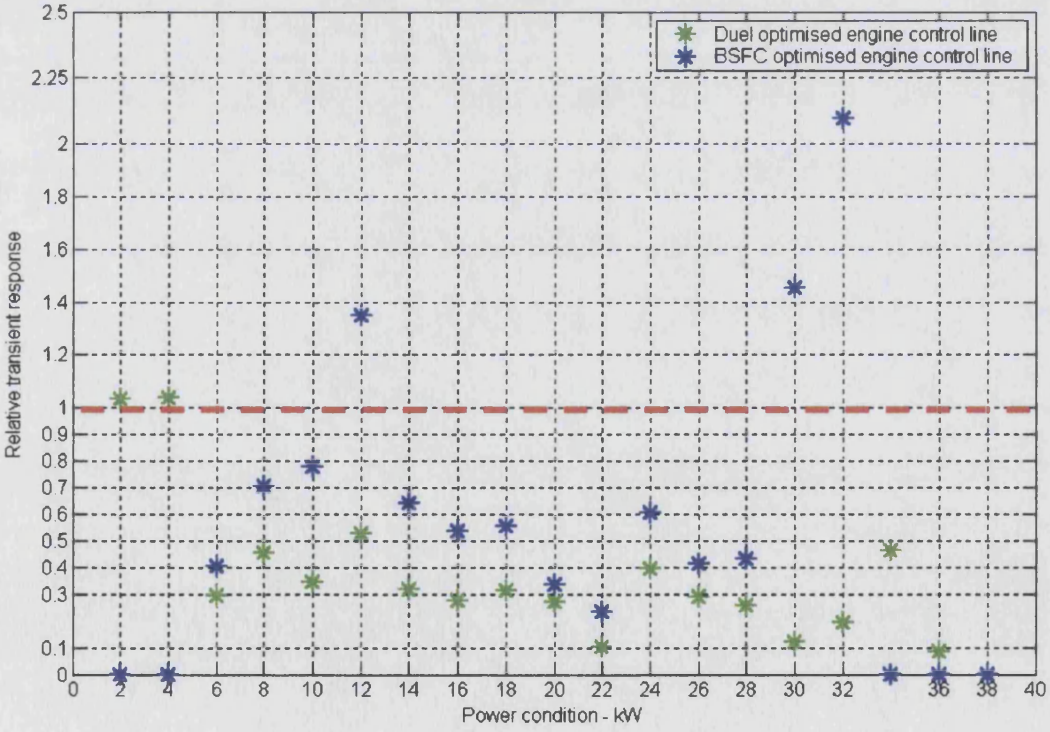


**Figure 7-14 Transient response characteristics for dilution control strategies**

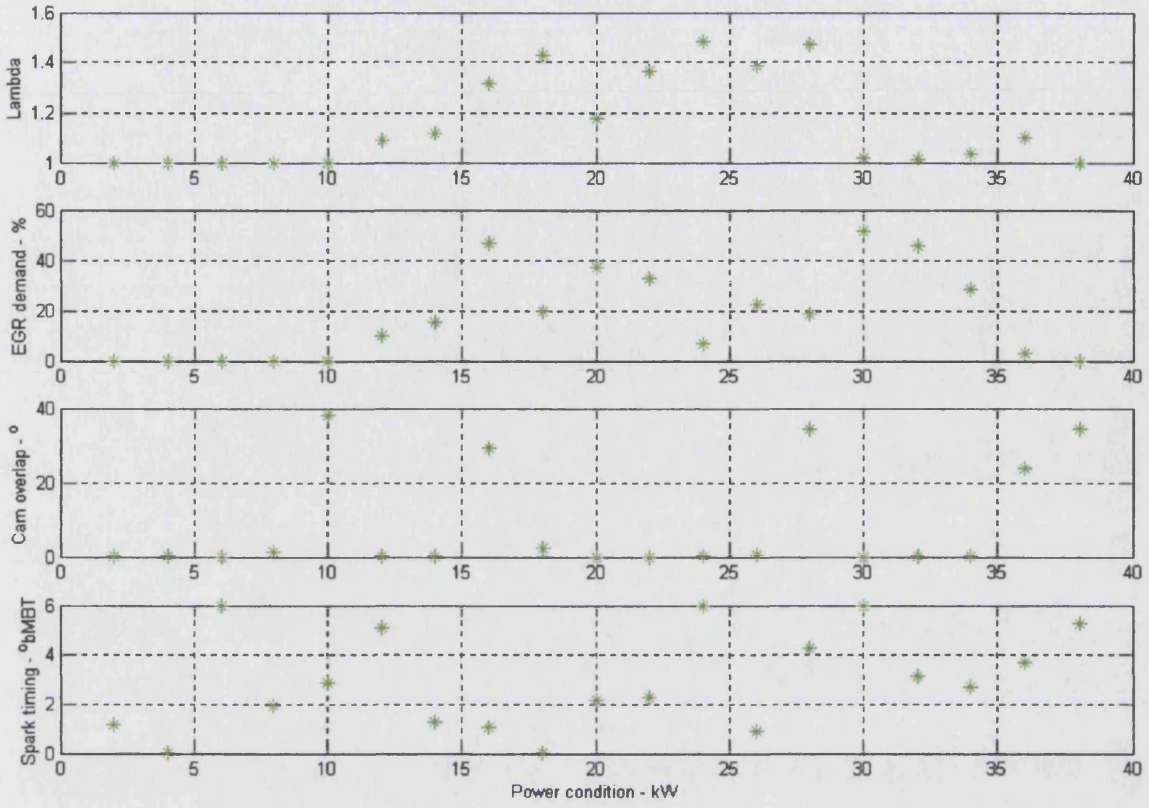


**Figure 7-15 Dilution control conditions for combined control strategy**

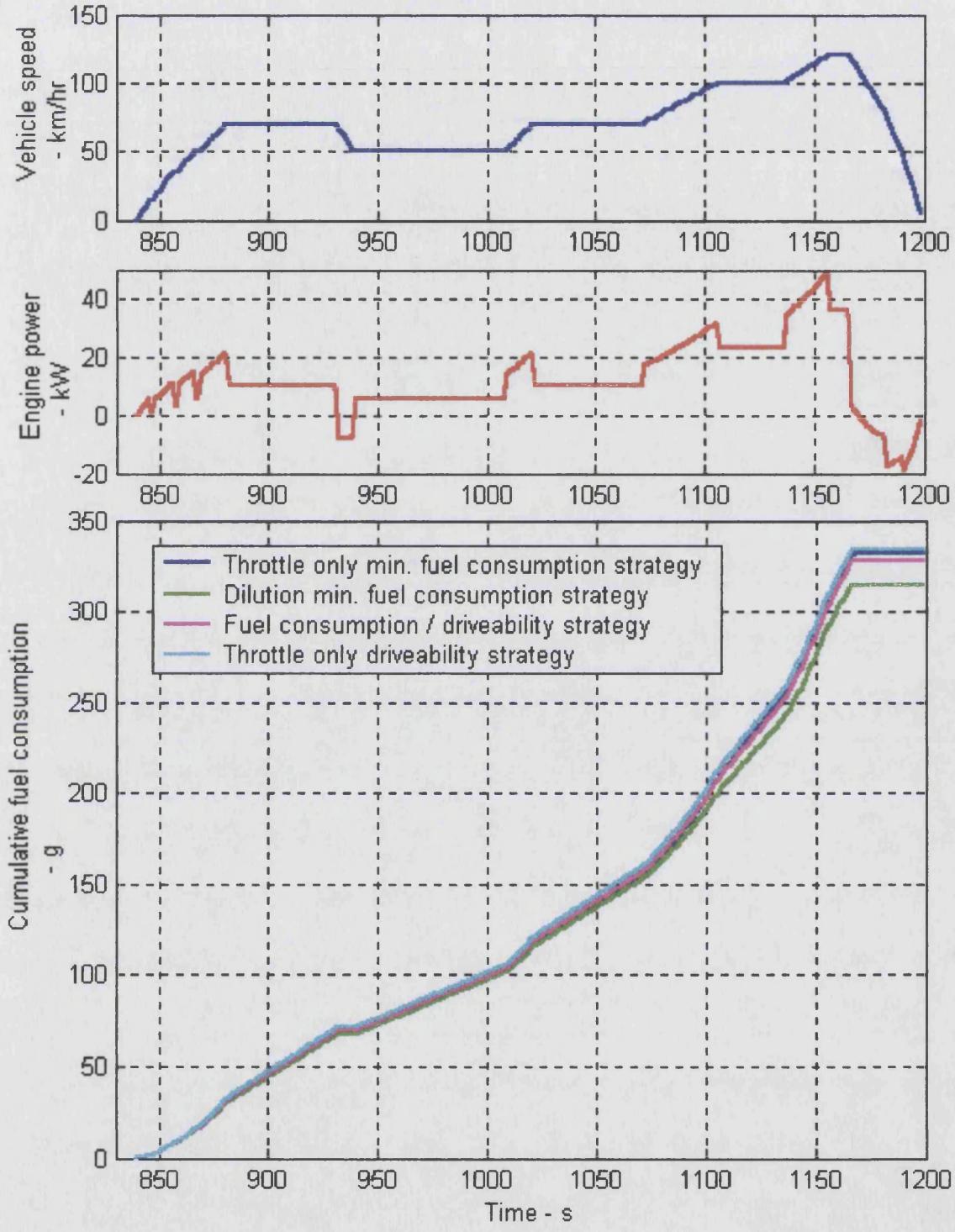


**Figure 7-16 Comparison of the effects of engine control strategy upon fuel consumption**

# 8 Conclusions

This chapter summarises the results obtained and conclusions drawn throughout the body of this work, identifying the novel contributions developed.

The work introduces the concept that continuously variable transmissions allow flexibility of engine operation highlighting how this flexibility has been used to develop engine control strategies for minimum fuel consumption. The work continues to show that in practice a compromised engine control strategy is used because optimal fuelling strategies provide unacceptable response times during transient operations due to the reduced levels of available torque margin.

This work then introduces the novel concept of charge dilution torque control. This is the use of gases excess to the combustion process which dilute the induced charge, thereby reducing the torque developed for a given throttle opening. The greater body of this work has determined the scope that charge dilution offers to reduce the driveability compromise suffered by an optimal fuel consumption engine control strategy. The charge diluents examined in this work are exhaust gas recirculation and lean charge combustion.

In order to assess the implications of charge dilution on steady state and transient operation, a gasoline engine test rig was developed. The test rig allowed the effect of five engine control variables, namely throttle position, cam timing, spark timing, charge fuelling, and EGR rate to be assessed. A design of experiments (DoE) testing methodology was developed in order to maximise the information derived from a given number of experiments. Classical application of DoE was investigated and a novel adaptation was developed. The latter was developed to improve high order model accuracy and used two second order regression models joined by a geometric spline. The two stage gradient matched method developed was then compared with a classical $5^{th}$ order regression model. The comparison was made by visual examination of the response results, and through scrutinising each model's accuracy in predicting a set of test data not used in the model development process. The use of an independent data set to test the accuracy of a model is novel to this field.

Using the developed DoE test program, the effect of charge dilution was investigated on the engine. It was found that external EGR and lean charge dilution have the potential to develop torque margins of 30 Nm and 40 Nm respectively at wide open throttle. It was found that whilst the torque margin developed through lean charge dilution was consistent throughout the throttle range, the torque margin developed via external EGR charge dilution peaked at 30° throttle opening. This work also showed that the torque margin that could be developed through internal EGR, with the VVA system fitted to the test engine, was insufficient to be usefully exploited.

Transient tests were conducted to enable a thorough understanding of transient response to be developed. This work showed that from any initial steady state point, lean charge transient operations where performed most rapidly. In transients occurring from low speed conditions, throttled transients occurred second quickest however as the higher engine speed increased EGR transients became the second quickest. The duration of transients involving cam phasing was consistently the greatest.

The final stage of the thesis was the development of optimal engine controls which maximised the potential provided by dilution torque control. In order to achieve this the regression models developed as a result of the testing program were incorporated into an engine model. Included within this engine model was an assessment of the performance of both a three-way catalyst and a $NO_x$ trap catalyst. The engine model was incorporated into a multi-variable, multi response objective function. The objective function was used to minimise fuel consumption and maximise vehicle driveability for sets of engine variables that met legislative emissions requirements. This multiple goal optimisation was achieved using sub-objective functions for legislative emissions, and transient responses to scale the fuel consumption output of the engine model.

To the author's knowledge, this is the first application of a multiple goal optimisation approach within engine research to include fuel consumption and a direct measure of vehicle driveability. The developed engine control line produced a 10% improvement in fuel consumption at any diluted operating point, compared to a conventional optimal engine control line. Additionally the transient response time of the dilution torque control was typically half that of a conventional operating point.

The effect of the optimised control variables was examined over the course of an extra urban drive cycle. It was shown that over the course of the cycle the dilution charge control developed a 6% fuel consumption saving while meeting specific emissions requirements.

# 9 Recommendations for further work

This chapter seeks to propose future areas where this work may be taken in order to fully examine the potential that dilution torque control offers. it is broken down into three areas, namely, enhancement of the work presented, implementation of current results and approaches to extend the scope of dilution torque control.

## *9.1 Enhancement of work presented*

The work presented in this study could be enhanced in a number of ways.

- Completion of the engine operating map

Extending the engine map to include high speed and deceleration engine regions.

- Improvements in the quality of the catalyst models

Improving these models will allow greater accuracy in the estimation of exhaust gas constituents. This may allow the use of conditions with greater engine $NO_x$ emissions, thereby extending the useful engine envelope.

- More complex optimisation arrangement

If an objective function could be constructed such that each operating point within a specified drive cycle could be optimised at once, then there is greater potential to utilise the whole engine performance possible within legislative emissions limits. It is possible to speculate as to the structure of such an objective function. If it were to be used to optimise a drive cycle consisting of 10 power conditions, then the objective function would consist of 10 sub-objective functions. The main objective function would be provided with information to establish the control variable setting for each power condition, i.e. in this case 600 items of information. Each sub objective function would evaluate the engine model for the specified sets of control variables. The emissions, fuel consumption and transient response results of each sub-objective function would be weighted and accumulated. Such an optimisation approach, however, would require substantial computing power

- Adapting the EGR system

In line with the works of Yoshizawa et al[43], Blank et al[44] the EGR system should be adapted to maximise homogeneous charge mixing whilst minimising transient implications of this feature. Additionally, taking the EGR tubing directly over the crank case and into specific engine ports may reduce transient lag, whilst maximising the charge reduction due to bulk charge heating.

- The development of a fully dynamic CVT, vehicle model

The development of such a model would allow the optimisation of specific transient vehicle characteristics such as initial jerk. Additionally a combination of transient traits could be optimised by identifying an ideal vehicle acceleration profile, similar to that developed in the work of Wicke[18], and using this in the objective function for driveability. However, such an investigation would require considerable computing power if optimised using a genetic algorithm technique.

## *9.2 Implementation of current results*

Before a dilution torque control strategy can be implemented within a vehicle the following ECU control issues must be addressed.

- The control of an engine featuring dilution charge control.

Since dilution charge control can feature both EGR and lean burn dilution strategies it is unlikely that a torque based engine management controller, where the torque is inferred from the airflow past a hotwire anemometer, will be accurate enough to maintain suitable operating conditions. Interesting development in the use of in-cylinder pressure transducers to control engine parameters have been presented [131,132] and it is the belief of the author that such systems may offer an ideal approach to control parameter scheduling.

Research into the estimation of engine torque and control dilution levels from pressure signals is required in this field.

- Control of a drivetrain featuring dilution charge control

Currently within industry two approaches are being used with regard to the controller responsible for engine parameter scheduling within integrated powertrains proposes the use of a power demand signal to an engine controller which co-ordinates the throttle

position, and fuelling in order to meet the power demand. Murray[22] on the other hand proposes the use of a powerful master controller scheduling the position of all engine variables remote from the engine.

Research must be undertaken to identify which approach is more suitable for the application of a dilution control strategy.

## *9.3 Approaches to extend the scope of dilution torque control*

A number of approaches to extend an engine's tolerance to charge dilution, and consequently extend the scope of dilution torque control, have been touched upon in Chapter 2.

The most obvious application is that of a stratified direct injection engine. It would then be possible to investigate fully the lean charge dilution potential of an engine featuring specific design adaptations which enhance dilution tolerance.

However, in the author's opinion enhanced ignition energy systems and iEGR through additional cam lobes on the exhaust cam profile offer some of the most interesting opportunities. Both of these approaches could be implemented without deviating from the original premise that the engine must be cheap, such that the total cost of the application of a CVT can be offset. Additionally these technologies could allow the implementation of high dilution rates without the additional requirement of a $NO_x$ trap type catalyst, whilst still developing a rapid transient response.

# 10 References


1. **Botti J. J., & Miller C. E.,** "Powertrains of the future reducing the impact of transportation on the environment " SAE 1999-01-0991, SAE International publications, Warrendale USA 1999

2. **Shillington S. A. C.** "The unstoppable versus the immovable - a personal view of the future facing gasoline direct injection in face of Euro IV" IMechE S490/009/97 1997

3. **Zelenka P., Egert M., Cartelllieri W.,** "Ways to meet emissions standards for heavy sports utility vehicles - SUV" Seoul 2000 Fisita world automotive congress F2000H180-June 12-15 2000

4. **Gis W., & Bielaczyc,** "Emissions of $CO_2$ and fuel consumption for automotive vehicles" SAE 1999-01-1074, SAE International publications, Warrendale USA 1999

5. **Nohira H., Ito S., Paquet T.**, "The development of Toyota's direct injection gasoline engine" Spark Ignition Engine Emissions - course at Univ. Leeds 23 - 27 Nov. 1998 also presented in Proceeding of AVL Engine and Environment Conference, 1997

6. **Schechter M. M., & Levin M. B.,** "Camless engine" SAE 960581 SAE International publications, Warrendale USA 1996

7. **Crosse J.**, "Saab gets radical" PP36-40 December 2000 Automotive Engineer

8. **Mayflower corporation**, $e^3$ engine development homepage: http://www.mayflower-e3.com 2002

9. **Lotus engineering**, AVT engine homepage: http://www.lotuscars.co.uk/template.cfm?name=lotengresnewtechavt 2002

10. **Soyhan H. S., Lovas T. Mauss F.,** "A stochastic simulation of an HCCI engine using an automatically reduced mechanism" Proceedings of the 2001 Fall technical conference of the ASME internal combustion Engine division ASME 2001-ICE-416

11. **Kong S. C., & Reitz R. D.,** "Modelling direct injection gasoline HCCI combustion using detailed chemistry and CFD" Proceedings of the 2001 Fall technical conference of the ASME internal combustion Engine division ASME 2001-ICE-415

12. **Takiyama T., & Morita S.,** "Analysis of Improvement of Fuel Consumption by Engine-CVT Consolidated Control" AVEC '96 International Symposium on Advanced Vehicle Control, pp.1159-1167

13. **Hendriks E.,** "Qualitative and Quantitative Influence of a Fully Electronically Controlled CVT on Fuel Economy and Vehicle Performance" Van Doorne's Transmissie B.V., SAE 930668 SAE International publications, Warrendale USA 1993

14. **Kriegler W.,** "IC engines and CVT's in passenger cars: A system integration approach" Paper 4 IMechE S540 Advanced vehicle transmissions and powertrain management September 1997

15. **Heisler H.,** "Vehicle and Engine Technology" 2nd Edition Arnold Publishing 1999 ISBN 0-340-69186-7

16. **Setright L. J. K.,** "Progress without steps" Automotive Engineer March 1999

17. **Singh T., & Nair S. S.,** " A mathematical review of continuously variable transmissions" SAE 922107 SAE International publications, Warrendale USA 1992

18. **Wicke V.,** "Driveability and control aspects of vehicles with continuously variable transmissions" University of Bath School of Mech. Eng. PhD Thesis 2001

19. **Happian-Smith J.,** "An introduction to modern vehicle design" pp 403 – 453 Butterworth Heinemann 2002 ISBN 0-7506-5044-3

20. **Akehurst S.,** "An investigation into the loss mechanisms associated with a pushing metal v-belt continuously variable transmission" University of Bath School of Mech. Eng. PhD Thesis 2001

21. **Kluger M. A., & Fussner D. R.**, "An overview of current CVT mechanisms, forces and efficiencies" SAE 970688 SAE International publications, Warrendale USA 1997

22. **Murray S. W.,** "Control of an integrated IVT powertrain" IMechE S744 Conference on integrated powertrains and their control, Sept 2000, Univ. of Bath. S744

23. **Torotrak Development Ltd.**, Homepage: http://www.torotrak.com 2002

24. **Brace C. J., Deacon M., Vaughan N. D., Burrows C. R., Horrocks R. W.,** "Integrated passenger car diesel CVT powertrain control for economy and low emissions" Paper 3 IMechE S540 Advanced vehicle transmissions and powertrain management September 1997

25. **Brace C. J.,** "Transient Modelling of a DI TCI diesel Engine" PhD Thesis 1996, University of Bath

26. **Birch S.,** "Audi takes CVT's from the 15th century to the 21st century" Automotive Engineering 01/00 also found at http://www.sae.org/automag/techbriefs_01-00/03.htm

27. **Cuddy M. R., & Wipke K. B.,** "Analysis of the fuel economy benefits of drivetrain hybridisation" SAE 970289

28. **Nickel F.**, "ISAD – Integrated starter-alternator damper. What benefit is it for the user?" Proc. AVL Engine and Environment Graz 1998

29. **Katrasnik T., Trenc F., Rodman S., Hribernik A., Medica V.,** "Improvement of the dynamic characteristic of an automotive engine by a turbocharger assisted by an electric motor" Proceedings of the 2001 Fall technical conference of the ASME internal combustion Engine division ASME 2001-ICE-429

30. **Panting J., Pullen K. R., Martinez-Botas R. F.,** "Turbocharger motor-generator for improvement of transient performance in an internal combustion engine" Proc. Instn. Mech Eng. Vol 215 part D pp 369-83 IMechE 2001

31. **Serrarens A. F. A.,** "Driveability control of the ZI powertrain" International conference on Integrated powertrains and their control, Sept 2000, Univ. of Bath. S744

32. **Vroemen B., Serrarens A. Veldpaus F.,** "Hierarchical of the Zero Inertia powertrain" JSAE 20014506 JSAE review 22 pp 519-526 2001

33. **Serranens A. K. A., & Veldpaus F. E.,** "New concepts for control of power transients in flywheel assisted drivelines with a CVT" Proc. Of FISITA World Automotive Congress Seoul 2000. F2000 A129

34. **Stone R.,** "Introduction to internal combustion engines" 2nd edition Macmillian Press Ltd 1992 ISBN 0-333-55084-6

35. **Heywood J. B.,** "Internal combustion engine fundamentals" McGraw Hill International Editions 1988 ISBN 0-07-100499-8

36. **Murray S.,** "Proposed Exhaust Gas Recirculation (EGR) Strategy" Private Communication with Torotrak, October 1999

37. **Dorey R. E. & Martin E. J.,** "Vehicle driveability: The Development of an Objective Methodology" SAE 2000-01-1326, 2000

38. **List H. & Schoeggl P.,** "Objective Evaluation of Vehicle Driveability" SAE 980204 SAE International publications, Warrendale USA 1998

39. **Wicke V., Brace C. J., Vaughan N. D.,** "Preliminary results from driveability investigations of vehicles with continuously variable transmissions". Proc CVT '99 - Int. con. On continuously variable transmissions pp 9-14 Eindhoven Univ. Technology, The Netherlands, 1999

40. **Jackson N. S.,** "Exhaust Gas recirculation for Good Fuel Economy" Spark Ignition Engine Emissions - course at Univ. Leeds 23 - 27 Nov. 1998

41. **Diana S., Giglio V., Iorio B., Police G.,** "A strategy to improve the efficiency of stoichiometric spark ignition engines" SAE 961953 (SP 1204) SAE International publications, Warrendale USA 1996

42. **Tabata M., Yamamoto T., Fukube T.,** " Improving $NO_x$ and fuel consumption for mixture injected SI engine with EGR" SAE 950684 SAE International publications, Warrendale USA 1995

43. **Yoshizawa K., Mori K., Matayoshi Y., Kimura S.,** "Development of an EGR Distribution prediction method using three-dimensional flow analysis and its application" Proceedings of the 2001 Fall technical conference of the ASME internal combustion Engine division ASME 2001-ICE-425

44. **Blank H, Dismon H, Kochs M. W., Sanders M., Golden J. E.,** "EGR and air management for direct injection gasoline engines" SAE 2002-01-0707 SAE International publications, Warrendale USA 2002

**45.** **Nakajima Y., Sugihara K., Takagi Y., Muranaka S.,** "Effects of exhaust gas recirculation on fuel consumption" Proc. Instn Mech Engrs. Vol 195 PP.369 – 376 IMechE 1981

46. **Olbrot A. W., Berri M. H., Asik J. R.,** "Parameter scheduling controller for exhaust gas recirculation (EGR) system" SAE 970620 SAE International publications, Warrendale USA 1997

47. **Osses M., Clarke P., Andrews G., Ounzain A., Robertson G.,** "Enhanced Exhaust Gas Recirculation Using Exhaust Throttling for $NO_x$ Reduction" IMechE C517/011/96, 1996

48. **Ahmad T. & Theobald M. A.,** "A survey of variable-valve-actuation technology" SAE 891674 SAE International publications, Warrendale USA 1989

49. **Stone R. & Kwan E.,** " Variable valve actuation and the potential for their application" SAE 890673 International publications, Warrendale USA 1989

50. **Gray C.,** "A review of variable engine valve timing" SAE 880386 International publications, Warrendale USA 1988

51. **Stein R. A., Galietti K. M., Leone T. G.,** "Dual equal VCT - A variable camshaft timing strategy for improved fuel economy and emissions" SAE 950975 International publications, Warrendale USA 1995

52. **Leone T. G., Christenson E. J., Stein R. A.** "Comparison of variable camshaft timing strategies at part load" SAE 960584 SAE International publications, Warrendale USA 1996

53. **Jankovic M., Frischmuth F., Stefanopoulou A., Cook J. A.,** "Torque management of engines with variable cam timing" IEEE trans. on control systems vol. 7 paper no. 0272-1708 October 1998

54. **Stefanopoulou A. G., & Kolmanovsky I.,** "Analysis and control of transient torque response in engines with internal exhaust gas recirculation" IEEE trans on control systems vol 7 no 5. pp 555-565 Sept. 1999

55. **Rao V. K., Bardon M. F., Gardiner D. P.,** "A method of assisting cold-starts, improving fuel economy and reducing emissions of engines at cold temperatures" SAE 890001 SAE International publications, Warrendale USA 1989

56. **Edwards S. P., Frankle G. R., Wirbeleit F., Raab A.,** " The potential of a combined miller cycle and internal EGR engine for future heavy duty truck applications" SAE 980180 SAE International publications, Warrendale USA 1998

57. **Horie K., Nishizawa K., Ogawa T., Akazaki S., Miura K.,** "The development of a high performance four-valve lean burn engine" SAE 920455 SAE International publications, Warrendale USA 1992

58. **Ladommatos N., Abdelhalim S. M., Zhao H.,** "The effects of carbon dioxide in EGR on diesel engine emissions" IMechE C517/028/96 1996

59. **Eng J. A., Leppard W. R., Dryer F. L.,** " Experimental hydrocarbon consumption from a spark ignition engine" SAE 972888 International publications, Warrendale USA 1997

60. **Hacohen J., Ashcroft S. J., Belmont M. R.,** " Lean burn versus EGR S. I. Engine" SAE 951902 SAE International publications, Warrendale USA 1995

61. **Neame G. R., Gardiner D. P., Mallory R. W., Rao V. K., Bardon M. F., Battista V.**, "Improving the fuel Economy of stoichiometrically fuelled S.I. engines by means of EGR and enhanced ignition – A comparison of gasoline, methanol and natural gas" SAE 952376 SAE International publications, Warrendale USA 1995

62. **Wijetunge R. S., Brace C. J., Hawley J. G., Vaughan N. D., Horrocks R. W., Bird G. L.,** "Dynamic behaviour of a high speed direct injection diesel engine" SAE 1999-01-0829 SAE International publications, Warrendale USA 1999

63. **Wijetunge R.S.**, "Transient optimisation of a diesel engine" PhD Thesis 1996, University of Bath

64. **Stokes J., Lake T. H., Christie M. J., Denbratt I.,** "Improving the $NO_x$/fuel economy trade-off for gasoline engines with the CCVS combustion system" SAE 940482 SAE International publications, Warrendale USA 1994

**65.** **Mikulic L., Quissek F., Fraidl G. K.,** "Development of low emissions high performance four valve engine" SAE 90157 International publications, Warrendale USA 1990

66. **Ando H.** "Combustion Control Technologies for Gasoline Engines" Lean Burn Combustion Engines Seminar S433/001/96 IMechE Publications, 3 - 4 Dec. 1996

67. **Sadler M., Stokes J., Edwards S. P., Zhan H., Ladommatos N.,** "Optimisation of the combustion system for a direct injection gasoline engine, using a high speed in-cylinder sampling valve" S490/010/97 IMechE 1997

68. **Ma T. H., Finlay I. C.,** "Modal assessment of exhaust emissions potential of a lean burn petrol engined vehicle" C465/030/93 IMechE 1993

69. **Shayler P. J., Horn G., Eade D.,** "Predictions of fuel economy for types of DISI and MPI spark ignition engines" IMechE C575/026/99 1999

70. **Shiga S., Kobayashi K., Hayakawa E., Matsuura T., Nakamura H., Ishima T.,** "Effect of injection rate on the performance and emissions of a direct-injection gasoline engine in comparison with the port-injected operation" 2000-ICE-405

71. **Kolmanovsky I., Sun J., Wang L.,** "Co-ordinated control of lean burn gasoline engines with continuously variable transmissions" Proceedings of the American control conference pp 2673-2677 June 1999

72. **Gradin B., & Angstrom H.,** "Replacing Fuel Enrichment in a turbocharged SI engine: Lean Burn or cooled EGR" SAE 1999-01-3505

73. **Gschweitl K.,** "Cameo in online engine optimisation using statistical methods" 5th International symposium for vehicle diagnostics pp 241-251 ICE 2001 Sept 2001

74. **Fraidi G. K., Quissek F., Winklhofer E.,** "Improvement of LEV / ULEV potential of fuel efficient high performance Engines" SAE 920416 SAE International publications, Warrendale USA 1992

75. **Arcoumanis C., Hu Z., Validis C., Whitelaw J. H.,** "Tumble motion: A mechanism for turbulence enhancement in spark-ignition engines" SAE 900060 SAE International publications, Warrendale USA 1990

76. **Evans R. L.,** " Combustion chamber design for a lean burn SI engine" SAE 921545 SAE International publications, Warrendale USA 1992

77. **Asik J. R., Paitkowski P., Foucher M. J., Rado W. G.,** "Design of a plasma jet ignition system for automotive application" SAE 770355 SAE International publications, Warrendale USA 1977

78. **Geiger J., Pischinger S., Bowing R., Kob H., Thiemann J.**, "Ignition systems for highly diluted mixtures in SI engines" SAE 1999-01-0799 SAE International publications, Warrendale USA 1999

79. **Heuser G., Oppel R., Eden M., Farenden G, Warren G., Menne R.,** 'The new 1.7L Zetec SE engine for Ford's sports coupe Puma' MTZ Motorechnishe Zeitschrift 58 Vol. 4, 1997

**80. Rendell J.,** "New Fiesta to outgun polo" Autocar pp52 – 55 12th July 1995

81. **Moriya Y., Watanabe A., Ude H., Kawamura H., Yoshioka M., Adachi M.,** "A newly developed intelligent variable valve timing system – continuously controlled cam phasing as applied to a new 3 liter inline 6 engine" SAE 960579 SAE International publications, Warrendale USA 1996

82. **Hoy A.,** Engine Management and Control strategy for a Zetec 1.7 L-SE Internal Ford Document 1998

83. **British Standard**, " Road vehicles - Engine test code - Gross power" BS ISO 2534:1998 British standards institution London Second edition 1998

84. **British standard,** "Reciprocating internal combustion engines - Exhaust emissions measurement" Part 1, BS ISO 8178-1:1996 British standards institution London 1996

85. **Spindt R. S.,** "Air-fuel ratio from exhaust gas analysis" SAE 650507 International publications, Warrendale USA 1988

**86. Farenden G.** "97MY Zetec-S VCT Engine (LVPP) - A Brief Technical Appraisal Internal Ford Report 1996

87. **Goulburn J. R., Brown D. G., Case R.**, "Computer-controller non-steady-state engine testing" Int. Journ. Of Vehicle Design Vol. 12 1991 pp 50-60

88. **Ward M., Brace C. J., Vaughan N. D, Ceen R., Hale T., Kennedy G.,** "Investigation of 'sweep' mapping approach on engine test bed" SAE 2002-01-615 International publications, Warrendale USA 1989

89. **Pilley A. D., Beaumont A. J., Robinson D., Mowll D.,** " Design of experiments for optimisation of engines to meet future emissions targets" Intn. Symposium on advanced transportation applications. Paper 94EN014 1994

90. **Mowll D., Robinson D. R., Pilley A. D.,** "Bayesian experimental design and it application to engine research and development" SAE 961157 SAE International publications, Warrendale USA 1996

91. **Mowll D., Robinson D. R., Pilley A. D.,** "Optimising engine performance and emissions using Bayesian techniques" SAE 971612 SAE International publications, Warrendale USA 1997

92. **Brace C. J. & Ward M. C.,** "Bayesian statistics in engine mapping" International conference on statistical and analytical methods in automotive engineering 24 – 25 Sept 2002

93. **Muller R., Schneider B.,** " Approximation and control of the engine torque using neural networks" SAE 2000-01-0929 SAE International publications, Warrendale USA 2000

94. **Bacon A., Shayler P. J., Ma T.,** "Potential for engine control using neural networks" IMechE C338/057 1992

95. **Mhller N., Hafner M. & Isermann R.,** "A Neuro-Fuzzy Based Method for the design of Combustion Engine Dynamometer Experiments" SAE 2000-01-1262, 2000

96. **Mhller N., Hafner M., Isermann R.,** " A neuro-fuzzy method for the design of combustion engine dynamometer experiments" SAE 2000-01-1262 SAE International publications, Warrendale USA 2000

97. **Brunson D., & Baker J.,** " Statistical Modelling of engine systems" Statistics for Engine optimisation Seminar IMechE London Dec. 1998

98. **Stevens S. P., Shayler P. J., Ma T. H.**, "Experimental data processing techniques to map the performance of a spark ignition engine" Proc. Of Instn Mech Engrs Vol 209 pp 297-306 IMechE 1995

99. **Edwards S. P., Clarke D. P., Pilley A. D., Anderson P. E.,** "The role of statistics in the engine development process". Statistics for Engine optimisation Seminar IMechE London Dec. 1998

100. **Yan J., Rogalla R., Kramer T.,** "Diesel combustion and transient emissions optimisation using taguchi methods" SAE 930600 SAE International publications, Warrendale USA 1993

101. **Ahlinder S., Sjolander P., Sward P., Fuxin F., Kihlander B., Asberg A.**, "Smart testing – reaping the benefits of DoE" Volvo Technology report No. 2 1997

102. **Edwards S. P., Pilley A. D., Michon S., Fournier G.**, "The optimisation of common rail FIE equipped engines through the use of statistical experimental design mathematical modelling and genetic algorithms" SAE 970346 SAE International publications, Warrendale USA 1997

103. **Lee T., Reitz R. D.,** "Response surface method optimisation of a HSDI Diesel engine equipped with a common rail injection system" Proceedings of the 2001 Fall technical conference of the ASME Internal Combustion Engine Division ASME 2001-ice-401

**104.** **Seabrooke J. F.**, "Combustion and emissions optimisation in a high-performance SI engine" PhD Thesis University College London, Department of Mechanical Engineering 1995

105. **Houghton C.,** "Application of design of experiments: optimisation of DI diesel engine" University of Bath, MEng final year project 2001

106. **Seabrooke J.,** 'Application of design of experiments in engine development' Proc. of "Statistics for Engine optimisation" Seminar 2nd Dec. 1998

107. **Stuhler H., Kruse T., Stuber A., Gschweitl K., Horst P., Lick P.**, "Automated model-based GDI engine calibration adaptive online approach" SAE 2002-01-0708 SAE International publications, Warrendale USA 2002

108. **Haines S. N. M., Dicken C. S., Gallacher A. M.**, "The application of an automatic calibration optimisation tool to direct-injection diesels" 5th International symposium for vehicle diagnostics pp 322-331 ICE 2001 Sept 2001

109. **Bartee E. M.,** "Engineering Experimental Design Fundamentals" Prentice-Hall 1968

**110. Umetri AB,** "Introduction to design of experiments" Draft copy Umetri AB 1998

111. **Atkinson & Donev** "Optimum Experimental Designs" Oxford Clarenden Press 1992

112. **De Boor C.,** "Spline toolbox - Users guide version 3" The MathWorks Inc Sept 2000

113. **Shayler P. J., Winborn L. D., Hill M. J., Eade D.,** "The influence of gas/ fuel ratio on combustion stability and misfire limits of spark ignition engines" SAE 2000-01-1208 SAE International publications, Warrendale USA 2000

114. **Patrick R. S., & Powell J. D.,** "A technique for the real-time estimation of air-fuel ratio using molecular weight ratio" SAE 900260 SAE International publications, Warrendale USA 1990

115. **Maugham R. D., Vaughan N. D., Brace C. J., Murray S. W.**, "Preliminary investigations in dilution torque control" Proceedings of the 2001 Fall technical conference of the ASME Internal Combustion Engine division ASME 2001-ICE-428

116. **Garbett K. S.,** "Multi-objective scheduling and control of a non-linear automotive powertrain" University of Warwick, Department of engineering 1991

117. **Fonseca C. M. M.,** "Multi-objective genetic algorithms with application to control engineering problems" Department of Automatic control and systems Engineering. The University of Sheffield PhD 1995

118. **Cello C. A. C.**, "An updated survey of multiobjective evolutionary optimisation: State of the art and future trends" Special session on multi-objective optimisation, Congress on Evolutionary Computing Vol. 1 pp 3 - 13 IEEE March 1999

119. **D'Errico G., Ferrari G., Onorati A., "**Numerical Modelling of unsteady reacting flows in the exhaust system of a S.I. Engine including catalytic converter" F2000A423

**120. Shamim T., Medisetty V. C.,** "Dynamic response of automotive catalytic converters to variations in air-fuel ratio" ASME 2001-ICE-424

121. **Gidlow M.** "A Hydrogen Bomb under Your Seat" IMechE AD Chairman's Address 2000 3rd Feb. 2000

122. **Brogan M. S., Will N. S., Twigg M. V., Wilkins A. J. J., Jordan K., Brisley R. J.,** "Advances in DENOx catalyst technology for European stage IV emissions levels" IMechE S490/012/97

123. **Hepburn J. G., Thanaslu E., Dobson D. A., Watkins W.,** " Experimental and modelling investigations of $NO_x$ trap performance" SAE 962051 SAE International publications, Warrendale USA 1996

124. **Brogan M. S., Brisley R. J., Moore J. S., Clark A. D.,** "Evaluation of NOx absorber catalysts systems to reduce emissions of lean running gasoline engines"

125. **Ketfi-cherif A., Von Wissel D., Buerthey S., Sorine M.,** "Modelling and control of a NOx trap catalyst" SAE 200-01-1198

126. **Hepburn J. S., Thanasiu E., Dobson D. A., Watkins W. L.,** " Experimental and modelling investigations of NOx trap performance" SAE 96051

127. **Hartick J., Moore J. S., Brogan M. S.**, "Temperature control of exhaust gas from a lean tune gasoline engine to help meet stringent emissions requirements" IMechE S490/013/97 1997

128. **Marshall R. A., Gregory D., Eves B., Peirce G., Taylor T., Cornis S., Dearth M., Hepburn J.**, "Optimising the aftertreatment configuration for $NO_x$ regeneration on a lean-$NO_x$ trap" SAE 1999-01-349 SAE International publications, Warrendale USA 1999

129. **Schoggl P., Koegeler H. M., Gschweitl K., Kokal H., Williams P., Hulak K.**, "Automated EMS calibration using objective driveability assessment and computer aided optimisation methods" SAE 2002-01-0849 SAE International publications, Warrendale USA 2002

130. **Ketfi-Cherif A., Von Wissel D., Beurthley S., Sorina M.**, "Modelling and control of a $NO_x$ trap catalyst" SAE 2001-1198 SAE International publications, Warrendale USA 2001

131. **Mladek M., Onder C. H.**, " A model for the estimation of induced air mass and residual gas fraction using cylinder pressure measurements" SAE 2000-01-0958 SAE International publications, Warrendale USA 2000

132. **Muller R., Hari M., Truscott A., Noble A., Krotz G., Eickhoff M., Cavalloni C., Gnielka M.**, " Combustion pressure based engine management systems" SAE OOP-301 1998

# A. Appendix A

Unified dilution measure

## *A 1 Conventional approaches to dilution measurement*

Conventionally the measures for lean and EGR charge dilution are separated. The conventional measure used to describe a lean charge dilution is the lambda ratio. This is the ratio of the current diluted air / fuel condition with an equivalent stoichiometric condition.

$$\lambda_{lean} = \frac{AFR_{lean}}{AFR_{stoich}} \qquad \text{...(Eqn A- 1)}$$

Where: $AFR_{lean}$ is the air fuel ratio at the diluted condition

$AFR_{stoichi}$ is a stoichiometric air fuel ratio

While charge dilution through the induction of EGR is measured by a ratio of the $CO_2$ percentage in the inlet and exhaust gases.

$$EGR_{\%} = \frac{EGR_{inlet} - EGR_{ambient}}{EGR_{exhaust} - EGR_{ambient}} \qquad \text{...(Eqn A- 2)}$$

Shillington[2] has alluded to the concept that this relationship maybe expressed in a lambda form. Where lambda is a ratio of the total induced charge and the combustible charge

$$\lambda_{EGR} = \frac{Mass_{total}}{Mass_{stoichi}} \qquad \text{...(Eqn A- 3)}$$

Where: $Mass_{total}$ is the mass of the combustible mixture and the recirculated exhaust. The relative mass of the EGR is determined through emissions analysis of inlet and exhaust $CO_2$.

$Mass_{stoichi}$ Is the mass of combustible mixture

Figure A-1 shows the relationship between charge dilution and torque for a conventional dilution measure. The lean dilution condition is represented by a blue line while the EGR dilution condition is represented by a purple line. It can be seen that a maximum EGR dilution condition occurs at lambda 1.25. At this point the torque is 85Nm, which is 40 Nm less than a non-diluted condition and 20 Nm less than an apparently similarly diluted lean mixture. The dilution limit by the current measure for excess air is lambda 1.5. Using this measure it would appear that per unit volume of combustible gas replaced by exhaust gases there is a greater effect on output torque than the reduction of charge fuelling which causes excess air dilution. Exhaust gases have a greater

specific heat capacity and are inert, however it is not apparent that these features of EGR charge dilution should cause this greater torque reduction effect.

Furthermore, it is not apparent that when using conventional measures of dilution how it is possible to combine them in order to assess the dilution of a mixture featuring a combination of EGR.

A reason for the large disparity in the effect of EGR and lean dilution conditions with classical measures is because these measures only consider the dilution of the charge resident in the cylinder. They do not consider the diluent effect of the charge heating upon the quantity of combustible charge drawn into the cylinder. Therefore the effect on emissions and fuel consumption for a given EGR dilution will vary if the exhaust gases are cooled prior to induction into the inlet manifold.

A further aspect of these relationships is that they have been simplified to ease their application, this however has meant that it is not apparent by which means conventional dilution measures may be combined.

Other dilution measures have been developed by Shayler et al[113] and Partick & Powell[114]. The work of Shayler[113] examined the gas fuel ratio, this is a ratio of gases to the fuelling in the combustion chamber. The work of Patrick & Powell[113] produced a similar measure based upon the molecular weights, cylinder pressures and temperatures. The benefit of the work of Patrick & Powell[114] is that it may be evaluate in real time in order to affect fuelling control.

### *A 2 Further examination of dilution measures*

This work, through the comparison of the composition of exhaust gases and knowledge of the quantities of induced air and fuel seeks primarily to validate conventional dilution measures. Additionally an examination of this type allows the potential to determine an appropriate method to combine dilution methods. A final motivation for this study is that a chemical analysis allows the potential to include a thermal adaptation such that there is more consistency between EGR and excess air dilution measures. .

### *A 3 Chemical examination*

In order to perform a chemical analysis of the combustion process it is necessary to formulate the composition of the inlet, and exhaust charges. The inlet charge consists of fresh air, a fuelling pulse, and recirculated gases:-

$$\mathrm{Inlet\_gases} = X\{\mathrm{air}\} + Y\{\mathrm{Exhaust\_gases}\} + Z\{\mathrm{Fuel}\} \qquad \ldots(\text{Eqn A- 4})$$

Where: Exhaust_gas is defined in Equation A-5

| | |
|---|---|
| Air | Is taken to consist of 79% nitrogen and 21% oxygen |
| Fuel | is taken to be $C_{10}H_{18}$ from the C:H ratio used for gasoline by gas analysers for Spindt calculations |

The exhaust gases consist of nitrogen, carbon dioxide, carbon monoxide, unburnt fuel, oxygen, oxides of nitrogen, water.

$$Exhaust\_gases = \beta_{N_2}N_2 + \beta_{CO_2}CO_2 + \beta_{CO}CO + \beta_{uHC}uHC + \beta_{NO}NO + \beta_{H_2O}H_2O + \beta_{O_2}0_2$$

$$Exhaust\_gases = \beta_{N_2}N_2 + \beta_{CO_2}CO_2 + \beta_{CO}CO + \beta_{uHC}uHC + \beta_{NO}NO + \beta_{H_2O}H_2O + \beta_{O_2}0_2$$

Where: $\beta$ Are the number of moles of each exhaust constituent ...(Eqn A- 5)

$NO_x$ emissions consist principally of NO and $NO_2$ emissions. However, since the gas analyser used experimentally measures total NO it is used here to represent all $NO_x$ emissions. Equally uHC emissions consist of many fractions of $C_xH_y$. However, the emissions analyser measures methane ($C_4H_8$) and is therefore used to represent all uHC emissions.

A technique typically used to determine the quantities of exhaust emissions is through balancing the components of the inlet and exhaust gases. Chemical balances are developed here for carbon, nitrogen, oxygen, and hydrogen components.

Balancing carbon components:-

$$Y\{\beta_{CO_2} + \beta_{CO} + 4\beta_{uHC}\} + Z10 = \beta_{CO_2} + \beta_{CO} + 4\beta_{uHC} \quad \text{...(Eqn A- 6)}$$

Balancing $N_2$ components:-

$$0.79X + Y\{\beta_{N_2} + \beta_{NO}/2\} = \beta_{N_2} + \beta_{NO}/2 \quad \text{...(Eqn A- 7)}$$

Balancing $O_2$ components:-

$$0.21X + Y\left\{\beta_{CO_2} + \frac{\beta_{CO}}{2} + \frac{\beta_{NO}}{2} + \beta_{O_2} + \frac{\beta_{H_2O}}{2}\right\} = \beta_{CO_2} + \frac{\beta_{CO}}{2} + \frac{\beta_{NO}}{2} + \beta_{O_2} + \frac{\beta_{H_2O}}{2}$$

...(Eqn A- 8)

Balancing hydrogen components:-

$$Y\{2\beta_{H_2O} + 8\beta_{uHC}\} + Z18 = 2\beta_{H_2O} + 8\beta_{uHC} \quad \text{...(Eqn A- 9)}$$

Furthermore using the emissions analyser it is possible to develop relationships between the relative percentages of exhaust emissions.

$K_1 = \frac{\beta_{CO}}{\beta_{CO_2}}$ ... (Eqn A- 10); $K_2 = \frac{\beta_{O_2}}{\beta_{CO_2}}$ ...(Eqn A- 11); $K_3 = \frac{\beta_{uHC}}{\beta_{CO_2}}$ ...(Eqn A- 12)

However, a similar relationship for the relative size of $NO_x$ is not possible since $NO_x$ is measured in the wet exhaust stream, while all other analysers examine dry emissions.

Rearranging Equation A-6 and including Equations A-10, A-11, and A-12 it is possible to determine the number of moles of $CO_2$ in the exhaust.

$$\beta_{CO_2} = \left\{\frac{10Z}{1-Y}\right\}.[1+K_1+K_2] \quad \text{...(Eqn A- 13)}$$

Subsequently using Equations A-10, A-11, and A-12 it is possible to evaluate the number of moles of uHC, CO, and $O_2$.

Rearranging Equation A-9 it is possible to evaluate the number of moles of water in the exhaust stream

$$\beta_{H_2O} = \frac{1}{2}\left\{\left[\frac{18Z}{1-Y}\right].-8\beta_{uHC}\right\} \quad \text{...(Eqn A- 14)}$$

From Equation A-8 it is possible to establish the number of moles of $NO_x$ in the exhaust stream:

$$\beta_{NO} = 2.\left\{\left[\frac{0.21.X}{1-Y}\right]-\left[\beta_{CO_2}+\frac{\beta_{CO}}{2}+\beta_{O_2}+\frac{\beta_{H_2O}}{2}\right]\right\} \quad \text{...(Eqn A- 15)}$$

Finally using Equation A-7. it is possible to determine the number of moles of $N_2$

$$\beta_{N_2} = \left\{\left[\frac{0.79.X}{1-Y}\right]-\frac{\beta_{NO}}{2}\right\} \quad \text{...(Eqn A- 16)}$$

The emissions analyser also measures inlet $CO_2$ therefore it is possible to determine the value of Y. Since there can be no net difference in the number of moles induced and exhausted from the engine it is accurate to propose that:-

$$Y = \frac{CO_{2\_inlet}}{CO_{2\_exhaust}} \quad \text{...(Eqn A- 17)}$$

Lambda is defined as the ratio of the induced charges AFR with that of a stoichiometrically fuelled charge. For a charge purely diluted by excess air, lambda may be determined simply through a ratio of the number of moles of $O_2$ in the induced charge compared with that required for a

stoichiometric mixture. For a charge diluted purely by EGR, this ratio maybe considered to be a ratio of the $N_2$ induced with that in a stoichiometric charge. Therefore:

$$\lambda = \frac{afr_{cur}}{afr_{stoichi}} = \frac{N_{2\_charge}}{N_{2\_stoichi}} = \frac{O_{2\_charge}}{O_{2\_stoichi}} \quad \text{...(Eqn A- 18)}$$

The number of moles of air required for a stoichiometric charge can be determined by:

$$X_{stoichi} = 70.28.Z \quad \text{...(Eqn A- 19)}$$

Where the 70.28 multiplication factor is determined by performing a similar molar analysis to this, for a mixture which does not have EGR, and where there is complete combustion. From Equation A-19 stoichiometric levels of $N_2$ and $O_2$ are developed:

$$N_{2\_stoichi} = 0.79.X_{stoichi} \quad \text{...(Eqn A- 20)}$$

$$O_{2\_stoichi} = 0.21.X_{stoichi} \quad \text{...(Eqn A- 21)}$$

The relationship between a measured quantity and the number of moles is given by:

$$mols. = \frac{mass}{molar\_mass} \quad \text{...(Eqn A- 22)}$$

Where:

| | | |
|---|---|---|
| | $Molar\_mass_{air}$ | is 28.89 kg/kmol |
| | $Molar\_mass_{fuel}$ | is 138 kg/kmol |
| | $Mass_{air}$ | recorded by Yokagawa |
| | $Mass_{fuel}$ | recorded by ECU |

and the total number of moles of $O_2$ and $N_2$ in the diluted mixture is determined by accumulating the quantity of the induced inlet air and the recirculated gases

$$O_{2\_charge} = O_{2\_induced} + O_{2\_EGR} = 0.21.X + Y.\beta_4 \quad \text{...(Eqn A- 23)}$$

$$N_{2\_charge} = N_{2\_induced} + N_{2\_EGR} = 0.79.X + Y.\beta_1 \quad \text{...(Eqn A- 24)}$$

It can be seen from Table A-1 that the lean dilution ratio is eqivelent to a conventional measure. However there is a significant difference between inlet EGR rate and the $N_2$ dilution measure. Shillington[2] simply added the EGR rate to 1 in order to develop a dilution measure. It can be seen

that this would not work, the measure developed by Shillington it is not a ratio of the total gases to the non-diluted gases.

### *A 4 Thermal examination*

However these dilution relationships do not take into account the charge heating effect of EGR gases upon the induced charge. Although engine testing results are corrected for ambient temperature / pressure conditions, conventional relationships do not consider the heating effect of EGR upon bulk gases.

Using the perfect gas law, the effect of charge heating upon the volume of induced charge can be assessed.

$$V_2 = V_1 \frac{T_2}{T_1} \qquad \text{...(Eqn A- 25)}$$

Where: $T_1$ is the bulk inlet temperature

$T_2$ is the ambient temperature {25°C [Error! Reference source not found.]}

$\frac{V_2}{V_1}$ is the ratio of volumes

It is assumed that if the charge were to be cooled and then the cylinder was filled at ambient temperature / pressure conditions, then the additional gases would be consistent in mixture to those that were cooled. Using the ideal gas laws for a second time it is possible to determine a ratio of the number of moles that may be induced at standard temperature / pressure conditions.

$$\frac{V_2}{V_3} = \frac{n_2}{n_3} \qquad \text{...(Eqn A- 26)}$$

Where: $n_1$ is the number of moles in induced charge

$n_2$ is the number of moles in corrected charge

$\frac{V_2}{V_1}$ is the ratio of volumes

The ratio of the number of moles is equivalent to a dilution measure:

$$\lambda_{thermal} = \frac{n_1}{n_2}$$

### *A 5 Combination of dilution measures*

The combination of the three dilution ratios is key to the validity of the new dilution measure. Accumulating the dilution measures seems to be the most logical means to combine these measures since an EGR charge dilution will reduce the amount of combustible mixture irrespective of the lean dilution rate.

$$\lambda = 1 + (\lambda_{O_2} - 1) + (\lambda_{N_2} - 1) + (\lambda_{thermal} - 1)$$

Furthermore, since $NO_x$ maybe considered to be very small incomparison to $N_2$, $\lambda_{N2}$ can be reduced to:-

$$\lambda_{N2} = 1/(1\text{-}EGR_{per})$$

### A 6 Validity of new approach

Figure A-2 shows a dilution torque relationship for increasing EGR (purple line) and lean (blue line) dilutions. The dilution measure used to define this relationship is the new thermally corrected measure described above. It can be seen that there is very good correlation between torque reduction and dilution rate for both means of charge dilution. Furthermore there is good correlation between the two dilution methods, such that a charge diluted to lambda 1.2 develops the same torque as an EGR diluted charge.

Also plotted upon Figure A-2 are a number of points which feature a combination of charge diluents, these are the points 7 and 8 on Table A-1. It can be seen that these points also have good correlation with pure lean and EGR dilution results when plotted upon these axes. It is therefore the concluded that the chosen approach taken to combine the dilution measures is appropriate.

Table A- 1 Comparison of dilution measures

| Test point | Conventional Lambda | Conventional EGR | $N_2$ ratio | $O_2$ ratio | Thermal ratio | Combined ratio |
|---|---|---|---|---|---|---|
| 1 | 1.09 | 1.00 | 1.00 | 1.1 | 1.01 | 1.11 |
| 2 | 1.26 | 1.00 | 1.00 | 1.23 | 1.01 | 1.25 |
| 3 | 1.48 | 1.00 | 1.00 | 1.43 | 1.01 | 1.44 |
| 4 | 1.01 | 1.06 | 1.06 | 1.01 | 1.08 | 1.15 |
| 5 | 1.03 | 1.16 | 1.19 | 1.02 | 1.19 | 1.40 |
| 6 | 1.02 | 1.25 | 1.34 | 1.04 | 1.31 | 1.69 |
| 7 | 1.11 | 1.19 | 1.14 | 1.16 | 1.17 | 1.47 |
| 8 | 1.15 | 1.12 | 1.24 | 1.13 | 1.21 | 1.59 |

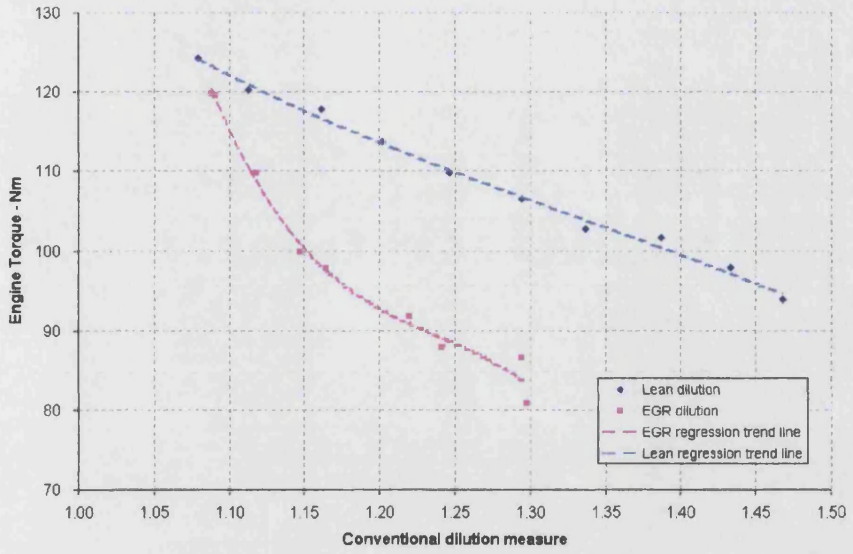


**Figure A- 1 Dilution effect on engine output torque - conventional dilution measures**

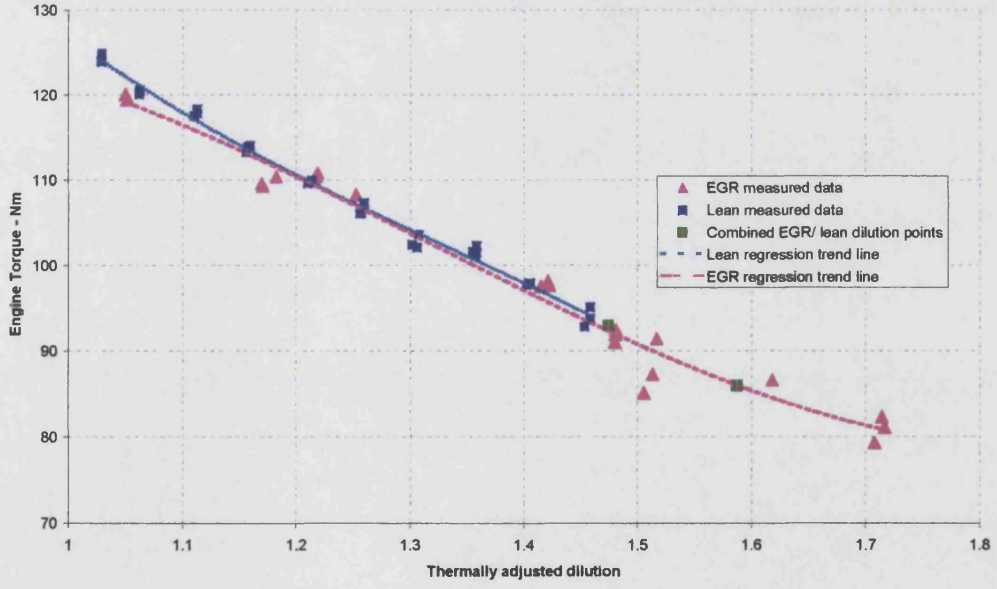


**Figure A- 2 Dilution effect on engine output torque - unified dilution measure**

# B. APPENDIX B

DoE test schedule showing major responses

Variables highlighted in blue are control variables, while variables highlighted in red are responses

| Throttle pos | EGR demand | Fuelling rate | Cam overlap | Spark timing | EGR flow | Torque | BSFC | BSNOx | BSuHC | BSCO2 | BSO2 | BSCO | COVimep | Comb pres |
|---|---|---|---|---|---|---|---|---|---|---|---|---|---|---|
| % | % | Lambda | degree | degree | % | Nm | g/kwhr | g/kWhr | g/kWhr | kg/kWhr | kg/kWhr | kg/kWhr | % | bar |
| 23.00 | 35.78 | 1.15 | 20.21 | 3.00 | 13.17 | 90.46 | 234.12 | 8.97 | 1.28 | 9.70 | 1.52 | 0.02 | 4.92 | 27.60 |
| 25.00 | 70.78 | 1.01 | 13.24 | 0.00 | 23.70 | 84.21 | 231.97 | 3.24 | 1.62 | 9.96 | 0.29 | 0.18 | 7.29 | 28.60 |
| 24.00 | 68.71 | 1.01 | 12.91 | 6.00 | 23.59 | 82.78 | 240.28 | 2.18 | 1.65 | 10.15 | 0.29 | 0.19 | 8.20 | 25.40 |
| 25.00 | 71.82 | 1.07 | 13.24 | 4.00 | 23.57 | 76.65 | 243.83 | 2.73 | 1.77 | 10.47 | 0.84 | 0.03 | 8.23 | 25.70 |
| 30.00 | 85.33 | 1.06 | 40.16 | 0.00 | 24.66 | 85.68 | 236.14 | 3.61 | 1.71 | 10.16 | 0.76 | 0.03 | 7.99 | 29.20 |
| 30.00 | 90.00 | 1.01 | 40.00 | 4.00 | 24.98 | 86.18 | 243.74 | 1.97 | 1.69 | 10.39 | 0.31 | 0.21 | 7.63 | 28.20 |
| 30.00 | 90.00 | 1.01 | 0.00 | 0.00 | 25.20 | 76.42 | 235.80 | 3.44 | 1.74 | 10.65 | 0.33 | 0.20 | 6.44 | 30.60 |
| 23.00 | 34.00 | 1.15 | 20.21 | 3.00 | 12.73 | 92.68 | 228.50 | 7.91 | 1.29 | 9.47 | 1.49 | 0.02 | 4.92 | 27.60 |
| 23.00 | 35.78 | 1.15 | 20.21 | 3.00 | 13.17 | 90.46 | 234.12 | 8.97 | 1.28 | 9.70 | 1.52 | 0.02 | 4.92 | 27.60 |
| 25.00 | 70.78 | 1.01 | 13.24 | 0.00 | 23.70 | 84.21 | 231.97 | 3.24 | 1.62 | 9.96 | 0.29 | 0.18 | 7.29 | 28.60 |
| 25.00 | 68.71 | 1.01 | 12.91 | 6.00 | 23.59 | 82.78 | 240.28 | 2.18 | 1.65 | 10.15 | 0.29 | 0.19 | 8.20 | 25.40 |
| 25.00 | 71.82 | 1.07 | 13.24 | 4.00 | 23.57 | 76.65 | 243.83 | 2.73 | 1.77 | 10.47 | 0.84 | 0.03 | 8.23 | 25.70 |
| 30.00 | 85.33 | 1.06 | 40.16 | 0.00 | 24.66 | 85.68 | 236.14 | 3.61 | 1.71 | 10.16 | 0.76 | 0.03 | 7.99 | 29.20 |
| 30.00 | 90.00 | 1.01 | 40.00 | 4.00 | 24.98 | 86.18 | 243.74 | 1.97 | 1.69 | 10.39 | 0.31 | 0.21 | 7.63 | 28.20 |
| 30.00 | 90.00 | 1.01 | 0.00 | 0.00 | 25.20 | 76.42 | 235.80 | 3.44 | 1.74 | 10.65 | 0.33 | 0.20 | 6.44 | 30.60 |
| 30.00 | 59.70 | 1.01 | 0.00 | 6.00 | 19.36 | 82.58 | 239.98 | 4.15 | 1.68 | 10.61 | 0.34 | 0.18 | 6.06 | 26.80 |
| 10.00 | 0.00 | 1.01 | 40.02 | 0.00 | 0.17 | 85.04 | 257.31 | 10.11 | 1.08 | 10.36 | 0.27 | 0.18 | 2.87 | 25.40 |
| 10.00 | 0.00 | 1.01 | 13.02 | 6.00 | 0.17 | 84.46 | 268.35 | 15.93 | 1.10 | 10.70 | 0.29 | 0.22 | 2.98 | 22.30 |
| 15.00 | 0.00 | 1.22 | 39.94 | 0.00 | 0.28 | 89.40 | 230.90 | 11.31 | 1.08 | 9.32 | 2.08 | 0.02 | 3.39 | 27.30 |
| 30.00 | 0.00 | 1.25 | 0.00 | 6.00 | 0.21 | 90.49 | 234.14 | 15.35 | 1.18 | 9.55 | 2.42 | 0.02 | 2.42 | 28.50 |
| 30.00 | 0.00 | 1.43 | 0.00 | 0.00 | 0.24 | 84.13 | 220.46 | 17.35 | 1.64 | 8.77 | 3.91 | 0.03 | 1.33 | 39.60 |
| 30.00 | 0.00 | 1.48 | 39.93 | 6.00 | 0.25 | 86.41 | 241.87 | 1.93 | 1.88 | 9.31 | 4.58 | 0.03 | 7.59 | 26.50 |
| 30.00 | 0.00 | 1.01 | 39.99 | 6.00 | 0.17 | 105.68 | 272.86 | 14.85 | 0.99 | 11.03 | 0.28 | 0.22 | 3.22 | 22.70 |
| 23.00 | 32.00 | 1.14 | 20.13 | 3.00 | 13.40 | 89.08 | 235.84 | 5.46 | 1.21 | 9.70 | 1.37 | 0.02 | 5.92 | 24.90 |
| 30.00 | 39.73 | 1.22 | 0.00 | 0.00 | 13.92 | 81.86 | 226.61 | 11.35 | 1.54 | 9.64 | 2.18 | 0.03 | 3.18 | 34.70 |
| 15.00 | 46.88 | 1.01 | 0.00 | 0.00 | 21.13 | 77.44 | 237.64 | 4.89 | 1.59 | 9.77 | 0.27 | 0.19 | 3.79 | 34.40 |
| 10.00 | 20.00 | 1.01 | 0.00 | 0.00 | 16.78 | 74.81 | 254.59 | 7.14 | 1.59 | 10.25 | 0.29 | 0.17 | 4.81 | 29.20 |
| 10.00 | 21.00 | 1.01 | 0.00 | 6.00 | 16.76 | 71.97 | 267.88 | 3.19 | 1.64 | 10.74 | 0.29 | 0.19 | 10.69 | 21.10 |
| 10.00 | 17.88 | 1.01 | 39.90 | 4.00 | 16.63 | 75.77 | 265.70 | 2.60 | 1.54 | 10.74 | 0.28 | 0.18 | 14.35 | 22.30 |
| 10.00 | 20.00 | 1.01 | 39.99 | 2.00 | 16.39 | 78.49 | 253.87 | 1.50 | 1.43 | 10.30 | 0.26 | 0.17 | 10.56 | 22.90 |
| 10.00 | 20.45 | 1.16 | 39.99 | 0.00 | 17.43 | 69.28 | 250.69 | 3.48 | 1.85 | 10.10 | 1.79 | 0.03 | 9.37 | 27.60 |
| 10.00 | 20.38 | 1.17 | 40.03 | 4.00 | 17.13 | 69.15 | 251.01 | 1.26 | 1.87 | 10.04 | 1.84 | 0.03 | 9.78 | 27.20 |
| 20.00 | 63.00 | 1.01 | 39.88 | 0.00 | 25.40 | 81.67 | 233.86 | 1.58 | 1.55 | 9.51 | 0.29 | 0.22 | 13.06 | 26.10 |
| 30.00 | 0.00 | 1.01 | 26.02 | 0.00 | 0.17 | 115.68 | 243.62 | 18.83 | 1.00 | 9.87 | 0.27 | 0.21 | 2.09 | 33.70 |
| 30.00 | 0.00 | 1.13 | 39.95 | 0.00 | 0.19 | 109.52 | 238.45 | 22.19 | 0.86 | 9.76 | 1.25 | 0.02 | 2.25 | 31.00 |
| 30.00 | 0.00 | 1.01 | 0.00 | 4.00 | 0.17 | 103.16 | 246.22 | 19.44 | 1.17 | 10.08 | 0.30 | 0.22 | 1.94 | 31.90 |
| 30.00 | 0.00 | 1.01 | 26.90 | 0.00 | 0.17 | 115.09 | 247.65 | 18.02 | 0.95 | 9.89 | 0.26 | 0.20 | 2.44 | 31.30 |
| 23.00 | 0.00 | 1.01 | 0.00 | 0.00 | 0.17 | 106.21 | 234.21 | 20.46 | 1.24 | 9.59 | 0.30 | 0.22 | 1.29 | 37.40 |
| 10.00 | 0.00 | 1.13 | 0.00 | 2.00 | 0.19 | 86.58 | 232.97 | 26.95 | 1.15 | 9.45 | 1.32 | 0.02 | 1.56 | 34.40 |
| 10.00 | 20.73 | 1.13 | 13.01 | 0.00 | 18.03 | 76.08 | 234.50 | 7.08 | 1.55 | 9.47 | 1.36 | 0.03 | 7.40 | 29.20 |
| 22.00 | 35.00 | 1.14 | 19.81 | 3.00 | 14.21 | 83.86 | 244.32 | 4.57 | 1.36 | 9.92 | 1.44 | 0.02 | 6.08 | 24.40 |
| 30.00 | 60.25 | 1.17 | 39.84 | 6.00 | 21.00 | 77.57 | 255.25 | 2.03 | 1.99 | 10.51 | 1.93 | 0.03 | 11.40 | 25.70 |
| 30.00 | 76.50 | 0.98 | 27.13 | 6.00 | 25.47 | 85.09 | 245.06 | 1.50 | 1.66 | 9.97 | 0.16 | 0.41 | 8.24 | 25.20 |
| 22.00 | 38.56 | 1.16 | 20.23 | 6.00 | 13.50 | 83.70 | 242.76 | 5.02 | 1.30 | 9.92 | 1.67 | 0.02 | 6.43 | 25.60 |
| 25.00 | 11.10 | 1.42 | 40.00 | 0.00 | 7.63 | 83.90 | 231.04 | 3.00 | 1.82 | 8.98 | 3.86 | 0.03 | 7.02 | 29.00 |
| 26.00 | 13.00 | 1.38 | 0.00 | 6.00 | 8.61 | 77.34 | 226.69 | 7.30 | 1.90 | 9.06 | 3.56 | 0.03 | 2.94 | 32.00 |
| | | | | | | | | | | | | | | |
| 100.00 | 0.00 | 1.01 | 0.00 | 6.00 | 0.85 | 104.10 | 245.65 | 19.29 | 1.29 | 10.58 | 0.29 | 0.18 | 1.41 | 29.10 |
| 100.00 | 0.00 | 1.22 | 0.00 | 0.00 | 0.77 | 95.36 | 226.33 | 25.09 | 1.26 | 9.67 | 2.18 | 0.03 | 1.43 | 37.90 |
| 100.00 | 100.00 | 1.15 | 26.02 | 0.00 | 17.87 | 91.65 | 226.18 | 6.65 | 1.51 | 10.11 | 1.56 | 0.03 | 4.72 | 28.80 |
| 100.00 | 100.00 | 1.00 | 40.11 | 4.00 | 16.44 | 95.27 | 253.37 | 3.71 | 1.79 | 11.02 | 0.25 | 0.27 | 4.10 | 26.00 |
| 40.00 | 100.00 | 1.00 | 26.10 | 6.00 | 21.99 | 87.98 | 245.49 | 2.34 | 1.54 | 10.53 | 0.27 | 0.21 | 5.12 | 26.70 |
| 40.00 | 99.00 | 1.01 | 12.82 | 0.00 | 21.77 | 88.08 | 239.27 | 3.49 | 1.60 | 10.25 | 0.26 | 0.17 | 3.41 | 31.70 |
| 40.00 | 98.00 | 0.98 | 39.89 | 2.00 | 21.70 | 94.89 | 229.79 | 3.28 | 1.63 | 9.91 | 0.16 | 0.37 | 2.43 | 32.10 |
| 40.00 | 98.00 | 1.07 | 39.94 | 2.00 | 21.75 | 87.79 | 241.52 | 3.74 | 1.76 | 10.39 | 0.87 | 0.03 | 4.84 | 28.60 |
| 40.00 | 99.50 | 1.07 | 0.00 | 4.00 | 21.76 | 77.83 | 235.45 | 4.58 | 1.80 | 10.86 | 0.90 | 0.03 | 4.62 | 26.70 |
| 80.00 | 98.00 | 1.07 | 39.86 | 0.00 | 16.10 | 95.85 | 234.51 | 6.36 | 1.76 | 10.38 | 0.89 | 0.03 | 4.33 | 29.30 |
| 70.00 | 38.00 | 1.15 | 19.85 | 3.00 | 7.10 | 97.96 | 238.40 | 12.24 | 1.02 | 10.13 | 1.51 | 0.02 | 3.18 | 27.70 |
| 52.00 | 26.00 | 1.36 | 39.96 | 6.00 | 5.82 | 88.91 | 245.70 | 2.39 | 2.04 | 9.64 | 3.55 | 0.03 | 5.47 | 25.60 |
| 71.00 | 38.00 | 1.15 | 19.76 | 3.00 | 7.13 | 99.23 | 237.19 | 10.53 | 1.02 | 10.09 | 1.55 | 0.02 | 3.98 | 26.10 |
| 40.00 | 33.00 | 1.01 | 40.02 | 0.00 | 7.70 | 110.07 | 246.57 | 11.18 | 1.33 | 10.05 | 0.25 | 0.19 | 3.01 | 30.80 |
| 60.00 | 100.00 | 1.00 | 0.00 | 6.00 | 18.28 | 83.27 | 246.21 | 2.97 | 1.73 | 11.53 | 0.26 | 0.23 | 6.28 | 22.00 |
| 40.00 | 0.00 | 1.38 | 0.00 | 6.00 | 0.70 | 83.79 | 226.86 | 6.91 | 1.64 | 9.25 | 3.65 | 0.03 | 3.22 | 27.20 |
| 40.00 | 0.00 | 1.01 | 0.00 | 0.00 | 0.65 | 105.15 | 241.89 | 19.62 | 1.28 | 10.06 | 0.30 | 0.21 | 1.47 | 33.90 |
| 100.00 | 0.00 | 1.01 | 39.94 | 0.00 | 0.85 | 115.44 | 254.26 | 18.51 | 1.27 | 10.43 | 0.30 | 0.17 | 1.92 | 30.60 |
| 70.00 | 0.00 | 1.23 | 20.20 | 3.00 | 0.86 | 101.35 | 234.06 | 13.75 | 1.04 | 9.55 | 2.24 | 0.03 | 2.49 | 25.80 |
| 100.00 | 85.25 | 1.02 | 39.87 | 6.00 | 13.07 | 96.25 | 265.81 | 4.88 | 1.55 | 11.47 | 0.35 | 0.14 | 4.60 | 21.00 |
| 100.00 | 100.00 | 1.06 | 13.18 | 6.00 | 16.62 | 85.71 | 280.42 | 3.67 | 1.48 | 11.67 | 0.77 | 0.04 | 5.93 | 21.90 |
| 100.00 | 66.50 | 1.01 | 0.00 | 0.00 | 12.78 | 95.49 | 232.28 | 11.33 | 1.56 | 10.85 | 0.29 | 0.20 | 1.90 | 35.50 |
| 100.00 | 68.86 | 1.20 | 0.00 | 6.00 | 13.80 | 79.06 | 236.80 | 5.07 | 1.80 | 11.08 | 2.29 | 0.03 | 10.52 | 22.80 |
| 72.00 | 52.57 | 1.21 | 19.88 | 3.00 | 9.72 | 90.98 | 237.37 | 7.03 | 1.36 | 10.16 | 2.23 | 0.03 | 4.30 | 27.70 |
| 71.00 | 33.29 | 1.17 | 19.86 | 3.00 | 6.83 | 96.43 | 239.30 | 9.45 | 1.03 | 10.21 | 1.78 | 0.02 | 3.26 | 25.00 |
| 40.00 | 36.33 | 1.25 | 0.00 | 0.00 | 8.91 | 85.59 | 223.62 | 12.80 | 1.49 | 9.52 | 2.50 | 0.03 | 2.50 | 33.20 |
| 40.00 | 35.33 | 1.01 | 0.00 | 6.00 | 7.54 | 96.17 | 245.33 | 11.21 | 1.35 | 10.43 | 0.29 | 0.20 | 2.57 | 28.50 |
| 100.00 | 10.43 | 1.43 | 0.00 | 6.00 | 3.67 | 81.82 | 223.24 | 7.91 | 1.99 | 9.31 | 4.20 | 0.03 | 2.29 | 33.40 |
| 100.00 | 10.33 | 1.46 | 39.94 | 0.00 | 3.64 | 95.62 | 223.52 | 5.48 | 2.05 | 8.61 | 4.11 | 0.03 | 4.61 | 32.00 |
| 84.00 | 7.00 | 1.47 | 39.95 | 6.00 | 3.46 | 83.32 | 259.11 | 1.20 | 2.37 | 9.92 | 4.83 | 0.04 | 8.69 | 25.60 |
| 76.00 | 0.00 | 1.45 | 0.00 | 0.00 | 0.94 | 84.16 | 221.10 | 18.76 | 1.76 | 9.01 | 4.21 | 0.03 | 1.51 | 42.70 |
| 40.00 | 0.00 | 1.33 | 35.20 | 0.00 | 0.67 | 102.57 | 226.07 | 11.73 | 1.41 | 8.97 | 3.04 | 0.03 | 2.36 | 32.70 |
| 40.00 | 0.00 | 1.01 | 40.06 | 6.00 | 0.51 | 103.95 | 283.83 | 15.12 | 1.14 | 11.57 | 0.27 | 0.24 | 3.91 | 21.70 |
| 100.00 | 0.00 | 1.11 | 40.07 | 6.00 | 0.69 | 96.21 | 280.54 | 14.38 | 0.76 | 11.69 | 1.33 | 0.05 | 3.98 | 21.80 |

**Table B- 1 DoE test program for 1200 rev/min**

| Throttle pos | EGR demand | Fuelling rate | Cam overlap | Spark timing | EGR flow | Torque | BSFC | BSNOx | BSuHC | BSCO2 | BSO2 | BSCO | COVimep | Comb pres |
|---|---|---|---|---|---|---|---|---|---|---|---|---|---|---|
| % | % | Lambda | degree | degree | % | Nm | g/kwhr | g/kWhr | g/kWhr | kg/kWhr | kg/kWhr | kg/kWhr | % | bar |
| 20.00 | 0.00 | 1.17 | 20.03 | 5.00 | 0.27 | 100.69 | 233.20 | 19.03 | 0.97 | 9.74 | 1.68 | 0.03 | 3.36 | 29.10 |
| 30.00 | 0.00 | 1.42 | 40.03 | 6.00 | 0.33 | 92.05 | 236.03 | 2.96 | 1.59 | 9.48 | 4.11 | 0.03 | 4.23 | 28.40 |
| 30.00 | 0.00 | 1.20 | 0.00 | 0.00 | 0.27 | 99.71 | 222.27 | 25.10 | 1.22 | 9.52 | 1.93 | 0.02 | 2.87 | 38.10 |
| 26.00 | 100.00 | 1.01 | 40.06 | 10.00 | 25.39 | 83.15 | 244.99 | 1.49 | 1.97 | 10.33 | 0.35 | 0.21 | 10.12 | 28.10 |
| 23.60 | 19.00 | 1.14 | 0.00 | 5.00 | 9.90 | 88.39 | 232.37 | 10.45 | 1.28 | 9.58 | 1.27 | 0.03 | 3.37 | 29.40 |
| 30.00 | 0.00 | 1.37 | 0.00 | 3.00 | 0.31 | 88.96 | 221.52 | 15.22 | 1.52 | 9.28 | 3.60 | 0.03 | 2.88 | 34.50 |
| 26.00 | 100.00 | 1.01 | 0.00 | 0.00 | 25.42 | 72.82 | 244.76 | 1.84 | 2.44 | 11.08 | 0.40 | 0.26 | 11.35 | 27.90 |
| 30.00 | 0.00 | 1.01 | 0.00 | 10.00 | 0.17 | 106.71 | 242.78 | 19.88 | 1.14 | 10.17 | 0.29 | 0.20 | 2.92 | 37.00 |
| 16.00 | 0.00 | 1.01 | 39.97 | 0.00 | 0.17 | 98.73 | 260.98 | 12.93 | 0.92 | 10.53 | 0.28 | 0.21 | 3.90 | 26.80 |
| 30.00 | 26.00 | 1.36 | 20.00 | 10.00 | 11.12 | 87.96 | 228.51 | 3.99 | 1.61 | 9.19 | 3.44 | 0.03 | 6.78 | 29.50 |
| 23.00 | 0.00 | 1.01 | 40.00 | 5.00 | 0.17 | 92.12 | 298.94 | 11.52 | 0.76 | 12.21 | 0.28 | 0.29 | 4.86 | 20.30 |
| 22.00 | 25.00 | 1.12 | 20.05 | 6.00 | 11.17 | 92.80 | 241.89 | 6.65 | 1.03 | 10.09 | 1.24 | 0.02 | 4.16 | 24.50 |
| 26.00 | 0.00 | 1.45 | 0.00 | 5.00 | 0.24 | 83.96 | 226.18 | 9.17 | 1.75 | 9.22 | 4.24 | 0.03 | 3.96 | 30.90 |
| 30.00 | 100.00 | 1.01 | 0.00 | 0.00 | 24.20 | 74.52 | 249.79 | 2.53 | 2.16 | 11.42 | 0.36 | 0.23 | 5.58 | 29.00 |
| 10.00 | 0.00 | 1.01 | 0.00 | 0.00 | 0.24 | 88.24 | 243.94 | 21.86 | 1.29 | 9.91 | 0.30 | 0.18 | 2.56 | 36.40 |
| 21.00 | 44.33 | 1.01 | 20.03 | 5.00 | 16.63 | 91.04 | 245.17 | 3.57 | 1.37 | 9.98 | 0.26 | 0.19 | 3.75 | 31.00 |
| 10.00 | 27.00 | 1.01 | 0.00 | 10.00 | 20.79 | 71.73 | 242.60 | 4.48 | 1.70 | 9.85 | 0.30 | 0.19 | 3.63 | 32.80 |
| 30.00 | 0.00 | 1.01 | 39.97 | 3.00 | 0.24 | 104.47 | 276.71 | 15.66 | 0.87 | 11.05 | 0.28 | 0.25 | 4.15 | 23.90 |
| 10.00 | 0.00 | 1.01 | 26.06 | 10.00 | 0.17 | 69.87 | 292.23 | 10.37 | 1.08 | 11.72 | 0.34 | 0.27 | 3.91 | 17.00 |
| 22.00 | 25.67 | 1.12 | 22.65 | 5.00 | 11.68 | 92.49 | 241.91 | 6.38 | 1.11 | 9.99 | 1.27 | 0.02 | 4.22 | 27.40 |
| 30.00 | 100.00 | 1.01 | 40.06 | 0.00 | 25.85 | 88.04 | 237.80 | 2.81 | 1.66 | 9.97 | 0.34 | 0.23 | 6.29 | 32.20 |
| 30.00 | 32.33 | 1.01 | 40.08 | 10.00 | 10.89 | 90.10 | 284.41 | 3.43 | 0.98 | 11.70 | 0.29 | 0.24 | 5.36 | 20.80 |
| 30.00 | 10.33 | 1.50 | 40.08 | 0.00 | 5.73 | 86.63 | 233.38 | 2.87 | 1.81 | 9.06 | 4.67 | 0.03 | 6.38 | 32.60 |
| 30.00 | 0.00 | 1.01 | 26.02 | 0.00 | 0.17 | 114.41 | 256.19 | 17.74 | 0.87 | 10.17 | 0.29 | 0.23 | 3.96 | 29.40 |
| 30.00 | 0.00 | 1.46 | 26.02 | 10.00 | 0.24 | 85.71 | 248.85 | 2.48 | 1.53 | 9.78 | 4.53 | 0.03 | 9.20 | 23.10 |
| 10.00 | 0.00 | 1.22 | 0.00 | 10.00 | 0.20 | 66.92 | 249.32 | 21.21 | 1.36 | 10.14 | 2.26 | 0.03 | 3.49 | 25.50 |
| 30.00 | 0.00 | 1.31 | 40.01 | 10.00 | 0.21 | 88.52 | 272.66 | 7.82 | 0.95 | 10.71 | 3.28 | 0.04 | 7.40 | 21.20 |
| 30.00 | 0.00 | 1.43 | 13.04 | 0.00 | 0.23 | 95.26 | 220.82 | 13.22 | 1.41 | 8.81 | 3.84 | 0.02 | 3.16 | 37.00 |
| 10.00 | 23.00 | 1.01 | 40.06 | 0.00 | 18.56 | 78.98 | 236.43 | 2.64 | 1.50 | 9.63 | 0.27 | 0.16 | 4.40 | 32.40 |
| 17.00 | 0.00 | 1.01 | 0.00 | 6.00 | 0.17 | 92.80 | 257.26 | 18.54 | 1.07 | 10.43 | 0.29 | 0.23 | 3.22 | 25.60 |
| 27.00 | 100.00 | 1.01 | 40.06 | 10.00 | 25.77 | 80.48 | 249.04 | 1.95 | 2.03 | 10.21 | 0.35 | 0.24 | 10.15 | 30.90 |
| 19.00 | 0.00 | 1.52 | 40.00 | 10.00 | 0.45 | 71.47 | 264.35 | 0.95 | 2.88 | 10.58 | 5.74 | 0.04 | 16.91 | 23.20 |
| 30.00 | 0.00 | 1.08 | 39.98 | 0.00 | 0.32 | 113.80 | 239.92 | 19.37 | 0.82 | 10.14 | 0.85 | 0.03 | 3.11 | 30.90 |
| 10.00 | 0.00 | 1.00 | 13.04 | 0.00 | 0.31 | 91.77 | 241.42 | 18.70 | 1.26 | 9.96 | 0.27 | 0.27 | 2.89 | 35.60 |
| 30.00 | 70.00 | 0.99 | 40.05 | 0.00 | 19.69 | 95.62 | 243.97 | 4.35 | 1.46 | 10.03 | 0.25 | 0.33 | 5.51 | 32.50 |
| 10.00 | 0.00 | 1.00 | 0.00 | 3.33 | 0.37 | 82.14 | 247.93 | 20.61 | 1.37 | 10.26 | 0.26 | 0.23 | 2.99 | 32.70 |
| 30.00 | 66.00 | 0.99 | 40.05 | 0.00 | 19.67 | 97.96 | 238.19 | 4.26 | 1.43 | 9.80 | 0.24 | 0.31 | 5.51 | 32.50 |
| 30.00 | 21.00 | 1.31 | 0.00 | 10.00 | 10.26 | 83.77 | 223.42 | 9.12 | 1.65 | 9.53 | 3.08 | 0.03 | 4.96 | 33.70 |
| | | | | | | | | | | | | | | |
| 40.00 | 0.00 | 1.53 | 0.00 | 0.00 | 0.54 | 84.14 | 220.27 | 15.12 | -0.07 | 8.98 | 4.61 | 0.03 | 2.95 | 38.70 |
| 100.00 | 0.00 | 1.47 | 39.98 | 6.00 | 0.62 | 98.55 | 226.73 | 4.51 | -0.07 | 8.99 | 4.06 | 0.03 | 4.52 | 29.80 |
| 80.00 | 0.00 | 1.45 | 0.00 | 6.00 | 0.71 | 88.52 | 220.97 | 20.09 | -0.07 | 9.43 | 4.10 | 0.03 | 2.76 | 41.00 |
| 70.00 | 44.33 | 1.28 | 20.05 | 3.00 | 9.79 | 93.63 | 230.99 | 6.94 | -0.07 | 9.77 | 2.59 | 0.03 | 6.05 | 28.10 |
| 40.00 | 60.00 | 1.02 | 39.92 | 4.00 | 15.97 | 101.50 | 246.61 | 5.21 | -0.06 | 10.09 | 0.30 | 0.27 | 4.26 | 29.30 |
| 50.00 | 69.00 | 1.03 | 0.00 | 6.00 | 18.72 | 84.30 | 249.26 | 5.07 | -0.07 | 11.62 | 0.41 | 0.22 | 5.17 | 27.80 |
| 100.00 | 100.00 | 1.19 | 13.01 | 6.00 | 18.41 | 81.10 | 239.55 | 3.97 | -0.07 | 11.32 | 2.03 | 0.03 | 7.50 | 25.20 |
| 40.00 | 10.00 | 1.50 | 26.03 | 6.00 | 5.57 | 90.82 | 223.50 | 2.67 | -0.07 | 8.72 | 4.26 | 0.03 | 9.10 | 28.90 |
| 40.00 | 0.00 | 1.13 | 39.93 | 0.00 | 0.33 | 112.44 | 240.23 | 20.31 | -0.06 | 9.82 | 1.23 | 0.03 | 3.51 | 28.30 |
| 40.00 | 0.00 | 1.38 | 0.00 | 6.00 | 0.40 | 88.86 | 227.65 | 11.91 | -0.07 | 9.37 | 3.40 | 0.03 | 3.25 | 30.70 |
| 40.00 | 0.00 | 1.02 | 40.04 | 6.00 | 0.31 | 102.57 | 291.07 | 14.33 | -0.06 | 11.52 | 0.28 | 0.29 | 3.80 | 21.20 |
| 70.00 | 0.00 | 1.22 | 20.00 | 3.00 | 0.59 | 105.46 | 236.24 | 16.67 | -0.06 | 9.62 | 2.04 | 0.03 | 3.71 | 25.40 |
| 70.00 | 48.00 | 1.18 | 20.07 | 3.00 | 10.43 | 97.11 | 236.38 | 7.95 | -0.07 | 10.19 | 1.70 | 0.03 | 5.54 | 26.10 |
| 90.00 | 100.00 | 1.00 | 36.31 | 6.00 | 19.56 | 89.88 | 265.32 | 2.29 | -0.07 | 11.52 | 0.26 | 0.43 | 6.69 | 22.70 |
| 100.00 | 100.00 | 1.03 | 0.00 | 6.00 | 18.90 | 84.22 | 241.55 | 3.93 | -0.07 | 12.17 | 0.43 | 0.21 | 4.03 | 25.40 |
| 70.00 | 99.00 | 1.08 | 0.00 | 0.00 | 17.36 | 84.82 | 231.26 | 8.20 | -0.07 | 11.78 | 0.83 | 0.05 | 4.08 | 31.90 |
| 70.00 | 39.33 | 1.30 | 0.00 | 6.00 | 8.77 | 84.33 | 225.66 | 7.22 | -0.07 | 10.18 | 2.96 | 0.03 | 4.12 | 29.50 |
| 40.00 | 61.33 | 1.10 | 0.00 | 4.00 | 16.17 | 85.76 | 233.76 | 7.78 | -0.07 | 10.88 | 0.97 | 0.03 | 5.42 | 28.90 |
| 40.00 | 58.67 | 1.24 | 26.11 | 4.00 | 16.79 | 87.27 | 235.78 | 4.13 | -0.07 | 9.79 | 2.20 | 0.03 | 5.15 | 28.30 |
| 40.00 | 0.00 | 1.02 | 0.00 | 2.00 | 0.51 | 106.73 | 245.95 | 19.71 | -0.06 | 10.19 | 0.29 | 0.24 | 2.79 | 37.80 |
| 40.00 | 0.00 | 1.02 | 25.98 | 6.00 | 0.44 | 107.60 | 268.51 | 15.19 | -0.06 | 10.77 | 0.29 | 0.26 | 3.66 | 22.90 |
| 40.00 | 0.00 | 1.47 | 40.00 | 2.00 | 0.52 | 98.18 | 225.22 | 5.42 | -0.07 | 8.88 | 4.00 | 0.03 | 3.49 | 33.30 |
| 100.00 | 0.00 | 1.02 | 40.00 | 0.00 | 0.78 | 117.50 | 252.83 | 18.17 | -0.06 | 10.26 | 0.28 | 0.22 | 2.57 | 31.30 |
| 100.00 | 0.00 | 1.41 | 0.00 | 0.00 | 0.86 | 95.80 | 207.01 | 21.61 | -0.06 | 9.15 | 2.13 | 0.03 | 2.96 | 32.30 |
| 100.00 | 0.00 | 1.20 | 0.00 | 0.00 | 0.72 | 100.59 | 226.40 | 28.27 | -0.06 | 10.10 | 1.63 | 0.03 | 2.86 | 36.80 |
| 60.00 | 0.00 | 1.02 | 0.00 | 0.00 | 0.78 | 107.66 | 238.14 | 20.66 | -0.06 | 10.38 | 0.29 | 0.23 | 2.56 | 37.00 |
| 70.00 | 100.00 | 1.04 | 39.95 | 2.00 | 19.74 | 91.79 | 248.88 | 3.50 | -0.06 | 10.97 | 0.44 | 0.14 | 5.98 | 25.60 |
| 100.00 | 100.00 | 1.08 | 40.05 | 0.00 | 19.34 | 94.03 | 237.03 | 6.46 | -0.06 | 10.58 | 0.78 | 0.04 | 6.08 | 29.30 |
| 70.00 | 40.00 | 1.11 | 19.98 | 3.00 | 9.64 | 104.20 | 231.05 | 13.20 | -0.06 | 10.10 | 1.02 | 0.03 | 4.84 | 28.10 |
| 100.00 | 61.00 | 1.02 | 0.00 | 0.00 | 14.22 | 92.98 | 233.94 | 11.31 | -0.06 | 11.41 | 0.33 | 0.24 | 2.65 | 36.00 |
| 100.00 | 17.00 | 1.48 | 12.98 | 0.00 | 4.96 | 88.59 | 222.51 | 7.96 | -0.07 | 9.13 | 4.23 | 0.03 | 6.17 | 33.50 |
| 80.00 | 16.00 | 1.50 | 40.04 | 0.00 | 3.84 | 94.36 | 223.53 | 5.18 | -0.07 | 8.79 | 4.23 | 0.03 | 5.53 | 34.20 |
| 40.00 | 58.00 | 1.02 | 13.01 | 0.00 | 17.42 | 92.72 | 245.54 | 4.28 | -0.06 | 10.43 | 0.33 | 0.27 | 5.96 | 27.20 |
| 40.00 | 62.00 | 1.26 | 40.17 | 6.00 | 17.27 | 83.38 | 246.27 | 2.47 | -0.07 | 10.18 | 2.49 | 0.03 | 11.22 | 26.80 |

**Table B- 2 DoE test program for 1400 rev/min**

| Throttle pos | EGR demand | Fuelling rate | Cam overlap | Spark timing | EGR flow | Torque | BSFC | BSNOx | BSuHC | BSCO2 | BSO2 | BSCO | COVimep | Comb pres |
|---|---|---|---|---|---|---|---|---|---|---|---|---|---|---|
| % | % | Lambda | degree | degree | % | Nm | g/kwhr | g/kWhr | g/kWhr | kg/kWhr | kg/kWhr | kg/kWhr | % | bar |
| 17.00 | 0.00 | 1.01 | 0.00 | 0.00 | 0.17 | 102.31 | 236.11 | 19.51 | 1.25 | 9.37 | 0.26 | 0.22 | 1.13 | 39.00 |
| 10.00 | 0.00 | 1.17 | 0.00 | 0.00 | 0.19 | 74.48 | 235.88 | 31.03 | 1.44 | 9.55 | 1.69 | 0.03 | 1.33 | 38.00 |
| 21.00 | 0.00 | 1.44 | 0.00 | 6.00 | 0.24 | 78.92 | 226.27 | 6.47 | 1.86 | 8.84 | 4.03 | 0.03 | 4.08 | 30.40 |
| 21.00 | 0.00 | 1.45 | 39.98 | 0.00 | 0.25 | 85.38 | 223.63 | 4.68 | 1.74 | 8.67 | 4.03 | 0.03 | 3.96 | 35.10 |
| 30.00 | 14.67 | 1.40 | 0.00 | 0.00 | 7.91 | 77.36 | 223.71 | 6.24 | 2.01 | 8.87 | 3.76 | 0.04 | 11.97 | 31.50 |
| 30.00 | 12.56 | 1.44 | 39.99 | 6.00 | 8.04 | 83.24 | 233.70 | 1.87 | 2.14 | 9.00 | 4.18 | 0.03 | 8.23 | 32.40 |
| 30.00 | 100.00 | 1.00 | 39.95 | 2.00 | 25.05 | 84.39 | 240.00 | 2.52 | 1.64 | 9.94 | 0.29 | 0.25 | 8.01 | 29.30 |
| 20.00 | 68.57 | 1.00 | 39.96 | 6.00 | 25.00 | 73.13 | 255.74 | 1.31 | 1.71 | 10.41 | 0.30 | 0.23 | 10.89 | 26.50 |
| 20.00 | 62.75 | 1.00 | 0.00 | 0.00 | 22.29 | 71.58 | 241.31 | 2.72 | 1.66 | 10.10 | 0.29 | 0.22 | 7.50 | 27.90 |
| 30.00 | 100.00 | 1.01 | 13.39 | 6.00 | 25.09 | 75.32 | 250.21 | 1.89 | 1.76 | 10.64 | 0.35 | 0.25 | 10.48 | 25.60 |
| 30.00 | 99.00 | 1.01 | 26.03 | 0.00 | 25.04 | 80.64 | 241.60 | 2.22 | 1.67 | 10.12 | 0.31 | 0.24 | 5.32 | 28.00 |
| 30.00 | 96.00 | 1.01 | 39.98 | 0.00 | 24.76 | 83.05 | 237.64 | 2.71 | 1.61 | 10.02 | 0.30 | 0.20 | 6.30 | 29.00 |
| 30.00 | 96.50 | 0.93 | 0.00 | 6.00 | 22.14 | 73.63 | 254.78 | 2.34 | 1.76 | 9.96 | 0.12 | 1.09 | 1.78 | 34.20 |
| 22.00 | 37.00 | 1.12 | 19.92 | 3.00 | 14.53 | 80.59 | 247.15 | 4.04 | 1.23 | 10.15 | 1.29 | 0.03 | 7.53 | 23.20 |
| 30.00 | 0.00 | 1.36 | 0.00 | 0.00 | 0.23 | 88.89 | 217.57 | 18.81 | 1.52 | 8.69 | 3.19 | 0.03 | 2.05 | 39.10 |
| 30.00 | 0.00 | 1.50 | 13.26 | 0.00 | 0.26 | 88.56 | 216.92 | 7.71 | 1.76 | 8.37 | 4.31 | 0.03 | 2.48 | 37.90 |
| 30.00 | 0.00 | 1.47 | 40.03 | 6.00 | 0.25 | 89.52 | 228.10 | 2.97 | 1.76 | 8.80 | 4.24 | 0.03 | 6.81 | 29.80 |
| 10.00 | 24.00 | 1.01 | 40.02 | 0.00 | 20.01 | 72.25 | 240.33 | 2.69 | 1.58 | 9.63 | 0.26 | 0.18 | 4.57 | 31.50 |
| 10.00 | 25.00 | 1.01 | 0.00 | 6.00 | 19.93 | 69.32 | 243.83 | 6.46 | 1.59 | 9.67 | 0.29 | 0.20 | 1.77 | 33.90 |
| 23.00 | 25.00 | 1.13 | 19.86 | 3.00 | 11.64 | 88.75 | 235.52 | 5.91 | 1.23 | 9.54 | 1.31 | 0.03 | 5.36 | 25.30 |
| 31.00 | 66.29 | 1.00 | 39.96 | 6.00 | 20.98 | 86.01 | 252.92 | 2.08 | 1.50 | 10.22 | 0.31 | 0.29 | 7.59 | 23.90 |
| 31.00 | 67.75 | 1.00 | 0.00 | 0.00 | 17.86 | 80.29 | 238.10 | 5.78 | 1.68 | 10.18 | 0.30 | 0.26 | 3.57 | 31.30 |
| 30.00 | 0.00 | 1.01 | 39.85 | 0.00 | 0.24 | 106.24 | 262.19 | 14.25 | 0.96 | 10.40 | 0.26 | 0.24 | 2.98 | 22.40 |
| 30.00 | 0.00 | 1.01 | 0.00 | 2.00 | 0.24 | 104.50 | 243.33 | 19.38 | 1.20 | 9.76 | 0.27 | 0.21 | 2.45 | 34.00 |
| 30.00 | 0.00 | 1.01 | 26.94 | 6.00 | 0.24 | 98.71 | 265.13 | 14.14 | 0.78 | 11.26 | 0.26 | 0.26 | 3.78 | 21.70 |
| 10.00 | 0.00 | 1.01 | 26.95 | 0.00 | 0.24 | 85.53 | 250.57 | 15.76 | 1.18 | 9.85 | 0.28 | 0.22 | 2.75 | 28.30 |
| 10.00 | 0.00 | 1.01 | 39.99 | 4.00 | 0.17 | 76.40 | 269.96 | 6.86 | 1.07 | 10.77 | 0.28 | 0.23 | 3.83 | 21.00 |
| 23.00 | 0.00 | 1.01 | 39.84 | 6.00 | 0.17 | 94.45 | 281.91 | 10.07 | 0.72 | 11.25 | 0.25 | 0.26 | 5.00 | 20.40 |
| 10.00 | 0.00 | 1.01 | 0.00 | 6.00 | 0.24 | 83.73 | 240.05 | 20.27 | 1.34 | 9.72 | 0.28 | 0.22 | 1.32 | 32.20 |
| 10.00 | 0.00 | 1.17 | 39.93 | 6.00 | 0.19 | 62.65 | 260.59 | 4.84 | 1.25 | 10.54 | 1.84 | 0.03 | 5.04 | 19.90 |
| 30.00 | 0.00 | 1.10 | 39.86 | 0.00 | 0.18 | 105.55 | 245.14 | 18.18 | 0.75 | 9.96 | 1.05 | 0.03 | 9.39 | 27.40 |
| 30.00 | 30.25 | 1.01 | 0.00 | 6.00 | 12.26 | 95.27 | 236.91 | 8.59 | 1.29 | 9.79 | 0.28 | 0.18 | 3.52 | 29.70 |
| 22.00 | 36.78 | 1.13 | 19.98 | 3.00 | 14.18 | 85.08 | 239.13 | 4.34 | 1.34 | 9.67 | 1.36 | 0.03 | 5.89 | 26.20 |
| | | | | | | | | | | | | | | |
| 40.00 | 0.00 | 1.50 | 13.35 | 6.00 | 0.35 | 90.36 | 223.08 | 4.68 | 1.76 | 8.49 | 4.21 | 0.03 | 3.61 | 33.20 |
| 40.00 | 0.00 | 1.48 | 39.89 | 4.00 | 0.36 | 96.87 | 223.11 | 5.26 | 1.76 | 8.45 | 4.01 | 0.03 | 3.47 | 35.80 |
| 60.00 | 0.00 | 1.43 | 0.00 | 0.00 | 0.62 | 88.32 | 217.25 | 20.01 | 1.59 | 8.85 | 3.74 | 0.03 | 2.87 | 42.20 |
| 100.00 | 0.00 | 1.44 | 0.00 | 4.00 | 0.61 | 88.81 | 216.91 | 12.82 | 1.63 | 8.92 | 3.67 | 0.03 | 2.16 | 35.70 |
| 100.00 | 0.00 | 1.47 | 39.99 | 0.00 | 0.64 | 101.10 | 217.30 | 9.04 | 1.77 | 8.31 | 3.84 | 0.03 | 2.04 | 38.40 |
| 70.00 | 0.00 | 1.28 | 25.46 | 0.75 | 0.54 | 104.79 | 230.71 | 12.63 | 1.01 | 9.15 | 2.32 | 0.03 | 3.09 | 30.50 |
| 100.00 | 0.00 | 1.04 | 0.00 | 0.00 | 0.58 | 110.54 | 231.65 | 22.56 | 1.22 | 9.63 | 0.35 | 0.10 | 1.40 | 38.30 |
| 100.00 | 0.00 | 1.02 | 39.97 | 0.00 | 0.59 | 116.19 | 257.68 | 17.28 | 1.38 | 10.20 | 0.25 | 0.21 | 2.03 | 30.00 |
| 100.00 | 0.00 | 1.04 | 26.36 | 0.00 | 0.65 | 120.53 | 239.42 | 18.41 | 1.05 | 9.69 | 0.26 | 0.17 | 1.74 | 32.70 |
| 40.00 | 100.00 | 0.89 | 0.00 | 0.00 | 21.51 | 80.28 | 236.31 | 5.15 | 1.79 | 10.91 | 0.32 | 0.24 | 2.37 | 34.90 |
| 40.00 | 100.00 | 0.97 | 39.60 | 6.00 | 23.76 | 84.07 | 261.04 | 2.12 | 1.66 | 10.67 | 0.30 | 0.26 | 6.34 | 24.90 |
| 40.00 | 100.00 | 0.98 | 39.78 | 2.00 | 23.60 | 86.15 | 253.66 | 2.47 | 1.58 | 10.36 | 0.23 | 0.32 | 4.98 | 27.60 |
| 40.00 | 42.50 | 1.18 | 20.00 | 3.00 | 12.98 | 89.17 | 239.33 | 5.26 | 1.09 | 9.68 | 1.66 | 0.03 | 5.35 | 25.30 |
| 100.00 | 41.56 | 1.19 | 0.00 | 0.00 | 9.75 | 90.32 | 222.02 | 17.35 | 1.35 | 9.82 | 1.79 | 0.03 | 2.66 | 33.80 |
| 40.00 | 40.83 | 1.35 | 39.86 | 0.00 | 12.83 | 88.97 | 226.93 | 3.91 | 1.69 | 8.81 | 3.00 | 0.03 | 7.67 | 31.30 |
| 40.00 | 100.00 | 0.98 | 39.63 | 6.00 | 23.88 | 88.50 | 249.77 | 2.07 | 1.59 | 10.19 | 0.30 | 0.24 | 5.15 | 25.70 |
| 80.00 | 99.00 | 0.99 | 39.83 | 0.00 | 19.06 | 97.37 | 239.39 | 5.38 | 1.61 | 10.25 | 0.26 | 0.25 | 3.24 | 30.00 |
| 100.00 | 100.00 | 0.93 | 0.00 | 6.00 | 17.73 | 86.79 | 234.27 | 5.78 | 1.69 | 11.07 | 0.24 | 0.26 | 1.63 | 32.70 |
| 100.00 | 98.00 | 1.13 | 13.43 | 0.00 | 17.51 | 85.33 | 230.83 | 6.94 | 1.54 | 10.46 | 1.47 | 0.03 | 4.13 | 31.00 |
| 100.00 | 97.00 | 1.12 | 39.88 | 4.00 | 18.27 | 87.61 | 245.91 | 3.97 | 1.49 | 10.84 | 1.14 | 0.03 | 4.70 | 26.00 |
| 60.00 | 97.00 | 1.03 | 0.00 | 6.00 | 18.62 | 78.18 | 238.24 | 4.60 | 1.69 | 11.53 | 1.03 | 0.03 | 4.09 | 25.10 |
| 100.00 | 66.57 | 1.03 | 39.87 | 6.00 | 13.91 | 91.81 | 263.33 | 4.62 | 1.32 | 11.24 | 0.35 | 0.13 | 3.00 | 22.00 |
| 70.00 | 69.17 | 1.09 | 20.04 | 3.00 | 14.94 | 93.48 | 232.34 | 7.18 | 1.21 | 10.39 | 0.83 | 0.03 | 4.11 | 28.40 |
| 40.00 | 0.00 | 1.05 | 0.00 | 6.00 | 0.38 | 104.89 | 242.75 | 17.93 | 1.19 | 9.96 | 0.26 | 0.22 | 2.05 | 29.10 |
| 70.00 | 41.00 | 1.29 | 20.02 | 3.00 | 9.54 | 94.72 | 225.88 | 5.53 | 1.37 | 9.24 | 2.34 | 0.03 | 5.44 | 29.00 |
| 40.00 | 71.14 | 0.99 | 0.00 | 6.00 | 17.84 | 86.04 | 231.92 | 6.01 | 1.64 | 10.62 | 0.40 | 0.13 | 3.19 | 31.40 |
| 100.00 | 33.71 | 1.03 | 39.95 | 0.00 | 6.64 | 112.65 | 244.39 | 13.20 | 1.40 | 9.97 | 0.28 | 0.17 | 2.45 | 32.10 |
| 100.00 | 10.33 | 1.50 | 26.38 | 6.00 | 3.85 | 89.23 | 228.30 | 2.85 | 1.91 | 8.76 | 4.17 | 0.03 | 5.18 | 31.40 |
| 40.00 | 9.83 | 1.49 | 26.05 | 0.00 | 5.67 | 91.19 | 219.31 | 5.88 | 1.71 | 8.28 | 3.97 | 0.03 | 4.28 | 37.80 |
| 40.00 | 11.00 | 1.45 | 0.00 | 2.00 | 5.73 | 82.12 | 220.85 | 11.39 | 1.84 | 8.72 | 3.77 | 0.03 | 3.37 | 37.90 |
| 80.00 | 9.67 | 1.51 | 39.85 | 6.00 | 3.71 | 91.76 | 226.95 | 3.76 | 2.07 | 8.58 | 4.23 | 0.03 | 4.82 | 31.60 |
| 70.00 | 40.57 | 1.16 | 20.41 | 3.00 | 9.29 | 102.22 | 229.22 | 11.68 | 1.06 | 9.45 | 1.42 | 0.02 | 2.72 | 33.30 |
| 100.00 | 3.00 | 1.11 | 0.00 | 6.00 | 2.60 | 98.49 | 242.64 | 20.70 | 0.98 | 10.52 | 0.86 | 0.03 | 2.15 | 27.70 |
| 40.00 | 0.00 | 1.12 | 0.00 | 0.00 | 0.47 | 105.65 | 226.53 | 26.40 | 1.06 | 9.42 | 0.86 | 0.02 | 1.66 | 39.10 |
| 40.00 | 0.00 | 1.17 | 40.05 | 6.00 | 0.41 | 112.98 | 234.17 | 21.36 | 0.94 | 9.30 | 1.28 | 0.02 | 2.03 | 33.20 |
| 40.00 | 0.00 | 1.02 | 39.98 | 0.00 | 0.38 | 115.25 | 255.54 | 16.21 | 1.11 | 9.89 | 0.26 | 0.24 | 2.20 | 27.30 |

**Table B- 3 DoE test program for 1500 rev/min**

| Throttle pos | EGR demand | Fuelling rate | Cam overlap | Spark timing | EGR flow | Torque | BSFC | BSNOx | BSuHC | BSCO2 | BSO2 | BSCO | COVimep | Comb pres |
|---|---|---|---|---|---|---|---|---|---|---|---|---|---|---|
| % | % | Lambda | degree | degree | % | Nm | g/kwhr | g/kWhr | g/kWhr | kg/kWhr | kg/kWhr | kg/kWhr | % | bar |
| 17.00 | 0.00 | 1.01 | 0.00 | 0.00 | 0.17 | 97.96 | 235.56 | 20.16 | 1.25 | 9.43 | 0.30 | 0.22 | 0.91 | 39.30 |
| 10.00 | 0.00 | 1.23 | 0.00 | 0.00 | 0.21 | 65.50 | 245.52 | 34.05 | 1.51 | 9.69 | 2.33 | 0.03 | 1.36 | 39.80 |
| 10.00 | 0.00 | 1.23 | 40.00 | 0.00 | 0.21 | 66.57 | 241.11 | 11.04 | 1.46 | 9.54 | 2.30 | 0.03 | 4.21 | 26.00 |
| 10.00 | 0.00 | 1.23 | 39.99 | 6.00 | 0.21 | 64.63 | 248.31 | 6.37 | 1.40 | 9.81 | 2.37 | 0.03 | 4.30 | 22.80 |
| 10.00 | 0.00 | 1.01 | 39.92 | 4.00 | 0.17 | 72.82 | 268.01 | 7.51 | 1.09 | 10.56 | 0.29 | 0.19 | 3.56 | 19.00 |
| 10.00 | 0.00 | 1.01 | 0.00 | 6.00 | 0.17 | 78.96 | 246.07 | 19.48 | 1.35 | 9.67 | 0.31 | 0.22 | 1.66 | 30.40 |
| 10.00 | 24.00 | 1.01 | 0.00 | 6.00 | 19.10 | 68.29 | 248.49 | 8.12 | 1.60 | 9.73 | 0.27 | 0.19 | 2.13 | 32.80 |
| 10.00 | 19.00 | 1.01 | 40.10 | 0.00 | 17.12 | 71.01 | 243.91 | 4.44 | 1.57 | 9.66 | 0.29 | 0.18 | 3.77 | 32.30 |
| 20.00 | 56.50 | 1.01 | 39.94 | 6.00 | 22.22 | 71.35 | 262.42 | 1.45 | 1.72 | 10.47 | 0.30 | 0.20 | 14.86 | 25.50 |
| 20.00 | 55.00 | 1.00 | 0.00 | 0.00 | 22.10 | 71.62 | 243.82 | 3.35 | 1.61 | 9.80 | 0.27 | 0.20 | 7.49 | 27.70 |
| 30.00 | 67.00 | 1.00 | 0.00 | 0.00 | 18.32 | 81.33 | 239.41 | 5.86 | 1.63 | 10.05 | 0.27 | 0.25 | 2.07 | 34.10 |
| 30.00 | 69.57 | 1.00 | 40.10 | 6.00 | 19.07 | 75.69 | 283.13 | 2.09 | 1.50 | 11.34 | 0.30 | 0.27 | 11.66 | 22.70 |
| 30.00 | 100.00 | 1.00 | 39.95 | 2.00 | 25.29 | 79.09 | 242.41 | 2.19 | 1.66 | 10.01 | 0.31 | 0.24 | 8.35 | 26.60 |
| 30.00 | 100.00 | 1.01 | 26.96 | 0.00 | 25.22 | 79.88 | 241.41 | 2.78 | 1.64 | 9.91 | 0.30 | 0.22 | 7.66 | 27.90 |
| 30.00 | 100.00 | 1.00 | 13.00 | 6.00 | 24.98 | 75.45 | 248.21 | 2.16 | 1.72 | 10.41 | 0.32 | 0.24 | 6.96 | 27.50 |
| 30.00 | 92.00 | 1.05 | 40.00 | 6.00 | 23.57 | 74.75 | 254.28 | 2.03 | 1.80 | 10.65 | 0.71 | 0.05 | 12.59 | 25.30 |
| 22.00 | 36.00 | 1.14 | 20.00 | 3.00 | 14.43 | 80.28 | 241.43 | 4.98 | 1.28 | 9.65 | 1.41 | 0.03 | 6.98 | 25.70 |
| 30.00 | 34.33 | 1.01 | 0.00 | 6.00 | 12.11 | 88.18 | 251.75 | 8.17 | 1.24 | 10.53 | 0.30 | 0.19 | 3.62 | 26.50 |
| 30.00 | 100.00 | 1.05 | 40.09 | 0.00 | 25.16 | 78.28 | 241.00 | 2.91 | 1.70 | 10.07 | 0.85 | 0.05 | 7.77 | 28.10 |
| 21.00 | 36.56 | 1.14 | 20.01 | 3.00 | 14.95 | 81.04 | 239.54 | 4.59 | 1.28 | 9.58 | 1.40 | 0.03 | 4.87 | 28.00 |
| 30.00 | 17.50 | 1.44 | 40.03 | 0.00 | 7.85 | 82.50 | 233.16 | 2.22 | 1.95 | 8.84 | 4.06 | 0.03 | 7.94 | 31.40 |
| 23.00 | 0.00 | 1.01 | 40.04 | 6.00 | 0.17 | 100.50 | 258.12 | 0.00 | 0.95 | 10.49 | 0.24 | 0.20 | 3.73 | 23.80 |
| 23.00 | 37.70 | 1.13 | 19.94 | 3.00 | 13.91 | 85.61 | 236.13 | 5.27 | 1.31 | 9.61 | 1.31 | 0.03 | 5.23 | 26.30 |
| 30.00 | 15.57 | 1.39 | 0.00 | 0.00 | 7.23 | 79.33 | 223.28 | 13.90 | 1.76 | 9.14 | 3.69 | 0.03 | 2.84 | 39.00 |
| 30.00 | 0.00 | 1.43 | 12.93 | 0.00 | 0.34 | 92.78 | 214.43 | 17.31 | 1.53 | 8.43 | 3.73 | 0.03 | 4.46 | 38.90 |
| 30.00 | 0.00 | 1.45 | 40.00 | 4.00 | 0.24 | 91.20 | 220.84 | 4.58 | 1.62 | 8.55 | 3.98 | 0.03 | 5.26 | 32.50 |
| 21.00 | 0.00 | 1.44 | 40.01 | 0.00 | 0.24 | 84.22 | 222.18 | 6.90 | 1.63 | 8.70 | 3.93 | 0.03 | 2.89 | 34.70 |
| 21.00 | 0.00 | 1.41 | 0.00 | 6.00 | 0.24 | 81.49 | 220.39 | 17.57 | 1.64 | 8.66 | 3.73 | 0.03 | 1.55 | 38.70 |
| 21.00 | 0.00 | 1.26 | 0.00 | 6.00 | 0.21 | 88.70 | 224.79 | 17.61 | 1.25 | 9.24 | 2.44 | 0.03 | 2.45 | 32.10 |
| 21.00 | 0.00 | 1.12 | 40.00 | 0.00 | 0.18 | 101.36 | 230.59 | 18.96 | 0.84 | 9.47 | 1.12 | 0.02 | 1.91 | 34.00 |
| 21.00 | 0.00 | 1.01 | 39.99 | 0.00 | 0.17 | 104.31 | 242.52 | 14.00 | 0.95 | 9.90 | 0.24 | 0.20 | 2.58 | 29.70 |
| 30.00 | 0.00 | 1.01 | 0.00 | 2.00 | 0.17 | 108.80 | 234.02 | 20.19 | 1.19 | 9.97 | 0.29 | 0.23 | 1.38 | 37.10 |
| 30.00 | 0.00 | 1.01 | 39.95 | 0.00 | 0.17 | 112.06 | 254.48 | 15.60 | 0.99 | 10.00 | 0.25 | 0.22 | 2.36 | 30.90 |
| 30.00 | 0.00 | 1.01 | 26.87 | 6.00 | 0.17 | 106.99 | 259.95 | 15.06 | 0.96 | 10.45 | 0.24 | 0.21 | 3.36 | 24.20 |
| 30.00 | 0.00 | 1.01 | 26.95 | 0.00 | 0.24 | 117.98 | 238.85 | 17.87 | 1.07 | 9.44 | 0.24 | 0.20 | 2.24 | 34.70 |
| 23.00 | 0.00 | 1.01 | 40.11 | 6.00 | 0.17 | 96.44 | 269.38 | 11.71 | 0.86 | 10.86 | 0.25 | 0.22 | 3.87 | 22.60 |
| 30.00 | 0.00 | 1.18 | 39.93 | 0.00 | 0.19 | 106.45 | 225.45 | 18.46 | 0.84 | 9.10 | 1.69 | 0.03 | 2.57 | 34.70 |
| 30.00 | 0.00 | 1.27 | 0.00 | 6.00 | 0.21 | 92.34 | 224.16 | 16.21 | 1.24 | 9.47 | 2.64 | 0.03 | 2.08 | 32.80 |
| 22.00 | 37.33 | 1.14 | 19.91 | 3.00 | 13.94 | 87.06 | 230.59 | 6.63 | 1.26 | 9.31 | 1.33 | 0.02 | 4.69 | 29.50 |
| 30.00 | 16.63 | 1.43 | 40.02 | 6.00 | 8.46 | 83.39 | 227.85 | 2.64 | 2.04 | 8.77 | 3.98 | 0.03 | 7.13 | 32.00 |
| | | | | | | | | | | | | | | |
| 40.00 | 0.00 | 1.47 | 12.97 | 6.00 | 0.35 | 92.40 | 218.15 | 6.47 | 1.66 | 8.36 | 4.03 | 0.03 | 3.91 | 34.20 |
| 40.00 | 0.00 | 1.47 | 29.94 | 4.00 | 0.36 | 96.46 | 215.95 | 7.50 | 1.61 | 8.17 | 3.98 | 0.03 | 3.00 | 39.00 |
| 40.00 | 0.00 | 1.47 | 40.09 | 4.00 | 0.25 | 96.04 | 217.99 | 5.70 | 1.57 | 8.23 | 4.01 | 0.03 | 2.97 | 37.20 |
| 60.00 | 0.00 | 1.30 | 0.00 | 0.00 | 0.48 | 95.21 | 216.99 | 25.33 | 1.40 | 9.43 | 2.89 | 0.03 | 1.82 | 40.10 |
| 100.00 | 0.00 | 1.42 | 0.00 | 4.00 | 0.63 | 87.19 | 217.04 | 17.31 | 1.76 | 9.57 | 4.11 | 0.03 | 1.85 | 37.80 |
| 100.00 | 0.00 | 1.46 | 40.02 | 0.00 | 0.65 | 99.36 | 216.11 | 7.00 | 1.64 | 8.40 | 4.00 | 0.02 | 3.42 | 38.00 |
| 70.00 | 43.33 | 1.11 | 19.93 | 3.00 | 9.34 | 102.29 | 229.14 | 10.49 | 1.07 | 10.02 | 1.18 | 0.02 | 4.77 | 30.70 |
| 100.00 | 41.88 | 1.23 | 0.00 | 0.00 | 9.26 | 87.92 | 221.51 | 18.66 | 1.46 | 9.89 | 2.31 | 0.03 | 2.20 | 39.10 |
| 40.00 | 43.17 | 1.30 | 39.98 | 0.00 | 12.70 | 91.20 | 223.68 | 5.10 | 1.43 | 8.73 | 2.71 | 0.03 | 4.28 | 35.20 |
| 70.00 | 42.13 | 1.08 | 19.89 | 3.00 | 10.24 | 104.65 | 227.80 | 14.26 | 1.02 | 10.05 | 0.81 | 0.03 | 2.44 | 35.70 |
| 40.00 | 100.00 | 1.00 | 0.00 | 0.00 | 20.72 | 79.73 | 236.63 | 5.92 | 1.78 | 10.89 | 0.30 | 0.24 | 3.53 | 33.00 |
| 40.00 | 100.00 | 1.01 | 40.16 | 6.00 | 22.75 | 81.21 | 259.89 | 1.97 | 1.59 | 11.21 | 0.31 | 0.23 | 9.27 | 25.60 |
| 40.00 | 100.00 | 0.95 | 39.97 | 2.00 | 22.56 | 88.96 | 249.01 | 1.97 | 1.55 | 9.75 | 0.11 | 0.76 | 4.66 | 30.00 |
| 60.00 | 100.00 | 1.09 | 0.00 | 6.00 | 18.05 | 75.69 | 238.01 | 4.60 | 1.84 | 12.01 | 1.17 | 0.04 | 3.67 | 26.30 |
| 80.00 | 99.00 | 1.01 | 39.96 | 0.00 | 17.91 | 91.36 | 245.33 | 3.74 | 1.38 | 10.75 | 0.29 | 0.18 | 3.07 | 29.20 |
| 100.00 | 99.00 | 1.08 | 39.97 | 4.00 | 19.80 | 91.76 | 230.15 | 6.13 | 1.32 | 10.15 | 0.90 | 0.03 | 4.68 | 29.30 |
| 100.00 | 99.00 | 1.06 | 12.98 | 0.00 | 18.93 | 87.35 | 231.26 | 6.60 | 1.44 | 11.22 | 0.78 | 0.03 | 4.40 | 30.40 |
| 100.00 | 0.00 | 1.00 | 40.01 | 6.00 | 0.58 | 110.78 | 267.30 | 17.02 | 1.41 | 11.59 | 0.22 | 0.29 | 3.24 | 25.90 |
| 100.00 | 0.00 | 1.02 | 0.00 | 0.00 | 0.58 | 111.54 | 227.10 | 24.89 | 1.27 | 10.58 | 0.35 | 0.16 | 0.92 | 43.10 |
| 40.00 | 0.00 | 1.00 | 39.93 | 0.00 | 0.31 | 117.84 | 243.67 | 16.44 | 0.94 | 9.48 | 0.22 | 0.23 | 2.40 | 32.50 |
| 40.00 | 0.00 | 1.01 | 0.00 | 6.00 | 0.31 | 106.33 | 241.33 | 18.99 | 1.00 | 10.11 | 0.27 | 0.23 | 2.65 | 30.60 |
| 70.00 | 0.00 | 1.22 | 20.05 | 3.00 | 0.53 | 104.38 | 230.17 | 14.97 | 0.82 | 9.39 | 2.09 | 0.03 | 4.08 | 29.70 |
| 70.00 | 42.11 | 1.26 | 20.03 | 3.00 | 10.30 | 94.93 | 225.14 | 6.02 | 1.27 | 9.40 | 2.46 | 0.02 | 4.97 | 32.10 |
| 70.00 | 50.57 | 1.00 | 19.99 | 3.00 | 11.92 | 103.13 | 240.46 | 8.61 | 1.21 | 10.30 | 0.26 | 0.24 | 3.33 | 30.50 |
| 40.00 | 70.89 | 1.14 | 0.00 | 6.00 | 17.61 | 75.89 | 235.93 | 4.46 | 1.69 | 10.72 | 1.65 | 0.03 | 5.16 | 26.60 |
| 40.00 | 11.14 | 1.43 | 0.00 | 2.00 | 5.40 | 81.53 | 221.90 | 14.99 | 1.62 | 8.88 | 3.89 | 0.03 | 3.87 | 36.10 |
| 40.00 | 11.75 | 1.47 | 26.93 | 0.00 | 5.18 | 92.49 | 215.77 | 7.30 | 1.50 | 8.11 | 3.89 | 0.03 | 3.52 | 38.30 |
| 80.00 | 12.00 | 1.48 | 40.04 | 6.00 | 3.63 | 87.09 | 237.86 | 1.60 | 1.91 | 8.97 | 4.45 | 0.03 | 8.08 | 31.70 |
| 100.00 | 11.00 | 1.46 | 26.99 | 6.00 | 3.76 | 92.16 | 220.67 | 4.16 | 1.63 | 8.53 | 4.06 | 0.03 | 4.23 | 35.40 |
| 100.00 | 33.14 | 1.01 | 40.04 | 0.00 | 6.45 | 116.63 | 233.64 | 14.16 | 1.14 | 9.57 | 0.25 | 0.14 | 2.27 | 35.10 |
| 100.00 | 65.60 | 1.01 | 40.01 | 6.00 | 14.88 | 93.91 | 257.55 | 4.11 | 1.27 | 11.07 | 0.23 | 0.18 | 3.76 | 23.30 |
| 100.00 | 100.00 | 1.02 | 0.00 | 6.00 | 18.87 | 81.69 | 236.38 | 5.27 | 1.64 | 11.85 | 0.40 | 0.13 | 2.94 | 28.90 |
| 70.00 | 42.00 | 1.13 | 19.92 | 3.00 | 9.86 | 95.04 | 238.27 | 9.28 | 0.98 | 10.38 | 1.32 | 0.02 | 4.66 | 25.70 |

**Table B- 4 DoE test program for 1700 rev/min**

| Throttle pos | EGR demand | Fuelling rate | Cam overlap | Spark timing | EGR flow | Torque | BSFC | BSNOx | BSuHC | BSCO2 | BSO2 | BSCO | COVimep | Comb pres |
|---|---|---|---|---|---|---|---|---|---|---|---|---|---|---|
| % | % | Lambda | degree | degree | % | Nm | g/kwhr | g/kWhr | g/kWhr | kg/kWhr | kg/kWhr | kg/kWhr | % | bar |
| 10.02 | 0.00 | 1.01 | 39.92 | 0.00 | 0.19 | 62.55 | 254.55 | 12.59 | 1.37 | 10.18 | 0.28 | 0.20 | 2.44 | 27.95 |
| 10.00 | 0.00 | 1.17 | 0.00 | 2.00 | 0.19 | 61.86 | 254.12 | 32.72 | 1.38 | 10.13 | 1.76 | 0.03 | 3.51 | 39.80 |
| 15.00 | 35.01 | 1.00 | 0.00 | 6.00 | 20.02 | 72.42 | 240.27 | 5.76 | 1.47 | 9.55 | 0.23 | 0.19 | 5.23 | 30.80 |
| 30.00 | 39.90 | 1.28 | 0.00 | 0.00 | 15.37 | 78.70 | 226.24 | 9.17 | 1.54 | 9.19 | 2.67 | 0.03 | 8.56 | 31.40 |
| 22.00 | 33.04 | 1.21 | 19.92 | 3.00 | 13.76 | 86.46 | 231.59 | 5.64 | 1.29 | 9.10 | 1.95 | 0.03 | 6.27 | 29.10 |
| 30.00 | 69.85 | 1.19 | 39.98 | 6.00 | 19.97 | 75.92 | 245.08 | 1.94 | 1.77 | 9.87 | 1.95 | 0.03 | 13.60 | 27.20 |
| 30.00 | 65.50 | 1.00 | 0.00 | 6.00 | 18.38 | 82.45 | 238.54 | 4.07 | 1.50 | 10.20 | 0.21 | 0.23 | 4.68 | 26.90 |
| 30.00 | 95.20 | 1.00 | 0.00 | 0.00 | 24.39 | 75.65 | 239.28 | 3.97 | 1.63 | 10.52 | 0.26 | 0.22 | 10.00 | 28.10 |
| 30.00 | 0.00 | 1.00 | 40.03 | 6.00 | 0.17 | 114.58 | 248.58 | 16.06 | 1.17 | 9.79 | 0.21 | 0.21 | 2.48 | 30.10 |
| 30.00 | 100.00 | 1.00 | 40.03 | 4.00 | 24.77 | 87.56 | 236.19 | 3.29 | 1.57 | 9.61 | 0.26 | 0.26 | 6.17 | 32.80 |
| 30.00 | 100.00 | 1.05 | 39.98 | 0.00 | 24.41 | 84.07 | 231.33 | 3.59 | 1.56 | 9.74 | 0.57 | 0.06 | 9.61 | 29.80 |
| 25.00 | 80.23 | 1.05 | 0.00 | 4.00 | 22.42 | 73.28 | 238.48 | 4.92 | 1.73 | 10.43 | 0.61 | 0.05 | 12.71 | 27.00 |
| 23.00 | 36.86 | 1.20 | 20.03 | 3.00 | 13.88 | 81.38 | 241.85 | 5.03 | 1.39 | 9.50 | 2.00 | 0.03 | 5.78 | 27.40 |
| 15.03 | 22.39 | 1.17 | 40.02 | 6.00 | 17.24 | 65.52 | 258.96 | 1.86 | 1.88 | 10.00 | 1.85 | 0.03 | 10.42 | 25.49 |
| 15.00 | 28.25 | 1.16 | 13.04 | 0.00 | 17.46 | 69.32 | 240.78 | 5.72 | 1.57 | 9.42 | 1.65 | 0.03 | 11.19 | 25.30 |
| 15.00 | 29.44 | 1.01 | 40.13 | 2.00 | 16.84 | 76.37 | 249.65 | 3.24 | 1.38 | 9.73 | 0.27 | 0.18 | 7.80 | 27.10 |
| 15.00 | 29.46 | 1.00 | 0.00 | 6.00 | 16.58 | 76.66 | 239.93 | 8.11 | 1.43 | 9.36 | 0.24 | 0.19 | 3.49 | 29.80 |
| 22.00 | 32.49 | 1.21 | 19.92 | 3.00 | 14.07 | 83.46 | 230.86 | 5.36 | 1.35 | 9.02 | 1.95 | 0.03 | 5.90 | 28.80 |
| 20.00 | 67.50 | 1.01 | 39.97 | 0.00 | 26.04 | 71.53 | 265.28 | 1.85 | 1.62 | 9.91 | 0.30 | 0.23 | 13.84 | 26.30 |
| 10.00 | 1.10 | 1.01 | 12.96 | 0.00 | 0.17 | 70.31 | 266.38 | 23.47 | 1.35 | 9.90 | 0.31 | 0.22 | 2.15 | 32.70 |
| 10.00 | 1.00 | 1.01 | 12.87 | 6.00 | 0.17 | 70.06 | 257.95 | 20.07 | 1.32 | 9.97 | 0.30 | 0.24 | 2.57 | 27.80 |
| 16.00 | 0.80 | 1.28 | 39.89 | 0.00 | 0.21 | 73.98 | 233.29 | 10.30 | 1.27 | 8.96 | 2.58 | 0.03 | 4.56 | 29.40 |
| 30.00 | 0.30 | 1.26 | 0.00 | 6.00 | 0.21 | 96.88 | 220.35 | 20.99 | 1.12 | 8.77 | 2.35 | 0.03 | 2.11 | 39.10 |
| 30.00 | 0.30 | 1.45 | 0.00 | 0.00 | 0.25 | 86.04 | 218.77 | 23.04 | 1.52 | 8.48 | 3.90 | 0.03 | 4.11 | 44.70 |
| 30.00 | 0.30 | 1.48 | 40.00 | 6.00 | 0.25 | 91.70 | 222.36 | 4.97 | 1.61 | 8.28 | 4.12 | 0.03 | 5.79 | 33.20 |
| 30.00 | 0.20 | 1.14 | 40.00 | 0.00 | 0.19 | 114.04 | 223.37 | 22.91 | 0.82 | 8.84 | 1.24 | 0.02 | 1.87 | 40.10 |
| 30.00 | 0.10 | 1.00 | 27.03 | 0.00 | 0.17 | 120.99 | 236.82 | 18.46 | 1.11 | 9.21 | 0.22 | 0.19 | 2.17 | 36.70 |
| 30.00 | 0.00 | 1.01 | 0.00 | 4.00 | 0.17 | 113.20 | 229.57 | 20.22 | 1.14 | 9.15 | 0.27 | 0.22 | 1.54 | 42.70 |
| 23.00 | 0.00 | 1.01 | 0.00 | 0.00 | 0.17 | 111.01 | 226.56 | 20.57 | 1.16 | 8.92 | 0.27 | 0.22 | 2.10 | 45.50 |
| 16.70 | 0.00 | 1.01 | 39.98 | 6.00 | 0.17 | 90.12 | 256.36 | 11.01 | 0.92 | 10.01 | 0.22 | 0.19 | 3.53 | 22.81 |
| 22.00 | 33.03 | 1.22 | 19.96 | 3.00 | 13.46 | 86.94 | 226.13 | 7.12 | 1.34 | 8.76 | 1.97 | 0.03 | 7.86 | 31.00 |
| 25.00 | 75.48 | 1.00 | 12.91 | 6.00 | 24.42 | 81.63 | 241.72 | 3.78 | 1.58 | 9.67 | 0.27 | 0.21 | 7.40 | 30.50 |
| 25.00 | 79.29 | 1.05 | 26.96 | 6.00 | 25.77 | 78.77 | 237.48 | 3.77 | 1.62 | 9.70 | 0.64 | 0.04 | 8.95 | 30.00 |
| 26.00 | 9.17 | 1.41 | 39.91 | 0.00 | 8.09 | 90.23 | 211.57 | 6.57 | 1.60 | 7.99 | 3.41 | 0.03 | 8.75 | 33.20 |
| 26.00 | 11.88 | 1.39 | 0.00 | 6.00 | 6.98 | 81.84 | 221.10 | 14.91 | 1.55 | 8.50 | 3.39 | 0.03 | 14.25 | 36.80 |
| | | | | | | | | | | | | | | |
| 70.00 | 46.00 | 1.04 | 19.97 | 3.00 | 11.45 | 104.52 | 242.85 | 9.60 | 1.60 | 11.76 | 0.25 | 0.27 | 2.97 | 31.10 |
| 40.00 | 68.00 | 1.01 | 39.98 | 6.00 | 17.80 | 92.14 | 266.88 | 3.50 | 1.43 | 10.76 | 0.27 | 0.27 | 4.88 | 25.30 |
| 70.00 | 40.67 | 1.30 | 19.99 | 3.00 | 9.40 | 91.43 | 232.64 | 5.62 | 1.52 | 10.67 | 3.13 | 0.03 | 3.15 | 32.20 |
| 100.00 | 98.00 | 1.09 | 25.96 | 3.00 | 19.01 | 91.63 | 234.03 | 6.12 | 1.65 | 12.52 | 0.90 | 0.07 | 5.64 | 31.30 |
| 70.00 | 0.00 | 1.20 | 19.93 | 3.00 | 0.50 | 113.34 | 227.00 | 22.72 | 1.05 | 9.95 | 1.84 | 0.03 | 2.66 | 36.60 |
| 40.00 | 0.00 | 1.45 | 0.00 | 0.00 | 0.34 | 88.29 | 218.09 | 17.74 | 1.57 | 8.73 | 4.12 | 0.03 | 3.93 | 36.50 |
| 60.00 | 20.00 | 1.38 | 0.00 | 6.00 | 6.58 | 87.88 | 219.55 | 15.02 | 1.70 | 9.96 | 3.79 | 0.03 | 3.74 | 34.20 |
| 40.00 | 100.00 | 1.04 | 0.00 | 6.00 | 20.39 | 81.02 | 234.71 | 5.37 | -0.06 | 11.41 | 0.43 | 0.18 | 5.07 | 31.60 |
| 40.00 | 96.00 | 1.03 | 13.05 | 0.00 | 21.77 | 84.67 | 244.22 | 2.77 | -0.06 | 10.93 | 0.34 | 0.21 | 7.01 | 26.70 |
| 100.00 | 10.00 | 1.38 | 0.00 | 2.00 | 3.08 | 90.56 | 217.15 | 21.56 | -0.08 | 11.10 | 4.05 | 0.04 | 2.56 | 37.90 |
| 100.00 | 0.00 | 1.02 | 39.87 | 6.00 | 0.44 | 116.59 | 265.67 | 18.85 | -0.07 | 12.34 | 0.26 | 0.39 | 3.40 | 25.90 |
| 80.00 | 97.00 | 1.06 | 39.98 | 6.00 | 17.48 | 88.46 | 254.11 | 3.37 | -0.07 | 12.43 | 0.78 | 0.14 | 4.56 | 25.70 |
| 100.00 | 100.00 | 1.03 | 0.00 | 6.00 | 18.64 | 85.57 | 235.87 | 6.51 | -0.08 | 14.80 | 0.43 | 0.33 | 2.14 | 34.00 |
| 40.00 | 97.00 | 1.03 | 39.99 | 0.00 | 21.79 | 92.19 | 235.76 | 4.08 | -0.06 | 10.36 | 0.32 | 0.23 | 5.12 | 32.80 |
| 40.00 | 69.67 | 1.02 | 0.00 | 6.00 | 17.42 | 83.57 | 245.86 | 4.50 | -0.06 | 11.61 | 0.30 | 0.32 | 3.69 | 27.70 |
| 70.00 | 43.33 | 1.26 | 19.92 | 3.00 | 8.94 | 94.33 | 231.46 | 8.47 | -0.07 | 10.59 | 2.75 | 0.03 | 3.35 | 31.60 |
| 80.00 | 0.00 | 1.21 | 0.00 | 0.00 | 0.50 | 104.98 | 219.92 | 33.70 | -0.07 | 11.32 | 2.00 | 0.03 | 1.58 | 43.90 |
| 100.00 | 0.00 | 1.05 | 0.00 | 0.00 | 0.45 | 113.37 | 227.71 | 27.58 | -0.07 | 12.11 | 0.46 | 0.22 | 1.43 | 42.60 |
| 100.00 | 33.67 | 1.05 | 40.01 | 0.00 | 6.49 | 118.37 | 237.31 | 17.15 | -0.06 | 10.63 | 0.40 | 0.13 | 2.09 | 34.30 |
| 60.00 | 100.00 | 1.06 | 0.00 | 0.00 | 18.09 | 80.14 | 237.25 | 5.62 | -0.07 | 12.85 | 0.89 | 0.07 | 3.73 | 28.70 |
| 40.00 | 33.00 | 1.04 | 0.00 | 0.00 | 10.04 | 103.07 | 229.76 | 14.37 | -0.06 | 9.79 | 0.37 | 0.23 | 2.26 | 40.10 |
| 100.00 | 100.00 | 1.05 | 39.94 | 0.00 | 20.30 | 95.31 | 238.08 | 4.23 | -0.07 | 11.74 | 0.44 | 0.17 | 5.14 | 29.30 |
| 80.00 | 99.00 | 1.02 | 0.00 | 0.00 | 14.89 | 84.51 | 235.12 | 8.17 | -0.08 | 14.29 | 0.43 | 0.40 | 2.97 | 33.00 |
| 40.00 | 0.00 | 1.03 | 0.00 | 4.00 | 0.31 | 107.98 | 238.27 | 20.00 | -0.06 | 9.63 | 0.34 | 0.25 | 1.77 | 35.20 |
| 40.00 | 0.00 | 1.17 | 39.99 | 6.00 | 0.26 | 101.49 | 253.38 | 13.98 | -0.06 | 10.27 | 1.59 | 0.04 | 5.26 | 23.60 |
| 40.00 | 39.67 | 1.45 | 39.97 | 0.00 | 11.50 | 83.99 | 231.39 | 3.10 | -0.07 | 8.82 | 4.38 | 0.03 | 14.60 | 32.90 |
| 70.00 | 41.67 | 1.22 | 19.98 | 3.00 | 8.04 | 100.60 | 228.91 | 11.23 | -0.07 | 10.69 | 2.27 | 0.02 | 2.61 | 36.90 |
| 100.00 | 100.00 | 1.01 | 12.93 | 0.00 | 19.92 | 92.50 | 237.59 | 4.70 | -0.07 | 13.01 | 0.24 | 0.52 | 2.46 | 33.00 |
| 40.00 | 0.00 | 1.03 | 39.99 | 0.00 | 0.24 | 118.13 | 243.92 | 17.29 | -0.05 | 9.71 | 0.26 | 0.25 | 3.67 | 32.80 |
| 40.00 | 0.00 | 1.45 | 39.98 | 4.00 | 0.34 | 95.57 | 224.07 | 3.71 | -0.07 | 8.67 | 4.20 | 0.02 | 8.46 | 30.70 |
| 40.00 | 24.00 | 1.43 | 26.00 | 6.00 | 7.32 | 85.57 | 238.94 | 1.77 | -0.07 | 9.25 | 4.33 | 0.03 | 10.16 | 28.90 |
| 100.00 | 0.00 | 1.07 | 0.00 | 6.00 | 0.49 | 110.28 | 226.99 | 32.14 | -0.07 | 12.19 | 0.92 | 0.06 | 1.50 | 42.68 |
| 100.00 | 0.00 | 1.37 | 40.01 | 0.00 | 0.59 | 108.32 | 220.18 | 10.30 | -0.07 | 9.46 | 3.73 | 0.03 | 3.12 | 37.70 |
| 100.00 | 0.00 | 1.36 | 40.03 | 6.00 | 0.50 | 101.16 | 236.93 | 5.92 | -0.08 | 10.25 | 3.95 | 0.03 | 3.56 | 28.90 |
| 100.00 | 0.00 | 1.05 | 25.93 | 0.00 | 0.44 | 122.69 | 238.65 | 24.36 | 1.21 | 11.28 | 0.35 | 0.12 | 1.81 | 36.70 |
| 80.00 | 0.00 | 1.05 | 25.96 | 0.00 | 0.44 | 124.24 | 236.93 | 23.05 | 1.20 | 10.95 | 0.29 | 0.15 | 1.70 | 35.10 |
| 60.00 | 0.00 | 1.04 | 26.00 | 0.00 | 0.44 | 118.82 | 245.04 | 17.75 | 1.26 | 10.04 | 0.23 | 0.22 | 2.24 | 32.60 |
| 40.00 | 0.00 | 1.04 | 25.95 | 0.00 | 0.24 | 119.64 | 240.66 | 17.23 | 1.14 | 9.35 | 0.22 | 0.21 | 2.26 | 34.60 |
| 100.00 | 0.00 | 1.52 | 19.95 | 0.00 | 0.56 | 95.88 | 211.18 | 14.91 | 1.66 | 9.11 | 4.61 | 0.03 | 2.44 | 43.30 |
| 100.00 | 95.60 | 1.06 | 20.00 | 0.00 | 19.66 | 91.32 | 229.73 | 7.08 | 1.71 | 12.60 | 0.43 | 0.12 | 2.78 | 33.10 |
| 100.00 | 95.60 | 1.05 | 20.00 | 0.00 | 19.64 | 92.77 | 226.16 | 6.98 | 1.67 | 12.40 | 0.43 | 0.12 | 2.78 | 33.10 |
| 50.00 | 95.02 | 1.01 | 20.01 | 0.00 | 21.95 | 89.94 | 231.58 | 5.37 | 1.46 | 10.34 | 0.28 | 0.22 | 3.88 | 32.20 |
| 100.00 | 40.67 | 1.30 | 19.99 | 3.00 | 9.40 | 91.43 | 232.64 | 5.62 | 1.52 | 10.67 | 3.13 | 0.03 | 3.15 | 32.20 |

**Table B- 5 DoE test program for 1800 rev/min**

| Throttle pos | EGR demand | Fuelling rate | Cam overlap | Spark timing | EGR flow | Torque | BSFC | BSNOx | BSuHC | BSCO2 | BSO2 | BSCO | COVimep | Comb pres |
|---|---|---|---|---|---|---|---|---|---|---|---|---|---|---|
| % | % | Lambda | degree | degree | % | Nm | g/kwhr | g/kWhr | g/kWhr | kg/kWhr | kg/kWhr | kg/kWhr | % | bar |
| 30.00 | 66.00 | 1.10 | 39.95 | 6.00 | 19.44 | 85.91 | 227.53 | 4.02 | 1.50 | 9.45 | 1.16 | 0.03 | 6.28 | 28.90 |
| 24.96 | 100.00 | 1.05 | 0.00 | 4.00 | 25.43 | 65.34 | 251.71 | 2.50 | 2.57 | 10.85 | 0.83 | 0.09 | 6.37 | 29.62 |
| 30.00 | 74.00 | 1.10 | 39.95 | 6.00 | 19.29 | 86.82 | 225.14 | 4.01 | 1.48 | 9.35 | 1.15 | 0.03 | 6.28 | 28.90 |
| 30.00 | 66.00 | 1.10 | 39.95 | 6.00 | 19.44 | 85.91 | 227.53 | 4.02 | 1.50 | 9.45 | 1.16 | 0.03 | 6.28 | 28.90 |
| 24.96 | 100.00 | 1.05 | 0.00 | 4.00 | 25.43 | 65.34 | 251.71 | 2.50 | 2.57 | 10.85 | 0.83 | 0.09 | 6.37 | 29.62 |
| 25.00 | 100.00 | 1.01 | 13.15 | 6.00 | 25.66 | 75.07 | 244.14 | 2.71 | 1.90 | 10.07 | 0.35 | 0.27 | 9.87 | 26.70 |
| 25.00 | 33.80 | 1.16 | 20.94 | 3.00 | 12.86 | 89.07 | 230.04 | 8.09 | 1.17 | 9.32 | 1.61 | 0.03 | 5.47 | 28.10 |
| 10.00 | 20.00 | 0.95 | 0.00 | 6.00 | 19.37 | 58.42 | 254.79 | 3.95 | 1.89 | 10.22 | 0.34 | 0.22 | 2.56 | 27.30 |
| 10.00 | 0.02 | 1.07 | 39.87 | 2.00 | 0.47 | 63.51 | 237.19 | 12.14 | 1.33 | 9.41 | 0.26 | 0.24 | 8.37 | 23.54 |
| 30.00 | 0.00 | 1.14 | 40.11 | 0.00 | 0.26 | 108.93 | 224.90 | 19.53 | 0.84 | 9.15 | 1.29 | 0.03 | 2.14 | 32.70 |
| 30.00 | 0.00 | 1.42 | 0.00 | 0.00 | 0.34 | 82.92 | 221.46 | 22.25 | 1.53 | 8.54 | 4.09 | 0.03 | 4.72 | 42.70 |
| 30.00 | 0.00 | 1.01 | 27.31 | 0.00 | 0.24 | 119.07 | 232.27 | 18.64 | 1.07 | 9.21 | 0.26 | 0.27 | 1.21 | 39.10 |
| 10.00 | 0.00 | 0.98 | 39.89 | 0.00 | 0.24 | 71.27 | 252.41 | 13.02 | 1.32 | 9.92 | 0.27 | 0.30 | 1.36 | 28.20 |
| 10.00 | 0.00 | 1.13 | 0.00 | 2.00 | 0.27 | 55.28 | 260.56 | 33.08 | 1.54 | 10.39 | 1.85 | 0.03 | 1.22 | 33.70 |
| 10.00 | 20.00 | 0.98 | 13.71 | 0.00 | 19.11 | 58.47 | 255.55 | 4.43 | 1.89 | 10.39 | 0.55 | 0.07 | 9.55 | 21.90 |
| 10.00 | 8.00 | 0.97 | 39.77 | 0.00 | 13.25 | 57.63 | 254.56 | 7.86 | 1.63 | 10.37 | 0.57 | 0.05 | 3.07 | 28.20 |
| 22.00 | 33.00 | 1.15 | 20.73 | 3.00 | 12.88 | 82.58 | 234.11 | 6.26 | 1.32 | 9.38 | 1.67 | 0.03 | 5.35 | 27.60 |
| 30.00 | 39.00 | 1.21 | 0.00 | 0.00 | 14.68 | 83.02 | 223.09 | 13.96 | 1.35 | 9.14 | 2.06 | 0.03 | 2.25 | 36.70 |
| 30.00 | 100.00 | 0.99 | 0.00 | 0.00 | 23.58 | 73.67 | 243.96 | 3.62 | 1.89 | 10.35 | 0.37 | 0.25 | 5.36 | 29.90 |
| 30.00 | 0.00 | 1.00 | 40.01 | 6.00 | 0.24 | 108.24 | 263.04 | 13.84 | 1.10 | 10.38 | 0.25 | 0.27 | 2.78 | 24.00 |
| 30.00 | 100.00 | 1.00 | 39.82 | 4.00 | 24.89 | 84.93 | 235.74 | 4.02 | 1.56 | 9.61 | 0.30 | 0.26 | 5.74 | 32.50 |
| 30.00 | 100.00 | 0.99 | 39.96 | 0.00 | 25.32 | 82.73 | 238.73 | 3.97 | 1.55 | 9.72 | 0.27 | 0.33 | 4.52 | 33.70 |
| 25.00 | 100.00 | 0.99 | 28.61 | 6.00 | 25.63 | 78.04 | 241.18 | 3.19 | 1.65 | 9.85 | 0.31 | 0.26 | 6.94 | 28.40 |
| 20.00 | 75.00 | 0.98 | 39.88 | 0.00 | 24.87 | 72.20 | 246.42 | 2.78 | 1.77 | 9.86 | 0.30 | 0.24 | 14.39 | 26.60 |
| 30.00 | 67.00 | 1.00 | 0.00 | 6.00 | 17.36 | 78.98 | 241.23 | 4.47 | 1.52 | 10.00 | 0.30 | 0.31 | 4.43 | 28.10 |
| 30.00 | 31.67 | 1.14 | 20.75 | 3.00 | 12.26 | 92.97 | 230.03 | 8.65 | 1.06 | 9.32 | 1.40 | 0.02 | 3.99 | 27.50 |
| 30.00 | 0.00 | 1.01 | 0.00 | 4.00 | 0.24 | 106.64 | 239.54 | 18.74 | 1.04 | 9.29 | 0.32 | 0.26 | 1.12 | 38.40 |
| 23.00 | 0.00 | 1.01 | 0.00 | 0.00 | 0.24 | 108.65 | 229.66 | 19.71 | 1.08 | 9.02 | 0.31 | 0.26 | 1.20 | 45.00 |
| 10.00 | 0.00 | 0.99 | 13.19 | 6.00 | 0.24 | 71.16 | 255.21 | 21.05 | 1.40 | 9.97 | 0.33 | 0.31 | 1.73 | 30.31 |
| 15.00 | 0.00 | 1.24 | 39.93 | 0.00 | 0.29 | 73.15 | 232.47 | 13.46 | 1.68 | 9.16 | 2.50 | 0.03 | 1.39 | 35.10 |
| 17.00 | 0.00 | 0.99 | 39.95 | 6.00 | 0.24 | 87.61 | 255.24 | 11.42 | 1.20 | 9.98 | 0.25 | 0.30 | 3.19 | 26.20 |
| 23.00 | 33.00 | 1.13 | 20.70 | 3.00 | 12.58 | 90.06 | 226.54 | 8.71 | 1.26 | 9.12 | 1.45 | 0.02 | 5.99 | 29.20 |
| 30.00 | 0.00 | 1.42 | 39.97 | 6.00 | 0.34 | 94.36 | 219.53 | 6.97 | 1.50 | 8.47 | 4.12 | 0.03 | 8.67 | 38.40 |
| 30.00 | 0.00 | 1.26 | 0.00 | 6.00 | 0.30 | 93.96 | 220.77 | 21.61 | 1.22 | 8.69 | 2.62 | 0.03 | 0.99 | 42.80 |
| 23.00 | 33.00 | 1.15 | 20.68 | 3.00 | 12.15 | 95.76 | 224.54 | 10.34 | 1.19 | 9.02 | 1.59 | 0.02 | 2.68 | 35.80 |
| 25.00 | 16.89 | 1.32 | 0.00 | 6.00 | 8.34 | 80.76 | 223.29 | 15.63 | 1.49 | 8.77 | 3.25 | 0.03 | 3.18 | 38.10 |
| | | | | | | | | | | | | | | |
| 40.00 | 43.00 | 1.39 | 40.00 | 0.00 | 11.90 | 93.30 | 214.00 | 4.67 | 1.73 | 8.30 | 3.28 | 0.03 | 5.63 | 38.90 |
| 40.00 | 68.30 | 1.05 | 0.00 | 6.00 | 16.70 | 87.70 | 232.00 | 5.59 | 1.63 | 10.60 | 0.41 | 0.19 | 3.08 | 32.40 |
| 40.00 | 100.00 | 1.03 | 0.00 | 0.00 | 20.80 | 81.50 | 234.00 | 4.95 | 1.84 | 11.10 | 0.36 | 0.25 | 7.93 | 30.50 |
| 70.00 | 55.00 | 1.08 | 20.40 | 3.00 | 10.90 | 104.00 | 243.00 | 11.50 | 1.81 | 13.20 | 0.61 | 0.12 | 3.30 | 29.90 |
| 70.00 | 43.30 | 1.19 | 20.40 | 3.00 | 9.35 | 101.00 | 235.00 | 11.50 | 1.62 | 12.20 | 2.10 | 0.03 | 2.04 | 30.00 |
| 70.00 | 0.00 | 1.30 | 20.70 | 3.00 | 0.47 | 106.00 | 227.00 | 12.40 | 1.25 | 9.02 | 2.66 | 0.03 | 2.49 | 32.20 |
| 40.00 | 0.00 | 1.46 | 39.90 | 2.00 | 0.35 | 101.00 | 216.00 | 7.08 | 1.75 | 8.21 | 4.09 | 0.03 | 2.48 | 39.60 |
| 40.00 | 0.00 | 1.46 | 0.00 | 0.00 | 0.34 | 86.40 | 220.00 | 23.30 | 1.55 | 8.38 | 4.01 | 0.03 | 5.40 | 44.50 |
| 80.00 | 0.00 | 1.03 | 40.00 | 6.00 | 0.66 | 117.00 | 264.00 | 18.50 | 1.82 | 10.80 | 0.43 | 0.16 | 3.45 | 26.20 |
| 100.00 | 0.00 | 1.05 | 0.00 | 0.00 | 0.52 | 115.00 | 226.00 | 24.30 | 1.46 | 10.60 | 0.40 | 0.20 | 0.95 | 45.90 |
| 100.00 | 0.00 | 1.03 | 13.50 | 6.00 | 0.45 | 116.00 | 251.00 | 19.00 | 1.39 | 10.90 | 0.32 | 0.23 | 2.02 | 29.60 |
| 100.00 | 0.00 | 1.03 | 40.00 | 4.00 | 0.45 | 121.00 | 256.00 | 18.80 | 2.08 | 10.70 | 0.35 | 0.20 | 2.94 | 28.10 |
| 100.00 | 0.00 | 1.30 | 40.00 | 6.00 | 0.48 | 111.00 | 230.00 | 10.70 | 1.68 | 9.13 | 2.84 | 0.03 | 2.79 | 22.10 |
| 100.00 | 0.00 | 1.12 | 40.00 | 0.00 | 0.48 | 125.00 | 232.00 | 23.50 | 1.72 | 9.57 | 1.13 | 0.04 | 2.51 | 35.40 |
| 60.00 | 0.00 | 1.02 | 40.00 | 0.00 | 0.38 | 128.00 | 243.00 | 18.40 | 1.83 | 9.08 | 0.28 | 0.24 | 2.42 | 34.40 |
| 40.00 | 0.00 | 1.02 | 26.60 | 0.00 | 0.24 | 126.00 | 232.00 | 18.40 | 1.37 | 8.94 | 0.26 | 0.24 | 1.52 | 38.70 |
| 40.00 | 0.00 | 1.02 | 0.00 | 6.00 | 0.24 | 111.00 | 236.00 | 17.90 | 1.25 | 9.10 | 0.31 | 0.26 | 1.39 | 37.70 |
| 100.00 | 0.00 | 1.46 | 0.00 | 6.00 | 0.54 | 87.60 | 219.00 | 19.10 | 1.94 | 9.58 | 4.63 | 0.03 | 1.57 | 44.60 |
| 100.00 | 5.00 | 1.40 | 0.00 | 2.00 | 2.71 | 93.00 | 215.00 | 27.50 | 2.04 | 11.50 | 4.40 | 0.04 | 1.34 | 44.80 |
| 100.00 | 6.00 | 1.43 | 39.90 | 4.00 | 2.34 | 106.00 | 221.00 | 8.78 | 2.27 | 9.55 | 4.21 | 0.04 | 2.15 | 38.80 |
| 40.00 | 100.00 | 0.89 | 40.00 | 6.00 | 22.60 | 92.00 | 272.00 | 1.38 | 2.58 | 8.64 | 0.07 | 1.99 | 2.97 | 31.70 |
| 40.00 | 100.00 | 1.07 | 40.10 | 0.00 | 22.40 | 85.20 | 241.00 | 3.65 | 1.69 | 10.60 | 0.58 | 0.09 | 4.65 | 29.90 |
| 40.00 | 93.80 | 1.02 | 39.90 | 0.00 | 21.90 | 83.50 | 256.00 | 2.49 | 1.78 | 11.00 | 0.33 | 0.24 | 6.30 | 25.90 |
| 40.00 | 0.00 | 1.19 | 40.00 | 6.00 | 0.27 | 102.00 | 244.00 | 14.30 | 0.96 | 9.82 | 1.67 | 0.04 | 3.39 | 25.80 |
| 40.00 | 10.00 | 1.46 | 13.60 | 6.00 | 4.85 | 89.90 | 220.00 | 7.45 | 1.83 | 8.33 | 4.00 | 0.03 | 5.31 | 35.00 |
| 40.00 | 10.70 | 1.43 | 40.00 | 6.00 | 5.15 | 88.00 | 238.00 | 1.88 | 2.10 | 9.04 | 4.23 | 0.04 | 6.55 | 28.60 |
| 60.00 | 9.71 | 1.43 | 40.00 | 6.00 | 4.09 | 97.30 | 229.00 | 3.39 | 2.00 | 9.04 | 3.99 | 0.03 | 5.07 | 33.10 |
| 100.00 | 100.00 | 1.03 | 38.70 | 0.00 | 18.00 | 99.00 | 243.00 | 5.12 | 2.94 | 15.00 | 0.44 | 0.25 | 2.82 | 29.60 |
| 85.00 | 69.30 | 1.07 | 20.30 | 4.50 | 13.30 | 96.00 | 259.00 | 8.94 | 2.16 | 14.10 | 1.24 | 0.06 | 4.15 | 26.60 |
| 100.00 | 42.70 | 1.20 | 5.21 | 0.00 | 7.34 | 101.00 | 221.00 | 25.60 | 1.97 | 13.70 | 2.44 | 0.04 | 1.78 | 38.60 |
| 80.00 | 100.00 | 1.06 | 5.28 | 0.00 | 15.60 | 92.80 | 227.00 | 10.10 | 2.55 | 16.10 | 0.84 | 0.14 | 1.82 | 34.60 |
| 86.00 | 90.00 | 1.02 | 5.49 | 5.00 | 15.00 | 90.40 | 241.00 | 7.00 | 2.67 | 17.30 | 0.45 | 0.39 | 2.75 | 29.50 |
| 100.00 | 9.00 | 1.52 | 26.10 | 0.00 | 3.22 | 96.00 | 216.00 | 9.99 | 2.37 | 10.20 | 5.54 | 0.04 | 1.94 | 43.50 |

**Table B- 6 DoE test program for 2000 rev/min**

| Throttle pos | EGR demand | Fuelling rate | Cam overlap | Spark timing | EGR flow | Torque | BSFC | BSNOx | BSuHC | BSCO2 | BSO2 | BSCO | COVimep | Comb pres |
|---|---|---|---|---|---|---|---|---|---|---|---|---|---|---|
| % | % | Lambda | degree | degree | % | Nm | g/kwhr | g/kWhr | g/kWhr | kg/kWhr | kg/kWhr | kg/kWhr | % | bar |
| 25.00 | 100.00 | 1.03 | 16.60 | 6.00 | 25.60 | 72.40 | 256.00 | 1.93 | 1.93 | 10.60 | 0.36 | 0.28 | 14.60 | 23.90 |
| 25.00 | 100.00 | 1.02 | 18.00 | 6.00 | 25.50 | 75.50 | 243.00 | 3.64 | 1.68 | 10.10 | 0.34 | 0.26 | 11.10 | 27.30 |
| 10.00 | 21.00 | 1.01 | 39.90 | 2.00 | 17.30 | 59.30 | 253.00 | 5.28 | 1.60 | 10.10 | 0.27 | 0.22 | 5.98 | 27.20 |
| 10.00 | 0.00 | 1.03 | 39.90 | 0.00 | 0.24 | 67.80 | 257.00 | 14.20 | 1.26 | 10.10 | 0.28 | 0.26 | 4.23 | 28.60 |
| 10.00 | 0.00 | 1.19 | 0.00 | 2.00 | 0.28 | 59.00 | 254.00 | 32.00 | 1.45 | 10.10 | 2.06 | 0.03 | 4.87 | 33.70 |
| 30.00 | 0.00 | 1.00 | 22.80 | 0.00 | 0.24 | 121.00 | 236.00 | 18.70 | 1.01 | 9.30 | 0.30 | 0.26 | 3.03 | 38.50 |
| 30.00 | 0.00 | 1.00 | 0.00 | 4.00 | 0.24 | 110.00 | 236.00 | 18.70 | 1.07 | 9.24 | 0.36 | 0.31 | 3.07 | 38.00 |
| 30.00 | 0.00 | 1.14 | 40.00 | 0.00 | 0.26 | 111.00 | 228.00 | 20.30 | 0.84 | 9.39 | 1.42 | 0.02 | 3.51 | 34.60 |
| 30.00 | 0.00 | 1.38 | 0.00 | 0.00 | 0.33 | 87.70 | 222.00 | 23.70 | 1.51 | 8.66 | 3.88 | 0.02 | 3.68 | 39.00 |
| 30.00 | 66.00 | 1.14 | 40.00 | 6.00 | 19.20 | 79.90 | 242.00 | 2.97 | 1.75 | 9.85 | 1.82 | 0.02 | 14.70 | 27.80 |
| 15.00 | 46.00 | 0.99 | 0.00 | 0.00 | 18.20 | 71.10 | 247.00 | 4.85 | 1.65 | 9.60 | 0.33 | 0.27 | 6.54 | 29.10 |
| 10.00 | 20.70 | 1.13 | 40.00 | 6.00 | 17.40 | 51.20 | 266.00 | 2.78 | 2.62 | 10.50 | 1.83 | 0.03 | 19.50 | 22.70 |
| 10.00 | 19.70 | 1.14 | 13.10 | 0.00 | 17.20 | 53.30 | 261.00 | 5.48 | 1.97 | 10.40 | 1.72 | 0.02 | 16.80 | 22.00 |
| 22.00 | 34.30 | 1.15 | 19.90 | 3.00 | 12.40 | 85.70 | 232.00 | 9.79 | 1.19 | 9.28 | 1.64 | 0.02 | 5.63 | 29.30 |
| 30.00 | 39.30 | 1.21 | 0.00 | 0.00 | 13.90 | 82.80 | 225.00 | 9.33 | 1.34 | 9.19 | 2.29 | 0.02 | 6.42 | 32.30 |
| 30.00 | 65.00 | 0.99 | 0.00 | 6.00 | 16.70 | 83.60 | 238.00 | 7.41 | 1.41 | 9.74 | 0.35 | 0.33 | 4.24 | 34.20 |
| 30.00 | 100.00 | 0.98 | 39.90 | 4.00 | 25.00 | 81.70 | 248.00 | 2.73 | 1.48 | 9.97 | 0.34 | 0.23 | 10.80 | 26.60 |
| 30.00 | 100.00 | 1.01 | 0.00 | 0.00 | 22.80 | 72.00 | 245.00 | 3.75 | 1.75 | 10.50 | 0.41 | 0.31 | 6.53 | 27.70 |
| 30.00 | 97.00 | 1.03 | 39.90 | 4.00 | 23.80 | 76.60 | 252.00 | 2.73 | 1.62 | 10.50 | 0.62 | 0.09 | 9.29 | 26.40 |
| 25.00 | 89.00 | 1.04 | 26.10 | 6.00 | 24.80 | 72.40 | 247.00 | 2.57 | 1.91 | 10.20 | 0.83 | 0.04 | 11.10 | 25.50 |
| 22.00 | 31.70 | 1.17 | 20.90 | 3.00 | 12.20 | 83.30 | 234.00 | 6.07 | 1.15 | 9.34 | 1.93 | 0.02 | 8.13 | 25.20 |
| 30.00 | 0.00 | 1.01 | 39.90 | 6.00 | 0.24 | 107.00 | 262.00 | 14.80 | 0.76 | 10.40 | 0.28 | 0.22 | 3.62 | 25.50 |
| 17.00 | 0.00 | 1.00 | 39.90 | 6.00 | 0.24 | 92.50 | 249.00 | 13.90 | 0.94 | 9.78 | 0.26 | 0.23 | 4.83 | 28.30 |
| 23.00 | 0.00 | 0.89 | 0.00 | 0.00 | 0.25 | 105.00 | 262.00 | 20.40 | 1.11 | 8.92 | 0.36 | 0.33 | 2.77 | 45.00 |
| 10.00 | 0.00 | 0.99 | 13.00 | 6.00 | 0.24 | 62.20 | 277.00 | 15.90 | 1.10 | 10.70 | 0.34 | 0.29 | 5.49 | 20.90 |
| 30.00 | 0.00 | 1.30 | 0.00 | 6.00 | 0.25 | 93.30 | 221.00 | 25.80 | 1.25 | 8.66 | 2.99 | 0.02 | 3.72 | 42.30 |
| 30.00 | 0.00 | 1.43 | 40.20 | 6.00 | 0.25 | 93.60 | 222.00 | 6.24 | 1.46 | 8.54 | 4.21 | 0.02 | 5.66 | 32.80 |
| 15.00 | 0.00 | 1.25 | 39.90 | 0.00 | 0.21 | 86.10 | 228.00 | 16.20 | 1.10 | 8.91 | 2.60 | 0.02 | 3.81 | 35.90 |
| 22.00 | 35.30 | 1.16 | 20.00 | 3.00 | 12.90 | 82.70 | 231.00 | 10.90 | 1.32 | 9.14 | 1.97 | 0.02 | 6.88 | 32.90 |
| 25.00 | 14.00 | 1.35 | 40.00 | 0.00 | 7.52 | 81.50 | 232.00 | 4.78 | 1.68 | 9.07 | 3.75 | 0.02 | 10.40 | 32.20 |
| 20.00 | 71.70 | 0.99 | 39.90 | 0.00 | 24.10 | 74.40 | 246.00 | 3.50 | 1.66 | 9.78 | 0.28 | 0.23 | 13.30 | 30.30 |
| | | | | | | | | | | | | | | |
| 40.00 | 0.00 | 1.45 | 40.01 | 0.00 | 0.34 | 103.74 | 212.32 | 10.78 | -0.07 | 8.29 | 3.88 | 0.03 | 4.73 | 38.20 |
| 40.00 | 0.00 | 1.00 | 39.98 | 6.00 | 0.24 | 115.87 | 260.46 | 15.52 | -0.06 | 10.40 | 0.31 | 0.23 | 5.24 | 25.80 |
| 100.00 | 0.00 | 1.04 | 39.86 | 0.00 | 0.38 | 132.98 | 238.36 | 25.22 | -0.06 | 11.61 | 0.48 | 0.13 | 4.02 | 34.60 |
| 100.00 | 0.00 | 1.02 | 0.00 | 6.00 | 0.31 | 115.17 | 243.02 | 20.46 | -0.07 | 11.64 | 0.30 | 0.41 | 2.78 | 33.80 |
| 40.00 | 0.00 | 1.02 | 0.00 | 0.00 | 0.24 | 116.88 | 227.11 | 20.09 | -0.05 | 9.00 | 0.35 | 0.30 | 2.11 | 45.30 |
| 40.00 | 0.00 | 1.43 | 39.98 | 4.00 | 0.34 | 99.94 | 218.50 | 5.93 | -0.07 | 8.45 | 4.06 | 0.03 | 8.76 | 33.00 |
| 80.00 | 0.00 | 1.46 | 0.00 | 0.00 | 0.34 | 92.58 | 214.39 | 19.52 | -0.08 | 9.77 | 4.85 | 0.03 | 4.07 | 44.20 |
| 40.00 | 41.25 | 1.23 | 0.00 | 0.00 | 12.14 | 87.63 | 221.47 | 14.90 | -0.06 | 9.14 | 2.37 | 0.03 | 6.08 | 36.60 |
| 70.00 | 37.67 | 1.03 | 20.02 | 3.00 | 9.21 | 110.45 | 241.26 | 10.81 | -0.06 | 11.09 | 0.36 | 0.21 | 4.11 | 30.10 |
| 100.00 | 41.33 | 1.23 | 39.98 | 0.00 | 6.92 | 106.95 | 221.31 | 11.40 | -0.07 | 9.99 | 2.32 | 0.03 | 4.72 | 34.00 |
| 100.00 | 71.33 | 1.13 | 0.00 | 6.00 | 12.93 | 85.06 | 239.93 | 8.17 | -0.09 | 14.50 | 1.89 | 0.04 | 5.64 | 27.90 |
| 100.00 | 100.00 | 1.09 | 39.95 | 2.00 | 17.62 | 92.19 | 242.25 | 5.42 | -0.07 | 12.34 | 1.12 | 0.04 | 7.01 | 27.90 |
| 60.00 | 96.00 | 1.04 | 0.00 | 6.00 | 16.63 | 82.29 | 242.45 | 5.10 | -0.08 | 13.17 | 0.70 | 0.15 | 6.22 | 27.50 |
| 40.00 | 87.00 | 1.00 | 11.11 | 0.00 | 20.53 | 84.56 | 247.38 | 5.48 | -0.06 | 10.32 | 0.54 | 0.12 | 5.39 | 31.20 |
| 40.00 | 100.00 | 1.01 | 0.00 | 2.00 | 20.47 | 78.41 | 243.33 | 6.27 | -0.06 | 10.65 | 0.38 | 0.28 | 5.07 | 34.40 |
| 40.00 | 100.00 | 1.00 | 27.09 | 6.00 | 22.29 | 86.06 | 248.62 | 3.56 | -0.06 | 10.27 | 0.33 | 0.23 | 6.97 | 27.70 |
| 40.00 | 66.00 | 1.03 | 0.00 | 6.00 | 15.55 | 82.66 | 243.50 | 5.02 | -0.06 | 10.36 | 0.36 | 0.31 | 5.84 | 28.80 |
| 70.00 | 50.00 | 1.03 | 20.04 | 3.00 | 11.18 | 106.31 | 236.97 | 9.29 | -0.06 | 10.96 | 0.28 | 0.34 | 3.90 | 30.30 |
| 70.00 | 40.67 | 1.13 | 20.50 | 3.00 | 9.46 | 103.43 | 235.12 | 11.22 | -0.07 | 10.79 | 1.24 | 0.03 | 4.57 | 28.60 |
| 40.00 | 0.00 | 1.40 | 0.00 | 6.00 | 0.32 | 90.88 | 216.54 | 15.97 | -0.07 | 8.48 | 3.48 | 0.03 | 4.09 | 36.50 |
| 100.00 | 0.00 | 1.12 | 0.00 | 0.00 | 0.41 | 127.20 | 208.93 | 14.21 | -0.06 | 8.92 | 0.37 | 1.06 | 2.93 | 44.50 |
| 100.00 | 0.00 | 1.11 | 39.97 | 6.00 | 0.47 | 119.65 | 255.70 | 22.58 | -0.08 | 12.45 | 1.16 | 0.07 | 4.53 | 25.20 |
| 100.00 | 0.00 | 1.47 | 27.08 | 6.00 | 0.44 | 106.10 | 219.87 | 5.82 | -0.08 | 9.86 | 4.78 | 0.03 | 6.99 | 32.60 |
| 100.00 | 0.00 | 1.47 | 12.98 | 0.00 | 0.54 | 104.98 | 211.02 | 16.97 | -0.08 | 9.54 | 4.70 | 0.03 | 4.15 | 44.30 |
| 100.00 | 16.00 | 1.40 | 0.00 | 4.00 | 4.38 | 94.95 | 216.11 | 15.45 | -0.08 | 9.98 | 4.18 | 0.03 | 4.27 | 39.50 |
| 80.00 | 14.00 | 1.41 | 39.97 | 6.00 | 4.46 | 97.36 | 233.64 | 3.24 | -0.08 | 9.52 | 4.31 | 0.03 | 9.71 | 30.10 |
| 100.00 | 100.00 | 1.00 | 40.01 | 6.00 | 18.37 | 96.38 | 252.53 | 3.37 | -0.08 | 12.74 | 0.19 | 0.63 | 4.79 | 26.40 |
| 100.00 | 100.00 | 1.01 | 0.00 | 0.00 | 17.36 | 89.05 | 234.27 | 7.38 | -0.09 | 15.45 | 0.44 | 0.49 | 4.35 | 33.60 |
| 40.00 | 10.33 | 1.41 | 13.04 | 6.00 | 6.04 | 90.66 | 219.22 | 7.77 | -0.07 | 8.33 | 3.98 | 0.03 | 7.75 | 34.10 |
| 40.00 | 73.00 | 1.16 | 39.95 | 6.00 | 18.62 | 87.67 | 235.76 | 3.48 | -0.06 | 9.74 | 1.60 | 0.02 | 8.58 | 29.00 |
| 40.00 | 34.00 | 1.03 | 39.98 | 0.00 | 10.34 | 108.86 | 234.99 | 11.60 | -0.06 | 9.47 | 0.30 | 0.22 | 4.56 | 32.30 |
| 60.00 | 100.00 | 1.02 | 39.94 | 0.00 | 19.37 | 96.49 | 236.50 | 4.86 | -0.06 | 10.87 | 0.32 | 0.32 | 4.33 | 30.60 |
| 60.00 | 40.67 | 1.15 | 20.00 | 3.00 | 10.58 | 96.88 | 236.10 | 8.98 | -0.07 | 10.54 | 1.63 | 0.03 | 5.30 | 27.20 |
| 70.00 | 0.00 | 1.10 | 20.03 | 3.00 | 0.40 | 119.99 | 240.11 | 25.25 | -0.07 | 10.96 | 1.08 | 0.03 | 3.89 | 32.40 |

**Table B- 7 DoE test program for 2200 rev/min**

| Throttle pos | EGR demand | Fuelling rate | Cam overlap | Spark timing | EGR flow | Torque | BSFC | BSNOx | BSuHC | BSCO2 | BSO2 | BSCO | COVimep | Comb pres |
|---|---|---|---|---|---|---|---|---|---|---|---|---|---|---|
| % | % | Lambda | degree | degree | % | Nm | g/kwhr | g/kWhr | g/kWhr | kg/kWhr | kg/kWhr | kg/kWhr | % | bar |
| 17.00 | 0.00 | 1.27 | 39.80 | 0.00 | 0.21 | 71.45 | 232.26 | 18.28 | 1.20 | 9.20 | 2.29 | 0.03 | 2.37 | 34.10 |
| 10.00 | 0.00 | 1.16 | 0.00 | 4.00 | 0.19 | 51.47 | 268.25 | 33.61 | 1.48 | 10.71 | 1.55 | 0.04 | 14.58 | 32.60 |
| 10.00 | 0.00 | 1.16 | 25.96 | 6.00 | 0.19 | 51.09 | 267.13 | 31.74 | 1.46 | 10.64 | 1.53 | 0.03 | 14.35 | 32.70 |
| 10.00 | 0.00 | 1.03 | 39.61 | 0.00 | 0.17 | 58.50 | 260.90 | 16.17 | 1.40 | 10.13 | 0.36 | 0.25 | 10.27 | 31.30 |
| 10.00 | 0.00 | 1.13 | 26.04 | 6.00 | 0.19 | 52.88 | 265.56 | 31.97 | 1.46 | 10.54 | 1.34 | 0.04 | 14.60 | 34.70 |
| 10.00 | 0.00 | 1.13 | 0.00 | 4.00 | 0.19 | 51.27 | 271.14 | 34.30 | 1.46 | 10.68 | 1.43 | 0.04 | 13.37 | 32.10 |
| 18.00 | 36.17 | 1.19 | 39.84 | 6.00 | 14.90 | 66.31 | 239.04 | 4.96 | 1.73 | 9.26 | 1.90 | 0.03 | 13.25 | 28.20 |
| 27.00 | 26.00 | 1.22 | 20.03 | 3.00 | 10.87 | 88.34 | 225.46 | 11.80 | 1.10 | 8.81 | 1.82 | 0.03 | 4.24 | 34.80 |
| 30.00 | 100.00 | 1.01 | 0.00 | 6.00 | 22.47 | 64.74 | 269.33 | 2.13 | 1.87 | 11.26 | 0.40 | 0.34 | 16.36 | 23.00 |
| 30.00 | 100.00 | 1.00 | 39.80 | 0.00 | 23.80 | 80.98 | 240.99 | 5.59 | 1.36 | 9.42 | 0.27 | 0.25 | 11.66 | 32.10 |
| 35.00 | 100.00 | 0.99 | 39.84 | 6.00 | 22.81 | 80.95 | 254.74 | 3.61 | 1.36 | 9.98 | 0.29 | 0.28 | 10.26 | 26.10 |
| 35.00 | 100.00 | 0.98 | 0.00 | 0.00 | 21.16 | 74.14 | 254.77 | 5.56 | 1.63 | 10.37 | 0.34 | 0.41 | 11.82 | 28.00 |
| 10.00 | 0.00 | 0.99 | 0.00 | 0.00 | 0.18 | 44.10 | 297.92 | 26.54 | 1.66 | 11.37 | 0.44 | 0.34 | 13.33 | 26.40 |
| 35.00 | 0.00 | 1.03 | 0.00 | 6.00 | 0.17 | 113.26 | 229.04 | 18.49 | 0.99 | 8.79 | 0.30 | 0.26 | 1.67 | 42.20 |
| 18.00 | 0.00 | 1.04 | 39.78 | 6.00 | 0.17 | 91.66 | 241.85 | 13.41 | 0.91 | 9.39 | 0.26 | 0.20 | 5.85 | 28.20 |
| 35.00 | 0.00 | 1.30 | 0.00 | 0.00 | 0.22 | 95.64 | 216.80 | 23.33 | 1.06 | 8.39 | 2.51 | 0.03 | 9.06 | 42.50 |
| 35.00 | 0.00 | 1.14 | 39.96 | 6.00 | 0.19 | 108.04 | 235.56 | 16.09 | 0.63 | 9.32 | 1.19 | 0.03 | 4.00 | 29.70 |
| 27.00 | 0.00 | 1.03 | 0.00 | 0.00 | 0.17 | 109.63 | 226.99 | 20.13 | 0.98 | 8.63 | 0.30 | 0.27 | 7.40 | 47.00 |
| 17.00 | 0.00 | 1.25 | 39.77 | 0.00 | 0.20 | 79.97 | 226.11 | 19.92 | 1.02 | 8.84 | 1.98 | 0.03 | 3.55 | 36.20 |
| 36.01 | 0.00 | 1.49 | 12.96 | 6.00 | 0.27 | 92.17 | 214.62 | 12.24 | 1.42 | 8.06 | 3.83 | 0.03 | 6.95 | 41.70 |
| 30.00 | 0.00 | 1.48 | 26.03 | 0.00 | 0.25 | 92.42 | 213.61 | 18.78 | 1.30 | 8.08 | 3.77 | 0.03 | 4.84 | 45.40 |
| 35.00 | 0.00 | 1.47 | 39.88 | 4.00 | 0.25 | 95.26 | 212.38 | 12.29 | 1.29 | 8.06 | 3.70 | 0.03 | 7.50 | 42.60 |
| 35.02 | 66.86 | 1.26 | 39.83 | 6.00 | 16.42 | 96.01 | 239.53 | 5.16 | 1.35 | 9.66 | 0.27 | 0.24 | 8.16 | 27.90 |
| 35.00 | 69.50 | 1.41 | 0.00 | 6.00 | 16.02 | 84.90 | 233.64 | 7.86 | 1.31 | 10.24 | 0.56 | 0.12 | 8.52 | 31.50 |
| 27.00 | 25.00 | 1.23 | 19.89 | 3.00 | 10.33 | 91.73 | 222.43 | 10.32 | 1.06 | 8.62 | 1.91 | 0.03 | 8.42 | 33.70 |
| 30.00 | 50.83 | 1.22 | 20.02 | 3.00 | 15.98 | 83.46 | 227.65 | 6.45 | 1.31 | 9.06 | 1.92 | 0.03 | 11.82 | 32.50 |
| 19.00 | 35.50 | 1.22 | 0.00 | 0.00 | 13.69 | 68.60 | 236.00 | 8.11 | 1.55 | 9.33 | 2.04 | 0.03 | 12.57 | 27.70 |
| 27.00 | 24.33 | 1.23 | 19.95 | 3.00 | 10.77 | 89.33 | 222.60 | 10.17 | 1.07 | 8.61 | 1.93 | 0.03 | 7.19 | 35.30 |
| 35.00 | 35.67 | 1.31 | 39.90 | 0.00 | 11.15 | 89.34 | 225.77 | 5.56 | 1.22 | 8.98 | 2.53 | 0.03 | 5.74 | 33.30 |
| 36.00 | 35.00 | 1.04 | 0.00 | 0.00 | 11.60 | 97.48 | 231.16 | 12.13 | 1.07 | 9.35 | 0.32 | 0.24 | 8.20 | 34.00 |
| 17.00 | 33.83 | 1.01 | 0.00 | 6.00 | 15.62 | 66.35 | 259.84 | 3.45 | 1.38 | 10.13 | 0.30 | 0.27 | 7.45 | 24.00 |
| 23.00 | 0.00 | 1.37 | 0.00 | 6.00 | 0.23 | 79.92 | 224.41 | 19.20 | 1.28 | 8.64 | 3.22 | 0.03 | 3.41 | 35.30 |
| 17.00 | 29.14 | 1.10 | 20.13 | 3.00 | 14.64 | 73.64 | 232.05 | 12.86 | 1.18 | 9.31 | 0.94 | 0.02 | 3.75 | 31.00 |
| 35.00 | 0.00 | 1.01 | 39.91 | 0.00 | 0.24 | 120.16 | 238.99 | 17.49 | 0.94 | 9.26 | 0.25 | 0.22 | 7.28 | 33.50 |
| | | | | | | | | | | | | | | |
| 70.00 | 51.20 | 1.01 | 20.06 | 3.00 | 9.89 | 116.76 | 232.53 | 12.18 | 1.38 | 9.50 | 0.28 | 0.25 | 3.82 | 37.30 |
| 80.00 | 100.00 | 1.00 | 0.00 | 6.00 | 15.75 | 94.23 | 237.29 | 6.36 | 1.60 | 10.77 | 0.20 | 0.65 | 5.73 | 36.50 |
| 80.00 | 100.00 | 1.08 | 0.00 | 6.00 | 15.55 | 86.56 | 239.30 | 5.89 | 1.42 | 11.85 | 0.76 | 0.08 | 7.64 | 27.50 |
| 100.00 | 100.00 | 1.10 | 0.00 | 2.00 | 14.73 | 88.05 | 230.69 | 9.29 | 1.38 | 11.47 | 1.02 | 0.04 | 7.46 | 33.40 |
| 60.00 | 99.00 | 1.01 | 0.00 | 6.00 | 15.72 | 86.71 | 238.55 | 6.32 | 1.47 | 11.04 | 0.34 | 0.31 | 10.02 | 31.40 |
| 60.00 | 39.67 | 1.42 | 39.96 | 6.00 | 9.28 | 88.96 | 232.18 | 3.51 | 1.74 | 9.28 | 3.61 | 0.03 | 9.14 | 32.20 |
| 60.00 | 10.00 | 1.51 | 0.00 | 0.00 | 3.10 | 84.70 | 223.16 | 8.39 | 1.78 | 8.82 | 4.46 | 0.04 | 11.83 | 36.00 |
| 100.00 | 10.83 | 1.43 | 27.02 | 6.00 | 2.68 | 105.10 | 214.71 | 7.82 | 1.55 | 8.47 | 3.58 | 0.03 | 8.92 | 40.90 |
| 100.00 | 32.50 | 1.01 | 0.00 | 6.00 | 6.21 | 115.17 | 229.06 | 16.46 | 1.22 | 9.65 | 0.28 | 0.36 | 6.83 | 44.70 |
| 100.00 | 37.67 | 1.30 | 39.91 | 0.00 | 7.18 | 108.13 | 215.91 | 10.18 | 1.48 | 9.04 | 2.42 | 0.03 | 3.63 | 43.00 |
| 70.00 | 41.50 | 1.16 | 20.11 | 3.00 | 8.33 | 111.45 | 223.24 | 13.07 | 1.24 | 9.49 | 1.11 | 0.03 | 5.08 | 35.50 |
| 100.00 | 0.00 | 1.45 | 0.00 | 0.00 | 0.43 | 99.54 | 212.83 | 21.68 | 1.37 | 8.94 | 3.74 | 0.03 | 2.58 | 47.90 |
| 80.00 | 0.00 | 1.49 | 39.90 | 6.00 | 0.44 | 104.77 | 217.42 | 5.48 | 1.80 | 8.82 | 4.13 | 0.03 | 5.90 | 40.80 |
| 40.00 | 0.00 | 1.48 | 39.92 | 2.00 | 0.34 | 101.10 | 212.72 | 10.59 | 1.37 | 8.17 | 3.74 | 0.03 | 4.20 | 45.30 |
| 100.00 | 0.00 | 0.99 | 39.84 | 0.00 | 0.39 | 139.92 | 236.94 | 17.90 | 1.59 | 9.46 | 0.18 | 0.54 | 6.62 | 39.20 |
| 100.00 | 0.00 | 0.83 | 39.89 | 4.00 | 0.50 | 134.95 | 293.98 | 3.00 | 1.67 | 7.75 | 0.05 | 2.72 | 7.68 | 34.20 |
| 100.00 | 0.00 | 0.84 | 12.96 | 6.00 | 0.49 | 136.15 | 280.34 | 3.66 | 1.59 | 7.45 | 0.06 | 2.51 | 6.49 | 41.10 |
| 100.00 | 0.00 | 1.02 | 0.00 | 0.00 | 0.38 | 127.86 | 227.17 | 20.82 | 1.12 | 9.55 | 0.33 | 0.30 | 1.65 | 48.70 |
| 100.00 | 0.00 | 1.24 | 0.00 | 6.00 | 0.40 | 110.91 | 219.58 | 21.52 | 0.92 | 9.51 | 1.99 | 0.04 | 3.36 | 37.40 |
| 100.00 | 0.00 | 0.99 | 12.91 | 6.00 | 0.38 | 133.58 | 238.64 | 17.46 | 1.36 | 9.63 | 0.17 | 0.48 | 7.22 | 37.60 |
| 100.00 | 0.00 | 1.02 | 39.88 | 4.00 | 0.38 | 127.75 | 248.66 | 19.26 | 1.58 | 10.69 | 0.29 | 0.29 | 3.61 | 29.00 |
| 40.00 | 0.00 | 1.16 | 39.97 | 6.00 | 0.26 | 114.52 | 231.95 | 16.40 | 0.71 | 9.14 | 1.40 | 0.04 | 8.26 | 30.10 |
| 40.00 | 0.00 | 1.01 | 39.94 | 0.00 | 0.24 | 129.83 | 230.21 | 18.91 | 1.11 | 8.90 | 0.26 | 0.22 | 2.69 | 40.20 |
| 40.00 | 0.00 | 1.01 | 27.03 | 6.00 | 0.31 | 126.27 | 237.85 | 17.82 | 1.12 | 9.17 | 0.26 | 0.24 | 5.69 | 36.60 |
| 40.00 | 0.00 | 1.48 | 27.10 | 0.00 | 0.35 | 100.83 | 210.39 | 15.42 | 1.34 | 8.00 | 3.84 | 0.03 | 8.38 | 46.60 |
| 40.00 | 0.00 | 1.53 | 0.00 | 6.00 | 0.36 | 83.85 | 225.27 | 9.31 | 1.74 | 8.48 | 4.57 | 0.04 | 9.68 | 36.90 |
| 40.00 | 0.00 | 1.02 | 0.00 | 4.00 | 0.24 | 117.32 | 232.43 | 18.93 | 0.97 | 8.97 | 0.30 | 0.26 | 7.42 | 40.40 |
| 70.00 | 42.83 | 1.23 | 19.99 | 3.00 | 8.60 | 103.31 | 225.15 | 10.63 | 1.19 | 9.21 | 2.03 | 0.03 | 3.02 | 39.50 |
| 40.00 | 68.63 | 1.12 | 0.00 | 0.00 | 16.06 | 86.36 | 226.25 | 12.99 | 1.24 | 10.00 | 1.05 | 0.03 | 9.46 | 34.90 |
| 40.00 | 100.00 | 1.01 | 0.00 | 0.00 | 20.02 | 85.43 | 235.54 | 7.37 | 1.52 | 10.32 | 0.38 | 0.29 | 6.20 | 36.60 |
| 40.00 | 98.00 | 1.05 | 12.98 | 6.00 | 20.27 | 87.00 | 240.19 | 5.08 | 1.38 | 10.18 | 0.49 | 0.13 | 5.37 | 29.70 |
| 40.00 | 96.00 | 1.03 | 39.88 | 4.00 | 20.64 | 85.86 | 253.75 | 3.69 | 1.35 | 10.36 | 0.34 | 0.25 | 12.99 | 24.70 |
| 70.00 | 41.33 | 1.16 | 20.04 | 3.00 | 8.92 | 103.93 | 229.01 | 12.71 | 0.99 | 9.65 | 1.30 | 0.03 | 6.68 | 31.70 |
| 100.00 | 100.00 | 1.00 | 13.03 | 0.00 | 16.20 | 102.21 | 233.89 | 7.47 | 1.47 | 10.20 | 0.17 | 0.44 | 4.36 | 38.20 |
| 100.00 | 100.00 | 1.03 | 39.93 | 6.00 | 16.73 | 88.60 | 264.63 | 3.53 | 1.33 | 11.70 | 0.34 | 0.22 | 8.12 | 23.30 |
| 80.00 | 98.00 | 1.04 | 39.98 | 0.00 | 16.63 | 97.68 | 238.01 | 7.23 | 1.25 | 10.47 | 0.39 | 0.16 | 6.46 | 30.10 |
| 60.00 | 96.50 | 1.07 | 39.90 | 0.00 | 16.91 | 94.22 | 235.88 | 7.29 | 1.19 | 10.27 | 0.70 | 0.06 | 9.21 | 29.90 |

**Table B- 8 DoE test program for 2400 rev/min**

| Throttle pos | EGR demand | Fuelling rate | Cam overlap | Spark timing | EGR flow | Torque | BSFC | BSNOx | BSuHC | BSCO2 | BSO2 | BSCO | COVimep | Comb pres |
|---|---|---|---|---|---|---|---|---|---|---|---|---|---|---|
| % | % | Lambda | degree | degree | % | Nm | g/kwhr | g/kWhr | g/kWhr | kg/kWhr | kg/kWhr | kg/kWhr | % | bar |
| 18.00 | 100.00 | 1.02 | 0.00 | 6.00 | 11.47 | 83.54 | 240.64 | 5.51 | -0.05 | 9.49 | 0.25 | 0.23 | 11.44 | 31.50 |
| 18.03 | 100.00 | 1.22 | 0.00 | 2.00 | 12.42 | 72.61 | 231.69 | 8.36 | -0.06 | 9.23 | 1.96 | 0.03 | 11.27 | 33.00 |
| 18.00 | 100.00 | 1.23 | 0.00 | 0.00 | 12.58 | 72.26 | 232.43 | 11.95 | -0.06 | 9.22 | 1.98 | 0.03 | 12.83 | 29.60 |
| 24.00 | 0.00 | 1.17 | 0.00 | 3.00 | 11.08 | 84.54 | 228.20 | 11.77 | -0.06 | 9.14 | 1.49 | 0.03 | 11.04 | 31.60 |
| 24.00 | 30.00 | 1.02 | 39.69 | 0.00 | 19.61 | 72.11 | 240.69 | 4.65 | -0.06 | 9.64 | 0.32 | 0.30 | 16.06 | 28.80 |
| 30.00 | 30.00 | 1.01 | 39.69 | 6.00 | 16.37 | 80.64 | 241.85 | 4.79 | -0.06 | 9.85 | 0.31 | 0.34 | 12.93 | 26.00 |
| 30.00 | 30.00 | 1.02 | 39.69 | 6.00 | 21.43 | 77.96 | 247.95 | 3.83 | -0.06 | 9.92 | 0.32 | 0.30 | 13.08 | 28.20 |
| 30.00 | 29.78 | 1.02 | 39.67 | 0.00 | 0.24 | 111.36 | 227.78 | 20.82 | -0.05 | 8.84 | 0.34 | 0.29 | 8.27 | 45.10 |
| 30.00 | 35.94 | 1.50 | 39.67 | 2.00 | 0.34 | 84.80 | 220.71 | 17.78 | -0.07 | 8.41 | 4.07 | 0.04 | 11.23 | 37.30 |
| 30.00 | 29.19 | 1.49 | 39.67 | 0.00 | 0.34 | 93.54 | 216.40 | 16.76 | -0.07 | 8.29 | 3.91 | 0.03 | 10.70 | 39.00 |
| 30.00 | 36.44 | 1.18 | 39.67 | 0.00 | 16.51 | 79.47 | 211.10 | 6.84 | -0.06 | 9.80 | 0.83 | 0.06 | 0.00 | 29.13 |
| 13.00 | 30.00 | 1.19 | 12.98 | 6.00 | 0.27 | 51.85 | 261.29 | 15.61 | -0.07 | 10.43 | 1.84 | 0.04 | 16.92 | 24.90 |
| 22.00 | 36.00 | 1.41 | 12.98 | 0.00 | 0.32 | 81.35 | 224.11 | 15.29 | -0.07 | 8.63 | 3.38 | 0.03 | 11.25 | 37.20 |
| 22.00 | 36.00 | 1.41 | 12.98 | 3.00 | 0.32 | 83.50 | 223.38 | 21.32 | -0.07 | 8.56 | 3.40 | 0.03 | 11.34 | 33.80 |
| 30.00 | 36.00 | 1.02 | 12.98 | 6.00 | 0.24 | 107.21 | 255.63 | 13.18 | -0.06 | 9.90 | 0.29 | 0.28 | 9.96 | 26.20 |
| 30.00 | 30.00 | 1.52 | 12.98 | 4.00 | 0.36 | 89.97 | 217.60 | 11.67 | -0.07 | 8.31 | 4.21 | 0.03 | 10.84 | 41.00 |
| 13.00 | 28.00 | 1.02 | 20.03 | 6.00 | 0.24 | 58.16 | 266.07 | 22.74 | -0.06 | 10.28 | 0.39 | 0.32 | 14.73 | 30.00 |
| 24.50 | 28.00 | 1.14 | 20.03 | 0.00 | 0.24 | 99.18 | 212.59 | 18.90 | -0.05 | 8.17 | 0.31 | 0.26 | 9.48 | 41.90 |
| 30.00 | 71.00 | 1.28 | 0.00 | 6.00 | 10.84 | 90.52 | 225.59 | 6.17 | -0.06 | 8.67 | 2.41 | 0.03 | 11.15 | 33.90 |
| 30.00 | 61.00 | 1.02 | 0.00 | 4.00 | 10.31 | 103.86 | 236.05 | 9.83 | -0.05 | 9.32 | 0.30 | 0.21 | 8.78 | 32.50 |
| 30.00 | 61.00 | 1.02 | 0.00 | 4.00 | 10.53 | 106.05 | 229.50 | 12.20 | -0.05 | 9.06 | 0.29 | 0.22 | 8.76 | 32.50 |
| 30.00 | 72.00 | 1.02 | 0.00 | 4.00 | 21.77 | 81.38 | 242.13 | 3.71 | -0.06 | 9.74 | 0.30 | 0.28 | 13.61 | 28.90 |
| 30.00 | 60.00 | 1.02 | 0.00 | 0.00 | 21.64 | 81.25 | 242.87 | 4.83 | -0.06 | 9.71 | 0.30 | 0.26 | 11.76 | 30.10 |
| 28.00 | 60.00 | 1.02 | 0.00 | 2.00 | 20.15 | 70.98 | 252.46 | 3.85 | -0.06 | 10.38 | 0.36 | 0.34 | 13.20 | 26.70 |
| 30.00 | 71.00 | 1.09 | 0.00 | 0.00 | 16.43 | 80.60 | 232.24 | 8.49 | -0.06 | 9.68 | 0.82 | 0.05 | 11.86 | 29.10 |
| 30.00 | 0.00 | 1.34 | 0.00 | 6.00 | 0.30 | 93.44 | 221.84 | 20.38 | -0.06 | 8.56 | 2.78 | 0.03 | 9.38 | 39.10 |
| 30.00 | 0.00 | 1.15 | 0.00 | 0.00 | 0.26 | 111.04 | 224.01 | 21.73 | -0.06 | 8.67 | 1.26 | 0.03 | 8.43 | 38.20 |
| 25.00 | 0.00 | 1.06 | 0.00 | 6.00 | 19.36 | 81.75 | 242.27 | 4.05 | -0.06 | 9.80 | 0.54 | 0.08 | 11.98 | 29.20 |
| 25.00 | 0.00 | 1.17 | 0.00 | 3.00 | 11.04 | 91.68 | 230.36 | 11.03 | -0.06 | 9.18 | 1.44 | 0.03 | 10.56 | 29.20 |
| 18.00 | 0.00 | 1.24 | 0.00 | 6.00 | 12.00 | 69.26 | 235.44 | 10.98 | -0.06 | 9.24 | 2.12 | 0.03 | 14.20 | 31.60 |
| 25.00 | 0.00 | 1.02 | 0.00 | 3.00 | 15.59 | 87.10 | 241.18 | 7.91 | -0.05 | 9.37 | 0.27 | 0.26 | 12.95 | 31.10 |
| 20.00 | 0.00 | 1.02 | 0.00 | 0.00 | 0.24 | 98.61 | 239.95 | 17.69 | -0.05 | 9.24 | 0.30 | 0.24 | 9.89 | 34.90 |
| | | | | | | | | | | | | | | |
| 35.00 | 0.00 | 1.01 | 0.00 | 6.00 | 0.17 | 118.13 | 235.03 | 18.55 | 1.03 | 8.90 | 0.29 | 0.22 | 8.11 | 39.90 |
| 35.00 | 0.00 | 1.44 | 0.00 | 0.00 | 0.24 | 89.82 | 221.18 | 17.22 | 1.32 | 8.36 | 3.76 | 0.03 | 11.50 | 36.60 |
| 35.00 | 0.00 | 1.47 | 12.93 | 6.00 | 0.25 | 95.18 | 215.45 | 16.77 | 1.40 | 8.14 | 3.93 | 0.03 | 10.14 | 41.70 |
| 57.00 | 0.00 | 1.46 | 39.83 | 0.00 | 0.35 | 105.70 | 211.34 | 15.78 | 1.28 | 8.01 | 3.78 | 0.02 | 10.06 | 44.10 |
| 100.00 | 0.00 | 1.41 | 39.81 | 6.00 | 0.43 | 105.99 | 221.36 | 7.28 | 1.46 | 8.70 | 3.68 | 0.03 | 10.38 | 35.40 |
| 100.00 | 0.00 | 1.00 | 39.73 | 6.00 | 0.38 | 123.50 | 257.48 | 16.60 | 1.37 | 10.18 | 0.25 | 0.32 | 8.76 | 27.40 |
| 100.00 | 41.50 | 1.26 | 39.89 | 0.00 | 7.97 | 105.68 | 219.06 | 10.88 | 1.19 | 8.94 | 2.37 | 0.03 | 8.70 | 40.60 |
| 67.00 | 42.75 | 1.17 | 20.07 | 3.00 | 9.52 | 106.86 | 222.90 | 11.97 | 1.07 | 9.09 | 1.60 | 0.03 | 9.32 | 35.30 |
| 35.00 | 70.00 | 1.14 | 0.00 | 0.00 | 16.17 | 82.71 | 229.78 | 10.74 | 1.17 | 9.60 | 1.36 | 0.03 | 11.32 | 33.70 |
| 100.00 | 66.14 | 0.99 | 39.79 | 0.00 | 12.69 | 110.69 | 236.36 | 8.83 | 1.37 | 9.62 | 0.20 | 0.32 | 8.60 | 36.00 |
| 78.00 | 100.00 | 1.01 | 39.80 | 0.00 | 18.43 | 99.45 | 235.35 | 7.47 | 1.26 | 10.04 | 0.32 | 0.23 | 9.31 | 34.30 |
| 100.00 | 100.00 | 1.10 | 39.83 | 4.00 | 17.30 | 89.68 | 243.27 | 5.15 | 1.16 | 10.57 | 1.11 | 0.04 | 10.89 | 30.10 |
| 100.00 | 100.00 | 1.00 | 27.05 | 6.00 | 17.68 | 92.29 | 253.46 | 4.41 | 1.25 | 10.74 | 0.29 | 0.28 | 11.66 | 26.80 |
| 100.00 | 100.00 | 1.01 | 0.00 | 0.00 | 17.16 | 89.68 | 239.04 | 7.17 | 1.25 | 10.76 | 0.35 | 0.22 | 10.01 | 33.20 |
| 78.00 | 100.00 | 1.11 | 0.00 | 6.00 | 17.39 | 81.75 | 242.56 | 5.79 | 1.23 | 11.00 | 1.29 | 0.03 | 11.77 | 29.60 |
| 35.00 | 99.00 | 1.13 | 26.98 | 0.00 | 20.52 | 82.74 | 233.77 | 4.92 | 1.20 | 9.50 | 1.29 | 0.03 | 12.74 | 31.00 |
| 35.00 | 39.89 | 1.34 | 39.88 | 6.00 | 11.95 | 82.49 | 238.66 | 2.69 | 1.61 | 9.16 | 3.25 | 0.03 | 13.26 | 30.50 |
| 67.00 | 43.40 | 1.17 | 20.07 | 3.00 | 9.35 | 105.04 | 225.26 | 11.59 | 0.91 | 9.17 | 1.60 | 0.03 | 9.48 | 34.70 |
| 100.00 | 34.00 | 1.01 | 0.00 | 6.00 | 7.28 | 111.19 | 242.12 | 12.58 | 1.05 | 9.78 | 0.29 | 0.28 | 8.62 | 34.00 |
| 35.00 | 32.78 | 0.99 | 0.00 | 0.00 | 10.36 | 107.96 | 229.77 | 14.73 | 1.05 | 8.80 | 0.21 | 0.36 | 8.45 | 46.10 |
| 35.00 | 19.00 | 1.40 | 39.83 | 2.00 | 6.75 | 95.10 | 217.34 | 12.17 | 1.23 | 8.29 | 3.37 | 0.02 | 10.45 | 39.90 |
| 57.00 | 15.88 | 1.36 | 0.00 | 6.00 | 4.82 | 94.74 | 219.12 | 20.11 | 1.13 | 8.43 | 3.10 | 0.02 | 10.91 | 42.30 |
| 100.00 | 9.60 | 1.38 | 0.00 | 2.00 | 3.31 | 99.43 | 215.33 | 20.01 | 1.17 | 8.44 | 3.26 | 0.03 | 9.69 | 43.10 |
| 100.00 | 11.33 | 1.42 | 12.93 | 0.00 | 3.48 | 103.76 | 212.99 | 20.89 | 1.15 | 8.30 | 3.55 | 0.02 | 8.96 | 51.70 |
| 68.00 | 43.00 | 1.18 | 20.06 | 3.00 | 9.45 | 106.95 | 223.68 | 13.25 | 1.02 | 9.05 | 1.65 | 0.03 | 8.60 | 37.00 |
| 35.00 | 100.00 | 1.00 | 39.66 | 6.00 | 21.84 | 87.21 | 248.79 | 4.30 | 1.26 | 9.89 | 0.29 | 0.27 | 12.30 | 29.30 |
| 35.00 | 100.00 | 1.01 | 0.00 | 4.00 | 21.44 | 80.57 | 241.23 | 5.68 | 1.31 | 10.21 | 0.37 | 0.28 | 11.66 | 29.70 |
| 100.00 | 0.00 | 1.12 | 39.72 | 0.00 | 0.41 | 129.71 | 222.91 | 24.64 | 1.06 | 9.09 | 1.17 | 0.04 | 7.10 | 43.20 |
| 35.00 | 0.00 | 1.17 | 39.72 | 6.00 | 0.27 | 108.04 | 239.53 | 12.91 | 0.60 | 9.33 | 1.63 | 0.04 | 9.42 | 28.20 |
| 35.00 | 0.00 | 1.01 | 39.67 | 0.00 | 0.24 | 124.17 | 236.29 | 17.93 | 0.87 | 9.00 | 0.26 | 0.24 | 8.14 | 39.20 |
| 100.00 | 0.00 | 1.26 | 0.00 | 6.00 | 0.38 | 106.27 | 227.57 | 15.46 | 0.72 | 9.24 | 2.37 | 0.04 | 9.34 | 33.80 |
| 67.00 | 0.00 | 1.20 | 19.97 | 3.00 | 0.36 | 122.64 | 221.59 | 21.78 | 0.83 | 8.77 | 1.77 | 0.03 | 7.94 | 40.80 |
| 67.00 | 47.80 | 1.01 | 20.00 | 3.00 | 10.77 | 118.80 | 229.82 | 12.11 | 1.20 | 9.16 | 0.27 | 0.23 | 8.01 | 36.50 |
| 67.00 | 42.20 | 1.22 | 20.03 | 3.00 | 9.07 | 104.36 | 220.47 | 10.94 | 1.05 | 8.91 | 2.03 | 0.03 | 9.14 | 36.60 |

**Table B- 9 DoE test program for 2600 rev/min**

| Throttle pos | EGR demand | Fuelling rate | Cam overlap | Spark timing | EGR flow | Torque | BSFC | BSNOx | BSuHC | BSCO2 | BSO2 | BSCO | COVimep | Comb pres |
|---|---|---|---|---|---|---|---|---|---|---|---|---|---|---|
| % | % | Lambda | degree | degree | % | Nm | g/kwhr | g/kWhr | g/kWhr | kg/kWhr | kg/kWhr | kg/kWhr | % | bar |
| 40.00 | 33.67 | 1.01 | 39.46 | 6.00 | 8.12 | 112.98 | 243.10 | 10.77 | 1.26 | 9.32 | 0.27 | 0.19 | 2.98 | 40.80 |
| 40.00 | 100.00 | 1.00 | 39.41 | 6.00 | 17.74 | 89.67 | 246.03 | 5.01 | 1.32 | 9.62 | 0.26 | 0.30 | 7.67 | 27.90 |
| 40.00 | 100.00 | 1.00 | 0.00 | 2.00 | 17.30 | 82.27 | 239.04 | 7.72 | 1.21 | 9.65 | 0.29 | 0.29 | 4.08 | 33.20 |
| 35.00 | 100.00 | 1.13 | 12.98 | 6.00 | 18.91 | 73.24 | 246.53 | 3.88 | 1.40 | 10.01 | 1.36 | 0.03 | 5.88 | 29.40 |
| 35.00 | 100.00 | 1.14 | 39.57 | 2.00 | 18.98 | 74.36 | 246.32 | 3.49 | 1.42 | 9.84 | 1.49 | 0.03 | 10.25 | 27.20 |
| 35.00 | 100.00 | 1.10 | 0.00 | 0.00 | 17.98 | 73.21 | 237.52 | 8.15 | 1.26 | 9.93 | 1.05 | 0.03 | 9.67 | 28.60 |
| 10.00 | 0.00 | 1.23 | 0.00 | 6.00 | 0.21 | 35.90 | 304.42 | 16.68 | 1.40 | 11.72 | 2.82 | 0.06 | 5.51 | 20.40 |
| 10.00 | 0.00 | 1.19 | 39.56 | 0.00 | 0.20 | 38.23 | 283.20 | 17.81 | 1.41 | 11.35 | 2.27 | 0.04 | 6.40 | 21.60 |
| 26.00 | 0.00 | 1.21 | 20.03 | 3.00 | 0.27 | 94.38 | 224.36 | 28.63 | 0.84 | 8.62 | 1.80 | 0.02 | 0.86 | 46.30 |
| 28.00 | 33.50 | 1.20 | 20.07 | 3.00 | 11.73 | 88.41 | 223.93 | 19.23 | 0.95 | 8.64 | 1.76 | 0.02 | 2.39 | 41.80 |
| 40.00 | 70.00 | 1.19 | 39.58 | 0.00 | 16.79 | 87.24 | 227.56 | 8.90 | 1.07 | 8.88 | 1.69 | 0.02 | 5.08 | 37.30 |
| 22.00 | 48.00 | 1.13 | 19.94 | 3.00 | 15.70 | 72.48 | 236.59 | 11.24 | 1.16 | 9.20 | 1.24 | 0.02 | 5.73 | 32.70 |
| 22.00 | 35.00 | 1.29 | 26.01 | 6.00 | 12.56 | 63.89 | 249.44 | 4.57 | 1.76 | 9.38 | 2.66 | 0.03 | 10.95 | 28.10 |
| 22.00 | 35.00 | 1.28 | 0.00 | 6.00 | 12.54 | 60.49 | 249.61 | 4.34 | 1.98 | 9.40 | 2.83 | 0.03 | 7.62 | 27.70 |
| 28.00 | 34.63 | 1.21 | 19.97 | 3.00 | 11.83 | 85.23 | 227.11 | 13.78 | 0.96 | 8.73 | 1.82 | 0.02 | 3.48 | 35.30 |
| 40.00 | 71.43 | 1.14 | 0.00 | 6.00 | 16.18 | 77.74 | 237.27 | 8.11 | 1.11 | 9.65 | 1.43 | 0.03 | 4.57 | 31.00 |
| 27.00 | 67.71 | 1.00 | 39.53 | 0.00 | 16.76 | 82.86 | 242.16 | 6.54 | 1.10 | 9.23 | 0.24 | 0.28 | 4.27 | 29.70 |
| 27.00 | 66.57 | 1.00 | 0.00 | 6.00 | 17.04 | 73.91 | 253.40 | 6.40 | 1.16 | 9.78 | 0.26 | 0.30 | 5.47 | 27.80 |
| 27.00 | 34.33 | 1.20 | 19.98 | 3.00 | 11.92 | 83.08 | 229.08 | 11.72 | 0.91 | 8.84 | 1.79 | 0.03 | 5.12 | 34.10 |
| 40.00 | 0.00 | 1.00 | 39.59 | 4.00 | 0.24 | 120.71 | 239.48 | 16.89 | 0.91 | 9.04 | 0.23 | 0.23 | 3.51 | 36.80 |
| 40.00 | 0.00 | 1.33 | 39.59 | 6.00 | 0.31 | 104.14 | 215.01 | 18.27 | 0.93 | 8.17 | 2.71 | 0.03 | 1.92 | 43.90 |
| 39.98 | 34.88 | 1.01 | 0.00 | 0.00 | 9.10 | 104.36 | 225.55 | 17.98 | 0.89 | 8.71 | 0.27 | 0.19 | 1.33 | 48.14 |
| 36.00 | 100.00 | 1.00 | 0.00 | 0.00 | 18.51 | 80.06 | 238.88 | 7.95 | 1.17 | 9.67 | 0.26 | 0.28 | 2.75 | 32.80 |
| 40.00 | 100.00 | 1.00 | 27.01 | 0.00 | 18.42 | 88.94 | 239.39 | 7.33 | 1.09 | 9.23 | 0.26 | 0.32 | 5.25 | 31.60 |
| 30.00 | 0.00 | 1.49 | 0.00 | 2.00 | 0.36 | 72.75 | 237.03 | 4.86 | 1.69 | 8.74 | 4.44 | 0.03 | 6.67 | 28.10 |
| 40.00 | 0.00 | 1.50 | 12.95 | 0.00 | 0.36 | 90.12 | 218.83 | 9.73 | 1.33 | 8.05 | 4.11 | 0.03 | 2.15 | 41.70 |
| 40.00 | 11.00 | 1.44 | 39.61 | 0.00 | 4.81 | 89.94 | 223.43 | 6.30 | 1.54 | 8.32 | 3.80 | 0.03 | 7.89 | 38.70 |
| 40.00 | 10.00 | 1.46 | 0.00 | 6.00 | 3.75 | 78.58 | 231.52 | 6.65 | 1.53 | 8.51 | 4.03 | 0.03 | 7.81 | 33.60 |
| 22.00 | 34.00 | 1.29 | 39.38 | 4.00 | 12.60 | 63.67 | 254.70 | 2.76 | 2.02 | 9.51 | 2.94 | 0.03 | 10.88 | 27.70 |
| 22.00 | 0.00 | 1.16 | 0.00 | 0.00 | 0.27 | 82.50 | 230.31 | 25.59 | 0.74 | 8.91 | 1.40 | 0.02 | 4.28 | 36.30 |
| 13.00 | 0.00 | 1.01 | 13.01 | 0.00 | 0.24 | 45.42 | 293.43 | 26.14 | 1.31 | 11.12 | 0.36 | 0.28 | 5.35 | 26.10 |
| 13.00 | 0.00 | 1.01 | 0.00 | 0.00 | 0.24 | 45.53 | 292.00 | 23.94 | 1.32 | 11.06 | 0.34 | 0.26 | 5.19 | 25.70 |
| 20.00 | 0.00 | 1.01 | 39.51 | 0.00 | 0.24 | 85.03 | 240.90 | 19.92 | 0.89 | 9.05 | 0.24 | 0.23 | 2.02 | 39.30 |
| 40.00 | 0.00 | 1.16 | 0.00 | 0.00 | 0.27 | 103.09 | 220.33 | 27.52 | 0.69 | 8.44 | 1.39 | 0.02 | 1.06 | 48.40 |
| 10.00 | 0.00 | 1.01 | 39.50 | 6.00 | 0.17 | 43.46 | 299.38 | 8.51 | 1.19 | 11.72 | 0.29 | 0.25 | 11.01 | 20.10 |
| 20.00 | 0.00 | 1.01 | 0.00 | 0.00 | 0.17 | 84.51 | 239.76 | 17.69 | 0.95 | 9.15 | 0.23 | 0.22 | 4.26 | 37.30 |
| 20.00 | 0.00 | 1.01 | 0.00 | 6.00 | 0.17 | 81.01 | 250.11 | 18.22 | 0.96 | 9.51 | 0.26 | 0.23 | 1.58 | 32.10 |
| 40.00 | 0.00 | 1.01 | 0.00 | 6.00 | 0.24 | 110.76 | 237.64 | 18.70 | 0.81 | 8.87 | 0.23 | 0.22 | 3.06 | 39.20 |
| 40.00 | 0.00 | 1.00 | 39.59 | 0.00 | 0.24 | 122.92 | 233.47 | 18.93 | 0.92 | 8.86 | 0.22 | 0.23 | 2.26 | 41.20 |
| | | | | | | | | | | | | | | |
| 45.00 | 0.00 | 0.99 | 39.48 | 0.00 | 0.31 | 133.49 | 229.16 | 17.88 | 1.07 | 8.53 | 0.15 | 0.30 | 2.40 | 48.30 |
| 45.00 | 0.00 | 1.16 | 39.53 | 6.00 | 0.35 | 119.88 | 221.08 | 22.21 | 0.87 | 8.51 | 1.40 | 0.03 | 2.46 | 42.20 |
| 45.00 | 0.00 | 1.01 | 39.56 | 0.00 | 0.31 | 130.64 | 226.59 | 20.14 | 0.90 | 8.70 | 0.25 | 0.15 | 3.27 | 43.80 |
| 45.00 | 67.00 | 1.01 | 39.57 | 6.00 | 14.43 | 91.92 | 260.65 | 6.41 | 1.09 | 10.07 | 0.28 | 0.20 | 7.35 | 24.30 |
| 45.00 | 0.00 | 1.03 | 39.49 | 0.00 | 0.24 | 128.02 | 229.23 | 21.49 | 0.84 | 8.84 | 0.32 | 0.09 | 1.63 | 44.70 |
| 45.00 | 0.00 | 1.02 | 0.00 | 6.00 | 0.24 | 113.92 | 236.92 | 19.57 | 0.73 | 9.04 | 0.27 | 0.14 | 2.99 | 39.70 |
| 45.00 | 0.00 | 1.16 | 0.00 | 0.00 | 0.27 | 107.32 | 218.56 | 28.47 | 0.68 | 8.49 | 1.35 | 0.02 | 1.56 | 50.80 |
| 100.00 | 0.00 | 1.02 | 39.53 | 6.00 | 0.37 | 126.23 | 240.19 | 19.00 | 0.98 | 9.45 | 0.31 | 0.14 | 3.07 | 34.60 |
| 100.00 | 100.00 | 1.00 | 39.47 | 6.00 | 15.37 | 103.04 | 232.90 | 10.17 | 1.13 | 9.33 | 0.23 | 0.22 | 2.34 | 36.40 |
| 100.00 | 100.00 | 1.00 | 27.29 | 0.00 | 15.18 | 101.96 | 234.69 | 9.87 | 1.12 | 9.45 | 0.24 | 0.23 | 2.74 | 37.50 |
| 82.00 | 100.00 | 1.01 | 0.00 | 6.00 | 16.07 | 87.37 | 243.76 | 7.12 | 1.02 | 10.39 | 0.29 | 0.20 | 5.99 | 28.20 |
| 100.00 | 100.00 | 1.11 | 0.00 | 2.00 | 14.41 | 84.49 | 233.56 | 10.04 | 0.97 | 10.08 | 1.10 | 0.03 | 5.64 | 31.30 |
| 45.00 | 100.00 | 1.18 | 27.20 | 6.00 | 16.84 | 78.91 | 245.29 | 3.52 | 1.24 | 9.81 | 1.86 | 0.03 | 8.58 | 27.50 |
| 45.00 | 100.00 | 1.00 | 0.00 | 0.00 | 17.33 | 84.42 | 242.69 | 8.21 | 1.08 | 10.01 | 0.24 | 0.28 | 5.00 | 30.20 |
| 63.00 | 100.00 | 1.11 | 39.54 | 0.00 | 16.95 | 88.12 | 239.76 | 7.02 | 1.00 | 9.86 | 1.15 | 0.03 | 6.17 | 29.30 |
| 72.00 | 48.63 | 1.01 | 20.38 | 3.00 | 10.00 | 115.36 | 232.61 | 13.90 | 0.98 | 9.03 | 0.23 | 0.22 | 2.29 | 39.20 |
| 72.00 | 42.57 | 1.22 | 20.18 | 3.00 | 8.33 | 103.66 | 221.83 | 12.72 | 0.89 | 8.66 | 1.89 | 0.02 | 2.80 | 38.40 |
| 45.00 | 68.70 | 1.16 | 0.00 | 6.00 | 14.59 | 81.83 | 235.10 | 8.69 | 0.98 | 9.64 | 1.56 | 0.03 | 8.69 | 31.40 |
| 73.00 | 42.44 | 1.21 | 20.40 | 3.00 | 8.62 | 98.52 | 230.57 | 9.76 | 0.84 | 8.99 | 1.93 | 0.03 | 5.07 | 34.80 |
| 100.00 | 43.08 | 1.29 | 0.00 | 0.00 | 9.51 | 88.29 | 222.52 | 16.30 | 0.99 | 9.02 | 2.64 | 0.03 | 3.72 | 36.90 |
| 73.00 | 41.57 | 1.25 | 18.74 | 3.00 | 8.55 | 99.61 | 223.66 | 11.23 | 0.92 | 8.71 | 2.22 | 0.03 | 5.54 | 38.20 |
| 100.00 | 10.13 | 1.47 | 13.23 | 6.00 | 3.44 | 94.11 | 219.06 | 8.74 | 1.36 | 8.29 | 3.98 | 0.03 | 5.07 | 40.80 |
| 45.00 | 0.00 | 1.50 | 13.40 | 0.00 | 0.35 | 94.17 | 217.88 | 9.74 | 1.40 | 8.11 | 4.12 | 0.03 | 6.81 | 42.10 |
| 100.00 | 0.00 | 1.48 | 39.46 | 0.00 | 0.45 | 101.83 | 214.67 | 9.02 | 1.46 | 8.04 | 4.00 | 0.03 | 5.26 | 42.40 |
| 100.00 | 0.00 | 1.45 | 0.00 | 6.00 | 0.34 | 90.92 | 219.11 | 16.47 | 1.19 | 8.48 | 3.85 | 0.02 | 2.80 | 42.60 |
| 72.00 | 0.00 | 1.27 | 20.37 | 3.00 | 0.38 | 115.65 | 215.82 | 24.36 | 0.91 | 8.27 | 2.24 | 0.02 | 1.16 | 47.60 |
| 100.00 | 0.00 | 1.01 | 0.00 | 0.00 | 0.31 | 122.45 | 226.68 | 21.93 | 0.75 | 8.93 | 0.25 | 0.18 | 0.88 | 47.40 |
| 45.00 | 0.00 | 1.34 | 0.00 | 6.00 | 0.31 | 95.43 | 218.37 | 20.97 | 0.91 | 8.25 | 2.82 | 0.03 | 1.88 | 43.00 |
| 100.00 | 34.14 | 1.04 | 39.55 | 0.00 | 7.36 | 123.79 | 225.00 | 20.30 | 0.90 | 8.84 | 0.45 | 0.07 | 2.85 | 44.50 |
| 100.00 | 36.00 | 1.00 | 0.00 | 6.00 | 7.62 | 110.31 | 234.92 | 16.19 | 0.89 | 9.35 | 0.22 | 0.24 | 1.47 | 40.80 |
| 64.00 | 17.22 | 1.44 | 39.53 | 6.00 | 3.57 | 98.43 | 215.87 | 12.79 | 1.20 | 8.11 | 3.66 | 0.03 | 4.94 | 42.80 |
| 45.00 | 18.00 | 1.43 | 0.00 | 4.00 | 5.14 | 83.52 | 225.20 | 10.26 | 1.24 | 8.46 | 3.68 | 0.03 | 3.40 | 37.90 |
| 82.00 | 15.29 | 1.39 | 0.00 | 0.00 | 3.32 | 91.41 | 217.79 | 19.54 | 1.05 | 8.52 | 3.38 | 0.02 | 3.77 | 43.20 |
| 45.00 | 40.09 | 1.36 | 39.53 | 0.00 | 10.17 | 93.90 | 219.00 | 11.02 | 1.13 | 8.29 | 3.04 | 0.02 | 4.80 | 42.40 |

**Table B- 10 DoE test program for 3000 rev/min**

# C. APPENDIX C

Regression CoefficientsFifth order regression coefficients

| Torque | ENGINE SPEED (rev/min) | | | | | | | | | |
|---|---|---|---|---|---|---|---|---|---|---|
| COEFFICIENTS | 1200 | 1400 | 1500 | 1700 | 1800 | 2000 | 2200 | 2400 | 2600 | 3000 |
| const | 1.133E+02 | -4.951E+01 | 9.549E+01 | 1.947E+02 | 6.496E+01 | 6.240E+01 | -6.907E+01 | 6.162E+00 | -1.028E+01 | -7.436E+01 |
| Throt; | 3.939E+00 | 6.060E+00 | 4.463E+00 | 3.087E+00 | 1.168E+01 | 1.026E+01 | 1.144E+01 | 8.867E+00 | 8.339E+00 | 9.416E+00 |
| Throt^2; | -1.188E-01 | -2.325E-01 | -1.327E-01 | -1.894E-01 | -4.073E-01 | -3.436E-01 | -4.340E-01 | -2.135E-01 | -2.085E-01 | -2.126E-01 |
| Throt^3; | 1.958E-03 | 4.387E-03 | 2.170E-03 | 5.134E-03 | 6.945E-03 | 5.761E-03 | 8.345E-03 | 2.458E-03 | 3.082E-03 | 2.336E-03 |
| Throt^4; | -1.750E-05 | -4.042E-05 | -1.869E-05 | -6.469E-05 | -5.723E-05 | -4.770E-05 | -7.850E-05 | -1.209E-05 | -2.440E-05 | -1.174E-05 |
| Throt^5; | 6.356E-08 | 1.429E-07 | 6.414E-08 | 2.793E-07 | 1.816E-07 | 1.540E-07 | 2.826E-07 | 1.615E-08 | 7.986E-08 | 2.002E-08 |
| EGR; | -3.725E-01 | 1.960E-01 | -3.516E-01 | 8.458E-02 | -6.301E-01 | -9.828E-01 | 5.020E-02 | -9.922E-01 | -5.717E-01 | 9.620E-03 |
| EGR^2; | 5.790E-04 | -5.039E-04 | 3.538E-04 | -2.485E-04 | 1.516E-03 | 1.491E-03 | 8.293E-04 | 1.142E-03 | 1.899E-03 | 6.891E-05 |
| Fuel; | -5.670E+01 | 1.872E+02 | -3.549E+01 | -2.201E+02 | -9.136E+01 | -6.726E+01 | 1.465E+02 | 3.453E+00 | 2.827E+01 | 9.680E+01 |
| Fuel^2; | -7.609E-01 | -9.612E+01 | -1.060E+01 | 8.289E+01 | 1.248E+01 | -2.409E+00 | -8.948E+01 | -2.565E+01 | -2.233E+01 | -6.033E+01 |
| CAM; | 1.083E-01 | 1.234E-01 | -3.685E-01 | 1.421E+00 | -4.875E-02 | -5.157E-02 | -1.469E-01 | 3.916E-01 | 3.996E-01 | 4.549E-01 |
| CAM^2; | -9.020E-03 | -9.431E-03 | -7.439E-03 | -7.804E-03 | -7.411E-03 | -1.066E-02 | -4.617E-03 | -1.038E-02 | -1.977E-02 | -7.299E-03 |
| SPK; | -7.700E-01 | -3.222E+00 | -2.854E+00 | -2.540E+00 | 6.198E-02 | -2.119E+00 | -4.014E+00 | -1.457E+00 | -3.026E+00 | -3.783E-01 |
| SPK^2 ; | -1.806E-01 | 3.238E-02 | 1.404E-02 | 3.733E-02 | -1.554E-01 | -8.423E-03 | 7.241E-03 | 7.305E-02 | 2.511E-02 | -5.233E-02 |
| Throt * EGR; | 2.004E-03 | 9.118E-04 | 1.500E-03 | -1.917E-03 | 8.632E-04 | 1.283E-03 | 3.888E-04 | 1.035E-04 | -3.142E-03 | 3.504E-04 |
| Throt * Fuel; | 5.764E-02 | 9.985E-02 | 2.789E-02 | -2.392E-01 | -1.715E-02 | 8.518E-02 | 1.614E-01 | -1.477E-01 | -5.304E-01 | -1.764E-01 |
| Throt * CAM; | 1.065E-03 | 2.125E-03 | 1.414E-03 | -1.296E-03 | 2.581E-03 | 2.133E-03 | 9.923E-04 | -5.182E-04 | 4.365E-03 | 1.702E-03 |
| Throt * SPK; | -6.062E-03 | 5.113E-04 | -1.115E-02 | -5.496E-03 | -4.915E-03 | -8.893E-03 | -1.126E-02 | -1.321E-02 | -5.751E-03 | -8.459E-03 |
| EGR * Fuel; | -8.647E-02 | -5.261E-01 | -1.450E-01 | -1.097E-02 | 6.817E-02 | 3.881E-01 | -5.492E-01 | 4.894E-01 | 2.446E-01 | -3.365E-01 |
| EGR * CAM; | 1.903E-03 | 2.779E-03 | 3.549E-03 | -3.400E-03 | 1.523E-03 | 1.387E-03 | 9.982E-04 | 3.000E-05 | -1.466E-03 | -8.403E-04 |
| EGR * SPK; | 5.555E-03 | 1.650E-02 | 1.038E-02 | -1.649E-02 | 4.396E-03 | 1.234E-02 | 1.410E-02 | 1.114E-03 | 2.387E-02 | -7.808E-04 |
| Fuel * CAM; | 3.078E-01 | 3.107E-01 | 6.182E-01 | -4.834E-01 | 3.165E-01 | 4.537E-01 | 3.687E-01 | 2.152E-01 | 3.056E-01 | 3.830E-02 |
| Fuel * SPK; | 1.234E+00 | 1.929E+00 | 2.421E+00 | 2.230E+00 | 7.155E-01 | 1.505E+00 | 2.839E+00 | 1.504E+00 | 1.916E+00 | 8.905E-01 |
| CAM * SPK; | -2.124E-02 | -2.806E-02 | -2.527E-02 | -1.795E-02 | -1.863E-02 | -1.927E-03 | 4.007E-03 | -2.101E-02 | -3.980E-02 | -7.981E-03 |

| BSFC | ENGINE SPEED (rev/min) | | | | | | | | | |
|---|---|---|---|---|---|---|---|---|---|---|
| COEFFICIENTS | 1200 | 1400 | 1500 | 1700 | 1800 | 2000 | 2200 | 2400 | 2600 | 3000 |
| const | 4.513E+02 | 6.735E+02 | 4.207E+02 | 4.718E+02 | 4.028E+02 | 4.692E+02 | 5.838E+02 | 6.693E+02 | 6.035E+02 | 7.141E+02 |
| Throt; | -6.187E+00 | 2.271E+00 | 2.338E+00 | -3.013E+00 | -1.212E+01 | -4.953E+00 | -9.120E+00 | -1.296E+01 | -2.180E+01 | -1.961E+01 |
| Throt^2; | 2.980E-01 | 1.121E-02 | -1.036E-01 | 2.015E-01 | 5.272E-01 | 1.837E-01 | 3.947E-01 | 4.871E-01 | 9.706E-01 | 7.001E-01 |
| Throt^3; | -6.482E-03 | -1.896E-03 | 1.899E-03 | -5.951E-03 | -1.020E-02 | -2.811E-03 | -8.072E-03 | -8.610E-03 | -1.982E-02 | -1.181E-02 |
| Throt^4; | 6.545E-05 | 3.300E-05 | -1.524E-05 | 7.443E-05 | 9.140E-05 | 1.994E-05 | 7.876E-05 | 7.248E-05 | 1.887E-04 | 9.630E-05 |
| Throt^5; | -2.460E-07 | -1.639E-07 | 4.498E-08 | -3.230E-07 | -3.081E-07 | -5.403E-08 | -2.904E-07 | -2.330E-07 | -6.728E-07 | -3.038E-07 |
| EGR; | -9.993E-01 | -3.407E+00 | -1.400E+00 | -5.043E-01 | -9.250E-02 | 3.569E-01 | -1.215E+00 | -6.713E-01 | -2.235E-01 | -5.353E-01 |
| EGR^2; | 1.032E-03 | 4.102E-03 | 3.243E-03 | 8.442E-04 | -1.601E-03 | 3.450E-04 | 2.079E-03 | 1.560E-03 | 2.443E-04 | 6.240E-04 |
| Fuel; | -2.440E+02 | -7.168E+02 | -3.068E+02 | -3.429E+02 | -1.001E+02 | -3.109E+02 | -4.225E+02 | -4.849E+02 | -2.783E+02 | -4.476E+02 |
| Fuel^2; | 8.256E+01 | 2.744E+02 | 1.126E+02 | 1.321E+02 | 3.264E+01 | 1.277E+02 | 1.634E+02 | 1.904E+02 | 9.868E+01 | 1.814E+02 |
| CAM; | 2.707E-01 | 7.872E-01 | 1.724E+00 | 5.446E-01 | 7.363E-01 | 8.867E-01 | 5.901E-01 | -2.605E-01 | -2.995E-01 | 1.033E-01 |
| CAM^2; | 4.445E-03 | 9.095E-03 | -1.790E-03 | 2.538E-03 | 7.154E-04 | -3.415E-04 | -6.298E-03 | 8.737E-03 | 1.449E-03 | 5.493E-03 |
| SPK; | 2.645E+00 | 3.898E+00 | 6.432E+00 | 7.717E+00 | -3.868E-02 | 5.495E+00 | 5.245E+00 | 4.132E+00 | 3.375E+00 | 3.204E+00 |
| SPK^2 ; | 2.789E-01 | 3.205E-02 | -8.564E-02 | 2.626E-01 | 7.636E-02 | -2.534E-01 | 8.119E-02 | -1.641E-01 | -4.601E-02 | -1.782E-01 |
| Throt * EGR; | -5.006E-04 | -3.458E-04 | -1.414E-03 | -8.494E-04 | -1.018E-03 | -7.728E-04 | -8.577E-04 | -1.588E-03 | 2.427E-04 | -2.075E-03 |
| Throt * Fuel; | -1.619E-01 | -7.442E-01 | -1.536E-01 | -5.049E-02 | -2.686E-01 | -4.266E-01 | -3.234E-01 | -2.825E-01 | -2.519E-01 | -3.440E-01 |
| Throt * CAM; | 3.085E-03 | -2.543E-04 | 3.266E-03 | 2.928E-03 | 2.742E-03 | 4.667E-03 | 3.637E-03 | 6.079E-03 | -4.297E-04 | 7.988E-04 |
| Throt * SPK; | 1.380E-02 | 1.296E-02 | 1.518E-02 | 8.592E-03 | 1.134E-02 | 2.060E-02 | 2.930E-02 | 1.465E-02 | 6.386E-03 | -4.146E-03 |
| EGR * Fuel; | 8.857E-01 | 2.891E+00 | 1.170E+00 | 4.224E-01 | 3.636E-01 | -2.092E-01 | 1.148E+00 | 6.655E-01 | 1.902E-01 | 6.554E-01 |
| EGR * CAM; | -4.156E-03 | -4.755E-03 | -5.324E-03 | 2.172E-04 | -2.977E-03 | -2.418E-03 | -1.888E-03 | 5.661E-04 | 3.122E-04 | 8.367E-04 |
| EGR * SPK; | -1.078E-02 | -3.748E-02 | -1.428E-02 | -1.957E-03 | -4.136E-03 | -1.938E-02 | -1.782E-02 | 4.861E-03 | -5.355E-03 | 4.429E-03 |
| Fuel * CAM; | -2.694E-01 | -9.029E-01 | -1.266E+00 | -6.994E-01 | -6.186E-01 | -8.380E-01 | -3.497E-01 | -4.049E-01 | 1.140E-01 | -3.516E-01 |
| Fuel * SPK; | -2.709E+00 | -3.653E+00 | -4.513E+00 | -6.959E+00 | -6.782E-01 | -3.078E+00 | -4.937E+00 | -3.156E+00 | -2.374E+00 | -8.710E-01 |
| CAM * SPK; | 5.956E-02 | 1.047E-01 | 4.834E-02 | 1.259E-02 | 5.981E-02 | 2.004E-02 | 2.484E-02 | 4.267E-02 | 5.437E-02 | -1.392E-03 |

| BSNOx | ENGINE SPEED (rev/min) | | | | | | | | | |
|---|---|---|---|---|---|---|---|---|---|---|
| COEFFICIENTS | 1200 | 1400 | 1500 | 1700 | 1800 | 2000 | 2200 | 2400 | 2600 | 3000 |
| const | -9.000E+01 | -2.441E+01 | -9.698E+01 | -7.185E+01 | -3.825E+01 | -1.317E+02 | -9.785E+01 | -1.199E+02 | 5.984E+01 | -1.800E+02 |
| Throt; | 7.311E-01 | -1.678E-01 | -2.088E+00 | -5.557E-01 | -3.970E+00 | -1.477E+00 | 1.316E+00 | -6.940E+00 | -1.043E+01 | -8.243E-01 |
| Throt^2; | -7.557E-03 | 1.719E-02 | 1.104E-01 | -1.109E-02 | 2.169E-01 | 8.300E-02 | -5.389E-02 | 3.194E-01 | 4.757E-01 | 4.988E-02 |
| Throt^3; | -2.261E-04 | -5.044E-04 | -2.416E-03 | 1.491E-03 | -4.864E-03 | -1.944E-03 | 9.976E-04 | -6.338E-03 | -9.693E-03 | -1.275E-03 |
| Throt^4; | 4.994E-06 | 5.986E-06 | 2.334E-05 | -2.479E-05 | 4.943E-05 | 2.034E-05 | -8.411E-06 | 5.763E-05 | 9.048E-05 | 1.337E-05 |
| Throt^5; | -2.577E-08 | -2.506E-08 | -8.291E-08 | 1.190E-07 | -1.849E-07 | -7.753E-08 | 2.613E-08 | -1.959E-07 | -3.146E-07 | -4.975E-08 |
| EGR; | -4.231E-01 | -2.848E-01 | -1.687E-01 | -2.024E-03 | -4.264E-01 | -3.994E-01 | -3.883E-01 | -2.003E-01 | -2.766E-01 | 1.255E-01 |
| EGR^2; | 1.735E-03 | 1.857E-03 | 1.555E-03 | 8.180E-04 | 2.148E-03 | 1.829E-03 | 2.284E-03 | 2.029E-03 | 3.607E-04 | 4.674E-04 |
| Fuel; | 1.797E+02 | 8.793E+01 | 2.340E+02 | 1.393E+02 | 1.395E+02 | 2.648E+02 | 1.817E+02 | 3.191E+02 | 5.157E+01 | 3.655E+02 |
| Fuel^2; | -8.002E+01 | -4.472E+01 | -1.043E+02 | -4.930E+01 | -5.487E+01 | -1.060E+02 | -7.422E+01 | -1.281E+02 | -1.485E+01 | -1.614E+02 |
| CAM; | -5.618E-02 | -1.219E-01 | -4.609E-01 | 4.125E-01 | 2.226E-01 | 3.082E-01 | 3.185E-01 | 7.346E-02 | 8.697E-01 | -1.682E-01 |
| CAM^2; | 1.473E-03 | 5.275E-04 | 2.525E-03 | 7.122E-03 | 6.586E-04 | 2.870E-03 | 3.612E-03 | -2.989E-03 | -8.934E-03 | -2.539E-03 |
| SPK; | 9.507E-01 | -4.982E-01 | -1.878E+00 | -1.394E+00 | 1.265E+00 | 1.297E+00 | 2.153E+00 | 8.488E-03 | 3.621E-01 | -2.663E+00 |
| SPK^2 ; | -1.641E-02 | 6.374E-03 | 1.662E-01 | 2.251E-01 | -3.983E-02 | 5.304E-03 | -1.539E-01 | -4.137E-03 | -3.305E-02 | 7.684E-02 |
| Throt * EGR; | 3.625E-04 | 2.000E-04 | 4.301E-04 | -1.811E-03 | -6.816E-04 | 6.936E-05 | 9.075E-05 | -1.025E-04 | -1.126E-04 | 8.454E-04 |
| Throt * Fuel; | 1.601E-02 | 8.307E-02 | 6.432E-02 | -2.982E-01 | -1.855E-01 | 2.696E-02 | -1.173E-02 | -1.489E-01 | -4.808E-02 | 1.678E-01 |
| Throt * CAM; | -7.766E-05 | -6.905E-04 | 5.729E-04 | -3.213E-03 | -6.868E-04 | -1.647E-04 | 2.562E-03 | 1.160E-04 | 6.943E-04 | 6.634E-04 |
| Throt * SPK; | -4.372E-03 | -8.149E-03 | 2.130E-03 | 2.351E-03 | -1.845E-03 | -8.552E-03 | -1.668E-03 | -6.719E-03 | 3.979E-03 | 9.322E-03 |
| EGR * Fuel; | 4.729E-02 | -9.068E-02 | -1.809E-01 | -5.450E-04 | 4.434E-02 | 3.516E-02 | -1.623E-03 | -1.338E-01 | 1.355E-01 | -3.711E-01 |
| EGR * CAM; | 1.095E-03 | 1.397E-03 | 1.454E-03 | -1.284E-03 | 1.826E-03 | 1.327E-03 | -1.853E-04 | 6.853E-04 | -1.004E-03 | 6.957E-04 |
| EGR * SPK; | 3.277E-03 | 4.055E-03 | 3.942E-03 | -1.428E-02 | 1.747E-03 | 4.275E-03 | 2.190E-03 | 1.613E-03 | 6.516E-03 | 1.550E-03 |
| Fuel * CAM; | -1.516E-01 | -2.735E-02 | 1.161E-01 | -4.341E-01 | -3.780E-01 | -5.555E-01 | -5.789E-01 | -6.723E-02 | -4.389E-01 | 1.113E-01 |
| Fuel * SPK; | -1.351E+00 | 2.676E-01 | -6.242E-02 | -2.354E-01 | -1.007E+00 | -1.525E+00 | -1.079E+00 | -3.678E-02 | -7.365E-01 | 8.415E-01 |
| CAM * SPK; | 9.758E-03 | -4.263E-03 | 1.053E-02 | 9.112E-04 | -8.516E-03 | 8.485E-03 | -1.518E-02 | -2.613E-03 | -2.260E-02 | 8.785E-03 |

| CO | ENGINE SPEED (rev/min) | | | | | | | | | |
|---|---|---|---|---|---|---|---|---|---|---|
| COEFFICIENTS | 1200 | 1400 | 1500 | 1700 | 1800 | 2000 | 2200 | 2400 | 2600 | 3000 |
| const | -7.990E+00 | 3.345E+00 | -7.113E+00 | -1.017E+01 | -7.818E+00 | -4.502E+00 | -3.715E-02 | -3.987E+00 | -1.788E+00 | -7.083E+00 |
| Throt; | -7.706E-02 | 2.975E-02 | 6.939E-02 | 3.092E-03 | -1.005E-01 | -1.406E-02 | 9.563E-02 | 1.479E-01 | -1.649E-01 | -9.869E-02 |
| Throt^2; | 4.273E-03 | -1.713E-03 | -4.057E-03 | -2.563E-04 | 3.092E-03 | -5.106E-04 | -5.147E-03 | -9.979E-03 | 7.580E-03 | 3.844E-03 |
| Throt^3; | -1.051E-04 | 4.273E-05 | 9.888E-05 | 4.519E-06 | -5.799E-05 | -4.032E-06 | 9.196E-05 | 2.573E-04 | -1.583E-04 | -6.761E-05 |
| Throt^4; | 1.154E-06 | -4.126E-07 | -1.050E-06 | -1.355E-08 | 5.072E-07 | 2.444E-07 | -6.751E-07 | -2.818E-06 | 1.580E-06 | 5.872E-07 |
| Throt^5; | -4.579E-09 | 1.340E-09 | 4.028E-09 | -9.931E-11 | -1.670E-09 | -1.617E-09 | 1.685E-09 | 1.097E-08 | -5.947E-09 | -1.980E-09 |
| EGR; | -4.161E-03 | -4.596E-03 | 1.631E-02 | 6.086E-03 | -1.484E-02 | 3.312E-02 | -4.171E-02 | 6.707E-02 | -1.644E-02 | -2.982E-04 |
| EGR^2; | -7.984E-06 | 3.778E-05 | 1.855E-05 | -1.185E-05 | -1.688E-05 | -8.652E-05 | 1.049E-05 | -5.976E-05 | -1.715E-05 | 3.077E-06 |
| Fuel; | 8.780E+00 | -1.080E+01 | 5.900E+00 | 1.161E+01 | 9.486E+00 | 2.809E+00 | -6.222E+00 | 6.023E-01 | 4.624E-01 | 7.994E+00 |
| Fuel^2; | -1.311E-01 | 7.871E+00 | 1.107E+00 | -1.264E+00 | -7.594E-01 | 2.275E+00 | 6.226E+00 | 3.076E+00 | 3.205E+00 | 3.052E-01 |
| CAM; | -7.909E-03 | -3.048E-02 | -2.560E-03 | -1.253E-02 | -1.387E-02 | -3.989E-03 | -3.152E-03 | -5.342E-03 | -3.400E-02 | 2.298E-03 |
| CAM^2; | 7.766E-05 | -1.654E-05 | 1.685E-04 | 4.474E-04 | 2.353E-04 | 1.054E-04 | 3.615E-05 | 2.951E-05 | 4.854E-04 | 1.629E-04 |
| SPK; | -1.190E-01 | -2.145E-02 | -6.463E-02 | -2.446E-02 | -7.169E-02 | -6.322E-02 | 1.499E-02 | 2.022E-01 | 3.170E-02 | -9.730E-03 |
| SPK^2 ; | 2.717E-03 | 3.093E-03 | -1.975E-04 | 1.061E-03 | -1.800E-03 | 4.364E-03 | -4.984E-04 | -9.723E-03 | -3.487E-03 | -3.254E-03 |
| Throt * EGR; | -6.549E-06 | -5.077E-07 | 3.588E-05 | -1.676E-05 | -8.888E-06 | 1.719E-05 | 3.219E-05 | -6.800E-06 | -1.429E-05 | -2.893E-05 |
| Throt * Fuel; | 1.563E-03 | -1.008E-02 | -3.558E-03 | 1.901E-03 | 2.191E-02 | 1.880E-02 | 8.070E-03 | 1.258E-03 | -9.023E-03 | -8.682E-03 |
| Throt * CAM; | -2.656E-05 | -2.988E-05 | -3.919E-05 | -6.004E-05 | -1.942E-05 | 2.555E-05 | 3.092E-05 | 6.769E-05 | 1.598E-05 | -6.624E-06 |
| Throt * SPK; | 1.136E-04 | 7.874E-04 | -1.950E-04 | 1.787E-04 | 4.168E-04 | -4.021E-04 | 6.158E-04 | 5.660E-04 | -4.451E-04 | -1.816E-04 |
| EGR * Fuel; | 5.472E-03 | 7.580E-03 | -1.374E-02 | -3.408E-03 | 1.767E-02 | -2.446E-02 | 4.022E-02 | -5.687E-02 | 1.687E-02 | 2.690E-03 |
| EGR * CAM; | -2.315E-06 | -6.985E-05 | -9.803E-05 | 2.699E-05 | -5.127E-06 | 2.452E-05 | -1.523E-05 | -2.422E-05 | 6.754E-05 | 1.424E-06 |
| EGR * SPK; | 1.360E-04 | -5.993E-04 | 1.319E-04 | -9.172E-05 | -1.347E-04 | 9.957E-05 | -1.940E-04 | -7.378E-04 | -1.635E-04 | 9.818E-05 |
| Fuel * CAM; | 4.593E-03 | 2.645E-02 | -2.424E-03 | -4.378E-03 | 2.515E-03 | -4.945E-03 | -2.222E-03 | 1.676E-04 | 5.071E-03 | -6.627E-03 |
| Fuel * SPK; | 8.787E-02 | 1.626E-02 | 5.441E-02 | 1.824E-02 | 6.043E-02 | 3.252E-02 | -3.495E-02 | -1.474E-01 | 1.355E-02 | 4.177E-02 |
| CAM * SPK; | 4.239E-04 | -1.237E-04 | 4.306E-04 | -8.852E-05 | 5.564E-04 | 6.847E-04 | 4.056E-04 | 7.418E-04 | 1.130E-03 | -4.282E-04 |

| uHC | ENGINE SPEED (rev/min) | | | | | | | | | |
|---|---|---|---|---|---|---|---|---|---|---|
| COEFFICIENTS | 1200 | 1400 | 1500 | 1700 | 1800 | 2000 | 2200 | 2400 | 2600 | 3000 |
| const | 1.162E+01 | 1.793E+01 | 1.003E+01 | 8.623E+00 | 1.222E+01 | 1.247E+01 | 1.383E+01 | 1.124E+00 | 1.214E+01 | 2.157E+01 |
| Throt; | -2.064E-01 | 9.878E-02 | 2.654E-01 | -4.170E-02 | -7.400E-01 | -2.575E-01 | -1.909E-01 | -6.960E-01 | -8.220E-01 | -7.839E-01 |
| Throt^2; | 1.141E-02 | -2.331E-03 | -1.440E-02 | 6.356E-03 | 3.563E-02 | 1.152E-02 | 7.677E-03 | 2.721E-02 | 3.704E-02 | 2.744E-02 |
| Throt^3; | -2.647E-04 | 3.183E-05 | 3.495E-04 | -2.051E-04 | -7.250E-04 | -2.686E-04 | -1.188E-04 | -4.911E-04 | -8.094E-04 | -4.483E-04 |
| Throt^4; | 2.813E-06 | -1.145E-07 | -3.737E-06 | 2.679E-06 | 6.941E-06 | 3.141E-06 | 1.051E-06 | 4.153E-06 | 8.179E-06 | 3.525E-06 |
| Throt^5; | -1.099E-08 | -2.914E-10 | 1.445E-08 | -1.196E-08 | -2.508E-08 | -1.356E-08 | -3.985E-09 | -1.335E-08 | -3.062E-08 | -1.073E-08 |
| EGR; | -3.200E-02 | -7.196E-02 | -3.837E-02 | -1.899E-02 | -3.063E-03 | -3.757E-02 | -4.398E-02 | -6.417E-03 | 7.273E-03 | -2.320E-02 |
| EGR^2; | 7.322E-05 | 1.354E-04 | 1.390E-04 | 1.471E-04 | 1.428E-05 | 1.362E-05 | 1.702E-04 | 1.562E-04 | -2.418E-06 | 8.898E-05 |
| Fuel; | 8.804E-01 | -1.324E+01 | -1.958E+00 | 2.687E+00 | 4.771E+00 | -5.660E-01 | -5.303E+00 | 2.476E+01 | 7.087E+00 | -6.939E+00 |
| Fuel^2; | -1.274E+00 | 4.752E+00 | 1.175E-01 | -1.665E+00 | -2.247E+00 | -6.017E-01 | 2.707E+00 | -1.058E+01 | -3.703E+00 | 2.757E+00 |
| CAM; | 6.025E-03 | 2.473E-02 | 5.277E-02 | 4.296E-03 | 1.685E-02 | 2.302E-02 | 1.030E-01 | -1.990E-02 | 2.147E-02 | 5.071E-03 |
| CAM^2; | 6.250E-04 | 8.546E-04 | 2.449E-04 | 4.383E-04 | 6.700E-04 | 1.584E-04 | -2.371E-04 | 7.546E-04 | 2.208E-04 | 4.078E-04 |
| SPK; | 1.874E-01 | 1.772E-01 | 2.197E-01 | 3.077E-01 | 9.784E-02 | 2.746E-01 | 2.861E-01 | -8.619E-02 | 3.159E-01 | 2.052E-01 |
| SPK^2 ; | 3.336E-03 | -1.952E-03 | 1.319E-03 | 1.886E-02 | -3.645E-03 | -2.180E-02 | 3.204E-03 | 1.631E-03 | -4.073E-03 | -6.826E-03 |
| Throt * EGR; | 1.245E-05 | 1.040E-04 | 1.620E-05 | 3.823E-05 | 3.934E-05 | 6.793E-04 | 1.949E-04 | 3.260E-05 | 2.193E-04 | -7.612E-05 |
| Throt * Fuel; | -1.221E-02 | -2.558E-02 | -1.227E-02 | -1.570E-02 | -3.217E-02 | 3.707E-03 | -4.617E-02 | 6.338E-03 | 2.037E-02 | -1.298E-02 |
| Throt * CAM; | -1.321E-05 | -2.007E-04 | -8.466E-06 | -1.237E-04 | -4.630E-04 | -4.375E-04 | -1.705E-04 | 1.685E-04 | 2.139E-05 | -1.692E-05 |
| Throt * SPK; | 8.297E-04 | -5.943E-05 | 1.177E-03 | 5.213E-05 | 1.050E-03 | -3.678E-04 | 1.667E-03 | 1.331E-06 | 1.232E-03 | 9.594E-06 |
| EGR * Fuel; | 3.410E-02 | 6.586E-02 | 3.590E-02 | 6.807E-03 | 1.907E-02 | 3.418E-02 | 4.428E-02 | 3.289E-03 | -4.406E-03 | 2.888E-02 |
| EGR * CAM; | -3.286E-04 | -4.542E-04 | -3.176E-04 | -1.723E-04 | -3.749E-04 | -3.439E-04 | -5.853E-04 | -1.642E-04 | -2.079E-04 | -9.434E-05 |
| EGR * SPK; | -4.872E-04 | -1.346E-03 | -1.128E-03 | 8.096E-04 | -2.681E-04 | -1.089E-03 | -7.864E-04 | 1.079E-03 | -8.721E-04 | 1.315E-04 |
| Fuel * CAM; | -2.020E-02 | -4.335E-02 | -4.779E-02 | -2.241E-02 | -2.471E-02 | -1.154E-02 | -6.217E-02 | -1.897E-02 | -1.998E-02 | -2.003E-02 |
| Fuel * SPK; | -1.436E-01 | -1.220E-01 | -1.817E-01 | -3.125E-01 | -8.900E-02 | -7.728E-02 | -2.507E-01 | 6.155E-02 | -2.310E-01 | -1.186E-01 |
| CAM * SPK; | 2.094E-03 | 3.903E-03 | 2.077E-03 | 1.009E-03 | 2.574E-03 | 4.969E-04 | 1.314E-04 | 7.571E-04 | 9.096E-04 | 2.018E-04 |

| BSCO2 | ENGINE SPEED (rev/min) | | | | | | | | | |
|---|---|---|---|---|---|---|---|---|---|---|
| COEFFICIENTS | 1200 | 1400 | 1500 | 1700 | 1800 | 2000 | 2200 | 2400 | 2600 | 3000 |
| const | 2.160E+01 | -9.080E+00 | 2.710E+01 | -4.868E+01 | -3.390E+01 | 5.968E+01 | 3.651E+01 | 8.041E+00 | -7.991E+01 | -1.620E+01 |
| Throt; | -1.397E+00 | -1.460E+00 | -8.057E-01 | 1.751E+00 | 2.897E+00 | -1.045E+00 | -1.860E+00 | 8.984E-01 | 1.025E+01 | 6.081E-01 |
| Throt^2; | 5.782E-02 | 6.702E-02 | 3.397E-02 | -2.056E-02 | -1.516E-01 | 4.269E-02 | 9.167E-02 | -3.614E-02 | -4.838E-01 | -1.895E-02 |
| Throt^3; | -1.292E-03 | -1.429E-03 | -7.384E-04 | -1.050E-03 | 3.363E-03 | -8.916E-04 | -1.980E-03 | 5.047E-04 | 1.008E-02 | 2.097E-04 |
| Throt^4; | 1.394E-05 | 1.388E-05 | 7.531E-06 | 2.142E-05 | -3.342E-05 | 9.083E-06 | 1.990E-05 | -2.583E-06 | -9.659E-05 | -5.154E-07 |
| Throt^5; | -5.510E-08 | -4.941E-08 | -2.823E-08 | -1.074E-07 | 1.225E-07 | -3.471E-08 | -7.395E-08 | 2.773E-09 | 3.445E-07 | -2.118E-09 |
| EGR; | 5.381E-01 | 6.085E-01 | 4.492E-01 | -5.529E-02 | 6.599E-01 | 5.870E-01 | 5.022E-01 | 4.819E-01 | 3.962E-01 | 3.659E-01 |
| EGR^2; | -1.617E-03 | -1.799E-03 | -2.079E-03 | -6.508E-04 | -2.000E-03 | -2.162E-03 | -1.819E-03 | -1.662E-03 | -4.030E-04 | -1.357E-03 |
| Fuel; | -1.513E+01 | 3.369E+01 | -3.284E+01 | 9.897E+01 | 2.860E+01 | -7.900E+01 | -4.162E+01 | -2.293E+01 | 1.934E+01 | 1.720E+01 |
| Fuel^2; | 8.653E+00 | -1.328E+01 | 1.367E+01 | -5.659E+01 | -1.053E+01 | 3.221E+01 | 2.176E+01 | 9.278E+00 | -1.631E+01 | -6.064E+00 |
| CAM; | 5.046E-02 | 2.205E-02 | 2.023E-02 | -1.061E+00 | -8.846E-03 | -1.870E-02 | 2.095E-01 | 3.406E-02 | -5.446E-01 | 2.152E-02 |
| CAM^2; | -2.056E-04 | -3.340E-05 | 1.835E-04 | -2.728E-03 | -1.276E-03 | -3.932E-04 | -2.211E-03 | -4.000E-04 | 1.294E-02 | -5.927E-04 |
| SPK; | -2.390E-01 | -1.502E-01 | -3.374E-01 | 3.346E-01 | -4.453E-01 | -1.505E+00 | -9.661E-01 | 3.403E-01 | 1.945E+00 | -8.355E-02 |
| SPK^2 ; | 5.854E-02 | 6.105E-03 | 6.976E-02 | -1.863E-01 | 1.333E-01 | 4.324E-02 | 1.396E-02 | -3.888E-02 | -1.289E-01 | 1.363E-02 |
| Throt * EGR; | -1.806E-03 | -1.087E-03 | -1.165E-03 | 1.604E-03 | -8.175E-04 | -1.765E-03 | -1.345E-03 | -9.398E-04 | 7.054E-04 | -6.060E-04 |
| Throt * Fuel; | -3.287E-02 | -2.778E-03 | 1.478E-02 | 2.330E-01 | -2.481E-02 | -3.758E-02 | -1.619E-01 | 2.763E-02 | 2.740E-01 | -3.174E-02 |
| Throt * CAM; | -2.775E-04 | -1.376E-04 | -6.221E-04 | 2.296E-03 | -3.269E-04 | 1.032E-03 | 6.086E-04 | 6.398E-05 | -9.434E-04 | -1.337E-04 |
| Throt * SPK; | -3.342E-04 | -4.587E-04 | -2.598E-04 | 3.163E-03 | -7.448E-04 | -2.305E-03 | 1.633E-03 | -8.248E-04 | -7.383E-03 | -5.351E-04 |
| EGR * Fuel; | -5.211E-02 | -1.553E-01 | 1.728E-02 | 3.968E-02 | -2.026E-01 | -8.182E-02 | -4.034E-02 | -7.078E-02 | -2.235E-01 | -2.407E-02 |
| EGR * CAM; | 7.247E-05 | 1.247E-04 | 7.754E-04 | 3.691E-03 | 7.175E-04 | 4.019E-04 | 4.656E-04 | 2.832E-04 | 1.378E-03 | 4.128E-05 |
| EGR * SPK; | 2.085E-04 | 2.918E-03 | 1.113E-03 | 1.414E-02 | -1.134E-03 | -1.387E-03 | -3.553E-04 | -8.773E-05 | -1.035E-02 | -2.160E-04 |
| Fuel * CAM; | -3.022E-02 | 1.983E-02 | 1.791E-04 | 7.131E-01 | 5.199E-02 | -1.480E-02 | -9.931E-02 | -2.791E-02 | 4.326E-03 | 2.436E-02 |
| Fuel * SPK; | -1.503E-01 | 2.269E-01 | 6.887E-03 | 1.752E-01 | -2.312E-01 | 1.183E+00 | 4.854E-01 | -8.768E-02 | -4.142E-01 | 1.089E-01 |
| CAM * SPK; | 3.746E-03 | -9.463E-03 | -5.301E-03 | 2.459E-03 | -5.468E-04 | -2.147E-03 | 1.036E-02 | 3.047E-03 | 1.526E-02 | -3.493E-03 |

## Second order regression coefficients

**Low Model - Torque**

| | ENGINE SPEED (rev/min) | | | | | | | | | |
|---|---|---|---|---|---|---|---|---|---|---|
| COEFFICIENTS | 1200 | 1400 | 1500 | 1700 | 1800 | 2000 | 2200 | 2400 | 2600 | 3000 |
| Const | 3.859E+01 | -1.159E+02 | 1.117E+02 | 1.076E+02 | 3.717E+01 | 6.104E+01 | -1.015E+02 | 1.161E+02 | -2.933E+01 | -1.807E+02 |
| Throt; | 3.246E+00 | 3.557E+00 | 2.470E+00 | 3.725E+00 | 7.226E+00 | 7.820E+00 | 6.327E+00 | 8.523E+00 | 5.059E+00 | 7.028E+00 |
| EGR; | 1.496E-01 | 4.852E-01 | -2.051E-01 | -6.985E-01 | -1.948E-01 | -4.034E-01 | 6.971E-01 | -1.635E+00 | -1.365E-01 | 3.034E-01 |
| Fuel; | 7.545E+01 | 3.065E+02 | -2.599E+01 | -4.987E+01 | -6.987E-01 | -5.074E+01 | 2.484E+02 | -2.060E+02 | 1.017E+02 | 2.866E+02 |
| CAM; | -7.467E-02 | 1.039E-01 | -4.533E-01 | -5.073E-03 | -3.318E-01 | -1.462E-01 | -1.480E-01 | 1.814E-01 | 1.072E+00 | 6.087E-01 |
| SPK; | -1.267E+00 | -1.263E+00 | -2.472E+00 | -3.142E+00 | 1.195E+00 | -6.922E+00 | -3.853E+00 | 1.170E+00 | -5.938E+00 | 3.712E+00 |
| Throt^2; | -5.345E-02 | -1.155E-02 | -9.025E-02 | -6.946E-02 | -1.256E-01 | -9.016E-02 | -1.006E-01 | -8.850E-02 | -2.849E-02 | -8.052E-02 |
| EGR^2; | -1.584E-03 | 4.407E-04 | -8.910E-04 | 2.172E-03 | 4.787E-04 | 0.000E+00 | 0.000E+00 | 1.363E-03 | -1.850E-04 | -4.581E-04 |
| Fuel^2; | -5.446E+01 | -1.164E+02 | -3.478E+01 | -1.180E+01 | -2.485E+01 | 0.000E+00 | -1.324E+02 | 8.455E+01 | -4.863E+01 | -1.295E+02 |
| CAM^2; | -8.152E-03 | -1.524E-02 | -8.383E-03 | -1.245E-02 | -7.905E-03 | -6.865E-03 | -4.724E-03 | 0.000E+00 | -7.090E-03 | -4.431E-03 |
| SPK^2; | -1.392E-01 | 0.000E+00 | 0.000E+00 | 0.000E+00 | -2.215E-01 | 0.000E+00 | 0.000E+00 | -1.872E-01 | 0.000E+00 | 0.000E+00 |
| Throt * EGR; | 1.111E-02 | 7.200E-03 | 1.444E-02 | 2.354E-03 | 6.983E-03 | -2.411E-03 | 0.000E+00 | 0.000E+00 | -4.338E-03 | 0.000E+00 |
| Throt * Fuel; | 0.000E+00 | -2.270E+00 | 2.066E+00 | 5.547E-01 | 0.000E+00 | -1.397E+00 | 0.000E+00 | -1.915E+00 | -1.264E+00 | -4.284E-01 |
| Throt * CAM; | 8.420E-03 | 4.907E-03 | 5.603E-03 | 4.662E-03 | 1.653E-02 | 0.000E+00 | 0.000E+00 | -1.798E-03 | -4.473E-03 | 4.793E-03 |
| Throt * SPK; | -3.370E-02 | 4.792E-02 | 0.000E+00 | -4.360E-02 | -4.501E-02 | -1.462E-01 | 0.000E+00 | -1.838E-02 | -6.787E-02 | -2.868E-02 |
| EGR * Fuel; | -6.979E-01 | -9.984E-01 | -5.538E-01 | 0.000E+00 | -4.669E-01 | 0.000E+00 | -1.096E+00 | 1.059E+00 | -1.125E-01 | -5.590E-01 |
| EGR * CAM; | 1.863E-03 | 1.208E-03 | 4.901E-03 | 1.828E-03 | 1.813E-03 | 2.087E-03 | 0.000E+00 | 1.557E-03 | 0.000E+00 | 0.000E+00 |
| EGR * SPK; | 7.956E-03 | 1.803E-02 | 1.221E-02 | 1.094E-02 | 1.935E-03 | 2.226E-02 | 1.522E-02 | -4.722E-03 | 2.464E-02 | -4.247E-03 |
| Fuel * CAM; | 2.818E-01 | 5.532E-01 | 6.300E-01 | 4.130E-01 | 2.656E-01 | 3.924E-01 | 3.944E-01 | 0.000E+00 | -4.568E-01 | -3.630E-01 |
| Fuel * SPK; | 1.589E+00 | 0.000E+00 | 1.964E+00 | 3.290E+00 | 6.119E-01 | 8.111E+00 | 2.738E+00 | 5.237E-01 | 5.390E+00 | -2.551E+00 |
| CAM * SPK; | 0.000E+00 | -4.944E-02 | -3.785E-02 | -2.239E-02 | 0.000E+00 | 2.300E-02 | 0.000E+00 | 0.000E+00 | 1.841E-02 | 0.000E+00 |

**High Model - Torque**

| | ENGINE SPEED (rev/min) | | | | | | | | | |
|---|---|---|---|---|---|---|---|---|---|---|
| COEFFICIENTS | 1200 | 1400 | 1500 | 1700 | 1800 | 2000 | 2200 | 2400 | 2600 | 3000 |
| Const | 1.984E+02 | 1.554E+02 | 1.298E+02 | 3.240E+02 | 1.166E+02 | 2.145E+02 | 1.462E+02 | 1.745E+02 | 1.608E+02 | 1.513E+02 |
| Throt; | 2.372E-01 | -1.306E-01 | 3.082E-01 | 3.066E-01 | 4.523E-01 | 1.672E-01 | 2.822E-01 | 3.160E-01 | 6.087E-01 | 5.290E-01 |
| EGR; | -2.135E-01 | -1.247E-01 | -1.688E-01 | -8.658E-01 | -3.219E-01 | -6.819E-01 | -5.042E-01 | -1.456E-01 | -1.833E-01 | -3.123E-01 |
| Fuel; | -1.344E+02 | -4.126E+01 | -1.266E+01 | -3.350E+02 | 6.886E+00 | -1.174E+02 | -2.419E+01 | -6.209E+01 | -5.172E+01 | -3.432E+01 |
| CAM; | 3.576E-01 | 5.226E-01 | 1.534E-01 | 6.466E-01 | 3.110E-01 | -1.193E-01 | 3.792E-01 | 3.392E-01 | 2.686E-01 | 4.161E-01 |
| SPK; | 1.286E-01 | -3.308E+00 | -1.360E+00 | -1.974E+00 | -1.245E+00 | -3.609E+00 | -3.866E+00 | -1.641E+00 | -8.262E-02 | -2.362E+00 |
| Throt^2; | -3.795E-04 | -3.130E-04 | -2.564E-03 | -6.256E-04 | -1.883E-03 | -2.253E-03 | -1.003E-03 | -2.066E-03 | -4.217E-03 | -1.608E-03 |
| EGR^2; | -6.840E-04 | -9.455E-04 | -4.589E-04 | 5.740E-04 | 1.515E-04 | 0.000E+00 | 1.271E-03 | -2.219E-04 | 2.354E-04 | 2.835E-04 |
| Fuel^2; | 3.839E+01 | -6.248E+00 | -1.992E+01 | 1.176E+02 | -2.274E+01 | 1.604E+01 | -1.454E+01 | -6.908E+00 | -8.134E+00 | -9.813E+00 |
| CAM^2; | -8.838E-03 | -6.512E-03 | -6.892E-03 | -1.376E-02 | -6.369E-03 | -6.795E-03 | -7.339E-03 | -1.160E-02 | -1.240E-02 | -8.442E-03 |
| SPK^2; | -4.702E-02 | -3.688E-01 | 0.000E+00 | -3.093E-01 | 0.000E+00 | 0.000E+00 | 0.000E+00 | 1.530E-01 | -1.268E-01 | -1.434E-01 |
| Throt * EGR; | 7.002E-04 | 1.874E-03 | 2.103E-03 | 0.000E+00 | 1.130E-04 | 1.152E-03 | 0.000E+00 | 2.793E-04 | 0.000E+00 | 1.006E-03 |
| Throt * Fuel; | -1.340E-01 | 1.690E-01 | 1.065E-01 | -1.507E-01 | -1.100E-01 | 1.368E-01 | 0.000E+00 | 1.293E-01 | 8.482E-02 | -1.938E-01 |
| Throt * CAM; | -7.678E-04 | 4.619E-05 | -1.400E-03 | 1.946E-03 | 1.458E-03 | 2.627E-03 | 0.000E+00 | -9.180E-04 | 8.265E-04 | 0.000E+00 |
| Throt * SPK; | -5.763E-03 | 0.000E+00 | -2.536E-02 | 0.000E+00 | 0.000E+00 | 0.000E+00 | 0.000E+00 | -1.004E-02 | -9.382E-03 | 0.000E+00 |
| EGR * Fuel; | 0.000E+00 | -2.440E-01 | -2.463E-01 | 4.709E-01 | 0.000E+00 | 2.578E-01 | 0.000E+00 | -1.833E-01 | -2.179E-01 | -1.182E-01 |
| EGR * CAM; | 1.391E-03 | 1.635E-03 | 1.399E-03 | 7.365E-04 | 4.231E-04 | 0.000E+00 | 6.581E-04 | -1.030E-03 | 8.684E-04 | -6.011E-04 |
| EGR * SPK; | 4.238E-03 | 1.538E-02 | 7.745E-03 | 1.434E-02 | 0.000E+00 | 1.320E-02 | 1.184E-02 | 1.035E-03 | 3.382E-03 | 3.648E-03 |
| Fuel * CAM; | 2.603E-01 | 0.000E+00 | 3.840E-01 | 0.000E+00 | 9.405E-02 | 3.698E-01 | 1.507E-01 | 4.316E-01 | 3.138E-01 | 2.274E-01 |
| Fuel * SPK; | 0.000E+00 | 3.781E+00 | 2.123E+00 | 2.378E+00 | 9.396E-01 | 1.883E+00 | 2.370E+00 | 1.116E+00 | 9.146E-01 | 2.397E+00 |
| CAM * SPK; | -3.548E-02 | -1.437E-02 | -1.615E-02 | -3.370E-02 | -3.023E-02 | 0.000E+00 | -1.041E-02 | -3.401E-02 | -2.414E-02 | -1.235E-02 |

Low Model - BSFC

| | ENGINE SPEED (rev/min) | | | | | | | | | |
|---|---|---|---|---|---|---|---|---|---|---|
| COEFFICIENTS | 1200 | 1400 | 1500 | 1700 | 1800 | 2000 | 2200 | 2400 | 2600 | 3000 |
| Const | 5.384E+02 | 9.429E+02 | 5.229E+02 | 4.080E+02 | 3.522E+02 | 4.530E+02 | 7.462E+02 | 3.079E+02 | 5.375E+02 | 8.703E+02 |
| Throt; | -2.914E+00 | 2.789E-01 | 3.839E+00 | 4.701E-01 | -3.132E+00 | -6.158E-01 | -1.091E+00 | -6.705E+00 | -2.708E+00 | -5.939E+00 |
| EGR; | -3.028E+00 | -2.633E+00 | -2.217E+00 | -9.568E-01 | 2.489E-01 | -4.466E-01 | -2.900E+00 | 1.529E-03 | -1.608E+00 | -1.008E+00 |
| Fuel; | -4.078E+02 | -1.098E+03 | -5.214E+02 | -2.891E+02 | -1.240E+02 | -3.427E+02 | -8.186E+02 | 4.657E+01 | -4.416E+02 | -8.804E+02 |
| CAM; | 6.171E-01 | 6.884E-01 | 1.645E+00 | 7.470E-01 | 9.092E-01 | 1.416E+00 | 6.678E-01 | -1.792E-01 | 8.337E-01 | -9.660E-01 |
| SPK; | 2.301E-01 | 6.193E-01 | 2.907E+00 | 7.970E+00 | -4.790E+00 | 8.151E+00 | 8.248E-01 | 2.688E+00 | 1.370E+01 | -4.116E+00 |
| Throt^2; | 4.973E-02 | -1.479E-01 | 3.930E-02 | 5.658E-02 | 1.380E-01 | 0.000E+00 | 1.139E-01 | 1.047E-01 | 6.416E-02 | 1.444E-01 |
| EGR^2; | 6.999E-03 | 1.868E-03 | 6.141E-03 | -1.188E-03 | -1.074E-03 | 3.790E-03 | 4.674E-03 | 2.619E-03 | 4.477E-03 | 2.729E-03 |
| Fuel^2; | 1.499E+02 | 3.542E+02 | 2.491E+02 | 1.452E+02 | 7.392E+01 | 1.633E+02 | 3.747E+02 | -3.497E+01 | 1.853E+02 | 3.979E+02 |
| CAM^2; | 8.020E-03 | 1.820E-02 | 0.000E+00 | 9.124E-03 | 3.232E-03 | -8.052E-03 | 0.000E+00 | 1.878E-03 | -4.447E-03 | 0.000E+00 |
| SPK^2; | 3.569E-01 | 1.642E-01 | 0.000E+00 | 0.000E+00 | 2.830E-01 | 0.000E+00 | 0.000E+00 | 2.476E-01 | -1.077E-01 | 0.000E+00 |
| Throt * EGR; | -1.387E-02 | -6.756E-04 | -1.701E-02 | 0.000E+00 | -1.459E-02 | 0.000E+00 | -1.306E-02 | 0.000E+00 | 0.000E+00 | -9.126E-03 |
| Throt * Fuel; | 0.000E+00 | 6.051E+00 | -5.114E+00 | -3.232E+00 | -3.244E+00 | -1.255E+00 | -4.342E+00 | 4.279E-01 | -9.892E-01 | -3.668E+00 |
| Throt * CAM; | 1.295E-02 | 1.725E-02 | 1.021E-02 | 1.156E-02 | -6.516E-03 | 3.120E-02 | 0.000E+00 | 1.930E-02 | -4.879E-03 | 5.778E-03 |
| Throt * SPK; | 0.000E+00 | -1.060E-01 | 0.000E+00 | 6.353E-02 | 0.000E+00 | 2.236E-01 | 0.000E+00 | -6.653E-02 | 0.000E+00 | 4.856E-02 |
| EGR * Fuel; | 2.776E+00 | 2.346E+00 | 2.169E+00 | 1.189E+00 | 3.414E-01 | 3.523E-01 | 2.832E+00 | 0.000E+00 | 1.418E+00 | 1.181E+00 |
| EGR * CAM; | -5.635E-03 | -5.789E-03 | -1.003E-02 | -4.895E-03 | -1.665E-03 | -6.956E-03 | 0.000E+00 | -4.482E-03 | -3.931E-03 | 0.000E+00 |
| EGR * SPK; | 0.000E+00 | -4.177E-02 | 0.000E+00 | -1.599E-02 | 0.000E+00 | -3.702E-02 | 0.000E+00 | 1.732E-02 | -4.223E-02 | 0.000E+00 |
| Fuel * CAM; | -8.968E-01 | -1.563E+00 | -1.446E+00 | -1.034E+00 | -7.838E-01 | -1.523E+00 | -5.663E-01 | -3.028E-01 | -3.892E-01 | 7.245E-01 |
| Fuel * SPK; | 0.000E+00 | 1.645E-01 | -2.658E+00 | -7.397E+00 | 2.354E+00 | -1.060E+01 | 0.000E+00 | -1.399E+00 | -9.225E+00 | 3.470E+00 |
| CAM * SPK; | 3.167E-02 | 1.321E-01 | 9.697E-02 | 4.361E-02 | 7.027E-02 | 0.000E+00 | 0.000E+00 | -1.145E-02 | 0.000E+00 | 0.000E+00 |

High Model - BSFC

| | ENGINE SPEED (rev/min) | | | | | | | | | |
|---|---|---|---|---|---|---|---|---|---|---|
| COEFFICIENTS | 1200 | 1400 | 1500 | 1700 | 1800 | 2000 | 2200 | 2400 | 2600 | 3000 |
| Const | 2.725E+02 | 4.870E+02 | 3.711E+02 | 4.035E+02 | 5.376E+02 | 3.948E+02 | 4.699E+02 | 4.989E+02 | 3.573E+02 | 4.581E+02 |
| Throt; | 8.474E-02 | 4.418E-01 | -2.753E-01 | 9.936E-01 | -4.725E-01 | 7.185E-01 | 2.035E-01 | 4.831E-01 | 4.823E-01 | 1.601E-01 |
| EGR; | -1.620E-01 | -1.677E+00 | -9.013E-01 | -3.211E-01 | -9.140E-01 | 8.243E-01 | -9.339E-01 | -1.360E+00 | -9.806E-01 | -8.764E-01 |
| Fuel; | -1.486E+01 | -3.844E+02 | -1.772E+02 | -3.343E+02 | -4.580E+02 | -3.018E+02 | -3.897E+02 | -4.568E+02 | -1.915E+02 | -3.763E+02 |
| CAM; | 3.068E-01 | 1.075E+00 | 1.133E+00 | 1.039E+00 | 1.164E+00 | 1.398E+00 | 1.097E+00 | 8.342E-01 | -1.875E-02 | 4.139E-01 |
| SPK; | -2.162E+00 | 8.696E+00 | -1.399E+00 | 4.675E+00 | 2.640E+00 | 5.010E+00 | 7.226E+00 | 5.020E+00 | -9.083E-01 | 4.396E+00 |
| Throt^2; | -4.525E-03 | -1.872E-04 | 2.729E-03 | -7.114E-03 | 0.000E+00 | -2.384E-03 | -2.512E-03 | -5.777E-04 | 1.074E-03 | -1.319E-03 |
| EGR^2; | 1.279E-03 | 2.520E-03 | 1.793E-03 | 5.171E-04 | 0.000E+00 | -2.709E-03 | 1.517E-03 | 3.200E-03 | 2.267E-03 | 2.068E-03 |
| Fuel^2; | -2.581E+01 | 1.423E+02 | 5.836E+01 | 1.296E+02 | 1.635E+02 | 1.203E+02 | 1.455E+02 | 1.855E+02 | 6.963E+01 | 1.433E+02 |
| CAM^2; | 8.089E-03 | -5.238E-03 | 0.000E+00 | 8.896E-03 | -1.050E-02 | 0.000E+00 | -4.971E-03 | 0.000E+00 | 6.270E-03 | -1.620E-03 |
| SPK^2; | 3.964E-01 | 5.968E-01 | 1.093E-01 | 5.040E-01 | 6.183E-01 | 0.000E+00 | 0.000E+00 | -4.367E-01 | 2.929E-01 | 0.000E+00 |
| Throt * EGR; | 9.862E-04 | -1.525E-03 | -1.730E-03 | -1.175E-03 | 8.496E-04 | 0.000E+00 | 0.000E+00 | -7.690E-04 | -5.866E-04 | -1.563E-03 |
| Throt * Fuel; | 3.758E-01 | -3.900E-01 | -1.753E-01 | 0.000E+00 | 3.464E-01 | -3.117E-01 | 0.000E+00 | -3.995E-01 | -4.838E-01 | 0.000E+00 |
| Throt * CAM; | 3.394E-03 | 0.000E+00 | 3.023E-03 | 0.000E+00 | 0.000E+00 | 0.000E+00 | 3.562E-03 | 2.811E-03 | -1.650E-03 | 2.432E-03 |
| Throt * SPK; | 1.893E-02 | 2.333E-02 | 3.260E-02 | 0.000E+00 | 0.000E+00 | 0.000E+00 | 2.350E-02 | 1.367E-02 | 7.128E-03 | 4.742E-03 |
| EGR * Fuel; | 0.000E+00 | 1.381E+00 | 7.608E-01 | 4.343E-01 | 8.805E-01 | -4.681E-01 | 9.236E-01 | 1.103E+00 | 7.677E-01 | 8.708E-01 |
| EGR * CAM; | -5.749E-03 | 5.106E-04 | 0.000E+00 | -2.519E-03 | -2.610E-03 | 0.000E+00 | -4.547E-03 | 1.616E-03 | 0.000E+00 | -6.569E-04 |
| EGR * SPK; | -9.529E-03 | -3.300E-02 | 0.000E+00 | -1.977E-02 | -1.455E-02 | -2.619E-02 | -2.138E-02 | 0.000E+00 | 6.059E-03 | -6.025E-03 |
| Fuel * CAM; | -4.457E-01 | -5.722E-01 | -8.696E-01 | -1.031E+00 | -4.765E-01 | -1.007E+00 | -7.406E-01 | -9.482E-01 | -1.977E-01 | -4.750E-01 |
| Fuel * SPK; | 0.000E+00 | -9.888E+00 | 0.000E+00 | -5.084E+00 | -4.738E+00 | -2.799E+00 | -5.583E+00 | -2.395E+00 | -1.015E+00 | -3.144E+00 |
| CAM * SPK; | 8.462E-02 | 4.101E-02 | 0.000E+00 | 4.649E-02 | 7.103E-02 | 3.834E-02 | 2.256E-02 | 6.275E-02 | 5.694E-02 | 0.000E+00 |

**Low Model - Nox Emissions**

| | ENGINE SPEED (rev/min) | | | | | | | | | |
|---|---|---|---|---|---|---|---|---|---|---|
| COEFFICIENTS | 1200 | 1400 | 1500 | 1700 | 1800 | 2000 | 2200 | 2400 | 2600 | 3000 |
| Const | -1.189E+02 | -1.180E+02 | -7.754E+01 | -6.384E+01 | -9.215E+01 | -1.776E+02 | -1.341E+02 | -5.463E+01 | -6.819E+00 | -2.095E+02 |
| Throt; | -1.205E+00 | 1.220E+00 | -3.731E-01 | 4.645E-01 | -1.827E+00 | 5.592E-01 | 2.802E+00 | -2.941E-01 | -1.783E+00 | -5.527E-01 |
| EGR; | -2.276E-01 | -6.141E-01 | -1.737E-01 | -4.905E-01 | -1.857E-01 | -2.229E-01 | -1.494E-01 | -1.283E+00 | -2.190E-01 | 2.362E-01 |
| Fuel; | 2.623E+02 | 2.220E+02 | 2.032E+02 | 1.407E+02 | 2.259E+02 | 3.222E+02 | 2.214E+02 | 1.361E+02 | 8.686E+01 | 4.213E+02 |
| CAM; | -3.764E-01 | -2.171E-01 | -6.660E-01 | -1.525E-02 | 9.037E-02 | 4.051E-01 | 5.771E-01 | -1.533E-01 | 2.844E-01 | 1.496E-01 |
| SPK; | 3.856E+00 | -3.423E-01 | -2.108E+00 | -1.246E+00 | 8.171E-02 | -2.235E-01 | -4.657E+00 | 1.542E+00 | -2.230E+00 | -1.776E+00 |
| Throt^2; | -5.371E-03 | 0.000E+00 | -2.662E-02 | -8.993E-03 | 2.268E-02 | 0.000E+00 | -4.791E-02 | 4.103E-02 | 4.917E-02 | -5.646E-03 |
| EGR^2; | 2.226E-03 | 2.273E-03 | 1.733E-03 | 1.797E-03 | 3.119E-03 | 2.377E-03 | 1.659E-03 | 5.487E-03 | 9.261E-04 | 6.561E-04 |
| Fuel^2; | -1.327E+02 | -8.207E+01 | -1.101E+02 | -6.093E+01 | -9.810E+01 | -1.214E+02 | -8.145E+01 | -4.051E+01 | -3.279E+01 | -1.921E+02 |
| CAM^2; | -4.547E-03 | -1.841E-03 | 0.000E+00 | -3.871E-04 | 6.566E-04 | 0.000E+00 | 6.421E-03 | -9.569E-03 | -5.880E-03 | -7.484E-03 |
| SPK^2; | 3.792E-02 | 5.559E-02 | 2.249E-01 | 1.734E-01 | -9.764E-02 | 0.000E+00 | 9.158E-02 | -1.025E-01 | -1.174E-01 | -4.910E-02 |
| Throt * EGR; | 0.000E+00 | 6.993E-03 | 6.160E-03 | 3.674E-03 | 5.895E-04 | 4.108E-03 | 9.496E-03 | 0.000E+00 | 5.192E-03 | 3.338E-03 |
| Throt * Fuel; | 1.709E+00 | -1.256E+00 | 1.425E+00 | 0.000E+00 | 6.512E-01 | -7.114E-01 | -8.255E-01 | -1.562E+00 | -5.800E-01 | 8.094E-01 |
| Throt * CAM; | 0.000E+00 | 5.901E-03 | 3.858E-03 | 4.775E-03 | 1.279E-02 | 9.493E-03 | 7.052E-03 | 2.867E-03 | 4.952E-03 | 2.317E-03 |
| Throt * SPK; | 0.000E+00 | 1.427E-02 | 0.000E+00 | -1.737E-02 | -6.953E-03 | 0.000E+00 | -2.435E-02 | -5.776E-02 | 0.000E+00 | 2.439E-02 |
| EGR * Fuel; | -1.717E-01 | 0.000E+00 | -4.129E-01 | 0.000E+00 | -3.102E-01 | -2.821E-01 | -4.909E-01 | 5.590E-01 | -1.828E-01 | -5.566E-01 |
| EGR * CAM; | 1.455E-03 | 1.459E-03 | 3.078E-03 | 1.498E-03 | 4.571E-04 | 1.182E-03 | 7.984E-04 | 1.872E-03 | 0.000E+00 | 0.000E+00 |
| EGR * SPK; | 0.000E+00 | 4.810E-03 | 9.622E-03 | 7.428E-03 | 1.178E-02 | 0.000E+00 | 1.276E-02 | 2.557E-03 | 2.015E-03 | 0.000E+00 |
| Fuel * CAM; | 3.971E-01 | 0.000E+00 | 3.304E-01 | -2.315E-01 | -5.358E-01 | -7.385E-01 | -1.047E+00 | 2.385E-01 | -1.801E-01 | 0.000E+00 |
| Fuel * SPK; | -4.462E+00 | -8.271E-01 | 0.000E+00 | 0.000E+00 | 0.000E+00 | 0.000E+00 | 4.084E+00 | 0.000E+00 | 2.350E+00 | 6.217E-01 |
| CAM * SPK; | 8.878E-03 | -6.007E-03 | 0.000E+00 | 0.000E+00 | 0.000E+00 | 0.000E+00 | -1.396E-02 | 7.362E-03 | -1.650E-02 | 0.000E+00 |

**High Model - NOx Emissions**

| | ENGINE SPEED (rev/min) | | | | | | | | | |
|---|---|---|---|---|---|---|---|---|---|---|
| COEFFICIENTS | 1200 | 1400 | 1500 | 1700 | 1800 | 2000 | 2200 | 2400 | 2600 | 3000 |
| Const | -3.782E+01 | -8.934E+01 | -3.845E+01 | 6.295E+01 | -2.184E+02 | -7.865E+01 | -6.097E+01 | -1.557E+02 | -2.846E+01 | -1.886E+02 |
| Throt; | 2.652E-01 | 2.081E-01 | 3.165E-01 | 5.154E-01 | 6.170E-01 | -8.440E-02 | 5.486E-02 | -5.654E-02 | 1.091E-02 | 2.611E-01 |
| EGR; | -3.497E-01 | -1.327E-01 | -2.207E-01 | -8.323E-01 | -2.272E-01 | 0.000E+00 | -7.251E-01 | 2.369E-01 | 2.737E-02 | 2.509E-01 |
| Fuel; | 9.187E+01 | 1.764E+02 | 9.316E+01 | -4.758E+01 | 3.751E+02 | 1.621E+02 | 1.307E+02 | 3.002E+02 | 5.941E+01 | 3.525E+02 |
| CAM; | 7.249E-02 | 1.902E-01 | -2.107E-01 | -8.529E-01 | 1.963E-01 | 6.817E-01 | 9.042E-01 | 7.332E-02 | 6.551E-01 | -3.160E-01 |
| SPK; | 1.407E+00 | -2.488E-01 | 5.864E-01 | -3.666E+00 | 1.421E+00 | 1.149E+00 | 1.658E+00 | -2.200E-01 | 4.116E+00 | -3.327E+00 |
| Throt^2; | -1.340E-03 | -1.364E-03 | -1.774E-03 | 1.941E-04 | -3.147E-04 | 1.215E-03 | -6.442E-04 | 7.519E-04 | -1.210E-03 | -1.135E-03 |
| EGR^2; | 8.061E-04 | 1.565E-03 | 5.329E-04 | 1.636E-03 | 9.534E-04 | -8.724E-04 | 2.305E-03 | 0.000E+00 | 0.000E+00 | 0.000E+00 |
| Fuel^2; | -4.258E+01 | -7.648E+01 | -4.344E+01 | 1.136E+01 | -1.463E+02 | -6.247E+01 | -5.208E+01 | -1.228E+02 | -1.386E+01 | -1.470E+02 |
| CAM^2; | 2.543E-03 | 4.077E-03 | 7.338E-03 | 3.511E-03 | 5.752E-03 | 6.005E-03 | -2.364E-03 | 1.742E-03 | 5.624E-04 | 6.010E-03 |
| SPK^2; | 4.237E-02 | -1.765E-02 | 6.902E-02 | -1.434E-01 | 0.000E+00 | 0.000E+00 | 0.000E+00 | 8.245E-02 | -7.144E-02 | 1.326E-01 |
| Throt * EGR; | -2.734E-04 | -8.523E-05 | 4.679E-04 | -1.216E-03 | -9.169E-04 | 5.714E-04 | 0.000E+00 | 1.443E-04 | 9.294E-04 | 4.458E-04 |
| Throt * Fuel; | 0.000E+00 | 6.197E-02 | 0.000E+00 | -3.486E-01 | -3.951E-01 | 0.000E+00 | 0.000E+00 | -3.214E-02 | 5.557E-02 | -8.080E-02 |
| Throt * CAM; | -1.041E-03 | -2.121E-03 | -1.477E-03 | -9.022E-04 | -1.798E-03 | -1.569E-03 | 1.440E-03 | -6.594E-04 | 9.434E-04 | 0.000E+00 |
| Throt * SPK; | -3.865E-03 | -7.022E-03 | -8.535E-03 | 0.000E+00 | 0.000E+00 | 0.000E+00 | 8.515E-03 | 0.000E+00 | 2.367E-03 | 3.577E-03 |
| EGR * Fuel; | 1.351E-01 | -1.460E-01 | 0.000E+00 | 4.435E-01 | 0.000E+00 | 0.000E+00 | 3.687E-01 | -3.608E-01 | -1.808E-01 | -4.097E-01 |
| EGR * CAM; | 6.391E-04 | 8.711E-05 | 0.000E+00 | 3.205E-03 | 1.274E-03 | -6.285E-04 | -1.694E-03 | 0.000E+00 | 0.000E+00 | 5.337E-04 |
| EGR * SPK; | 0.000E+00 | 3.899E-03 | -3.974E-03 | 1.583E-02 | 0.000E+00 | 0.000E+00 | 0.000E+00 | 0.000E+00 | -3.919E-03 | 0.000E+00 |
| Fuel * CAM; | -2.284E-01 | -2.943E-01 | -1.280E-01 | 3.179E-01 | -4.285E-01 | -8.478E-01 | -7.558E-01 | -1.365E-01 | -7.238E-01 | 0.000E+00 |
| Fuel * SPK; | -2.073E+00 | 0.000E+00 | -9.762E-01 | 2.140E+00 | -1.448E+00 | -1.850E+00 | -2.194E+00 | -5.877E-01 | -3.562E+00 | 1.460E+00 |
| CAM * SPK; | 1.276E-02 | 1.625E-03 | 1.990E-02 | 2.010E-02 | -1.247E-02 | 1.164E-02 | -1.304E-02 | -6.371E-03 | -3.444E-03 | 8.143E-03 |

**Low Model - CO2 emissions**

| | ENGINE SPEED (rev/min) | | | | | | | | | |
|---|---|---|---|---|---|---|---|---|---|---|
| COEFFICIENTS | 1200 | 1400 | 1500 | 1700 | 1800 | 2000 | 2200 | 2400 | 2600 | 3000 |
| Const | 2.981E+00 | 4.634E+00 | 5.219E+00 | 4.336E+00 | 3.872E+00 | 3.517E+00 | 5.067E+00 | 3.934E+00 | 5.983E+00 | 4.338E+00 |
| Throt; | 1.692E-02 | -1.378E-02 | 1.007E-02 | -2.350E-04 | 1.159E-02 | 6.302E-02 | -1.457E-02 | -4.177E-03 | 7.129E-04 | -1.000E-02 |
| EGR; | 1.077E-02 | -2.757E-03 | -6.776E-03 | 6.398E-03 | 8.766E-04 | 4.773E-03 | 1.137E-03 | -5.809E-03 | -8.663E-03 | 7.523E-03 |
| Fuel; | -4.670E+00 | -6.859E+00 | -8.222E+00 | -6.744E+00 | -6.111E+00 | -6.594E+00 | -7.863E+00 | -5.437E+00 | -9.135E+00 | -6.323E+00 |
| CAM; | -1.131E-04 | 3.733E-03 | 5.302E-04 | 9.827E-04 | 6.275E-04 | 1.402E-03 | 2.388E-03 | -1.115E-02 | -7.276E-03 | -2.721E-03 |
| SPK; | -1.977E-02 | -1.099E-02 | -2.056E-02 | 6.859E-04 | 3.784E-03 | 1.211E-02 | 4.495E-02 | -5.332E-02 | 3.447E-02 | -8.283E-03 |
| Throt^2; | -1.701E-05 | -5.649E-05 | -9.296E-05 | 1.052E-04 | -9.922E-05 | 0.000E+00 | 3.522E-04 | -2.879E-04 | 1.960E-04 | 1.087E-04 |
| EGR^2; | -2.265E-05 | 2.872E-06 | 6.804E-06 | -1.202E-05 | -3.336E-05 | 0.000E+00 | 0.000E+00 | 0.000E+00 | 2.059E-05 | -6.676E-06 |
| Fuel^2; | 1.865E+00 | 2.431E+00 | 3.231E+00 | 2.667E+00 | 2.410E+00 | 3.027E+00 | 3.107E+00 | 1.730E+00 | 3.613E+00 | 2.333E+00 |
| CAM^2; | 0.000E+00 | 3.395E-05 | 2.610E-05 | 0.000E+00 | -3.984E-05 | 6.052E-05 | 0.000E+00 | 8.425E-05 | 0.000E+00 | 0.000E+00 |
| SPK^2; | 2.921E-03 | 5.533E-04 | 2.539E-03 | -3.056E-04 | 1.878E-03 | 0.000E+00 | 0.000E+00 | 3.963E-03 | -1.883E-03 | -1.301E-03 |
| Throt * EGR; | 6.407E-05 | 9.483E-05 | 4.860E-05 | 7.886E-05 | 2.074E-04 | 0.000E+00 | 0.000E+00 | 1.417E-04 | 0.000E+00 | 0.000E+00 |
| Throt * Fuel; | -1.309E-02 | 1.653E-02 | -5.988E-03 | -3.794E-03 | -7.031E-03 | -4.997E-02 | 0.000E+00 | 1.629E-02 | -1.192E-02 | 2.155E-03 |
| Throt * CAM; | -7.910E-05 | 5.237E-05 | 0.000E+00 | 0.000E+00 | -3.779E-05 | -1.552E-04 | -5.241E-05 | -3.449E-05 | -8.017E-05 | 2.946E-05 |
| Throt * SPK; | -1.479E-04 | -3.478E-04 | 0.000E+00 | 0.000E+00 | 0.000E+00 | -1.535E-03 | 4.501E-04 | 0.000E+00 | 1.488E-03 | -1.326E-04 |
| EGR * Fuel; | -1.138E-02 | 0.000E+00 | 4.735E-03 | -7.516E-03 | -3.825E-03 | -5.291E-03 | 0.000E+00 | 1.528E-03 | 6.506E-03 | -6.327E-03 |
| EGR * CAM; | 2.200E-05 | -1.076E-05 | 0.000E+00 | -4.075E-06 | 3.949E-05 | 0.000E+00 | -2.970E-05 | 0.000E+00 | 1.654E-05 | 5.546E-06 |
| EGR * SPK; | 0.000E+00 | -2.064E-05 | 0.000E+00 | 0.000E+00 | -2.291E-04 | 0.000E+00 | -1.268E-04 | 1.002E-04 | -2.303E-04 | 0.000E+00 |
| Fuel * CAM; | 0.000E+00 | -5.471E-03 | -2.410E-03 | -1.370E-03 | 1.222E-03 | 0.000E+00 | 0.000E+00 | 6.765E-03 | 7.326E-03 | 2.174E-03 |
| Fuel * SPK; | 0.000E+00 | 1.301E-02 | 0.000E+00 | 0.000E+00 | -7.619E-03 | 2.781E-02 | -3.779E-02 | 2.363E-02 | -4.083E-02 | 2.270E-02 |
| CAM * SPK; | 3.907E-04 | 8.168E-05 | 3.358E-04 | 9.021E-05 | -1.425E-04 | 0.000E+00 | -4.146E-04 | 0.000E+00 | -2.420E-04 | -1.731E-04 |

**High Model - CO2 emissions**

| | ENGINE SPEED (rev/min) | | | | | | | | | |
|---|---|---|---|---|---|---|---|---|---|---|
| COEFFICIENTS | 1200 | 1400 | 1500 | 1700 | 1800 | 2000 | 2200 | 2400 | 2600 | 3000 |
| Const | 4.030E+00 | 5.132E+00 | 4.839E+00 | 3.864E+00 | 1.067E+01 | 4.246E+00 | 1.011E+01 | 6.127E+00 | 4.813E+00 | 3.658E+00 |
| Throt; | -2.924E-03 | 1.196E-03 | -8.693E-04 | -7.437E-05 | 1.369E-03 | -7.372E-04 | 1.123E-02 | 5.404E-03 | -1.013E-03 | 2.233E-04 |
| EGR; | 1.095E-04 | -9.563E-03 | -4.948E-03 | 8.030E-04 | -2.078E-03 | 0.000E+00 | 3.178E-03 | 1.007E-02 | 5.910E-03 | 4.807E-03 |
| Fuel; | -5.999E+00 | -7.800E+00 | -7.574E+00 | -5.998E+00 | -1.704E+01 | -6.173E+00 | -1.651E+01 | -9.735E+00 | -7.289E+00 | -5.593E+00 |
| CAM; | 1.369E-03 | 2.522E-03 | 9.354E-03 | 3.028E-03 | 7.649E-03 | -9.110E-03 | -1.821E-02 | -6.685E-03 | -1.823E-03 | 8.203E-04 |
| SPK; | -8.663E-03 | -4.015E-03 | 4.907E-02 | 2.664E-02 | -3.523E-02 | -1.124E-02 | -6.637E-03 | 3.268E-02 | -8.618E-03 | -1.371E-02 |
| Throt^2; | 1.678E-05 | -4.402E-06 | -1.292E-05 | -9.400E-06 | -6.799E-05 | 0.000E+00 | 0.000E+00 | 0.000E+00 | 1.016E-05 | -3.731E-06 |
| EGR^2; | 0.000E+00 | -2.196E-05 | 0.000E+00 | 0.000E+00 | 0.000E+00 | 1.348E-05 | -4.706E-05 | -1.869E-05 | -1.966E-05 | -1.063E-05 |
| Fuel^2; | 2.305E+00 | 2.920E+00 | 2.893E+00 | 2.311E+00 | 6.532E+00 | 2.282E+00 | 6.682E+00 | 3.727E+00 | 2.766E+00 | 2.140E+00 |
| CAM^2; | -5.866E-05 | 0.000E+00 | 0.000E+00 | 5.221E-05 | -2.030E-04 | 6.937E-05 | 1.797E-04 | 2.842E-05 | 4.068E-05 | -1.894E-05 |
| SPK^2; | 9.907E-04 | -2.581E-03 | -1.406E-03 | 1.300E-03 | 6.456E-03 | 0.000E+00 | 0.000E+00 | 0.000E+00 | 2.549E-04 | 0.000E+00 |
| Throt * EGR; | 1.859E-05 | 3.242E-05 | 7.260E-06 | -1.171E-05 | 2.222E-05 | 1.495E-05 | 8.661E-06 | -1.125E-05 | -3.024E-06 | 0.000E+00 |
| Throt * Fuel; | 0.000E+00 | 0.000E+00 | 2.330E-03 | 1.139E-03 | 7.286E-03 | 0.000E+00 | -8.823E-03 | -2.399E-03 | 0.000E+00 | 0.000E+00 |
| Throt * CAM; | -1.277E-05 | 0.000E+00 | -2.363E-05 | -1.990E-05 | 0.000E+00 | 0.000E+00 | 0.000E+00 | 0.000E+00 | -4.171E-06 | -1.387E-05 |
| Throt * SPK; | 0.000E+00 | -1.297E-04 | 0.000E+00 | 1.127E-04 | 0.000E+00 | 1.611E-04 | 0.000E+00 | -1.901E-04 | 1.941E-05 | 6.909E-05 |
| EGR * Fuel; | -1.852E-03 | 4.686E-03 | 3.490E-03 | 0.000E+00 | 0.000E+00 | 0.000E+00 | 0.000E+00 | -7.036E-03 | -3.924E-03 | -3.318E-03 |
| EGR * CAM; | 0.000E+00 | 6.566E-05 | 1.513E-05 | 0.000E+00 | 0.000E+00 | 0.000E+00 | 5.271E-05 | -2.027E-05 | 4.218E-06 | 3.419E-06 |
| EGR * SPK; | 1.082E-04 | 2.993E-04 | -1.062E-04 | -1.612E-04 | 0.000E+00 | 1.027E-04 | 0.000E+00 | 0.000E+00 | 0.000E+00 | 0.000E+00 |
| Fuel * CAM; | 1.085E-03 | -2.890E-03 | -5.550E-03 | -3.491E-03 | 0.000E+00 | 4.637E-03 | 5.423E-03 | 5.522E-03 | 0.000E+00 | 0.000E+00 |
| Fuel * SPK; | 0.000E+00 | 2.409E-02 | -3.028E-02 | -3.245E-02 | 0.000E+00 | 0.000E+00 | 0.000E+00 | -1.546E-02 | 4.441E-03 | 5.248E-03 |
| CAM * SPK; | 9.270E-05 | 1.707E-04 | -2.133E-04 | 1.089E-04 | 0.000E+00 | 0.000E+00 | 5.730E-04 | 0.000E+00 | 1.331E-04 | 1.383E-04 |

Low Model - CO emissions

| | ENGINE SPEED (rev/min) | | | | | | | | | |
|---|---|---|---|---|---|---|---|---|---|---|
| COEFFICIENTS | 1200 | 1400 | 1500 | 1700 | 1800 | 2000 | 2200 | 2400 | 2600 | 3000 |
| Const | -8.455E+00 | -5.605E+00 | -8.783E+00 | -8.628E+00 | -9.337E+00 | 1.225E+00 | 1.705E+00 | -1.385E+01 | -4.184E+00 | -4.833E+00 |
| Throt; | -2.593E-03 | 4.675E-02 | -5.689E-03 | 1.081E-02 | -2.706E-04 | -4.845E-02 | 2.043E-01 | -3.055E-02 | -3.979E-02 | 6.777E-02 |
| EGR; | -5.426E-03 | 1.359E-03 | -4.026E-03 | -1.353E-02 | 4.285E-04 | -9.162E-03 | -5.267E-02 | 1.287E-01 | 5.839E-02 | -9.463E-03 |
| Fuel; | 8.769E+00 | 3.279E+00 | 9.155E+00 | 8.770E+00 | 1.041E+01 | -6.239E+00 | -1.254E+01 | 1.833E+01 | 9.711E-01 | 1.334E+00 |
| CAM; | -1.070E-02 | -1.674E-02 | -7.231E-03 | -3.051E-03 | -2.729E-03 | -1.707E-02 | -1.417E-02 | 1.012E-02 | 4.670E-02 | -2.134E-02 |
| SPK; | -1.124E-01 | -1.204E-01 | 8.527E-03 | -3.537E-02 | -6.190E-02 | 2.802E-02 | -4.004E-02 | 1.130E-01 | -1.329E-01 | -1.347E-01 |
| Throt^2; | 5.548E-04 | -3.793E-04 | 5.457E-04 | 5.249E-04 | 1.223E-03 | -1.541E-03 | -6.039E-04 | 4.815E-04 | 3.997E-03 | 5.498E-04 |
| EGR^2; | 5.338E-06 | 0.000E+00 | 2.375E-05 | 5.004E-06 | -3.060E-05 | 0.000E+00 | -2.680E-05 | -1.095E-04 | -5.384E-05 | 2.189E-05 |
| Fuel^2; | 0.000E+00 | 2.501E+00 | 0.000E+00 | 2.361E-01 | -4.377E-01 | 5.828E+00 | 1.079E+01 | -4.032E+00 | 4.917E+00 | 4.089E+00 |
| CAM^2; | 8.027E-06 | 1.181E-04 | 2.209E-04 | 1.272E-04 | 9.012E-05 | 0.000E+00 | 2.333E-04 | -1.952E-04 | -3.176E-04 | 1.547E-04 |
| SPK^2; | 7.100E-03 | 1.764E-03 | -1.832E-03 | 3.146E-03 | 1.685E-03 | 0.000E+00 | 0.000E+00 | -6.523E-03 | 0.000E+00 | 3.371E-03 |
| Throt * EGR; | -1.356E-04 | -4.576E-05 | -2.302E-05 | -4.257E-05 | -8.494E-05 | 3.832E-04 | 0.000E+00 | -4.268E-04 | -7.368E-04 | 0.000E+00 |
| Throt * Fuel; | -1.418E-02 | -3.177E-02 | -1.838E-02 | -3.017E-02 | -4.659E-02 | 6.755E-02 | -1.631E-01 | 0.000E+00 | -1.355E-01 | -9.846E-02 |
| Throt * CAM; | -1.883E-04 | 6.810E-05 | -3.514E-05 | -7.746E-05 | -1.383E-04 | 7.378E-04 | 0.000E+00 | 2.549E-04 | 0.000E+00 | 0.000E+00 |
| Throt * SPK; | -1.336E-04 | 0.000E+00 | 5.959E-04 | 0.000E+00 | -4.731E-04 | 4.231E-03 | -2.652E-03 | 0.000E+00 | 0.000E+00 | -1.451E-04 |
| EGR * Fuel; | 8.336E-03 | 0.000E+00 | 5.857E-03 | 1.467E-02 | 4.305E-03 | 0.000E+00 | 5.189E-02 | -9.979E-02 | -2.993E-02 | 8.212E-03 |
| EGR * CAM; | 3.525E-05 | 2.261E-05 | -6.963E-05 | 0.000E+00 | 3.398E-05 | 0.000E+00 | 9.664E-05 | 0.000E+00 | -5.893E-05 | 0.000E+00 |
| EGR * SPK; | 1.182E-04 | -1.426E-04 | 0.000E+00 | 1.229E-05 | 1.299E-04 | 0.000E+00 | 0.000E+00 | -3.426E-04 | 2.343E-04 | 1.274E-04 |
| Fuel * CAM; | 1.136E-02 | 8.454E-03 | 0.000E+00 | -1.836E-03 | -1.423E-03 | 0.000E+00 | 0.000E+00 | -8.637E-03 | -2.282E-02 | 1.547E-02 |
| Fuel * SPK; | 6.371E-02 | 9.531E-02 | 0.000E+00 | 1.280E-02 | 4.172E-02 | -9.968E-02 | 9.068E-02 | -8.110E-02 | 1.566E-01 | 1.183E-01 |
| CAM * SPK; | 5.303E-04 | 3.222E-04 | 6.655E-05 | 2.196E-04 | 8.043E-04 | -1.360E-03 | 0.000E+00 | 0.000E+00 | -1.766E-03 | -4.603E-04 |

High Model - CO emissions

| | ENGINE SPEED (rev/min) | | | | | | | | | |
|---|---|---|---|---|---|---|---|---|---|---|
| COEFFICIENTS | 1200 | 1400 | 1500 | 1700 | 1800 | 2000 | 2200 | 2400 | 2600 | 3000 |
| Const | -8.226E+00 | -3.447E+00 | -8.960E+00 | -1.119E+01 | -2.826E+00 | -9.255E-01 | -8.682E-02 | 2.450E+00 | -3.567E+00 | -5.998E+00 |
| Throt; | 4.864E-03 | 1.063E-02 | 4.635E-03 | 4.047E-03 | -2.601E-02 | -4.413E-02 | -4.916E-03 | 9.401E-03 | 7.013E-03 | -5.065E-03 |
| EGR; | -1.112E-02 | 2.630E-02 | 2.131E-02 | 3.756E-03 | -2.107E-02 | 0.000E+00 | -5.631E-02 | -2.815E-02 | -2.528E-02 | -9.843E-03 |
| Fuel; | 8.328E+00 | -1.405E+00 | 8.873E+00 | 1.258E+01 | -5.974E-01 | -2.300E+00 | -5.787E+00 | -9.712E+00 | 1.508E+00 | 4.968E+00 |
| CAM; | -1.070E-02 | 3.798E-02 | 6.080E-03 | 9.666E-03 | 2.530E-03 | 5.130E-03 | 2.601E-02 | 1.510E-02 | -2.607E-02 | 1.414E-02 |
| SPK; | -1.896E-01 | -1.638E-01 | -1.248E-01 | 5.472E-02 | -8.178E-02 | -2.451E-02 | -9.617E-02 | 4.349E-02 | -1.492E-01 | 1.857E-02 |
| Throt^2; | -5.425E-05 | -1.015E-04 | 0.000E+00 | -9.260E-05 | -1.877E-05 | 8.305E-05 | -7.784E-05 | -7.123E-05 | 0.000E+00 | 1.885E-05 |
| EGR^2; | 1.168E-05 | -1.813E-05 | 4.028E-05 | -5.622E-06 | 0.000E+00 | -7.286E-05 | 7.227E-05 | 2.275E-05 | 1.042E-05 | 7.680E-06 |
| Fuel^2; | 0.000E+00 | 4.428E+00 | 0.000E+00 | -1.761E+00 | 3.436E+00 | 3.782E+00 | 5.840E+00 | 7.026E+00 | 2.412E+00 | 1.220E+00 |
| CAM^2; | 9.584E-05 | 2.563E-04 | 1.423E-04 | 4.835E-04 | -6.516E-05 | 0.000E+00 | -1.537E-04 | 0.000E+00 | 2.221E-04 | -5.169E-05 |
| SPK^2; | 4.419E-03 | 4.148E-03 | 5.248E-03 | -2.641E-03 | 1.067E-02 | 0.000E+00 | 7.400E-03 | 0.000E+00 | 2.223E-03 | 0.000E+00 |
| Throt * EGR; | 3.768E-06 | -6.050E-05 | -5.634E-05 | -9.691E-06 | 0.000E+00 | 8.373E-05 | 0.000E+00 | -1.749E-05 | -3.657E-05 | -1.108E-05 |
| Throt * Fuel; | 2.204E-03 | 2.156E-03 | -4.106E-03 | 1.012E-02 | 2.847E-02 | 3.233E-02 | 1.425E-02 | 2.750E-03 | -4.043E-03 | 2.809E-03 |
| Throt * CAM; | 0.000E+00 | 0.000E+00 | 0.000E+00 | -8.831E-05 | -4.972E-05 | -1.338E-04 | 0.000E+00 | -3.938E-05 | -2.129E-05 | -1.188E-05 |
| Throt * SPK; | 2.212E-04 | 4.221E-04 | 4.522E-04 | -2.220E-04 | 0.000E+00 | 0.000E+00 | 5.829E-04 | 0.000E+00 | 0.000E+00 | -6.061E-05 |
| EGR * Fuel; | 9.497E-03 | -5.841E-03 | -1.141E-02 | 0.000E+00 | 2.166E-02 | 0.000E+00 | 5.163E-02 | 2.762E-02 | 2.361E-02 | 1.055E-02 |
| EGR * CAM; | 0.000E+00 | -3.247E-04 | -1.609E-04 | -4.322E-05 | 0.000E+00 | 0.000E+00 | -1.209E-04 | -4.739E-05 | 5.306E-05 | -7.463E-06 |
| EGR * SPK; | 1.697E-04 | 0.000E+00 | 0.000E+00 | -3.986E-04 | -2.575E-04 | 0.000E+00 | 0.000E+00 | -3.808E-04 | 3.442E-04 | 0.000E+00 |
| Fuel * CAM; | 4.249E-03 | -4.042E-02 | -9.455E-03 | -2.066E-02 | 0.000E+00 | 0.000E+00 | -1.747E-02 | -1.174E-02 | 1.151E-02 | -1.062E-02 |
| Fuel * SPK; | 1.291E-01 | 1.058E-01 | 4.291E-02 | 0.000E+00 | 3.188E-02 | 0.000E+00 | 0.000E+00 | -2.388E-02 | 9.506E-02 | -1.101E-02 |
| CAM * SPK; | 6.381E-04 | 6.289E-04 | 3.671E-04 | 3.670E-04 | 5.532E-04 | 1.377E-03 | 7.073E-04 | 5.684E-04 | 8.499E-04 | 5.498E-05 |

**Low Model - uHC emissions**

| | ENGINE SPEED (rev/min) | | | | | | | | | |
|---|---|---|---|---|---|---|---|---|---|---|
| COEFFICIENTS | 1200 | 1400 | 1500 | 1700 | 1800 | 2000 | 2200 | 2400 | 2600 | 3000 |
| Const | -2.204E+01 | -2.613E+01 | 3.253E+01 | 5.184E+01 | 2.308E+00 | 1.065E+02 | 6.265E+01 | 7.612E+00 | -9.221E+00 | 5.721E-01 |
| Throt; | -1.426E+00 | -8.046E-01 | -1.064E+00 | -9.646E-01 | 5.570E-01 | -1.670E+00 | -6.170E-02 | 5.719E-02 | -5.729E-02 | -1.768E-02 |
| EGR; | 9.882E-01 | 6.447E-01 | 3.012E-01 | 5.871E-01 | 8.054E-01 | 2.898E-01 | 3.901E-01 | 7.357E-01 | 4.857E-01 | 3.781E-01 |
| Fuel; | 6.381E+01 | 5.426E+01 | -3.951E+01 | -7.083E+01 | -1.808E+01 | -1.476E+02 | -1.229E+02 | -1.343E+01 | 1.844E+01 | -1.776E-01 |
| CAM; | -2.949E-01 | 4.254E-03 | -3.056E-02 | 5.950E-02 | -1.400E-01 | -7.243E-03 | 1.318E-01 | 8.984E-02 | 1.755E-02 | -8.095E-03 |
| SPK; | -1.000E-01 | 2.075E-01 | -3.741E-01 | -9.939E-01 | -3.291E-01 | 1.160E-01 | 1.056E+00 | 2.656E-01 | -3.620E-01 | 1.353E-01 |
| Throt^2; | 3.664E-02 | 1.828E-02 | 2.458E-02 | 1.584E-02 | 1.161E-02 | 1.646E-02 | 4.550E-02 | -1.451E-03 | 0.000E+00 | 4.568E-04 |
| EGR^2; | -2.082E-03 | -1.622E-03 | -1.609E-03 | -1.018E-03 | -2.471E-03 | -1.853E-03 | -1.713E-03 | -2.347E-03 | -1.511E-03 | -1.635E-03 |
| Fuel^2; | -2.903E+01 | -2.141E+01 | 1.661E+01 | 2.721E+01 | 1.762E+01 | 5.386E+01 | 7.570E+01 | 5.567E+00 | -7.575E+00 | -1.666E-01 |
| CAM^2; | 1.944E-03 | 1.658E-03 | 2.068E-03 | 7.314E-04 | 2.264E-03 | -1.260E-03 | 2.363E-03 | -8.816E-04 | -8.580E-04 | -9.785E-04 |
| SPK^2; | 4.829E-02 | 0.000E+00 | 9.660E-02 | 8.993E-02 | 1.488E-01 | 0.000E+00 | -7.316E-02 | -5.022E-02 | 1.150E-03 | -4.139E-02 |
| Throt * EGR; | -1.239E-02 | -1.412E-02 | -1.209E-02 | -1.491E-02 | -1.160E-02 | -5.609E-03 | -1.173E-02 | -4.316E-03 | -4.493E-03 | -2.211E-03 |
| Throt * Fuel; | 0.000E+00 | 0.000E+00 | 0.000E+00 | 2.117E-01 | -8.919E-01 | 7.312E-01 | -1.801E+00 | 0.000E+00 | 0.000E+00 | 0.000E+00 |
| Throt * CAM; | -3.695E-03 | 8.855E-04 | -7.531E-04 | 0.000E+00 | -1.531E-03 | 3.711E-03 | 2.633E-03 | 0.000E+00 | 1.923E-03 | 0.000E+00 |
| Throt * SPK; | -2.101E-02 | 0.000E+00 | 1.567E-02 | 1.158E-02 | -2.824E-02 | 1.481E-02 | -2.702E-02 | 1.751E-03 | 0.000E+00 | -4.313E-03 |
| EGR * Fuel; | -1.853E-01 | 1.719E-01 | 4.437E-01 | 2.025E-01 | 0.000E+00 | 2.926E-01 | 3.443E-01 | -1.456E-01 | 0.000E+00 | 4.111E-02 |
| EGR * CAM; | 9.724E-04 | 0.000E+00 | 6.222E-04 | 0.000E+00 | 8.214E-04 | 2.742E-04 | 0.000E+00 | 1.987E-04 | 2.154E-04 | 1.491E-04 |
| EGR * SPK; | 2.802E-03 | -8.276E-04 | 0.000E+00 | 0.000E+00 | -1.219E-03 | -2.043E-03 | 1.355E-03 | 7.249E-04 | 5.108E-04 | 9.369E-04 |
| Fuel * CAM; | 2.380E-01 | -3.598E-02 | 0.000E+00 | -5.519E-02 | 5.594E-02 | 0.000E+00 | -2.468E-01 | -4.532E-02 | -2.639E-02 | 4.702E-02 |
| Fuel * SPK; | 0.000E+00 | 0.000E+00 | -1.996E-01 | 3.394E-01 | 0.000E+00 | -2.899E-01 | 0.000E+00 | 0.000E+00 | 3.227E-01 | 2.276E-01 |
| CAM * SPK; | 1.252E-02 | -1.102E-02 | -1.378E-02 | -9.143E-03 | 5.401E-03 | -1.464E-02 | 0.000E+00 | 0.000E+00 | -1.482E-03 | -2.679E-03 |

**High Model - uHC emissions**

| | ENGINE SPEED (rev/min) | | | | | | | | | |
|---|---|---|---|---|---|---|---|---|---|---|
| COEFFICIENTS | 1200 | 1400 | 1500 | 1700 | 1800 | 2000 | 2200 | 2400 | 2600 | 3000 |
| Const | -2.204E+01 | -2.613E+01 | 3.253E+01 | 5.184E+01 | 2.308E+00 | 1.065E+02 | 6.265E+01 | 7.612E+00 | -9.221E+00 | 5.721E-01 |
| Throt; | -1.426E+00 | -8.046E-01 | -1.064E+00 | -9.646E-01 | 5.570E-01 | -1.670E+00 | -6.170E-02 | 5.719E-02 | -5.729E-02 | -1.768E-02 |
| EGR; | 9.882E-01 | 6.447E-01 | 3.012E-01 | 5.871E-01 | 8.054E-01 | 2.898E-01 | 3.901E-01 | 7.357E-01 | 4.857E-01 | 3.781E-01 |
| Fuel; | 6.381E+01 | 5.426E+01 | -3.951E+01 | -7.083E+01 | -1.808E+01 | -1.476E+02 | -1.229E+02 | -1.343E+01 | 1.844E+01 | -1.776E-01 |
| CAM; | -2.949E-01 | 4.254E-03 | -3.056E-02 | 5.950E-02 | -1.400E-01 | -7.243E-03 | 1.318E-01 | 8.984E-02 | 1.755E-02 | -8.095E-03 |
| SPK; | -1.000E-01 | 2.075E-01 | -3.741E-01 | -9.939E-01 | -3.291E-01 | 1.160E-01 | 1.056E+00 | 2.656E-01 | -3.620E-01 | 1.353E-01 |
| Throt^2; | 3.664E-02 | 1.828E-02 | 2.458E-02 | 1.584E-02 | 1.161E-02 | 1.646E-02 | 4.550E-02 | -1.451E-03 | 0.000E+00 | 4.568E-04 |
| EGR^2; | -2.082E-03 | -1.622E-03 | -1.609E-03 | -1.018E-03 | -2.471E-03 | -1.853E-03 | -1.713E-03 | -2.347E-03 | -1.511E-03 | -1.635E-03 |
| Fuel^2; | -2.903E+01 | -2.141E+01 | 1.661E+01 | 2.721E+01 | 1.762E+01 | 5.386E+01 | 7.570E+01 | 5.567E+00 | -7.575E+00 | -1.666E-01 |
| CAM^2; | 1.944E-03 | 1.658E-03 | 2.068E-03 | 7.314E-04 | 2.264E-03 | -1.260E-03 | 2.363E-03 | -8.816E-04 | -8.580E-04 | -9.785E-04 |
| SPK^2; | 4.829E-02 | 0.000E+00 | 9.660E-02 | 8.993E-02 | 1.488E-01 | 0.000E+00 | -7.316E-02 | -5.022E-02 | 1.150E-03 | -4.139E-02 |
| Throt * EGR; | -1.239E-02 | -1.412E-02 | -1.209E-02 | -1.491E-02 | -1.160E-02 | -5.609E-03 | -1.173E-02 | -4.316E-03 | -4.493E-03 | -2.211E-03 |
| Throt * Fuel; | 0.000E+00 | 0.000E+00 | 0.000E+00 | 2.117E-01 | -8.919E-01 | 7.312E-01 | -1.801E+00 | 0.000E+00 | 0.000E+00 | 0.000E+00 |
| Throt * CAM; | -3.695E-03 | 8.855E-04 | -7.531E-04 | 0.000E+00 | -1.531E-03 | 3.711E-03 | 2.633E-03 | 0.000E+00 | 1.923E-03 | 0.000E+00 |
| Throt * SPK; | -2.101E-02 | 0.000E+00 | 1.567E-02 | 1.158E-02 | -2.824E-02 | 1.481E-02 | -2.702E-02 | 1.751E-03 | 0.000E+00 | -4.313E-03 |
| EGR * Fuel; | -1.853E-01 | 1.719E-01 | 4.437E-01 | 2.025E-01 | 0.000E+00 | 2.926E-01 | 3.443E-01 | -1.456E-01 | 0.000E+00 | 4.111E-02 |
| EGR * CAM; | 9.724E-04 | 0.000E+00 | 6.222E-04 | 0.000E+00 | 8.214E-04 | 2.742E-04 | 0.000E+00 | 1.987E-04 | 2.154E-04 | 1.491E-04 |
| EGR * SPK; | 2.802E-03 | -8.276E-04 | 0.000E+00 | 0.000E+00 | -1.219E-03 | -2.043E-03 | 1.355E-03 | 7.249E-04 | 5.108E-04 | 9.369E-04 |
| Fuel * CAM; | 2.380E-01 | -3.598E-02 | 0.000E+00 | -5.519E-02 | 5.594E-02 | 0.000E+00 | -2.468E-01 | -4.532E-02 | -2.639E-02 | 4.702E-02 |
| Fuel * SPK; | 0.000E+00 | 0.000E+00 | -1.996E-01 | 3.394E-01 | 0.000E+00 | -2.899E-01 | 0.000E+00 | 0.000E+00 | 3.227E-01 | 2.276E-01 |
| CAM * SPK; | 1.252E-02 | -1.102E-02 | -1.378E-02 | -9.143E-03 | 5.401E-03 | -1.464E-02 | 0.000E+00 | 0.000E+00 | -1.482E-03 | -2.679E-03 |

# D. Appendix D

Matlab objective function

**The Matlab code consists of 5 major functions :**

- **GA code**
- **Objective function**
- **Spline fitting code**
- **TWC catalyst code**
- **De-Nox code**
- **Imposing dilution limits**
- **Transient response code**

**The following pages are the documented code which was been used.**

## Main body of GA

```
% Simple Genetic Algorithm - sga
%
% This script implements the Simple Genetic Algorithm described
% in the examples section of the GA Toolbox manual.
%
% Author:     Andrew Chipperfield
% Adapted by  R. D. Maugham
% History:    23-Mar-94     file created
%             03-Jan-02     modified University of bath to be used with DoE engine model
%=======================================================================================
%set global variables - done to speed up processing time
global power_demand
global x
global BSFCmin;
global BSFCmin2;
global Speed_min;
global Throttle_pos_opt;
global torque_opt;
global spark;
global cam_opt;
global BSFCMAP;
global Speed_pos;
global Opt_details
global Emiss_limits
global Eng_model;
global Uhc;
global relative_transient_performance
global glob_score
global speed_demand
global P_throt_time_torque
global P_EGR_time_torque
global P_fuel_time_torque
global P_cam_time_torque
global P_throt_torque_time
global P_EGR_torque_time
global P_fuel_torque_time
global P_cam_torque_time
%=======================================================================================
% define arrays as empty
Uhc=[];
Eng_model=[];
Opt_all_details=[];
Opt_all_details_speed=[];
%=======================================================================================
```

```
% load variables
load Uhc;               %uhc model from saved data
load Eng_model;         %other engine responses from engine model saved data
load Opt_details.mat;   %optimal base line engine conditions fuel=1 EGR=0 cam=max power; throt & spark only variables
load Emiss_limits.mat;  %emissions limits and catalyst efficiencys from EUDC 1.6l focus tests
load P
%=========================================================================
% Power tables - table of at which the engine performance is to be optimised
power_cond_table=[4 6 8 10 12 14 16 18 20 22 24 26 28 30 32 34 36 38 40];
%=========================================================================
% For engine speed loops - the model optimises individual power conditions at individual speeds
for j=10
    speed_demand=j;
    Opt_all_details=[];
    %=====================================================================
    % Power condition loop - power condition taken from power condition table
        for i=1:length(power_cond_table)
                power_demand=power_cond_table(i)
                NIND = 15;           % Number of individuals per subpopulations
                MAXGEN = 250;        % maximum Number of generations
                GGAP = .9;           % Generation gap, how many new individuals are created
                NVAR = 4;          % Generation gap, how many new individuals are created
                PRECI = 10;          % Precision of binary representation
                % Build field descriptor
                FieldD = [rep([PRECI],[1, NVAR]); rep([0;100],[1, NVAR]);...
              rep([1; 0; 1 ;1], [1, NVAR])];
                % Initialise population
                Chrom = crtbp(NIND, NVAR*PRECI);
                % Reset counters
                Best = NaN*ones(MAXGEN,1);    % best in current population
                gen = 0;                      % generational counter
                % Evaluate initial population
                ObjV = MyfirstOBJFUN1_noswitch(bs2rv(Chrom,FieldD));
                % Track best individual and display convergence
                Best(gen+1) = min(ObjV);
                plot(log10(Best),'ro');xlabel('generation'); ylabel('log10(f(x))');
                text(0.5,0.95,['Best = ', num2str(Best(gen+1))],'Units','normalized');
                drawnow;
    %=====================================================================
    % Set zeros for generational loop counters
                trig=0;
                cnts=0;
                cnts2=0;
    BSFCmin_old=0;
    BSFCmin_abs=9000;
    glob_score_old=0;
    glob_score_abs=10000;
    x_min=0;
    %=====================================================================
    % Generational loop
      while trig<1
        if gen>MAXGEN
            break
        end
                        % Assign fitness-value to entire population
          FitnV = ranking(ObjV);
                        % Select individuals for breeding
          SelCh = select('sus', Chrom, FitnV, GGAP);
                        % Recombine selected individuals (crossover)
          SelCh = recombin('xovsp',SelCh,0.7);
                        % Perform mutation on offspring
          SelCh = mut(SelCh);
                        % Evaluate offspring, call objective function
          ObjVSel = MyfirstOBJFUN1_noswitch(bs2rv(SelCh,FieldD));
          [min_score x_min_pos]=min(ObjVSel);
          x_min=bs2rv(SelCh(x_min_pos,:),FieldD);
                        % Reinsert offspring into current population
```

```
            [Chrom ObjV]=reins(Chrom,SelCh,1,1,ObjV,ObjVSel);
                        % Increment generational counter
            gen = gen+1;
                        % Update display and record current best individual
            Best(gen+1) = min(ObjV);
            plot(log10(Best),'ro'); xlabel('generation'); ylabel('log10(f(x))');
            text(0.5,0.95,['Best = ', num2str(Best(gen+1))],'Units','normalized');
            drawnow;
        % determine if a solution has converged
         BSFCmin=min_score;
         %=================================================================================
% determine if solution is not going to reached - if solution is not going to be reached set results          %to zero
        if (BSFCmin>9000) & (gen>50)
            BSFCmin=0; BSFCmin2=0; Speed_min=0; relative_transient_performance=0; Throttle_pos_opt=0;
            torque_opt=0; spark=0; cam_opt=0; cnts2=cnts2+1;
            %stop current power condition if solution is not possible
            if cnts2>10
              opt_all_details=[x_min';BSFCmin2;BSFCmin;Speed_min;relative_transient_performance;...
                 Throttle_pos_opt;torque_opt;spark;cam_opt];
                break
            end
        end
        %=================================================================================
        % convergance of generation loop - this loop trys to speed up the optimisation process.
        % it compares the current best with the global best. if the current best is close to the
        % global best and 50 generations have been processed then the counter is incremented by one
        % if the current is 2 better than the previous best then a new chromosone has been probably
        % been found and the counter is reset. When the counter reaches 16 it is deemed that the
        % power condition has been optimised.
        abs(BSFCmin-BSFCmin_abs) %displays the diffence
        if (abs(BSFCmin-BSFCmin_abs)<1.5) & gen>50
                %checks whether the current best solution is close to the absolute minimum
                cnts=cnts+1                         %increments counter by one
                if cnts>12
                    trig=1;
       %when counter reaches 16 trigger is set and power condition is deem to have been optimised
                end
            end
                            BSFCmin_old=BSFCmin;
            if (BSFCmin_old<BSFCmin_abs)
                 %check for large changes in BSFC and sets the variables to be recorded.
                BSFCmin_abs=BSFCmin_old;            %resets the absolute best solution
                opt_all_details=[x_min';BSFCmin2;BSFCmin;Speed_min;relative_transient_performance...
                          ;Throttle_pos_opt;torque_opt;spark;cam_opt];
                                                    % defines the variables to be recorded
                if (abs(BSFCmin_old-BSFCmin_abs)>5)
                    cnts=0                          %resets counter to zero
                end
            end
        end
        Opt_all_details=[Opt_all_details, opt_all_details];
        % End of GA
        end
    % if loop used to save approapriate speed information
    if speed_demand==1;
            Opt_all_details_1=Opt_all_details;
            save Opt_all_details_1 Opt_all_details_1;
        elseif speed_demand==2
            Opt_all_details_2=Opt_all_details;
            save Opt_all_details_2 Opt_all_details_2;
        elseif speed_demand==3
            Opt_all_details_3=Opt_all_details;
            save Opt_all_details_3 Opt_all_details_3;
        elseif speed_demand==4
            Opt_all_details_4=Opt_all_details;
            save Opt_all_details_4 Opt_all_details_4;
        elseif speed_demand==5
```

```
            Opt_all_details_5=Opt_all_details;
            save Opt_all_details_5 Opt_all_details_5;
        elseif speed_demand==6
            Opt_all_details_6=Opt_all_details;
            save Opt_all_details_6 Opt_all_details_6;
        elseif speed_demand==7
            Opt_all_details_7=Opt_all_details;
            save Opt_all_details_7 Opt_all_details_7;
        elseif speed_demand==8
            Opt_all_details_8=Opt_all_details;
            save Opt_all_details_8 Opt_all_details_8;
        elseif speed_demand==9
            Opt_all_details_9=Opt_all_details;
            save Opt_all_details_9 Opt_all_details_9;
        elseif speed_demand==10
            Opt_all_details_10=Opt_all_details;
            save Opt_all_details_10 Opt_all_details_10;
        end
end
%concatonates speed results into a single matrix
Opt_all_details_speed_10=cat(3,Opt_all_details_1,Opt_all_details_2,Opt_all_details_3,Opt_all_details_4,Opt_all_details_5,O
pt_all_details_6,Opt_all_details_7...
        ,Opt_all_details_8,Opt_all_details_9,Opt_all_details_10)
    save Opt_all_details_speed_10 Opt_all_details_speed_10
```

## Main objective function

```
function glob_score=fnctest2j(x,speed,torque_demand,speed_high_low)
%program structure -
%   1.  Load coefficients
%   2.  check a solution is possible
%   3.  determine join details for high low models and spline details
%   4.  determine where the join should be between high low models
%   5.  determine throttle setting for a given Torque requirement
%   6.  Evaluate other variables
%   7.  evalute uHC response
%   8.  Evaluate transient response variable
%   9.  Evlauate emissions response variable
%   10. Evaluate global response
%-------------------------------------------------------------------------------------------------------------------
% read / set global variables
global cam_opt;
global spark;
global torque_opt;
global Throttle_pos_opt;
global Speed_min;
global BSFCmin;
global BSFCmin2;
global BSFCMAP;
global power_demand;
global Speed_pos;
global relative_transient_performance
global glob_score
global Eng_model
%-------------------------------------------------------------------------------------------------------------------
%2. defines control variables and check limits
%make sure that there is a solution
glob_score=10000;
%-------------------------------------------------------------
%define control variables from chromosone
Fuel_per=x(1);
EGR_per=x(2);
CAM=(x(3)/100)*40;
SPK=(x(4)/100)*6;
%-------------------------------------------------------------
% 2. initial check
passfail1=check(Fuel_per,EGR_per,CAM,SPK,speed,torque_demand);
if passfail1==0
    glob_score=10000;
    return;
end
%-------------------------------------------------------------------------------------------------------------------
%3. calls join_variable_point_spline - to determine point of join and details of spline
%   Throt_high_low  - join details for all variables
%   pp              - spline details for all variables
%-------------------------------------------------------------------------------------------------------------------
[Throt_high_low,pp]=join_variable_point_spline(Fuel_per,EGR_per,SPK,CAM,speed);
%-------------------------------------------------------------------------------------------------------------------
% 4. Determine the throttle position for a given desired Torque at a given engine speed
%               this is achieved by iterating to find torques which fit with in logical limits
%               the largest throttle position for a given engine speed is the one recorded.
%-------------------------------------------------------------------------------------------------------------------
% Throttlepos       - the throttle position at which a required torque can be achieved
% Speed_pos         - the speeds at which a torque can be achieved
Speed_pos=[];
[Throttlepos,Speed_pos]=throttle_position_torque(Fuel_per,EGR_per,SPK,CAM,Throt_high_low,torque_demand,speed,pp);
%-------------------------------------------------------------------------
% exists objective function if no speed can achieve required power
if isempty(Speed_pos)
    glob_score=10000;
```

```
    return
else if Speed_pos==0;
    glob_score=10000;
    return
end
%_____________________________________________________________________________________________
% 5. Evaluate other responses at the throttle conditions for a given torque
%      - First we need to zero the matrixes again
%      - then impose the dilution bounds
%      - then evaluate the variables
% note for use with two stage gradient based solution model
% To use Eng_model array call Eng_model(u,v,w,x) where:-
%   u - is high or low (1 or 2 )
%   v - the ceofficient (1-21)
%   w - is the speed (1=1400; 2=1800; 2=2000; 4=2200, 5=2600)
%   x - is the response being examined (1=Torque; 2=BSFC; 3=FuelFlow; 4=Power; 5=NOx;
%                                       6=CO; 7=O2; 8=CO2; 9=Exhaust_press, 10=Exhaust_temp; Inletpress)
%=============================================================
% zero response arrays
TORQUEMAP=[]; BSFCMAP=[]; FUELFLOWMAP=[]; POWERMAP=[]; NOXMAP=[]; COMAP=[]; O2MAP=[]; CO2MAP=[];
EXHPRESSMAP=[]; EXHTEMPMAP=[]; INLPRESSMAP=[]; YOKAMAP=[]; UHCMAP=[]; spk=[]; cam=[]; vari_table=[];
%_____________________________________
%evaluate all variables
% defines the variables to be evaluated
vari_table=[1 2 3 4 5 6 7 8 9 10 11 16];
for variables=1:length(vari_table);
    vari=vari_table(variables);             %sets variable in question
    for speed=speed;                        %loop for test speed
                for Throt=Throttlepos;
                        %loop for throttle condition required to achieve require torque
            CALCULATED_VAL=[];                          % zeros calculated_val
            %switches between high and low models at approapriate throttle condition
            clip=Throt_high_low(variables);
            if Throt>clip;
                high_low=2;
            else
                high_low=1;
            end
            %_____________________________________________________________________________________
            % impose dilution boundary conditions
            [Fuel,EGR]=limits2(Fuel_per,EGR_per,Throt);
            for i=1:21;
                coefficient_index=(i);
                c(i)=0;
                c(i)=Eng_model(high_low,coefficient_index,speed,vari); %load variable coefficients
            end;
            %evaluate model at given condition
            f1 = c(2) * Throt;
            f2 = c(3) * EGR;
            f3 = c(4) * Fuel;
            f4 = c(5) * CAM;
            f5 = c(6) * SPK;
            f6 = c(7) * Throt^2;
            f7 = c(8) * EGR^2;
            f8 = c(9) * Fuel^2;
            f9 = c(10) * CAM^2;
            f10 = c(11) * SPK^2;
            f11 = c(12) * Throt * EGR;
            f12 = c(13) * Throt * Fuel;
            f13 = c(14) * Throt * CAM;
            f14 = c(15) * Throt * SPK;
            f15 = c(16) * EGR * Fuel;
            f16 = c(17) * EGR * CAM;
            f17 = c(18) * EGR * SPK;
            f18 = c(19) * Fuel * CAM;
            f19 = c(20) * Fuel * SPK;
            f20 = c(21) * CAM * SPK;
```

```
            Calculated_val = c(1) + f1 + f2 + f3 + f4 + f5 + f6 + f7 + f8 + f9 + f10 + f11 + ...
                    f12 + f13 + f14 + f15 + f16 + f17 + f18 + f19 + f20;
            %impose spline effects on approapriate operating conditions
            if Throt_high_low(variables)<7
                if Throt>=Throt_high_low(variables) & Throt<=Throt_high_low(variables)+5
                    Calculated_val=ppval(pp(variables),Throt);
                end
            elseif Throt_high_low(variables)>=7
                if Throt>=Throt_high_low(variables)-7 & Throt<=Throt_high_low(variables)+6
                    Calculated_val=ppval(pp(variables),Throt+1);
                end
            end
            CALCULATED_VAL=[CALCULATED_VAL Calculated_val];
        end
        %save results for approapraite variables
        if vari==1
            TORQUEMAP=[TORQUEMAP ; CALCULATED_VAL];
        elseif vari==2
            BSFCMAP=[BSFCMAP ; CALCULATED_VAL];
        elseif vari==3
            FUELFLOWMAP=[FUELFLOWMAP ; CALCULATED_VAL];
        elseif vari==4
            POWERMAP=[POWERMAP ; CALCULATED_VAL];
        elseif vari==5
            NOXMAP=[NOXMAP ; CALCULATED_VAL];
        elseif vari==6
            COMAP=[COMAP ; CALCULATED_VAL];
        elseif vari==7
            O2MAP=[O2MAP ; CALCULATED_VAL];
        elseif vari==8
            CO2MAP=[CO2MAP ; CALCULATED_VAL];
        elseif vari==9
            EXHPRESSMAP=[EXHPRESSMAP ; CALCULATED_VAL];
        elseif vari==10
            EXHTEMPMAP=[EXHTEMPMAP ; CALCULATED_VAL];
        elseif vari==11
            INLPRESSMAP=[INLPRESSMAP ; CALCULATED_VAL];
        elseif vari==16
            YOKAMAP=[YOKAMAP ; CALCULATED_VAL];
        end %variable
    end % throttle
end %speed
%_____________________________________________________________________________________________-
%7. evaluate unburnt hydrocarbons response and record uHC response
Uhc_pred=uhcmodel1(Speed_pos,Throttlepos,Fuel,Fuel_per,EGR,EGR_per,CAM,SPK);
UHCMAP=[UHCMAP Uhc_pred];
%_____________________________________________________________________________________________-
%8. evaluate torque response ability
% determines the relative transient response, either sets a minimum torque margin for throttle only control or
% determines the relative duration of torque margin liberation and engine acceleration
Relative_transient_performance=[];
if isempty(Speed_pos)
    Relative_transient_performance=[10000];
else

[relative_transient_performance]=driveabilty_version2(Speed_pos,TORQUEMAP,Throttlepos,CAM,EGR,SPK,power_demand,Fuel,speed_
high_low);
    Relative_transient_performance=[Relative_transient_performance relative_transient_performance];
end
%_____________________________________________________________________________________________-
%9. evaluate emissions response
% determines if the control conditions develop a condition where catalysts can reduce exhaust
% emissions to levels which meet legislative limits
Passfail=[];
if  isempty(Speed_pos)
    Passfail=[1000];
else
```

```
    [passfail]=catalyst_model(NOXMAP,COMAP,CO2MAP,UHCMAP,O2MAP,power_demand,EXHTEMPMAP,Fuel,YOKAMAP);
    Passfail=[Passfail passfail];
end
%_____________________________________
%change variable names
BSFCmin=BSFCMAP;
BSFCmin2=BSFCmin;
Pass=Passfail;
transient_performance=Relative_transient_performance;
Speed_min=Speed_pos;
Throttle_pos_opt=Throttlepos;
torque_opt=TORQUEMAP;
spark=spk;
cam_opt=cam;
%_____________________________________________________________________________________________-
%10. evaluate global score
%glob_score=(BSFCmin)*Pass;
glob_score=(BSFCmin+transient_performance*250)*Pass;
BSFCmin=glob_score;
return
end
```

## Spline fitting subroutine

```
function [Throt_high_low,pp]=join_variable_point_spline(Fuel_per,EGR_per,SPK,CAM,speed_range);
% set globals variables
global PP;
global Eng_model
%Structure of this section
%1. run both sets of Coefficients across throttle range
%2. Identify the direction of the variable (not required for just Torque calculations
%3. compare the maximum value of the lower range with the coresponding value of the upper range
%4. determine throttle position required for step change
%5. create spline for point where models join
%=========================================================================================
% stage 1.run both sets of cefficients over their full range
Throt_high_low=[];
pp=[];
variable_table=[1:11 16];
for vari_i=1:length(variable_table)
    vari=variable_table(vari_i);
    speed=speed_range;
    Torque_low=[];
    Torque_high=[];
    for high_low=1:2;
        cnts=0;
        throtl_high_low=0;
        for i=1:21; %evaluate coefficients
                coefficient_index=(i);
                c(i)=0;
                c(i)=Eng_model(high_low,coefficient_index,speed,vari);
         end;
         for Throt=0:1:80;
            %_____________________________________________________________________________________
            % impose dilution boundary conditions
            [Fuel,EGR]=limits2(Fuel_per,EGR_per,Throt);
            %_____________________________________________________________________________________
                        f1 = c(2) * Throt;
                        f2 = c(3) * EGR;
                        f3 = c(4) * Fuel;
                        f4 = c(5) * CAM;
                        f5 = c(6) * SPK;
                        f6 = c(7) * Throt^2;
                        f7 = c(8) * EGR^2;
                        f8 = c(9) * Fuel^2;
                        f9 = c(10) * CAM^2;
                        f10 = c(11) * SPK^2;
                        f11 = c(12) * Throt * EGR;
                        f12 = c(13) * Throt * Fuel;
                        f13 = c(14) * Throt * CAM;
                        f14 = c(15) * Throt * SPK;
                        f15 = c(16) * EGR * Fuel;
                        f16 = c(17) * EGR * CAM;
                        f17 = c(18) * EGR * SPK;
                        f18 = c(19) * Fuel * CAM;
                        f19 = c(20) * Fuel * SPK;
                        f20 = c(21) * CAM * SPK;
                        torque = c(1) + f1 + f2 + f3 + f4 + f5 + f6 + f7 + f8 + f9 + f10 + f11 + ...
                              f12 + f13 + f14 + f15 + f16 + f17 + f18 + f19 + f20;
                        if high_low==1;
                              Torque_low=[Torque_low torque]; %high throttle range
                      elseif high_low==2;
                              Torque_high=[Torque_high torque]; % low throttle range
                        End
        end % end throttle loop
    end     % end high low loop
%=========================================================================================
% Stage 2 - 3 - 4 identfiy general form of response; Then identify where curves meet
```

```
    throtl=2; % reset base value
    while (cnts<1) & (throtl<72)
        Torque_low(1)=Torque_low(2);
            if Torque_low(2)-Torque_low(3)<0;
                    %initially trace is accelerating i.e. becoming greater with throttle
                    % determine if lower region breaks through the high region
                if Torque_low(throtl)>Torque_high(throtl) & cnts<1;
                    cnts=1;
                    throt_high_low=throtl;
                %determine if lower rgion does not break the high region where the maximum of the lower region is
                elseif Torque_low(throtl)<Torque_low(throtl-1) & cnts<1 & throtl>15;
                    cnts=1;
                    throt_high_low=throtl-1;
                end
            else Torque_low(2)-Torque_low(3)>0;
                    % initially the trace is decelerative i.e. becoming smaller with throttle
                    % determine if lower region breaks through the high region
                if Torque_low(throtl)<Torque_high(throtl) & cnts<1;
                    cnts=1;
                    throt_high_low=throtl;
                %determine if lower rgion does not break the high region where the maximum of the lower region is
                elseif Torque_low(throtl)>Torque_low(throtl-1) & cnts<1 & throtl>15;
                    cnts=1;
                    throt_high_low=throtl-1;
                end
            end
        throtl=throtl+1;
    end %end throtl loop
    %=============================================================================================
    % Stage 5 - gradient fitting spline
          % count back 5 deg from point of throtl join. determine the gradient at this point
          % count forward on the high line 5 from join and determine the gradient there
          % then fit a spline between these points
    if throt_high_low>7
        %If the model joins mid-range then use large data area to determine local gradients
        low_start=Torque_low(throt_high_low-5);
                    gradient_low=(Torque_low(throt_high_low-5)-Torque_low(throt_high_low-7))/3;
                    high_start=Torque_high(throtl_high_low+5);
                    gradient_high=(Torque_high(throt_high_low+5)-Torque_high(throt_high_low+7))/3;
                    X=[throt_high_low-7 throt_high_low-5 throt_high_low+5 throt_high_low+7];
                    Y=[gradient_low Torque_low(throt_high_low-7) Torque_low(throt_high_low-5)…
                              .Torque_high(throt_high_low+5) Torque_high(throt_high_low+7) gradient_high];
                    PP = SPLINE(X,Y);
    else
           %If the model joins close to the minimum throttle possition, then only use
            % minimum data to determine gradient
                    low_start=Torque_low(throt_high_low-1);
                    gradient_low=(Torque_low(throt_high_low)-Torque_low(throt_high_low-1))/1;
                    high_start=Torque_high(throtl_high_low+5);
                    gradient_high=(Torque_high(throt_high_low+5)-Torque_high(throt_high_low+7))/3;
                    X=[throt_high_low-1 throt_high_low throt_high_low+5 throt_high_low+7];
                    Y=[gradient_low Torque_low(throt_high_low-1) Torque_low(throt_high_low)…
                               Torque_high(throt_high_low+5) Torque_high(throt_high_low+7) gradient_high];
                    PP = SPLINE(X,Y);
    end
    % Concatinate throttle join details to send to back to the main program
    Throt_high_low=[Throt_high_low throt_high_low];
    % Concatinate spline details to send to back to the main program
    pp=[pp PP];
end %end speed loop
return
%_____________________________________________________________________________________________
```

## De-NOx catalyst model

```
function [tailpipe_NOx]=de_nox_cat(post_TWC_NOx,exhaust_temp,mdot_air)
% De-NOx Cat model

% De-Nox Cataylst store NOx emissions. As with all stores they have a finite capacity. As a result their
% ability to store NOx deteriorates with time (or rather more specifically with duration and rate of NOx
% emissions and mass flow rate out of the engine). Once a De-NOx cataylst has reached a certain fraction of its
% capacity it is regenerated. During this process the engine runs in a rich manor, the excess fuel and CO is thus % used
to convert NOx to N2 and other gasious components (h2o, CO2 etc)

% Modelling:
% there is quite a large body of work which has been dedicated to modelling De-NOx cats. However they have taken a % very
fundemental and detailed approach which would not be approapriate for use in an optimiseation objective
% function

% Summary of basic factors that effect the performance of a De-NOx Cat.
% temperature - temperature has a very significant effect on absorption efficiency (maximum efficiency around 250 % deg C)
i.e. temperature determines the number of NOx storage location sites available. Rate of NOx emissions -
% since there are a finte number of locations available to store the NOx. Exhaust Mass flow rate - Again since
% there are only a finite number of NOx storage locations

% this model in its first iteration will try to determine the effects of temperature on the De-NOx cataylst
% efficiency. it will not concern itself with the effects of NOx rate or flow rate, it is assumed that the engine %
control will have some knowledge of the DE-NOx cat efficiency and as a result schedule regeneration cycles to
% maintain a certain level of NOx efficiency. However if the model is developed it should be modified to include
% some estimation of the total number of NOx absorption sites, this would allow an estimation to be made of the
% rate of regenerations required, and therefore it would be possible to determine the fuel consumption
% implications of the use of a De-NOx cataylst.

% temperature concerns
% typically the DE-NOx cat has it s greatest efficiency around 250 deg C, since engine out and post TWC emissions % are
typically of the order of 500 - 900 deg C it is necessary to position the De-NOx cat as far from the TWC
% outlet as possible (in passenger vehicles at any rate). A number of papers have investigated various methods to
% cool or control the cooling of the exhaust emissions before the De-NOx cataylst However here a simple heat
% release relationship will be examined. SAE paper 1999-01-349* examined the use of different exhaust systems to
% identify a configureation for optimal thermal efficiency. Within this paper are details of an exhaust system
% listing Diameters, and temperatures at the TWC outlet and the inlet to the De-NOx cat. Using this information it
% was possible to determine an approximate heat transfer coefficient for use with in determining inlet temperature % to
the DE-NOX.

heat_tranf_coeffic= 1.372;
% this value is very small, however this could be caused by power airflow in force convection
area_exhaust=  0.2639;
% m^2
% this is determined from SAE paper where the test vehicle was an Escort diameter is given as 48mm
% exhaust has a length of 1.750m between TWC outlet and DE-NOx cat inlet
CP= 1.107;                          % mean value estimate
exhaust_temp_k=exhaust_temp+273;
temp_inlet_denox_k=exhaust_temp_k-(((exhaust_temp_k-293)*heat_tranf_coeffic*area_exhaust)/((mdot_air/60)*CP));
% table of de-nox cat efficiency based again taken from SAE paper 1999-01-349*
temp_inlet_denox=temp_inlet_denox_k-273;
Temperature_deno_in=[0 50 150 200 250 300 350 400 450 500 550 600 700 800 900];
DENOX_eff_bytemp=[0 20 27 48 72 88 91 92 89 66 40 20 20 20 20];
% values taken here are for a 80000 km aged DE-NOx trap
xi = temp_inlet_denox;
yi = interp1(Temperature_deno_in,DENOX_eff_bytemp,xi);
Max_denox_eff=yi;
% as mentioned earlier we shall assume that the ECU has some understanding of the Cataylst efficieny and that it
% changes fuelling in order to regernerate the catalyst. The iterature does not discuss the lower level that will
% cause a de-nox regen. Therefore for this work we shall assume that it is 50% of the original maximum conversion
%efficincy.
min_denox_eff=Max_denox_eff*0.65;
mean_denox_eff=mean([Max_denox_eff min_denox_eff]);
% this is where a number of regenerations would be determined if it where required
tailpipe_NOx=post_TWC_NOx-post_TWC_NOx*mean_denox_eff/100;
```

```
return
```

## EGR and lean burn limits

```
function [Fuel,EGR]=limits2(Fuel_per,EGR_per,throt);
%_____________________________________________________________________________________________-
% This function is used to Impose maximum dilution limits
% the engine cannot actually tolerate the full range of dilutions across its full working envelope
% instead it is necessary to use a demanded dilution level and impose a dilution limit upon this
% From now on our inputs will be %lean and % EGR these are the maximum % tolerable for a given throttle speed
% combination and a given lean dilution
%==========================
% zero matrices
TOTAL=[];
FUEL=[];
Egr=[];
FUEL=[];
EGR=[];
%_____________________________________________________
%define maximum limits
Max_lean_low=1.5;
Max_lean_high = 1.5;
Max_EGR_low=100;
Max_EGR_high=100;
Max_comb_lean=10;
Max_comb_EGR=1.1;
%_____________________________________________________
%determine suitable dilution levels
if throt<30;
    % any condition less than 10% can not sustain any dilution
    if throt<10;
       EGR=0;
       Fuel=1;
    % if throttle is less than 30% the dilution limits increase with throttle possition to the maximum limit
    else
       Max_Fuel=(0.5)*((throt-10)/(30-10));
       Max_EGR=(100)*((throt-10)/(30-10));
    % dilution limits are set such that fuel is defined as a percentage of the maximum and throttle condition
    % while EGR is defined as a percentage of what is left of the maximum dilution potential
       Fuel=1+(Fuel_per/100)*Max_Fuel;
       Max_comb=(1.6-Fuel)*(throt-10)/((30-10));
       EGR=((EGR_per/100)*(Max_comb/0.6))*100;
    end
    % for throttle conditions greater than 30% the fuel is defined as a percentage of the maximum
    % and EGR is determined as a percentage of the dilution potential that is left
elseif Fuel_per>40
       Max_Fuel=0.5;
       Max_EGR=100;
       Fuel=1+(Fuel_per/100)*Max_Fuel;
       Max_comb=1.6-Fuel;
       EGR=((EGR_per/100)*(Max_comb/0.6))*100;
else
        Max_Fuel=0.5;
        Max_EGR=100;
        Fuel=1+(Fuel_per/100)*Max_Fuel;
        Max_comb=1.6-Fuel;
        EGR=((EGR_per/100)*(Max_comb/0.6))*100;
end
return
%_____________________________________________________________________________________________
```

## TWC function

```
function [passfail]=catalyst_model(raw_nox,raw_co,raw_co2,raw_uhc,raw_o2,power_condition,exh_temp,lambda,mdot_air)
%Catalyst model
% this function reads in the emissions as measured (and the lambda ratio & exhaust temperature)
%   ==> subsequently if the engine is operating in a stoichiometric manor it applies either the approaprtiate
% conversion efficientcy from rolling road data, or else it applies standard model conversion efficiecys.

CO_raw
CO2_raw
uHC_raw
O2_raw
NOx_raw
lambda
power
Exh_temp

j=0
load max_emissions&TWC_eff.txt
power_conds=max_emissions&TWC_eff(3)
%_____________________________________________________________
% looks for the current power condition.
[i,j]=find(power_conds==power)

%_____________________________________________________________
% if the current power condition is one of the specified one and the lambda value is within tolerable limits then we can
use the
% catalyst efficiency derived from work on the 1.6 L ford focus.
% the details of these relationships can be found in file powerlevels2.xls

if (j>0) & (lambda<1.1) %the current power condition is one of the ones on the EUDC which can be modelled by this work

    % conversion efficiency if determined from the EUDC trace. For steady state points the results were averaged over
similar points
    % for transient point the eficienies are the instantanious efficiency.


    conversion_eff_uhc=max_emissions&TWC_eff(9,j)   % conversion efficinecy of uHC
    conversion_eff_NOx=max_emissions&TWC_eff(10,j) % conversion efficiency of NOx
    conversion_eff_CO=max_emissions&TWC_eff(7,j)   % Conversion efficiency of CO
    conversion_eff_CO2=max_emissions&TWC_eff(8,j)  % conversion efficiency of CO2


%_____________________________________________________________
% if not the power condition is not one of the specified ones or else the engine is operating lean then the catalyst
efficincy can be
% modelled
% by standard catalyst efficiencies
else
        if lambda<1.2
                conversion_eff_NOx=      133333.3333318610*lambda^4      -      533571.4285655360*lambda^3      +
800160.9523721170*lambda^2 -
                … 532948.3571369720*lambda + 133026.4499985310
%polynomial developed by examination of conversion efficiecncy recorded in literature
        else
                conversion_eff_NOx=0
        end
        conversion_eff_CO = -704693.8082275390*lambda^5 + 3546050.3329715700*lambda^4 - 7135033.3799192000*lambda^3 +
        …7175646.9893343200*lambda^2 - 3606925.8018480600*lambda + 724956.6244838560
        conversion_eff_uhc = -704693.8082275390*lambda^5 + 3546050.3329715700*lambda^4 - 7135033.3799192000*lambda^3 +
        …7175646.9893343200*lambda^2 - 3606925.8018480600*lambda + 724956.6244838560
        conversion_eff_CO2=100/CO_eff
end
post_TWC_nox=raw_NOx-conversion_eff_NOx*raw_NOx
```

```
%_____________________________________________________________
% if the engine is operating lean then a DE_nox catalyst can be used to reduce the tailpipe nox emissions
if lambda>1.1
    tailpipe_NOx=de_nox_cat(post_TWC_nox,exhaust_temp,mdot_air)
else
    tailpipe_NOx=post_TWC_NOx
end

%_____________________________________________________________
% the quantity of other emissions can be determined as follows

tailpipe_uhc=raw_uhc-conversion_eff_uhc*raw_uhc
tailpipe_CO=raw_CO-conversion_eff_CO*raw_CO
tailpipe_CO2=raw_CO2-conversion_eff_CO2*raw_CO2
tailpipe_O2=raw_O2      % assume that it is not effected by TWC - obviously this is rather shallow

%_____________________________________________________________
% emissions reading considered upto now have been on a g/kwhr basis. However the emissions limits for individual powers
are on a mass basis
% therefore we need to transform the tail_pipe readings to a g/hr reading.

[tailpipe_NOx_g,                    tailpipe_uHC_g,                    tailpipe_CO2_g,                    tailpipe_CO_g,
tailpipe_O2_g]=emissions_correction(tailpipe_NOx,tailpipe_uHC,tailpipe_CO2,tailpipe_CO,tail_pipe_O2,power)

%_____________________________________________________________
% It is possible to determine the emissions limits for specific powers through scaling the rate of emissions production,
% during the course of a drive cycle to legislative limits. This approach has the benifits that it in effect takes into
account the engine warm-up
% process. However in scaling every value it does have the draw back of reducing the flexibility of the model
% the following arrays are the scaled legislative drive cycles for specific emissions. the development work for these can
be found in
% powerlevels2.xls

emissions_limits_power_NOx=max_emissions&TWC_eff(5,j)
emissions_limits_power_uhc=max_emissions&TWC_eff(6,j)
emissions_limits_power_CO=max_emissions&TWC_eff(4,j)

%_____________________________________________________________
% Pass ~ fail bit: if the tail pipe emissions are higher than the legislative limits then the operating condition is poor.
% A multiplier is passed back to the main program which will make these solutions appear comparitively very poor.
% future iterations of this code will enable a rather more judgemental approach, i.e. scaling the mutliplication factor as
measured
% emissions approach the legislative limits.

if      (tailpipe_uhc_g>emissions_limits_power_uhc(i))      |      (tailpipe_NOx_g>emissions_limits_power_NOx(i))      |
(tailpipe_CO_g>emissions_limits_power_CO(i))
       passfail=100
else
       passfail=1
end
return
```

## Transient response code

```
function [relative_transient_performance]=driveabilty(SPEED,torque,throt,cam,egr_demand,spk,power,lambda,speed_high_low)
speed_table=[1200 1400 1500 1700 1800 2000 2200 2400 2600 3000];
speed=speed_table(SPEED);
fuelling_duration=0;

global Opt_details
global P_throt_time_torque
global P_EGR_time_torque
global P_fuel_time_torque
global P_cam_time_torque
global P_throt_torque_time
global P_EGR_torque_time
global P_fuel_torque_time
global P_cam_torque_time


% driveability factor 2
% this function takes previously defined rate of transient response models defined through
% thorough testing across operating region of engine and subsequently determines the duration of each transient
% additionally it evaluates the torque margin available as a result of each torque step.

% Stages:
%   1. evaluates torque margin
%   2. determine the time required for each transient independantly
%   3. determine the greatest transient duration
%   4. compares this to a standard throttle transient
%   5. outputs a driveability factor


%_____________________________________________________________
% Evaluate torque margin
%   use WOT torque up look table for each speed to determine torque margin
WOT_TORQUE=[115 121 125 128 132 134 145 149 138 139]; %nomianal values
torque_margin=WOT_TORQUE(SPEED)-torque;

%_____________________________________________________________
% Determine the transient time required for each individual component of a transient event
% to achieve the response of the physical system is approximated by mathematical relaions ships

%------------------ Throttling --------------------------------
% duration of a standard throttle transient can be represented by an exponetial decay and an offset
% the exponential decay represents the throttle, manifold, filling dynamics. The offset represents the system
% lag to a demand.

% for every speed condition the offset will remain the same, however the characteristics of the exponential will
% alter with engine speed due to filling dynamics. However for a first approximation simply scaling the exponential factor
% will suffice. The curve was determined for 2600 rev/min

y0=0.08943;
a1=0.75324;
t1=5.88706;
a2=0.50985;
t2=72.37884;
scaling_factor=[0.55 0.589 0.52 0.395 0.375 0.44 0.581 0.7 0.7 0.59];
throttle_duration=0;

if throt<50
    throttle_duration=((a1*exp(-throt/t1)+a2*exp(-throt/t2))*scaling_factor(SPEED))+y0;
    %from unit curve we can identify the duration until it reaches 62%
end

%---------------------fuelling ---------------------------------------
% Examination of a range of lean dilution transients has shown that the duration of a lean
```

```
% transient is fairly independantly fuelling step it is simply a system lag. Following a system delay the
% fuelling dmand is changed, it is then necessary to wait for another firing event before the torque response
% can happen thue it is dependant upon speed. it can be represented by a series of system lags determined for each speed
% from experimental data
fuelling_lags=[0.37 0.289     0.26      0.211     0.194     0.17      0.165364762         0.17      0.17      0.184];
fuelling_duration=0;
if lambda>1.1
    fuelling_duration=fuelling_lags(SPEED);
end

%-------------------- EGR --------------------------------------------
% EGR transient duration is rather more complicated - there are value dynamic, manifold dynamics (including throttling
effects)
% and system lags to consider.

% Valve Dynamics - it is reasonable to suppose that the valve has a dead band just before at low and high demand
positions.
% For this work we will say that there is a dead band from 0-5% demand and from 90 - 100% demand.
% Additionally it does not close instantaneously and will be affected by the magnitude of inlet and exhaust manifold
pressure states.
% However if the start of transient is identified from the inlet manifold signal, the effect of valve and gas dynamics can
be
% negated.

% Manifold dynamics - for a given throttle position the effect of varying EGR should be linear with EGR position. The
maximum level
% of induced EGR will occur around 30 % throttle since this is the lowest throttle position where 100% EGR valve opening
is allowed.
c3=       -7.28E-06;
c2=       2.05E-03;
c1=       -1.92E-01;
c0=       7.01E+00;
demand_lag=0.02;
EGR_duration=0;
if egr_demand>10
          if throt>30
                    EGR_throttle_factor=c0+(c1*throt)+(c2*throt^2)+(c3*throt^3);
          else
                    EGR_throttle_factor=c0+(c1*30)+(c2*30^2)+(c3*30^3);
          end

          EGR_speed_factor=[0.49        0.460038072         0.44      0.400559279         0.376660019         0.33
          0.270229769         0.21      0.19      0.190815398];

          if egr_demand<10;
                    EGR_duration= demand_lag;
          elseif egr_demand>90;
                    EGR_duration= ((egr_demand-10)/100) * 0.9*EGR_throttle_factor * EGR_speed_factor(SPEED) + demand_lag;
          else
          %   effect of valve position
                    EGR_duration=   ((100-egr_demand-10)/100)   *   0.9*EGR_throttle_factor   *   EGR_speed_factor(SPEED)   +
demand_lag;
          end
end
%------------------ Cam ------------------------------------------------
% Following a transient demand the cam position, will be varied independly of speed, and throttle condition.
% its response will consist of a dead band (control system dynamics) followed by a continious ramp from
% the operating condition to the maximum torque condition
system_lag=2;
cam_max_torque=[0 10 24 26 26 26 30 32 32 25]; %from ECU lookup tables
if cam<cam_max_torque(SPEED)
    cam_duration=abs((cam_max_torque(SPEED)-cam)/cam_max_torque(SPEED))*((-1.4545454545E-04*speed)+6.6818181818E-01);
else
    cam_duration=0;
end

%----------------- Spark ----------------------------------------------
```

```
% the effect of spark timing on torque and subsequently driveability is small (maximum ~ 5 Nm)
% At this stage is sufficient to ignore the transient effect of spark timing, however if it was to be
% considered it would have the same transient response as a small lean step.
%=========================================================================
% determineation of relative transient duration
%_________________________________________________________________________
% In this section we try to find a relative transient duration factor.
% this is achieved by determining the greatest transient duration of the individual transient components
% then comparing the duration with that of a similarly size throttle only torque step.

%--------------- determine the greatest transient duration ----------
%determine which transient has the  greatest duration, such that the total engine transient may be evaluated
durations=[throttle_duration;EGR_duration;fuelling_duration;cam_duration];
[max_duration,index]=max(durations);
if index==1
    P_time_torque=P_throt_time_torque;
    P_torque_time=P_throt_torque_time;
elseif index==2
    P_time_torque=P_EGR_time_torque;
    P_torque_time=P_EGR_torque_time;
elseif index==3 | index==4
    P_time_torque=P_fuel_time_torque;
    P_torque_time=P_fuel_torque_time;
elseif index==4
     P_time_torque=P_cam_time_torque;
     P_torque_time=P_cam_torque_time;
else
%error no worst transient duration therefore there is no transient possible
    combined_transient_time=100;
    relative_transient_performance=1000;
    return
end
%_____________________________________________________________________________________________
% transient duration calculator
if max_duration>0
         trans_62per_unit=polyval(P_time_torque,0.62);
%subsequently by comparing real time and the unit time it is possible to predict the full duration of the transient event
         delta_unit_time=trans_62per_unit/max_duration;
% therefore for each time increment (- 0.01 seconds) the unit model increments 1 unit_time
% now we have to run through a transient event, evaluating the torque and incrementing the engine speed until the demanded
power is
% met
         trans_power=(speed*2*pi/60)*torque;
         i_max=10000 ;
         real_time=0;
         unit_time=0;
         max_unit_time=1000;
         engine_inertia=0.2; %flywheel inertia is approximately 0.157 however torotrak has an additional inertia effect
         delta_real_time=0.01;
         max_speed=3000;
         max_torque_speed=2600;
         max_speed_rad=3000*2*pi/60;
         max_torque_speed_rad=2600*2*pi;
         i=0;
         initial_torque=torque;
         cur_speed_rad=speed*2*pi/60;
         min_speed_rad=cur_speed_rad;
         while trans_power<42000 & i<i_max
                  if cur_speed_rad<max_torque_speed_rad
                    speed_torque_factor1=(max(WOT_TORQUE)-WOT_TORQUE(SPEED))*((cur_speed_rad-min_speed_rad)/...
                  ...(max_torque_speed_rad-min_speed_rad));
                    speed_torque_factor2=0;
                elseif cur_speed_rad<max_speed_rad
                    speed_torque_factor1=max(WOT_TORQUE)-WOT_TORQUE(SPEED);
                    speed_torque_factor2=(WOT_TORQUE(max_speed)-max(WOT_TORQUE))*((cur_speed_rad...
                  ...-max_torque_speed_rad)/(max_speed_rad-max_torque_speed_rad));
                else
```

```
                    speed_torque_factor1=max(WOT_TORQUE)-WOT_TORQUE(SPEED);
                    speed_torque_factor2=(WOT_TORQUE(max_speed)-max(WOT_TORQUE));
                end
% speed_torque_factor1 represents the increase in torque available as the engine speed increases upto 2600 rpm
% speed_torque_factor2 represents the decrease in torque present as the engine speed increases from 2600 to 3000
% note although the torque does rise again after the engine speed reaches 3000rpm it is not presented within these
calculations
                if unit_time<max_unit_time %the throttling transient has not been completed yet

        eng_torque=torque_margin*polyval(P_torque_time,unit_time)+speed_torque_factor1+speed_torque_factor2;
                    if eng_torque<0
                            eng_torque=0;
                    end
                else
                    eng_torque=torque_margin+speed_torque_factor1+speed_torque_factor2;
                end
               delta_torque=eng_torque;
% assume that all of the available torque margin will be used to solely accelerate the engine - thus leaving horrible
vehicle
% dynamics well alone
                alpha=delta_torque/engine_inertia; % alpha is the engine acceleration
                delta_speed=alpha*delta_real_time; % increase in speed caused by the available torque during the last
time period
                cur_speed_rad=cur_speed_rad+delta_speed; % recalculation of engine speed
                real_time=real_time+delta_real_time;
                unit_time=unit_time+delta_unit_time*delta_real_time;
                i=i+1;
                trans_power=(cur_speed_rad)*(eng_torque+initial_torque);
        end
        combined_transient_time=real_time;
end
%=========================================================================
% combination of driveability factor effects
% There is a difficulty in determining the relative importance of torque margin compared to transient response time.
% The torque margin represents the engines potential to accelerate to the final power condition. The transient response
represents
% initial jerk of vehicle following a transient demand.
% There is an additional complication since with changes in engine speed there is an accompanying change in both torque
margin and
% rate of change of torque.
% A method of combining the effects of torque margin and rate of change of torque is to determine a total transient time
from the
% operating
% condition to another operating point. For this work the final power demand condition is WOT at 3000 rev/min.
% to achieve this we have to determine the increase in engine speed required.
%=========================================================================
% Comparison of combined transient time with a control
% in this case the control that has been taken is transient performance of a similar vehicle operating a minimum fuel
consumption
% strategy
% To achieve this the optimisation program was run with fixed fuelling (lambda =1), fixed EGR (EGR=0) and individual power
conditions
% were investigated. The following table has been produced, which identifies the engine speed, throttle condition, cam
timing and
% spark timing required for
% a standard optimal fuel consumption strategy.
control_power_table=[2 4 6 8 10 12 14 16 18 20 22 24 26 28 30 32 34 36 38 40 42 44 46 48];
control_speed_table=Opt_details(7,:);
control_throttle_table=Opt_details(9,:);
control_cam_table=Opt_details(12,:);
control_spark_table=Opt_details(11,:);
control_torque_table=Opt_details(10,:);

[q,power_num]=find(control_power_table==power);
control_speed=control_speed_table(power_num);
control_throttle=control_throttle_table(power_num);
control_cam=control_cam_table(power_num);
```

```
control_spark=control_spark_table(power_num);
control_torque=control_torque_table(power_num);

if speed_high_low==1
    control_speed=fix(control_speed)-1;
elseif speed_high_low==2
    control_speed=fix(control_speed);
else
    control_speed=control_speed;
end

if control_speed>10
    control_speed=10;
end
%--- Evaluate torque margin
%   use WOT torque up look table for each speed to determine torque margin
SPEED_table=[1200 1400 1500 1700 1800 2000 2200 2400 2600 3000];
WOT_TORQUE=[115 121 125 128 132 134 145 149 138 139]; %nomianal values
control_torque_margin=WOT_TORQUE(control_speed)-control_torque;
control_speed_rpm=SPEED_table(control_speed);

%--- determine the throttle duration for this control transient
y0=0.08943;
a1=0.75324;
t1=5.88706;
a2=0.50985;
t2=72.37884;
scaling_factor=[0.55 0.589 0.52 0.395 0.375 0.44 0.581 0.7 0.7 0.59];
control_throttle_duration=((a1*exp(-control_throttle/t1)+a2*exp(-control_throttle/t2))*scaling_factor(control_speed))+y0;

%--- determine the cam transient duration for this control transient
system_lag=2;
cam_max_torque=[0 10 24 26 26 26 30 32 32 25]; %from ECU lookup tables
if control_cam<cam_max_torque(control_speed)
    control_cam_duration=abs((cam_max_torque(control_speed)-control_cam)/cam_max_torque(control_speed))*-1.4545454545E-
    …04*speed_table(control_speed)+6.6818181818E-01;
else
    control_cam_duration=0;
end
control_duration=[control_cam_duration control_throttle_duration];

%---- determine the length of the maximum transient duration
[max_duration2,index2]=max(control_duration);
if index2==2
    P_time_torque=P_throt_time_torque;
    P_torque_time=P_throt_torque_time;
elseif index2==3
    P_time_torque=P_EGR_time_torque;
    P_torque_time=P_EGR_torque_time;
elseif index2==4
    P_time_torque=P_fuel_time_torque;
    P_torque_time=P_fuel_torque_time;
elseif index2==1
    P_time_torque=P_cam_time_torque;
    P_torque_time=P_cam_torque_time;
else
%error no worst transient duration therefore there is no transient possible
    control_combined_transient_time=100;
end

%_____________________________________________________________________________
% transient duration calculator
if max_duration2>0
        trans_62per_unit=polyval(P_time_torque,0.62);
%subsequently by comparing real time and the unit time it is possible to predict the full duration of the transient event
        delta_unit_time=trans_62per_unit/max_duration;
%delta_unit_time2=throttle_62per_duration/throttle_62per_unit -- to deduce the total duration of the transient
```

```
%therefore for each time increment (- 0.01 seconds) the unit model increments 1 unit_time
%now we have to run through a transient event, evaluating the torque and incrementing the engine speed until the demanded
power met
        trans_power=(speed*2*pi/60)*torque;
        i_max=10000 ;
        real_time=0;
        unit_time=0;
        max_unit_time=1000;
        engine_inertia=0.2; %flywheel inertia is approximately 0.157 however torotrak has an additional inertia effect
        delta_real_time=0.01;
        max_speed=3000;
        max_torque_speed=2600;
        max_speed_rad=3000*2*pi/60;
        max_torque_speed_rad=2600*2*pi;
        i=0;
        initial_torque=control_torque;
        cur_speed_rad=control_speed_rpm*2*pi/60;
        min_speed_rad=cur_speed_rad;

        while trans_power<42000 & i<i_max
                if cur_speed_rad<max_torque_speed_rad
                        speed_torque_factor1=(max(WOT_TORQUE)-WOT_TORQUE(control_speed))*((cur_speed_rad…
                        …-min_speed_rad)/(max_torque_speed_rad-min_speed_rad));
                        speed_torque_factor2=0;
                        elseif cur_speed_rad<max_speed_rad
                        speed_torque_factor1=max(WOT_TORQUE)-WOT_TORQUE(control_speed);
                        speed_torque_factor2=(WOT_TORQUE(max_speed)-max(WOT_TORQUE))*((cur_speed_rad-…
                        …max_torque_speed_rad)/(max_speed_rad-max_torque_speed_rad));
                else
                        speed_torque_factor1=max(WOT_TORQUE)-WOT_TORQUE(control_speed);
                        speed_torque_factor2=(WOT_TORQUE(max_speed)-max(WOT_TORQUE));
                end
% speed_torque_factor1 represents the increase in torque available as the engine speed increases upto 2600 rpm
% speed_torque_factor2 represents the decrease in torque present as the engine speed increases from 2600 to 3000
% note although the torque does rise again after the engine speed reaches 3000rpm it is not presented within these
calculations
                if unit_time<max_unit_time %the throttling transient has not been completed yet;
                        eng_torque=control_torque_margin*polyval(P_torque_time,unit_time)+…
                        …speed_torque_factor1+speed_torque_factor2;
                else
                        eng_torque=control_torque_margin+speed_torque_factor1+speed_torque_factor2;
                end
                delta_torque=eng_torque;
% assume that all of the available torque margin will be used to solely accelerate the engine - thus leaving horrible
vehicle
% dynamics well alone
                alpha=delta_torque/engine_inertia; % alpha is the engine acceleration
                delta_speed=alpha*delta_real_time; % increase in speed caused by the available torque during the last
        time period
                cur_speed_rad=cur_speed_rad+delta_speed; % recalculation of engine speed
                real_time=real_time+delta_real_time;
                unit_time=unit_time+delta_unit_time*delta_real_time;
                i=i+1;
                trans_power=(cur_speed_rad)*(eng_torque+initial_torque);
        end
        control_combined_transient_time=real_time;
end

%=============================================================================================
% Determine relative transient performance
%=============================================================================================
relative_transient_performance=combined_transient_time/control_combined_transient_time;
```